Loss allocation in a distribution system with distributed generation units

Lund, T.; Nielsen, A.H.; Sørensen, Poul Ejnar

Published in:
Proceedings

Publication date:
2007

Document Version
Publisher's PDF, also known as Version of record

Risø-R-Report

Proceedings
Nordic Wind Power Conference
Risø National Laboratory
1-2 November 2007

Nicolaos Cutululis and Poul Sørensen (eds.)

Risø-R-1624(EN)

Risø National Laboratory
Technical University of Denmark
Roskilde, Denmark
November 2007

Author: Nicolaos Cutululis and Poul Sørensen (eds.)
Title: Proceedings Nordic Wind Power Conference Risø National Laboratory 1-2 November 2007
Department: Wind Energy Department

Risø-R-1624(EN)
November 2007

Abstract (max. 2000 char.):

This fourth Nordic Wind Power Conference was focused on power system integration and electrical systems of wind turbines and wind farms.
NWPC presents the newest research results related to technical electrical aspects of wind power, spanning from power system integration to electrical design and control of wind turbines.
The first NWPC was held in Trondheim (2000), Norway, the second in Gothenburg (2004), Sweden and the third in Espoo (2006), Finland.
Invited speakers, oral presentation of papers and poster sessions ensured this to be a valuable event for professionals and high-level students wanting to strengthen their knowledge on wind power integration and electrical systems.

ISSN 0106-2840
ISBN 978-87-550-3640-6

Contract no.:

Group's own reg. no.:
(Føniks PSP-element)

Sponsorship:

Cover :

Pages: 270
Tables:
References:

Information Service Department
Risø National Laboratory
Technical University of Denmark
P.O.Box 49
DK-4000 Roskilde
Denmark
Telephone +45 46774004
bibl@risoe.dk
Fax +45 46774013
www.risoe.dk

Contents

7. Poster session

Bulk Energy Transport Assessment on Wind Power
Case Study on utilizing Wind Power as a part of Intended Island Operation
The transport sectors potential contribution to the flexibility in the power sector required by large scale wind power integration
Analysis of electric networks in island operation with a large penetration of wind power
Load flow analysis considering wind turbine generator power uncertainties
Increasing Wind Power Penetration by Advanced Control of Cold Store Temperatures
A Load-Management Research Facility (FlexHouse) in Distributed Power Systems
Modelling of wind turbine cut outs in a power system region
State Space Averaging Modeling and Analysis of Disturbance Injection Method of Maximum Power Point Tracking for Small Wind Turbine Generating Systems
Modelling of floating wind turbine foundations for controller design
Capacity Credits of Wind Power in Germany
Wind Farm Repowering: A Case of Study
Wind Power in Power Markets: Opportunities and Challenges
Design aspects for a fullbridge converter thought for an application in a DC-based wind farm
A Model for the Assessment of Wind Farm Reliability based on Sequential Monte Carlo Simulation
Adaptive Markov-switching modelling for offshore wind power fluctuations
Real-time digital simulation of a VSC-connected offshore wind farm
Analysis of the experimental spectral coherence in the Nysted Wind Farm

Performance of Automatic Generation Control Mechanisms with Large-Scale Wind Power

Bart C. Ummels[1), *)], Madeleine Gibescu[1)], Wil L. Kling[1), 2)], Gerardus C. Paap[1)]
[1)] Delft University of Technology, Mekelweg 4, 2628 CD, The Netherlands
[*)] T +31 15 2784051, @ b.c.ummels@tudelft.nl
[2)] Transmission Operations Department of TenneT bv, TSO of the Netherlands, Utrechtseweg 310, 6812 AR Arnhem, The Netherlands

Abstract — The unpredictability and variability of wind power increasingly challenges real-time balancing of supply and demand in electric power systems. In liberalised markets, balancing is a responsibility jointly held by the TSO (real-time power balancing) and PRPs (energy programs).
In this paper, a procedure is developed for the simulation of power system balancing and the assessment of AGC performance in the presence of large-scale wind power, using the Dutch control zone as a case study. The simulation results show that the performance of existing AGC-mechanisms is adequate for keeping ACE within acceptable bounds. At higher wind power penetrations, however, the capabilities of the generation mix are increasingly challenged and additional reserves are required for keeping ACE at the same level.
Index Terms — Wind Power, System Integration, Secondary Control, Automatic Generation Control, Dynamic Simulation

1. Introduction

In the past decade wind power has become a generation technology of significance in a number of European countries. With further development of wind power on the horizon, the impacts of wind power on power system operation will increase as well. In particular the unpredictability and variability of wind power challenge real-time balancing of supply and demand in electric power systems. This is because significant amounts of wind power not only introduce additional power variations and uncertainty but may also decrease generation capacity available for secondary control. For balancing the fluctuations of wind power, additional power reserves may be required on top of power reserves already held for managing existing power variations in the system, which are caused by load variations and unscheduled generation outages.

In liberalized markets throughout Europe, participants have been made free to make arrangements for trading power in a number of forward markets. In order to guarantee a balanced power system, generation, load and energy trades are scheduled on beforehand and laid down in energy programs, which are sent to the system operator (TSO). In the Netherlands, the responsibility for maintaining the power balance in the system lies not only with the TSO but also with market participants responsible for delivering according to their energy programs. Based on the energy exchange programs received from these program responsible parties (PRPs) day-ahead, the TSO takes care of all real-time power imbalances using reserve power. PRPs are penalized for energy exchanges with the system different from specified in their energy program. Interestingly, in the Netherlands, wind power is subject to program responsibility as well, compared to the more common priority dispatch. Failure of a Dutch PRP to balance the partial predictability and variability of wind power with other generation/load in its portfolio therefore results in the payment of an imbalance price to the TSO [1]. Wind power will therefore impact the secondary control actions performed by PRPs.

Little research has been performed on the impacts of wind power on secondary control performance in general, and the integration of wind power into liberalized electricity markets in particular. Dynamic interactions between wind power and system frequency have been investigated in [2]. It is shown that the displacement of conventional generation with wind results in increased rates of change of system frequency for that particular system. However, for larger systems, system inertia may be considerably larger and impacts of wind power on this can be delineated as being less severe or absent [3]. Impacts of wind power on secondary control and the need for spinning reserves [3], [4] may however be more significant, also at low wind power penetration levels. Quantifying these using classical models for power-frequency control (Automatic Generation Control, AGC) does not consider energy program responsibility since these approaches implicitly assume a direct physical link between a secondary control signal by the TSO and a generator set-point change. Furthermore, any strategic behaviour by market participants is assumed to be absent. It is the objective of this paper to demonstrate a possible extension of existing models with such aspects and to illustrate the impacts wind power may have when fully integrated into program responsibility.

This research is focused on modelling load-frequency control dynamics in the presence of large-scale wind power subject to program responsibility. Simulation results are presented for different variants with wind power balancing by separate conventional generation portfolios subject to program responsibility, such as the case in the current market design in the Netherlands. A two-area power system model, representing a control area as part of a large interconnection, is set-up based on realistic data for generation units, loads, wind power production and forecasts. The novel contribution of this work consists in modelling the imbalance control by PRPs via minimization of their energy program deviations. The impact is assessed of different market designs on the total amount of reserve and regulation applied for balancing wind power and on Area Control Error performance.

This paper is organised as follows. First, the Dutch market design and its impact on wind power are briefly re-introduced in Section 2. Section 3 describes the development of a dynamic power system model for frequency stability and secondary control adequacy assessment, from both the perspective of the TSO and PRPs. In Sections 4 and 5, the set-up and the results obtained from the simulations are covered. Conclusions and an outlook on further work a presented in Section 6.

2. Market Integration of Wind Power

The responsibility for balancing large interconnected systems such as UCTE is typically divided between different transmission system operators (TSOs), each responsible for balancing its respective area (control zone). The whole process of power system balancing comprises many stages, starting with energy trade en ending with real-time balancing of unscheduled power exchanges of market participants with the system. In order to organise trade and guarantee a balanced system on beforehand, the concept of program responsibility is applied. This is illustrated and discussed in more detail below for the Netherlands.

2.1. Program Responsibility

With program responsibility, PRPs or program responsible parties (PRPs) have been made responsible for keeping their own energy balance. Each customer (generator or load) connected to the system is associated to a PRP. A PRP must maintain its energy balance (MWh) for each market settlement period or program time-unit (PTU). Program responsibility requires program responsible parties to provide energy programs (e-programs) to the TSO, describing the energy exchange with the system for each PTU, and to act accordingly. The e-programs in fact contain the sums of all scheduled generation, load and trade of one PRP with other PRPs: generation is delivered to the power system only if there is a load to match it. The sum of all e-programs of all PRPs should add up to zero.

PRPs have different markets to their disposal for trade, comprising bilateral contracts (blocks for long terms for physical position settlement), spot markets (up to one day preceding operation) and adjustment markets (up to one or a few hours before the hour of operation). At gate closure, all trading for the physical delivery of electrical energy ceases: PRPs submit their final schedules to the TSO. The schedules contain their intended energy exchanges with the system for each trading period. It is then the TSO who manages power reserves for maintaining the system balance. On top of the automated primary actions for system security, the TSO continuously manages secondary (available within 15 minutes) and tertiary reserves (available after 15 minutes) in order to maintain the balance in the system in real-time. Secondary and tertiary reserves are in general made available by PRPs submitting bids for operating reserves to the TSO. Since the capacity for system balancing is made available by PRPs who themselves must keep their energy balance as well, it should be noted that secondary control actions by the TSO and PRPs will coincide or, occasionally, interfere during operation. Furthermore, it is important to realise that program responsibility is based on economic incentives: the balancing costs encountered by the TSO are passed on to PRPs deviating from their submitted energy programs. Thus, PRPs will behave strategically in order to minimize their imbalance costs.

2.2. Program Responsibility for Wind Power

In the Netherlands, wind power is subject to program responsibility, just like conventional generation, which is unlike most market designs for wind power. PRPs are thereby financially encouraged to limit possible imbalances resulting from wind power variability and partial unpredictability: a power imbalance as a result of wind power implies an energy program deviation. In order to prevent imbalance costs, Dutch PRPs therefore monitor and manage their unit portfolio taking into account wind power predictions and real-time measurements.

Balancing wind power output deviations can be done by adjusting generation or load within the PRPs' portfolio or by taking precautionary measures on the market [1]. In order to be able to do so, wind power unpredictability and variability must be taken into account during unit commitment and dispatch calculations of an individual PRP with wind power in its portfolio. Wind power thereby is part of the overall operating decisions continuously made by PRPs.

As the amount of wind power increases, individual PRPs will be inclined to reserve more of the generation capacity within their portfolio for minimization of energy program deviations, while the TSO may not need significant extra reserves for balancing wind power. At the same time, any imbalances remaining after secondary control actions by PRPs must still be matched by the TSO, using the capacity made available by the PRPs. Wind power therefore challenges existing AGC-mechanisms applied both by PRPs and by the TSO for imbalance minimization.

3. Power System Model Development

In order to assess the impacts of wind power on the performance of secondary control or automatic generation control (AGC) mechanisms, a power system simulation model for the UCTE-area is developed. This dynamic model can be used for the simulation of long-term frequency stability, i.e. the ability of a power system to maintain steady frequency following a severe system upset, resulting in a significant imbalance between generation and load [5]. As an immediate consequence of such power imbalances, the system frequency changes and an area control error (ACE) is introduced. The TSO will then send out signals to selected PRPs for secondary response in order to re-install the system frequency at the set value. Below, the development of the model is described.

3.1. System Inertia and Primary Control

From a system point of view, frequency stability is determined by two system parameters comprising the response of the system as a whole: power system inertia and the system power frequency characteristic.

The model developed here effectively describes the power system as a mass rotating at a speed of 50 Hz. The actual rotational speed is dependent on the amounts of mechanical power added to or taken from this mass. A uniform frequency is assumed using an aggregated inertia constant of an equivalent one-machine infinite bus system, such as applied in [6]. The power frequency characteristic (the overall dynamic response of generation and load to a power balance) consists of a load self-regulation factor of 1 and an aggregated primary response of generators in the UCTE as a whole. Detailed primary responses of 70 units in the Dutch system have been modelled explicitly using historical unit models available to the authors. The resulting aggregated primary response of the model has been compared to frequency data supplied by Dutch TSO TenneT, using an approach as presented in [7].

For the estimation of system inertia and primary response of the UCTE-interconnection, 4s. frequency deviation measurements were obtained for 88 significant instantaneous

power imbalances in the UCTE-interconnection from 10/2004 to 12/2006. The power frequency characteristic was found to lie between 19·10e3 MW/Hz and 47·10e3 MW/Hz, with a mean of 26·10e3 MW/Hz and a standard deviation of 9·10e3 MW/Hz. With an allowable measurement inaccuracy of 10 mHz in place for generators on primary control, a primary response of the model is obtained as shown in Fig. 1, illustrated with a small number of recordings representative of the full data set.

3.2. Secondary Control

The area control error (ACE) represents the total power deviation of a system (MW) and comprises unscheduled power exchanges of the area with neighbouring areas and the frequency deviation of the system. For secondary control purposes, ACE is typically processed using a PI-controller (processed ACE, PACE) before it is sent to units on secondary control. The PACE-logic has the objective of minimizing ACE while neglecting fast dynamics in system frequency, which would result in unnecessary, fast changes in demands for secondary control. In this model, it is assumed that ACE occur in the Dutch area only and that Dutch secondary control alone returns ACE to zero. The rest of the UCTE-system is balanced but will contribute to primary reaction in case of significant frequency deviations. Dutch ACE and PACE have been modelled using the mechanisms developed and currently applied by Dutch TSO TenneT. A power frequency characteristic of 900 MW obtained from operational experiences of the TSO is applied, which is then compared to a two-stage threshold for fast response to significant events. Also, PACE is set such that its integral term does not increase (decrease) further in case ACE is positive (negative) but decreasing (increasing).

For real-time power system balancing, the TSO applies secondary reserves made available by PRPs through a bidding ladder (selection of cheapest bids). Bids are orderly arranged based on price in a power reserve bidding ladder, a separate ladder for upward and downward reserves. During real-time operation, the TSO continuously determines the amount of reserve power that is needed, based on the actual PACE. Using the bidding ladder, the amount of required reserves is mirrored onto the available bids which are then called off by the TSO. This is done by sending a *delta*-signal (MW-set point) to the PRP associated with each bid called, using a separate delta for both upward and downward reserves. The rate-of-change of delta does not exceed a ramp-rate value pre-specified by the associated PRP. Every four seconds, the PACE is re-calculated to determine whether the sum of all bids called (MW) is sufficient for balancing the control zone and which bid should be used up to which extent. In case PACE drops below an active bid's threshold and the bid is no longer necessary, the bid is reduced with a ramp rate no more than the maximum specified in the bid. Because of this ramp rate limitation, positive and negative bids may be active simultaneously. It is the responsibility of the market party associated with the bid called off to adjust its generation operating points and/or load schedules accordingly.

3.3. Energy Program Responsibility

When a power imbalance is picked up by the TSO (i.e. ACE) and secondary control is activated, the generation/load deviations from scheduled values causing it will also be picked up by the PRP responsible for it. Simultaneously with secondary control at the system level, the PRP will take measures in order to minimize its energy program deviation (not necessarily its power imbalance) in order to avoid imbalance costs. The PRP will not only monitor its power imbalance (MW), but also physical position within the PTU (MWh). The actual power imbalance of each PRP is constantly assessed by monitoring generation and load deviations from scheduled values while settling the secondary control signal received from the TSO. For imbalance minimization, a fraction of the actual power imbalance is integrated and subtracted from the set-point of generation units selected by the PRP for imbalance management. Because participation in secondary control is taken into account in calculating its imbalance, both the PRPs' imbalance and the system imbalance are eventually returned to zero.

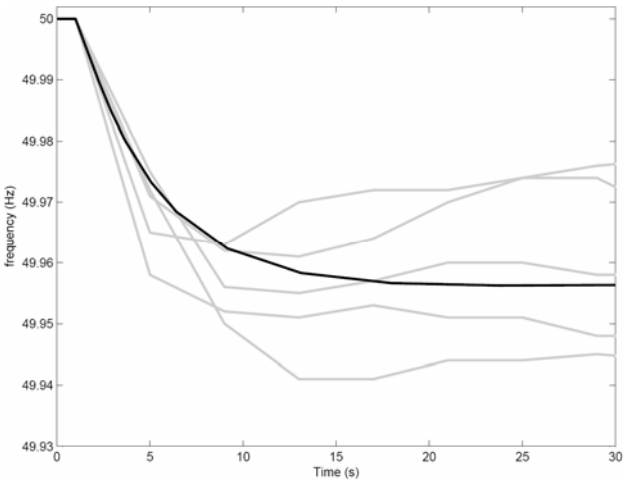

Fig. 1. Validation of system inertia and power frequency characteristic

Since imbalance costs are settled not on a MW but on an MWh/PTU basis, the energy imbalance for each PTU is the most relevant parameter for a PRP. The MWh-value specified in the PRPs' energy program is the operational objective: during each PTU, the overall energy deficit or surplus compared to the energy program must be minimized. For the counter-balancing of power deviations, different operating strategies for imbalance minimization may be applied in order to reach the energy value objective, as shown in Fig. 2 (area under all three modi is equal). Interviews by the authors with Dutch PRPs have revealed that the preferable operation modus is the most gradual one (B), even though this involves a continuous adjustment of operation set-points of units under secondary control, which could partially be prevented by opting for strategies A and C, or other. In the model, the energy program deviation is constantly calculated and fed back into the secondary control signal. At the start of each PTU, the energy-program deviation is reset to zero.

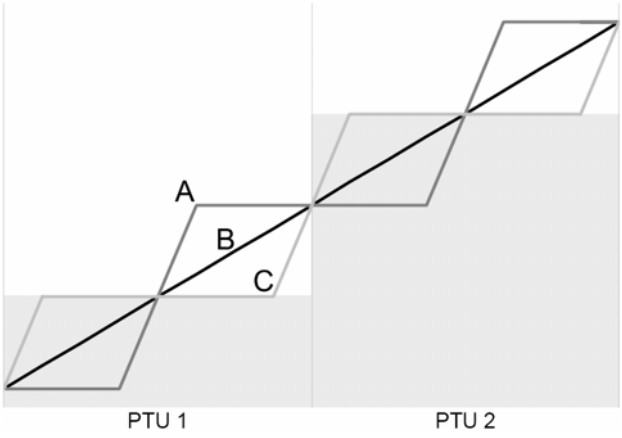

Fig. 2. Different operating strategies between energy-programme set-points

3.4. Generation Units

A number of existing dynamic generation unit models for Dutch plant have been compared to literature models [8]. It is found that, for long-term frequency control simulations, a differentiation must be made between initial responses and more persistent ones. The former are determined mainly by the governing system (valve positions) while in the longer term, the physical processes in the boiler become more important. For unit start-up or shut-down, these physical processes may require hours up to days, which must be taken into account when calculating the unit commitment and economic dispatch (UC-ED) of these units.

In this work, dynamic response (seconds) and primary reaction of 70 Dutch units part of PRPs' portfolios have been modelled explicitly. The models incorporate typical aspects as primary reaction and speed, power-frequency, turbine and fuel control. Longer-term physical aspects (minutes) have been delineated; instead, fixed ramp-rates not governed by physical limitations but by controls have been assumed, as is current practice for all units part of the PRPs' dispatch. UC-ED (weeks to hours) of the main Dutch generation units is calculated using a commercial optimization tool previously applied in [9].

As an example of the dynamic models of the generation units, Fig. 3 shows the simulated responses of some unit models developed for this research: a coal unit, a combined cycle gas turbine (CCGT) and a cokes gas unit in the Dutch system. All units are at a 0.6 p.u. operating set-point. At t = 0 s., a frequency drop of 0.004 p.u. is introduced, leading to a primary response of all units (a dead zone of 0.002 p.u. is assumed), resulting in a full primary response within 10-20 seconds. As can clearly be seen, the units all show a fast initial and a slower, more persistent response. At t = 30 s., the operating set-point is stepped up from 0.6 to 0.65 p.u. In this case, the dynamic response of the unit is governed by the unit ramp-rate controls. More detailed modelling of the unit dynamics therefore does not translate into added value for the simulations and have therefore not been incorporated. Notably, several Dutch PRPs have indicated to the authors that detailed physical models of their units are in fact not available to them.

3.5. Wind Power

With the modelling of wind power, it has been borne in mind that it is the objective this work to investigate the impacts of wind power on automatic generation control performance. Since the overall power fluctuations of wind power clusters are of importance here, detailed models for wind turbines fall outside of the scope of this paper. Wind speeds at representative locations of Dutch wind parks onshore and offshore have been developed using wind speed data obtained from the Royal Dutch Meteorological Institute (KNMI). The data concerns 10-minute wind speed averages with a resolution of 0.1 m/s for 18 locations in the Netherlands (9 onshore, 3 coastal and 6 offshore) measured between June 1, 2004 and May 31, 2005. Wind speed time series for the study period are created for 15-minute time intervals in such a way that the spatial correlation between the sites is taken into account. The development of wind speed data is described in more detail in [9]. For simplification, it has been assumed that the effects of turbulence on the aggregated output of each wind farm within each 15 min. interval are small because of smoothing of fluctuations [10].

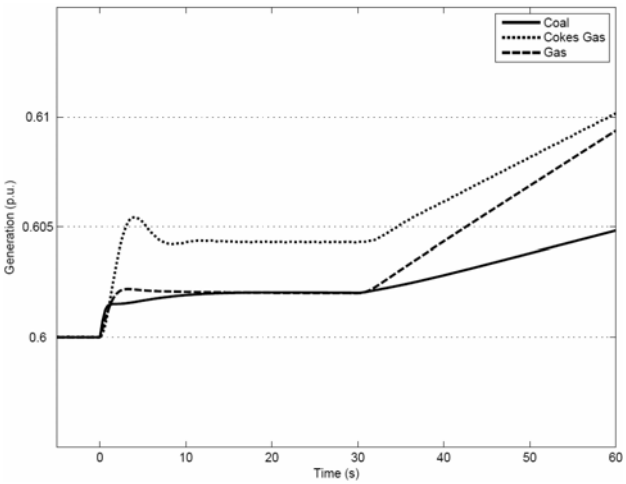

Fig. 3. Simulated responses of three generation unit responses to frequency and a operating set-point steps

4. Simulation Set-Up

4.1. Simulation Method

The operation schedules of conventional generation units are governed by a number of longer-term aspects which fall outside the scope of the dynamic simulation model developed here. These aspects include scheduling of maintenance, market trading and settlement procedures of markets, which lead to the calculation of UC-ED schedules for each unit in the system. In order to arrive at a realistic starting point for the dynamic simulations, the following simulation set-up is applied:

- *Calculation of UC-ED*: A chronological UC-ED model with the same make-up as the dynamic model (generation units, wind power etc.) is run for a week or any longer period of time using a 15-min. time step. Steady-state operating set-points for each generation unit are obtained and saved.
- *Select cases*: The output of the UC-ED model is analysed and interesting cases for dynamic simulation (simultaneous wind power drop and load increase, generation outages etc.) are selected. A small number of

consecutive states including the selected state are isolated.

- *Import of unit set-points*: The operating set-points for all units are imported into the dynamic model. Interpolation is applied to obtain continuous operating signals serving as an input for the dynamic model of each unit.
- *Initialization and dynamic simulation*: The dynamic model is initialised around the operating points of the first state and then run. Power deviations occurring in real-time may be simulated by adding these deviations (i.e. wind gusts or random noise) to the set-points imported from the UC-ED-results. Valid parameters such as system frequency, ACE and PACE and power imbalances and energy program deviations of PRPs are reported.

For each PRP, one or more units are selected for AGC by the PRP, based on daily operating routines of Dutch PRPs. Furthermore, PRPs make bids available to the TSO for secondary reserves, which are then taken into account with the scheduling of UC-ED. Notably, PRPs prefer to use base-load coal units – if available within the portfolio of the PRP – for managing e-program deviations.

4.2. Simulated Variants

The following simulations are run:

a) System operation without wind power
b) Large variation of 2 GW wind power
c) Forecast error and large variation of 2 GW wind power
d) Large variation of 4 GW wind power
e) Forecast error and large variation of 4 GW wind power

Simulation a) is used to provide a base-case for comparison with the simulations with wind power. Since for this simulation, no data are added compared to the set-points imported from the UC-ED-model and no wind power is present, the power imbalance at any moment in time should be small, resulting in a small ACE and PACE. Also, the results imported from UC-ED will be different since wind power will impact the scheduling of conventional units.

In simulations b) and c), wind power increases between t = 450s. and t = 1350s from 553 MW to 1207 MW (+654 MW) and then decreases between t = 1350s. and t = 3150s. to 707 MW. In simulation b) it is assumed that wind power is perfectly predicted and no real-time deviations occur. Therefore, the UC-ED will incorporate wind power and ACE and e-program deviations resulting from wind power imbalances can be expected to be small, although a more dynamic operation of conventional units is expected. In simulation c), a 'real-time deviation' signal of wind power is added to the wind power set-points imported from the UC-ED-results in order to simulate unscheduled wind power output. Thus, PRPs and the TSO will apply secondary reserves to balance forecast errors and ACE as a result of it. PRPs experiencing wind power deviations in real-time apply secondary control in order to avoid energy program deviations.

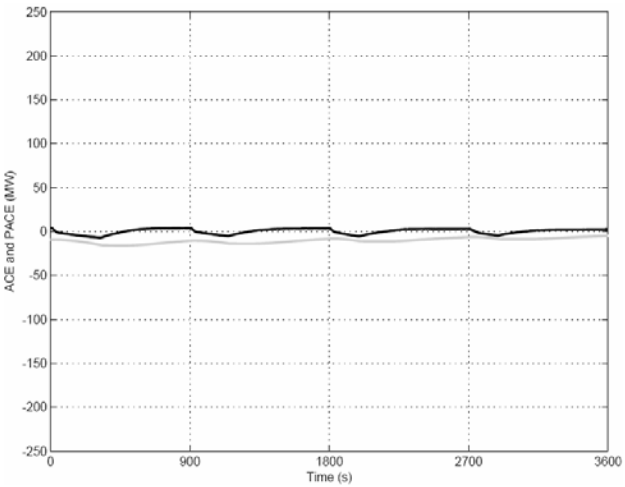

Fig. 4. Area Control Error (ACE, black line) and Processed Area Control Error (PACE, grey line) of the Dutch control zone with 0 GW wind power.

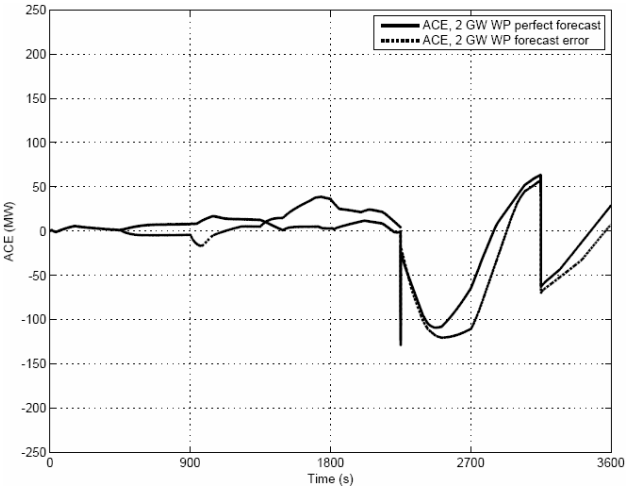

Fig. 5. ACE for the Dutch control zone with 2 GW wind power with perfect forecast b)(line) and with forecast error c)(dotted line).

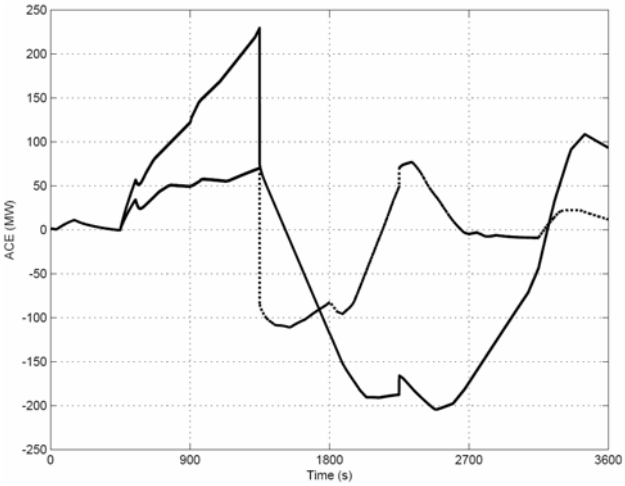

Fig. 6. ACE for the Dutch control zone with 4 GW wind power with perfect forecast d)(line) and with forecast errors e) (dotted line).

In simulations d) and e), wind power increases between t = 450s. and t = 1350s from 983 MW to 1736 MW (+753 MW) and then decreases between t = 1350s. and t = 3150s. back to 743 MW. In simulation d) it is assumed that wind power is perfectly predicted, in simulation e) wind power deviates in real-time from scheduled values.

5. Simulation Results

5.1. System Perspective: ACE

In Fig. 4, the simulation results for a selected one-hour simulation period of the model is shown. Since for this simulation model, the generation and load set-point results from the UC-ED calculations are directly imported into the dynamic program and no sudden changes in unit output are present, ACE is very close to zero. As a result, PACE is also small.

Fig. 5 shows the simulation results of the same one-hour period, but now with 2 GW wind power. The UC-ED of other units in the system is scheduled to respond to this. As a result of the significant wind power variations, the UC-ED is changed compared to the situation without wind power: two units are now taken out of operation (t = 2250s. and t = 3150s.) and one unit starts operation (t = 1350s). Since these conventional generation units have a minimum power output level, committing or de-committing these units results in a sudden steps in ACE. ACE is also influenced by wind power forecast errors: apparently, PRPs are unable to take these into account fast enough as to prevent power imbalances, which directly result in an increase of ACE, as can be seen in the figure.

In simulation variants d) and e), the variations of wind power are even higher than in simulation variants b) and c) and therefore a different UC-ED schedule has been chosen. At t = 1350s, one large unit is taken out of operation while at t = 2250s. a smaller unit is committed. Because of the large wind power variations, ACE significantly increases between t = 450s. and t = 1350s. Apparently, the reserves committed for balancing the wind power variations (Fig. 6) are not sufficient to keep ACE within a range comparable to Fig. 5.

It can be noted that for simulation e), the forecast errors actually improve ACE performance. For some PRPs, forecast wind power variations were actually larger than actual wind power variations. Because of this, more capacity was available for secondary control actions requested by the TSO. It can also be noted that UC-ED calculates the de-commitment of a large unit at t = 1350s. Apart from the high possible risk for a PRP actually doing so, ACE performance would suggest the commitment of more power reserves.

5.2. Market Perspective: E-Program Deviation

In Fig. 7, above, scheduled generation and total generation level delivered during real-time operation are shown for one program responsible party, PRP1, for simulation b) (2 GW wind power, perfect wind power prediction). The scheduled total generation of this PRP is rather constant. Because PRP1 does have wind power in its portfolio, its other generation units have apparently been scheduled in such a way that wind power variations are balanced. Initially, PRP1 stays very close to its scheduled generation output, but at t = 450s. it increases its generation. This can be explained by considering the demand for secondary control by the TSO, to which PRP1 then responds by increasing generation units selected for this and by any secondary control actions of PRP1 itself in order to minimize energy program deviations.

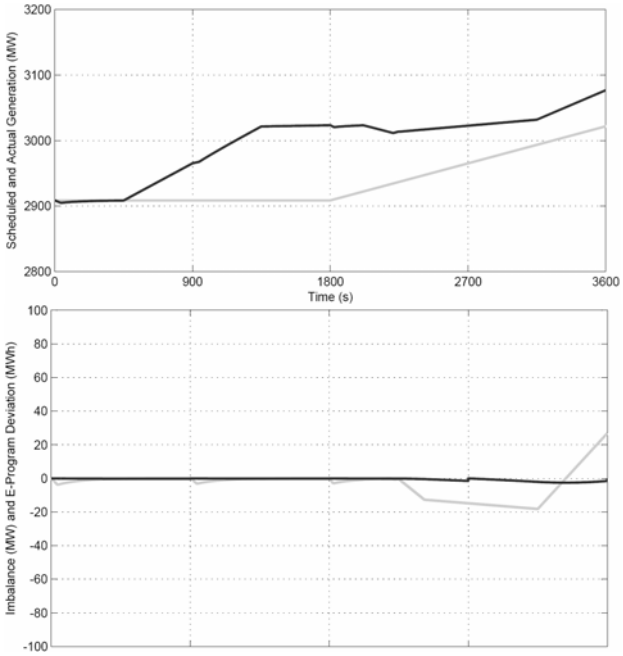

Fig. 7. Above: Scheduled (MW, grey line) and actual generation (MW, black line). Below: power imbalance (MW, grey line) and energy program deviation (MWh, black line). All for PRP 1 for simulation b).

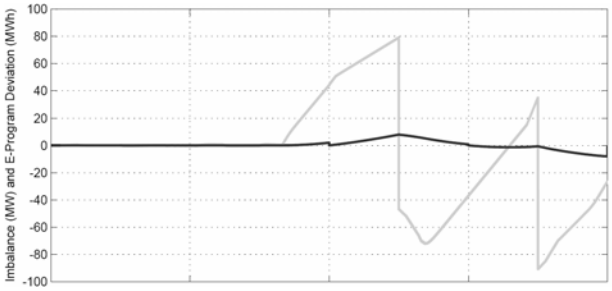

Fig. 8. Power imbalance (MW, grey line) and energy program deviation (MWh, black line) .for PRP 1 for simulation b)

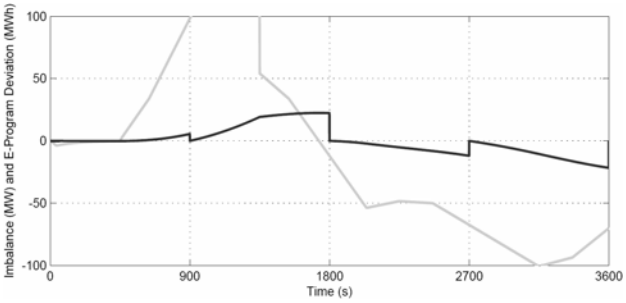

Fig. 9. Power imbalance (MW, grey line) and energy program deviation (MWh, black line) .for PRP 2 for simulation d).

In the lower graph of Fig. 7, the real-time power imbalance and energy program deviation of PRP1 are shown for the same simulation. Clearly, PRP1 is initially very successful in minimizing its real-time power imbalance and energy program deviations. After t = 2250s., however, the real-time

imbalance increases considerably, although strategic imbalancing between t = 2700s. and t = 3600s. still keeps the energy program deviation small. It should be noted that the energy program deviation at the end of each PTU (900s., 1800s., 2700s., 3600s.) is the value which the final imbalance costs are based upon. At the beginning of each PTU, the e-program deviation is reset.

Fig. 8 shows PRP2 who intends to minimize its energy deviation by strategically timing its power imbalance. Since this PRP has chosen to take two large units out of operation during this period in order to balance the foreseen wind power decrease between t = 1350s. and t = 3150s. In order to minimize its energy program deviation, PRP2 first overshoots, then takes its first unit out of operation, after which it reduces its imbalance again. The overall result of these actions is that the energy program deviation at the end of PTU 3 is very close to zero. However, PRP2's control actions have an impact on ACE as can be seen in Fig. 5.

In case PRP2 has more wind power in its portfolio, a different UC-ED is chosen. Apparently, it is now more optimal to de-commit one unit at t = 1350s., compared to the two units in simulation b) / Fig. 8. However, PRP2 is not able to balance its own portfolio including wind power while responding to secondary control signals from the TSO at the same time. Since its ramping capabilities for balancing wind power balances are already heavily used, PRP2 runs into a large power imbalance since it is unable to respond to the TSO signal. The secondary control actions upwards and downwards are not enough to prevent significant energy program deviations. PRP2 needs larger amounts of secondary reserves and/or reserves with higher ramp rates in order to prevent this.

6. Conclusions

A model has been developed for the simulation of power system balancing and the assessment of AGC performance in the presence of wind power. The Dutch control zone is used as a case study for the integration of wind power under program responsibility. The simulation results show that the performance of existing AGC-mechanisms of both TSO and program responsible parties are adequate for returning ACE to small values within one PTU (15 min.) and energy program deviations within bounds. It is shown that the variability of wind power may lead to higher ACE, especially if insufficient amounts of reserves are taken into account during the unit commitment and economic dispatch calculations.

A notable simulation result is that the variability of wind power not only has a direct impact on ACE and power imbalances of program responsible parties, but also an indirect one. Significant wind power variations are shown to have an impact on commit and de-commit decisions of conventional units in the system, which in turn trigger strategic imbalancing by PRPs. The ACE as a result of this then requires the TSO to apply additional secondary reserves. Thus, even though the steady-steady UC-ED schedule is in balance for each state, variations in real-time as well as demands for secondary control by the TSO may require additional ramping capabilities of the units. These must be taken into account in the UC-ED in order to minimize power imbalances during operation.

Acknowledgement

This work is part of the project PhD@Sea, which is funded under the BSIK-program of the Dutch Government and supported by the consortium we@sea, http://www.we-at-sea.org/. The authors acknowledge the use of system data provided by the Dutch TSO TenneT. The Royal Dutch Meteorological Institute (KNMI) is acknowledged for the use of wind speed and HIRLAM data.

References

[1] B.C. Ummels, M. Gibescu, W.L. Kling, and G.C. Paap. Integration of Wind Power in the Liberalized Dutch Electricity Market. *Wind Energy*, 9(6): 579–590, Nov.–Dec. 2006

[2] G. Lalor, A. Mullane, and M. J. O'Malley. Frequency Control and Wind Turbine Technologies. *IEEE Transactions on Power Systems*, 20(4): 1905–1913, Nov. 2005

[3] G. Dany. Kraftwerksreserve in elektrischen Verbundsystemen mit hohem Windenergieanteil (in German). Ph.D.-thesis, RWTH Aachen, 2000

[4] R. Doherty and M. J. O'Malley, Quantifying Reserve Demands due to Increasing Wind Penetration, Proc. IEEE Bologna PowerTech Conference, June 23–26, 2003, 5 pp.

[5] P. Kundur. Power System Stability. McGraw-Hill Inc. 1994

[6] P. M. Anderson and M. Mirheydar. A Low-Order System Frequency Response Model. *IEEE Transactions on Power Systems*, 5(3): 720-729, Aug. 1990

[7] J. O'Sullivan, M. Power, M. Flynn and M. J. O'Malley. Modelling of Frequency Control in an Island System. Proc. IEEE Power Engineering Society 1999 Winter Meeting, Jan. 31–Feb. 4, 1999, pp. 574–579

[8] F. P. de Mello, R. J. Mills, and W. F. B'Rells. Automatic Generation Control Part I - Process Modeling. *IEEE Transactions on Power Systems*, PAS-92(2): 710–715, 1973

[9] B. C. Ummels, M. Gibescu, E Pelgrum, W. L. Kling and A. J. Brand. Impacts of Wind Power on Thermal Generation Unit Commitment and Dispatch. *IEEE Transactions on Energy Conversion*, 22(1): 44–51, Mar. 2007

[10] T. Nanahara, M. Asari, T. Sato, K. Yamaguchi, M. Shibata and T. Maejima. Smoothing Effects of Distributed Wind Turbines. Part 1. Coherence and Smoothing Effects at a Wind Farm. *Wind Energy*, 7: 61–74, 2004

Integration of large-scale offshore wind power in the Norwegian power system

Magnus Korpås*), Thomas Trötcher, John Olav Giæver Tande
SINTEF Energy Research, N-7365 Trondheim, Norway
*) tlf. +47 7359 7229, e-mail magnus.korpas@sintef.no

Abstract — Deep sea offshore wind farms may be developed to constitute a significant part of the total power system generation. This paper describes a simulation study of integrating 5500 MW offshore wind power in the Norwegian power system, using a power market model of North-Western Europe. The results illustrates that wind energy has the potential to effectively relieve constrained energy situations in Norway. When also considering the possible increase in onshore wind generation and hydro generation, the simulations indicate a need for increasing the cross-border transfer capacities in order to avoid hydro spillage and thus enhancing the possibilities of exporting large amounts of renewable energy to the continent.

Index Terms — hydro power, offshore wind power, power exchange, power market.

1. Introduction

There are vast wind energy resources outside the Norwegian coastline. In contrast to offshore wind farms that today are built at shallow waters with relatively short transmission distances to the mainland, the most promising prospects outside Norway are at water depths from 30 to 150 meters, located more than 50 km from shore. This is manly because of public opposition against wind farms close to shore and onshore, and because the majority of areas outside the Norwegian coastline are at deep sea. There are several ongoing research and development projects on the design of different bottom-supported and floating wind turbines, giving hopes for future exploitation of the enormous offshore wind potential at deeper waters.

Deep sea offshore wind farms may be developed to constitute a significant part of the total power system generation. This implies that there are system wide impacts related to transmission planning and system operation that need to be addressed. Since the existing power supply consists almost entirely of hydro power plants, a high wind penetration will raise new challenges in how to optimally utilize the hydro reservoirs with respect to balancing short-term and seasonal wind variations. In contrast to dispersed regional onshore wind farm development, the offshore wind scenario implies large blocks of wind farms connected to relatively few central grid nodes. Thus, handling of transmission bottlenecks in the central grid becomes especially important, including utilization of interconnections to other countries.

This work addresses system implications of large-scale offshore wind power integrated in the Norwegian power system. A scenario with 5500 MW offshore wind power in Norway has been studied regarding the impact on electricity price, transmission bottlenecks and hydro power utilization. With an estimated capacity factor as high as 50%, the scenario gives an annual generation of 25 TWh, which corresponds to about 17% of today's inland consumption.

2. Prospects for offshore wind power in Norway

2.1. Offshore wind turbine concepts for deeper waters

Offshore wind farms have so far been installed at shallow waters (-30 m) using gravity base structures or mono-piles. However, the potential at deeper water is huge provided that costs can be reduced to a competitive level. The relevant technologies for foundation appear to be tripod or jacket support structures (-70 m) and floating concepts for greater depths.

The use of tripod and jacket foundations are well known from the offshore oil and gas industry, but these must be scaled in size and costs to fit offshore wind turbines. OWEC Tower AS has designed a jacket substructure which was selected for the Beatrice Demonstrator Project [1], while Aker Kværner is to deliver substructures for wind turbines off the coast of Germany and France [2]. Hydro has recently released ambitious plans for their floating concept HyWind [3]. The concept is simple in the sense that it may use any state-of-the-art wind turbine which will be fixed to a floating concrete substructure and then only requires some additions to the wind turbine control system. An alternative floating concept is promoted by SWAY [4]. Here a downwind turbine is assumed, and the upper part of the tower is streamlined to minimize the disturbance of the wind acting on the rotor. The tower is stiffened by a taut cable arrangement on the upwind side of the tower.

2.2. Grid integration

Development of deep sea offshore wind farms in sizes of some tens of MWs is interesting for supply to offshore oilrigs. But in the long run deep sea offshore wind farms connected to the main grid may be developed to constitute a significant part of the total power system generation. A very large offshore wind farm, say 1000 MW, is likely not built in one block, but rather as five blocks a 200 MW (or in that order). The reason for this is partly that a large block would appear as a roughness element in the sea and by that reducing the wind resource over the site. At a block size smaller than 200 MW this effect is less pronounced. Other reasons are limitations of electrical equipment to handle such high power and for improving the technical availability.

The most important factor for choosing grid structure is the size of the wind farm and the distance to the connection point. Until a recently it has been a well established "fact" that the use of conventional AC cable transmission is limited to relatively short distances. The reasoning was mainly

because of the cable capacitance (F/km) that causes reactive current and hence reduction of the cable capacity to transport active power. Using reactors or similar to counteract on this makes it however viable to transmit power on AC over longer distances. HVDC is still an alternative, either based on Line Commutated Converters (LCC) or Voltage Source Converters (VSC).

2.3. Wind conditions

There are enormous areas at deeper waters outside the Norwegian coastline which could be available for developing offshore wind farms. Knowing that the wind conditions at the Norwegian coastline are among the most favorable in Europe and that the average wind speeds generally increases with the distance from the shore, it is expected that offshore wind farms located 50 km or more off the coast will achieve very high average production pr MW installed.

To estimate the production potential, hourly wind series for year 2005 from five representative measurement stations has been combined with a normalized wind power curve based on a state-of-the-art wind turbine suitable for high wind speed sites. Figure 1 and Figure 2 compare the normalized sum of production with a similar onshore wind power series and the actual wind generation in Denmark-West. The estimated utilization factor for offshore wind power is about 50%. This is indeed much higher than what could be expected for onshore wind power in Norway, with typical utilization factors ranging from 30% to 40%. Taking all uncertainties into account, it is emphasized that the estimated utilization factor for offshore wind power is indicative only, but it is nevertheless reasonable to expect that that the production potential pr MW installed is much higher than onshore.

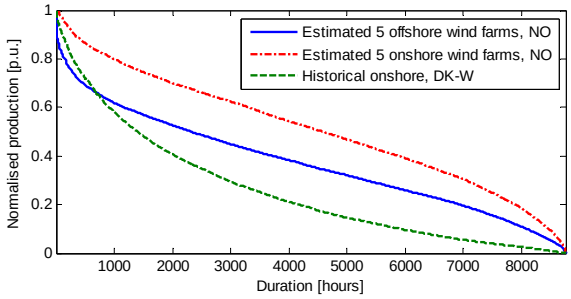

Figure 1. Duration curves for estimated offshore and onshore wind power in Norway, and for actual production in Denmark-West, 2005.

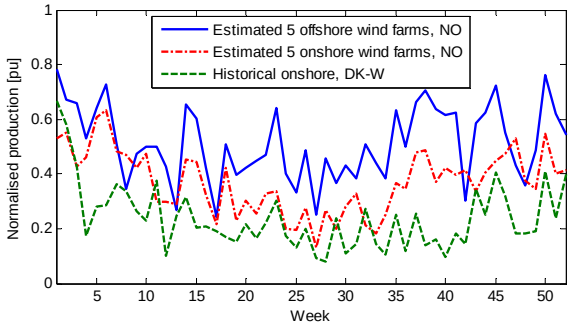

Figure 2. Weekly average power output for estimated offshore and onshore wind power in Norway, and for actual production in Denmark-West, 2005.

3. POWER MARKET MODEL

The analysis uses a new power market model of North-Western Europe [5]. The model was originally developed for studying the impact of wind power on the power prices in Western Denmark, but expanded and adapted for the purposes of this paper. A throughout description of the model, and the basic model parameters used, such as installed generation, power exchange limits and marginal generating costs, are given in [5]. The model consists of six price areas, shown in Figure 3, connected by transmission lines constrained by active power limits. To calculate the optimal dispatch of generators, a quadratic programming model is used where each generator is defined by its quadratic cost function and upper bounds on generation capacity.

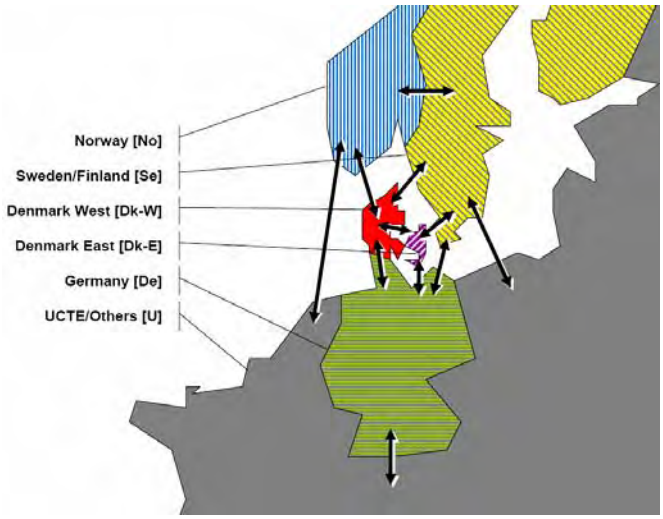

Figure 3. Price areas and their interconnections, as defined in the power market model. Copy from [5].

Wind power is modelled as having zero marginal cost and wind power in Norway is represented by the time series described in Chapter 2. Historical production data is used for the wind generation in Denmark-West and Denmark-East. Due to lack of specific data, German wind power is simply modelled by up-scaling and shifting the time-series for Denmark-West a certain number of hours [5].

Reference [6] shows how hourly variations in wind power output from turbines are correlated depending on spatial distribution. For the Nordic countries, with distance d between the wind farms, the correlation coefficient c_f is found to approximate:

$$c_f = \mathrm{e}^{-d/500} \quad (1)$$

To prepare wind power data for Germany, up-scaled wind data for Denmark-West is used, only shifted by a number of hours such that the correlation coefficient becomes 0.55, corresponding to an approximate average distance of 300 km between main wind sites in Germany and Denmark-West.

Hydro power, which dominates in Norway and Sweden, is modelled based on actual observed operation of hydro power in Scandinavia, also taking into account variations in inflow and utilization of hydro reservoirs. The marginal cost is set equal to the water value, calculated from a regression model

described in [5] which captures well the scheduling of hydro power on an aggregate level without performing a full stochastic dynamic optimization of all hydro reservoirs. See Figure 4 for a comparison of historical prices and simulated water values, and Figure 5 for a comparison of historical and simulated hydro reservoir levels.

Hour by hour, the model goes through four steps; First, normalised wind power output is set according to synthetic or historical data-series and multiplied with the installed capacity. Next, water values are calculated based on current reservoir levels. Then, the optimal generator dispatch that satisfies the loads in all areas is found, and the solution is stored for the particular hour. Finally, the level in all hydro reservoirs for the next hour is updated based on inflow, production, and spillage during the current hour. Simulation results are area prices, power flow on tie-lines and generator outputs for each hour of a whole year or several years.

For the simulations described in this paper, 21 years of chronological hydro inflow data has been used for capturing the year-to-year hydro power variations and long-term development of the hydro reservoir levels. The time series for wind and load are held constant from year to year, using 2005 data as a reference case. For Norway, the total consumption in 2005 was about 120 TWh, which equals to the average yearly hydro inflow. Assuming the same wind for all years is a rough approximation, since the annual wind generation may in reality vary ± 20% [7]. Results obtained here are still considered reasonable for the purposes of this study, but future work will include analyses of the impact of year-to-year variations in wind generation.

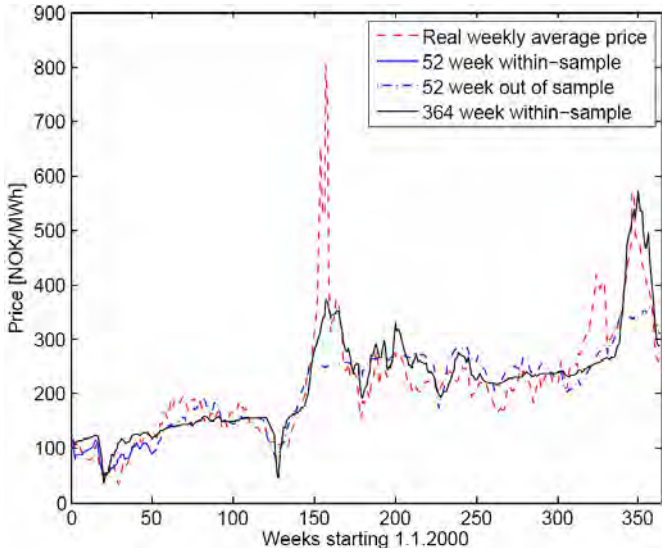

Figure 4. Observed and simulated water values. The 364 week model fit (soild line) is used in the simulations. Copy from [5].

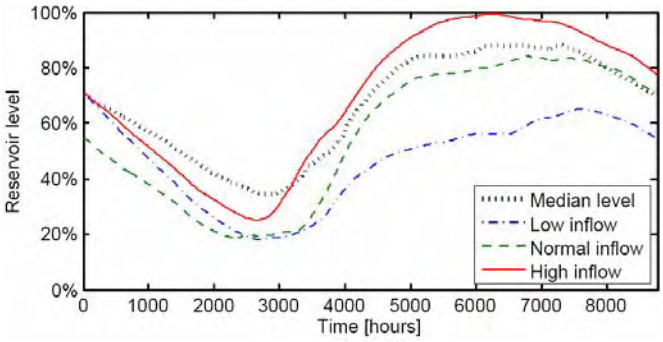

Figure 5. Simulated reservoir level for Norway for three different inflow series plotted together with the real historical median. Copy from [5].

4. Simulation cases

The aim of using the power market model in this work is to study some possible system impacts of integrating 5500 MW offshore wind power in Norway, based on wind speed measurements representative for offshore wind conditions. As described in Chapter 2, the estimated capacity factor is as high as 50%, resulting in an annual generation of approximately 25 TWh. The timeline for developing and building offshore wind farms at deep waters are of course very uncertain, but nevertheless we believe that large-scale offshore wind development within year 2025 could be plausible. Therefore, year 2025 has been chosen as a reference year for the simulations.

Five possible cases for the situation in 2025 have been defined. Construction of detailed scenarios have not been the focus here, it has rather been chosen to highlight some important factors that will impact on the way offshore wind power is integrated in the system. The simulation cases (in addition to the reference case for year 2005 described in the previous chapter) are listed below:

- Case A
  - As the reference case for year 2005 but with 15 TWh annual load increase in Norway.
- Case B
  - As Case A but added 5500 MW (25 TWh) offshore wind and 3100 (10 TWh) onshore wind in Norway.
- Case C
  - As Case B but added 10 TWh small hydro and 10 TWh conventional hydro in Norway.
- Case D
  - As Case C but including a 3-fold increase in wind power production in Germany and Denmark
- Case E
  - As Case D but added three new sub-sea interconnections: 1200 MW to UK, 1400 MW to DE and 600 MW to DK-W (UK is a part of price area 'U' in Figure 3).

A load increase of 15 TWh, added to the 120 TWh actually consumed in 2005, is assumed in all cases. In a 'ideal' future situation with a much higher share of renewable power, it could be argued that the electricity consumption should decrease due to higher environmental consciousness and

more efficiency energy end-use, exemplified by more use of heat pumps instead of direct electrical heating in houses. On the other hand, more renewable power generation could also trigger shifts from fossil fuels to electricity especially for covering the energy demands in the offshore sector (oil and gas rigs) and in the transport sector (more use of electric vehicles).

The cases are structured for being illustrative and only weakly based on plausible future developments. Case A represents a tight power balance situation with no new generating units in Norway. Case B adds a total of 35 TWh wind generation, whereof 10 TWh is onshore wind. Although the main focus of this work is offshore wind, it is important also to take into account that Norway has a very high onshore wind power potential. There are plans for large onshore wind farms along the coastline from south to north, and it is plausible that a many of these projects will be realised the next 5-15 years. Similarly, there are a good potential for small-scale hydro and for upgrading existing conventional hydro. By also accounting for the predicted increase in inflow due to climate change, it is reasonable to expect at least 20 TWh new hydro generation, as suggested in Case C.

Since the ambitions for building wind farms in Germany and Denmark have been much higher than in Norway, a future with large-scale development of offshore and onshore wind power in Norway would most probably also imply further expansion of wind power in those countries. Based on scenarios presented in [8]-[9], Case D assumes a 3-fold increase in wind generation in Germany and Denmark. Although this part of the analysis is strongly simplified due to the chosen system boundaries for the simulations, is it nevertheless interesting to investigate how new wind power in Denmark and Germany will affect the simulation results.

Case E includes new interconnections which add up to 3200 MW exchange capacity to and from Norway. This is based on a scenario described by the Norwegian TSO in [10], where the role of Norwegian hydro power as flexible generation in the European power system is enhanced. Equally important, new interconnections will increase the possibilities for exporting Norwegian offshore wind power to countries with a high share of fossil power plants, and thus reduce CO_2-emmisions and electricity prices.

5. Results

5.1. Wind impact on hydro reservoir

With no load increase, i.e. the reference case, there is a balance between production and consumption in an 'average' hydro inflow year. On the other hand, the yearly inflow may vary up to ± 30% of the average value, causing a risk for low reservoir levels in late winter before the snow melting season. A load increase of 15 TWh will worsen the situation, and may give rise to undesirable price levels, especially consecutive dry years are critical. Figure 6 shows the simulated reservoir levels for Case A with 15 TWh load increase. For comparison, the median level from simulating the system with no load increase (reference case) is also shown.

The seasonal production pattern for Norwegian wind power roughly follows the load pattern, as opposed to hydro inflow. Moreover, earlier studies of the long-term variations in wind generation and hydro inflow shows a low correlation between dry years and years with low average wind speeds [7]. The results from Case B with 35 TWh added wind energy, shown in Figure 7, clearly illustrates the benefits of integrating wind farms in the Norwegian power system. The median reservoir level is significantly higher than for the reference case and Case A. Compared to Case A (Figure 6), the minimum simulated level is raised from 6% to 16% of the reservoir capacity, illustrating that wind power has the potential to effectively relieve constrained energy situations in Norway.

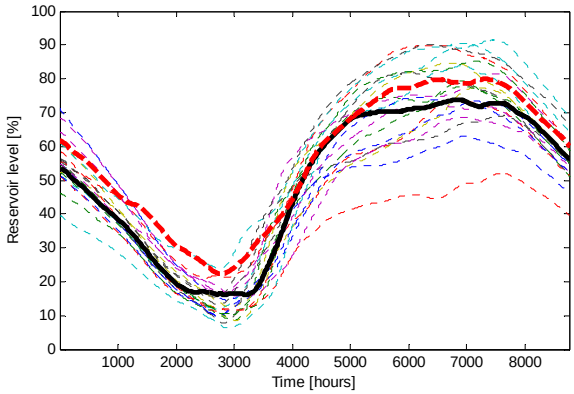

Figure 6. Simulated hydro reservoir level in Case A (15 TWh load increase), using 21 consecutive years of inflow data. The solid thick line is the median level. The dotted thick line is the median level for the reference case.

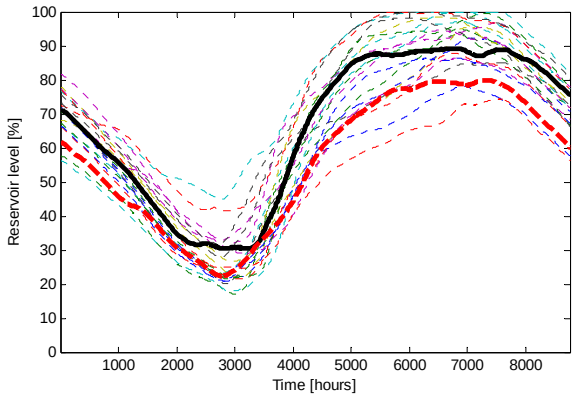

Figure 7. Simulated hydro reservoir level in Case B (15 TWh load increase and 35 TWh wind generation), using 21 consecutive years of inflow data. The solid thick line is the median level. The dotted thick line is the median level for the reference case.

5.2. Wind impact on electricity price

Since the Norwegian power system is almost entirely based on hydro power, electricity prices are especially sensitive to low reservoir levels, which cause risks for energy shortages in the winter. Historically, high prices are therefore observed in autumns and winters with lower reservoir levels than normal, since most of the precipitation in the winter season cannot be utilized for power production until the snow melting begins in the spring.

Since wind power reduces the needs for using the stored hydro energy in the winter, it will most likely have a very positive effect on the winter prices. This effect is indicated by Figure 8, which shows that the winter peak prices are significantly lower when introducing a high share of wind power in the system. In the summer season of wet years, wind power will contribute to very low price levels. Figure 8 shows some occurrences of zeros price, caused by completely filled reservoirs.

As a comment to the parameters used in the simulation model, it is observed from Figure 8 that the summer prices very seldom are between zero and 200 NOK/MWh, although expected in situations with high degree of reservoir filling. The discrepancy can be explained by how the water value function is tuned based on historical prices and reservoir data, see [5] for further details. Future modelling work will therefore include a further refining and tuning of the water value equations.

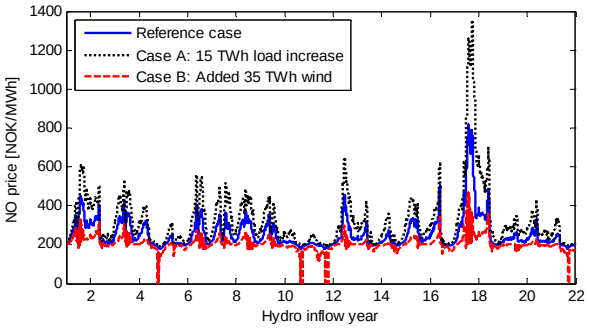

Figure 8. Simulated price in Norway for Case A and Case B.

Figure 7 shows that Case B with 35 TWh wind generation causes some occurrences of full reservoirs and this explains the periods with zero price. With 20 TWh new hydro, as simulated in Case C, there will be a higher tendency of hydro spillage, as can be read from the price duration curve in Figure 9. Furthermore, a 3-fold increase in wind generation in the neighbouring countries Germany and Denmark (Case D) gives less possibility for exporting excess power in wet years, but the small difference between Case C and D in Figure 9 indicates that this have a relatively low effect on the simulated prices in for Norway. One explanation is the high value used for cross-border capacity between Germany and the rest of the UCTE (14650 MW), calculated as the sum of the Net Transfer Capacities found in [11]. Hence, new wind power in Germany will mostly displace fossil plants.

Adding a total of 55 TWh of new generation in Norway was seen to cause zero prices during parts of the summer as a result of hydro spillage, meaning that potential hydro energy will be wasted. By strengthening the cross-border capacity between Norway and the neighbouring countries, it is possible to utilize more renewable energy. Figure 9 shows that the total share of zero price hours over the 21 simulated years is reduced from 14% to 6% by adding a total of 3200 MW exchange capacity (going from Case D to E). A further reduction of hydro spillage should be possible by including long-term wind power forecasting in the water value calculations. The results presented here are conservative in this sense, as the water values are updated each time step as a function of the reservoir level only.

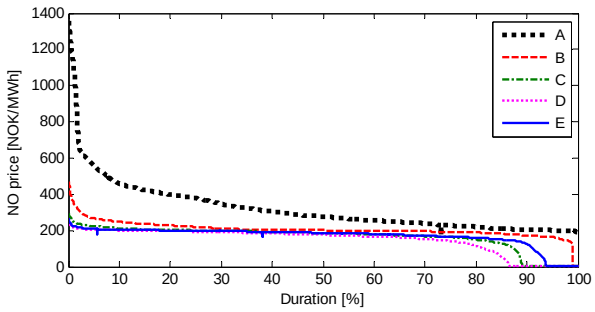

Figure 9. Duration curve for price in Norway for simulation cases A-E.

5.3. Wind impact on power exchange

In the reference case, there is balance between consumption and generation in Norway when considering the 21 simulated years as a whole. In Case A, the energy balance is shifted negatively by 15 TWh. Due to the variations in hydro inflow, the net power exchange is not constant from year to year. Figure 10 (Case A) shows a negative balance of 30 TWh in the worst year, and only two years with a slightly positive balance. By adding 35 TWh of wind (Case B), the shape of the curve is almost unchanged, shifted 35 TWh in a positive direction. This further strengthens the observation that the Norwegian power system is capable of handling large amounts of wind energy, although it is emphasized that this study assumes no year-to-year wind variations and no internal bottlenecks in the Norwegian grid. Knowing that the integration of wind farms in e.g. the Northern parts of the country is limited due to low power transfer capacities, a scenario with 35 TWh wind may imply extensive grid reinforcements at transmission level.

An interesting effect is observed when further adding 20 TWh hydro (Case C). The yearly export pattern is altered since the new hydro power include run-of-river plants fully correlated to the existing hydro power regarding the inflow, thus giving higher yearly exchange variations. Furthermore the average yearly export is not increased fully by 20 TWh due to hydro spillage. This is especially evident for wet years (year 11 and 21 in the figure). Increasing the cross-border capacity thus has a very positive effect in the wet years, as seen when comparing cases C/D with E.

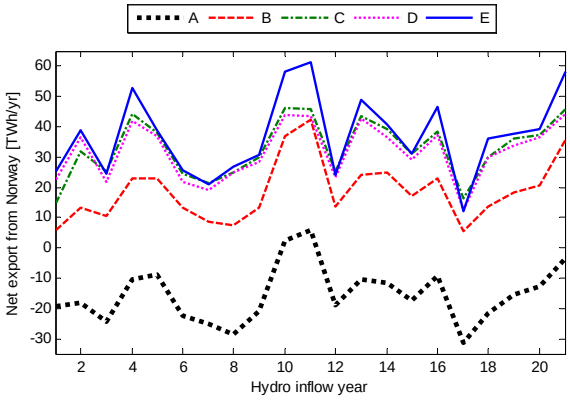

Figure 10. Net yearly energy exported from Norway to the neighboring countries for simulation cases A-E.

Comparing Case C and D in Figure 10, new wind power in Germany and Denmark has little effect on the net export from Norway. It is also seen from Figure 11 that yearly export to Sweden is not remarkable affected. However, an

interesting observation is that the export to Sweden is reduced when simulating the system with new interconnections between Norway and the neighbouring countries. Since the generating capacity in Sweden is dominated by cheap hydro and nuclear power, it is more cost effective to export renewable power to the other countries, and thus release capacity on the power lines between Norway and Sweden.

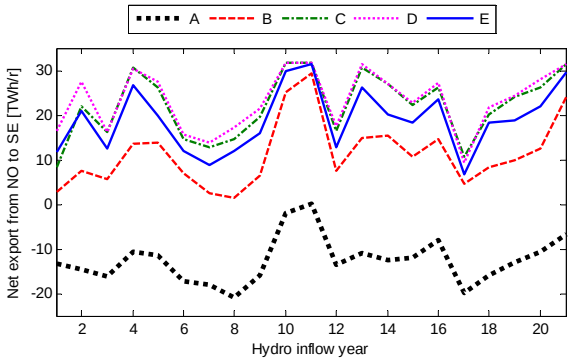

Figure 11. Net yearly power export from Norway to Sweden for simulation cases A-E.

6. Conclusions

Deep sea offshore wind farms may be developed to constitute a significant part of the total power system generation. There are several ongoing research and development projects on the design of different bottom-supported and floating wind turbines, giving hopes for future exploitation of the enormous offshore wind potential at deeper waters. This paper has presented a simulation study of integrating 5500 MW of offshore wind power in the Norwegian power system, and also taking into account further development of onshore wind farms and increased utilization of the inland hydro power potential.

The analysis uses a power market model of North-Western Europe, adapted for the purposes of this work. The model consists of six price areas, connected by transmission lines constrained by exchange limits. The system has been simulated hour-hour using 21 years of hydro inflow data. The time series for wind is held constant from year to year, which is a rough estimation. However, based on experience from previous studies, the results here obtained by using one-year wind data is considered fair for the purposes of this paper. Future work will include analyses of the year-to-year variations in wind generation, further refining and tuning of the water-value calculations, and increasing the number of price areas in the model to analyse the impact of limited power transfer capability within each country.

The results illustrates that wind power has the potential to effectively relieve the constrained energy situations in Norway, exemplified here with 35 TWh offshore and 10 TWh onshore wind generation. When also taking into account a plausible scenario with 20 TWh increase in hydro generation, the results indicate a need for increasing the cross-border transfer capacities. This is in order to reduce occurrences of hydro spillage due to inland energy surplus, thus enhancing the possibilities of exporting large amounts of renewable energy to the continent.

Acknowledgement

This work is part of the project "Deep sea offshore wind turbine technology" financed by the Research Council of Norway and Norwegian industry. See [12] for project info.

References

[1] Homepages of OWEC: http://www.owectower.no
[2] Homepages of Aker Kværner: http://www.akerkvaerner.com
[3] Homepages of StatoilHydro: http://www.statoilhydro.com/
[4] Homepages of SWAY: http://sway.no
[5] T. Trötscher. Large-scale wind power integration in a hydro-thermal power market. Master Thesis. Norwegian University of Science and Technology, Trondheim, Norway, 2007.
[6] P. Nørgaard, H. Holttinen. A multi-turbine power curve approach. In: Proc. Nordic Wind Power Conference, Gotenburg, Sweden, 2004.
[7] J.O.G. Tande, K.O. Vogstad. Operational implications of wind power in a hydro based power system. In: Proc. European Wind Energy Conference, Noce, France, 1999.
[8] Deutsche Energie-Agentur. Planning of the grid integration of wind energy in Germany onshore and offshore up to the year 2020 (dena grid study). 2005. Available at: http://www.dena.de
[9] The Committee for Future Offshore Wind Power Sites. Future Offshore Wind Power Sites -2025. Danish Energy Authority, 2007. Available at: http://www.ens.dk
[10] Statnett. Kraftsystemutredning for sentralnettet 2006-2025 (in Norwegian). 2007. Available at: http://statnett.no
[11] European Transmission System Operators (ETSO). Indicative values for Net Transfer Capacities (NTC) in Europe, 2006. Available online at: http://www.etso-net.org.
[12] http://www.sintef.no/wind

50 % WIND POWER IN DENMARK

A PLAN FOR ESTABLISHING THE NECESSARY ELECTRICAL INFRASTRUCTUREC

Niels Andersen[1], **Claus Overgaard Jensen** [2]
SEAS-NVE, Denmark

Hans Henrik Lindboe[3]Ea Energy Analyses, Denmark

***Abstract* – On 19 January 2007 the Danish Government published "A visionary Danish energy policy" outlining energy policy objectives towards 2025. One long term goal is to make Denmark independent on fossil fuels and the proposal includes an aim for 2025 of doubling the share of renewable energy in the energy supply to 30 pct. In the proposal it is mentioned that an important contribution could come from doubling the wind power capacity from 3000 MW to 6.000 MW in 2025 thus covering 50 pct. of the Danish power demand.**

SEAS-NVE and Ea Energy Analyses has conducted a study on how to physically incorporate the increased wind capacity in the Danish electricity system without constructing new high voltage overhead lines. It has been assumed that there is an upper limit of 3500 MW regarding possible land based capacity in Denmark. This means that a major part of the increase in wind capacity will be off shore. To reach the goal of 50 % wind power in 2025 the study assumes that another 2.250 MW off shore windpower shall be established around Denmark.

This paper concludes that it is possible to establish more than 2000 MW off shore wind farms in Denmark without construction of new overhead lines and at an integration cost of DKK 3,5 mill. per MW wind. It is proposed in this study to make extensive use of HVDC-VSC technology for the reason of economy and to increase active power control in a system with an extensive wind penetration.

Index Terms— 50% wind power, power system development, grid re-inforcement, Environment, FACTS, VSC HVDC.

I. System Description

A well functioning and sufficient grid is an assumption to secure supply and serve the need of the market to accommodate renewable energy and to handle the electric supply readiness [3].

II. Grid development

The principles of grid control contain two parameters: the active and reactive power. Main focus is on active power control and the reactive power is assumed to be controlled by the central power units connected at the 400 kV grid as well as smaller mechanical switched devices.

When the share of wind power grows the production from the large thermal units (centralised units) decreases. These units will more and more often be shut down due to low prices in the market or due to the system balance. Thereby the controllability of the system decreases. The use of grid enforcement can result in loss of huge areas of smaller production units with a total power well above the N-1 criteria for the area. When building more connections and make grid more meshed a fault in the grid will result in a voltage drop in a larger area, thereby more production units will be affected of the fault The central power units have traditionally been used for control of the voltage, but with more frequent disconnection of these traditional power units this service is required from elsewhere. The offshore wind farms can to some extent and costs supply the steady state demand but poorly the dynamic requirement.

FACTS are a collection of electronic controlled devices which are able to both support the grid and solve some of the above discussed disadvantages.

[1] Niels Andersen. Email: na@seas-nve.dk.
[2] Claus Overgaard Jensen. Email: coj@seas-nve.dk.
With SEAS-NVE, Phone: +45 70 29 29 29
Address: Slagterivej 25, 4690 Haslev, Denmark.

[3] Hans Henrik Lindboe. Email: hhl@eaea.dk.

Taking the above mentioned problems and possibilities into account, the map on page 1 shows the main solutions chosen in the grid development plan proposed in this project.

It is proposed to establish a total of nine offshore wind farms, of which five are located in Western Denmark and four in East. Seven of the farms are 250 MW in size and the remaining two 350 MW and 150 MW respectively. Three of the four farms in the East will be connected to strong points in the grid by use of HVDC-VSC. All five farms in western Denmark will be connected with 150 KV AC technology.

Wind farm	Size, MW	Total cable, Km	Technology
Denmark West			
Horns Rev 3	250	60	AC 150 kV
Horns Rev 4	250	60	AC 150 kV
Vestkyst 1	250	50–55	AC 150 kV
Vestkyst 2	250	50–55	AC 150 kV
Jammerbugt	250	70	AC 150 kV
Denmark East			
Rødsand 3	250	135	HVDC-VSC
Rødsand 4	250	135	HVDC-VSC
Kriegers flak	350	80	HVDC-VSC
St. Middelgr.	150	70-75	AC 132 kV

Apart from establishing and connecting the wind farms the most important feature in the plan is to move a planned DC link to Norway further south than planned and establish the connection as a DC Multi-terminal. In the following the different elements of the plan are presented and discussed.

400 kV connection Endrup and Galtho

The connection contains two major differences from today. The establishment of a 400 kV cable (1) and a new 400 kV station in Galto. The Galtho station shall serve as a collection station from three of the planned off-shore windfarms.

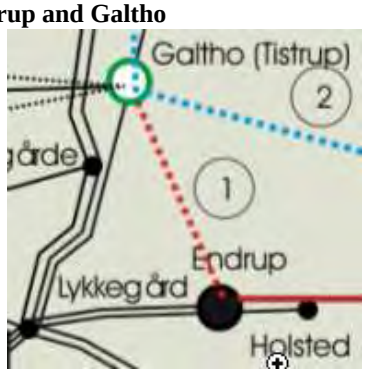

By establishing the 400 kV cable two main objectives are achieved. Firstly to avoid building overhead (OH) lines and secondly to avoid laying several 170 kV cables systems. The 400 kV cable is intended to be operated at 150 kV with Horns Rev 2 until Horns Rev 3 and 4 will be build and the cable is upgraded to 400 kV as the station in Galtho established.

DC connection Galtho – Landerupgård

The DC connection from Galtho to Landerupgård serves two purposes to export the wind power to a strong connection point and to stabilise the general 400 kV grid. The HVDC connection will not be with the traditional HVDC, but with the VSC HVDC which also can be used as a multi terminal (i.e. a DC link with more than two stations).

DC connection from Galtho to Idomlund/Norge

The connection Galtho to Norway is suggested instead of the planned Skagerrak 4 connection from Tjele. Thereby the transmission to Norway is established from another point than Tjele. Idomlund could become a fourth terminal in the DC backbone grid, if further detailed studies show the necessity.

The purpose of moving the DC link to Galtho also serves the aim to avoid a planned 400 kV OH line from Endrup to Idomlund. This solution makes it possible to utilise the North (Norway) – South (Germany) transmission as if the Skagerrak 4 was terminated in Tjele together with the Endrup – Idomlund OH line.

According to evaluations made in the study it will not be necessary to extend the grid on Zealand due to the new offshore wind farms. The HVDC VSC transmission top connected to the farms will serve the purpose to keep the grid in control with only a few central power plants in operation (Today six central power plants is needed in operation in Denmark as a whole and five will be needed when the Great Belt HVDC is in operation)

III. Connection of Offshore Wind Farms

The wind farms can be connected by either HVDC or HVAC. The connection method will depend on size and distance. As a rule of thumb the AC solution is preferred at distances below 50 km and DC is preferred at distances above 80 km. While the AC cable can transmit some 250-300 MW (largest cable transmission today is Nysted with 166 MW), the DC cable solution able to transmit up to 700 MW in one system (largest transmission planned today is Borkum 2 at 400 MW and 203 km).

Horns Rev

At Horns rev, two more wind farms with a total of 500 MW are planned in addition to Horns Rev 1 (in operation) and Horns Rev 2 (decided)

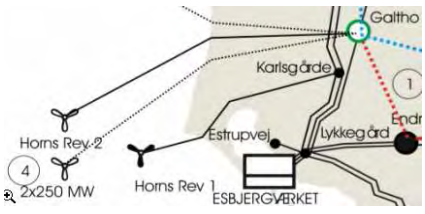

These will be connected in Galtho with a distance off app.

60-80 km. Further studies may show that a HVDC solution could be a feasible alternative. The AC cables are expected to be connected at 170 kV with a transformer both in the receiving end and at the wind farm. By using transformers in both ends of the cable transmission to shore, the voltage variation on the cable can be limited and the voltage can be kept close to the rated voltage during all operation conditions. This will ensure an increased transmission capacity of approximately 10%.

Kriegers Flak

Kriegers Flak is situated in the Baltic Sea some distance from the 400 kV transmission grid, which is quite strong and short in the eastern part of Denmark. The 132 kV grid is closer to Kriegers Flak, but with the construction of the Rødsand 2 the 132 kV grid is at its limit and can therefore not transmit substantially more power. Therefore new farms at Kriegers Flak or at Rødsand require either additional grid extensions or that the new wind farms are connected directly at the 400 kV grid.

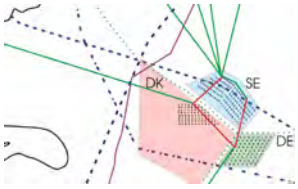

Kriegers Flak is situated at the border between Denmark, Sweden and Germany: The Swedish part has a potential 500-660 MW and the German part app. 330 MW. The cable distance to the Danish 400 kV grid will be some 80km, with 55 km sea cable and 25 km land cable.

It is estimated that connection of 600-800 MW wind power in Bjæverskov can be done without additional extension of the 400 kV grid.

When connecting the Kriegers Flak wind farm it is obvious at the same to connect the Swedish, German and Danish parts (red lines) and thereby establish an interconnection between the three countries. This interconnection does not require VSC HVDC technology for all three connections, but it might be the economically most feasible solution.

IV. DISCUSSIONS

The HVDC and HVDC-VSC

The conventional HVDC is a well proven technology based on Mercury arc valves since the mid 50s and thyristors since mid 70s. The technology is also termed line commutated HVDC. The technology is mainly suited for large point to point power transmissions above 300 MW with large distances 800-1000 km. The technology is also suited for asynchronous connections as well as cable transmissions above 50 km. Even though some articles claim that the conventional technology can be used for offshore wind farms connection, it is expected to involve great technical difficulties. Three companies supply the technique.

The HVDC-VSC is a relatively new technology based on IGBT converters with the first demonstration project in 1997. The technology is also called voltage source converter. The power level for HVDC-VSC range from 10 MW to 700 MW. The technology is suited for the same projects as conventional HVDC, but has additional advantages in offshore connection of windfarms, multiterminal DC grids and in weak grids. The additional mentioned advantages are expected to be used when the central power plants are not in operation.

The traditional HVDC will probably need additional investments in order to be able to function with an off-shore transmission. The table below shows the range where projects with the different technologies are most likely to be carried out.

	AC offshore	HVDC	HVDC-VSC
Voltage | kV	132-220	150-600	60-300
Transmission* | MW	200-300	200-2000	10-700
Length | km	10 - 100	30 – 580	30-580
Losses | 100 km,	medium	Low	medium
Technology	Known	Known	New
Delivery time	Long	Long	Medium
Cables	3	1 or 2	2
Multi terminal	Yes	Max 3	Yes
Design	Simple	Complex	Simple
Circulating currents in grid enforcement	Yes	No	No
Cable overload	Yes	No	No
Dyn. Reactive pwr support	No	No	Yes
Isolate disturbances	No	Yes	Yes
Black-start capability	Yes	No	Yes

Some other advantages which are important to mention in DC transmission compared to AC are:

Emergency power support and mutual assistance. Both AC and DC can support a grid, but with DC the support can predefined to match the actual capability of the connecting grid. This implies that it is possible to isolate the disturbances and have a ‘Fire-wall’ against cascading outages as well as give maximum support without jeopardize the supporting grid.

The HVDC-VSC generates/absorbs in addition to the power transmission VARs, which are needed to maintain system voltage and stability. This is supported in the AC grid through the centralised power plants.

The DC has no distance limitation. At full power the DC will have no additional reactive power. On the HV grid AC cables

will compensated using reactors which are likely to create resonances in the grid, which is expected to cause problems due to the very low losses.

Complementary to the DC connections the existing and new AC transmission combined with FACTS technology will to some extent be able to achieve the same capability as the DC except for the cables transfer capability.

Multiterminal

The HVDC-VSC technology is suited for so called multi-terminal technology. A multi-terminal HVDC Transmission System consist of three or more HVDC substations that are geographically separated with interconnecting transmission lines or cables.

The converters can be connected to different points in the AC grid or even to different AC grids. The choice of DC grids can be radial, meshed or a combination of both. In the future multi-terminal configurations and grid alterations might be done in a "plug and operate" fashion, with continued robust performance. However the extension of the backbone DC grid is restricted to the problem with selectivity on the DC side.

The main advantages of a multi-terminal configuration is that you can feed in or out several different places in the grid in a controlled manner.

With HVDC VSC technology it should be less challenging to develop a multi-terminal HVDC grid than with conventionally HVDC. In a “conventional” multi-terminal HVDC currents need to be balanced, but with HVDC VSC converters, which are voltage controlled, there is no need to balance the currents.

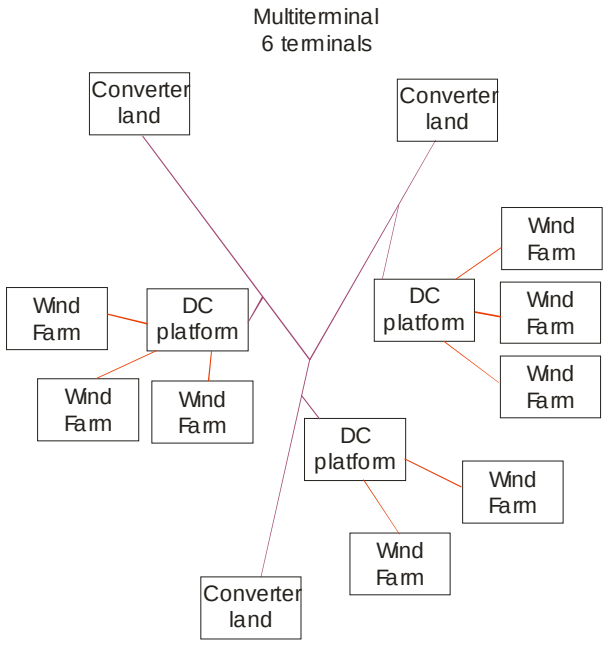

The shown example could be a layout on the Kriegers Flak.

The converter size could range from 300-700 MW. The suggested voltage could be some ±300 kV. With 1600 ¤CU cables the transmitted power in each cable par could be 1000 MW. With the technology it is possible to connect converters in parallel.

Losses

The losses of transmission are not fixed but will be optimised together with the capitalisation. When HVDC-VSC converters are brought into questions the focus is often on the losses. However one has to keep in mind that both AC and DC transmission causes losses. The losses are not only connected to the transmission to shore but also to the existing transmission grid, the step up transformers, the interturbine grid.

As an example a wind farm 120 km offshore of approximately 300 MW is used as an example for the losses

Losses in MW	**AC**	**DC**
Cables	2x132 kV three phase	2x150 kV single phase
WT transformers	2.1	
Inter turb cables	3.0	
Offshore Main Transformer	1.4	14
Transmission cable	15	
Grid transformer	1.4	
Total losses	23.1	19
	7.7 %	6.3%

By increasing the voltage to 220 kV the losses will decrease on the AC transmission cables and the cable might be reduced to one three phase cable but will still be comparable with the DC solution. The two largest three phase cables in operation are still the Nysted 132 kV and 165 MW cable and the Horns Rev 170 kV 160 MW cable.

By using the DC solution one might deliver reactive support and thereby increases the voltage in the on-shore grid, this will decrease the overall losses or with DC continue to a more suitable connection point and thereby avoid increased grid losses.

Economy

The table below shows the total costs to connect the offshore parks and reinforce the grid as described in the present paper. Regarding the investment for the connection to Norway (Skagerrak 4) it is the difference between the proposed (VSC) and the planned (Traditional) HVDC connection that is included. The investment allows for the integration of additionally 2,250 MW of off-shore in the Danish electricity system at a total of 7,940 mill. DKK. This corresponds to a cost of DKK 3.5 mill. per MW wind.

Total investment – mill. DKK			
Wind farm	Cable	Other	Total
Denmark West			
Horns Rev 3	470	165	635
Horns Rev 4	470	165	635
Vestkyst 1	370	165	535
Vestkyst 2	370	165	535
Jammerbugt	455	165	620
Grid enforcement			1060
Denmark East			
Rødsand 3+4	285	1350	1635
Kriegers flak	190	1350	1540
St. Middelgr.	595	150	745
Total			**7940**

V. Conclusion

This paper concludes that it is possible to establish more than 2000 MW off shore wind farms in Denmark without construction of new overhead lines and at an integration cost of DKK 3,5 mill. per MW wind. It is proposed in this study to make extensive use of HVDC-VSC technology for the reason of economy and to increase active power control in a system with an extensive wind penetration.

It is also proposed to establish a three terminal multi-terminal DC network as a joint Danish – Norwegian demonstration project. Full size multi-terminals have not yet been demonstrated anywhere in the world but are expected to have several advantages in future network designs both as dedicated DC nets and in DC/AC combinations.

VI. References

[1] 50 pct vindkraft i Danmark i 2025 – en teknisk-økonomisk analyse, May 2007 EA Energianaluse

[2] Anlægsrapport 2006 for el- og gastransmission I Danmark. Energinet.dk dec. 2006

[3] *Anlægsplan 2006 for eltransmission I Danmark.* . Energinet.dk., dec. 2005.

[4] Vindkraftspark – Kriegers Flak, underlag för utökat samråd, Niels Andersen, Peter Christensen NVE for Vattenfall, November 2003.

[5] Global experience curves for wind farms, M. Junginger*, A. Faaij, W.C. Turkenburg, Energy Policy 33 (2005) 133–150,

VII. Biographies

Claus Overgaard Jensen Larsen was born in 1972. He received his B.Sc. from the Odense University Collage of Engineering (IOT) in 1996. Since 1988 he has been employed at SEAS and is now team leader in the station and transmission department. His work includes system studies, design, preparations and erection of substations in the transmission grid.

Niels Andersen was born in 1961. He received his M.Sc. degree from the Technical University of Denmark (DTU) in 1988, and was employed at the ABB Power Systems (HVDC) until 1994. Since 1994 he has been employed by NVE where he has been working with HVDC and FACTS applications. The main areas of work are project management, system studies, feasibility studies and specification for HVDC/FACTS. From 1996-2003 he was a member of the CIGRE WG14-28 active filters for high voltage applications.

Hans Henrik Lindboe (MSc, Engineering) has extensive experience as project manager in the Nordic and Baltic area. Has focus on economy and security of supply in a liberalised electricity market. In recent years, Hans Henrik has contributed to analyses of the utility value of investments in the Nordic transmission grid, the economic conditions of integrating large amounts of RE in the electricity system and the challenges to the district heating sector. Hans Henrik was previously employed with the transmission system operator in Eastern Denmark (Elkraft), and before that with the Danish Energy Authority.

Comparison of Control Schemes of Wind Turbines with Doubly Fed Induction Generator

Abram Perdana[1*)] and Ola Carlson[1)]
[1)]Department of Energy and Environment
Chalmers University of Technology
S-412 96 Gothenburg, Sweden
[*)]Email:abram.perdana@chalmers.se

***Abstract*— Validity of wind turbine model for power system stability studies has been important as the penetration of wind power generation in the power system increases significantly. Variable speed wind turbines with doubly fed induction generator (DFIG) are the most common technologies used in today's wind power generation. So far, there is no agreement on generic model of this type of wind turbine. Different control schemes of wind turbine with DFIG have been presented in many publications. However, comparisons of the different control schemes and their influences on the stability study are rarely found in the papers. This paper investigates different control schemes implemented in wind turbine with DFIG for power stability studies, which include the speed/power controls and the pitch controls.**

***Index Terms*— Doubly fed induction generator, dynamic simulation, induction generator, voltage stability, wind turbine.**

I. Introduction

VALIDITY of wind turbine model for power system stability studies has been important as the penetration of wind power generation in the power system increases significantly. Variable speed wind turbines with doubly fed induction generator (DFIG) are the most common technologies used in today's wind power generation. Up to now, there has been no agreement on common models for this type of wind turbine. Different control schemes of wind turbine with DFIG have been presented in many publications [1] to [13]. Nevertheless, comparisons of the different control schemes and their influences on stability studies are rarely discussed.

This paper is aimed at investigating different control schemes implemented in wind turbine with DFIG for power stability studies. These control schemes include the speed and active power control, the pitch compensation controller and the torque controller. The significance of these different schemes on wind turbine response during disturbance is discussed. Based on the controller comparisons, some recommendations for developing generic or common models of wind turbines with DFIG are presented.

In this study, voltage and reactive power controllers are not discussed since the controllers presented in papers are relatively similar.

II. Overall model structure

General structure of a wind turbine model with DFIG is shown in Fig. 1. The main parts of the model include a generator and drive train, a rotor converter, a turbine rotor model, power/speed controller, a voltage and reactive power controller, a pitch controller and grid-side converter.

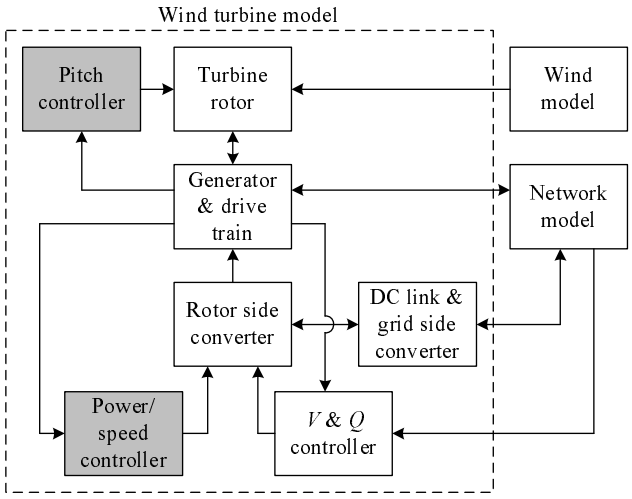

Fig. 1. General structure of model of wind turbine with DFIG

The generator and drive train models for wind turbines are relatively well established. The generator can be modeled either as a first-, second- or fifth-order induction generator model, depending on the nature of studies. The commonly used drive-train model for system stability studies is the two-mass model. Although one-mass model is also acceptable for long-term voltage stability studies. For stability studies, the turbine rotor is sufficiently modeled using a $Cp(\lambda, \beta)$ lookup table. The rotor and grid-side converter is modeled as a voltage source converter. The grid-side converter regulates the dc-link voltage according to a scheme shown in Fig. 2.

Regarding pitch controller and power-speed controller, so far, there is no agreement among authors. For that reason, in this study, different control schemes presented in literature are compared and evaluated.

III. Disturbance model

In order to compare response of the different control schemes, two types of disturbances are applied in simulations e.g. a wind gusts and grid faults. These disturbances are

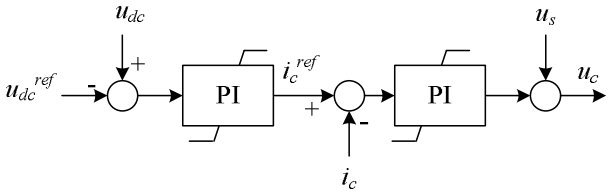

Fig. 2. Typical dc-link controller. Variable u and i denote the voltage and current, respectively. Subscript dc, c and s refer to the dc-link, grid-side converter and stator quantities, respectively. Superscript ref indicates the reference value

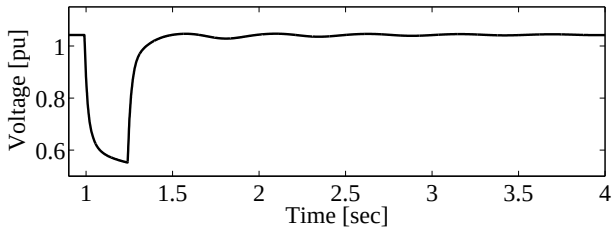

Fig. 3. Voltage profile

relevant for short-term stability studies related to wind turbines. The wind gust represents a moderate disturbance caused by an abrupt change of wind speed, which causes relatively slow dynamic responses. Wind gust profiles are appropriately chosen according to needs of controller investigations.

The fault represents a more severe disturbance, which involves relatively fast dynamics. The fault is simulated by applying a voltage dip on the wind turbine terminal. The voltage dip profile is shown in Fig. 3

An aggregated model of a wind farm consisting of 5x2MW wind turbines with DFIG is used in the simulation. The wind turbine and controller parameters are given in Appendix I.

IV. Active power and speed control

As presented in Fig. 4, active power and speed control of wind turbines with DFIG can be realized in different schemes. In this study, the different control schemes are denoted by type A to E, respectively. Each control scheme employs a speed control characteristic curve. The speed control characteristic is aimed at maximizing output of the turbine at low wind speed and limiting the electrical power or torque at wind speed above a certain level. The optimum power output corresponds to a tip speed ratio (λ) that produces maximum power. As shown in Fig. 5, the speed control characteristic curve can be presented as a power versus generator speed relationship, an electrical torque versus generator speed relationship or a wind speed versus generator speed relationship.

Type A was proposed in [1]–[3]. In this scheme, the measured generator speed ω_r is transformed into reference electrical torque ${T_e}^{ref}$ by means of a speed control characteristic curve in the form of electrical torque versus generator speed lookup table. The reference electrical torque is then transformed into reference current ${i_{rd}}^{ref}$ by means of the following expression

$$ {i_{rd}}^{ref} = \frac{{T_e}^{ref}(L_{ls} + L_m)}{|u_s|L_m} \tag{1} $$

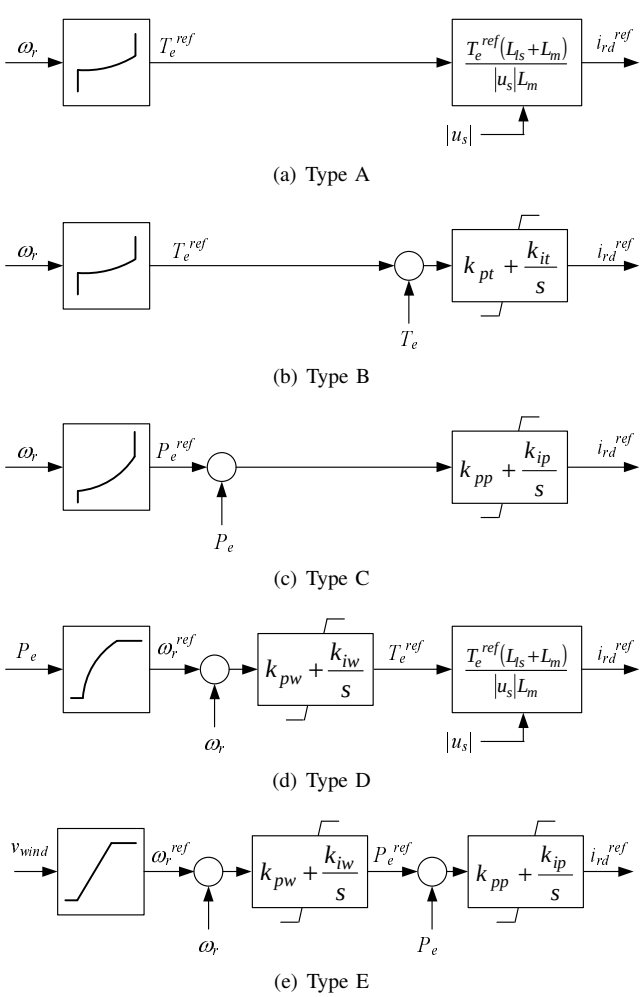

Fig. 4. Control schemes

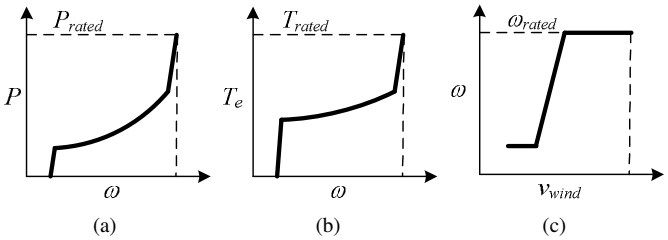

Fig. 5. Speed control characteristic curve: (a) generator power vs generator speed curve (b) electrical torque versus generator speed curve (c) generator speed versus wind speed curve

where T_e^{ref} is the reference electrical torque; u_s is the stator voltage; L_m is the magnetizing inductance and L_{ls} is the stator leakage inductance.

Type B control scheme is similar to type A control scheme, except the electrical torque T_e is regulated by means of a PI controller. This control scheme can be found in [4].

In type C control scheme, the speed control characteristic curve is implemented in the form of generator power versus generator speed lookup table. The reference electrical power ${P_e}^{ref}$ is then realized by means of a PI controller to produce corresponding rotor current. The scheme was proposed in [5].

Type D control scheme uses measured generator electrical

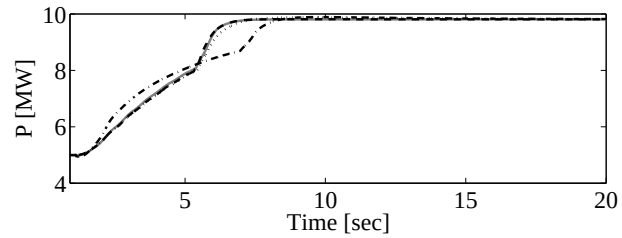

(a) Active power

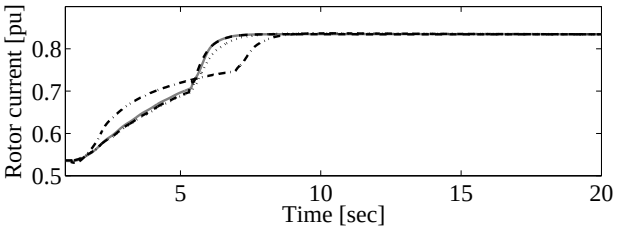

(b) Rotor current

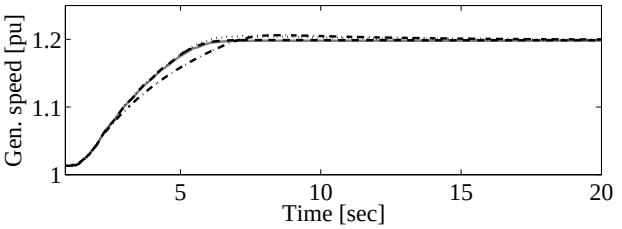

(c) Generator speed

Fig. 6. Response of wind turbine with different controller schemes to wind gust: type A (solid), type C (dashed), type D (dotted) and type E (dash-dotted)

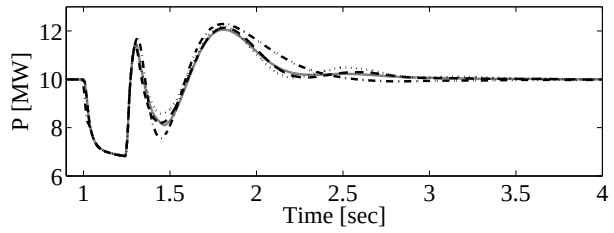

(a) Active power

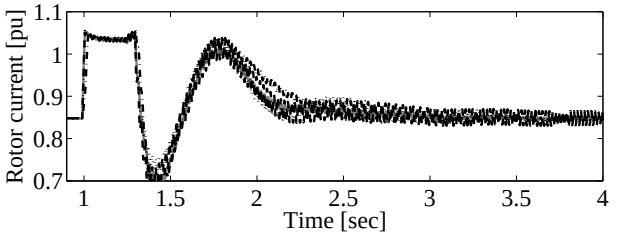

(b) Rotor current

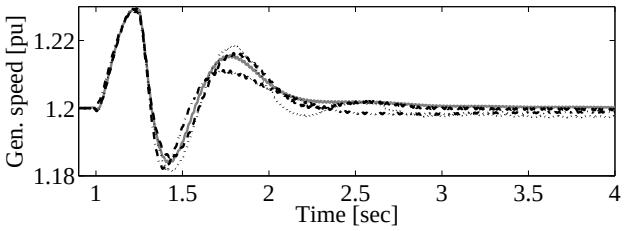

(c) Generator speed

Fig. 7. Response of wind turbine with different controller schemes to grid fault: type A (solid), type C (dashed), type D (dotted) and type E (dash-dotted)

power P_e as an input for the controller. By using speed control characteristic curve, the measured electrical power is transformed into reference generator speed ${\omega_r}^{ref}$. A scheme similar to type D control scheme was presented in [6] and to some extent was also presented in [7]–[9].

Unlike the other control schemes mentioned earlier, type E control scheme uses a different strategy. This controller uses wind speed v_{wind} as an input for the controller instead of using measured generator speed ω_r or generator power P_e. This scheme can be found in [11] and [10]

The responses of the control schemes to wind gust are shown in Fig. 6. The wind gust is simulated by ramping wind speed up from 8.9 ms^{-1} to 11.1 ms^{-1} within 1 second. The maximum wind speed is kept below the rated value in order to avoid interference with pitch controller operating region. In general, the different controller schemes have similar responses except for type E control scheme. A noticeable different response of type E control scheme is mainly due to difference in the speed control characteristic curve used.

The different control schemes are also compared by applying a grid fault. The PI controller gains are set to be relatively high to obtain fast response of the wind turbine. The pitch controller is locked during the simulations in order avoid actions of the pitch controller that may influence the turbine response. Simulation results are shown in Fig. 7. Note that since response of type A and B are quite similar, therefore only type A is presented in the results. Active power, rotor current and generator speed need to be observed in this investigation because these quantities determine the actions of protection systems. The active power is an important parameter in a grid interaction, the rotor current level determines action of the rotor side over-current protection and the generator speed influences the over-speed protection.

The response of the wind turbine is characterized by oscillations due to a non-stiff drive train. The results suggest that with relatively high controller gains, the responses of these controllers to a grid fault are similar. However, in some cases, the controller may not be too fast in order to consider sampling and time lag in the measurements as well as to maintain stability of the controllers. In such a case the turbine response is determined by the control parameters. A slower control response results in higher oscillations in the active power and rotor current and less oscillation on the generator speed (see Fig. 8). For type A control scheme, however, there is no possibility to adjust the controller parameters. Therefore this control scheme is not able to simulate a slower controller response unless additional time constant is introduced in the model.

V. Pitch Compensation

A basic pitch controller is depicted in Fig. 9. Some wind turbines with DFIG use pitch compensation to improve performance of the pitch controller during transient time, i.e. to reduce power overshoot due to wind gust.

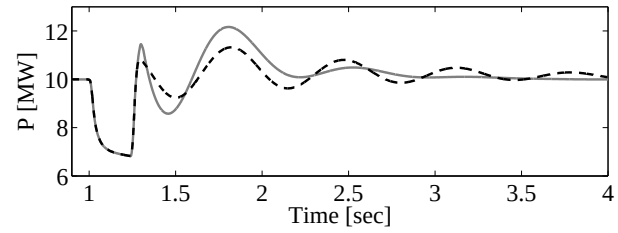

(a) Active power

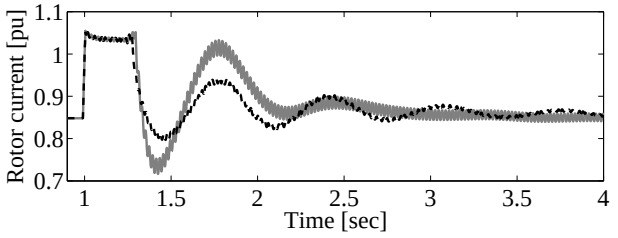

(b) Rotor current

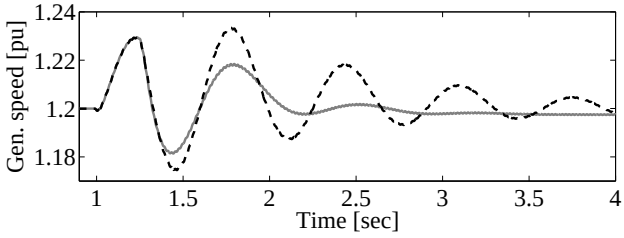

(c) Generator speed

Fig. 8. Response of wind turbine with type D control scheme to grid fault: fast controller (solid), slow controller (dashed)

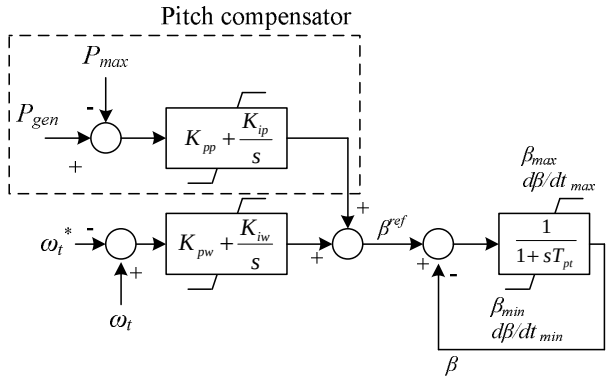

Fig. 9. Pitch controller

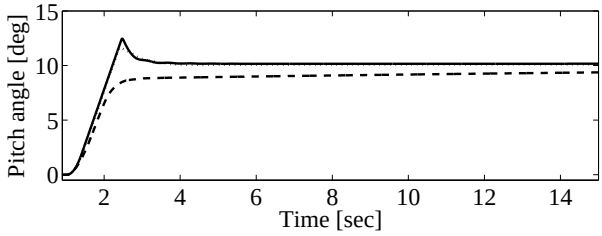

(a) Pitch angle

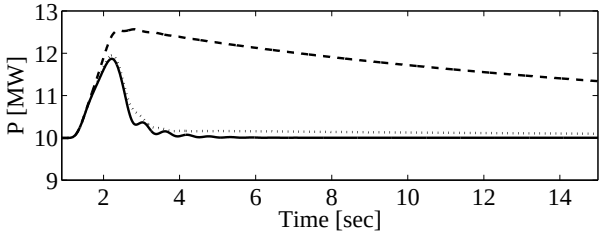

(b) Active power

Fig. 10. Response of wind turbine to wind gust: with pitch compensation (solid), no pitch compensation (dashed) and no pitch compensation with adjusted controller gain (dotted)

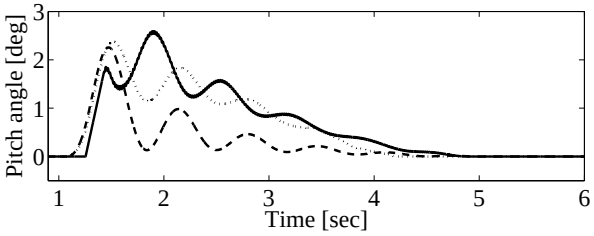

(a) Pitch angle

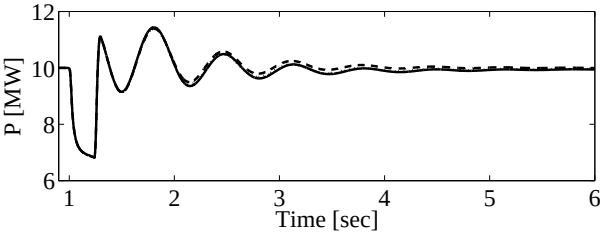

(b) Active power

Fig. 11. Response of wind turbine to grid fault: with pitch compensation (solid), no pitch compensation (dashed) and no pitch compensation with adjusted controller gain (dotted)

The difference of wind turbine response with and without pitch compensation to wind gust is shown in Fig. 10. In the simulation, the wind speed increases from 11.15 ms^{-1} (rated wind speed) to 15 ms^{-1} within 1 second. As shown in the figure, wind turbine with pitch compensation is able to recover the output power quickly. In contrast, active power output response of the wind turbine without pitch compensation exceeds rated value for a longer time. However, with gain adjustment, the pitch controller without pitch compensation is able to perform closely with the one with pitch compensation. The adjustment is normally done by increasing controller gains. This simulation suggests that the pitch controller without pitch compensation can be implemented for stability studies with some gain adjustments. It must be kept in mind, however, excessively high gains may lead to an instability.

The response of the two models to grid fault is shown in Fig. 11. The figure shows that the pitch compensation model is less influential in active power fault response despite significant difference in pitch response. This is because wind speed is assumed to be constant throughout the simulations.

VI. Conclusion

By assuming a relatively fast controller response, the simulation results indicate the different power-speed control schemes in wind turbine with DFIG are not influential for short-term voltage stability studies. However, with slower

responses of power-speed controllers the response of the wind turbine model depends very much on the controller parameters. That is to say, for such studies, an appropriate selection of control parameters is highly important regardless of control schemes used in the model. Type C and type D control schemes are more likely to be beneficial for short-term stability studies due to their simplicity in real implementation and parameter adjustability.

Inclusion of pitch compensation in wind turbine model is recommended although absence of the pitch compensation can be compensated by high pitch controller gains.

ACKNOWLEDGMENT

The authors would like to thank Nordic Energy Research, Svenska Krafnät and Vattenfall for financial support.

APPENDIX I
SIMULATION PARAMETERS

A. Generator parameters

Base power = 2 MW, R_s = 0.0082 pu, L_{ls} = 0.077 pu, L_m = 4.5 pu, R_r = 0.0062 pu, L_{lr} = 0.077 pu, H_g = 0.5 seconds

B. Turbine parameters

Rotor diameter = 80 m, Gearbox ratio = 90, rotor inertia constant = 2.5 seconds, shaft stiffness = 0.35 pu,

C. Rotor controller parameters

k_{pw} = 3, k_{iw} = 0.6, k_{pp} = 3, k_{ip} = 0.6, k_{pt} = 0.1, k_{it} = 50

D. Pitch controller parameters

T_{pt} = 0.02 = seconds, K_{pp} = 10, K_{ip} = 50, K_{pw} = 150, K_{iw} = 25, minimum pitch angle = 0 degree, maximum pitch angle = 45 degrees, minimum pitch rate = -10 degree/seconds, maximum pitch rate = 10 degree/seconds

REFERENCES

[1] J.B. Ekanayake, L. Holdsworth, X. Wu, N. Jenkins. "Dynamic modeling of doubly fed induction generator wind turbines," *IEEE Trans. Power Systems*, vol. 18, no. 2, May 2003, pp. 803-809.

[2] J.B. Ekanayake, L. Holdsworth, N. Jenkins. "Comparison of 5th order and 3rd order machine models for doubly fed induction generator (DFIG) wind turbines," *Electric Power Systems Research*, vol. 67, 2003, pp. 207-215.

[3] L. Holdsworth, X.G. Wu, J.B. Ekanayake, N. Jenkins. "Direct Solution method for initalising doubly-fed induction wind turbines in power system dynamic models," *IEE Proc. Generation, Transmission and Distribution*, vol. 150, no. 3, May 2003, pp. 334-342.

[4] B. Rabelo, W. Hofmann, "Control of an optimized power flow in wind power plants with doubly-fed induction generators." in *Proceeding of Power Electronics Specialist Conference (PESC), 2003*, vol 4, June 2003, pp. 1563 - 1568.

[5] M.A. Poller. "Doubly-fed induction machine models for stability assessment of wind farms," in *Proceeding of Power Tech Conference 2003*, vol. 3, June 2003.

[6] I. Erlich, J. Kretschmann, J. Fortmann, S. Mueller-Engelhardt, H. Wrede. "Modeling of wind turbines based on doubly-fed induction generators for power system stability studies," *IEEE Trans. Power Systems*, vol. 22, no. 3, Aug. 2007, pp. 909 - 919.

[7] S. Seman. "Transient performance analysis of wind-power induction generators," Ph.D. thesis, Helsinki University of Technology, Finland, 2006.

[8] N.W. Miller, J.J. Sanchez-Gasca, W.W. Price,R.W. Delmerico, "Dynamic modeling of GE 1.5 and 3.6 MW wind turbine-generators for stability simulations," in *Proceeding of Power Engineering Society General Meeting 2003*, vol. 3, July 2003, pp. 1977 - 1983.

[9] N.W. Miller, W.W. Price and J.J. Sanchez-Gasca. "Dynamic Modeling of GE 1.5 and 3.6 Wind Turbine-Generators," Technical Report, General Electric Company, Oct. 2003.

[10] S.M. Bolik, "Modelling and analysis of variable speed wind turbines with induction generator during grid fault," Ph.D. thesis, Aalborg University, Denmark, 2004.

[11] V. Akhmatov, "Modelling of variable speed wind turbines with doubly-fed induction generators in short-term stability investigations," in *Proceeding of International Workshop on Transmission networks for Offshore Wind Farms 2002*, Stockholm, Sweden, April.

[12] A. Petersson, "Analysis, modeling and control of doubly fed-induction generators for wind turbines," Ph.D. thesis, Chalmers University of Technology, Sweden, 2005.

[13] P. Ledesma and J. Usaola, "Doubly fed induction generator model for transient stability analysis," *IEEE Trans. Energy Conversion*, vol. 20, no. 2, June 2005, pp. 388-397.

Long-term voltage stability when connecting wind power

Marcia Martins[1*)], Evert Agneholm[1)2)], Ola Carlson [1)]
[1)] Chalmers University of Technology, Hörsalsvägen 11, 41309 - Gothenburg, Sweden
[*)] tlf. +46 317721638, e-mail marcia.martins@chalmers.se
[2)] Gothia Power AB, Gothenburg, Sweden

Abstract — This paper presents long-term voltage stability studies of a power system at different scenarios. The model of the system studied includes a production area, transmission lines and a load area. In the load area, the generated power is either based on thermal power, fixed speed wind turbines or a combination of thermal and wind power. The model of the system also includes a transformer tap-changer, a dynamic load and generator field and armature current limiters. The generators are dimensioned according to grid codes. Simulations have been performed with a variation in the active power generation of the production plants. For the wind parks, investigations have also been performed on different control strategies of the reactive power production. It has been demonstrated that these control strategies play an important role for the long-term voltage stability of the power system.

Index Terms — Fixed speed wind turbines, grid code, long-term voltage stability, voltage collapse.

1. Introduction

The introduction of large-scale wind power in power systems brings up a number of questions regarding various stability aspects. One of these is the long-term voltage instability that has been the reason for many voltages collapses during the years [5]. Historically many power systems have been based on hydro units and thermal units. Both of these production sources use synchronous generator that has the possibility either to produce or absorb reactive power and thereby continuously contribute to the voltage control of the power system. However, the generators used for large scale wind power applications are mostly based on fixed speed induction generators, double fed induction generators or generators equipped with full converters. These types of generators can produce and consume reactive power in various ways. The fixed speed induction generator can only consume reactive power and therefore it has to be combined with shunt capacitors or an SVC in order to fulfil the grid codes given by the independent system operator. In this paper the fixed speed induction generator will be studied in more detail and compared with conventional thermal power plants from a long-term voltage stability point of view. However, most of the principles analysed may also be valid for other types of wind turbine technologies.

Except the type of generation the long-term voltage stability will also be affected by parameter settings of the dynamic load, tap changers etc. However, it has not been the scope of this paper to analyse all these aspects and therefore typical settings have been used for the dynamic load and tap changers. The way of operation will also affect losses in the wind park and the power system. These losses and costs have not been analysed in this paper.

2. Long-term Voltage Stability

According to [4]-[5]-[6], long-term voltage stability involves slower acting equipment such as tap-changing transformers, thermostatically controlled loads and generator current limiters. The study period of interest is up to minutes, and long-term simulations are required for an analysis of the system dynamic performance. Stability is usually determined by the resulting outage of equipment, rather than the severity of the initial disturbance. Instability is due to the loss of long-term equilibrium (e.g., when loads try to restore their power beyond the capability of the transmission network and connected generation), the post-disturbance steady state operating point being small-disturbance unstable or a lack of attraction towards the stable post-disturbance equilibrium (e.g., when a remedial action is applied too late). The disturbance can also be a sustained load build up (e.g., morning load increase). In many cases static analysis can be used to estimate stability margins, covering a wide range of system conditions and scenarios. Where the timing of control actions is important, the analysis shall be complemented with quasi-steady-state time domain simulations.

3. Studied System

A power system comprises three parts: the transmission system, the generation system and the distribution system where the load demand is included. Using this approach a simplified network can be built to represent any power system, for instance the Swedish system with a significant amount of power supply coming from the north of the country combined with the thermal power plants in the south where also a possible integration of wind power into the grid is analysed. A system as in Figure1 has been modelled by using the Digsilent Power Factory power system analysis package. The transmission corridor consists of two 400 kV transmission lines of 300 km length. Area 1 has been modelled as an infinite source. The load is situated at the 24 kV level and has been varied to find the operational limits of the system. During voltage instability the impact of the load voltage dependency is essential to consider. Therefore, a dynamic load model is used to model the load recovery [3]. A 400/24 kV transformer with 15% reactance has been included to model the reactive power losses between the transmission system and the 24 kV load. It is important to represent the transformer tap-changers since they can be the cause of long-term voltage instability in their attempt to restore the voltage and thereby the power on the load level.

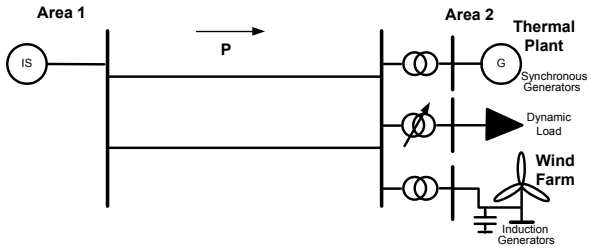

Figure1. The studied system.

Voltage collapse is rarely a concern when all lines are in operation. The transmission system security is typically guaranteed such that the loss of any single component will not lead to any violation of the operational limits. Thus, even after loss of one of the two lines the system should be stable for a certain load level. Therefore the system after a loss of one of the two transmission lines will be analysed in this paper.

3.1. Thermal Unit

A 283 MVA, 255 MW synchronous generator represents the thermal unit. Since voltage problems can be due to generators performance, it is important to consider the reactive capability limit of synchronous generators in long-term voltage stability studies.

From the stability point of view the performance of synchronous generators have certain limitations related to their construction. Such limitations are related to the limits in the reactive power generation capabilities like the field current limit and the armature current limit. Therefore these limiters are included in the voltage regulator of the synchronous generator.

A capability diagram displays possible operating areas where the generator thermal limits are not violated.

In Figure 2 the capability diagram including the field and armature current limiters are presented.

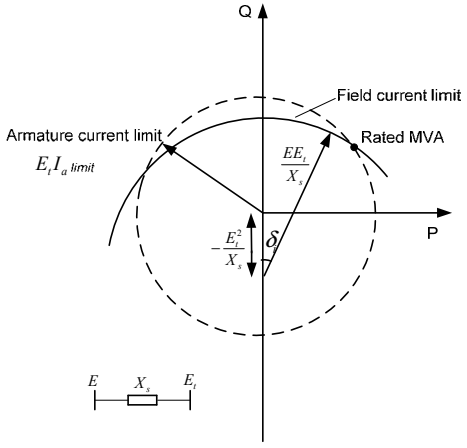

Figure 2. Synchronous generator reactive capability curve.

3.1.1. Field Current Limiter:

The purpose of having a field current limiter is to protect the field winding from overheating due to prolonged field overcurrent. The data used to model the field current limiter is shown in Appendix.

The interaction between the current limited and the load characteristic occurs if for some reason a system has a deficiency of transmission capacity leading to a voltage stability problem and the current limiter is activated after further load increase. The generator may then be seen as a fixed voltage source behind a reactance. From the system point of view it will be like an increase of the reactance in the system which will weaken the system leading to a risk for a voltage collapse. A description is given in [1].

3.1.2. Armature Current Limiter

The armature current results in an RI^2 power loss and the energy associated with this loss must be removed in order to limit the increase in temperature of the generator. If the armature current limiter is exceeded the voltage regulator will reduce the excitation of the generator and thereby the reactive power production. The output signal from the armature current limiter is going to a "Min limiter" together with the output signal from the field current limiter and the output signal from the voltage regulator. The data used to model the armature current limiter is shown in Appendix.

3.2. Dynamic Load

During voltage instability the impact of the load is essential to consider. Therefore, a dynamic load model is used to model the load recovery.

The load model used in this paper is based on field measurements performed in the south of Sweden [3]-[10]. The investigations performed in this paper mainly focus on the features of the wind power generation. Further investigations on variations of load model parameters can be seen in [3].

The recovery time, T_p, or T_q of the model is in the time frame of minutes. The load model includes a static part of the active $P_s(V)$ and reactive power $Q_s(V)$ and a transient part of the active $P_t(V)$ and reactive power $Q_t(V)$. In [2] a load state is introduced as:

$$x_p = T_p\left(P_d - P_t(V)\right)$$

$$x_q = T_q\left(Q_d - Q_t(V)\right)$$

Here P_d is the active power demand and Q_d the reactive power demand. The exponential load recovery is then given by:

$$\dot{x}_p = \frac{1}{T_p}x_p - P_t(V) + P_s(V) = -P_d + P_s(V)$$

$$\dot{x}_q = \frac{1}{T_q}x_q - Q_t(V) + Q_s(V) = -Q_d + Q_s(V)$$

The static load voltage dependent characteristics give the stationary and transient behaviour as:

$$P_s(V) = P_0\left(\frac{V}{V_0}\right)^{\alpha_s},\ Q_s(V) = Q_0\left(\frac{V}{V_0}\right)^{\beta_s}$$

$$P_t(V) = P_0\left(\frac{V}{V_0}\right)^{\alpha_t},\ Q_t(V) = Q_0\left(\frac{V}{V_0}\right)^{\beta_t}$$

Here: P_0, Q_0 are the active and reactive power consumption at pre-fault voltage, V is the supplying voltage [kV], V_0 is the pre-fault value of the supplying voltage [kV], α_s, β_s are the steady state active and reactive load voltage dependence respectively and α_t, β_t are the transient active and reactive load voltage dependence respectively.

Examples of dynamic loads in the distribution networks that are included in the model are: electrical heating, air conditioning, refrigerators and freezers.

3.3. Transformer on-load tap changer

Tap-changers provide voltage control by restoring the load voltage level. They can be the cause of long-term voltage instability in their attempt to restore the load voltage. During this process the transmission level voltage is deteriorated with a possible voltage collapse. The time delay of the tap-changer model for the studies in this paper has been set to 30 seconds per step.

Based on simulations performed it can be observed that if no tap-changer is included in the transformer model, the voltage collapse will take longer time to occur even for critical levels of load demand. The time it takes for the system to collapse can be prolonged with 30 to 50 minutes. The simulations also show that the voltage collapse can happen gradually, i.e. the voltage will keep declining for longer time reaching unacceptable levels. It means that the presence of the tap-changer not only contributes but can also speed up the voltage collapse in critical situations.

3.4. The fixed speed wind turbine

The investigations in this paper have used a fixed speed wind turbine as a model for all studies. A fixed speed wind turbine consists of an induction generator connected directly to the grid. For simulation purposes the mechanical model is represented as a one-mass model wind turbine. A one-mass model comprehends a lumped model where the masses of wind turbine, gear box and generator rotor are lumped into a single rotating mass. Since long-term voltage stability is studied the period of interest may be several or many minutes and therefore a lumped model is adequate to be used for this purpose. However, for short-term voltage stability purposes a two-mass model would be required to accurately represent the electro mechanical oscillations [7].

When using induction generators the reactive power demand increases with the loading of the machine (Figure 3). In order to compensate this reactive power, shunt capacitors or a SVC can be used. In this paper shunt capacitors are installed in order to be able to fully compensate at 100% loading and 90% voltage. This is in accordance with the grid codes [9], see section IV.

During the simulations two alternatives of using the shunt capacitors have been applied: reactive power control and voltage control of the wind park.

Reactive power control is used for compensating the reactive losses in the wind park and transformer. In the point of connection to the grid the reactive power is 0 MVAr irrespectively of the voltage.

Voltage control is used for controlling the voltage in the point of connection to the grid. In case of an active power production less than maximum available shunt capacitors are connected and disconnected at various voltage levels. For severe voltage instability situations all shunt capacitors will be connected after the voltage decrease. This behaviour will also correspond to the behaviour of a SVC which acts very fast.

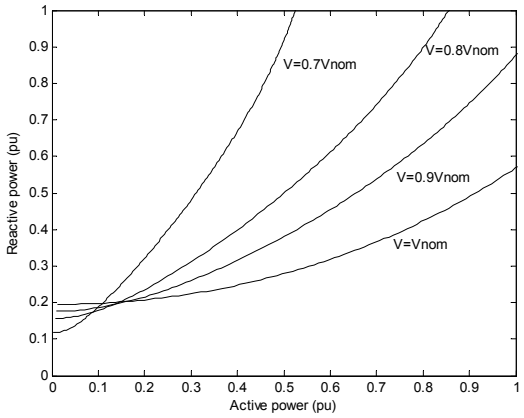

Figure 3. Reactive power consumed by an induction generator as a function of the generated active power for different voltage levels (Vnom = nominal voltage).

4. GRID CODES

Due to the deregulation of the electricity market and the large-scale introduction of wind power based on various technologies there has been a focus on introducing grid codes for production plants. The grid codes cover a variety of requirements during normal and disturbed conditions. When studying long-term voltage stability the requirements related to supplying and absorbing reactive power is important to consider. In this paper the Swedish grid code will be treated as an example. However, the method is general and can also be applied for other grid codes [9].

The Swedish grid code states that for thermal and hydro plants it shall be possible to produce and consume reactive power according to:

- Produce reactive power corresponding to a 1/3 of maximum active power when the voltage is within 90-100% of rated voltage. Both reactive power and voltage are referred to the high voltage side of the step-up transformer, i.e. the losses in the transformer must be taken into account.
- Produce reactive power corresponding to a 1/3 of maximum active power production when the voltage is above 100%. This shall be possible until the generator terminal voltage exceeds 105%.
- Thermal units shall be able to reduce the reactive power production to 0 MVAr seen from the upper side of the transformer.

For wind power the only requirement is that it shall be able to control the reactive power production and consumption to 0 MVAr at the connection point to the grid. No voltage levels are given in the grid codes but an assumption is that it

shall be possible to fulfil the requirement down to 90% voltage.

5. SIMULATION RESULTS

The simulations were performed using the system presented in Figure 1. Digsilent Power Factory simulator software was used to carry out all investigations. In order to analyse the long-term voltage stability, three different scenarios of the system in Figure 1 were used:

5.1. Area 2 supplied by only thermal power;
5.2. Area 2 supplied by only wind power;
5.3. Area 2 supplied by thermal plus wind power.

5.1. Area 2 supplied only by thermal power

The disturbance applied to the system (Figure 1) is initiated by the trip of one of the two transmission lines. As described in Section 3 the system will be exposed to a tap-changer action and load recovery until the current limiters are activated.

The voltage will instantaneously go down both on the load level and on the transmission level when the line is disconnected. As a result the active power demand will decrease. However, the load will recover and when also the tap changer starts to act the load will recover even more. As a result the voltage on the transmission level will drop, see Figure 5. Figure 4 shows the maximum load in Area 2 as a function of the active power production in the thermal unit. If for each production level the load is increased an additional MW, the voltage collapse will be a fact.

Normally thermal power plants are operated close to their maximum power production since the efficiency of the plant usually is designed for this point of operation. In Figure 4, however, it can be seen that if the active power production is reduced some, the total load in the load area can be higher as compared to if full active power production is achieved. This can be explained by the fact that when the active power production is reduced there will be access to more reactive power from the generator. This reactive power results in an increased voltage in the transmission system in the load area [1]. As the voltage increases it will be possible to transfer more power from Area 1 to Area 2.

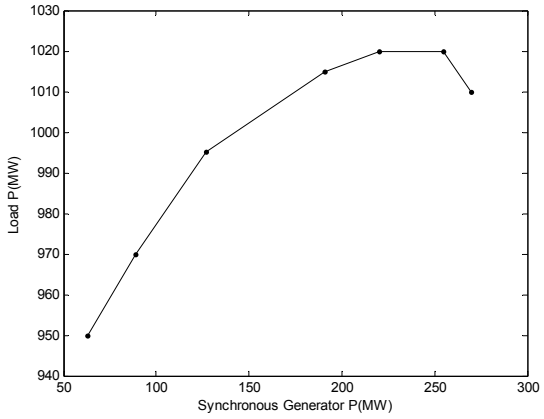

Figure 4. Relation between load limit level and synchronous generator active power production.

5.1.1. Interaction between dynamic load, tap changer and generator current limiters:

Using the models described for dynamic load, tap changer and generator current limiters a simulation was carried out to illustrate the phenomenon of voltage instability verifying the combined effects of these components. The disturbance on the system in Figure 1 is initiated by a trip of one of the two transmission lines (wind power is not included) at 100 seconds. At the instant when the line is disconnected, the voltage and power demand drop at the load side (Figure 5, 6). In [1] this phenomenon is analysed in detail.

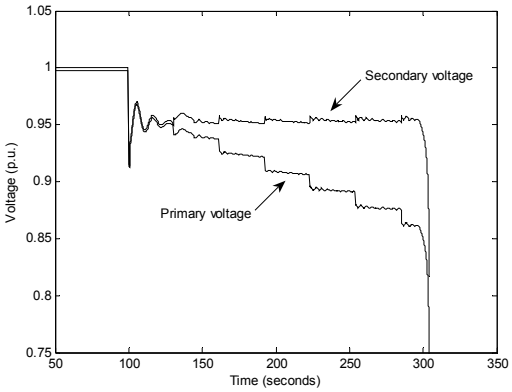

Figure 5. Voltage collapse seen on both sides of the transformer located at the load end.

Thirty seconds after the disturbance, the tap changer starts to restore the voltage level at the load side (Figure 7). For every tap step, the voltage at the load side increases and therefore the load power increases. This also leads to a current increase at the load side of the transformer. This increased current is amplified on the primary side by the transformer and as a result gives an increased voltage drop on the primary side. The field current limiter is activated at 140 seconds whereas the armature current limiter is activated at 280 seconds followed by the voltage collapse in the next 20 seconds (Figure 9). The generator reactive power production will be reduced when the current limiters are activated. When the generator reaches its field current limit, its terminal voltage drops. In addition to that the tap changer continues to restore the load voltage resulting in a current increase and an additional voltage drop on the primary side. At 310 seconds the voltage collapse is a fact.

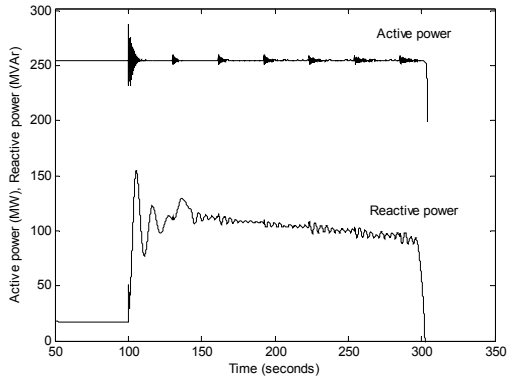

Figure 6. Synchronous generator active and reactive power.

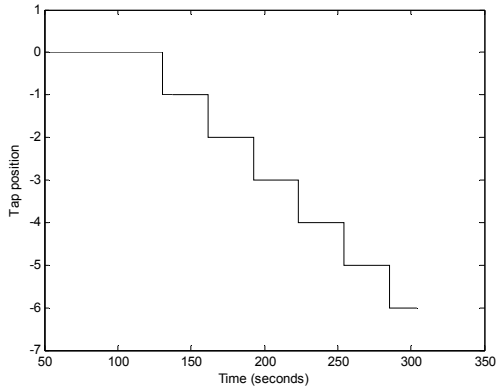

Figure 7. Tap changer activation.

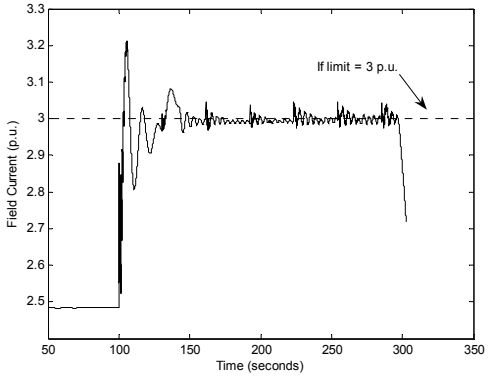

Figure 8. Field current limiter activation (current is limited to 3 p.u.).

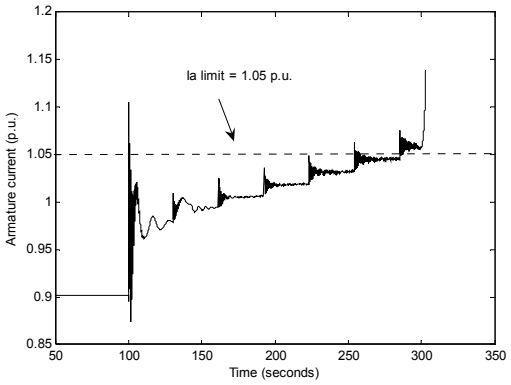

Figure 9. Armature current limiter activation (current is limited to 1.05 p.u.)

5.2. Area 2 supplied only by wind power

The simulations as performed when only having thermal power have been repeated when only having a large wind farm connected to Area 2 as shown in Figure 1. The wind farm is modelled as three aggregated induction generators and one 400/0.96 kV transformer. The wind farm has 250 wind turbines, of 2MW each, i.e. in total 500 MW.

The presence of the wind power installation leads to the injection of active power in the system and an increase of reactive power consumption. The solution chosen in this paper is to equip the wind farm with capacitor banks providing reactive power compensation. The studies were made considering the two situations mentioned in Section 3.4.

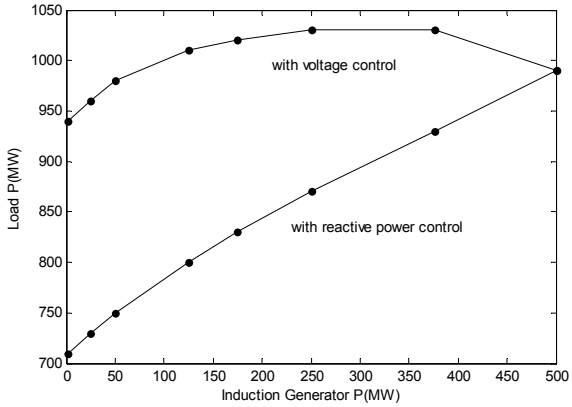

Figure 10. Relation between load and power generation of a system with only wind power input.

The curve with reactive power control demonstrates a considerable reduction on the load level supply when decreasing the active generated power. In this case the reactive power consumption by the induction generators is determining the voltage stability limit for the system. The reactive power consumption is well indicated by the non linear proportion between the load and the generated power presented in Figure 10.

The curve with voltage control shows a significant improvement. Higher amounts of loads can be supplied when the wind farm is producing from 25% to 75% of the total generated power. Even when no wind incidence will appear, i.e. if the wind farm would go down to around 0 MW power generation, still a considerable level of load could survive after loss of a line. It demonstrates that the wind farm can always provide reactive power to the grid regardless of the amount of wind. From the power system point of view wind power offers the benefit of operating as a voltage control for the system when not producing active power, i.e. during most of the time.

Figure 11 shows the behaviour of the voltage on primary and secondary sides when the wind farm is producing 150 MW, with a load demand of 900 MW. A simulation was done in order to compare the behaviour after a disturbance when having reactive power control and when having voltage control.

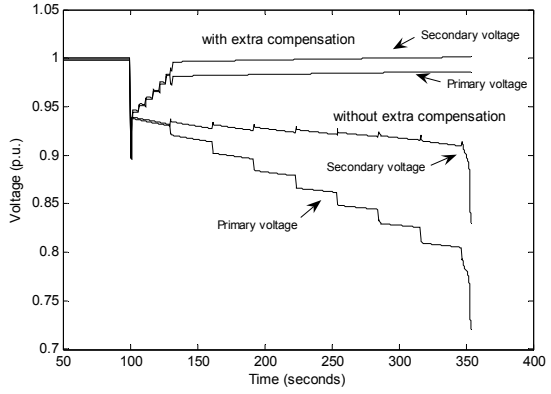

Figure 11. Secondary and primary voltages when the wind farm is having voltage and reactive power control.

5.3. Area 2 supplied by both wind and thermal power

In Figure 12 it is evident that the combination of both types of power suppliers raises the amount of load that the system can sustain after the disconnection of a transmission line. For the curve with voltage control, once again, it can be observed that even when the wind farm has very low incidence of wind the system can keep the voltage stable for high load levels after the loss of a transmission line. When comparing with a system with only thermal power the load levels are lower.

Once more it is shown that the wind farm will provide reactive power to the system even though the amount of wind is not sufficient to produce active power.

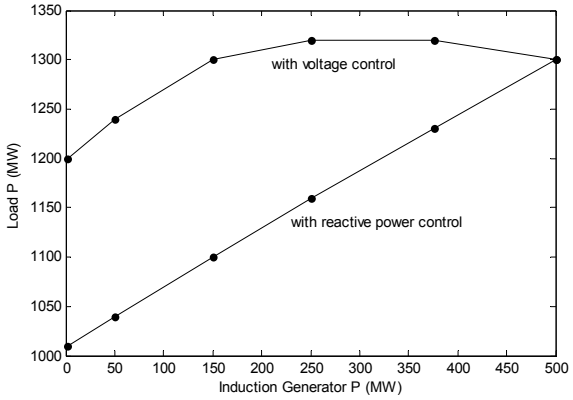

Figure 12. Relation between load and power generation of a system supplied by both thermal and wind power.

6. CONCLUSION

From the long-term voltage stability point of view wind farms do not have the same influence on the power system as a conventional power plant. Conventional power plants normally produce maximum or close to maximum active power whereas wind power normally produces much less than maximum active power. As the grid codes are related to maximum active power production, normally there will be a substantial amount of reactive power available from the wind farm. In this paper fixed speed wind turbines combined with shunt capacitors has been studied but other technologies with doubly fed induction generator or generators equipped with full converters can be applicable. Also a combination of these techniques with a SVC or connection via HVDC light can be possible.

However, the essential idea from the investigations done in this paper is to illustrate that the impact of the integration of a large wind farm acting as a voltage control is entirely helpful on the power system performance when referring to long-term voltage stability.

From the studies it can be noticed that wind power is able to supply highest amount of load demand when producing from 25% to 75% of the total wind power capacity. Considering wind variation, statistically the average of wind power production is around 30% of the rated capacity. Thus a wind farm at this level is capable to maintain voltage stability for its highest power demand.

Another relevant aspect is that, irrespective of the amount of the incidence of wind blowing, i.e. even if the active power production would be close to 0 MW the wind farm still can provide reactive power to the system. This means that the power system performance will be able to keep the voltage stable for a reasonable amount of load power demand.

All these considerations are made based on wind farms located in close proximity to the power system, i.e. the power system can take advantage of the reactive power.

Based on the analysis performed it is recommendable that the grid code includes a requirement stating that wind farms have to be equipped with voltage control and not only controlling reactive power.

APPENDIX

Dynamic load model:
$\alpha_s = 0.38$, $\alpha_t = 2.26$, $\beta_s = 2.68$, $\beta_t = 5.22$, $P_0 = 0.10$ p.u., $T_{pr} = 127.6$ s, $T_{qr} = 75.3$ s.

Transformer tap-changer model:
Controller time constant = 0.01 p.u., tap step = 0.01 p.u., time delay = 30 s.

Current Limiters model:
Field current limiter: I_f limit = 2.987 p.u., T = 10s, Tc = 4 s, VCMIN = -100 p.u., VCMAX = 100 p.u., KC = 10 p.u.

Armature current limiter: I_a limit = 1.05 p.u., T = 10s, Tc = 4 s, VCMIN = -100 p.u., VCMAX = 100 p.u., KC = 10 p.u..

ACKNOWLEDGEMENT

The authors thank Jaap Daalder for his valuable comments to this paper.

REFERENCES

[1] S. Johansson. Long-term voltage stability in power systems, Ph.D. dissertation, Dept. Electric Power Engineering. Chalmers University of Technology, Sweden, 1998.
[2] D. Hill. Nonlinear dynamic load models with recovery for voltage stability studies. Power Systems, IEEE Trans. Vol. 8. 1993
[3] D. Karlsson. Voltage stability simulations using detailed models based on field measurements. Ph.D. dissertation, Dept. Electric Power Engineering. Chalmers University of Technology, Sweden, 1992.
[4] P. Kundur, J. Paserba, V. Ajjarapu, G. Andersson, A. Bose, C. Canizares, N. Hatziargyriou, D. Hill, A. Stankovic, C. Taylor, T. Van Cutsem, V. Vittal. Definition and classification of power system stability IEEE/CIGRE joint task force on stability terms and definitions. Power Systems, IEEE Trans. Vol. 19. 2004; pp. 1387 – 1401.
[5] C. Taylor. Power systems voltage stability. McGraw-Hill Inc.: New York, 1994.
[6] P. Kundur. Power systems stability and control. McGraw-Hill Inc.: New York, 1994.
[7] A. Perdana, M. Martins, P. Ledesma, E. Agneholm, O. Carlson. Validation with a fixed speed wind turbine dynamic model with measured data. Renewable Energy Journal.
[8] Å. Larsson. The power quality of wind turbines. Ph.D. dissertation, Dept. Electric Power Engineering. Chalmers University of Technology, Sweden, 2000.
[9] Svenska Kraftnät. Grid code for wind power integration.
[10] G. le Dous, J. Daalder and D. Karlsson. Dynamic load measurement in a 2000 MW system in order to operate power systems close to their limits. CIGRÉ Rep. 39-107, Paris, France, Aug. 1998.

Grid faults' impact on wind turbine structural loads

Anca D. Hansen*, Nicolaos A. Cutululis*, Florin Iov+,
Poul Sørensen*, Torben J. Larsen*
* Risø National Laboratory, Technical University of Denmark, Wind Energy Department,
P.O. Box 49, DK-4000 Roskilde, Denmark
Email: anca.daniela.hansen@risoe.dk, nicolaos.cutululis@risoe.dk, poul.e.soerensen@risoe.dk

Abstract — The objective of this work is to illustrate the impact of the grid faults on the wind turbine structural loads.

Grid faults are typically simulated in detailed power system simulation tools, which by applying simplified mechanical models, are not able to provide a throughout insight on the structural loads caused by sudden disturbances on the grid. On the other hand, structural loads of the wind turbine are typically assessed in advanced aerolastic computer codes, which by applying simplified electrical models do not provide detailed electrical insight.

This paper presents a simulation strategy, where the focus is on how to access a proper combination of two complimentary simulations tools, such as the advanced aeroelastic computer code HAWC2 and the detailed power system simulation tool DIgSILENT, in order to provide a whole overview of both the structural and the electrical behaviour of the wind turbine during grid faults.

The effect of a grid fault on the wind turbine flexible structure is assessed for a typical fixed speed wind turbine, equipped with an induction generator.

Index Terms — grid faults, mechanical loads, grid connection requirements, aeroelastic computer code.

1. INTRODUCTION

As a result of the fast development of the wind energy industry in the last few years, the attention is directed toward the wind power impact on the power system. This aspect is also reflected in the wind turbine grid connection requirements [1], which are continuously subjected to periodic revisions.

The fulfillment of these requirements poses challenges for the design of both the electrical system and the mechanical structure of wind turbines.

From an electrical point of view, these challenges imply development of advanced controllers of wind turbines adapted to fulfil the grid requirements. However, the design of such controllers, suitable to ensure the fulfillment of the grid requirements, requires also a better understanding of their influence on the wind turbines structural loads.

This issue has not been sufficiently investigated in the relevant literature. Up to now, no clarified knowledge and investigations, on how the fulfillment of the new grid requirements affects the wind turbine structural loads, exist. Such investigations are very important in order to evaluate and define possible new directions in the certification process of future power plant wind turbines, namely wind turbines which participate actively in the stabilization of power systems.

This paper describes an ongoing research work [2] whose long term objective is to investigate into the consequences of the grid connection requirements on the fatigue and extreme loads of wind turbines. As a result of the fast development in wind turbine design, there is a lack in a long-term experience concerning the quantification of the grid faults' impact on the structural loads and thus on the lifetime of the wind turbine. The final goal of this research issue is therefore to identify new possible guidelines for design basis and certification which also take into account the fulfilment aspects of the new grid requirements. A procedure for the evaluation of the consequences of grid faults on the wind turbines' loads is to be developed and intended to be used directly in the certification of future wind turbines.

The paper presents the prior steps toward understanding how the fulfilment of the fault-ride through requirement affects the structure of the wind turbine itself. A set of simulations reflecting both the electrical and the structural dynamic response of a fixed speed wind turbine to a grid fault are presented and analysed in this paper.

2. GRID FAULTS AND GRID REQUIREMENTS

The first natural step in the evaluation of the grid faults impact on wind turbine loads is to assess an overview of the grid faults types and their frequency, in different countries.

Such a mapping of the grid faults and grid requirements in different countries is provided in the report [3], which is one result of the ongoing research project. In this report, statistics regarding, for example, the grid faults in the transmission system of the Nordic countries (Denmark, Finland, Norway and Sweden), are presented and analysed.

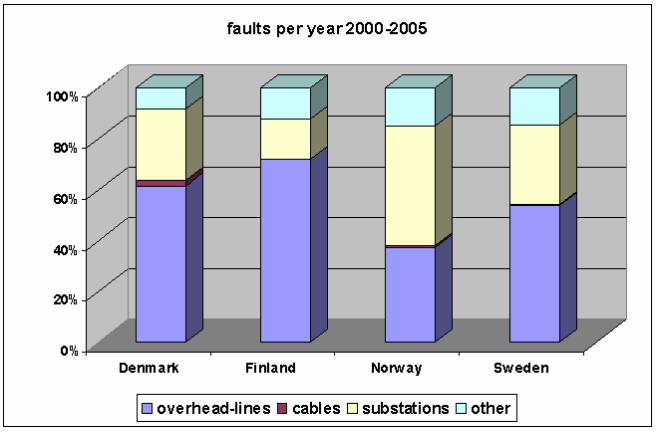

Figure 1. Types of faults in the Nordic countries transmission system – source [3].

Figure 1 illustrates for example that, in the Nordic countries excepting Norway, the most faults per year are located on overhead lines in the period 2000-2005. According to [3], in this period of time, the number of faults located in cables is less than 2.5% of the total number of faults.

Furthermore, in these Nordic countries, most of the faults on overhead lines in the period 1996-2005 are located on 132kV lines, while 400kV lines are less susceptible to faults – as illustrated in Figure 2.

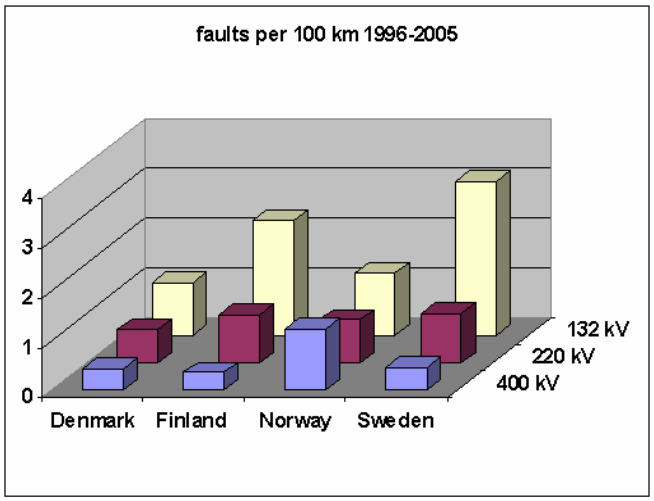

Figure 2. Number of faults per 100km in Nordic countries' overhead lines in the period 1996-2005 – source [3].

The analysis in [3] reveals also that, in Nordic countries, the single phase fault type has the highest probability to occur compared with other fault types, as illustrated in Figure 3.

An overview of the national grid codes in countries as Denmark, Ireland, Germany, Great Britain, Spain, Italy, USA and Canada is also provided in [3]. All these codes require fault ride-through capabilities for wind turbines.

The fault ride-through capability addresses primarily the design of the wind turbine controller in such a way that the wind turbine is able to remain grid-connected during voltage dips caused by grid faults. The fault ride-through requirement has been imposed in order to avoid significant loss of wind turbine production in the event of grid faults. Nowadays, with the increased wind power penetration in the power system, a large loss of power production would worsen an already critical grid situation by making the power system unstable and violating certain grid codes and security standards.

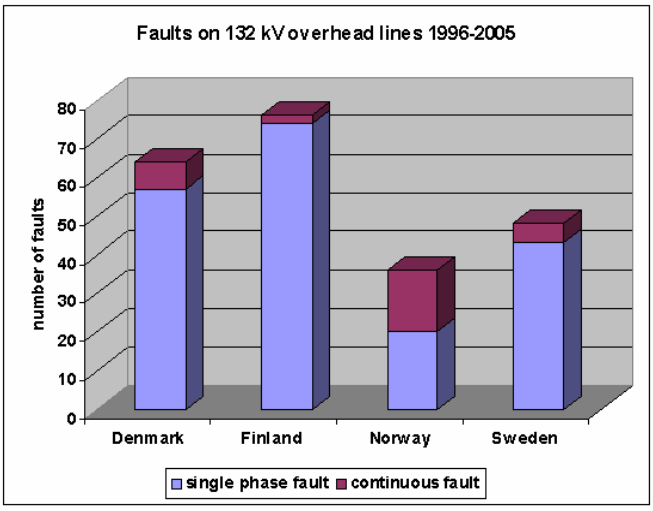

Figure 3. Frequency of different fault types on 132kV overheads lines – source [3].

A summary of the fault ride-through in different national grid codes is given in Table 1. Notice that some national grid codes e.g. Denmark and Ireland have specific fault ride-through requirements for distribution networks as well as for transmission ones, while other national grid codes have focus only on the transmission level. The voltage profiles in these national requirements are given specifying the depth of the voltage drop and the clearance time as well. In some of the grid requirements, as in Denmark, Íreland and Germany, the definition of the voltage profile is clearly specified regarding the type of the fault, i.e. symmetric or asymmetric.

Table 1.Summary of national fault ride-through requirements – source [3].

Country	Voltage Level	Fault ride-through capability				
		Fault duration	Voltage drop level	Recovery time	Voltage profile	Reactive current injection
Denmark	DS	100 msec	25%U_r	1 sec	2, 3-ph	no
	TS	100 msec	25%U_r	1 sec	1, 2, 3-ph	no
Ireland	DS/TS	625 msec	15%U_r	3 sec	1, 2, 3- ph	no
Germany	TS	150 msec	0%U_r	1.5 sec	generic	Up to 100%
Great Britain	TS	140msec	15%Ur	1.2sec	generic	no
Spain	TS	500 msec	20%U_r	1 sec	generic	Up to 100%
Italy	> 35 kV	500 msec	20%U_r	0.3 sec	generic	no
USA	TS	625 msec	15%U_r	2.3 sec	generic	no
Ontario	TS	625 msec	15%Ur	-	-	no
Quebec	TS	150 msec	0%U_r	0.18 sec	Positive-sequence	no

Notice that Ireland's code is very demanding regarding the fault duration, while Denmark has the lowest fault duration with only 100msec. However, Denmark's code requires the wind turbine to remain connected to the grid during successive faults. The German grid code requires the wind turbines to remain connected to the grid during voltage sags down to 0% from the rated voltage in the PCC for a duration of 150msec. Moreover, a reactive current injection up to 100% during fault is required, this requirement being also present in the Spanish grid code.

3. GRID FAULTS AND CERTIFICATION

Wind turbines connected to the grid are frequently subjected to grid faults. Grid faults are basically experienced by the wind turbine as changes in the voltage at the generator terminal. This causes typically transients in the generator electromagnetic torque, which result in significant stress of the wind turbine components, i.e. the drive train component.

Nowadays, analysis of wind turbine loads caused by grid faults is even more important especially in terms of lifetime of the wind turbines with regard to the fulfilment of the fault ride-through requirements. A typical design basis analysis of the loads and lifetime includes today the distribution of fatigue loads and extreme loads only for normal, start and shut-down operations. Besides these aspects, it is also relevant to know how different the wind turbine loads caused by grid faults are, compared to the wind turbines loads during shut-down and restart operations. A focus directed to loads caused during grid fault operation can thus provide a more complete understanding of the loads distribution during the whole wind turbine lifetime.

The fast development of the wind energy industry implies a continuous revision not only of the grid connection requirements, but also of the certification standards. These standards have to specify the essential wind turbine design requirements to ensure the engineering integrity of wind turbines. They have therefore to be adapted continuously

according to the progress of technology, knowledge and new requirements, such as the grid connection requirements.

At the moment, IEC 61400-1 certification standard, (paragraph 7.4) [4], presents a list with different design situations and load cases (i.e. faults during normal or parking operation). Loss of the electrical power network, voltage/frequency ranges, voltage unbalance are specified, but not really dealt with in certification. IEC 61400-1 certification standard stipulates the wind turbines to be designed to withstand electrical faults and any other type of abnormal operating conditions that may occur in the grid, but it does not state requirements in terms of specific faults to be considered, leaving this task to the designer and the certifier of the wind turbine.

4. COMPLIMENTARY SIMULATION TOOLS

At the moment, the design and the research of wind turbines take place in specific dedicated simulation tools, which are specialised either in the mechanical design area or in the electrical design area regarding grid integration issues of wind turbines. The expertise in these wind turbine design areas is thus built-up independently, with very specific focus and without any influence from one design area to another. In spite of this fact, practical experience shows that there is a considerable interplay between these design areas, which is necessary to take into account. It seems likely that the increased requirements regarding wind turbines response during grid faults may have significant influence on the structural loads of the wind turbine.

The attention in this paper is therefore directed to the design of a simulation approach able to assess the effect of grid fault on wind turbine structure, namely the real interaction between the electrical and the mechanical aspects of the wind turbine response during grid faults.

In this respect, in this work, two complimentary simulation tools, namely Power Factory from DIgSILENT and HAWC2 (Horizontal Axis Wind turbine Code) are considered. These and other similar simulation tools are used intensively by the wind energy industry at the moment to verify grid code compliance and structural loads respectively.

DIgSILENT is a dedicated electrical power system simulation tool used to model the dynamic behaviour of power systems and for assessment of power quality and analysis of wind turbines grid integration. DIgSILENT simulations are performed based on very detailed models for the electrical components of the wind turbine and the grid, but on simplified aerodynamic and mechanical models for the wind turbine. The simulations in DIgSILENT reflect thus the electrical interaction between wind turbines and grid, but they do not provide a detailed insight on the wind turbine structural loads.

HAWC2 is an aeroelastic simulation code, developed at Risø National Laboratory. The core of this code is an advanced model for the flexible structure of the wind turbines, taking the flexibility of the tower, blades and other components of the wind turbines into account. It contains thus detailed models for the aeroelastic and mechanical aspects in a wind turbine, while the models for the electrical components and control of the wind turbine are typically very simplified.

By using these two simulation tools with complimentary abilities in the attempt to put them to work together to the extent that is possible, it is achieved a complete combination of structural dynamics and generator dynamics. As illustrated in Figure 4, DIgSILENT is used to simulate the grid faults and the electrical interaction between the wind turbine and the grid, while HAWC2 is used to simulate and analyse the structural loads of the wind turbine.

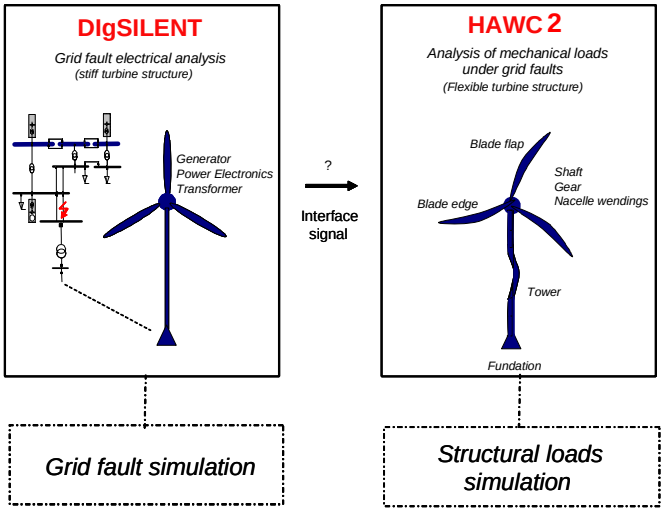

Figure 4. Complimentary simulation tools.

The combination of DIGSILENT and HAWC2 provides new insight into the structural as well as the electrical design and this is very important in order to quantify the loads' impact on the wind turbines' lifetime, during and after grid faults. Once the whole complex model in DIgSILENT and HAWC2 is established, it is possible to investigate sequentially the whole integrated wind turbine design.

The key to access a successful combination of these two complimentary simulation tools is strongly dependent on a proper definition of the interface signal in between them. In a previous stage of the work [5], it has been experienced that for wind turbines with directly connected squirrel-cage induction generators, it is not sufficient to use the electromagnetic generator torque, as interface signal between DIgSILENT and HAWC2, as there does not exist any close loop between the generator toque and the generator speed. It was concluded that in order to asses properly the wind turbine loads caused by grid faults it is necessary to consider the generator damping inside the aeroelastic code.

The attention in this paper is therefore drawn mainly to the approach where the generator dynamic model is directly considered inside HAWC2 environment. The reduced order generator model, implemented in HAWC2, is obtained by neglecting the electric transients of the stator and is written in the state space form only in terms of the rotor fluxes in dq synchronous reference frame [6], [7].

In the simulation scenario presented in this paper, the generator voltage signal simulated in DIgSILENT is used as interface signal, namely as input in the generator model of HAWC2. Such an approach opens the loop between grid voltage and grid current in the connection point. This approach is of course justified only on the condition that the generator currents, simulated in both simulation tools, are identically. This paper presents a set of simulations in order to check this assumption out.

5. SIMULATION SETUP

As a case study, a 2MW active stall wind turbine has been selected. It is equipped with a squirrel-cage induction generator. In order to analyse the wind turbine response during grid faults, the wind turbine benchmark model presented in [8], is used in DIgSILENT as a simplified simulation scenario of a short circuit in a reduced wind power installation. In the first stage of this research is assumed that the wind turbine is not equipped with any advanced fault ride-through controller. Such advanced controller, similar to that described in [9], will be included in the next step of the research.

The selected simulation scenario is illustrated in Figure 5. The wind turbine is connected to a typical-medium voltage (MV) distribution network.

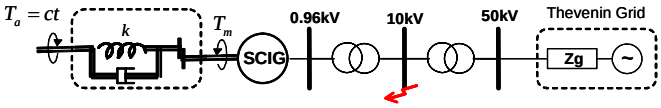

Figure 5. Single line diagram of active stall wind turbine used in DIgSILENT.

The mechanical system is represented in DIgSILENT as a simplified 2 mass-model [8], driven by a constant aerodynamic torque (T_a=ct). The aerodynamic torque is adjusted to give 2MW electrical power from the wind turbine generator and kept thus constant through and after the short circuit. As no advanced fault ride-through is used in this stage of the work, the pitch angle can be assumed constant during the grid fault.

The electric network is represented in Figure 5 by a Thevenin equivalent, consisting of a constant magnitude/frequency voltage source and a serial impedance. The 3 phase short circuit on 10kV busbar, with duration 100ms, is simulated in DIgSILENT using the RMS (electromechanical transient models) simulation feature for longer-term dynamics. Sørensen et. al. [8] confirms that the wind turbine mechanical torque shaft during grid faults is predicted in DIgSILENT in the same way no matter whether a detailed electromagnetic transients models (EMT) or a reduced RMS generator model is used.

In order to assess the maximum wind turbine structural stresses developed during grid faults, the worst scenario is simulated, i.e. wind turbines operates at rated power, minimum fault impedance and fault closest to the wind turbine. It is also assumed that in the case study the wind turbine protections are not taken into account, but they can be of course considered if their settings are well known.

6. SIMULATION RESULTS

Figure 6 shows the generator stator voltage during the grid fault, simulated in DIgSILENT.

This signal is used as input in HAWC2. As expected, the generator voltage drops right after the grid fault and recovers to its initial value when the fault is cleared after 100msec.

The components d- and q- of the generator stator current in the synchronous reference frame are illustrated Figure 7. Notice that the currents components simulated in DIgSILENT are almost identically with those simulated in HAWC2. This justifies the fact that the generator voltage can be used as interface signal between DIgSILENT and HAWC2 in order to asses a simultaneous insight in both

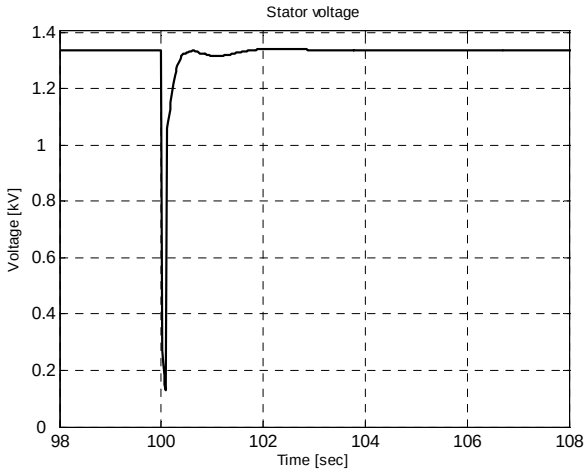

Figure 6. Generator stator voltage simulated DIgSILENT and used as input in HAWC2.

structural and electrical design aspects of the wind turbine during grid faults.

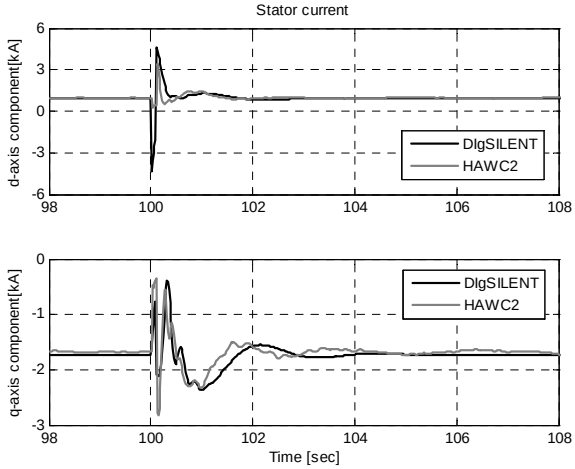

Figure 7. Components of the stator current on the d- and q- axis – simulated DIgSILENT and HAWC2.

Figure 8 illustrates the speed and the torque of the generator simulated in DIgSILENT and HAWC2, respectively.

Both simulation tools predict almost similarly the behaviour of these signals. During grid fault, the speed accelerates as the aerodynamic torque is no longer balanced

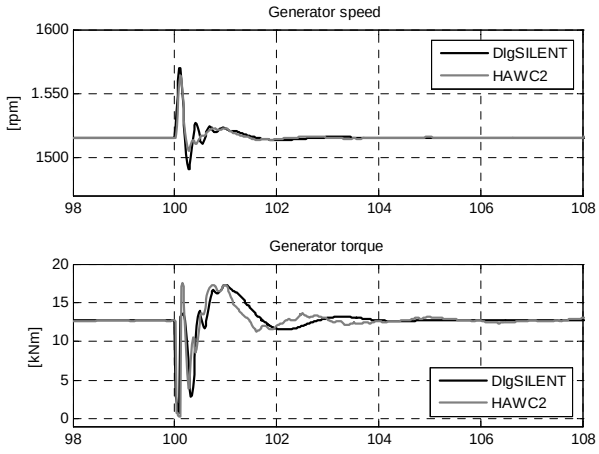

Figure 8. Generator speed and torque in DIgSILENT and HAWC2.

by the electromagnetic torque of the generator. Notice that as expected the grid fault causes also transients in the generator electromagnetic torque.

The behavior of the wind turbine shaft (drive train) torque is illustrated in Figure 9. It is predicted almost similarly by DIgSILENT and HAWC2, during and after the grid fault. Notice however that, there is a small delay between the signals simulated in DIgSILENT and HAWC2. It seems likely that there is a slight difference in the free-free frequency used in DIgSILENT and HAWC2. This frequency depends strongly on the inertias and shaft stiffness used inside wind turbine model.

The tower top torque is also presented in Figure 9. Notice that the grid faults do also affect the tower loads.

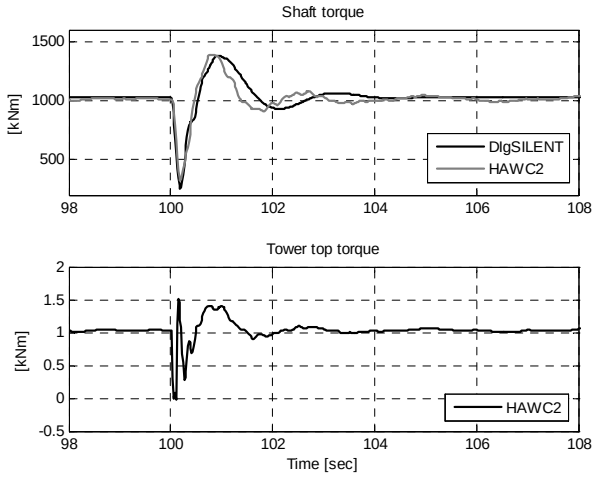

Figure 9. Shaft and tower top torques.

Apparently, the tower frequency is slightly visible in the tower top moment. It is clearly that the tower top torque (i.e. 2nd lateral tower bending mode) is affected by the grid fault. Moreover, as it resembles the electromagnetic torque of the generator simulated in HAWC2 – see Figure 8, the coupling from the generator down to the tower is also underlined.

The blade edgewise loads have also been investigated. They are however not illustrated in this paper, as no significant effect of the grid fault on the blade edgewise loads has been noticed.

7. Conclusions

Emphasis in this paper is on how to access a throughout insight on the grid faults impact on the wind turbine structural loads. The paper suggests a simulation approach between two dedicated simulation tools, which are complimentary, being specialised in two different wind turbine design areas. The goal with such approach is to be able to investigate the whole integrated wind turbine design with focus sequentially on both structural and electrical design aspects.

The strengths of two complimentary simulation tools, i.e. DIgSILENT and HAWC2 are thus combined. DIgSILENT has skills on detailed electrical modelling of the interaction between wind turbine and the electrical grid during grid fault, while HAWC2 has skills on detailed aeroelastic and mechanical loads modelling of wind turbines, respectively. The success of such combination is strongly dependent on the definition of the interface signal in between them.

This paper presents an investigation where the generator voltage signal is used as interface signal between DIgSILENT and HAWC2. The generator voltage is thus simulated first in DIgSILENT and then used as input in HAWC2. In this first stage investigation, it is assumed that the wind turbine is not equipped with any advanced fault ride-through controller, because the idea is to provide a quick insight on the wind turbine loads during grid faults, when the wind turbine has no fault ride-through capability.

As a case study, a 2MW active-stall wind turbine equipped with a squirrel-cage induction generator is considered. The quantitive results of this investigation are not necessarily representative for other wind turbines of the same type, since they depend critically on the drive train torsional characteristics, as well as on the generator parameters. However, as general reflection, it is illustrated that grid faults do affect the wind turbine shaft and tower loads, but not the blade edgewise loads.

The presented approach of using the generator voltage as the interface signal is justified by means of a set of simulations. As the generator current is simulated almost identically in both simulation tools, it means that the interaction between the electrical and the mechanical aspects of the wind turbine can be correctly assessed by using the presented simulation approach. As a preliminary result of this approach, it is illustrated that the grid faults do affect the shaft and the tower loads. In the next step of the work, is will be investigated whether the presence of advanced fault ride-through controller necessary to fulfil the increased grid codes, do have an even stronger impact the wind turbines structural loads.

Acknowledgement

This paper describes the ongoing results of the project titled "Grid fault and design-basis for wind turbines". The Danish Energy Agency is acknowledged for funding this work in contract number PSO-F&U 2006-1-6319. The work is carried out by the Wind Energy Department at Risø National Laboratory in cooperation with Aalborg University.

References

[1] "Wind turbines connected to grids with voltages above 100 kV - Technical regulations for the properties and the control of wind turbines,, Energinet.dk, Transmission System Operator of Denmark for Natural Gas and Electricity, Technical Regulations TF 3.2.5, 2004, 35 p. Available: www.energinet.dk

[2] PSO-F&U 2006-1-6319. "Grid fault and design-basis for wind turbines", Risø National Laboratory project, http:/risoe-staged.risoe.dk .

[3] Iov F, Hansen A.D., Sørensen P., Cutululis N.A. Mapping of grid faults and grid codes, Risø report, Risø-R-1617(EN).

[4] IEC 61400-1 Ed.3: Wind turbine – Part 1: Design requirements, International electrotechnical commission report 88/228/FDIS.

[5] Hansen A.D., Cutululis N., Sørensen P., Florin Iov, Torben J. Larsen, Simulation of a flexible wind turbine response to a grid fault, EWEC 2007, Milano.

[6] Larsen T.J., Hansen M.H., Iov F. Generator dynamics in aeroelastic analysis and simulations, Risø-R-1395(EN), 2003.
[7] Cutululis N. A., Larsen T. J., Sørensen P., Iov F., Hansen A.D., Electrical modelling and control in HAWC2, Risø-R-1587, 2007.
[8] Sørensen P., Hansen A.D., Christensen P., Meritz M., Bech J., Bak.Jensen B., Nielsen H. Simulation and verification of transient events in large wind power installations, Risø-R-1331(EN), Okt. 2003.
[9] Hansen, A.D.; Sørensen, P.; Iov,F.; Blaabjerg, F., Grid support of a wind farm with active stall wind turbines and AC grid connection. Wind Energy 2006, vol. 6, pp 341-359.

Network Topology Considerations When Connecting a Wind Farm into Distribution Network

Sami Repo*), Jussi Antikainen, Pekka Verho, Pertti Järventausta
Tampere University of Technology, P.O. Box 692, FI-33101 Tampere, Finland
*) e-mail sami.repo@tut.fi

Abstract —The paper will present introduction of distribution network topology options and their benefits and disadvantages. These options are then evaluated based on reliability and stochastic load-flow calculations of real-life example. The strengthening of network by network topology options (investments on primary network) is compared to active network management options (investments on secondary devices) like local voltage control and production curtailment. The benefits of active network management are calculated with a software prototype developed by research group. The paper will also include short descriptions of calculation tools used.

Index Terms — Active network management, distribution network reliability, network topology, wind farm

1. INTRODUCTION

The paper will consider distribution network (20 kV) topology options and issues influencing on those in case of connecting a wind farm (< 10 MW) into distribution network. This paper will not consider network topology options inside the wind farm. The term network topology contains both the network configuration and the switching arrangements of distribution network.

The wind farm will very probably be the most important customer for the rural distribution network company in the service area. The connection of wind farm is typically arranged based on so called worst case planning principle. This principle ensures full network capability all the time. Although the normal connection to wind farm is strong enough to handle all possible load and production situations, there exists situations when wind farm must be shut down due to network related reasons. The backup connections for outage situations at rural distribution network are typically weak.

Distribution network reliability improvement has become a very important topic due to customer's dependency on reliable power supply. The improvement of distribution networks have almost without exception handled by investing on primary equipments. However the management of distribution network could also be improved by controlling loads and production units. The control of reactive power and power production is profitable for a wind farm when alternative solution is a long interruption. The controllability of production unit is needed for active network management. The active network management assures that network technical constraints are not exceeded in changing network conditions. It is believed that active network management might provide overall cost advantages compared to traditional network development options [1].

The aim of this paper is to study relations between distribution network reliability and active network management when the network includes a wind farm. The issues of wind farm connection into distribution network are considered in general level in chapter two. The discussion focuses on network dimensioning, reliability and network operation. The aim of this chapter is to clarify how network topology and wind farm connection are related. The third chapter describes the options of distribution network topology. The chapter four introduces the evaluation tools used at example calculations at chapter five.

2. ISSUES OF WIND FARM CONNECTION INTO DISTRIBUTION NETWORK

2.1. Network dimensioning

The technical limitations of existing network when a wind farm is connected into distribution network are typically the thermal capacity of cables, the over-voltage problem at lightly loaded networks and the exceeding of fault current capacity of components. Typically the overhead medium voltage (MV) lines of rural distribution network require strengthening due to over-voltage problem when a wind farm is connected far from primary substation. Rotating machines will increase the fault current level at distribution network and this might cause exceeding of fault current capacity of components. This is more typical for urban networks than for rural networks, thereby not so important issues in case of a wind farm connection.

The connection of wind farm into existing distribution network does not necessarily exceed the technical limitations of network, but when it does, the costs of network strengthening might be very high due to replacement of existing components. Therefore it is very important to look for alternative options for network planning and operation principles, network topology and so. It should however keep in mind that every process (planning, operation, billing, etc.) and sub-processes (e.g. wind farm connection) of distribution network business must be standardized in order to work efficiently. In the end this means that tailored wind farm connections are more costly for a network company, and in the end for the customers of network company, than standardized connections.

The distribution network dimensioning is based on so called "fit and forget", "worst case planning principle" or "passive network" planning principle. These terms describe the same network planning principle which designs the capability of network for all statistically relevant loading conditions. The worst planning case for a wind farm is typically "minimum loading – maximum production" loading situation. The distribution network will be then fully capable to supply all loads and to absorb all power produced during normal network conditions. The traditional network planning will bring investments on hardware like wires, substations, etc. in order to support its duty.

The investments of electrical networks are always done beforehand. The network should also include some margin between current maximum loading condition and the technical capability of network due to safety reasons, but also due to stepwise investments in network development. The development of network (re-enforcement of existing network and construction of new network) is based on forecasted scenarios of the growth of load demand and power production. When the size of a new customer compared to other customers increases, the location of that customer will have a great influence on the development of network and the long-term forecasting of location of a large customer becomes very difficult. These issues must be kept in mind when the connection of wind farm is discussed.

The capability of network is dependent on feeder and customer (consumption and production) characteristics. The network capability may be characterised by the amount of maximum power flow to each customer. If the network includes only consumption customers, the capability of network is limited by voltage drop or thermal capacity. When the network includes also remarkable amount of production, the over-voltage may become a limiting factor at the production unit interconnection point. In weak distribution networks over-voltage problems are likely to occur during low demand periods when there is a large amount of distributed generation (DG) interconnected on a MV network [2].

There are some technical solutions like reinforcement of MV network to solve the voltage rise problem. However the utilisation of network may be poor especially in case of wind power due to low capacity factor of wind power production. In order to improve the utilisation of network, the planning and the operation of network should be developed to be able to consider the stochastic nature of power production. The structure and operating principle of the distribution network will move towards an active distribution network with several active components along the network. The active management of distribution network requires control of DG unit power factor or voltage, production curtailment or combination of these to avoid occasional network constraints [3-5]. Another form of controllability is load control which has traditionally applied in demand side management for example at peak shifting.

The active network management may benefit both the network and the production companies by allowing higher penetration of DG with less network investments. The control of DG unit is beneficial, if voltage rise problem appears occasionally, e.g. during light loading and high production. The probability of this kind of network condition is rare and may be evaluated based on e.g. load curves and wind statistics or measurements.

2.2. Reliability

The reliability of radial distribution network consists of the number, the duration and the spread of outages. The reliability of certain connection point is dependent on relative location of connection point and outage locations. Network topology has also a big influence on the reliability of connection point by alternative connection routes to customers. The network reliability is determined in the network planning phase and typical choices / selections are e.g.: [6]

1. choice of line type (bare overhead conductor, coved overhead conductor or cable) and line route (field, beside a road, forest) which will affect on the number of faults
2. use of protection devices like surge arresters and animal shields or earth fault compensation to reduce the need of automatic reclosing actions
3. network automation (substation automation, medium voltage feeder automation, fault location, fault restoration) and parallel network connections (double line, backup connections from neighbouring feeder or substation, ring network structure which is operated in radial way, or meshed network) are used to reduce the outage duration
4. choice of substation siting, number of feeders and other protection zone reduction methods like satellite switching stations and reclosers are used to reduce the spread of outages

The risk of unreliability of power supply is a product of unreliability and consequences of unreliability. In order to evaluate necessary investments there are needed a clear and transparent way of assess consequences of unreliability and proper analysis of all aspects of network reliability. The consequence of unreliability of network for a wind power producer is the loss of power production which is dependent on wind conditions and profit of power otherwise produced during network outages. The availability of wind power units is not very high compared to base load units and that is why the availability of wind power units should be taken into account in network reliability analysis. However there might be strong correlation (but unknown at least for authors) between wind power production and network outages.

2.3. Network operation

The topology of distribution network affects on possible choices of network operation especially during disturbances. The protection and automation of wind farm should be such that normal fault location and power supply restoration procedures like trial switching and utilisation of backup connections should be possible.

Trial switching is used to locate a permanent fault by opening a disconnector along the feeder and closing feeder breaker again in order to see if fault is located behind the opened disconnector. In such procedure there may appear many fault situations which may be harmful for wind turbines. Wind turbines will also produce fault current which will mislead computational fault location algorithms. It is better to disconnect the wind farm from the network for the period of trial switching. The best way to do this is to lock wind farm connection switch to open position by remote control of a network company. This means that the network company should have a right to shut down the wind farm and keep it disconnected during the disturbance clearance.

When the location of permanent fault has been found will the process of power supply restoration start. The area of non-supply will be minimised by opening disconnectors closest to fault. The restoration of power supply to customers "behind" the fault requires utilisation of backup connection (closing of normally open disconnector). This would be fine if the backup connection is at least equally strong (electrically) as the normal connection. Unfortunately this is seldom the case in rural distribution networks. When the wind farm locates "behind" the fault, there is typically limited capability to adopt wind power production to the network due to voltage rise or thermal capability problems.

Otherwise the normal and the backup connections should be dimensioned to the same ratings, which is not economically feasible. The wind farm disconnection and locking of disconnector to open position via remote control of network company is also a possible solution for this challenge.

Network capability problems may however be handled by much more sophisticated method. The controller of wind farm or alternatively the voltage relays of wind farm connection point may react to voltage rise problem by reducing the power production of wind farm in order to keep voltage below the acceptable limit [5]. The thermal capability problem is more complex because that cannot be detected directly from wind farm connection point measurements. A straightforward solution for this challenge is to determine the worst case network transfer capability limit in all possible or probable backup connection situations. This limit is then set to wind farm controller and it is applied when backup connection is in use. The remote control of distribution network must send a message to wind farm when backup connection is utilised. The wind power curtailment is acceptable because the network is in abnormal state at these situations and the curtailed power allows continuation of power production at least partly.

3. DISTRIBUTION NETWORK TOPOLOGY OPTIONS

The network topology of distribution network is typically a ring which is operated in radial way. In that case the design of network topology is basically the design of backup connections from neighbouring feeders or substations and the selection of open disconnectors. The probe design would also include consideration of network disturbances i.e. fault management and reliability issues. Other less used possibilities of network topology are ring operation of feeders and intended island operation.

3.1. Radial network topology options

The connection of wind farm into radial distribution network has several options which are

a) connection to existing network with short line (if network is strong enough),
b) connection to existing network and replacement of open disconnector,
c) connection with parallel circuit on existing poles or on extended corridor to strong and reliable enough network node,
d) splitting of production units into two existing feeders (open disconnector at wind farm busbar) and
e) connection directly to substation with dedicated connection feeder.

3.2. Topology options of existing network

The most obvious way of connecting wind farm into distribution network is a direct connection of wind farm with transformer and short line into existing medium voltage line. Feeder 3 in Figure 1 is an example of this kind of arrangement. At the same time other feeders are not connected into wind farm. This is a typical arrangement when the size of wind farm is small and there are not network strengthening requirements. This arrangement does not affect remarkably into reliability of distribution network (only slight worsening due to additional serial components in the network).

Reliability of distribution network at wind farm connection point is dependent on the location of connection point in the existing network. In principle the reliability of distribution network becomes worsen when the location of connection point gets further away from the substation in the radial network. The reliability of distribution network at wind farm connection point may be improved with network related arrangements discussed in chapter two.

The next topology option is a similar kind than previous one, but the location of open disconnector is reconsidered due to wind farm connection. From the network dimensioning point of view, the feeder including wind farm should have as much load as possible. This arrangement gives higher transfer capability for the feeder because the over voltage problem is not that severe. From the reliability, power quality and feeder protection point of views, the situation is opposite i.e. the feeder including wind farm should be as short as possible. In that case the reliability of wind farm connection point is not disturbed by long tail of feeder, the disturbances (fast changes in voltage level, harmonics, flicker, etc.) of wind farm will not affect on rest of the customers and feeder protection settings are easier to handle.

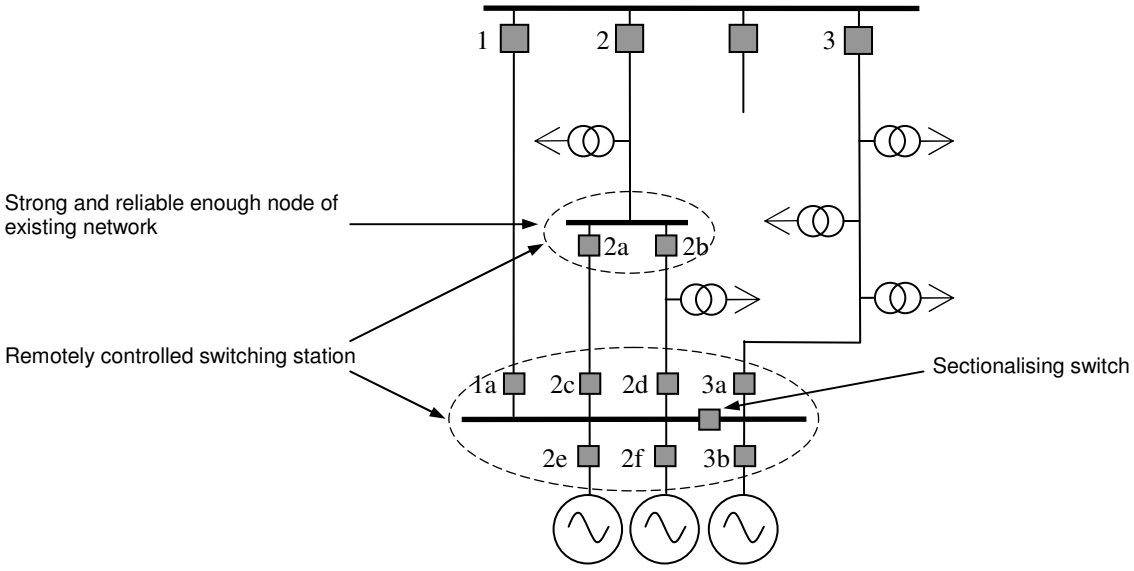

Figure 1. Possible network topologies.

3.3. Network re-enforcement options

The topology of distribution network influences on network strengthening requirements when a wind farm is connected into network. In rural distribution networks the voltage rise is typically the limiting factor for the size of wind farm at existing network. Parallel circuits and splitting of production units into two existing feeders are examples of network strengthening options to increase the capacity of network and the reliability of network at wind farm connection point when appropriate switching arrangement is provided.

Feeder 2 is an example of parallel circuits in Figure 1. Remotely controlled switches 2a and 2b along the feeder and 2c-2f and 3b at the wind farm connection point are utilised to remove permanent faults between circuits 2a-2c or 2b-2d and to disconnect some of wind turbines in order to reduce power production below the network capability limit. Switch 3a must be open in this case and it may provide a backup connection to wind farm.

The splitting of wind turbines into two feeders requires a sectionalising switch at wind farm connection point busbar. The sectionalising switch is normally open in order to distribute power production to the feeders according to their capabilities. This arrangement utilise the backup connection of previous example continuously. A dedicated cable connection directly to substation from wind farm connection point may be a reliable solution but also very expensive when distance to substation is remarkable.

4. CALCULATION TOOLS

4.1. Reliability based network analysis

The used calculation tool for reliability analysis was DIgSILENT PowerFactory (DSPF). DSPF is a computer aided engineering tool for the analysis of electrical power systems. In this study, DSPF is used to explore effects of different network topology options in a case of connection a new wind farm into distribution network. These options are discussed in chapter three. Reliability analysis is based on connectivity analysis. So, the power flow issues are not considered with DSPF.

The network of the example is modelled to a DSPF database (see chapter five). Used conductor types and constructions are fed to the database with their own reliability parameters. Parameters are presented in Table 1. This makes possible to calculate reliability indices at the wind farm connection point and also to the whole system.

In reliability analysis the wind turbines are modelled with two constant load units. The units have different capacities in simulations. The capacities are 2 MW and 4 MW with lagging power factor 0.92 or apparent power 0 VA to the turbines. This makes possible to calculate manually the amount of annual energy not supplied (ENS). Setting the turbines apparent power to zero does not have influence to reliability indices.

Table 1. Reliability calculation parameters for lines.

Line type	Permanent faults [per 100 km,a]	Repair time [h / fault]
Overhead line	6.0	3.0
Covered conductor line	2.3	3.0
Sea cable	0.2	100.0
Cable	0.5	4.0

4.2. Active network management

The statistical network planning method proposed in [5] takes into account the stochastic nature of load demand, power production and correlation between these. The planning of MV network and DG unit interconnection are not based on a single worst case but series of possible network conditions. When the output power of DG unit is dependent on weather conditions of a site and the probability of maximum output power of DG unit is low enough during a minimum loading condition of network, there is an opportunity to enhance network operation by controllability of DG unit. The idea is based on facts that the minimum loading of network occurs at summer nights (at least in Finland) and the mean value of wind turbine output is less at summertime than at wintertime. The "minimum loading – maximum production" planning condition is very conservative in that sense and some advantage may be achieved when the active network management is applied. The calculation method behind this method is described in [3-5] in detail.

The proposed method is based on stochastic load-flow computation. The hourly load-flows are calculated for a study period i.e. for 8760 hours. The stochastic part of calculations is based on statistical load and production curves which are time series for each customer type. Load and production curves have mean value and standard deviation. The Association of Finnish Electricity Utilities has published load curve models for 46 different customer groups. The expansion of hourly energy meters together with automatic meter reading will provide huge amount of data for load modelling purposes. Due to a lack of actual measurements and heavy dependence between power production and the location of wind turbine, the production curve is based on long-term statistics of wind speed.

The application of both the load and the production curves at load flow calculation makes it possible to simulate the hourly functioning of the distribution system including wind turbines. The planning of the distribution network is not restricted to certain fictive planning conditions, but a series of hourly conditions is considered. The load-flow simulations are used to analyse what kind of network conditions might exist. The correlation of power production and load demand is a very critical issue in network planning.

The active network management based on local voltage control of wind turbines is applied in the calculation tool. The voltage of wind turbine connection point may vary between 95-105 % of rated voltage. Between these limits wind turbines are operated at unity power factor. When a voltage limit is reached the control mode of wind turbine will be changed to constant voltage mode. The voltage setting is the value of voltage limit. The operation of constant voltage control mode may be continued until the reactive power limit of wind turbine is reached. If the voltage of connection point exceeds the voltage limit and the wind turbine operates at reactive power limit, the active power of wind turbine must be reduced i.e. wind power production must be curtailed.

A backup system for the local voltage control is realised by relay protection at wind turbine connection point. A voltage relay is typically installed to connection point in order to avoid intentional islanding of wind turbines. The settings of voltage relay must be co-ordinated with voltage control settings in order to avoid unnecessary interruptions.

The instantaneous over-voltage pickup limit (e.g. 110 %) must be above the over-voltage limit of local controller but less than damage limit of electrical devices. The delay of instantaneous operation must be very short or without delay due to safety reasons. The delayed over-voltage pickup limit (e.g. 106 %) must be between the over-voltage limit of local controller and the instantaneous over-voltage pickup limit. However the delay may be long (e.g. 60 s) without sacrificing the safety of network and there will also be time for operation of local voltage controller and slowly reacting voltage control equipments like on-load tap changers at primary substation. The instantaneous under-voltage setting is avoided because this will worsen the effect of voltage dips. The delayed under-voltage pickup limit (e.g. 90 %) is set below the under-voltage limit of local controller and the delay is determined by wind turbine's continuous under-voltage loading capability and characteristics of voltage control devices.

5. EXAMPLE

Example calculations are presented with a real-life distribution network from south-west Finland. The MV network examined consists of primary substation feeding two MV feeders. The wind turbines are connected 22 km away from the substation. The MV network has already over-voltage problems during low load demand periods due to about 70 km long sea cable. Examples include three 2 MW full converter variable-speed wind turbines. The power factor of wind turbines may be controlled between 0.92 and 1 leading or lagging at rated power.

The topology of MV network has been studied at 10 different cases. The topology options of example calculations are described in Table 2. Table 3 describes switching arrangements in normal and in backup connections. Figure 2 presents the outline of example network, topology options and switching arrangements.

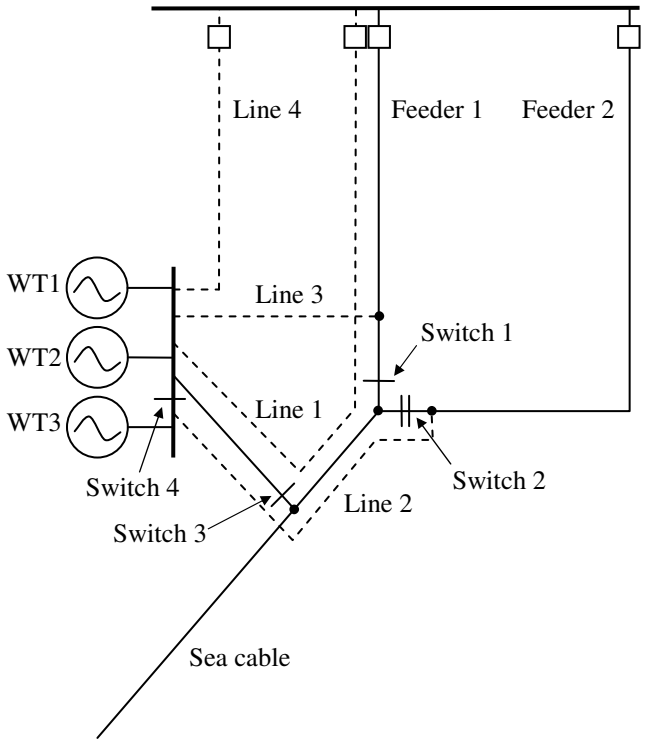

Figure 2. Example network.

Table 2. Topology options.

Cases	Description	Use of backup
Case 0.1 Case 0.2	Existing network	No Yes
Case 1.1 Case 1.2	Reinforcement of feeder 1 by duplicating feeder 1 from wind turbine connection point to primary substation	No Yes
Case 2.1 Case 2.2	Constructing a new connection of feeder 2 to wind turbine connection point. Two wind turbines are connected to feeder 1 and one wind turbine is connected to feeder 2.	No Yes
Case 3.1 Case 3.2	Reinforcement of feeder 1 by shortcut cable connection. Long sea cable at feeder 2.	No Yes
Case 4.1 Case 4.2	Dedicated cable feeder for wind turbines. Voltage limit of connection point is 107,5 %.	No Yes

Table 3. Switching arrangements at normal operation and at backup connection when it is allowed.

Cases	Normal operation	Backup connection
Case 0	Switch 2 is opened to separate feeder 1 and 2.	Switch 1 is opened to separate fault at the beginning of feeder 1. Swich 2 is closed to connect wind turbines to feeder 2.
Case 1	Line 1 is parallel with feeder 1.	If fault is at line 1, line 1 will be separated and wind turbines will be connected to feeder 1.
Case 2	Switch 4 is opened. Line 2 is used to connect wind turbine 3 to feeder 2.	If fault is at feeder 1 between substation and wind farm, fault will be separated and switch 4 is closed to connect wind turbines to feeder 2. If fault is at feeder 2 or at line 2, fault will be separated and switch 4 is closed to connect wind turbine to feeder 1.
Case 3	Switch 2 is closed and switches 1 and 3 opened. Line 3 is used to connect wind turbines to feeder 1.	If fault is at feeder 1 between substation and line 3 terminal or at line 3, fault will be separated and switch 3 is closed to connect wind turbines to feeder 2. If fault is at feeder 1 between switch 1 and line 3 terminal, fault will be separated and power supply continues via line 3 and feeder 1.
Case 4	Wind turbines are connected directly to primary substation via line 4.	If fault is at line 4, line 4 will be separated and switch 3 is closed to connect wind turbines to feeder 1.

5.1. Reliability analysis

Reliability analysis consists of five different cases. In the each case, the possibility of using backup connection to alternative power supply route is considered. The results are presented at Table 4. The results of reliability analysis are strongly dependent on the used reliability parameters. One of hardest parameter to estimate is the repair time of the sea cable. This will vary a lot depending on the time and the season when outage occurs. For example, in spring or in autumn, the repair time of a sea cable can be one to two months. Freezing or de-freezing of the sea and the movement of ice makes the sea cable repairing difficult or even impossible.

Variation of reliability indices SAIFI (system average interruption frequency index) and SAIDI (system average interruption duration index) are not very significant in the different cases. Naturally, system failure frequency will be increased if the length of the network grows. Because of constructing a new connection in the cases 2 and 3, SAIFI of the examined system increased slightly, when compared to SAIFI in the case 0. SAIDI grows in the cases 2.1 and in the case 3. This is consequence of the increased cabling: the repair time of a cable is more than the repair time of an overhead line or a covered conductor line. Decrease of SAIDI relates to possibilities of supplying power via a new backup connection. In that case, reliability indices of the system do not reveal a strong signal about the best solution to connect the wind farm. Variations of reliability indices are presented in Table 4.

From the wind farm point of view, indices at the connection point have more importance than indices of the system. In this study, average interruption time (AIT), average interruption frequency (AIF) and average interruption duration (AID) have been calculated to the wind turbine connection points. Energy not supplied (ENS) from wind turbines has been calculated too. The volumes of annual ENS are presented in Figure 3.

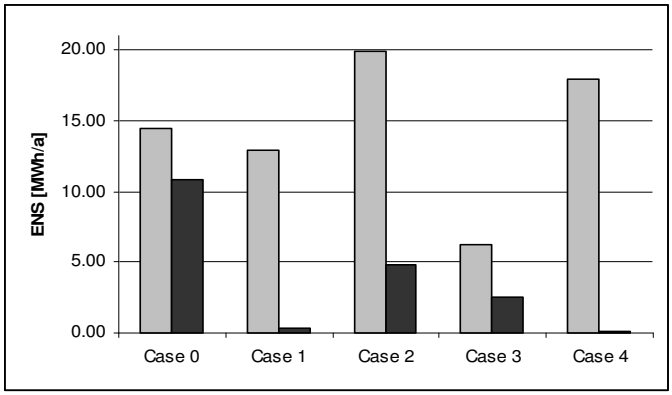

Figure 3. Energy not supplied. Gray bars are without backup and black bars are with backup connection.

In the case 0.1, ENS is 14.4 MWh/a without possibility of use of a backup connection. The backup connection diminishes the volume of ENS by about 25 %. In the case 1.1 without the backup, ENS is a little bit less than in the case 0.1. The difference can be explained by reinforcement of the feeder 1 which reduces AIT and AIF at the wind farm connection point. At the same time AID increases at the connection point. The average fault repair time at the reinforcement of the feeder 1 is 3.68 hours so the value of AID at the connection point has to be true. In the case 0.1, AID at the connection point depends on the construction of the whole feeder 1.

The role of the backup connection in the case 1.2 is now remarkable, compared to the case 0.2. ENS decreases by 97 %. It is important to note that the reinforcement has the same line route than the existing feeder 1. So, there can be correlation between outages at the feeder 1 and outages at the reinforcement. Besides, we do not consider independent second failures in this study. This means that the feeder 1 is always available when an outage occurs at the reinforcement and vice versa. These factors could distort the simulation results, but should be taken into account in practice.

In the case 2.1, ENS attained the highest value. The turbine 3 is now separated from turbines 1 and 2 and it is connected to the feeder 2 via a new connection. The length of the feeder 2 is more than the feeder 1. The turbines 1 and 2 do not suffer more outages than in the case 0.1 but the turbine 3 does. This increases AIF and AIT at the connection point of the turbine 3. The backup connection decreases AIT and AID so the volume of ENS diminishes greatly. Anyway, ENS in

Table 4. The results of reliability analysis.

	Case 0.1	Case 0.2	Case 1.1	Case 1.2	Case 2.1	Case 2.2	Case 3.1	Case 3.2	Case 4.1	Case 4.2
System										
SAIFI [1/a]	1.40	1.40	1.40	1.40	1.60	1.60	1.80	1.80	1.40	1.40
SAIDI [min/a]	3.68	3.68	3.68	3.52	3.88	3.61	3.70	3.70	3.66	3.50
ENS [MWh/a]	14.43	10.86	12.94	0.35	19.88	4.79	6.22	2.50	17.97	0.10
Turbine 1,2										
AIT [min/a]	2.41	1.81	2.16	0.06	2.41	0.58	1.04	0.42	3.00	0.00
AIF [1/a]	1.03	1.03	0.59	0.59	1.03	1.03	0.48	0.48	0.03	0.03
AID [h]	2.34	1.76	3.67	0.10	2.34	0.57	2.15	0.86	99.84	0.02
Turbine 3										
AIT [min/a]	2.41	1.81	2.16	0.06	5.13	1.23	1.04	0.42	3.00	0.00
AIF [1/a]	1.03	1.03	0.59	0.59	2.05	2.05	0.48	0.48	0.03	0.03
AID [h]	2.34	1.76	3.67	0.10	2.51	0.6	2.15	0.86	99.84	0.02

the case 2.2 is more than ENS in the case 1.2.

A shortcut sea cable in the case 3 reduces the distance between the supply system and the turbines. The shortcut cable shortens the connection of the turbines by 4.9 km, which is about 24 % of the length of the connection in the case 0. Besides, 4.7 km of this line, which is phased out, is overhead line. Therefore, the shortcut cable has very advantageous influence to the reliability at the wind farm connection point. The results show that ENS without or with the possibility of backup connections reached the lowest level compared to previous cases.

In the case 4.1 the calculated volume of ENS is quite same than in the case 2.1. At the turbines connection point, AIF reduced strongly but AIT and AID grown largely. ENS and also AID in that case are very speculative. That is because they are very sensitive to the used repair time for an outage at the sea cable. For roughly example, the magnitude of this repair time can vary between 10 hours and 1000 hours. So, based on these repair times ENS can vary between 1.8 MWh/a to 180.0 MWh/a. In this study, the used time was 100 h. If the backup connection is available to use in the case 4.2, ENS and reliability indices at the wind turbine connection point are the smallest.

The simulation results show that the backup connection is significant from the wind farm point of view. The significance of backup connection grows when the solution to connect the wind farm to the network is executed by a sea cable. Long repair time for the sea cable adds the risk of ENS. Along with ENS, AIF is important to notice in the comparison of the wind farm connection chances too. The great number of outages could harm the equipments of the wind farm. According to the results, the least values of ENS and AIF are in the cases 3 and 4. From the reliability point of view, the case 3 or 4 could be the best solution to connect the wind farm in this example.

5.2. Network capability calculations

The capability of network has been evaluated by stochastic load-flow method. The acceptability of network conditions has been decided based on voltage level of network. The maximum voltage has been 105 % i.e. 21 kV at MV network. If the voltage of wind turbine connection point (the highest voltage when wind turbines are in operation) exceeds the maximum voltage limit then controllability of wind turbines has been utilized. In the first case only the production curtailment is utilized in order to see the benefit of reactive power control utilized in second case. Finally the network conditions are always acceptable and the amount of production curtailment describes feasibility of network topology cases from technical constraints point of view.

The results of the first case are at Table 5. The amount of production curtailment is high in all cases. The differences between cases are due to differences in electrical distance from wind farm connection point to primary substation. Cases 1 to 4 are basically alternative ways to shorten the electrical distance between wind farm and primary substation when considered from load-flow point of view. The duration of production curtailment presents also how often over-voltages would appear due to wind power production if nothing is done.

The results of network capability calculations based on active network management have been presented at Table 6. Cases 1, 3 and 4 are the most interesting ones because the amount of production curtailment is zero. The existing network (case 0) is obviously the worst case. The network capability of case 0 with the worst case planning principle is only 2,25 MW. Similarly case 2 gets poor results because the network capability of feeder 2 is only 1,2 MW. Although the worst case network capability of cases 0 and 2 are higher than the average wind power production of wind turbines connected to these cases and the network capability increases when feeder loading increases, there still exists some hours when production curtailment is necessary.

The active network management has been realized as a local voltage control in this case. The reactive power control reacts to over-voltage and that is why it has a major role in this case. The benefit of reactive power control is clear when Tables 5 and 6 are compared. The controllability of reactive power avoids production curtailment in all situations at cases 1, 3 and 4 and reduces it remarkably in cases 0 and 2.

Table 5. Network capability without active network management.

	Case0	Case1	Case2	Case3	Case4
Production curtailment [%]	38,7	17,9	23,4	16,1	8,0
Duration of curtailment [h]	2780	1417	1872	1295	811

Table 6. Network capability based on active network management.

	Case0	Case1	Case2	Case3	Case4
Production curtailment [%]	2,4	0	0,0035	0	0
Duration of curtailment [h]	567	0	6	0	0
Control of reactive power [MVArh]	-3848	-1419	-2227	-1125	-1015
Duration of reactive power control [h]	2780	1417	1872	1295	811

5.3. Discussion of calculation results

Case 0 is not feasible network topology due to low network capability. The active network management does not reduce the amount of production curtailment enough in order to improve the situation. Either the reliability of this network topology is not good enough compared to other alternatives. This option would have been the cheapest one for everyone, if the output power of constructed wind farm would be smaller.

Case 1 is an expensive option although the network capability and the reliability characteristics are excellent when active network management and backup connection are utilized. This option provides a natural backup connection which is also very strong one from network capability point of view. One of the advantages of case 1 is also utilization of existing line route at network re-enforcement which would shorten the construction time by avoiding environmental impact assessment and by avoiding complaints hearing due to new line route.

Case 2 has a small risk of production curtailment with active network management. The amount of production curtailment would be higher when yearly wind conditions are higher than the average. Investment costs would however be about half of the costs of case 1. The reliability of case 2 is however worse than that of case 1.

Case 3 has many advantageous characteristics. The active network management together with line 3 investment would provide enough network capability to avoid production curtailment. Investment cost would be less than that of case 1 or case 4. The reliability of case 3 is good enough i.e. ENS is low even without backup connection. The drawback of this option is a remarkable increment of network losses due to increased transfer of reactive power. Case 3.1 have been decided to implement. This means that wind turbines must be disconnected during a backup connection via feeder 2.

Case 4 is not possible to consider at all due to very high cost. In this example high investment cost did not bring benefits which could not achieved by other less expensive options. Case 4 would be the best option if reactive power controllability of wind turbines would not be available. Other advantages of dedicated feeder for wind turbines would be straightforward operation of network and limitation of propagation of possible power quality problems.

ACKNOWLEDGEMENT

The authors are grateful to the partners of the Densy (Distributed Energy Systems R&D-program of Tekes) projects "Electricity distribution and distributed generation" and "Active network management in electricity distribution" for the interesting real life research topic, comments, funding and research co-operation.

6. REFERENCES

[1] Pudjianto, D., et al., Method for monetarisation of cost and benefits of DG options, Report D7 of project DG-GRID, 2006, On-line: www.dg-grid.org

[2] Masters, C.L., Voltage rise the big issue when connecting embedded generation to long 11 kV overhead lines, Power Engineering Journal, February 2002, pp 5-12.

[3] Repo, S. et al., Estimation of variable costs of electricity distribution company due to distributed generation, Proceedings of Probabilistic methods applied to power systems, 2006.

[4] Repo, S., Flexible Interconnection of Wind Power to Distribution Network, Proceedings of Nordic wind power conference, 2006.

[5] Repo, S., et al., Statistical short-team network planning of distribution system and distributed generation, Proceedings of Power system computation conference, 2005.

[6] Verho, P. et al., Applying reliability analysis in evaluation of life-cycle costs of alternative network solutions, European transactions on electrical power, 16, 2006.

Loss Allocation in a Distribution System with Distributed Generation Units

Torsten Lund[1*)], Arne Hejde Nielsen[2)], Poul Sørensen [3)]
[1)] Energinet.dk
[2)] Ørsted·DTU
[3)] Risø, DTU
[*)] phone +45 7622 4544, e-mail tld@energinet.dk

Abstract — **In Denmark, a large part of the electricity is produced by wind turbines and combined heat and power plants (CHPs). Most of them are connected to the network through distribution systems. This paper presents a new algorithm for allocation of the losses in a distribution system with distributed generation. The algorithm is based on a reduced impedance matrix of the network and current injections from loads and production units. With the algorithm, the effect of the covariance between production and consumption can be evaluated. To verify the theoretical results, a model of the distribution system in Brønderslev in Northern Jutland, including measurement data, has been studied.**

Index Terms — Distributed generation, wind power, loss allocation

1. Introduction

Since the mid eighties, a large number of wind turbines and distributed combined heat and power plants have been connected to the Danish power system. Especially in the Western part, comprising Jutland and Funen, the penetration is high compared to the load demand. In some periods the wind power alone can even cover the entire load demand.

Traditionally, the distributed generation (DG) units have to some extend been regarded as passive negative loads with the main purpose of producing energy and not disturbing the operation of the distribution systems.

Since the mid nineties, the Danish electrical power system, like most European power systems, has been going through a liberalization process, where services such as production, transmission, distribution, power balancing, ancillary services etc. are being unbundled. When evaluating the economy of DG, more aspects than the annual energy production must be taken into account. Dependent on the coincidence with the load demand and the location, the DG units can for example help reducing the power system losses in cases where they supply local consumers and work as peak shaving in high load periods.

The installation of DG in a distribution system affects the total system losses. In systems where the penetration of DG is low, the DG units are located close to load centers and there is a large coincidence between load and production, the DG units can contribute to reduction of the total system losses. On the other hand, if the power from the DG units connected to the MV or LV network has to be exported to the transmission system, because the local production exceeds the local demand, the total system losses will be higher than if the power were produced at a large power plant connected directly to the transmission system.

2. Loss allocation

Different loss allocation methods have been developed to quantify the influence of different participants on the total system losses. In a liberalized market, this knowledge can be used to avoid cross subsidizing in the transmission and distribution fees of consumers and producers [1], to generate incentives of the participants to change the consumption or production in periods with congestion [2;3] or to estimate the value of distributed generation in an area [4]. In systems where the investments and operation are partially or fully centrally controlled, the allocation of losses can be used to optimize the operation and investments and to minimize the losses. One of the problems about separating the cause of losses is their non linear nature.

In literature, the following main approaches of loss allocation based on deterministic methods are found [1;5-7]: Pro Rata procedures where the losses are allocated to producers and consumers proportionally to the delivered or consumed energy, Marginal Loss Allocation procedures where the losses are allocated according to the change in losses corresponding to a small change in production or consumption and Proportional Sharing procedures, also referred to as Tracing [6], where the losses are allocated according to the total power flows in the system generated by the participants. Further, the Z-Bus allocation method has been proposed in [8] where the losses are allocated based on the current flows in the system rather than the power flows.

2.1. Allocation based on current injections

A new method for loss allocation based on current injections rather than bus voltages or power flows is proposed here. The difference between this method and the method presented in [8] is that here, a single slack bus is assumed. This is considered reasonable in distribution systems which typically only has one infeed from the transmission system.

2.1.1. Mathematical formulation

The theory is based on the standard system impedance matrix as described for example in [9]. For the investigations, the network busses have been divided into three types: Fixed voltage busses, fixed current busses, and busses without sources. The relation between the voltage and the current in the fixed voltage and fixed current busses can be expressed with the full impedance matrix in (1). The rows and columns corresponding to busses without sources have been removed from the matrix.

$$\begin{bmatrix} \underline{\mathbf{V}}_V \\ \hline \underline{\mathbf{V}}_I \end{bmatrix} = \left[\begin{array}{c|c} \underline{\mathbf{Z}}_{11} & \underline{\mathbf{Z}}_{12} \\ \hline \underline{\mathbf{Z}}_{21} & \underline{\mathbf{Z}}_{22} \end{array}\right] \cdot \begin{bmatrix} \underline{\mathbf{I}}_V \\ \hline \underline{\mathbf{I}}_I \end{bmatrix} \tag{1}$$

The voltage at the busses with fixed current injections can be expressed as (2) where $\underline{\mathbf{Z}}_I$, defined in (3), is a reduced impedance matrix for the busses with fixed current injection

when the busses with fixed voltage have been short circuited. $\underline{\mathbf{K}_{21}}$, defined in (4), represents the relation between the voltage at the busses with fixed current infeed and the busses with fixed voltage. Analogously, the current injections at the constant voltage busses can be calculated using (5).

$$\overline{\mathbf{V}_\mathbf{I}} = \underline{\mathbf{Z}_\mathbf{I}} \cdot \overline{\mathbf{I}_\mathbf{I}} + \underline{\mathbf{K}_{21}}\,\overline{\mathbf{V}_\mathbf{V}} \tag{2}$$

$$\underline{\mathbf{Z}_\mathbf{I}} = \underline{\mathbf{Z}_{22}} - \underline{\mathbf{Z}_{21}} \cdot \underline{\mathbf{Z}_{11}}^{-1} \underline{\mathbf{Z}_{12}} \tag{3}$$

$$\underline{\mathbf{K}_{21}} = \underline{\mathbf{Z}_{21}} \cdot \underline{\mathbf{Z}_{11}}^{-1} \tag{4}$$

$$\overline{\mathbf{I}_\mathbf{V}} = \underline{\mathbf{Z}_{11}}^{-1} \overline{\mathbf{V}_\mathbf{V}} - \underline{\mathbf{K}_{12}} \cdot \overline{\mathbf{I}_\mathbf{I}} \tag{5}$$

$$\underline{\mathbf{K}_{12}} = \underline{\mathbf{Z}_{11}}^{-1} \underline{\mathbf{Z}_{12}} \tag{6}$$

For the loss allocation, all production units and loads are considered as fixed current injections, and a single slack bus with a fixed voltage magnitude and angle is assumed. The total system losses can be expressed as the sum of all power injections in the system (7).

$$\mathbf{S}_\mathbf{loss} = \mathbf{I}_\mathbf{SL}^{*} \mathbf{V}_\mathbf{SL} + \overline{\mathbf{I}_\mathbf{I}}^{H} \cdot \overline{\mathbf{V}_\mathbf{I}} \tag{7}$$

The current of the slack bus and the voltage of the load and generation busses can be eliminated using (2) and (5). After some manipulation and assuming that the reduced impedance matrix is symmetric, i.e. no phase shifting transformers are present, the losses in (7) can be reformulated as (8).

$$\mathbf{S}_\mathbf{loss} = \underbrace{\mathbf{V}_\mathbf{SL}\left(\underline{\mathbf{Z}_{11}}^{-1}\right)^{*} \mathbf{V}_\mathbf{SL}^{*}}_{\text{No-load losses}} + \underbrace{\overline{\mathbf{I}_\mathbf{I}}^{H} \underline{\mathbf{Z}_\mathbf{I}}\,\overline{\mathbf{I}_\mathbf{I}}}_{\text{Load dependent losses}} + \underbrace{j \cdot 2 \cdot \overline{\mathbf{I}_\mathbf{I}}^{H} \Im\left(\underline{\mathbf{K}_{21}}\right) \cdot \mathbf{V}_\mathbf{SL}}_{\text{Cross effect}} \tag{8}$$

The expression consists of three terms. The first term describes the no-load losses which are dependent only on the voltage at the slack bus. This includes shunt losses in transformers and series losses related to reactive power flows in the shunt elements. The second term represents the losses which are related to the square of the current infeeds. The last term represents a cross coupling between the two first terms. The last term describes the change in losses related to supplying the shunt elements from different busses. For example, one can think of a transformer with a large magnetizing current, located far away from the slack point. If a part of the magnetizing current is supplied at a connection point close to the transformer, it will contribute to reduction of the overall losses. This effect is not covered by the load dependent quadratic term. If the shunt impedances in the system are large compared to the series impedances, it can be seen that $\underline{\mathbf{K}_{21}}$ will be close to unity and the last term in (8) will be relatively small.

The most interesting term is the term describing the load dependent losses, because this term describes the effect of the power flows in the system. The second term in (8) only gives a scalar value. To separate the contributions from the individual participants and the cross couplings between them, the load dependent term can be reformulated as in (9). The factor in the square brackets is an *N* by *N* matrix where *N* is the number of current injections.

The real part of the diagonal elements will always be positive. This means that any traffic of active and reactive current in the system will cause active power losses. The real part of the off-diagonal elements can either be positive or negative, dependent on the loading of the network.

$$\mathbf{S}_\mathbf{loss-series} = \overline{\mathbf{I}_\mathbf{I}}^{H} \mathbf{Z}_\mathbf{I} \overline{\mathbf{I}_\mathbf{I}} = \bar{1}^{T} \cdot \left[\left(\overline{\mathbf{I}_\mathbf{I}} \cdot \overline{\mathbf{I}_\mathbf{I}}^{H}\right)^{*} [\,\bullet\,] \underline{\mathbf{Z}_\mathbf{I}}\right] \cdot \bar{1} \tag{9}$$

2.1.2. Allocation based on covariance and mean flows

The reduced impedance matrix, $\underline{\mathbf{Z}_\mathbf{I}}$, shows how the different cross products of the currents affect the losses. The contribution of the cross products to the mean losses is dependent on the simultaneity between activity of the different producers and consumers. A measure of the simultaneity is given by the covariance matrix. The covariance matrix of a random vector, $\overline{\mathbf{F}}$, is defined as (10), where E denotes the expected values [10]. The generalization of the theory to include complex random vectors is discussed in [11].

$$\mathrm{cov}\left[\overline{\mathbf{F}}\right] = \mathrm{E}\left[\left(\overline{\mathbf{F}} - \mathrm{E}\left[\overline{\mathbf{F}}\right]\right) \cdot \left(\overline{\mathbf{F}} - \mathrm{E}\left[\overline{\mathbf{F}}\right]\right)^{H}\right] \tag{10}$$

Rearranging (10), the expected value of the outer product of the vector with it self can be expressed as (11).

$$\mathrm{E}\left[\overline{\mathbf{F}} \cdot \overline{\mathbf{F}}^{H}\right] = \mathrm{cov}\left[\overline{\mathbf{F}}\right] + \mathrm{E}\left[\overline{\mathbf{F}}\right] \cdot \mathrm{E}\left[\overline{\mathbf{F}}\right]^{H} \tag{11}$$

If the current vector is treated as a vector of complex stochastic variables with a mean value and a variance, the expected value or the mean value of the losses can be formulated as (12) by combining (9) and (11).

$$\mathrm{E}\left[\mathbf{S}_\mathbf{loss-series}\right] = \bar{1}^{T} \cdot \left[\left(\underbrace{\mathrm{cov}\left[\overline{\mathbf{I}_\mathbf{I}}\right]}_{\text{Contr. from variance}} + \underbrace{\mathrm{E}\left[\overline{\mathbf{I}_\mathbf{I}}\right] \cdot \mathrm{E}\left[\overline{\mathbf{I}_\mathbf{I}}\right]^{H}}_{\text{Contr. from mean flows}}\right)^{*} [\,\bullet\,] \underline{\mathbf{Z}_\mathbf{I}}\right] \cdot \bar{1} \tag{12}$$

Equation (12) shows that the effect of the mean values of the current infeeds on the losses can be separated from the effect of the covariance between the current infeeds. The cross term of (8) could be considered a part of the losses related to the mean power flows, because if the voltage at the slack point is relatively constant, this term depends on the mean currents.

The real part of the term containing the mean values is difficult to change. The mean value of the production or consumption over longer period is given by the actual energy demand. The mean value of the reactive power can be changed, e.g. by installing or removing a capacitor or changing the power factor of a synchronous machine. The diagonal elements of the covariance matrix describe the variation of the consumption or production of each connection point. The off-diagonal elements describe the simultaneity of the variations of different current sources. Traditionally the information contained in the covariance matrix has been represented with a coincidence factor or Velander's coefficients [12]. The simultaneity between different loads and productions is caused by several effects with different time periods including hourly, daily, weekly and seasonal variations. An estimate of the mean values and covariances therefore only describes the behavior within the period where the measurements were taken.

The element wise product of the covariance matrix and the reduced impedance matrix can give an indication of where there is potential for power savings, e.g. by changing the production pattern of a CHP to better match the load pattern of a group of consumers in the vicinity. The impedance matrix may not be constant during the entire period under

consideration. For example, the position of the under load tap changers of the transformers changes from time to time. If the changes are relatively small, a mean value of the impedance matrix can be used. Alternatively, analyses can be performed separately for time periods with different network configurations.

2.1.3. Allocation based on linear regression

In cases where large sets of measurement data are available, but the network parameters are not exactly modeled, regression methods can be used to separate the causes of the active and reactive power losses from each other and to anticipate future losses based on prognoses. In [13] the causes of the Reactive power exchange between a distribution system and a transmission system have been allocated to the wind turbines, CHPs and consumers using a linear regression analysis. This approach has also been used in [14] to determine the impact of wind turbines on the reactive power losses in the distribution transformers of a system. [15;16] propose a cluster wise linear regression method based on fuzzy logic to anticipate and allocate active power losses in a distribution system.

The idea of the linear regression analysis is to represent the losses as a linear combination of a number of input variables. Generally, the linear regression problem can be specified as (13) [17]. $\bar{\hat{\mathbf{y}}}$ is a column vector with one sample of the estimated quantity per entry, $\underline{\mathbf{X}}$ is a matrix with a row for each observation and a column for each input parameter, $\bar{\mathbf{B}}$ is a column vector with one coefficient per input parameter, and $\bar{1}$ is an identity column vector with the same size as $\bar{\hat{\mathbf{y}}}$.

$$\bar{\hat{\mathbf{y}}} = \mathbf{b_0}\bar{1} + \mathbf{b_1}\overline{\mathbf{x_1}} + \mathbf{b_2}\overline{\mathbf{x_2}} + ... + \mathbf{b}_k\underline{\mathbf{x_k}} = \underline{\mathbf{X}} \cdot \bar{\mathbf{B}} \tag{13}$$

There are standard algorithms for determining the coefficient vector which leads to the smallest quadratic deviation between the measured and the estimated output. However, it is important to know the basic structure of the problem to select a set of input parameters which provide sufficient but not redundant information.

Reformulating (8) leads to the expression in (14). If there are no tap changing transformers and switchable capacitor batteries in the system, the model in (14) gives a complete description of the system. This means that if $\mathbf{S_{loss}}$ and $\bar{\mathbf{X}}$ are exactly known, for a large number of samples, and the input variables are not linearly dependent or constant, a regression analysis will give the $\bar{\mathbf{B}}$-vector in (14).

$$\hat{\mathbf{S}}_{\mathbf{loss}} = \bar{\mathbf{X}} \cdot \bar{\mathbf{B}} = \begin{bmatrix} \mathbf{V_{SL}} \cdot \mathbf{V_{SL}}^* \\ \left[\bar{\mathbf{I}}\right]_1^* \left[\bar{\mathbf{I}}\right]_1 \\ \left[\bar{\mathbf{I}}\right]_1^* \left[\bar{\mathbf{I}}\right]_2 + \left[\bar{\mathbf{I}}\right]_2^* \left[\bar{\mathbf{I}}\right]_1 \\ \vdots \\ \left[\bar{\mathbf{I}}\right]_N^* \left[\bar{\mathbf{I}}\right]_N \\ 2j \cdot \left[\bar{\mathbf{I}}\right]_1^* \mathbf{V_{SL}} \\ \vdots \\ 2j \cdot \left[\bar{\mathbf{I}}\right]_N^* \mathbf{V_{SL}} \end{bmatrix}^T \cdot \begin{bmatrix} \left(\mathbf{Z_{11}}^{-1}\right)^* \\ \left[\underline{\mathbf{Z_I}}\right]_{1,1} \\ \left[\underline{\mathbf{Z_I}}\right]_{1,2} \\ \vdots \\ \left[\underline{\mathbf{Z_I}}\right]_{N,N} \\ \Im\left(\left[\underline{\mathbf{K_{21}}}\right]_{1,1}\right) \\ \vdots \\ \Im\left(\left[\underline{\mathbf{K_{21}}}\right]_{N,1}\right) \end{bmatrix} \tag{14}$$

If the current infeeds are not known, they can be estimated using a load flow algorithm, or by assuming that the voltage has a magnitude of 1 p.u. and an angle of 0 in the entire system which is equivalent to inserting the conjugate of the complex power contributions.

One problem with the regression analysis is that many of the current injections are highly correlated with each other. For example wind farms, located close to each other. This problem is denoted multicollinearity and can lead to a large variance in the estimated coefficients when analyzing different sets of samples. The problem of multicollinearity can partly be overcome by applying a Ridge Regression or a Principal Component Regression, which can reduce the variance of the estimated coefficients at the cost of a bias in the estimated output vector [10;18;19].

2.1.4. Aggregation of current sources

In a real distribution system, there is usually a very large number of customers and production units. In the BOE case in Chapter 3, there are for example 721 aggregated loads, 65 induction machines and 29 synchronous machines in the model. With 815 current sources, (14) would require 333336 elements in the input vector, which would not be realistic. Further, there are not measurements of each of the 400 V loads in the system. Therefore, it is advantageous to group some of the sources together and assume that they behave as one lumped source, connected to one virtual node. The grouping of similar components also reduces the problem of multicollinearity.

Assuming that the current injections can be expressed as a linear combination of a reduced number of aggregated currents like in (15), the load dependent losses can be calculated exactly using (16) and (17)**.**

$$\overline{\mathbf{I_I}} = \underline{\mathbf{K_I}} \cdot \overline{\mathbf{I_{red}}} \tag{15}$$

$$\mathbf{S_{loss-series}} = \bar{\mathbf{I}}_{\mathbf{red}}^H \cdot \underline{\mathbf{K_I}}^H \cdot \underline{\mathbf{Z_I}} \cdot \underline{\mathbf{K_I}} \cdot \overline{\mathbf{I_{red}}} \tag{16}$$

$$\mathbf{S_{loss-cross}} = j \cdot 2 \cdot \bar{\mathbf{I}}_{\mathbf{red}}^H \underline{\mathbf{K_I}}^H \cdot \Im\left(\underline{\mathbf{K_{21}}}\right) \cdot \mathbf{V_{SL}} \tag{17}$$

When the reduced current vector is inserted in (14), the estimated $\bar{\mathbf{B}}$-vector will contain elements from $\underline{\mathbf{K_I}}^H \cdot \underline{\mathbf{Z_I}} \cdot \underline{\mathbf{K_I}}$ and $\underline{\mathbf{K_I}}^H \Im\left(\underline{\mathbf{K_{21}}}\right)$.

$\underline{\mathbf{K_I}}$ is a transformation matrix with a number of rows corresponding to the number of busses in the system and a number of columns corresponding to the number of aggregated currents.

One approach is to define an aggregated current for each feeder based on the sum of all loads of the feeder and another aggregated current based on the sum of all production of the feeder. Often, only the total power of the loads of a feeder is known. To estimate an aggregated current for the feeder, an aggregated voltage must be assumed. As a first approach, the voltages at the connection points of the feeders can be used as basis for calculating the current at the virtual nodes.

The method of loss allocation based on aggregated loads and consumers has been used in the investigation of the losses in the BOE network, presented in [20].

2.1.5.The influence from reactive power flows

The current dependent losses can be split into contributions from the active power transfer, the reactive power transfer and a cross effect between the two. Equation (18) shows the separation of the current injections into a part corresponding to the real power injections and a part corresponding to the reactive power injections. The changes in voltage caused by the current injections have not been considered.

$$\bar{\mathbf{I}}_{\mathbf{I}} = \bar{\mathbf{I}}_{\mathbf{P}} + \bar{\mathbf{I}}_{\mathbf{Q}} = \left(\overline{\mathbf{S}}[./]\overline{\mathbf{V}}\right)^{*} = \left(\overline{\mathbf{P}}[./]\overline{\mathbf{V}}\right)^{*} + \left(j\overline{\mathbf{Q}}[./]\overline{\mathbf{V}}\right)^{*} \tag{18}$$

$$\bar{\mathbf{I}}_{\mathbf{P}} = \left(\overline{\mathbf{P}}[./]\overline{\mathbf{V}}\right)^{*} \quad \text{and} \quad \bar{\mathbf{I}}_{\mathbf{Q}} = \left(j\overline{\mathbf{Q}}[./]\overline{\mathbf{V}}\right)^{*} \tag{19}$$

Inserting (18) in (9) yields (20)

$$\mathbf{S}_{\mathbf{loss-series}} = \bar{1}^{T} \cdot \left[\left(\underbrace{\bar{\mathbf{I}}_{\mathbf{P}} \cdot \bar{\mathbf{I}}_{\mathbf{P}}{}^{H}}_{\text{Contr. from P}} + \underbrace{\bar{\mathbf{I}}_{\mathbf{Q}} \cdot \bar{\mathbf{I}}_{\mathbf{Q}}{}^{H}}_{\text{Contr, from Q}} + \underbrace{\left(\bar{\mathbf{I}}_{\mathbf{Q}} \cdot \bar{\mathbf{I}}_{\mathbf{P}}{}^{H} + \bar{\mathbf{I}}_{\mathbf{P}} \cdot \bar{\mathbf{I}}_{\mathbf{Q}}{}^{H}\right)}_{\text{Cross effect}} \right)^{*} [.\bullet]\underline{\mathbf{Z}}_{\mathbf{I}} \right] \cdot \bar{1} \tag{20}$$

The three terms in (20) represent the contribution from the active power injections, the reactive power injections and the cross effect. Since the transfer of active power is usually regarded as the main objective, the cross effect could be considered a part of the losses, allocated to the reactive power.

3. CASE STUDY: BRØNDERSLEV OG OPLANDS ELFORSYNING

As case study, the distribution network in Brønderslev in Western Denmark has been investigated. A model of the 60 kV and 10 kV networks, including 65 wind turbines (total 40 MW), 29 synchronous generators (total 50 MW) and totally 1792 nodes has been implemented in PowerFactory®. The load demand is between 15 and 45 MW, which means that power is often exported to the transmission system. Fig. 1 shows an overview of the 60 and 10 kV network.

Ten months of 15 min measurement data have been obtained with the SCADA system. The data, containing for example active and reactive power flows through the 60 / 10 kV transformers, voltage measurement on the 150 kV infeed and production data from the wind turbines and CHPs, has been inserted as time scales in the model. The active and reactive loads and losses have been estimated by performing a series of load flows. The time dependent consumption and the losses have been estimated based on the power balance of each feeder. The procedure has been described in [14].

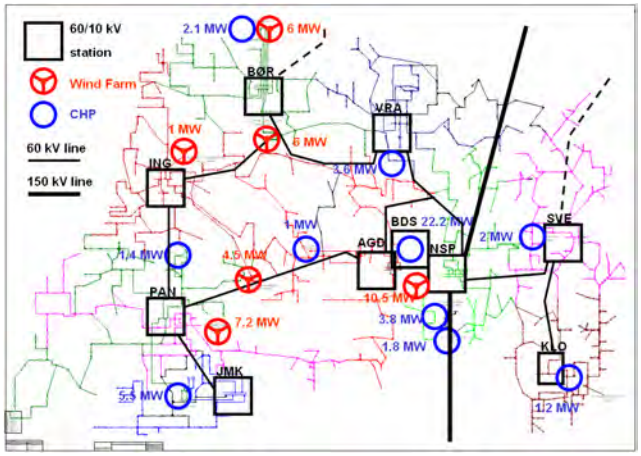

Fig. 1 The 60 and 10 kV network

3.1. Loss allocation

The losses of the system have been analyzed according to the methods described in Chapter 2. The aim of the analyses is twofold. Firstly, they are supposed to provide an overview of the losses in the distribution system. The following questions should be considered:

1. How large are the total losses compared to the load and production?
2. Where in the system are the losses dissipated?
3. What are the losses caused by the integration of DG?
4. What are the losses caused by the transfer of reactive power?
5. What are the potential savings in losses if the simultaneity between load and production is increased?

Secondly, the analyses will serve as a validation of the loss allocation methods presented in Chapter 2.

The analyses are based on measurements obtained in the period April 6th 2006 to February 6th 2007. During the period, a few days of data are missing due to communication problems in the SCADA system. The estimated mean values of losses etc. have not been corrected for the difference in load and production pattern between the missing two months and the rest of the year.

Fig. 2 shows an overview of the mean active power losses, divided into the components causing the losses. The total mean-losses make approximately 1.27 MW, from which 72 % is dissipated at 10 kV level and below. It should be noted that the real system also comprises a large number of 0.4 kV lines which have not been modeled. The shunt losses of the transformers which are practically independent of the loading, make 49 % of the total active power losses. The mean load dependent losses of the 150/60 kV transformers only amount to 5 kW.

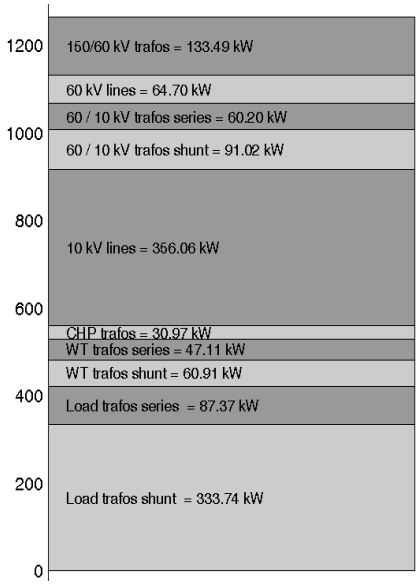

Fig. 2 Mean active power losses

The network comprises ten 60 / 10 kV stations. Three of the stations comprise two transformers which are not operated in parallel. Table 1 shows the mean load and production from CHPs and wind turbines of the feeders under each of the transformers.

	A Load	B Wind	C CHP	D Sum
AGD 2	-2.17	0	0.1	**-2.07**
AGD 1	-1.62	0.13	0.4	**-1.09**
BDS 2	0.00	0.00	7.72	**7.72**
BDS 1	-2.96	3.10	1.97	**2.11**
BØR	-3.09	3.26	0.62	**0.79**
ING	-2.28	1.37	0.60	**-0.31**
JMK	-2.69	0.03	2.51	**-0.16**
KLO	-1.34	0.03	0.68	**-0.63**
NSP	-3.10	0.05	0.00	**-3.05**
PAN 1	-2.00	1.66	0.00	**-0.34**
PAN 2	-2.29	0.22	0.52	**-1.55**
SVE	-1.39	0.05	0.81	**-0.53**
VRÅ	-3.73	0.04	0.56	**-3.13**
Sum	**-28.66**	**9.93**	**16.48**	**-2.25**

Table 1**:** Mean values of active power contributions of each feeder [MW]

To study the impact of the distributed generation, an allocation of the system losses is performed as described in Chapter 2. The following combination of the methods has been used:

Firstly, the losses of the 60 kV network, the 150 / 60 kV transformers and the 60 / 10 kV transformers are allocated to the individual feeders, based on the impedance matrix of that part of the network. For comparison, the allocation is made both using the marginal loss allocation method and the statistical method based on current injections.

Secondly, the losses at 10 kV level and below for each feeder are allocated to the four categories; loads, wind turbines, CHPs and shunt losses. The allocation is performed using the regression method using the apparent power as input and neglecting the cross effects.

Finally, the losses at 60 kV and above are allocated to the loads, wind turbines, CHPs and shunt losses of the individual feeders. The approach is that the load or generation of each category minus the low voltage losses allocated to the specific category are converted to an equivalent current injection on the 10 kV side of the 60 / 10 kV transformers, and the same approach as in step one is used.

Table 2 shows the allocation of the losses at 60 kV level and above, including the 60/10 kV transformers to the individual feeders. Column A contains the contribution from the mean power flows of the feeders. Column B shows the influence from the covariance. Column C shows the diagonal elements of the loss matrices. These losses correspond to the load dependent losses if only one of the feeders were connected. Column D is the sum of column A and B, representing the total losses allocated to each of the feeders. Column E represents the losses allocated to the different feeders using the sensitivity coefficients. The sum of the rows in column D is approximately equal to the sum of the rows in column E. The allocation to the individual feeders, however, deviates up to 5 %. The fundamental difference between the two methods is that the current injection method assumes a constant current where as the sensitivity method assumes a constant power infeed. This means that the sensitivity analysis takes the change in bus voltages and thereby changes in current injections caused by the change of a single power injection into account. The advantage of the current injection method is that it makes it possible to separate the influence from the mean values and the covariances. A comparison of column A and column B in Table 2 shows that the feeders with a high wind penetration like BDS 1, BØR, ING and PAN 1 have higher losses related to the covariance than those related to the mean value. The same applies for feeders with high penetration of CHP production like BDS 2 and JMK. For feeders with a relatively low penetration of distributed generation like AGD 2, NSP and VRÅ, the highest contribution comes from the mean value. For AGD 2, the contribution from the variance is even negative, because it is located close to the large CHP in Brønderslev.

	A Contribution from mean currents	B Contribution from the covariance	C Contribution from self-impedances	D Total allocated losses	E Marginal loss allocation
AGD 2	1.54	-0.04	2.29	1.50	1.44
AGD 1	1.07	0.32	1.29	1.38	1.45
BDS 2	11.92	23.56	37.98	35.47	35.00
BDS 1	1.90	5.93	6.80	7.83	7.76
BØR	-0.73	18.12	11.74	17.39	17.24
ING	1.08	10.53	5.10	11.61	11.90
JMK	0.52	7.28	5.69	7.80	8.02
KLO	1.11	0.80	1.47	1.90	1.96
NSP	3.85	0.44	4.39	4.29	4.34
PAN 1	1.17	10.36	5.70	11.53	11.41
PAN 2	5.34	4.35	5.46	9.69	9.93
SVE	0.58	0.98	1.12	1.56	1.58
VRÅ	11.21	1.44	11.52	12.65	12.54
Sum	**40.56**	**84.06**	**100.55**	**124.61**	**124.56**

Table 2**:** The load dependent losses of the 60 kV network, and the 150/60 kV and 60/10 kV transformers. The numbers represent the losses in kW

Table 3 shows the division of the losses at 60 kV and above in a part caused by the active power flows and a part caused by the reactive power flows. Column A and C have been calculated using the current injection algorithm, and column B and D have been calculated using the sensitivity algorithm. The total sum of losses allocated to the reactive power flows is similar for the two methods, but for the individual busses, the two methods give diverging results for the reactive power contribution in column C and D.

The problem with the current injection method here is that it assumes that the part of the current which is perpendicular to the bus voltage is related to the reactive power flow. The current injections, however, change the bus voltages.

With both methods, it is found that the reactive power injections only cause approximately 5 % of the load dependent losses at the 60 kV level and above.

	A Active power – current injection	B Active power – marginal allocation	C Reactive power – current injection	D Active power – marginal allocation
AGD 2	1.38	1.36	0.13	0.08
AGD 1	1.28	1.27	0.10	0.18
BDS 2	33.95	33.91	1.52	1.08
BDS 1	7.73	7.67	0.10	0.09
BØR	16.69	16.61	0.70	0.63
ING	10.85	10.87	0.76	1.03
JMK	7.55	7.53	0.25	0.50
KLO	1.61	1.61	0.29	0.35
NSP	3.78	3.77	0.51	0.57
PAN 1	11.01	10.94	0.52	0.47
PAN 2	9.33	9.43	0.36	0.50
SVE	1.50	1.50	0.07	0.08
VRÅ	11.84	11.94	0.81	0.60
Sum	**118.48**	**118.41**	**6.13**	**6.15**

Table 3**:** Separation of the losses on 60 kV level and above in contributions from active and reactive power flows kW

Table 4 shows the allocation of all the losses in the model to load, wind, CHP and constant shunt losses. The losses at 10 kV and below have been allocated using the linear regression method and the rest of the losses have been allocated using the current injection method. It can be seen that the no-load losses make approximately half the losses. In AGD 2 which has very little production from CHP units, the losses allocated to that category is negative and for JMK which has very little wind production, the losses allocated to wind power are negative. This means that these units actually contribute to reduction of the losses. Although the mean production from the CHPs is 65 % larger than from the wind turbines, the total losses allocated to the wind turbines are larger than the losses allocated to the CHPs. There are three main reasons for that. Firstly, all the wind turbines comprise a step up transformer, where as most of the larger CHPs are connected directly to the 10 kV network (or the transformer is not modeled). Secondly, nearly half the CHP production comes from the Brønderslev KVV which is located only half a kilometer from the substation, BDS 1. Thirdly, the ratio between the mean value and the standard deviation of the production is higher for the CHPs than for the wind turbines. The high correlation between the CHP production and the load demand is not assumed to have a large impact on the losses at 10 kV level and below, since most of the large CHPs have their own radials.

	A Shunt losses	B Load	C Wind	D CHP	E Sum
AGD 2	19.30	14.49	0	-0.11	**33.69**
AGD 1	32.67	16.48	0.89	5.74	**55.78**
BDS 2	0.05	0.00	0	47.48	**47.53**
BDS 1	53.53	11.62	68.62	13.78	**147.54**
BØR	33.63	35.07	49.90	1.11	**119.70**
ING	57.71	28.92	41.70	1.57	**129.89**
JMK	25.27	27.82	-0.12	16.05	**69.02**
KLO	27.44	9.17	0.21	5.79	**42.62**
NSP	48.96	29.85	0.10	0	**78.91**
PAN 1	29.98	36.51	29.92	0	**96.41**
PAN 2	31.52	52.82	3.46	2.94	**90.74**
SVE	28.61	8.41	0.31	10.31	**47.64**
VRÅ	35.84	48.32	0.19	3.29	**87.64**
60 kV	221.25	0	0	0	**221.25**
Sum	**645.76**	**319.5**	**195.18**	**107.94**	**1268.3**

Table 4**:** Allocation of all the losses in kW

To put the losses that have been allocated to the different categories into context, they have been presented in Table 5 as percentages of the total power flows and of the total system losses. Only the load dependent losses are allocated to participants with the loss allocation methods used above. Therefore, the no-load losses of the transformers related to the loads, wind turbines and CHPs are added to the losses allocated to the respective categories.

	A Allocated losses [kW]	B Mean Volume [MW]	C % of Volume	D % of all losses
Load	319.5	28.7	1.1	25.2
10/0.4 trafo no load	333.7	28.7	1.2	26.3
Load total	**653.2**	**28.7**	**2.3**	**51.5**
Wind	195.2	9.9	2.0	15.4
Wind trafo no load	60.9	9.9	0.6	4.8
Wind total	**256.1**	**9.9**	**2.6**	**20.2**
CHP	107.9	16.5	0.7	8.5
CHP trafo nl	11.7	16.5	0.1	0.9
CHP total	**119.7**	**16.5**	**0.7**	**9.4**
Rest	**239.4**			**18.9**
Total	**1268.4**	**55.1**	**2.3**	**100.0**

Table 5**:** The allocated losses relative to the total flows

4. CONCLUSION

The paper has described, how the losses in a distribution system can be allocated to load and distributed generation units. The marginal loss allocation method and the current injection method have been used in the case study to allocate the losses. For the 60 kV system, the results from current injection method have been compared to results from the sensitivity analysis, and the two algorithms show identical results. The advantages of the sensitivity analysis are firstly that the algorithm is a part of most power system simulation tools. In PowerFactory® the calculation of loss sensitivities, however, requires an invocation of the sensitivity tool for each bus under consideration. This can be automated, but it extends the total simulation time. Secondly, the interpretation is well suited for e.g. incentive generating price signals, since it directly gives the price of a small change in production / consumption. The advantages of the current injection method are firstly that it is based on the reduced impedance matrix, which contains the short circuit impedances. It is possible to make a rough estimate of the cost of transferring power from one place to another just by looking at the reduced impedance matrix. Like the sensitivity analysis, the algorithm requires a load flow calculation per measurement sample to determine the current infeeds. PowerFactory® does not directly support the export of the impedance matrix. It is, however, possible that it could get implemented in a future version of the tool.

The linear regression method is a simple way of getting an overview of the losses at 10 kV and below. It is, however, not possible to separate the losses related to components in the same feeder with similar load or production time profiles due to the multicollinearity problem.

For the 60 kV system and above, there is a clear synergy effect between production and load. These losses, however, only account for 10 % of the total system losses. For the 10

kV system, it is concluded that the cross effects between load and production make a relatively small part of the total system losses, because the larger wind farms and CHPs are connected to the 60 / 10 kV stations through their own radials. Based on the regression analysis of feeders with only a few smaller wind turbines and CHPs, it is, however, concluded that some of the smaller units do contribute to lowering the losses. The reactive power transfer through the 60/10 kV transformers and above only generates 5 % of the load dependent losses.

APPENDIX

Nomenclature

Symbol	Definition
$.$	Matrix product
$[./]$	Element wise vector or matrix division – equivalent to ./ in Matlab®
$[.\bullet]$	Element wise vector or matrix product equivalent to .* in Matlab®
$\mathbf{F}$	Complex quantity
$\mathbf{F}^*$	Complex conjugate
$\Re(\mathbf{F})$	Real part of a complex quantity
$\Im(\mathbf{F})$	Imaginary part of a complex quantity
$\overline{F}$	Column Vector
$\underline{F}$	Matrix
$\underline{F}^T$	Transposed vector or matrix
$\underline{\mathbf{F}}^H = \underline{\mathbf{F}}^{T*}$	Conjugate transposed vector or matrix
$[\underline{F}]_{i,j}$	Row *i*, column *j* of the matrix
$[\overline{F}]_i$	Element *i* of the vector
$\mathrm{E}(\mathbf{F})$	Estimate of mean value of a stochastic variable
$\mathrm{cov}(\overline{\mathbf{F}})$	Covariance matrix

ACKNOWLEDGEMENT

This work has been financed by the Danish transmission system operator, Energinet.dk and Nordic Energy Research. The data has peen provided by the distribution network operator BOE Net A/S.

REFERENCES

[1] Costa, P. M. and Matos, M. A., "Loss allocation in distribution networks with embedded generation," *IEEE Transactions on Power Systems*, vol. 19, no. 1, pp. 384-389, 2004.

[2] Cardell, J. B. Improved Marginal Loss Calculations During Hours of Transmission Congestion. 2005. 38th Annual Hawaii International Conference on System Sciences.

[3] Herter, K., "Residential implementation of critical-peak pricing of electricity," *Energy Policy*, vol. 35 pp. 2121-2130, 2007.

[4] Hoff, T. E., Perez, R., Braun, G., Kuhn, M., and Norris, B. The Value of Distributed Photovoltaics to Austin Energy and the City of Austin. 2006. Austin Energy.

[5] Conejo, A. J., Arroyo, J. M., Alguacil, N., and Guijarro, A. L., "Transmission loss allocation: a comparison of different practical algorithms," *IEEE Transactions on Power Systems*, vol. 17, no. 3, pp. 571-576, 2002.

[6] Al-Rajhi, A. N. and Bialek J.W. Marginal and Tracing Pricing of Transmission an Empirical Comparison. 2002. 14th Power Systems Computation Conference.

[7] Mutale, J., Strbac, G., Curcic, S., and Jenkins, N., "Allocation of losses in distribution systems with embedded generation," *IEE Proceedings-Generation Transmission and Distribution*, vol. 147, no. 1, pp. 7-14, 2000.

[8] Conejo, A. J., Galiana, F. D., and Kockar, I., "Z-bus loss allocation," *Power Systems, IEEE Transactions on*, vol. 16, no. 1, pp. 105-110, 2001.

[9] Glover, J. D. and Sarma, M. S., *Power System Analysis and Design* Brooks/Cole, 2002.

[10] Johnson, R. A. and Wichern, D. W., *Applied multivariate statistical analysis*, 5. ed. Prentice-Hall, Inc. Upper Saddle River, NJ, USA, 2002.

[11] Svensson, L. and Lundberg, M. Estimating complex covariance matrices. Thirty-Eighth Asilomar Conference on Signals, Systems and Computers , 2151-2154. 2004.

[12] Lakervi, E. and Holmes, E. J., *Electricity distribution network design* Peter Peregrinus Ltd, 1995.

[13] Østergaard, J. and Jensen, K. K. Ny Mvar-ordning. 506. 1-9-2004. DEFU.

[14] Lund, T., Nielsen, J. E., Hylle, P., Sørensen, P., Nielsen, A. H., and Sørensen, G., "Reactive Power Balance in a Distribution Network with Wind Farms and CHPs," *International Journal of Distributed Energy Resources*, vol. 3, no. 2, pp. 113-138, 2007.

[15] Hong, Y. Y., Chao, Z. T., and Yang, M. S., "A fuzzy multiple linear regression based loss formula in electric distribution systems," *Fuzzy Sets and Systems*, vol. 142, no. 2, pp. 293-306, 2004.

[16] Hong, Y. Y. and Chao, Z. T., "Development of energy loss formula for distribution systems using FCN algorithm and cluster-wise fuzzy regression," *Power Delivery, IEEE Transactions on*, vol. 17, no. 3, pp. 794-799, 2002.

[17] Mendenhall, W., Beaver, B. M., and Beaver, R. J., *Introduction to Probability and Statistics* Thomson Brooks/Cole, 2003.

[18] Draper, N. R. and Smith, H., *Applied Regression Analysis*, 2. ed. John Wiley & Sons New York, 1981.

[19] Jobson, J. D., *Applied Multivariate Data Analysis* Springer-Verlag, 1991.

[20] Lund, T. Measurement based analysis of active and reactive power losses in a distribution network with wind farms and CHPs. 2007. European Wind Energy Conference & Exhibition, Milan, EWEA.

Discussion on the Grid Disturbance on 4 November 2006 and its effects in a Spanish Wind Farm

Emilio Gómez, Miguel Cañas
Renewable Energy Research Institute
Dept. of Electrical, Electronic
and Control Eng. EPSA
Universidad de Castilla-La Mancha
02071 Albacete (SPAIN)
Email: emilio.gomez@uclm.es

Juan Álvaro Fuentes, Ángel Molina
Dept. of Electrical Eng.
Universidad Politécnica de Cartagena
30202 Cartagena (SPAIN)
Email: juanalvaro.fuentes@upct.es
angel.molina@upct.es

JuanMa Rodríguez
Red Eléctrica de España
P del Conde de los Gaitanes 177
ES-28109 Alcobendas (Madrid) (SPAIN)
Email: rodgarju@ree.es

***Abstract*— The main objective of this paper is the discussion of the grid disturbance occurred in Europe on the November 4, 2006, focusing the study on the consequences in Spain. So, countermeasures for avoiding similar events are being studied in Spain, being presented in the final paper. On the other hand, a discussion of the influence of this grid disturbance in a Spanish wind farm is done using the voltages and currents measured with a power quality analyzer placed in a wind turbine located in that wind farm.**

I. Introduction

The leader countries in wind power (Germany, Spain, Denmark) built up their wind power installations updating their objectives from year to year. Table I shows the Wind Power installed in Europe by end of 2006. Recently, and due to the installed wind power capacity figures, different studies on potential integration impacts have been performed, such is the case of Spain, [1], [2]. Therefore, utility managers and operators in those countries are studying the integration of more wind power, since it becomes more important at these levels.

National power systems are interconnected through transmission infrastructure with the main aim of assuring the security of supply by means of the mutual assistance between national subsystems. However, grid disturbances can be transmitted from one national subsystem to another. So, requirements imposed by Transmission System Operators (TSOs) years ago did not take into account the Power System Operation with Large Amounts of Wind Power, where faults and grid disturbances can be transmitted from one country to another. On the other hand, these grid disturbance effects could be even bigger in the future since wind power installed capacity is increasing year to year.

A grid disturbance occurred on 4 November 2006, when there were significant East-West power flows as a result of international power trade and the obligatory exchange of wind feed-in inside Germany. These flows were interrupted during the event. The tripping of several high-voltage lines, which started in Northern Germany, split the UCTE (union for the co-ordination of transmission of electricity) grid into three separate areas (West, North-East and South-East) with significant power imbalances in each area, figure 1. The Western Area was composed of Spain, Portugal, France, Italy, Belgium, Luxemburg, The Netherlands, a part of Germany, Switzerland, a part of Austria, Slovenia and a part of Croatia)

TABLE I
Europe Wind Energy Generating Capacity by end of 2006

Country	Capacity(MW)
Germany	20.622
Spain	11.615
Denmark	3.136
Italy	2.123
UK	1.983
Netherlands	1.560
Portugal	1.716
Austria	965
France	1.567
Greece	746
Sweden	572
Ireland	745
Belgium	193
Finland	86
Poland	152.5
Luxembourg	35
Estonia	32
Czech Republic	50
Latvia	27
Hungary	61
Lithuania	55.5
Slovakia	5
EU-25 total	48.027
Accesion Countries	68
EFTA Countries	325.6

Source: European Wind Energy Association (EWEA)

II. Grid disturbance effects in Europe

The power imbalance in the Western area induced a severe frequency drop that caused an interruption of supply for more than 15 million European households, [3].

In under-frequency areas (West and South-East), the imbalance between supply and demand as a result of the splitting was further increased in the first moment due to a significant

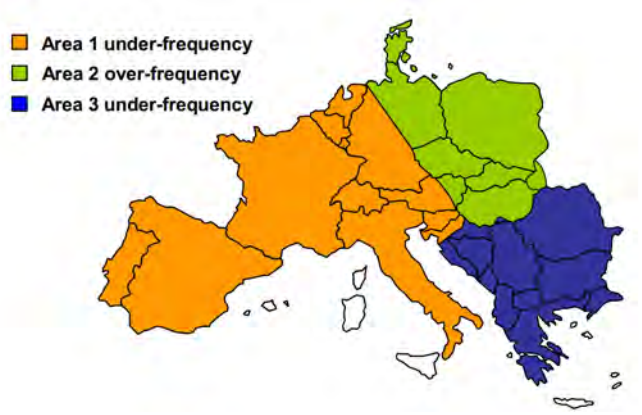

Fig. 1. Schematic map of UCTE area split into three areas

amount of tripped generation connected to the distribution grid. Full resynchronization of the UCTE system was completed 38 minutes after the splitting. The TSOs were able to re-establish a normal situation in all European countries in less than 2 hours. Due to the adequate performance of automatic countermeasures in each individual TSO control area and additional manual actions by TSOs a few minutes after the splitting, a further deterioration of the system conditions and a Europe-wide black-out could be avoided. In [3], a detailed study of the events, and solutions is presented.

The total generation of the Western area when it was disconnected from the other areas was 182.700 MW with a negative power imbalance of 8.940 MW caused by the lost from the power import from the East. This power imbalance and the trip of some groups of generation provoked a great fall of the frequency that required a great discharge to try maintaining the frequency in correct levels, this discharge was distributed in the next way: 6.460 MW in France, 2.912 MW in Italy, 2.107 MW in Spain, 800 MW in Belgium and 1.101 MW in Portugal. In the South-Eastern also occurred a fall of the frequency but was less important than in Western area due the power imbalance was only of 770 MW from the total generation of 29.100 MW. In the other hand, the North-East area suffered a high over-frequency due an excess of generation of more than 10.000 MW with an approximate total power generation of 58.900 MW (around 6.000 MW corresponded wind generation).

III. Grid disturbance effects in Spain

Spain was affected by the grid disturbance as it is shown in figure 1, being inside the under-frequency area. In Spain, this disturbance provoked:

- The interconnection lines between Morocco and Spain were tripped.
- Tripping of power installation CCGT de Arcos de la Frontera (728 MW)
- Tripping of 2.800 MW in wind power, figure 2(b). This figure shows the generated active power in tele-measured wind farms coloured in blue, whereas the total estimated wind generated active power is coloured in pink. Around 10:12 p.m., wind generated active power diminished from around 4.000 MW to 1.164 MW.
- 2.107 MW of load shedding, figure 2(a). This figure shows the real demand coloured in dark blue, whereas programmed demand is coloured in light blue and estimated actual demand is coloured in pink.

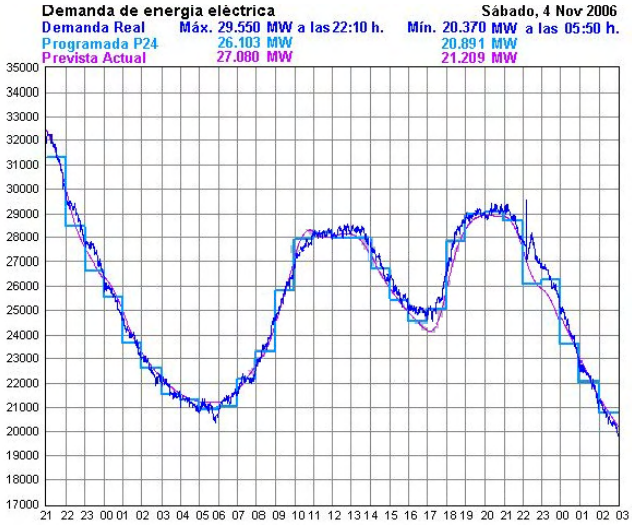

(a) Load demand

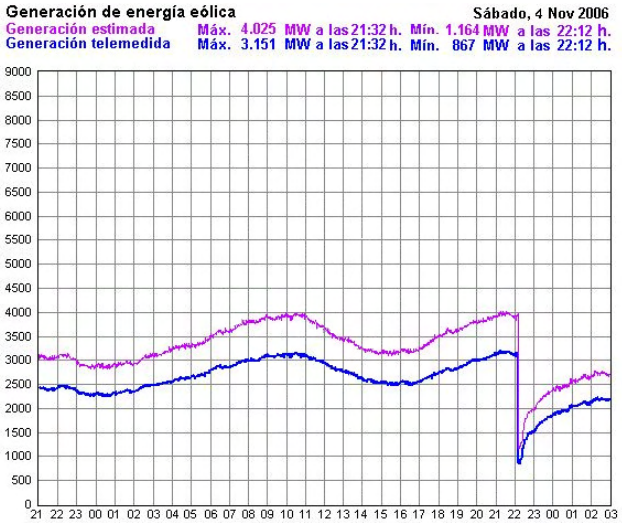

(b) Wind power

Fig. 2. Load demand and wind power in Spain on November 4, 2006. Source: REE

The rates of load shedding depends on the TSO, being in the case of Red Eléctrica de España (REE), [4]:

- 49.0 Hz: 15% of load shedding with no delay.
- 48.7 Hz: 15% of load shedding with no delay.
- 48.4 Hz: 10% of load shedding with no delay.
- 48.0 Hz: 10% of load shedding with no delay.

On the other hand, frequency relays are installed in wind turbines —maximum frequency (81M) at 51 Hz and minimum frequency (81m) at 49 Hz, complying, in that time the Spanish

requirements, [5].

IV. Grid disturbance effects in a Spanish wind farm

A power quality analyzer installed in a wind turbine, (model Topas 2000 from LEM, recently adquired by Fluke) located in a Spanish wind farm, measured voltages, currents and frequency during the disturbance, figures 3(a), 3(b) and 3(c).

Also, the power quality analyzer registers every 10 minutes V RMS and frequency, this gives the posibility to see when the system recovered its normal operation, 4(a) and 4(b)

The evolution of the voltages is seen in figure 5(a), by using a polar representation of the voltage space vector, [6]. From voltage space vector, the evolution of its amplitude is represented in figure 5(b).

As it can be seen in figure 3(c), the frequency is falling steadily until the 49 Hz level is reached, then the result of the load shedding scheme of REE, 15% of the load with no delay, is enough to restore the power balance between generation and load in the system. This relay of minimum frequency could be placed in the 132 kV line or in the substation transformer. As a comment, the small frequency oscillation just before the time 0.5s could be explained as a probably disconnection of a not very far protection adjusted to 49.5 Hz. Due to the conexion configuration of the power quality analyzer, when the voltage level reaches zero the frequency is fixed in 50 Hz. This effect can be observed comparing figures 3(a) and 3(c), the vertical dash-dot line place in both figures serves as time reference. It can be observed while voltage fall to zero the frequency increases from 49 Hz to the 50 Hz level.

The Topas 2000 determines the frequency in the next manner, [7]: for 10 s frequency values the sample data are filtered by 2^{nd} order infinite impulse response, the 3dB cut-off frequency is 50 Hz for 50 Hz nominal frequency. Based on the filtered signal whole periods within 10 s intervals (taken from the internal real time clock) are counted by detecting zero crossings. The frequency is calculated by dividing the number of whole periods by the duration of this number of whole periods. The time interval is derived from timestamps generated by the hardware of the first and the last sample within the block of whole periods.

Figures 3(a) and 3(b) shows the currents and voltages of the wind turbine. It can be seen that currents reduce to zero where there is an overvoltage of around a 1.3 pu as the result of the transients provoked by its disconnection. This process takes less than 0.1s.

In terms of protective relaying criteria, the recently approved regulation, [8], establishes that the minimum relaying protective devices in wind turbines must be coordinated with the load shedding system of the spanish peninsula power system, acting when frequency is going down of 48 Hz, at least during 3 seconds. On the other hand, maximum relaying protective devices can act if frequency rises 51 Hz, [8], with the timing established on the grid codes, being the proposal submitted to the regulars the following:

- 50.5 Hz: 5% installed capacity

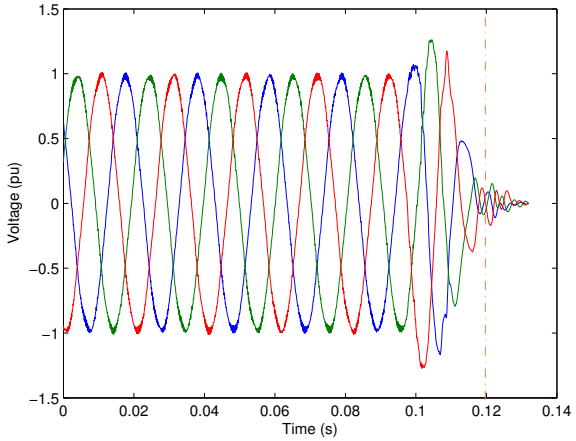

(a) Voltages

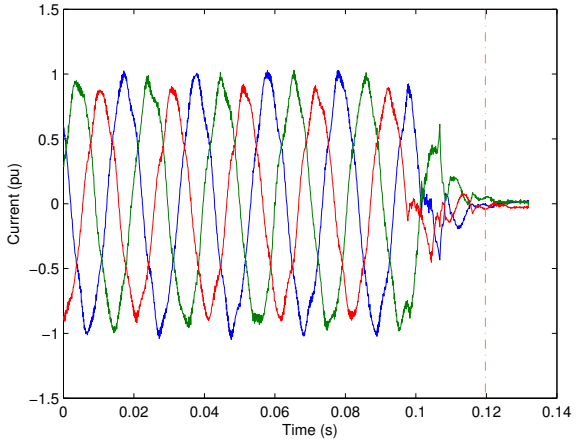

(b) Currents

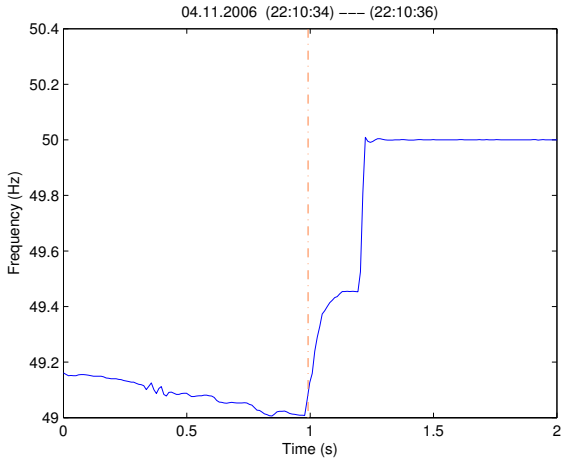

(c) Voltage frequency

Fig. 3. Measured voltages, currents and frequency in a wind turbine

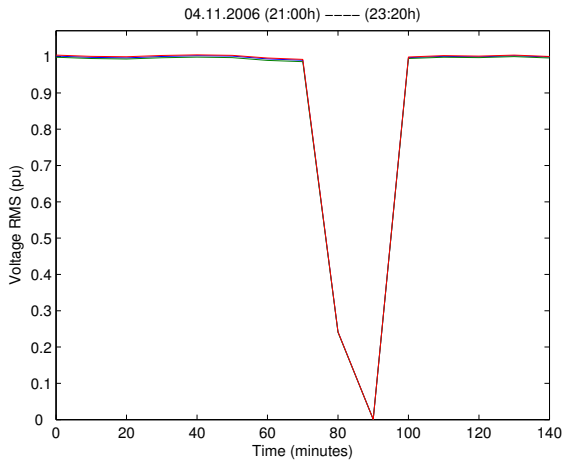

(a) Voltages

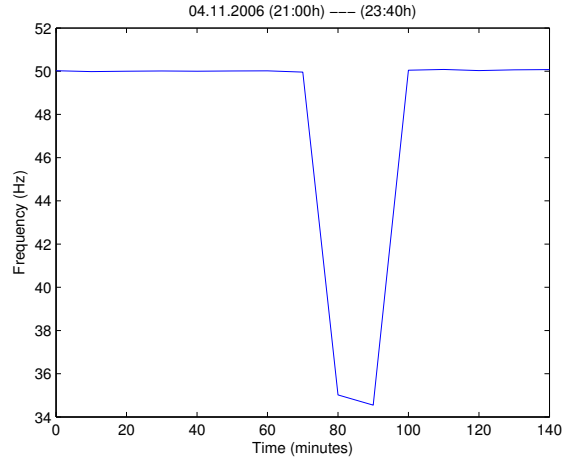

(b) Frequency

Fig. 4. Measured voltages RMS and frequency in a wind turbine

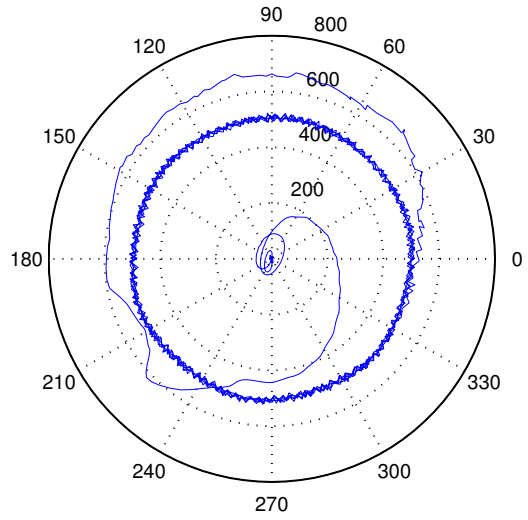

(a) Voltage space vector in polar coordinates

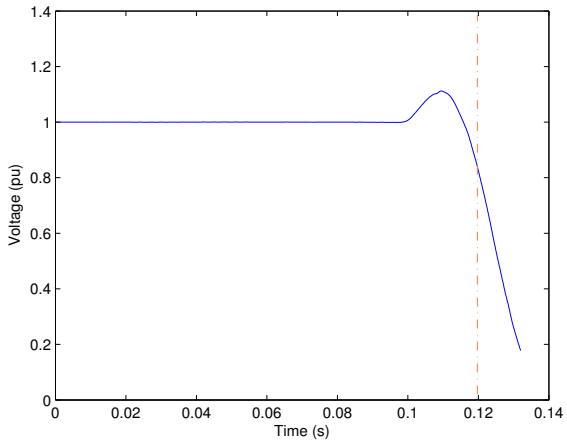

(b) Voltage space vector amplitude

Fig. 5. Voltage space vector

- 50.6 Hz: 10% installed capacity
- 50.7 Hz: 15% installed capacity
- 50.8 Hz: 20% installed capacity
- 50.9 Hz: 25% installed capacity
- 51.0 Hz: 25% installed capacity

In this way, the three second delay introduced in the minimum frequency relay could help minimise the effect of a premature disconnection of wind generation in case of a grid disturbance as the one discussed here.

ACKNOWLEDGMENT

The financial support provided by the "Ministerio de Educación y Ciencia" —ENE2006-15422-C02-01/ALT and ENE2006-15422-C02-02/ALT— and "Junta de Comunidades de Castilla-La Mancha" (PCI-05-024) is gratefully acknowledged. Authors also thank to Mr. Juan Manuel Abellán from "Dea y Energías Renovables", to the technicians of Moralejo wind farm —located in Alpera, Albacete (Spain)— and the Gamesa technicians.

REFERENCES

[1] REE, "Producción eólica técnicamente admisible en el sistema eléctrico peninsular ibérico, horizonte 2011," REE / REN / CNE / AEE, Tech. Rep., July 2006.

[2] ——, "Estudio de estabilidad eólica de la península ibérica. síntesis de criterios y metodologías," REE and REN, Tech. Rep., May 2005.

[3] UCTE, "Final report. system disturbance on 4 november 2006," Union for the co-ordination of transmission of electricity, Tech. Rep., 2007.

[4] REE, "Criterios generales de protección del sistema eléctrico peninsular español," 1995.

[5] Ministerio de Industria y Energía, "Normas administrativas y técnicas para funcionamiento y conexión a las redes eléctricas de centrales hidroeléctricas de hasta 5.000 kva y centrales de autogeneración eléctrica." B.O.E. 219, 12 September 1985.

[6] E. Gómez, J. Fuentes, A. Molina, F. Ruz, and F. Jiménez, "Field tests of wind turbines submitted to real voltage dips under the new spanish grid code requirements," *Wind Energy*, no. 483–495, 2007.

[7] *Power Quality Analyser Topas 2000, Operation Instructions*, Eo2000g rev a ed., LEM, Liebermannstrasse F01, CAMPUS 21, A-2345 Brunn am Gebirge, AUSTRIA, www.lem.com.

[8] RD661/2007, "Real decreto 661/2007, de 25 de mayo, por el que se regula la actividad de producción de energía eléctrica en régimen especial." 2007.

Automated power system restoration

Lars Lindgren[1*,2)], Bo Eliasson[1)], Olof Samuelsson[2)]
[1)] Malmo university / TS, Östra Varvsgatan 11 H, SE-205 06 Malmö, Sweden
[*)] tlf. +46 40 665 77 95, e-mail: lars.lindgren@ts.mah.se
[2)] Industrial Electrical Engineering and Automation, Lund University, Box 118, SE-221 00 LUND, Sweden

Abstract — Wind power and other distributed generation cause new possibilities and challenges in power system restoration. The increased number of units will increase the complexity and the need of tools for off-line studies, training, automation and decision support. As a first step, an algorithm has been developed that can take a system from total blackout to normal operation. The algotrithm uses static power flows to assess the sequence of actions. The algorithm has been successfully tested on a model of a transmission system, the modified version of the CIGRE NORDIC32 test network with 32 switch yards and 35 power units.

Index Terms — Automation, A*-search, Power system restoration.

1. INTRODUCTION

Worldwide, much effort has been taken to avoid blackouts by checking that power systems fulfil the (N–1)–criterion and by using automatic equipment that takes corrective action. Despite this, events, such as the blackouts in New York[1], Italy and Scandinavia[2] during autumn 2003, show that it is very important to be able to do a fast and reliable restoration after a blackout.

The increased use of distributed generation and remote control makes it possible to do faster power system restoration at a lower voltage level. On the other hand, distributed power generation creates more uncertainty and complexity during the restoration process.

Three cases where an automatic algorithm for power system restoration can be useful have been identified:

1) On-line automatic power system restoration.
2) On-line tool for supporting the operators in a restoration situation.
3) Off-line comparative studies of the difficulties and possibilities with power system restoration in different situations in the net, summer or winter, different amount of wind power etc.

This work mainly focuses on item three, but the algorithm can be applicable to other cases as well. The algorithm is computer-based so that it can be applied to systems with high numbers of generators such as wind turbine generators and other distributed generating units. Such a system is however not used in this paper.

2. WIND POWER IN RESTORATION

The power production from wind power will decrease the number of running thermal production units before a blackout and therefore the number of units available for hot restart after the blackout. This will increase the restoration time unless the wind power plants are used in the restoration.

To make use of wind power, the restoration process must be able to handle different wind patterns as well as different load patterns and other variations of the restoration situation.

This makes written static restoration plans harder to construct and use and is a strong motivation for more automated solutions that form the sequence of actions in real-time.

Depending on the controllability and size of the wind turbines or wind farms, wind power can take different roles, from being regarded as uncontrollable “negative loads” to highly controllable power plants with fast response in both active and reactive power.

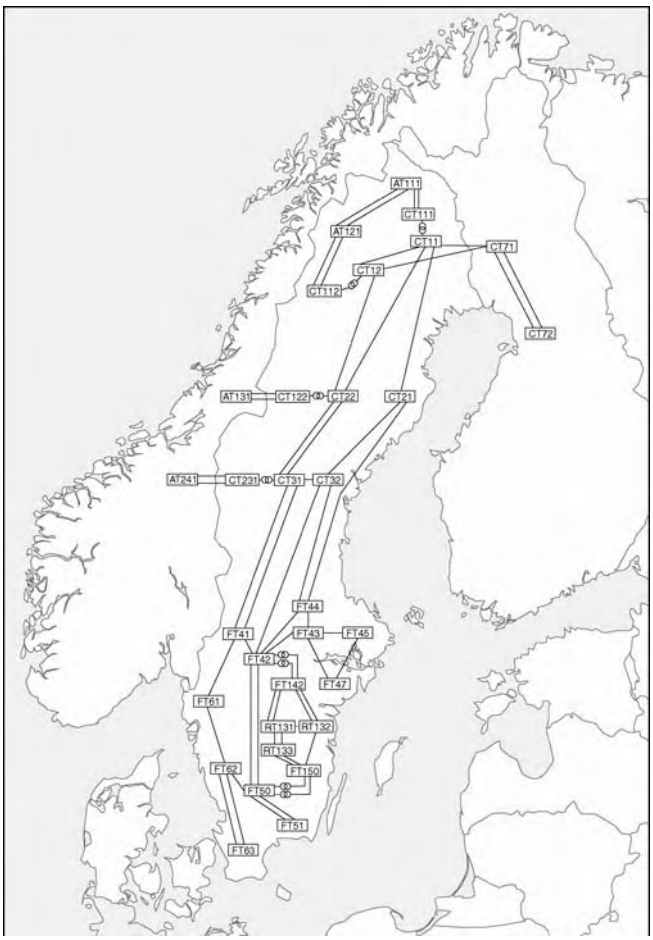

Figure 1. The CIGRE NORDIC32 is a model of a fictitious power system with certain similarities with the Nordel power system. The diagram shows the stations with their designations and all lines and transformers with approximate fictive geographic positions.

For small scale wind power the increased number of production units in it self increases the complexity of the restoration task. Altogether these factors increase the need for computer-based or even automatic restoration tools. This is the motivation for the algorithm presented here.

3. CONTRIBUTION

The main contribution of this article is to adopt a new and simple algorithmic approach to the over all restoration

problem and show that it can solve fairly complex restoration problems in reasonable time.

Table 1. Actions available to the algorithm.

Open a circuit-breaker
Close a circuit-breaker
Operate the tap changer on a transformer one step up
Operate the tap changer on a transformer one step down
Increase the set point for active power at a generating unit by 10 % of the control range
Decrease the set point for active power at a generating unit by 10 % of the control range
Increase the voltage set point at a generating unit by 1 %
Decrease the voltage set point at a generating unit by 1 %

4. MODELLING

A power flow model of the system is used for the calculations. Only the positive sequence is modelled and unsymmetries are thus disregarded. The algorithm can suggest a number of actions, see Table 1.The power system is simulated with a power flow calculation after every action in the search algorithm. The power flow calculation includes frequency calculation and limits on active and reactive power at power plants. The frequency calculation is developed from the concept of distributed slack bus. The frequency calculation assumes that all power units can be assigned frequency response characteristics in MW/Hz is applied over the entire control range.

The program also contains a complete topology calculation and handles several electrical islands running at the same time by performing a separate power flow calculation for each of them.

All connections and disconnections are made with explicitly modelled circuit-breakers. This includes the reconnection of load. Large loads have been sub-divided in smaller parts, typically 50 MW, that each is individually reconnected through the closing of a circuit-breaker. All automatics for on load tap changers, shunt reactors and shunt capacitors are assumed to be replaced with this algorithm during the restoration process.

A feasible state is a state in which the voltage and frequency at all energized nodes are within set limits and the current in all lines and transformers is below their thermal limits.

Circuit-breakers in non-energized parts of the power system are assumed to be open in the initial state, which is a fact when automatic zero-voltage tripping is employed. For a sequence of actions to be a valid solution to the problem, all intermediate states must be feasible. A state is described by:

- Circuit-breaker positions
- Tap changer settings
- Voltage set points of generating units
- Active power set points of generating units

Since the load in this model is determined only by the circuit breaker positions, no extra state variables are needed for the load. The initial state is not predetermined but a result of the power system incident.

5. ALGORITHM

In general, the starting point is a power system with an arbitrary operating state. From this state, the algorithm must find a sequence of actions that lead, in the final state, to all loads being connected.

The main difference between this problem and the planning problems normally studied in the artificial intelligence [3, part IV] domain is that the conditions that govern which actions are permitted cannot be expressed as explicit logical expressions. Instead they require a power flow calculation, after which it is possible to check whether variables such as voltages and frequency are within permitted limits.

Consequently, traditional planning algorithms such as partial order planning [3, section 11.3] cannot be used. Among other things, it is difficult to use the technology [3, page 384] to search backwards from the target state towards the initial state, since there is no fixed target state. For these reasons, a more direct method is used, namely to search for a sequence of actions from the initial state towards a goal state. The algorithm is based on the A*-algorithm [3, chapter 4] and has been adapted to the power system restoration problem. The algorithm maintains a list of all known actions and states. At the beginning this list only contains the initial state. During each iteration of the algorithm a state is chosen from the list based on the value of an evaluation function. This evaluation function is calculated from a number of variables, e.g.:

- Frequency
- Voltages
- The amount of connected loads and generators
- The number of actions in the sequences

A *second* evaluation function that contains a pseudo random term is used to select a suitable action to be applied on the chosen state; the resulting state is then calculated. The new action sequence with its resulting state is added to the list. The process continues until it finds a state where all loads are connected.

6. RESULT

The algorithm was tested using a modified version of NORDIC32 [4] with black start in north (CT72) and south (FT63) after a complete blackout. The model is shown in figure 1. The algorithm is able to find a sequence of actions that restores the power to all customers after about 800 actions. The algorithm tests about 1600 actions before it finds the final sequence.

On a PC with a 2 GHz CPU the search takes about 120 s for this model.

The algorithm is randomized and about 30% of the initiations of the pseudo random number generator succeed in connecting all loads in the power system in the first try, when it does not succeed in reconnecting all loads the algorithm can be rerun with an different initiation of the pseudo random number generator.

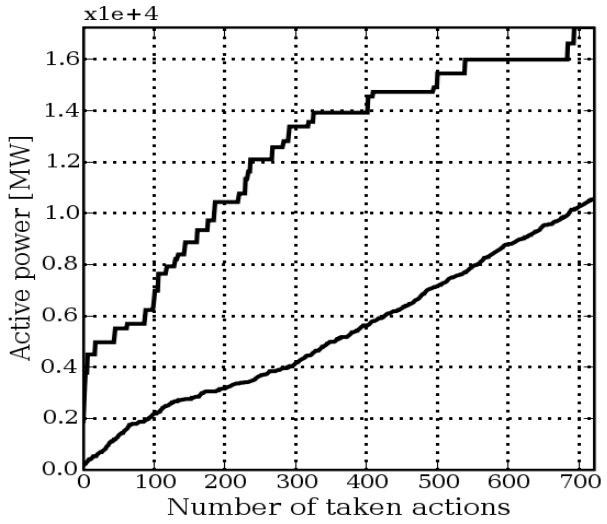

Figure 2. Result from restoration from north and south after a complete blackout in the NORDIC32 system. The upper line represents the amount of connected active generating capacity. Lower line represents the amount of connected active load. Both lines are plotted as a function of the number of actions taken in the final sequence. The total amount of load in the system is 10 900 MW.

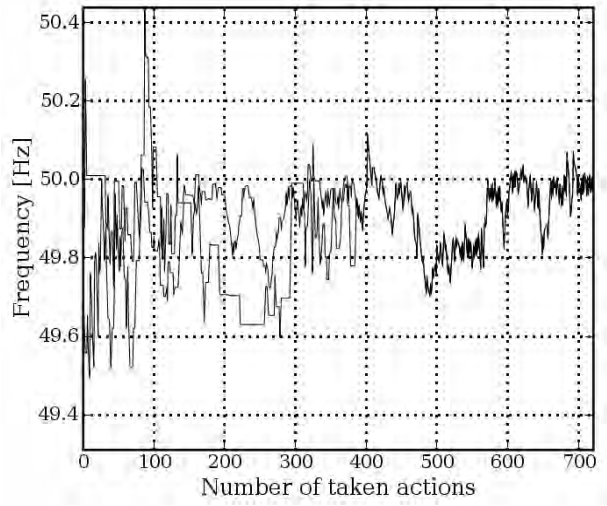

Figure 3. Frequencies as functions of number of actions applied in the final sequence.

Figure 2 shows the connection of load and generating capacity as the restoration progress.

Figure 3 shows the frequencies in the system during the restoration. As can be seen the two islands are synchronized after about 380 actions.

Figure 4 shows the search progress in the beginning of the search.

The algorithm tests a number of actions until a better state is found and then it tests to apply actions on that state. It is rather uncommon that the algorithm regrets a chosen state and tries to apply actions on an earlier state, but it is possible by this algorithm.

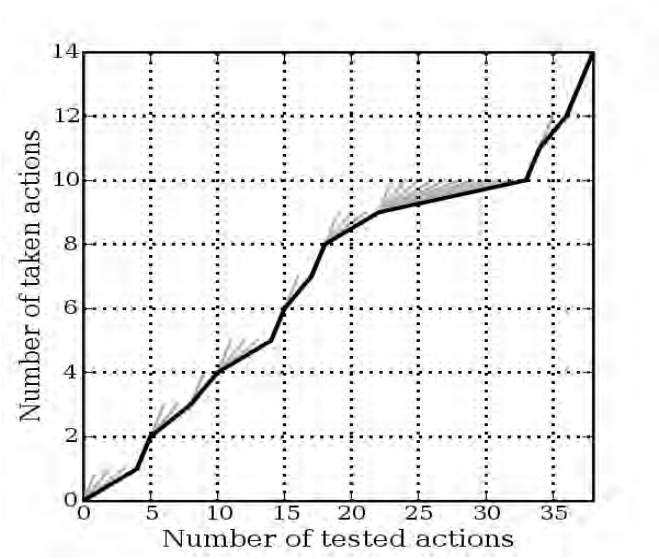

Figure 4. Length of sequence as function of number of investigated states zoomed in at the beginning of the sequence. Grey lines represent actions that are not used in the final sequence.

7. FUTURE WORK

The following future enhancements of the algorithm would be interesting to investigate:

1. Improve the algorithm so it will be able to succeed in shorter time and in more difficult cases. This can be done by a number of ways for example:
    a. Tune the parameters of the evaluation functions.
    b. Include the current number of actions tried on a state in the state evaluation function in order to promote the investigation of less closely related states.
    c. Improve the action evaluation function.
2. Use "energy not delivered" for optimization instead of "number of steps to all loads connected".
3. Make models of loads and power plants that include time dependencies such as, start time, ramping of power plants and cold load pick-up.
4. Improve the algorithm so it will be able to handle uncertainties in model data such as the size of loads and generation. This may also include handling of equipment malfunctions.
5. Verify restoration sequences in a dynamic power system simulator.
6. Interface this algorithm with a real time operator training simulator such as ARISTO[5].

Future studies on the impact of variations in different search parameters and model parameters are also needed.

One of the goals of the project is to study how distributed generation, not remotely controlled, affects the restoration process.

The algorithm is designed so that, given an arbitrary state, it attempts to find a sequence of actions that leads to a better state. For this to work satisfactorily, the evaluation function (prioritization function) must give clear guidance on which state appears best. Therefore, if modelling and evaluation

functions are adapted, situations other than restoration can be managed. This makes it possible to manage minor disturbances, adjust the voltage profile and so on.

The developed software with its source code will also be made available for other researchers.

8. CONCLUSION

The investigated algorithm gives promising results on this simplified restoration problem. Since no direct assumption of the over all restoration plan is done the algorithm should be able to adapt to very different restoration situations. As restoration processes are known to contain many unexpected events such as equipment malfunction, it is not realistic to rely on one pre-computed sequence of actions. In practice, the algorithm is instead re-run as soon as the result of a taken action differs significantly from the expected.

An algorithm like this could be used all the time to give the operators suggestions of actions, total restoration are just one of the more challenging situations to test such algorithm at.

ACKNOWLEDGEMENT

The project is funded by Energinet.dk and started in order to study the impact of distributed generation on the restoration process.

REFERENCES

[1] "Final Report on the August 14, 2003 Blackout in the United States and Canada: Causes and Recommendations," U.S.-Canada Power System Outage Task Force, April 5, 2004.

[2] Svenska Kraftnät, Rapport, Elavbrottet 23 september 2003 – händelser och åtgärder, Nr 1: 2003.

[3] Russell Stuart and Norvig Peter, Artificial Intelligence A Modern Approach, 2003, Prentice Hall, ISBN 0-13-080302-2.

[4] CIGRE TF 38.02.08, Long Term Dynamics Phase II, Final Report, March, 1995.

[5] A. Edström and K. Walve. The training simulator aristo - design and experiencies. In IEEE Power Enginering Society Winter Meeting, 1999.

GPS Synchronized high voltage measuring system

Leif S. Christensen[1)], Morten J. Ulletved[1)]
Poul Sørensen[2)], Troels Sørensen[3)], Torben Olsen[4)], Henny K. Nielsen[4)]

[1)]DELTA Dansk Elektronik, Lys & Akustik, Erhvervsvej 2 A, DK-8653 Them, Denmark. e-mail: LC@delta.dk,
[2)]Risø National Laboratory, Technical University of Denmark, VEA-118, P.O.Box 49, DK-4000 Roskilde,
[3)]DONG Energy, Teglholmen, A.C. Meyers Vænge 9, DK - 2450 København SV, Denmark.
[4)]Vattenfall A/S, Støberigade 14, 2450 København SV, Denmark

Abstract —This paper presents a measuring system build for documentation of voltage conditions in medium voltage (MV) systems and for verification of a high frequency simulation of transients in wind farm collection grids. The system consists of three units of measurement synchronized using GPS. Phase-earth voltages are measured using capacitive voltage sensors and phase currents using Rogowski-coils. The measurements are performed synchronously with 2.5 MHz sampling frequency in the three different measurement points in the grid. The measurement system runs on a Windows XP PC using National Instruments hardware and software developed in LabView for streaming data to an external FireWire harddisk.

Index terms — Transient measurements, wind farms, switching transients, synchronization, data sampling, and medium voltage (MV) systems.

1. Introduction

Although the wind power development is still mainly based on land sites, a number of large offshore wind farms have been developed, and there are significant plans for further offshore wind power development, e.g. in Denmark, Germany, the Netherlands and United Kingdom.
This development yields a need for accurate models of all main components in a wind farm (WF) as simulations are widely used to predict what happens in case of faults and switching operations in the grid and to verify design choices. The need for accurate simulations is major for offshore WFs as consequences of faults are more severe in terms of repair costs and lost revenue than for a land based WF. Transients from switching of circuit breakers (CB's) and fault situations in the MV collection grid can result in break down of components and therefore need to be addressed.
The result of simulations can always be questioned depending on the accuracy of the component models used in the simulation program, and validation of models and simulations with reliable measurements performed in a real large WF, makes it possible to verify and improve the simulations to give more reliable results.
Furthermore documentation of actual voltage conditions and current flow in a real WF gives useful information concerning the design parameters for the components and which level of stress they are going to have to withstand.

2. Defining the specification of the measuring system

The purpose of the measuring system is to document high frequency transients in large off-shore wind farms. The amplitude, the time derivative and the propagation time of the voltage and current transients are important and this reflects in the specifications for the measurement system. The number of measurement channels is given: Three voltages and three currents - totally six channels. The highest frequency simulated in [1] is 625 kHz, therefore the sampling frequency is selected to 2.5 MHz giving a Nyquist frequency of 1.25 MHz. The maximum amplitude of the transients in [1] is calculated to be below a maximum of 80 kV, this peak value sets the upper limit for measurement of the voltage. To be able to record propagation time of a transient in the MV collection grid, it is crucial that the measurement in the three different locations in the WF are synchronized within one sample e.g. 400 ns. To be able to record a switching transient in the WF, the measuring system then must record data continuously for up to 5 minutes, as the switching sequence has to be coordinated with the grid operator manually by phone and exact timing is not possible. To use the data, they must be stored on a harddisk and in a format that can be read and browsed at a reasonable speed.

3. Building the system

The measuring system consists of a recording system and transducers for measurement of voltage and current.

3.1. Data recording system

To meet the specification several solutions where discussed, from oscilloscopes to PXI-system, but the selected solution show in Figure 1 is based on PCI-cards and a stationary Windows PC, as this solution was the most cost efficient

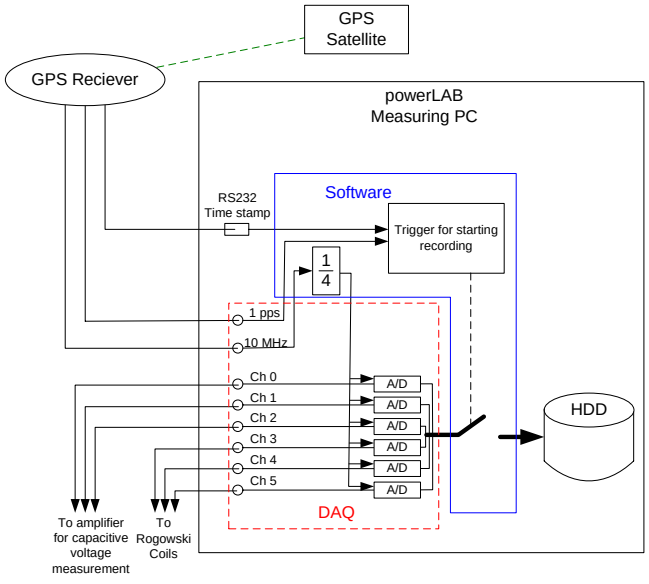

Figure 1 Principle diagram of measurement system

The system is an extension of DELTA's exciting measuring system for power quality measurements according to IEC 61400-21 [3]: powerLAB.
The data acquisition card is a PCI-card from National Instruments, it features simultaneous sampling of 8 channels at a maximum sampling rate of 2.5 MHz with a resolution of 14 bit. Saving data in LabView's TDMS-format gives 30 Mb data pr second from 6 channels. The operative system must be able to stream this amount of data to an external Firewire harddisk or an internal SATA harddisk.
The synchronization is based on a GPS timing device where one pulse per second and a 10 MHz clock signal are available together with a time stamp via serial interface. The precision of the GPS time is 100 nanoseconds. The time stamp is used for starting the measurement simultaneously in the three measuring points. The 10 MHz is divided by four to get a 2.5 MHz signal used for driving the AD-converters.
As break-out box NI suggest BNC-2110 Noise-Rejecting BNC I/O Connector Block, but test showed that the synchronization 10 MHz signal was easy disturbed in the connector block. The 10 MHz signal was disturbed by the measurement signals when switching with wind turbine and a new break out box was therefore designed, where all measuring signals and timing signals has a good ground reference. The new break-out box is also grounded together with the rest of the system.

3.2. Transducers

Measurement of high voltage at the transformer of a wind turbine involves some safety issues that have to be addressed, and furthermore connecting laboratory test equipment on a WT is generally not possible, therefore a capacitive voltage sensor system has been developed which utilizes standard high voltage equipement, thereby resolving the safety issues.
A standard high voltage T-connector is connected to the transformer as a "dead-end" and the phase to earth voltage is measured using a capacitive end-plug. The capacitive end-plug is normally used for control measurement only and not for precision measurement. The T-connector with capacitive end plug is shown in Figure 2. DELTA has developed and builds an amplifier for precision measuring with high frequency response on the end-plug. As the capacitance is very small, the measuring system is very sensitive to electrical fields and an efficient shielding is necessary to get a useful measurement. As the capacitive end-plug is not produced for precision measurements each end-plug / T-connector /amplifier combination has been calibrated with a known voltage signal before use.
The voltage measurement system consists of a standard T-connector with a capacitive end plug and an amplifier.
The specification of the system are: 20 nF input capacitance, giving a voltage ratio of 8500 : 1 depending on the end-plug, maximum input voltage of 85 kVpeak, output voltage ± 10 V, LF (3 dB) fL = 1 Hz and HF (3 dB) fH= 10 MHz.

Currents are measured with a Rogowski-coil sensor from Powertek. The flexible Rogowski-coils were chosen because the installation is very easy and it is always possible to get the coil around the cables. The specification is: 10 mV/A, peak current 600A, LF (3 dB) f_L = 0.55 Hz and HF (3 dB) f_H= 3.0 MHz.

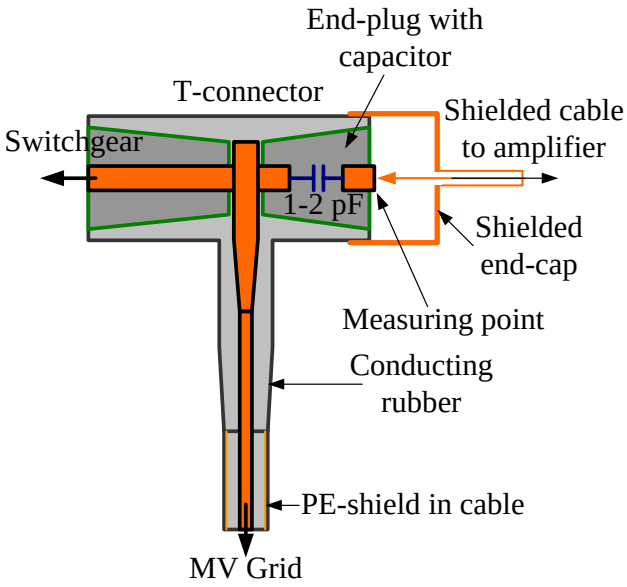

Figure 2 Capacitive measuring end-plug in standard T-connector.

3.3. Test of the system

Test of the system showed, that saving with 30 Mb/s is close to the limit of what can be possible on a Windows PC. To make the system continuously running, it was necessary to completely reinstall the PC and only have the must critical processes running. After this the data-recording runs continuously until the hard disk is full.
Synchronization was tested by setting up the three systems together and measuring the same signal. The three GPS receivers were placed on each side of the building, so the GPS receivers did not find the same satellites. After 5 minutes of recording the synchronization was still within one sample (400 ns) between the three systems.

The voltage sensor system is calibrated in the laboratory, and frequency response, temperature dependency and voltage linearity is documented.
Frequency response is tested using a network analyzer and the result shows that the system is linear up to 10 MHz (1 dB). In the high voltage laboratory the voltage linearity of the system is tested. The voltage ratio (input divided by output voltage) is linear up to 20 kV within 1 %. To determine the relation between temperature and the voltage ratio the system was cooled down to – 25°C and heated to +55°C. This showed the voltage ratio of the system is within 1 % in a temperature range from +10°C to +40°C and has a temperature coefficient on the voltage ratio -650 ppm with 20°C as reference temperature.

The data stored on the hard disk is easy to read and display using a standard LabView TDMS reader.

4. MEASUREMENT RESULTS

Measurements where made on Nysted Offshore Wind Farm, Denmark. The 72 off-shore wind turbines are placed in a parallelogram consisting of eight rows of nine wind turbines each. The wind turbines are delivered by the Danish wind turbine manufacturer Siemens Wind Power (BONUS). The tower is 69 m and the rotor has a diameter of 82 m. Each wind turbine has a max. production of 2.3 MW. The total output of the off-shore wind farm is 165.6 MW.
Measuring points were chosen to be (see Figure 3):

- At the transformer platform after the circuit breaker for radial A (the radial on the west side of the farm).
- At wind turbine A01, the first turbine in the radial A.
- At wind turbine A09, the last turbine in the radial A.

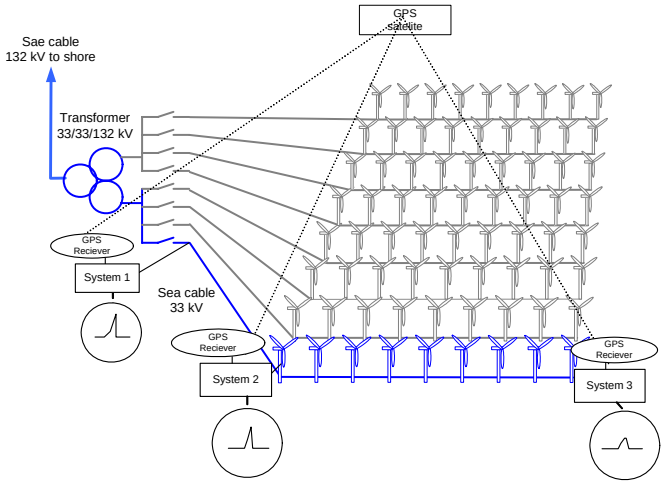

Figure 3 Measuring points at Nysted Offshore Wind Farm

Several switching transients where generated and recorded by switching the line breaker for the radial A and the load breaking switch in turbine A09.

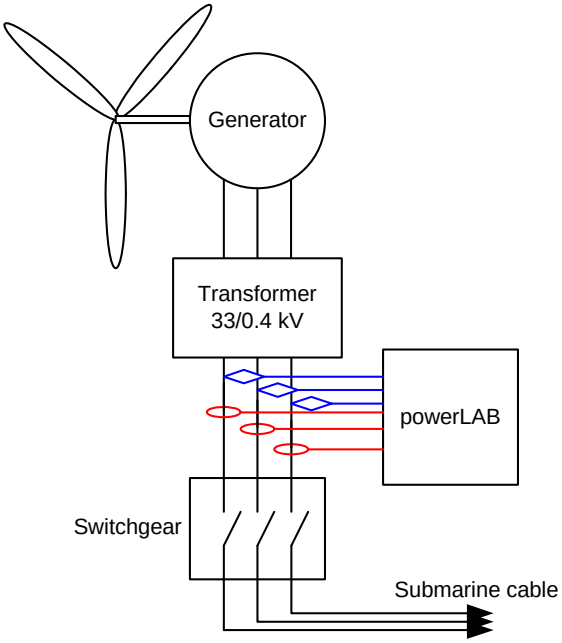

Figure 4 Measuring points in the wind turbine

4.1. Closing of line breaker radial A

The line breaker for the first row of wind turbines (radial A) was switched off and on to record the energisation of the radial cable and the magnetisation of the transformers in the nine wind turbines connected to the radial.
The opening of the breaker is not shown here. For the closing of the line breaker the voltages are shown Figure 5 and the currents in Figure 6. Time /div is 20 ms.
The voltages measured at the three locations are very similar at the ms time scale, and except for the first few milliseconds immediately following the energization the voltages appear not to be distorted (i.e. the short circuit power level is high enough to sustain the voltage during energization of a radial without significant distortion).

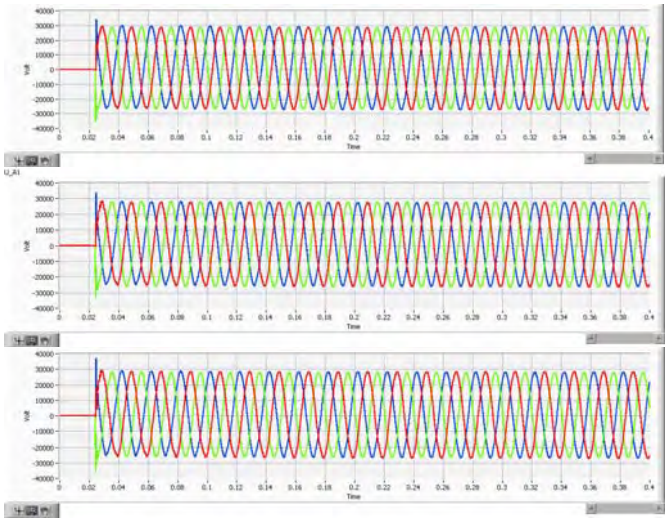

Figure 5 Voltage measurements at three locations during closing of the line breaker. Top: Transform platform, Middle: Turbine A01, Bottom: Turbine A09. Time: 20ms/div

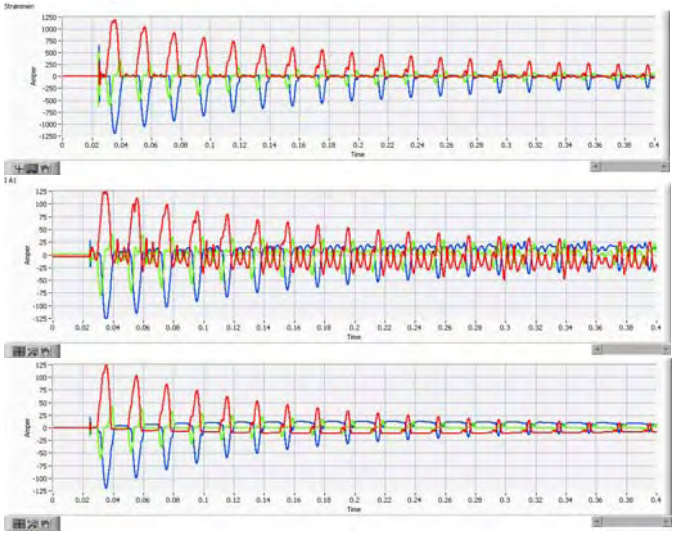

Figure 6 Current measurements at three locations during closing of the line breaker. Top: Transform platform, Middle: Turbine A01, Bottom: Turbine A09. Time: 20ms/div.

The currents measurements clearly show the effects of the saturation of the wind turbine transformers which results in very asymmetrical currents. In the wind turbines peak currents reach 125 A (i.e 2.2 p.u.) in the first period and decrease to under 1 p.u. after 10 periods. Although the wind

turbines are identical is the current more distorted in turbine A01 than in turbine A09.
On the transformer platform the measured current peaks at 1190 A (i.e. 2.3 p.u.)
With a 50µs/div resolution is it possible to see the voltage wave traveling from the transformer platform to turbine A01 and to A09 during the period after closing of the breaker. The closing of the breaker does not happen simultaneously for the three phases: there is a delay from phase 2 (green) is closed to phase 1 (red) of 227 µs and from phase 2 (red) to phase 3 (blue) another 140 µs. It can be noted that the energization of an individual phase doesn't affect the voltage of the other phases. This is because the phase cables are shielded and grounded individually, and therefore there is no appreciable capacitive coupling of the phases.
The amplitude of the voltage at the transformer platform is 18.3 kV and the front of the wave is very sharp.
It takes the wave 21 µs to travel from the platform to A01, where the front of the wave is rounded due to damping in the cable. The amplitude is of the front is 15.5 kV. It takes the wave 25 µs to travel from A01 to A09.
At A09 the wave meets an open end and the voltage is doubled to 27 kV and the front is rounded.
The wave travels back to A01 in 25 µs and from A01 to the transformer in 21 µs.
The corresponding current measurements, shown in Figure 8 show the primarily capacitive current charging the submarine cable of radial A measured at the platform reaching 600 A peak, and narrow 15 A to 30 A current peaks less than one microsecond wide measured at wind turbine A01 and A09 due to the charging the capacitances of the MV transformers in the wind turbines.

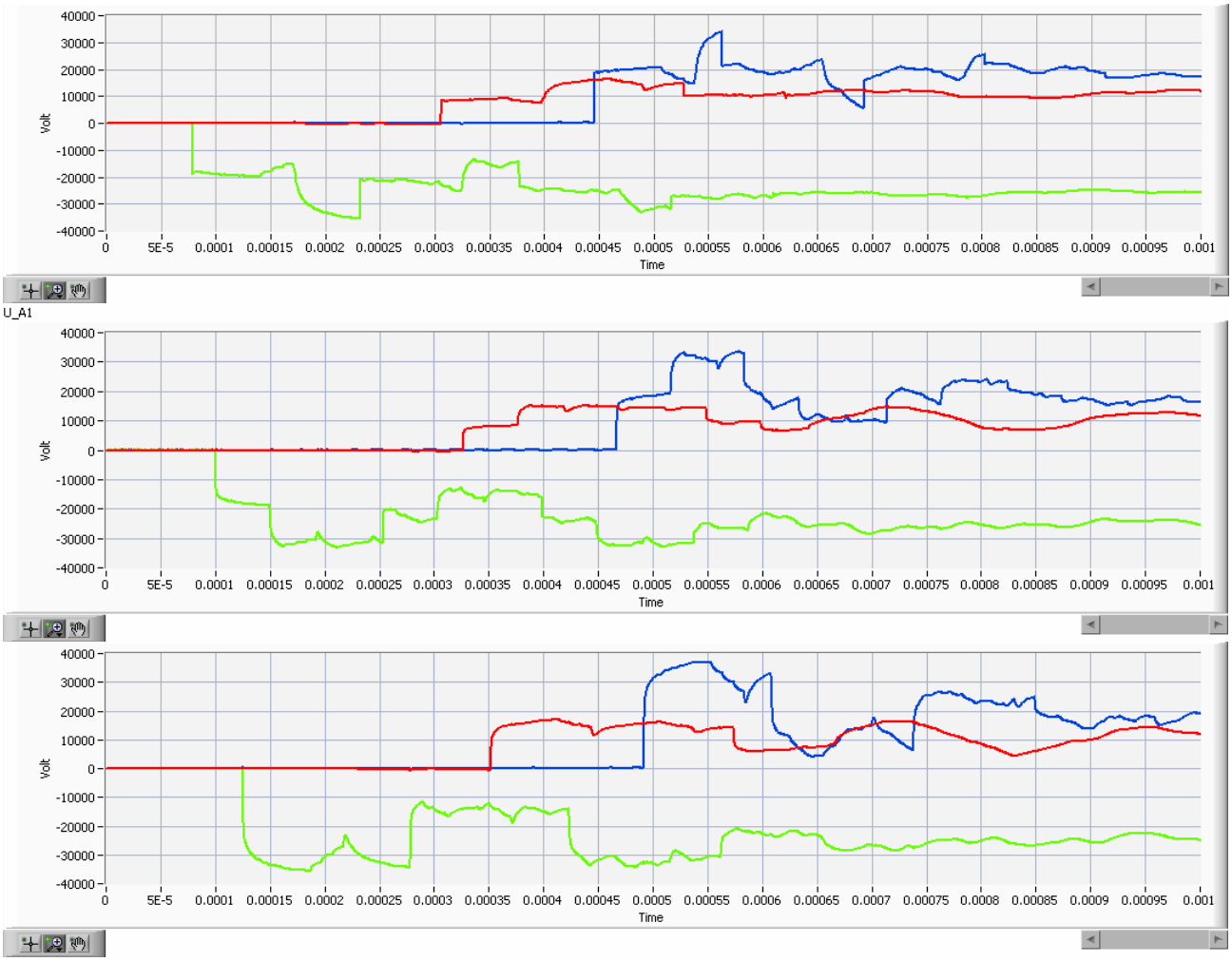

Figure 7 Voltage measurements at three locations during closing of the line breaker. Top: Transform platform, Middle: Turbine A01, Bottom: Turbine A09. Time: 50µs/div.

Figure 8 Current measurements at three locations during closing of the line breaker. Top: Transform platform, Middle: Turbine A01, Bottom: Turbine A09. Time: 50µs/div.

4.2. Closing of the load breaking switch in wind turbine A09

Opening and closing of the high voltage switch in a wind turbine is a normal operation that can happen many times during the life time of the offshore wind farm. It is therefore important to investigate if this practice produces any transients that can affect the wind turbine transformer or even the other turbines in the wind farm.

Figure 9 shows the voltage and Figure 10 shows the current in the three measuring points during closing of the switch in wind turbine A09. The other wind turbines of radial A including A01 were stopped during this test. There is no sign of any voltage transients from the switching on neither A01 nor at the transformer platform, as the short circuit power in the wind farm is high enough to hold the voltage during magnetization of the transformer of A09. The measurement in A09 show the current drawn for magnetization of the wind turbine transformer, which peaks above 125 A (the current probes saturates at 125 A) which is significantly higher than what was measured when switching with the line breaker for radial A. At wind turbine A09 the saturation of the transformers result in a very asymmetrical currents and peak currents above 125 A (i.e. 2.2 p.u.) in the first six periods. After 18 periods the peak current has fallen to below 1 p.u. The measurements performed in wind turbine A01, which was connected but not operating, show some distortion of the no load currents.

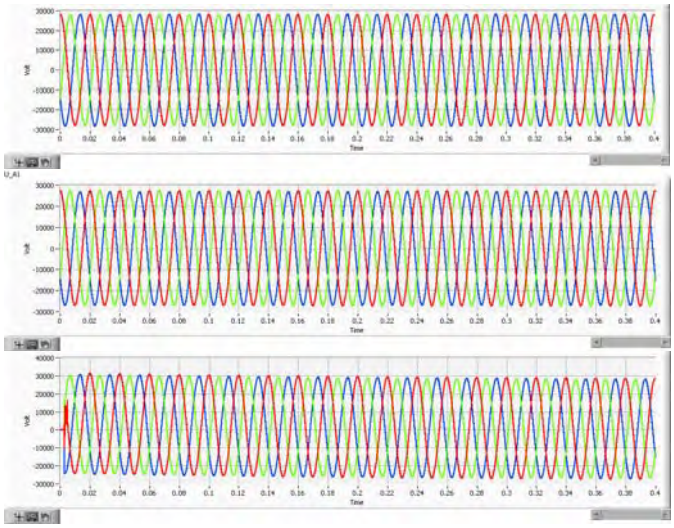

Figure 9 Voltage measurements at three locations during closing of switch in the wind turbine A09. Top: Transform platform, Middle: Turbine A01, Bottom: Turbine A09. Time: 20ms/div.

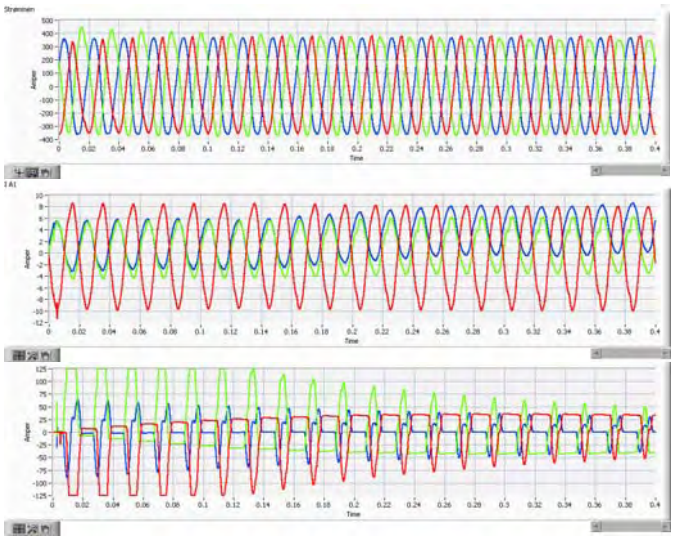

Figure 10 Current measurements at three locations during closing of switch in the wind turbine A09. Top: Transform platform, Middle: Turbine A01, Bottom: Turbine A09. Time: 20ms/div.

5. CONCLUSION

Three GPS synchronized measuring systems have been built and used for simultaneous measurement at three different locations in a large off-shore wind farm. The precision of the synchronisation is better than or equal to one sample (i.e. 400 ns). The sampling frequency has been set to 2.5 MHz and simultaneous recording of six channels at 14 bit resolution totally producing 32 Mb of data per second is recorded onto a harddisk. A voltage measuring system for medium voltage based on standard T-connectors with a capacitive end-plug and an amplifier has been developed for the measurements. The voltage measuring system has a linear frequency response up to 10 MHz, the voltage ratio is also linear up to 20 kV.

Measurements have been made with the three systems at Nysted Offshore Wind Farm, Denmark and measuring results has been presented.

The measurement results will be used for verification of simulation models of the wind farm thereby making it possible to have a more accurate determination of transient voltage conditions in a wind farm during faults and switching events.

ACKNOWLEDGEMENT

This paper describes the measurement system and the measurements performed within the project entitled "Voltage conditions and transient phenomena in medium voltage grids of modern wind farms", contract 2005-2-6345, funded by Energinet.dk. The project is carried out in a cooperation between DELTA (project manager), DONG Energy, Vattenfall and Risø National Laboratory

REFERENCES

[1] L. Liljestrand, A. Sannino, H. Breder, S. Johansson. "Transients in Collection Grids of Large Offshore Wind Parks". NORDIC WIND POWER CONFERENCE, 22-23 MAY, 2006, ESPOO, FINLAND

[2] P. Sørensen, A. D. Hansen, T. Sørensen, C. S. Nielsen, H. K. Nielsen, L. Christensen, M. Ulletved, "Switching transients in wind farm grids", European Wind Energy Conference & Exhibition, 7-10 May 2007, Milan, Italy

[3] IEC 61400-21. "Measurement and assessment of power quality characteristics of grid connected wind turbines". First edition. Dec 2001.

[4] Powertek, Current sensor CWT LF Data sheet: http://www.powertekuk.com/cwt_lf_ptk.pd

[5] Nysted Havmøllepark. http://www.nystedhavmoellepark.dk

Building Confidence in Computer Models of Wind Turbine Generators from a Utility Perspective

James Toal[1], Helge Urdal[2], Jonathan Horne[2], Yvonne Coughlan[3], Cornel Brozio[4], Brian Punton[5], Alistair Brown[6], Wojciech Wiechowski[7]

[(1)] JayTee Consulting (Scotland) (james@jayteeconsulting.co.uk)
[(2)] National Grid Electricity Transmission, [(3)] Eirgrid, [(4)] Scottish Power Energy Networks,
[(5)] Scottish Hydro-Electric Transmission, [(6)] Northern Ireland Electricity, [(7)] Energinet.dk

Abstract — Computer models of wind turbine generators for power system studies have recently been developed and supplied to power system operators worldwide. There appears however to be no consensus on the level of modelling detail required. Also, the models developed vary widely in complexity and performance. A number of TSOs, who operate in all four European networks, therefore decided to collaborate in comparing the response of wind turbine models in their respective power system simulation software packages.

This paper describes the process by which the TSOs were able to agree to collaborate in this effort without breaching their licence obligations in regard to confidentiality, and summarises the progress made to date in comparing and validating the performance of wind turbine models in multiple software packages.

Index Terms – Power System Planning Studies, Transmission System Operator, Wind Turbine Modelling.

1. Introduction

The rapid pace of development of wind turbine (WT) generation technology – particularly of the doubly-fed induction generator (DFIG) and full converter (FC) types – coupled with the growing level of applications to connect such new technology to the power network, increases the need of the host transmission system operator (TSO) to adequately represent these generators in its localised and system-wide simulation studies. Much valuable work has been done by manufacturers and research establishments to simulate the dynamic response of DFIG and FC machines to various types of disturbances, both from the mechanical (wind energy conversion) and electrical (network) sides of the machine. These have resulted in a broad measure of agreement on the modelling practices used to represent these technologies. However, in the authors' experience, these models tend to be very detailed, focusing on the manufacturers' own R&D objectives, and many are not well-suited to the requirements of utilities' multi-machine stability studies. Furthermore, manufacturers' legitimate desire to protect commercially sensitive information can inhibit the open disclosure of testing and verification of the models, which further limits the TSOs' confidence in the suitability of the models for utility applications.

Computer models of conventional synchronous machine have been developed to the stage where there is an industry-wide consensus as to what constitutes a valid and useable model. Also, the response of these models to network disturbances is well understood and familiar to users. The structure of many synchronous machine models including associated control systems are publicly available (e.g. in IEEE block diagram format), as are 'typical' machine and control system parameters (whilst remaining confidential in specific projects). This, together with the mature status of conventional machine modeling in commonly-available power system simulation packages, gives TSO users good reason to be confident in their system studies. This is not presently the case with wind turbine models.

Another difficulty faced by TSOs when including wind turbine models in their system studies is that they frequently receive these models as 'black box' elements to be incorporated into their power system simulation packages. Where problems develop with a particular model, or an inexplicable interaction occurs between several models, it is impossible to remedy or even investigate the cause. Even if a mathematical description of the model is available, the challenge for the TSO is to be sure that the encrypted code credibly reproduces the machine's actual response to network disturbances.

In addition, TSOs need such models to be compatible with other models used in multi-machine system studies. This implies not only comparable simplifying assumptions (especially as regards the model/network interface, and the neglect of very small time constants), but also that the maximum integration step should conform to their common practice in synchronous machine studies. In the authors' view, this is not the case with many current WT models.

All of these factors combine to reduce the confidence that TSOs have in the validity and reliability of their connection and system stability studies involving WTs.

2. Solution Adopted

To address this challenge constructively and methodically, the TSO members of the European Wind Turbine Model Validation Technical Panel (the EWTMVTP) agreed to collaborate on a programme of simulation studies to compare the response of wind turbine models in their respective power system simulation platforms, using commonly-agreed single- and multi-machine test networks. The members of the EWTMVTP – National Grid Electricity Transmission, Scottish Power Transmission, Scottish Hydro Electricity Transmission, Eirgrid, Northern Ireland Electricity/SONI and Energinet.dk – operate in all the four synchronous networks of Western Europe. The Panel also secured support from an independent Consultant with considerable experience and expertise in power systems modelling and simulation.

2.1. Preliminary Issues and Working Agreements

Before the Panel could begin their work, a number of issues had to be addressed. These included:-

- Drafting a multi-party collaboration agreement and Non-Disclosure Agreement (NDA) which allows the TSOs to co-operate to a defined and limited extent whilst respecting their licence obligations and preserving the confidentiality of the manufacturer's technical information. Key to this agreement is the Panel's undertaking to study a particular WT model only with the prior consent of the manufacturer concerned, and not to

publish their study results without the manufacturer's agreement.

- Securing the agreement of the relevant manufacturer for their WT model to be included in the study and for the participating TSOs to exchange such information on their respective versions of the model as was necessary to ensure like- for-like comparison.
- One of the factors the TSOs must take into account is that their interest in a particular WT usually begins with a connection application, which their licence conditions oblige them to keep confidential. The Panel therefore decided that each TSO should carry out their simulations for this exercise independently of each other using their own power system software, and designed the test network and conditions to be unrelated to any specific connection application.
- Agreeing Panel governance, including the financing of the work and each party's role. This included defining the test networks and test conditions, the studies to be performed, and procedures for the unbiased comparison and interpretation of study results and of investigating and resolving differences without breaching confidentiality.

2.2. Panel Membership and Organisation of Work

Initially, the Panel decided to limit its membership to TSOs with a direct interest in the WT models under consideration: principally in order to keep the management of its work simple. Thus windfarm developers and power system simulation software developers were not asked to participate in the work of the Panel, although we do welcome their support and cooperation.

Each Panel member covers its own costs and is expected to take on a reasonable share of the workload – which mainly comprises the working up and snagging of the models and data, and the execution of the simulations. Face-to-face meetings of the Panel are kept to a minimum: typically only to review results and reports, or to meet with the manufacturer concerned. The Panel's remaining workload mainly involves liaison with WT manufacturers to obtain their consent and cooperation, and the collation and reporting of multiple study results, which is carried out by the independent Consultant.

3. TEST NETWORKS AND TEST CONDITIONS

The Panel settled on two test networks:-

BN1 (figure 1). This is a simple single-machine/infinite bus network, similar to that used in calibrating excitation controllers of synchronous generator models and to the networks used in manufacturers' WT simulations.

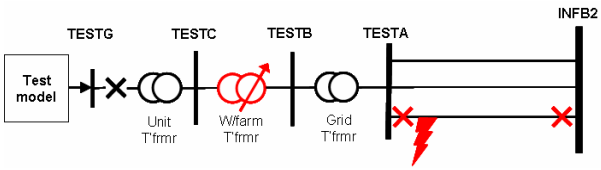

Figure 1. Test network BN1

Whilst not specifically representative of actual system conditions, it does permit the fault response of the WT model and the influence of its control systems to be simulated without introducing too many external complications. Also, by suitable choice of network parameters, it can represent conditions at the point of connection of a WT to the TSO's network. Thus the response of the model in this network can be made indicative of that observed in commissioning tests, although this is beyond the scope of work of the Panel.

BN2 (figure 2). This network captures some of the characteristics of a multi-machine system without requiring an excessive amount of data or introducing too many uncertainties as to its response to faults and/or circuit switching. The network allows the representation of up to three test models (windfarms) connected to the corresponding system HV busbar, and allows the Panel to examine their interaction with six groups of conventional synchronous machines (S2, S3, S5, S6.1, S6.3 and S7).

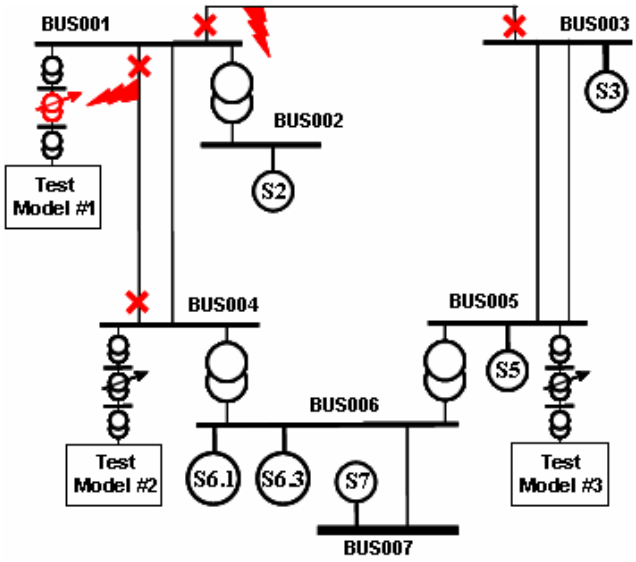

Figure 2: Test network BN2

With the parameters chosen, this system is known to exhibit a very lightly damped oscillatory response to faults such as those indicated. Thus it is expected to expose the test WT models to sustained transients and machine interactions of a kind that actually occur on large power systems. Also, as its complexity lies midway between that of BN1 and a full multi-machine system, it gives TSOs some indication of what to expect in a full system simulation with many windfarms represented.

3.1. Test Conditions

Both networks offer considerable scope to apply a variety of disturbances in systems of different strength.

For its initial studies, the Panel decided on the programme of tests listed in Table 1. These are designed to explore the WT model response to system conditions of particular interest to the TSOs. Transformer tap steps test the operation of WT MVAr/voltage controllers, whilst network faults allow comparison of its fault ride-through and transient stability performance.

Some of the tests defined for each network are designed to be similar in effect: this redundancy is intended to ease comparison and verify study continuity. Other tests will be

Table 1. Test conditions applied.

Test #	Net work	Test Model	Test Condition
1	BN1	100MW WT	Single tap increment to the windfarm transformer, TESTC-TESTB
2	BN1	100MW WT	3-phase fault at TESTA, cleared by opening one of the circuits TESTA-INFB2
5	BN2	100MW WT at BUS001	Single tap increment to the windfarm #1 transformer, TESTC-TESTB
6	BN2	100MW WT at BUS001	3-phase fault at BUS001, cleared by opening BUS001-BUS003 circuit
7	BN2	100MW WT at BUS001	3-phase fault at BUS001, cleared by opening BUS001-BUS004 circuit #1
11	BN2	100MW WTs at busses 1,4 & 5	Single tap increment to the windfarm transformer, TESTC-TESTB
12	BN2	100MW WTs at busses 1,4 & 5	3-phase fault at BUS001, cleared by opening BUS001-BUS003 circuit
13	BN2	100MW WTs at busses 1,4 & 5	3-phase fault at BUS001, cleared by opening BUS001-BUS004 circuit#1

added to the list as and when they are deemed necessary and appropriate to the particular WT model under examination.

Note that network BN2 offers the possibility of simulating unit tripping or load switching to investigate frequency response capability, or to explore interaction (if any) between different WT models. But again this is outwith the scope of the Panel's workplan.

In each test, the simulations are performed for a duration of 30s, using a 5ms integration timestep (fixed or maximum according to the simulation package), with the test disturbance applied at t=5s.

4. PRELIMINARY STUDIES

Before carrying out comparative simulations on WT models, the Panel's initial efforts were directed to rehearsing and fine-tuning the test procedures.

The aim of this step was to verify the equivalence of the test network data and conditions in each TSO's simulation software, before progressing to examine WT models. It was considered advisable for each TSO to satisfy themselves as to the viability of the planned test procedure on their own power system analysis software for a selected test case using conventional synchronous models.

In this initial phase, three simulation platforms were used – Siemens/PTI's PSS/E, DIgSILENT's PowerFactory and Tractebel's Eurostag. There is no significance to this choice: they are simply the software packages currently used by the participating TSOs.

In the event, this proved a very necessary step, as it allowed the Panel to verify the consistency of the network and model data, the initial conditions and the simulation parameters across each of the simulation platforms used with known models. Inevitably, even with 'identical' models and data, the different software packages gave slightly different answers when simulating the same test condition, due to many factors outside the TSOs' control – even when using conventional and well-understood models. Such factors as: the integration algorithms used; the treatment of the machine-network interface; the treatment of infinite busbars and reference frames; and the different modelling of loads and controllers, all cause the simulation results to diverge slightly.

Notwithstanding all of the above, the Panel were able by means of these preliminary studies to obtain a very good sense of the agreement that might reasonably be expected across the different simulation platforms. Figure 3 and 4, for example, show the response of test (synchronous) machine #1 generated real and reactive power in test #13 for each of the three simulation packages – identified here only as (1), (2) and (3). There is a small but noticeable difference in each case, but we consider the agreement is good enough for the Panel's purposes.

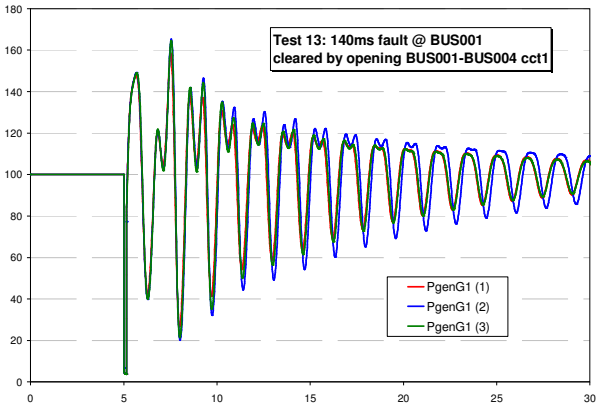

Figure 3: Real power of Test machine 1 in Test #13

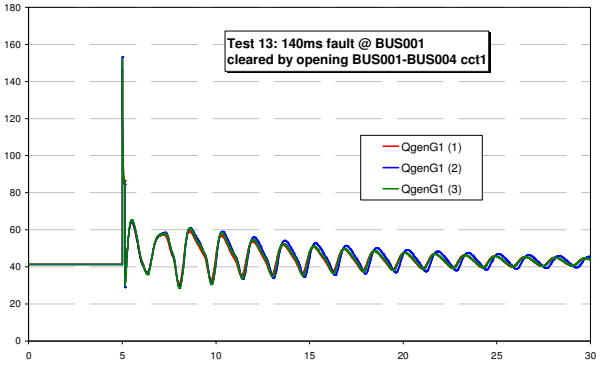

Figure 4: Reactive power of Test machine 1 in Test #13

5. WT MODEL STUDIES

The Panel is currently working on WT models from several manufacturers covering a variety of types of WT technology.

In compliance with the Panel's agreement to respect their confidentiality, the authors do not propose to name these

manufacturers, or to present results of our work on their models. Suffice it to say that they are among the major providers of new technology WTs in the European market, and that the results obtained so far give the Panel confidence that it is progressing in the right direction.

In reaching this stage of our work, the Panel has benefited greatly from the manufacturers' advice and cooperation. Other manufacturers are welcome to support our effort provided they have, or plan to have, wind turbines installed in at least one of the areas covered by the TSOs in the Panel, and they consent to the Panel's aims . This welcome is also extended to manufacturers of HVDC converters, including the VSC converter technology which is expected to play an increasing role in the connection of large scale offshore wind.

Manufacturers who do support the Panel's work are encouraged to take an active role in progressing their model through our tests. They will receive, in confidence, full details of the test networks and results relating to their own WT. We encourage them to compare our results to their own simulations and laboratory or site tests on actual WTs: we believe this is the ultimate validation of any model. They will also receive, if they wish, copies of models of their WTs that have been developed by the Panel in the course of this work, which they may release to third parties without any form of liability or service offered by the Panel.

The authors wish, however, to stress that the Panel's aim is not to compare WTs of different manufacture or technology, but to compare representations of a particular WT model in several power system simulation packages in order to satisfy themselves that these produce essentially the same, correct, response to network disturbances, preferably validated by comparison with tests on a real machine.

It is hoped that our cooperative efforts will lead to benefits for all concerned, TSOs and manufacturers, through a common understanding of the scope of application of the models, a shared confidence in their veracity, and – ultimately – to better and more reliable WT models.

6. PRELIMINARY CONCLUSIONS

The work of this project is not yet complete. Indeed it will not be for some time, given the rapid pace of technology developments in this field. However, some of our initial conclusions are summarised below:–

- We need clarity on the p.u. basis of the model data. Many models base the mechanical side data (turbine limits, pitch controllers, etc) on the rated power of the machine, and the electrical data on its rated MVA. Since the rated MVArs of a WT depend on its connection and application, the former might be the better choice, but consistency and clarity are needed.
- Controller limiters need to be better defined and implemented. In some cases these are non-windup limits, in other cases not. Several apparent differences in controller response (especially on the MVAr/ voltage controller side) were ultimately tracked down to differences in the representation of limits.
- It remains an open question how detailed the WT model needs to be. Many models include the highly non-linear wind-power characteristic, and with that the blade pitch controller dynamics. Yet in some cases, the authors have noted that the assumption of constant shaft mechanical power (which ignores all the above) gives practically the same dynamic response to network disturbances. Blade pitch dynamics may need to be represented if that is pertinent to the WT's fault ride-through response: this will be considered further. Nevertheless this simplifying assumption does lead to a simpler WT model, and is at least consistent with the assumption commonly made in simulating e.g. synchronous machine fault response.
- Very detailed or highly complex models cause difficulty in reliably and consistently initialising the WT model (especially from the loadflow terminal conditions: many assume a pre-knowledge of wind speed), rendering them impractical in multi-machine system studies.
- Great care has to be taken to ensure that the system load flows and model initial conditions are the same for the different software platforms, especially in regard to off-nominal transformer taps, voltage profiles and machine MVArs. Slight differences in these can give very misleading divergence in the WT's dynamic response.
- As discussed above, unavoidable differences between simulation packages means that perfect agreement between simulations will not be achieved. A reasonable degree of divergence in response has to be accepted. However, this should not be significantly more than can be ascribed to the differences in simulation software and efforts should be made to minimize these differences.

This paper has outlined a collaborative utility-led process that has been (and continues to be) successfully followed by a group of TSOs to test dynamic WT models on a variety of power system simulation platforms. Such models are essential for the accurate simulation of the transmission system as increasing volumes of new-technology wind generation are connected to the system. They will help to ensure that TSOs' simulations and planning studies reliably and credibly represent the effect of WTs on system stability and security, and fairly reflect their projected compliance with Grid Code requirements.

The legitimate desire of WT manufacturers to protect the confidentiality of their technology has sometimes acted to hinder utilities' efforts to assess and verify WT models suitable for use in transient stability studies or other dynamic network simulations. The Panel is very aware of the commercial sensitivity of much of the information provided by manufacturers and operates under the terms of an NDA that is strictly observed.

Comparative testing of a selected WT model proceeds only with the explicit consent of the relevant manufacturer. Each TSO with access to the model independently performs simulations according to the agreed test programme using their own power system software. The results are collated and compared, then reported only to the Panel and the relevant manufacturer.

ACKNOWLEDGEMENT

The authors wish to express their appreciation of the support, advice and assistance given to this project by several manufacturers of wind turbine generators.

Analysis of the Grid Connection Sequence of Stall- and Pitch-Controlled Wind Turbines

Gustavo Quinonez-Varela*), Andrew Cruden, Olimpo Anaya-Lara, Ryan Tumilty and James R. McDonald
Institute for Energy and Environment, University of Strathclyde,
204 George St., Glasgow, G1 1XW, UK
*) tlf. +44 141 548 2609, e-mail gustavo.quinonez@eee.strath.ac.uk

Abstract — The realistic modelling of wind turbines and wind farms is crucial in any form of power system analysis, and consequently, knowledge about their electrical characteristics and performance is also vital. One of the operating conditions producing major transient interaction between a wind turbine generator (WTG) and the local grid is the grid connection sequence itself, which is particularly significant in fixed-speed turbines. This paper presents experimental measurements of the grid connection sequence of both types of fixed speed wind turbines, i.e. stall- and pitch-controlled, via a soft-start device performed at two existing wind farms. Some of the results evidenced significant discrepancies between the actual soft-start operating intervals and those stated/suggested by open literature. The discussion of the paper focuses on highlighting the importance of accurate modelling of the grid connection sequence in order to avoid erroneous estimations of the interaction between the turbine and the grid during this operating state, or inappropriate design of the grid connection.

Index Terms — Wind power generation, power system analysis, wind farm design.

1. INTRODUCTION

The increasing penetration of wind power in existing power systems presents challenges on assessing the potential grid impacts such as stability and quality of supply. However, to assess the impact, knowledge about the electrical characteristics of the wind turbines is needed as otherwise the result could easily be an erroneous estimation of the interaction between the turbine and the grid, or an inappropriate design of the grid connection.

As a consequence, the realistic modelling of wind turbines and wind farms is crucial in any form of power system analysis. Constructing a suitable and reliable model requires model validation by comparing the model results against measurements of the actual wind turbine behaviour.

Although modelling of wind turbines have been the subject of numerous research works and a range of models are found in the open literature, experimental data is not easily available. In consequence, model validation becomes a complicated task.

A number of International efforts have been carried out, such as the IEA Annex XXI [1], in order to collect detailed wind turbine data, internal grid specifications and grid connection characteristics for accurate modelling. The data include experimental measurements of electrical characteristics (i.e. active and reactive power, voltage and currents) at the point of common coupling of the wind farm and at a number of the individual wind turbines.

According to the IEA Annex XXI documentation, experimental measurements have been focused on operating conditions during normal operation and response to voltage dips (i.e. grid faults).

One of the operating conditions producing major transient interaction between a wind turbine generator (WTG) and the local grid is the grid connection sequence itself. This condition is particularly significant in fixed-speed turbines.

Although the increasing presence of doubly-fed induction generators, a large number of fixed speed machines are currently in operation in power systems worldwide. For instance, in the UK, 75% of the total installed wind turbines (approximately 1067 machines) are fixed speed machines, accounting for a total of 756 MW [2]. In addition, a significant number of fixed speed wind turbines are available in the market from a number of manufacturers in a range of power capacity from 30 to 2300 kW [3].

This paper presents experimental measurements of the grid connection sequence of both types of fixed speed wind turbines, i.e. stall- and pitch-controlled, which were performed at two existing wind farm sites in Scotland. The presented experimental case studies have a high archival value since it provides utility engineers and researchers a better understanding of the transient interaction between fixed-speed wind turbines and the local grid during the grid connection sequence.

2. FIXED SPEED WIND TURBINE GENERATORS

In general, a fixed-speed wind turbine is equipped with a squirrel cage induction generator (SCIG) whose stator winding is directly connected to the local grid. Despite the term ‘fixed-speed’, the SCIG operates within a narrow range of rotational speed, which varies according to the generated output power (e.g. slips of about 1-2%) [4].

Figure 1 illustrates a schematic diagram of a typical fixed speed WTG equipped with a conventional SCIG, a thyristor-based soft-start module and its grid connection components.

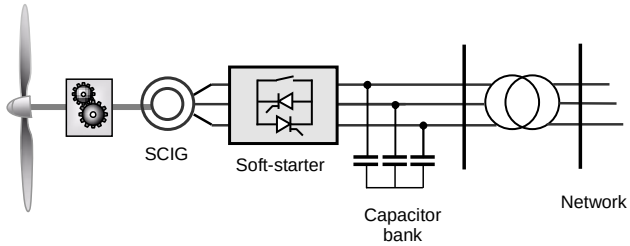

Figure 1. Schematic representation of a fixed-speed wind turbine

Due to its nature, a SCIG wind turbine requires a continuous source of reactive power, to feed its magnetic circuit, which is drawn from the local grid. A common solution to alleviate this condition is the utilisation of power factor compensation capacitors which supply the whole, or part, of this reactive power demand.

A soft-start module is normally utilised to minimise the inrush current required to magnetise the SCIG. Inrush current can result in overcurrents of between 4 to 6 times the magnitude of the rated current, and may be responsible for large starting torques in the drive train.

2.1. Stall-regulated Wind Turbines

Stall-controlled wind turbines have the rotor blades bolted onto the hub at a fixed angle. The rotor blade profile has been aerodynamically designed to ensure that the moment the wind speed becomes too high it creates turbulence on the side of the rotor blade which is not facing the wind. This stall prevents the lifting force of the rotor blade from acting on the rotor.

The literature [5],[6] refers that stall-regulated wind turbines must be rapidly connected to the power network since the turbine torque may exceed the maximum generator torque. This results in a turbine overspeed.

2.2. Pitch-regulated Wind Turbines

Pitch regulation means controlling the rotor blades angle via an electronic controller which checks the power output of the turbine constantly. When the power output becomes too high, the blade pitch mechanism immediately pitches (turns) the rotor blades slightly out of the wind. The rotor blades have to be able to turn around their longitudinal axis. This type of control does not only prevent damage to the turbines during strong winds but also maximises the turbine power output during these strong winds.

As pitch regulation provides a way of controlling the wind turbine torque, in [5],[6] it is stated that the connection of these type of turbines to the power network can be achieved in a smoother, more controlled fashion. Hence, a longer period of soft-starting is mentioned.

2.3. Soft-Starting

The soft-start module features a pair of thyristors connected in anti-parallel (back-to-back configuration) on each phase. To operate in a current limiting feature, delayed firing pulses are generated, with a trend of increasing the conduction angle of each thyristor. In this fashion, the phase current is increased from zero to rated current. Each thyristor in the anti-parallel array conducts on the appropriate positive half cycle of the supplied voltage, enabling full-wave control. Figure 2 illustrates the effect of modifying the thyristor conduction angle, which is related to the firing angle α by the relationship $\alpha = 180° - \theta$.

The soft-starter operates over a time interval and thereafter it is by-passed via a contactor in order to eliminate losses generated in the thyristors.

Generally, three types of soft-starter configurations are applicable in induction machines namely star, delta and branch delta [7]. In wind turbine applications, mainly the delta and star are utilised, having basically the same layout for the thyristor circuit but differentiated by the connection of the generator winding.

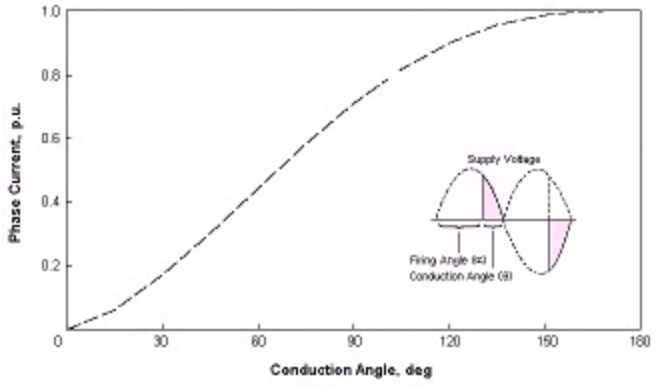

Figure 2. Evolution of the phase current with the variation of the conduction/firing angle of the thyristor.

3. HAGSHAW HILL (STALL-REGULATED TURBINES)

Hagshaw Hill wind farm is located on grass uplands South Lanarkshire, Scotland. The site has twenty-six Bonus 600MkI wind turbines (stall-regulated) rated at 600 kW, giving a total generation capacity of 15.6 MW. The turbines are standing 35m high, with a rotor diameter of 40m [8]. The site was commissioned in 1995 and was Scotland's first wind farm. It is owned by ScottishPower plc and is operated by Sinclair Knight Merz (SKM).

Figure 3 illustrates the wind farm layout at Hagshaw Hill and shows the monitored wind turbine.

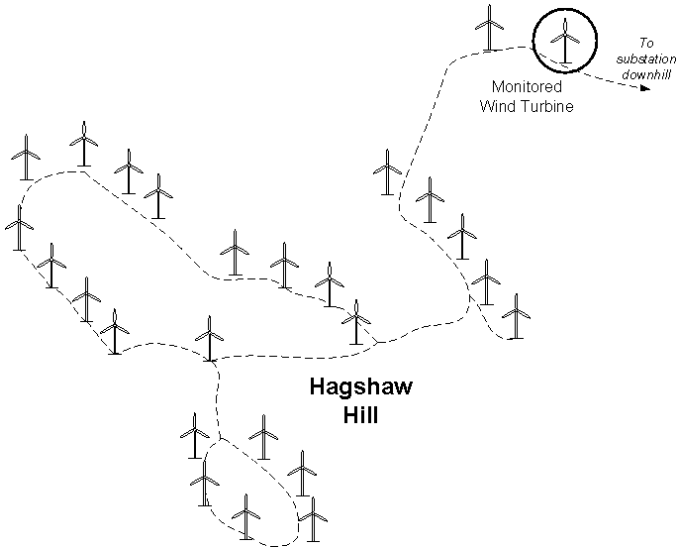

Figure 3. Monitored wind turbine within at Hagshaw Hill wind farm.

3.1. Test Equipment and Procedure

The measurements at Hagshaw Hill wind farm were carried out using an advanced power analyser, namely Dranetz BMI Power Platform PP-4300, with the capability to function as a DAQ [9]. The utilised 'Multi-DAQ Task Card' permitted logging short- and long-term waveform data at 128 samples/data per cycle (i.e. data logging at 6.4 kHz based on a 50 Hz signal).

This instrument comprises 4 differential voltage channels capable of directly measuring up to 600 Vrms (1000 Vpk), and 4 independent current channels to directly measure phase currents via non-intrusive clamp-type CT. A CT rated at 3 kA was utilised for this monitoring set-up, considering the in-rush current was above 1 kA.

The monitoring procedure comprised recording the instantaneous voltage and current waveforms during the turbine start and connection to the network. During the start up the rotor slowly accelerated from rest to cut-in wind speed and was then connected to the grid. This procedure was repeated a number of times.

3.2. Experimental Results

Once the wind speed is sufficient to self-start the turbine, the rotor is accelerated up to synchronous speed (i.e. at cut-in wind speed, which is 4 m/s in the case of the Bonus 600MkI), and the grid connection process is initiated by closure of the generator circuit breaker (by-passing the soft-starter).

Figure 4 illustrates a record of the instantaneous current in one of the phases during the initial cycles of the connection procedure. The action of the soft-start module in limiting the magnitude of the current during the initial cycles is clearly demonstrated in Figure 4. The thyristors operate over a period of 10 cycles (50 Hz system) before being by-passed by the main contactor.

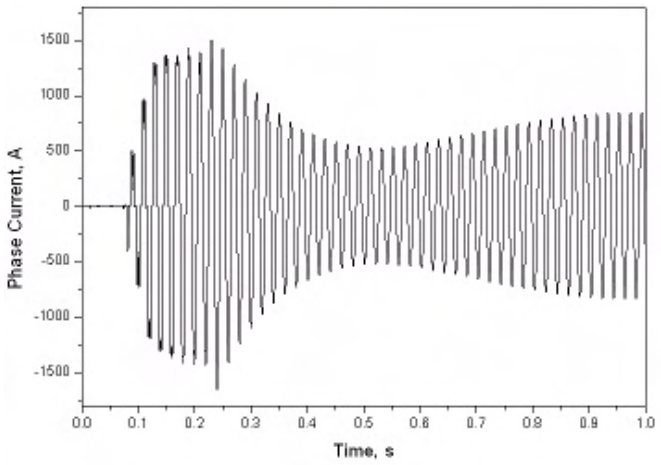

Figure 4. Instantaneous current waveform (phase A) during the soft-start stage, recorded at Hagshaw Hill.

The voltage across the thyristors was also experimentally measured and is illustrated in Figure 5. It clearly shows that the soft-starter thyristors are fired late in the voltage cycle and then the firing angle advanced (over the period of 10 cycles) until the entire AC voltage waveform is applied to the generator. After the by-pass, the voltage across the thyristor becomes zero.

The operation of the soft-start module produces varying harmonics as the firing angle of the thyristors is modified. Figure 5 evidently shows the harmonic distortion of the AC current waveform during the 10 cycles of soft-starter operation. The distortions are higher at the beginning and gradually lessen as the firing angle reduces and the thyristors move towards to full conduction. However, the soft-start module is only used for a very short period of time for which the effect of the harmonics is considered to be harmless and may be ignored, according to the International Standards.

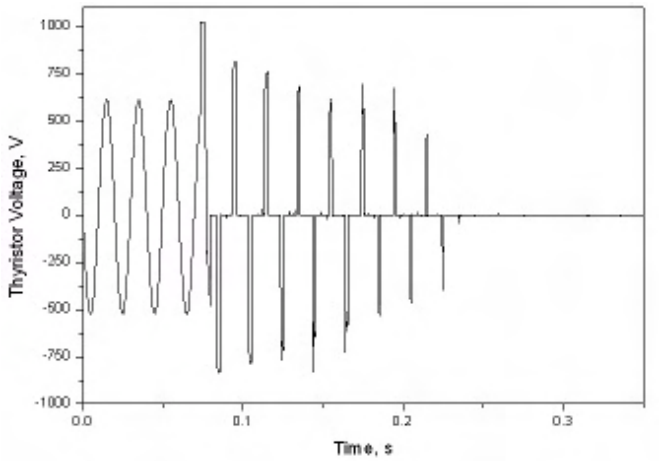

Figure 5. Instantaneous voltage across the thyristors (phase A) during the soft-start stage, recorded at Hagshaw Hill.

4. HARE HILL (PITCH-REGULATED TURBINES)

The wind farm at Hare Hill is situated on high level moorland close to New Cumnock in East Ayrshire, Scotland. The site has twenty Vestas V47 wind turbines (pitch-regulated) rated at 660 kW, giving a total generation capacity of 13.2 MW. The turbines are standing 40m high, with a rotor diameter of 47m [10]. Hare Hill was the first wind farm in the UK to be built without any renewable energy subsidy. The wind farm is owned by ScottishPower plc and is operated by B9 Energy O&M.

Figure 6 illustrates the wind farm layout at Hagshaw Hill and shows the monitored wind turbine.

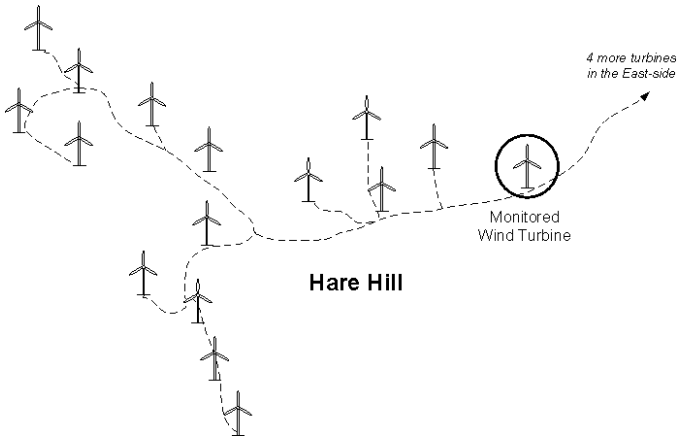

Figure 6. Monitored wind turbine within at Hare Hill wind farm.

4.1. Test Equipment and Procedure

For this experimental measurement, a THS730A handheld oscilloscope with 2 independently floating isolated channels was utilized for recording instantaneous voltages and currents waveforms [11]. The floating voltage channel is capable of directly measuring up to 600 Vrms (1000 Vpk). The current was measured in the second channel via a non-intrusive clamp-type CT. A CT rated at 1 kA each were

utilised for this monitoring set-up, considering the in-rush current was above 1 kA.

Similarly to the previous case, the monitoring procedure comprised repeatedly recording the voltage and current waveforms during the turbine start (from standstill) and its grid connection.

4.2. Experimental Results

The cut-in wind speed of the Vestas V47 is 4 m/s at which the turbine is accelerated up to synchronous speed and the grid connection process is initiated by closure of the generator circuit breaker (by-passing the soft-starter).

Figure 7 illustrates a record of the instantaneous current in one of the phases during the initial cycles of the connection procedure. In the case of the Vestas V47 the soft-starter thyristors are operated over a period of 34 cycles (50 Hz system) before being by-passed by the main contactor.

Despite the lower resolution of the oscilloscope unit in comparison to the power analyser used in Hagshaw Hill, the measurement provides a satisfactory illustration of the soft-starter operating interval.

The voltage across the thyristors is illustrated in Figure 8. It clearly shows that the progression of the thyristors firing angle until the full AC voltage waveform is applied to the generator. After this, the soft-starter is by-passed and the voltage across the thyristor becomes zero (after the determined period of 34 cycles).

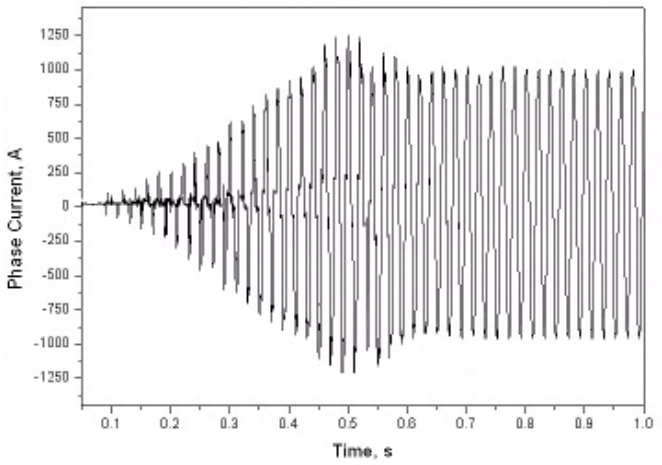

Figure 7. Instantaneous current waveform (phase A) during the soft-start stage, recorded at Hare Hill.

5. IMPACT OF SOFT-STARTER MODELLING

Some work published in the open literature suggest that soft-starters in fixed-speed wind turbines, disregarding wheter stall- or pitch-controlled turbine, normally operate for a period of 1-3 seconds [12]. Also, basic bibliography states that soft-start units operate for a period of "some seconds" [13] or "a few seconds" [14], also disregarding the type of fixed-speed turbine. For the specific case of pitch-regulated wind turbines, in [6] it is suggested that soft-starters in these type of turbine normally operates for a period between 2 to 3 seconds.

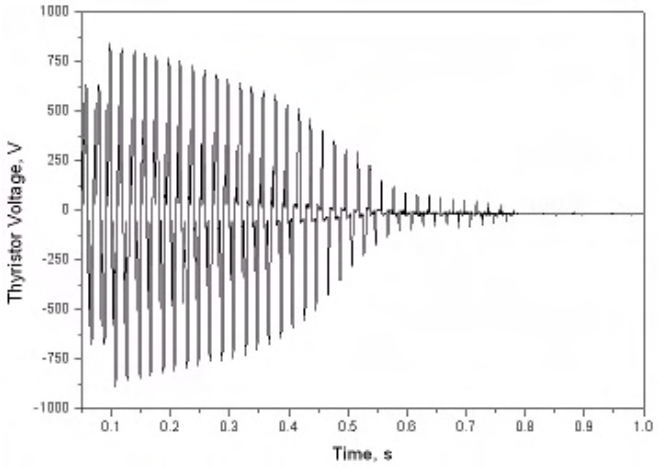

Figure 8. Instantaneous voltage across the thyristots (phase A) during the soft-start stage, recorded at Hare Hill.

The results presented in this paper demonstrate that the stall-regulated wind turbine under analysis (Bonus 600MkI) has a very short operating interval of soft-starting, determined to be 10-cycles. This agrees with the notion of fast connection in order to avoid overspeed [6]. However, this shows that the generalised suggestion in existing literature, as in [13] and [14] for instance, of "a few seconds" operation of soft-starters is ambiguous.

For the case of pitch-regulated, the results demonstrate that longer soft-starting, in comparison to stall-regulated turbines, might not be always the case. The determined soft-starting of the wind turbine under analysis (Vestas V47) was 34-cycles, which is approximately 3 times higher than that of the Bonus 600MkI. However, compared to the operating intervals suggested in literature for pitch-regulated turbines (up to a maximum of 3 seconds, suggested in [6]), the experimentally-determined interval is 4 times smaller.

As demonstrated in the above results, the erroneous or mistreated operation of wind turbine soft-starting will lead to inaccurate assumptions of the transient conditions of voltage drop and voltage recovery at the point of common coupling during the connection to the power network. This situation can potentially compromise the action of protection equipment by causing 'mystifying' nuisances such as misreading and miscoordination of protective devices.

6. CONCLUSION

One of the operating conditions producing major transient interaction between a wind turbine generator (WTG) and the local grid is the grid connection sequence itself, which is particularly significant in fixed-speed turbines. Therefore, to realistically model these types of wind turbines, a comprehensive knowledge about their electrical characteristics and performance is crucial.

This paper focused on an experimental analysis of the starting sequence of stall- and pitch-regulated fixed-speed wind turbines via thyristor-based soft-start devices. The turbines under consideration were a 600-kW Bonus 600MkI which is part of the 26- turbine Hagshaw Hill wind farm, and a 660-kW Vestas V47 which is part of a 20-turbines Hare Hill wind farm, both located in Scotland. Some of the results evidenced significant discrepancies between the actual soft-

start operating intervals and those stated/suggested by open literature, particularly in the case of pitch-regulated wind turbines The discussion of the paper focuses on highlighting the importance of accurate modelling of the grid connection sequence in order to avoid erroneous estimations of the interaction between the turbine and the grid during this operating state, or inappropriate design of the grid connection.

These experimental results are very useful to give engineers, operators and developers a good indication of the performance of these two wind turbine types during the connection to the power network. In addition, the results can be used in the validation of dynamic models of fixed-speed wind turbines to be used in power system studies.

ACKNOWLEDGEMENT

The authors acknowledge the assistance of ScottishPower Power Systems, ScottishPower Wind Farm Operations Group, Sinclair Knight Merz (SKM) and B9 Energy for allowing access and wind turbine measurements at Hagshaw Hill and Hare Hill wind farms.

REFERENCES

[1] J.O. Tande *et. al.* "Dynamic Models of Wind Farms for Power System Studies - Status by IEA Wind R&D Annex 21", in *Proc. of the European Wind Energy Conference and Exhibition EWEC '04*, 22-25 November, London UK, 2004.

[2] *Operational Wind Farms in the UK*, British Wind Energy Association (BWEA), 2006.

[3] *Wind Turbine Market 2006: Wind Turbine Market: Types, Technical Characteristics and Prices*, SunMedia Verlags-GmbH, ISBN 3-9810389-0-8, 2006.

[4] L. Holdsworth, X. Wu, J. B. Ekanayake and N. Jenkins, "Comparison of fixed speed and doubly-fed induction wind turbines during power system disturbances," IEE Proceedings Generation, Transmission and Distribution, 2003, Vol. 150, (3), pp. 343-352.

[5] A. Larsson. "Guidelines for Grid Connection of Wind Turbines". Proc. Of the 15th International Conference on Electricity Distribution, CIRED '99. 1-4 June, Nice, France, 1999.

[6] A. Larsson. "Flicker Emission of Wind Turbines caused by Switching Operations". IEEE Trans. On Energy Conversion, Vol. No. , pp.

[7] F. Iov, A.D. Hansen, F. Blaabjerg and R. Teodorescu. "Modelling of Soft-Starters for Wind Turbine Applications", in *Proc. of the Power Electronics Intelligent Motion Conference PCIM-2003, Power Quality*, Nuremberg, Germany, 20-22 May, pp. 179-184. 2003.

[8] *Bonus 600 kW MkI: The Wind Turbine Components and Operation*, Bonus Energy A/S, 1999

[9] *Power Platform PP-4300: MultiDAQ Taskcard User Manual*, Dranetz BMI, July 2002.

[10] *Vestas V47/660 kW: Wind Turbine Operating Manual*, Vestas, 1997.

[11] *THS730A Handheld Oscilloscope User Manual*, Tektronix, 2002.

[12] T. Thiringer. "Grid-Friendly Connecting og Constant-Speed Wind Turbines Using External Resistors". IEEE Trans. On Energy Conversion, Vol. 17, No. 4, pp. 537-542, 2002.

[13] N. Jenkins., R. Allan, P. Crossley, D. Kirschen. and G. Strbac. "Embedded Generation", IEE, London, UK, ISBN 0852967748, 2000.

[14] T. Burton, D. Sharpe, N. Jenkins and E. Bossanyi. *Wind Energy Handbook*, Wiley & Sons, ISBN 0-471-48997-2, 2001.

Fault ride-through and voltage support of permanent magnet synchronous generator wind turbines

Gabriele Michalke [1*)], Anca Daniela Hansen [2)], Thomas Hartkopf [1)]
[1)] Darmstadt Technical University, Department of Renewable Energies, Landgraf-Georg-Straße 4, 64283 Darmstadt, Germany
[*)] tlf. +49 6151 16 2367, e-mail gmichalke@re.tu-darmstadt.de
[2)] Risø DTU, VEA-118, P.O. Box 49, DK-4000 Roskilde, Denmark

Abstract — This paper presents a control strategy of direct driven multipole PMSG wind turbines, which enhances the fault ride-through and voltage support capability of such wind turbines during grid faults. A dynamic simulation model of the turbine is implemented in the simulation software DIgSILENT. Simulation results approve the effectiveness of the developed control strategy. It is shown that PMSG wind turbines equipped with such control even enable nearby connected conventional wind turbine to ride-through grid faults.

Index Terms — Permanent magnet synchronous generator wind turbine, fault ride-though, grid codes, grid fault, voltage support, DIgSILENT.

1. INTRODUCTION

The multipole permanent magnet synchronous generator concept (PMSG) with full-scale frequency converter is an appropriate solution for offshore wind turbines, as it requires low maintenance and at the same time it offers high efficiency and good controllability. PMSG wind turbines are thus anticipated to achieve an increased market penetration on the wind turbine market in the following years [1].

Due to the increasing penetration of wind power, the power system operators request newly installed wind turbines to ride-through and support the power system stability during grid faults. Fault ride-through capability is required in order to avoid significant loss of electrical power supply during grid faults. The goal of this paper is therefore to design a control strategy, which enhances the capability of wind farms based on multipole permanent magnet synchronous generator wind turbines to satisfy these new requirements.

The multipole PMSG wind turbine is connected via a full-scale frequency converter to the grid. As the converter decouples the generator from the grid, the generator and turbine system are not directly subjected to grid faults in contrast to direct grid connected wind turbine generators. It can thus be presumed that such full-scale converter connected wind turbine can easier accomplish fault ride-through and can support the grid during faults.

This paper presents an analysis of the PMSG wind turbine's dynamic behaviour during grid faults. Based on this, a control strategy for grid fault operation is developed.

The paper is organized as follows. First, the control strategy of the PMSG wind turbine for normal operation is briefly described. Then, an advanced control strategy developed for fault ride-through and voltage grid support is presented. The control strategy for a PMSG wind turbine during grid faults addresses both the control and protection of the frequency converter and the control of the wind turbine itself. An aggregated model for a large PMSG wind farm is presented and used to analyse the interaction of such wind farm and a generic power system. The investigations are carried out by means of a comprehensive dynamic simulation model in the software DIgSILENT Power Factory.

2. THE PMSG WIND TURBINE CONCEPT

The present paper deals with the direct driven multipole permanent magnet synchronous generator (PMSG) wind turbine concept with full-scale frequency converter. Direct drive wind turbines, characterized as high efficient and low maintenance solutions, offer high potentials for future applications [2], especially offshore. A direct driven multipole permanent magnet synchronous generator mounted in a wind turbine is shown in Figure 1 [2].

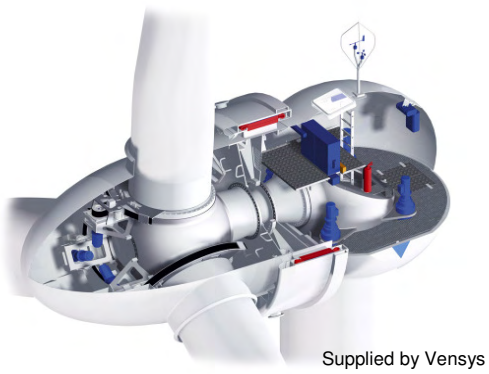

Figure 1: Wind turbine with multipole PMSG, supplied by Vensys [2]

A comprehensive dynamic simulation model of the PMSG wind turbine is implemented in the simulation software DIgSILENT Power Factory. The PMSG wind turbine model is sketched in Figure 2. It contains models for both the aerodynamic and mechanical part of the turbine as well as for the electrical system and its control structure. A detailed description of the turbine modelling and the control structure for normal operation of the PMSG wind turbine is presented in [3] and is therefore only briefly presented in the following.

2.1. Control Strategy of the PMSG wind turbine

The control of the PMSG wind turbine is realized by a coordinated control of the converter control and the wind turbine control. The frequency converter control is divided into two controllers: a control for the generator side converter and a control for the grid side converter, while the wind turbine control contains the blade angle control. The control task of the generator side converter is to maintain both a constant DC-link voltage as well as a constant stator voltage for the generator. At the same time the grid side

converter controls independently the active and reactive power production of the turbine in the wind turbine's point of common coupling. In wind turbines connected via a full converter the reactive power production of the grid side converter is independent of the reactive power set point of the generator. The active power reference value is provided by a maximum power point tracking look-up table, which assures operation at maximum aerodynamic efficiency of the wind turbine. A constant DC-link voltage guarantees that the generator power is transferred to the grid. Nevertheless, small variations of the DC-link voltage are allowed in order to damp torsional oscillations in the drive train whenever the system gets excited. Based on the generator speed signal a damping controller adds an oscillating offset to the DC-link voltage, which provokes in turn a torque component counteracting possible drive train oscillations. The blade angle control controls the speed of the system. For wind speeds below rated power, the blade angle control is not active, while the pitch angle is kept constant to its optimal value. As soon as rated wind speed is reached, the blade angle control controls the speed to its rated value and limits thus indirectly the power to its rated value, too. As indicated in Figure 2 the control for normal operation is extended by a control stage for grid faults.

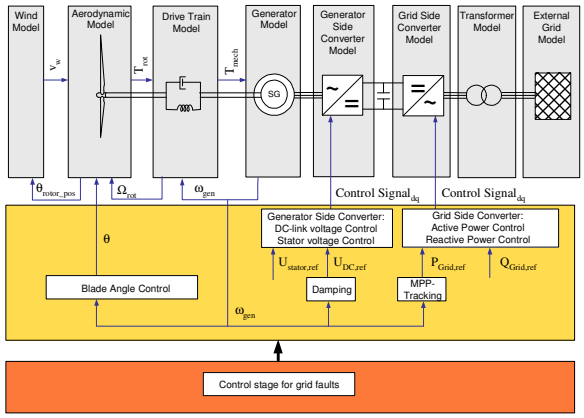

Figure 2: PMSG wind turbine dynamic simulation model and control strategy for normal operation and grid fault operation

3. Dynamic behaviour of the PMSG under grid faults

As the multipole PMSG wind turbine is grid connected via a full-scale frequency converter it can be presumed, that this wind turbine concept has very good grid support capability compared to any other wind turbine concept. Furthermore, the converter system decouples generator and turbine from the grid so that both are less subjected to the grid fault impact compared to turbines with direct grid connected generator. In order to confirm the above made assumptions the dynamic behaviour of PMSG wind turbines under grid faults and their fault ride-through and grid support capability is described and analysed in the following.

As a consequence of a grid fault the voltage at the PMSG terminal drops causing a drop of active power, too. The active power delivered to the grid by the grid side converter is thus reduced, while the wind turbine continues its power production. This leads to a power imbalance in the wind turbine system.

As long as the generator side converter continues to deliver the generated power from the generator to the DC-link, while the active power of the grid side converter is reduced, the power imbalance causes a charging of the DC-link capacitor. This can be represented by the following equation [5]:

$$U_{DC}(t) = \sqrt{U_{DC}^2(0) + \frac{2}{C}\int_0^t \left(P_{GenSC}(\tau) - P_{GridSC}(\tau)\right) d\tau} \qquad (1)$$

P_{GenSC} Power transferred by the generator side converter
P_{GridSC} Power transferred by the grid side converter
U_{DC} DC-link voltage
C DC-link capacitor

This power imbalance of the turbine must then be dissipated in the system. Different possible manners for that are itemized in the following [4]:

(i) In order to avoid the charging of the DC-link capacitor, which could cause overvoltages in the DC-link, a chopper can be applied to the DC-link. A chopper represents a parallel resistance, which is added parallel to the capacitor in the DC-link. The chopper is switched on if the DC-link voltage exceeds a critical level and the surplus power is burned in the chopper resistance.

(ii) In the present control strategy the control task of the generator side converter is to keep the DC-link voltage constant. During a fault the grid side converter transfers less power to the grid. As a consequence the generator side converter control will decrease its active current component in order to reduce the power flow into the DC-link. This causes a decrease of the stator current, so that the generator power decreases as well. The power imbalance is so transferred to the generator instead of the DC-link. When the generator power is decreased, while the turbine power stays constant, the power imbalance leads to an acceleration of generator and turbine. The power surplus is then buffered in rotational energy of the rotating masses.

(iii) If a power imbalance between turbine and generator power arises, as explained under (ii), the turbine starts to accelerate. If the speed increases above its rated value the pitch control increases the pitch angle, which reduces the aerodynamic power and counteracts the acceleration. However, the response time of the pitch system is very slow compared to the time frame of the fault. The action of the pitch system and the reduction of aerodynamic power becomes therefore relevant in case of long faults.

It has been mentioned before, that grid codes generally require voltage support and reactive power supply of the wind turbine during grid faults [6], [7]. This means, that the reactive current component in the control of the grid side converter has to be prioritized, while the active current component is limited. In the worst case, the active current component (d-current) is forced to zero and no active power can be fed to the grid during the fault. In this case the power imbalance between the turbine continuing its power production and the grid side converter transferring no power into the grid becomes maximum.

In order to enhance the fault ride-through capability of PMSG wind turbine in case of severe grid faults, several measures are proposed and described in the following section.

4. FAULT RIDE-THROUGH CAPABILTY

Fault ride-through enhanced by control

Two different control strategies for the converter system are illustrated in Figure 3 and compared in the following.

Figure 3a) shows the converter control, which is generally applied to full converter wind turbines [8], [9], [10] [11] with IGBT converter. DC-link voltage and reactive power are controlled by the grid side converter, while active power and stator voltage are controlled by the generator side converter. In contrast to this Figure 3b) shows the here applied control strategy. The DC-link voltage is instead controlled by the generator side converter while the power is controlled by the grid side converter. If the control strategy of Figure 3a) is applied, a grid fault causes the following conflict. First, a voltage drop limits the control capability of the grid side converter in general, as the voltage level is low during the fault and the converter limitations are therefore reached faster. Second, grid codes often require reactive power supply during a voltage drop to support the voltage level. This means, that reactive power control has first priority, which again limits the control capability for DC-voltage control. Moreover, the generator side converter continues to deliver power to the DC-link. Due to this reason, an additional coupling between generator side converter control and grid side converter control must be implemented to reduce the power flow from the generator side converter [8]. If however, the here developed control strategy of Figure 3b) is applied, no additional control for fault ride-through is necessary. The DC-link voltage can be kept constant by means of the generator side converter control, which has no limited control capability during the fault. This means that fault ride-through capability is already integrated in the implemented control strategy. Notice that such control is only possible if an active rectifier e.g. IGBT converter is used.

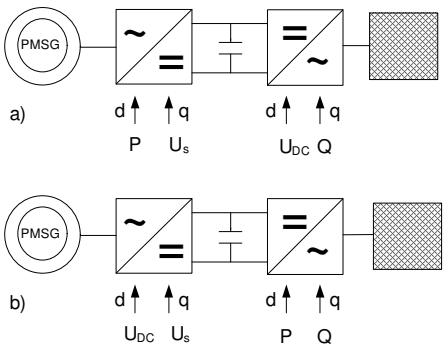

Figure 3: Two different control strategies for the power converter of the PMSG wind turbine.
a) The DC-voltage is controlled by the grid side converter.
b) The DC-voltage is controlled by the generator side converter.

Overspeed protection

When the DC-voltage is kept constant by the developed control system, the power imbalance is automatically transferred to the generator side and the generator starts to accelerate. In case of longer grid faults the acceleration can be counteracted by means of blade pitching. The pitch controller implemented in the presented model controls the generator speed and therefore it can directly be used as an overspeed protection. Note that the pitch angle control, illustrated in Figure 1, prevents over-speeding both in normal operation and during long grid faults. In case of over-speeding, the aerodynamic power is automatically reduced while the speed is controlled to its rated value. This means that there is no need to design an additional pitch control solution for grid faults.

Limitation of U_{DC}

In normal undisturbed operation the control tasks of the DC-voltage controller is to control the DC-voltage to a reference value, which is provided by a superiour damping controller. This damping controller operates similar to a power system stabilizer in a DC excited synchronous generator of large conventional power plants [12]. The damping controller, as shown in Figure 2 and Figure 7, interacts with the DC-voltage controller and causes DC-voltage variations around the constant DC-voltage reference value. However, when speed oscillations become too strong under grid faults, large DC-voltage variations are provoked and the DC-voltage must be limited. Overvoltages causing a damaging risk for the converter or undervoltages causing instability of the whole generator and converter system can then be avoided.

Chopper

The implementation of a chopper will enhance the turbine's fault ride-through capability even further. This is due to the following two aspects: (i) When the grid side converter prioritizes reactive power supply during a fault and the active power is forced to zero, the power imbalance in the turbine system becomes maximum. (ii) As the power imbalance is transferred to the generator side by the control the acceleration and speed oscillations followed by DC-voltage variations will be maximum, too.

In order to avoid, that the power imbalance is transferred to the generator and to prohibit an acceleration of the generator a chopper is implemented. As illustrated in Figure 4 the chopper is a resistance added parallel to the capacitor in the DC-link. The chopper resistance is switched on and off by means of the power electronic switch e.g. a single transistor with a switching frequency of 500 Hz [13].

When a fault happens and a power surplus in the wind turbine system occurs the DC-capacitor is charged and the DC-voltage rises. The chopper is switched on, if the DC-voltage exceeds a certain level [14], [15]. During the time, when the chopper is switched on, it burns the surplus power so that the capacitor discharges again and the DC-link voltage decreases below the threshold. This cycle is repeated with the switching frequency of the chopper. Since the surplus power is burned in the chopper both DC overvoltages and generator acceleration are avoided.

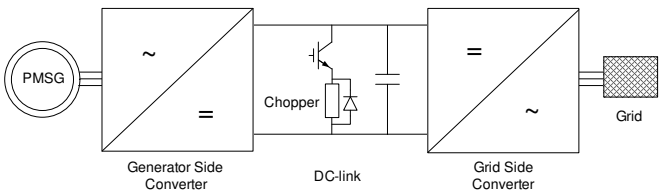

Figure 4: Chopper

In order to verify the effectiveness of the chopper a 3-phase short circuit at the point of common coupling of the PMSG wind turbine is simulated. The short circuit happens at 0 s and has a duration of 400 ms. The PMSG wind turbine

is connected to a grid, which is modelled as a Thevenin equivalent and the wind speed is kept constant during the simulation. Before the fault incident the turbine operates at rated power.

Figure 5 and Figure 6 depict the performance of the chopper action. In Figure 5a) the DC-voltage is plotted for 10 s after the fault incident. In addition to that, Figure 5b) shows a zoom of the DC-voltage signal for 600 ms after the fault. Due to the high frequent switching cycle of the chopper the DC-capacitor charges and discharges with the same frequency, which is visible in the DC-voltage signal (Figure 5b). When the speed oscillations are damped, the DC-voltage reaches its constant reference value.

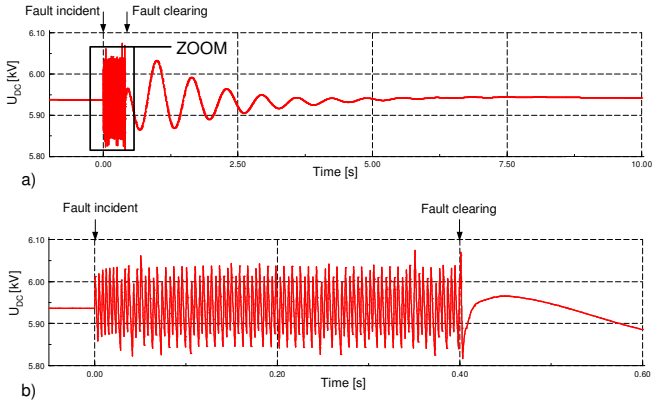

Figure 5: DC-voltage for a 400 ms three-phase fault at PMSG wind turbine's point of common coupling.

The simulation results of generator power and speed are illustrated in Figure 6. The signals are plotted for two cases: with and without the action of the chopper. Without chopper the converter control assures constant DC-voltage but transfers the power imbalance to the generator. This is visible in Figure 6, as the generator power drops. In this case the generator speed starts to oscillate. When however the chopper is applied to the system, the generator can continue the power production, as indicated by the power signal (red-solid line). This prevents in turn an acceleration of the generator and speed oscillation can be avoided. The chopper reduces thus effectively the grid fault impact on the generator and turbine system and enhances the PMSG wind turbine's fault ride-through capability.

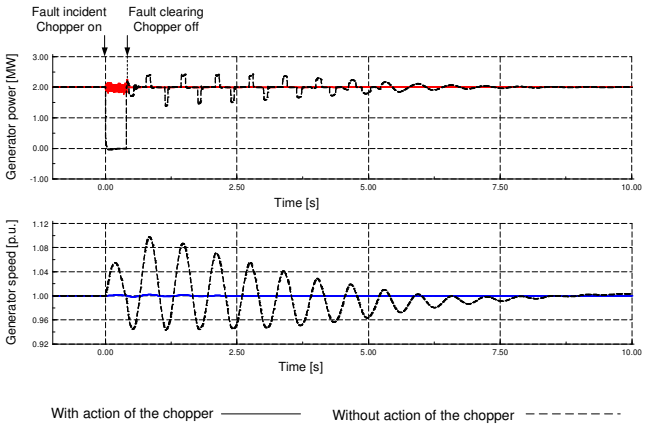

Figure 6: Generator active power and speed for a 400 ms three-phase fault at the PMSG wind turbine's point of common coupling for two cases: with and without chopper.

5. VOLTAGE CONTROL CAPABILTY

Besides fault ride-through capability grid codes also require reactive power supply. Due to the presence of the full-scale frequency converter in the considered PMSG wind turbine structure, reactive power supply can be realized by the grid side converter independently of the operational point of the generator.

The amount of reactive power supply is then only limited by the grid side converter rating:

$$Q_{Conv} = \sqrt{S_{Conv}^2 - P_{Conv}^2} \tag{2}$$

In order to accomplish voltage support, a voltage controller is added to the grid side converter control, as illustrated in Figure 7. The voltage controller is implemented in cascade to the inner reactive power control loop and the converter current control loop. Depending on the difference between the measured grid voltage and the reference voltage, the voltage controller demands thus the grid side converter controller to provide or to consume reactive power in order re-establish the grid voltage level.

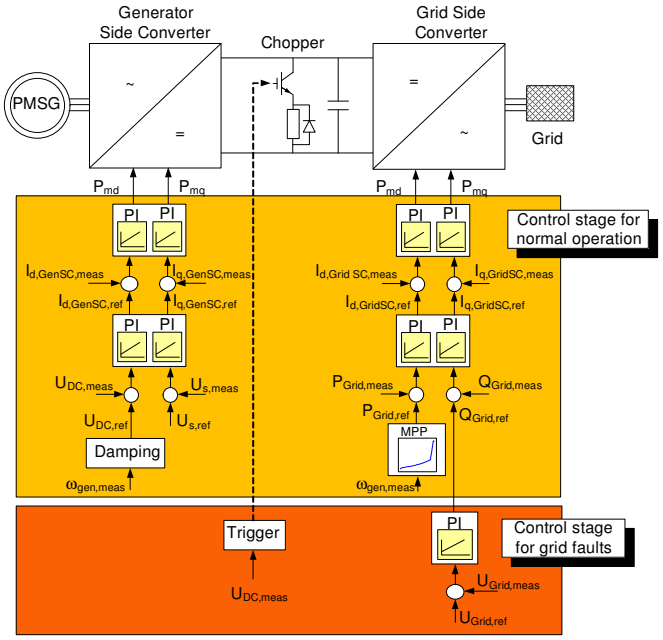

Figure 7: Control stages of the PMSG wind turbine for normal operation and grid faults

The action of the voltage controller can be exemplified by connecting e.g. an inductive load for 1 s to the point of common coupling (PCC) of the wind turbine system. Simulation results are illustrated in Figure 8. Two simulation cases can be compared: with and without voltage controller, respectively.

The inductive load coupling causes a reactive power imbalance so that the voltage drops down to a level of approximately 85 %. When the voltage controller is disabled no additional reactive power is supplied to the grid and the voltage stays at the lower level as long as the inductive load is connected. The active power can still be controlled to its reference value. After the inductive load is disconnected the voltage level recovers.

When the grid side converter voltage controller is active the converter starts to supply reactive power as soon as the

inductive load is connected. The converter can provide up to 1.5 MVar reactive power without active power reduction. The voltage level is immediately re-established to its reference value. When the inductive load is disconnected after 1 s the voltage controller reduces the reactive power supply to its original value.

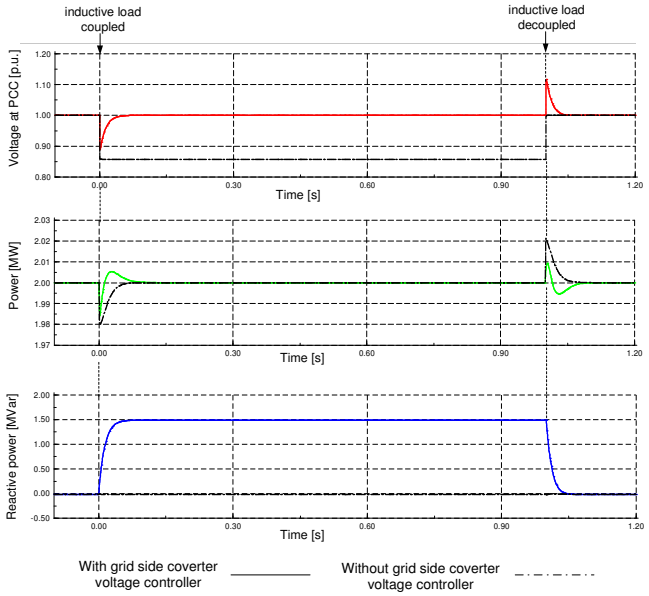

Figure 8: Voltage at the wind turbine's point of common coupling (PCC), grid side converter active and reactive power production for the simulation case, when an inductive load is coupled to the PCC for 1 s.

6. Power System Model

In order to emphasize the fault ride-through and grid support capability of PMSG wind turbines the dynamic interaction between permanent magnet synchronous generator based wind turbines and the power system in case of grid faults is analysed in the following.

A generic simplified transmission system model is implemented in the software DIgSILENT Power Factory (Figure 9). The transmission system model is based on a model, developed and provided by the Danish transmission system operator Energinet.dk [16]. The model embodies a generic representative transmission network and serves to simulate a realistic interaction between wind farm and transmission grid during grid faults.

The transmission system contains models for four central power plants and their control, several load centres and an aggregated model for local wind turbines with conventional technology based on asynchronous generators (Danish Concept). The transmission system model described in [16] is slightly modified in this paper. An aggregated 160 MW offshore wind farm composed of exclusively PMSG wind turbines is used instead of the active stall wind farm of the original transmission system model described in [16].

Aggregation methods reduce typically the complexity and simulation time without compromising the accuracy of the simulation results [17]. They can be used especially in power system studies concerning the impact of large wind farms on the power system.

In this paper 80 equal 2 MW PMSG wind turbines are aggregated to one equivalent lumped wind turbine with rescaled power capacity according to the entire wind farm power. DIgSILENT Power Factory provides a direct built-in aggregation technique for the electrical system. The generator and the transformer can be directly modelled by a certain number of parallel machines, while the other components, as e.g. the power converter or the mechanical power of the turbine rotor have to be up-scaled according to the wind farm power.

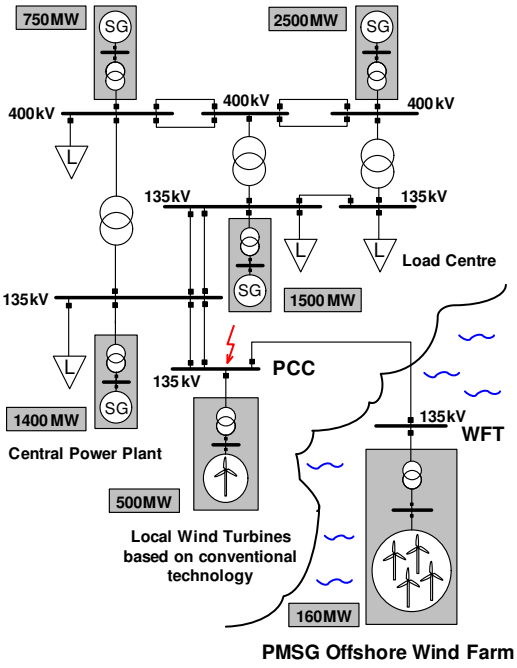

Figure 9: Generic power transmission system model

7. Simulation Results

In this section the developed control strategy of the PMSG wind turbine is assessed and analysed by means of simulations. A worst-case scenario is simulated in order to demonstrate the ability of the presented control strategy of the PMSG wind farm in terms of grid support during faults. A 3-phase short circuit at the PCC (see Figure 9) with a duration of 300 ms is performed. In the moment of the fault, the wind farm is assumed to work at its rated conditions. Due to its location close to the wind farm and its long duration, the fault scenario denotes a severe fault and critical situation for the grid and for the connected wind turbines. The following simulation results are shown in Figure 10:

- The voltage at the point of common coupling (PCC)
- The voltage at the wind farm terminal (WFT)
- The active and reactive power produced by one PMSG turbine in the wind farm
- The generator speed of a local wind turbine

Two simulations are compared in Figure 10:

- Case I (dashed line) shows the results without reactive power supply of the PMSG wind farm
- Case II (solid line) shows the results with reactive power supply of the PMSG wind farm

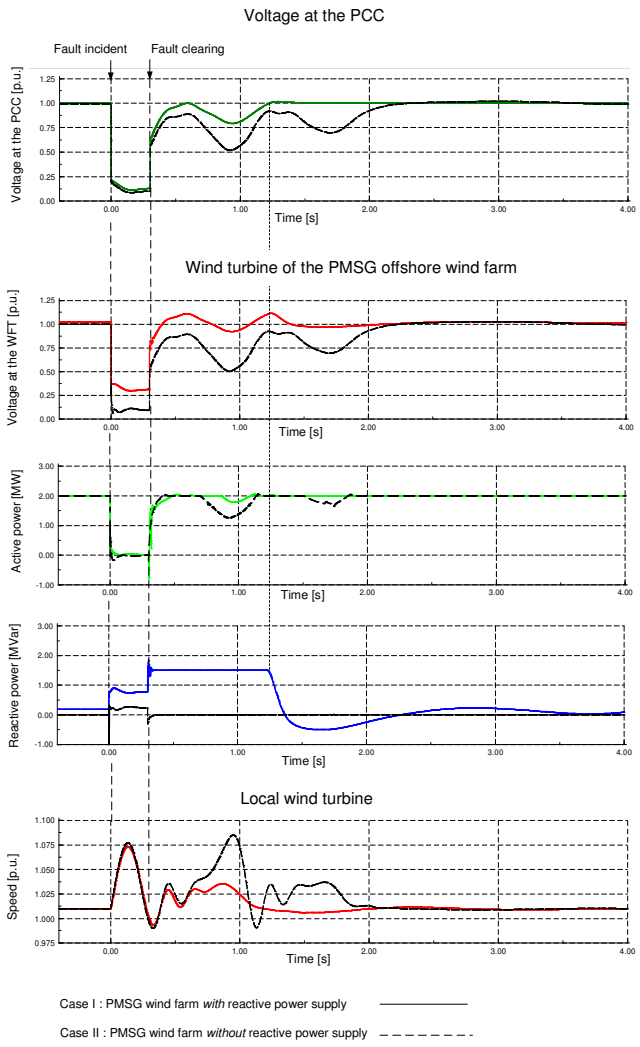

Figure 10: Generic power transmission system model

The short circuit causes a significant voltage drop at the PCC and at the wind farm terminal. This implies a drop in the grid side converter's active power production of the PMSG wind turbine. Because of the active power drop in the local wind turbines, which causes a reduction of the electromagnetic torque, the induction generators of the local wind turbines start to accelerate. As illustrated in Figure 10 the generator speed of the conventional (local) wind turbines is prone to heavy fluctuations in case I. These fluctuations are transferred to the voltage at the PCC. After the fault is cleared, the reactive power demand of the asynchronous generators of the local wind turbines has generally increased due to their acceleration. Moreover, the conventional wind turbines are subjected to high mechanical stresses in case of a grid fault. A tripping of the local wind turbines during grid faults, as it is common practice for conventional wind turbines today, is justifiable in this case. However, the tripping causes a significant loss of active power production, as the conventional wind turbines cannot immediately be reconnected after the fault is cleared.

In contrast to case I, case II shows the results when the wind farm is equipped with voltage control in the simulated fault case. As soon as the voltage has dropped, the grid side converter voltage controller provokes an increase of reactive power supply, which improves the voltage level at the wind farm terminal significantly during the fault. The improved voltage level causes an improvement of the active power, too. After the fault is cleared the grid side converter provides a much higher amount of reactive power due to the increased voltage level. As soon as the voltage at the PCC reaches its rated value the reactive power supply of the grid side converter is reduced. In contrast to case I the voltage and system stability can much faster be regained. The grid support of the PMSG wind turbines has furthermore a noticeable positive impact on the behaviour of the local wind turbines with conventional technique. The speed fluctuations are significantly reduced due to the control system of the PMSG wind farm.

The simulation results of case II show, that a tripping of the local wind turbines is no longer necessary if a nearby connected wind farm with PMSG wind turbines supports the power system stability by reactive power supply. The control system of the PMSG wind farm even facilitates a fault ride-through of the conventional wind turbines. This effect was also proven in the investigations presented in [18] and [19]. A significant loss of active power production can so be avoided.

The fault ride-through and grid support capability of PMSG wind turbines has thus been proven in the presented paper.

8. CONCLUSION

The paper presents a control strategy of permanent magnet generator wind turbines, which enables the turbines to accomplish fault ride-through and to provide grid support during grid faults.

The presented control strategy of the power converter is assessed to be very beneficial for fault ride-through. The DC-voltage is controlled by the generator side converter instead of the grid side converter. As the generator side converter is not coupled to the grid its control capability is not compromised during grid faults. With such control strategy the wind turbine is therefore able to ride-through faults even without any additional measures.

Nevertheless, a chopper is applied to the system, in order to enhance the fault ride-through capability further. A voltage controller is also added to the grid side converter control of the PMSG wind turbine to provide reactive power supply in case of grid faults.

Simulation results in DIgSILENT Power Factory exemplify how PMSG wind farms with such control strategy participate to re-establish the voltage during grid faults. Under grid faults the control can even improve the behaviour of local wind turbines with conventional technology, which are connected in vicinity to the PMSG offshore wind farm. A disconnection of the conventional wind turbines in case of grid faults is therefore not necessary anymore. This means, that significant power losses due to disconnection of conventional wind turbines during grid faults can be avoided.

REFERENCES

[1] A.D. Hansen, L. Hansen, "Wind Turbine Concept Market Penetration over 10 Years (1995-2004)", Wind Energy, Volume 10, Issue 1, Pages 81 – 97, January/February 2007.

[2] Jöckel S., VENSYS Energiesysteme GmbH, Germany, „High energy production plus built-in reliability – The new Vensys 70 / 77 gear-less wind turbines in the 1.5 MW class", European Wind Energy Conference EWEC, Athens, 2006.

[3] G. Michalke, A.D. Hansen, T. Hartkopf, "Control strategy of a variable speed wind turbine with multipole permanent magnet synchronous generator" European Wind Energy Conference EWEC, Milan–Italy, 7th –10th May 2007.

[4] E. Robles, J.L. Villate, S. Ceballos, I. Gabiola, I. Zubia, "Power electronics solutions for grid connection of wind farms", European Wind Energy Conference EWEC, Milan–Italy, 7th –10th May 2007.

[5] V. Akhmatov, "Modelling and Ride-through Capability of Variable Speed Wind Turbines with Permanent Magnet Generators". Wind Energy, Volume 9, Issue 4, Pages 313-326, July/August 2006.

[6] E.ON. Netz GmbH, "Netzanschlussregeln, Hoch- und Höchstspannung", www.eon-netz.com, 2006.

[7] Energinet.dk, "Wind Turbines Connected to Grids with Voltage above 100kV", Technical regulation TF 3.2.5, www.energinet.dk.

[8] V. Akhmatov, A.H. Nielsen, J. K. Pedersen, O. Nymann, „Variable-speed wind turbines with multipole synchronous permanent magnet generators. Part I. Modelling in dynamic simulation tools." Wind Engineering, Volume 27, No. 6, pp 531-548, 2003.

[9] P. Deglaire, S. Eriksson, A. Solum, "Simulation and control of a direct driven permanent magnet synchronous generator", Nordic PhD course on Wind Power, Smøla, Norway 5-11 June 2005, www.elkraft.ntnu.no/smola2005/Topics/2.pdf.

[10] D. Svechkarenko, "Simulations and Control of Direct Driven Permanent Magnet Synchronous Generator", ", Nordic PhD course on Wind Power, Smøla, Norway 5-11 June 2005, www.elkraft.ntnu.no/smola2005/Topics/18.pdf.

[11] M. Molinas, B. Naess, W. Gullvik, T. Undeland, "Control of Wind Turbines with Induction Generators Interfaced to the Grid with Power Electronis Converters", International Power Electronic Conference IPEC 2005, Niigata, Japan, 4 - 8 April 2005.

[12] P. Kundur, "Power System Stability and Control". McGraw Hill, 1994.

[13] G. Brando, A. Coccia, R. Rizzo, "Control method of a braking chopper to reduce voltage unbalance in a 3-level chopper", IEEE International Conference on Industrial Technology ICIT, 2004.

[14] N. Hennchen, "Wind turbine converter fits E.ON Regulation", Frisia Schaltanlagen GmbH, www.frisia-schaltanlagen.de/data/grid_integration_of_wind_turbines.pdf.

[15] V. Akhmatov, "Full-load Converter Connected Asynchronous Generators for MW Class Wind Turbines", Wind Engineering, Volume 29, No. 4, Pages 341-351, 2005.

[16] V Akhmatov, A. Nielsen, "A small test model for the transmission grid with a large offshore wind farm for education and research at Technical University of Denmark", Wind Engineering, Volume 3, No. 3, 2006.

[17] Pöller M., Achilles S., "Aggregated Wind Park Models for Analyzing Power System Dynamics", Forth International Workshop on Large Scale Integration of Wind Power and Transmission Networks, 20th and 21st October, Denmark, 2003.

[18] G. Michalke, A.D. Hansen, T. Hartkopf "Control of a wind park with doubly fed induction generators in support of power system stability in case of grid faults", European Wind Energy Conference EWEC, Milan–Italy, 7th –10th May 2007.

[19] A. Hansen, G. Michalke, P. Soerensen, T. Lund, F. Iov., "Co-ordinated voltage control of DFIG wind turbines in uninterrupted operation during grid faults", Wind Energy, Volume 10, Issue 1, Pages 51-68, January/February 2007.

Development of a method for evaluation of wind turbines ability to fulfill Swedish grid codes

Rolf Ottersten, Andreas Petersson, Evert Agneholm
Gothia Power AB, Aschebergsgatan 46, SE-411 33 Gothenburg, Sweden
tlph. +46 (0)31 209730, e-mail firstname.lastname@gothiapower.com

Abstract — This paper deals with grid code validation for wind power plants. An overview of some European grid code validation methods is given and the early progress of a possible Swedish validation plan is presented.

Index Terms — Wind power, grid codes, validation plan, VSC grid emulator

I. Introduction

Due to the large-scale integration of wind power in Europe in recent years, system operators and grid owner companies have renewed their grid codes for production plants. A common European grid code has not yet emerged, instead most countries have developed their own variants in order to suit their needs [1].

In addition to the codes being different within Europe, the validation requirements appear to vary as well. Only a few countries─the best examples are probably Germany [6], Spain [2] and Ireland [4]─appear to include or complement their grid codes with some kind of validation plan. With a validation plan, it is here implied a detailed description, leaving little or no room for free interpretations regarding how each requirement in a grid code should be validated, such as selection of test equipment and test algorithms, site conditions such as wind conditions and grid short-circuit power, variables that are to be monitored, etc.

This paper describes ongoing work in the project *Development of a method for evaluation of wind turbines ability to fulfill Swedish grid codes*, which objective is to develop a validation plan for the Swedish grid codes [11]−[13]. The work is funded by Vindforsk and the first phase of the project was recently completed. During the first phase, existing and validation methods under development were investigated and a suitable test equipment was selected.

II. Overview of Grid Code Validation Methods

This section provides an overview of the validation requirements in four European countries as stated in their applicable grid codes. A brief overview of an early working draft of the IEC-61400-21 standard, which currently is under revision, is also included.

A. Denmark

The Danish grid codes do not contain a detailed validation plan and simulation studies appears to be sufficient validation method for most of the grid-code requirements [8], [9]. Practical experiments should be conducted, though, for verification of that the wind turbine (WT) under test has sufficient battery backup to withstand six voltage dips within five minutes and the transient overvoltage should be recorded during a disconnection test.

B. Germany

In Germany, validation of system reliability requirements may be conducted by way of either simulation studies or full-scale tests on actual WTs [5]. For ride-through tests, though, full-scale testing appears to be mandatory.

A testing guideline is available for the German grid codes [6], [7]. It has not been possible to analyze this guideline in detail, but it appears that only single WTs, i.e., not farms, are covered and the main content of [6] appears to be:

- Instructions on how to conduct, analyze and document the validation tests.
- Test methods to validate voltage and frequency relays.
- Test methods for the setpoint control of active and reactive power.
- A methodology for measuring the active power capability as function of reactive power capability, i.e., the PQ diagram of a WT.
- Testing of low-voltage ride-through capability.

The latter ride-through test is conducted with a short-circuit emulator similar to that shown in Fig. 1, which consists of a number of reactors and breakers that can short-circuit one or several phases to ground. This equipment cannot increase the voltage nor vary the frequency. As the initiation of frequent short-circuits are not permitted in a public distribution system, the impedance closest to the grid in Fig. 1 must be designed to limit the grid inrush current during the short-circuit test.

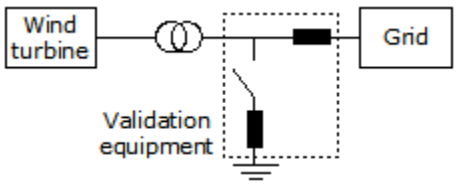

Fig. 1. German short-circuit emulator for ride-through tests.

C. Spain

In Spain, full-scale testing on actual WTs appears to be required for grid code validation. The testing itself is only one part of the validation, though, the entire WT validation process is in brief [2]:

- A single WT is subjected to various grid disturbances.
- A simulation model is developed for the WT and the model is tuned and validated against the previously conducted full scale test.
- The single WT simulation model is then further developed into an entire wind farm (WF) model, which is analyzed for various grid disturbances and operating conditions.

The Spanish ride-through test equipment appears to be similar to the German one in Fig. 1. For the test equipment described in [3], the voltage can be reduced in ten steps from 90 % to 0 % of nominal voltage, the rated voltage of the equipment is 30 kV and WTs rated up to 5 MW can be tested.

D. Ireland

The Irish validation requirements have a strong focus on simulation models. In order to connect to the grid, WT manufacturers must deliver a PSS/E simulation model of their WT, which is then to be reviewed by the system operator [4]. It is clearly specified which WT subsystems that must be included in the simulation models, full model documentation is required and it must be possible to easily aggregate a single WT model into a larger WF.

The simulation models must be validated against full-scale tests on actual WTs. It is not specified in detail how these tests are to be conducted, but both the test equipment and the test algorithms must be accepted by the system operator. In addition, the model must be validated for several different operating conditions, such as different short-circuit power at the point of common connection, short-circuits of various severity, various voltage and frequency deviations and different wind speeds.

E. IEC 61400-21

IEC 61400-21 is currently under revision and the new version, when released, may include the below new validation requirements [10].

The response of WTs, operating at 20 % and 100 % of nominal power, shall be tested during three- and two-phase short circuits to ground with duration of 400 ms. The remaining voltage during the short circuits should be 50 % and 90 %. The tests may be conducted using a short-circuit emulator similar to that in Fig. 1.

The WT reconnection time shall be measured, i.e., the time from that the voltage recovers until the WT starts to produce active power.

The ramp rate limitation mode for active power shall be measured and various tests for the set-point control of active and reactive power shall be conducted.

The reactive power capability, given as 10 min average values, shall be determined as a function of the active power output from 0 to 100 %.

The set operate values and the delay times shall be determined for voltage and frequency relays, zero active power output is permitted during these tests.

III. Development of Validation Method

The current Swedish grid codes do not contain a detailed validation plan. Full-scale testing on actual WTs is referred to as the most reliable validation method but, when such testing is inappropriate, technical calculations and simulations may be allowed as well [11]. In order to allow for full-scale testing to the largest possible extent for the Swedish grid codes, the test equipment shown in Fig. 2 has been found suitable. The equipment front end consists of a self-commutated voltage source converter (VSC) that is connected to the WT via an EMC filter, for PWM filtering, at the medium voltage level.

A. VSC Grid Emulator

The VSC is intended to operate as a grid emulator in the suggested test equipment. As such, the VSC is capable of generating any voltage waveforms, which can be either symmetrical or non-symmetrical. This allows testing not only the low-voltage ride-through capability but also how the WT behaves during slow (over)voltage and frequency variations. For certain WTs with direct coupling between the electric generator and the grid, an application of overvoltage and/or underfrequency in the VSC voltage waveforms enables, for instance, the possibility to verify the behaviour when the generator saturates magnetically.

For low-voltage ride-through testing, the VSC cannot only emulate a short-circuit fault but also the fault impedance. In consequence, the phase-angle jump during a short circuit can be controlled. A large phase-angle jump may be troublesome for a WT control system, since the new phase angle must be tracked as quickly as possible in order to achieve the intended production of active and reactive power. The VSC can also emulate grids with different short-circuit and X/R ratios.

Some European grid codes impose restrictions regarding when a disconnected WT is allowed to automatically reconnect to the grid. The Irish grid codes, for instance, specify that disconnected WTs are not permitted to connect to the grid if the frequency exceeds 50.2 Hz [4]. Such a requirement should preferably be validated on a full-scale actual WT and the VSC grid emulator can easily achieve this.

Requirements for setpoint and rate limitation control for active and reactive power are present in many grid codes and, in addition, requirements for voltage and frequency control are neither uncommon [4], [9]. The VSC grid emulator is capable of verifying such voltage and frequency control requirements—by emulating the grid response to active and reactive power—for a single WT only, but validation on an entire WF is prohibited due to VSC power limitations. In practice, though, these kinds of requirements should probably be validated on a WF. Given a voltage setpoint, for instance, the WF control system receives a voltage setpoint via remote control, measures the voltage at the point of common connection, calculates the voltage setpoint for each WT, sends the voltage setpoints to each WT and then the WTs should track these setpoints. This may take some time to accomplish and a proper droop control for each WT is probably required. Thus, validation of voltage and frequency control on single WTs possibly has limited value but it may identify major problems at an early phase. Furthermore, planned future work aims to investigate if the VSC can emulate not only the grid but also an entire WF or parts of a WF.

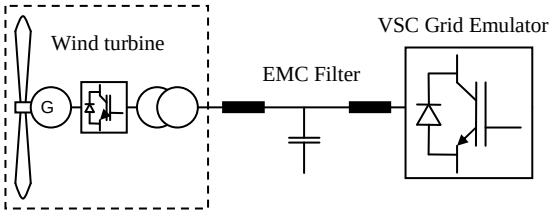

Fig. 2. Suitable test equipment: VSC grid emulator for code validation.

B. Validation Plan

A validation plan for the grid codes may be as important as the codes themselves, since a good validation plan leaves little or no room for free interpretations regarding how each requirement in a grid code should be validated, which insures that the code requirements are indeed satisfied. A small part of a very early possible Swedish validation plan is shown in Table I, which may provide an idea of the project scope. As shown, the validation plan is also intended to provide requirements for validation of WT/WF simulation models and for power system analysis, where the intention is to learn from the Irish and Spanish experiences.

C. Future Work

A follow-up project is planned, but has not yet been granted by Vindforsk, which is intended to contain at least the following work:

- The validation plan for the Swedish grid codes is to be further developed.
- Identify the Swedish grid code requirements that cannot be sufficiently validated with the VSC grid emulator. If possible, develop the VSC grid emulator such that more requirements can be validated.
- Derive requirements for hardware and software design of the VSC grid emulator.

IV. Conclusion

This paper has provided an overview of some European grid code validation methods and the early progress of a possible Swedish validation plan. A VSC grid emulator has been found suitable as test equipment and some of the advantages of this equipment were described. Parts of a very early validation plan were shown, which is intended to be significantly developed in a future project.

V. Acknowledgement

The research presented in this paper was carried out as a part of the Swedish wind energy research programme "Vindforsk – II", which was funded by ABB, the Norwegian based EBL-Kompetense, E.ON Sverige AB, Falkenberg Energi AB, Göteborg Energi, Jämtkraft AB, Karlstad Energi AB, Luleå Energi AB, Lunds Energi AB, Skellefteå Kraft AB, Svenska Kraftnät, Swedish Energy Agency, Tekniska Verken i Linköping AB, Umeå Energi AB, Vattenfall AB and Öresundskraft AB.

References

[1] C. Jauch, J. Matevosyan, T. Ackermann och S. Bolik, "International comparison of requirements for connection of wind turbines to power systems," Wind Energy, vol. 8, p. 295–306, July 2005
[2] Asociación Empresarial Eólica, "Procedimiento de medida y evaluación de la respuesta de las instalaciones eólicas ante huecos de tensión," www.aeolica.org
[3] A. Morales, "Unidad móvil de ensayo de huecos de tensión en aerogeneradores: ULISES," Energetica Power Generation Magazine, February 2006.
[4] EirGrid, "Grid code," ver. 2, January 2007, www.eirgrid.com
[5] Verband der Netzbetrieber, "EEG-Erzeugungsanlagen am hoch- und höchstspannungsnetz," August 2004, www.vdn-berlin.de
[6] Fördergesellschaft Windenergie, "FGW guidelines part 4: Determining the electrical properties − Power plant behaviour," November 2006, www.wind-fgw.de
[7] J. Möller, A. Tüxen, "Wind energy with power plant properties?,", in Proc. Risø Internat. Energy Conf., May 23–25, 2005, Risø, Denmark
[8] Energinet.dk, "Wind turbines connected to grids with voltages below 100 kV," May 2004, www.energinet.dk
[9] Energinet.dk, "Wind turbines connected to grids with voltages above 100 kV," December 2004, www.energinet.dk
[10] IEC 61400-21, "Measurement and assessment of power quality of grid connected wind turbines," IEC:200x, working draft
[11] Svenska Kraftnät, "Svenska Kraftnäts riktlinjer för vindkraftanslutningar," February 2007, www.svk.se
[12] Svensk Energi, "Anslutning av mindre produktionsanläggningar till elnätet (AMP)," 2002.
[13] Elforsk, "Anslutning av större produktionsanläggningar till elnätet (ASP), " Elforsk rapport 06:79, 2006, www.vindforsk.se

TABLE I
EXAMPLE OF SMALL PARTS OF EARLY VALIDATION PLAN.

Requirement	**Specification** *Validation method requirement*	**Comment**
Protection relays	AMP[12], ASP [13] *Parts of IEC 61400-21 [10], none*	An analysis of the WT protective systems should be done before test is carried out
Selectivity	To be identified *None*	
Slow voltage and frequency variations	SvKFS 2005:2 [11] *None*	Test duration of 30−60 minutes.
Voltage dips	SvKFS 2005:2 *None*	Three-, two, and single phase faults.
Voltage control	SvKFS 2005:2 *None*	
Reactive power setpoint control	SvKFS 2005:2 *IEC 61400-21*	
Real time communication (Voltage, active and reactive power production, operation status, power reserves)	SvKFS 2005:2 *None*	Delay time should be measured
Validation of WT/WF simulation models	*None*	
Power system analysis, PSS/E simulations	*None*	Transient stability, load flow, short-circuits…

Stochastic Assessment of Opportunities for Wind Power Curtailment

George Koustas, George Papaefthymiou, *Member IEEE*, Bart C.Ummels, *Member IEEE*
and Lou van der Sluis, *Senior Member IEEE*
Electrical Power System Laboratory (EPS), Faculty of Electrical Engineering, Mathematics & Computer Science,
Delft University of Technology (TU Delft), P.O. Box 5031, 2600 GA Delft, the Netherlands
e-mail:g.papaefthymiou@tudelft.nl.

***Abstract*—** An important characteristic of wind power is its stochastic and non-dispatchable nature. Because of the development of wind power in recent years, stochasticity is becoming a driving parameter in the power system. Unpredicted and excessive power flows in the power system may be a result of this, especially since the pace of wind power developments is faster than transmission system re-inforcements. These developments, in combination with the limited operational flexibility of the conventional generation units within short time-spans, makes the future integration of large-scale wind power in the power system a challenging task. Temporary curtailment of wind power might provide a favourable solution for this, especially if this lifts barriers for further growth of wind power capacity. This paper presents a stochastic methodology for the assessment of the advantages and disadvantages of wind power curtailment as a solution for system congestion in relation to increasing wind power penetration. The method is applied in a number of case studies and is shown to reduce line overloading risks and power flow distribution variability, thereby increasing the feasibility for further wind power development.

***Index Terms*—** Monte Carlo simulation, wind curtailment, power flow, wind power.

I. Introduction

In the past decade, wind power has become the fastest-growing generation technology for renewable energy. At the beginning of 2006, the worldwide installed capacity of wind power was about $60GW$, corresponding to an energy production of about $120TWh$ per year [1]. In Europe, wind power is becoming a generation technology of significance. In particular, as presented in the 2006 annual report of the European Wind Energy Association (EWEA), the total wind power capacity installed in 2006 reached $7.6GW$, corresponding to an increase of 23% compared to the previous year [2]. Such a large-scale integration of wind generation causes several challenges in the management of a power system due to the non-dispatchable nature of the wind. One of the main challenges for the future is to see how systems with significant wind power penetration can be operated and designed for efficient integration without violating system security.

In power systems there must be a continuous power balance between generation and load. Owing to the variability and unpredictability of wind power production, significant amounts of wind power complicate power system balancing [3]. In particular, when the share of wind energy in the system increases, there will be cases when wind power will cover or threaten to exceed system load. In such cases, the surplus of wind energy may be curtailed, i.e. some wind power plants have to be shut down, or several wind power plants have to decrease their production. In order to prevent wind power curtailment, large-scale energy storage solutions may be used to store excess wind energy, but these are often not available. Another solution is to use international interconnections to other regions to export this excess of power. In this case, the limiting factor is the transmission capacity between the neighboring regions and the ability of this region to absorb this excess of wind power [1].

Certainly, wind power curtailment has economic consequences due to opportunity losses. The wind power producer loses part of its revenue, which will have an impact on the investment payback time. Often, such possibilities are not taken into account in investment plannings for wind farm projects. As discussed in [4], as the total wind capacity in the system increases, the output of the conventional generation running at the same time will be reduced. Eventually, a limit is reached below which the conventional generation cannot be further reduced due to technical reasons (minimum output limitations) and wind curtailment is required [5]. The installation of additional wind parks in the system, even though leading to an increasing participation of wind energy in the total energy mix, will lead to more frequent occurences for curtailment in case flexibility measures in conventional generation plant are not applied. As presented in [4], for the case of Ireland at approximately $4000MW$ of wind generation, "the curtailment of the last wind turbine will be such that it can only operate for a few hours per year, near the times of system maximum demand".

For its assessment of the need for wind power curtailment in a specific system, a detailed analysis of the system load patterns in parallel to the allocation of the wind power resources is required. The matching between the system load and wind power is a central issue in this analysis, since it will define the frequency of cases when wind power exceeds the system load. In order to perform such an analysis, data records of a sufficiently long period should be used for the modeling of the stochasticity of the system load and wind power. One of the main problems here is the size of this dataset. Since the system load presents a high time-dependence (for a specific point in time the system load falls in the region of a time-conditional mean), its stochasticity may be captured without using large datasets [6]. Wind activity however is a

non time-dependent stochastic phenomenon, necessitating the use of large datasets for the deduction of statistically coherent results [7]. In order to tackle this problem, instead of the *chronological approach* of directly using recorded datasets for the analysis, the *stochastic approach* should be followed, i.e. simulation techniques should be used for the modeling of the system inputs stochasticity.

In this paper, the *Monte-Carlo Simulation (MCS)* methodology developed in [8] is applied for the system stochastic modeling. In section II, the sampling of the system stochastic inputs (loads and wind power) is performed based on the respective marginal distributions and the underlying stochastic dependencies. In section III the implementation of wind power curtailment to the system operation is presented, while in section IV the impact of wind power penetration and wind curtailment on a specific power system is elaborated.

II. Monte-Carlo Simulation Methodology

According to the probabilistic formulation of the problem, the stochastic system inputs (loads-wind generation) are modeled as *random variables* (r.v.'s) that follow specific probability distributions obtained by statistical analysis of related data [9]. These r.v.'s contain all necessary information for the stochastic assessment of wind curtailment to the power system. The proposed methodology for modelling the uncertainty of the stochastic inputs involves two basic steps [8]:

1) *Marginal distributions*: The system inputs are sampled based on the underlying distributions obtained by wind speed data. As is the general practice in MCS, for the sampling of a r.v. X with continuous invertible cumulative distribution function F_X, first a uniform random number U in $[0,1]$ is generated and then the transformation $x = F_X^{-1}(u)$ is applied, where u is a realization of U [10]. In this case the samples x follow the distribution F_X.
2) *Stochastic dependence structure*: The configuration of the dependence structure between the r.v.'s is derived. The point is to capture the prevailing dependence structure that holds between the stochastic inputs. For example, in case of the wind, the wind speed patterns in different sites are correlated. In order to capture the mutual dependencies, the rank correlation ρ_r is used and [11].

The sampling of the r.v.'s is performed based on the theory of *Joint Normal Transform methodology (JNT)*, in which the two main steps of MCS are combined. For the generation of n r.v.'s $X = [X_1, ..., X_n]$ correlated according to the $n \times n$ correlation matrix R, the following steps are followed [12]:

1) Generate a set of n normals $N = [N_1, ..., N_n]$, correlated based on correlation matrix R.
2) Transform the normals to uniforms. This is performed by the transformation $U = F_N(N)$ where F_N is the cumulative distribution function (cdf) of the corresponding normal and U is the resulted n-dimensional uniform distribution.
3) Transform the correlated uniforms U into the desired marginals X, by applying the inverse transformation $X_i = F_{X_i}^{-1}(U)$.

Specifically for the 2 stochastic inputs of this paper, the JNT has the following configuration:

- Concerning the wind power sampling, the wind speed marginal distributions at the generation sites are considered Weibull distributions and the wind speed patterns are highly correlated following a product moment correlation of 0.8. Hence, this will be the configuration of MCS for the sampled wind speed patterns concerning the marginals and the dependence structure. The wind speed distributions are transformed to wind power output using the static wind speed/power output characteristic of the wind turbine generators used [8].
- The MCS for the sampling of the stochastic load pattern shall take into account the fact that the load is highly time-dependent, following a periodical pattern with a period of one day. Hence, the stochastic behaviour of the loads is studied with the method of *Time Frames Analysis* (TFA) [6], according to which the period of the pattern is sliced in *Time Frames* (TF) where the load has similar statistical characteristics. The load in each TF is modelled by superimposing a random variable to the time-conditional mean. The practice in this study will be to slice the time period in 4 TFs; the load in each TF will follow a normal distribution with specific mean value and standard deviation, while within the TF the loads are almost independent following a product moment correlation of 0.3.

These distributions are propagated through the system model, which is in this case the steady-state system model [13], and the respective system state (node voltage) and output (line power flows) distributions are obtained.

III. Wind curtailment implementation

As discussed in the introduction, the first and most important task of the transmission system operator is to maintain the power balance in the system. As the output of wind generation is increased or the load demand is decreased, the output of CG units running at the time is reduced in order to keep the system in balance. Eventually, each CG unit will reach a limit below which its output cannot be reduced further. De-commitment of these units is often difficult from an operational point of view, and involves lengthy minimum down-times. In order to prevent excess power flows to neighboring systems, it may therefore be more preferable to temporarilty curtail wind generation.

The total amount of CG regulating power required at any time depends on the sum of the system load and the wind power. In order to determine the total amount of regulating power on the system scale, the wind power is regarded as negative load and the netload at each system bus can be defined as the load demand minus the wind power at this bus:

$$P_{NL}(i) = P_L(i) - P_W(i), \forall i \in [1, n_{bus} = 39] \qquad (1)$$

where P_L is the load and P_W is the injected wind power. In this context, $P_{NL}(i)$ actually corresponds to the power injection at the respective system bus i.

Since the wind power is considered as negative load, the curtailed wind power can be considered as positive load. With

the introduction of wind curtailment, the power balance for the whole system is performed according to the following equation:

$$\sum_{i=1}^{n_{bus}} P_{CG}(i) + P_{slack} = \sum_{i=1}^{n_{bus}} P_{NL}(i) + P_{losses} + DP_w \quad (2)$$

where DP_w is the curtailed wind power for the whole system.

The minimum operational setpoint of the CG units is set to 30% of their nominal power output. Due to this restriction, wind curtailment is necessary when the netload is so low that it pushes the CG setpoint to 30%. In these cases, there is excess of generated power (from the co-generation of CG and wind). With the application of wind curtailment, there power balance is restored in the system, so for each sample it holds:

$$\sum_{i=1}^{n_{bus}} P_{in}(i) = \sum_{i=1}^{n_{bus}} P_{out}(i) \Rightarrow$$

$$\sum_{i=1}^{n_{bus}} P_{CG}(i) = \sum_{i=1}^{n_{bus}} P_{NL}(i) + DP_w \Rightarrow$$

$$DP_w = 0.3 \cdot \sum_{i=1}^{n_{bus}} P_{CG,N}(i) - \sum_{i=1}^{n_{bus}} P_{NL}(i) \quad (3)$$

Algorithm 1 gives the regulation of setpoint x for the CG units and the wind power curtailed for each sample.

Algorithm 1 Regulation of the setpoint x of the CG units

for $i = 1 : allsamples$ **do**

if $30\% \leq \dfrac{\sum_{j=1}^{n_{bus}} P_{NL}(i)}{\sum_{j=1}^{n_{bus}} P_{CG,N}(i)} = x(i) \leq 100\%$ **then**

regulate CG, so that $P_{CG}(i,j) = x(i) \cdot P_{CG,N}(i,j)$, $\forall j \in [1, n_{CG} = 10]$

else

if $x(i) < 30\%$ **then**

regulate CG, so that $P_{CG}(i,j) = 30\% \cdot P_{CG,N}(i,j)$ and curtail wind: $DP_w = 0.3 \cdot \sum_{i=1}^{n_{bus}} P_{CG,N} - \sum_{i=1}^{n_{bus}} P_{NL}$

else

regulate CG, so that $x(i) = 1$

end if

end if

end for

IV. Application to a Power System with a High Wind Power Penetration

A. System Data

As a case study for the estimation of the impact of wind curtailment, the 39 bus - 46 branch IEEE New England test network of Fig. 1 is used [8]. The system is considered to be equipped with thermal CG units. Hydro-power, which is commonly regarded as an ideal solution for balancing wind power variations, is totally absent. Bus 31 is the slack bus and corresponds to the interconnections with the neighbouring

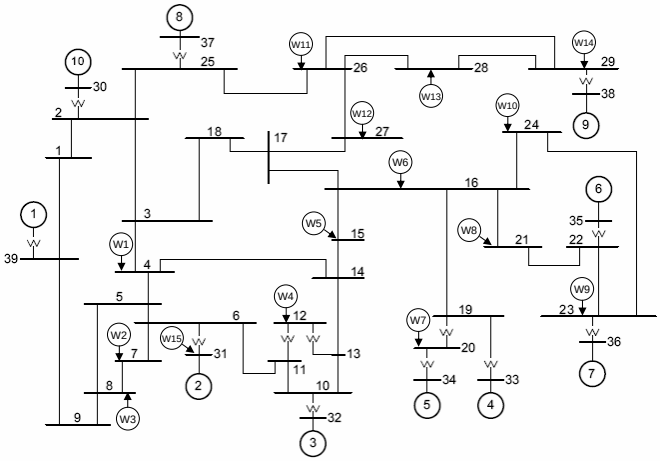

Fig. 1: IEEE New England Test System

systems. In this study, a distributed wind penetration scenario is investigated with the connection of 15 wind parks dispersed all over the power system. Each park is considered to be a uniform generation unit and all parks are of equal nominal power[1]. The wind penetration level is defined as the ratio of the total installed nominal wind power to the total installed CG:

$$x = \frac{\sum_{i=1}^{n_{bus}} P_{w,N}(i)}{\sum_{j=1}^{n_{bus}} P_{CG,N}(j)} \quad (4)$$

B. Stochastic wind generation

The total installed CG power is $P_{CG,tot} = 6000MW$, hence a $x\%$ wind penetration level means that the installed power of each wind park will be:

$$P_{w,N} = x\% \cdot \frac{P_{CG,tot}}{15} = x\% \cdot 400MW \quad (5)$$

The sampling of the system inputs is performed based on the MCS methodology described in section II.

C. Results

The Load Flow analysis was programmed in PSS/E. The output set is the 46 transmission lines power flow distributions, the slack bus power flow and the system losses. Nine study cases are considered, comprising of the no-wind-penetration case and 4 wind penetration scenarios with and without wind curtailment, in which the penetration level is ranging from 0% to 100% with a step of 25%.

[1] 'Uniform generation unit' means that the wind speed pattern is considered even all over the area of the wind park. Hence, the wind park is modelled as a single wind turbine with nominal power equal to the nominal power of the park. W_n is the n-th wind park

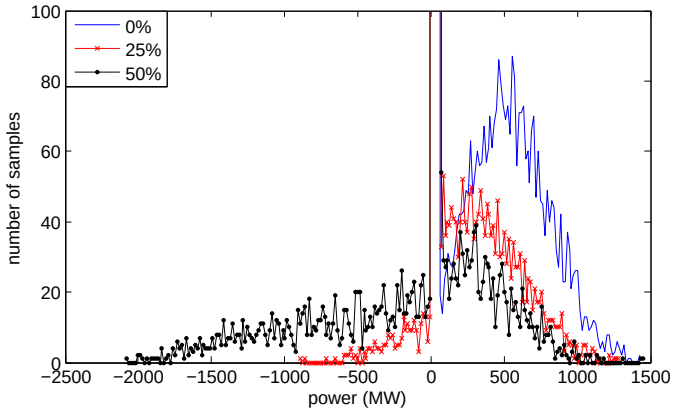

Fig. 2: Slack bus power flow distributions without curtailment.

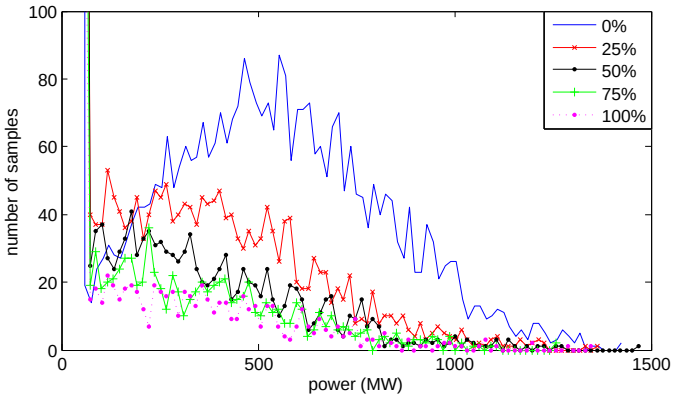

Fig. 3: Slack bus power flow distributions with curtailment.

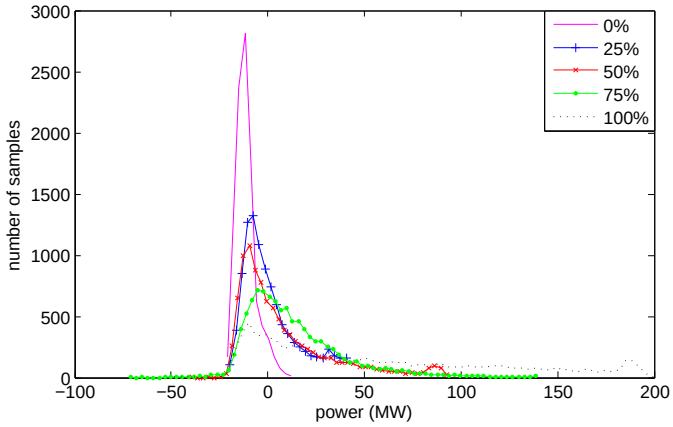

Fig. 4: Power flows in line 15 for all wind penetration levels.

1) Slack bus: The slack bus is responsible for restoring the power balance in the system; hence, its power flow distribution gives important information concerning the system behaviour. In Fig. 2, the slack bus power flow distributions for the study cases without wind curtailment are given. The study stops at 50% wind penetration level, because PSS/E faces a convergence error for higher penetration levels. This error comes from the excessive transmission lines power flows. The increase in wind penetration leads to an increase in the variability of the power flows at the slack bus due to the induced stochasticity of wind generation. The increase in wind penetration pushes the occurrences towards lower and negative power flow values. This means that the probability of import of power through the slack bus decreases. The thermal units are pushed towards their minimum setpoint and the excessive power is driven to the slack bus (negative power flows as seen from the slack bus) and the neighbouring systems.

Besides, there are about 2500 out of the 10.000 samples concentrated at the zero power flow at the slack bus for all the penetration levels, but it cannot be observed to Fig. 2 due to the limited y-axis range. This means that there is 25% probability that there is a power balance to the system, corresponding to 25% of the operational time.

The study cases of wind curtailment implementation, is depicted in Fig. 3. PSS/E converges even for 100% wind penetration due the relieved transmission lines power flows. Also, the slack bus power flows don't take negative values even for high levels of wind penetrations because the excess generated wind power is curtailed. A concentration of probability mass is observed in small values $(0 - 100MW)$, corresponding to the cases of the slack bus providing for the system losses. This occurs due to the increased system generation (CG+wind) which is sufficient to cover the load.

2) System power flows: The increasing wind penetration leads to an increase in the variability of the power flows for all the system lines. Fig. 4 gives the distributions of the power flows in line 15 for all wind penetration levels. The presence of stochastic generation in the system results to highly bi-directional power flows. The vertical system structure is changed to a horizontal one, where the distribution systems become active, exchanging power with the transmission system bidirectionally. This is justified by the bi-directional power flow distributions for line 15.

The impact of wind curtailment can be seen in Fig. 5 which gives the power flow distributions at line 13 for 50% wind penetration with and without curtailment. It can be seen that curtailment has the following result:

1) Decreases the power flow range (variability).
2) Shifts the power flow distributions towards lower absolute values.

Especially for the case of line 13 it seems that the whole distribution is shifted towards lower power flow values and the heavy tail of the distribution is cleared. The loadings of the lines are decreasing to values which are closer to the values obtained without wind. This is an important advantage since the overall generated power has been increased whereas the power flows have been kept to such low values that the lines are not overloaded.

The effects mentioned can be also depicted at Fig. 6, which gives the boxplot of power flows for specific lines for 50% wind penetration, without and with curtailment. For each transmission line 2 boxplots are given, the first one (from the left) is without wind curtailment and the second with curtailment.

The impact of wind curtailment to the overloading of the transmission lines is visualised in Fig. 7, which gives the bar

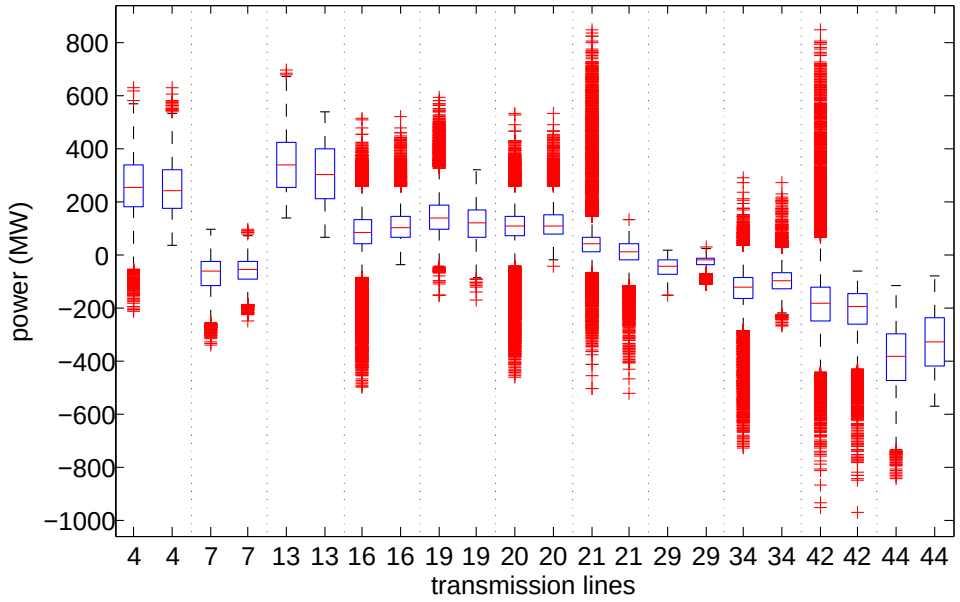

Fig. 6: Boxplot of transmission lines power flows, without and with curtailment.

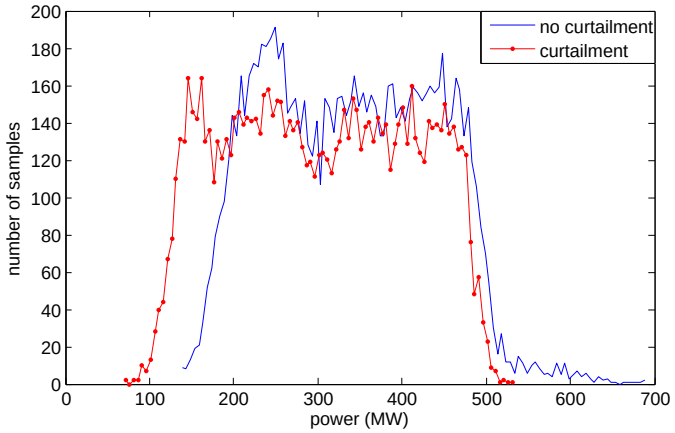

Fig. 5: Power flows in line 13 for 50% wind penetration.

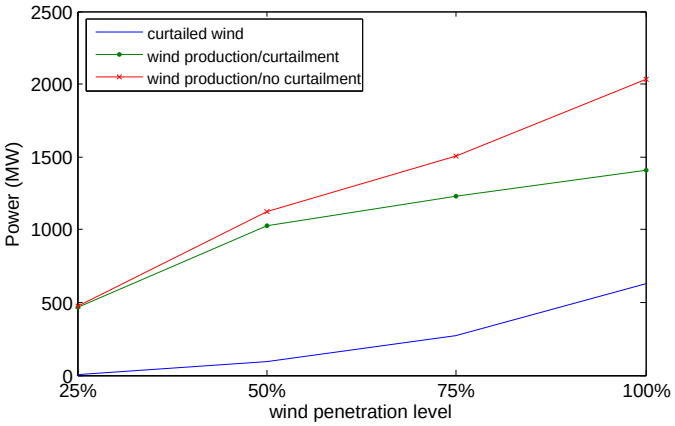

Fig. 8: Energy for several wind penetration levels

plot of the overloading probability for all lines for a wind penetration of 50% for 2 cases: without and with curtailment[2]. We can see that the heavily loaded lines are relieved due to curtailment, whereas for lines with low probability of overloading, the curtailment is less effective, leaving the overloading probability almost unchanged; hence, if we consider the response of the heavily loaded lines more critical for the evaluation of curtailment, we can accept wind curtailment as an adequate solution for limiting the excessive power flows in transmission lines.

3) Economic assessment of wind curtailment: When implementing a solution such as wind power curtailment, it is important to know the amount of energy loss and how much economically viable is this solution. When we deal with discrete time instances (samples of MCS), then the energy yield from the sum of the instances is given by:

$$E = \frac{1}{n}\sum_{i=1}^{n} \tag{6}$$

where n is the number of instances.

Eq. (6) corresponds actually the mean value of power $\overline{P}$ for a period of time. Hence, the mean value of a power distribution gives the energy yield for a specific period of time. Applying this procedure, we take the wind energy potential, the wind energy yield with curtailment and the energy loss due to curtailment for all wind penetration levels(Fig.8).

We can see that the wind energy yield and also the energy loss due to wind curtailment increases with wind penetration. As seen at Fig. 8, a 75% wind penetration gives $1230MW$ yield after curtailment, while for 50% we get $1120MW$ yield without curtailment. This is because during periods of low wind speed the higher wind power penetration gives a higher

[2]For the derivation of the transmission lines overloading limits, the following acknowledgement is taken into account: When the system is operating without wind penetration, the transmission lines are overloaded only for 5% of the samples.

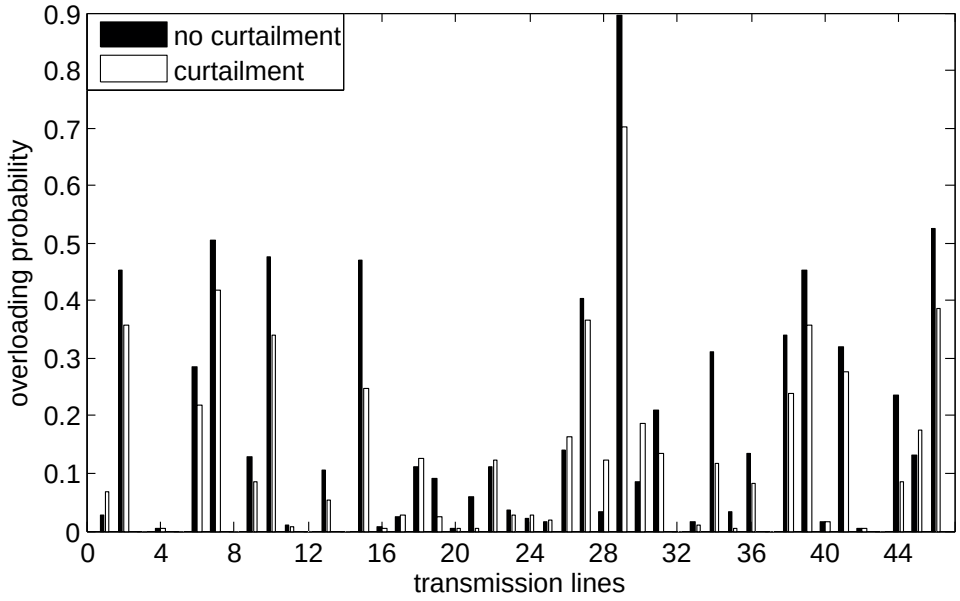

Fig. 7: Overloading probabilities of the transmission lines

power output even though wind power is curtailed in lower wind speeds compared with the lower wind power penetration. Also, the slopes are different for the 3 plots, for each interval between the wind penetration levels, which means that the share of energy loss due to curtailment changes with increasing wind penetration.

V. Conclusion

In this paper, a stochastic methodology assessment of wind curtailment in a power system is presented. The probabilistic system analysis shows that the injection of stochastic generation in a distributed scheme (fifteen wind parks connected all over the system) results to highly bi-directional power flows. The vertical system structure is changed to a horizontal one, where the distribution systems become active, exchanging power with the transmission system bi-directionally.

The method of wind curtailment is applied in the sense of maintaining the power balance in the system and prevent the excessive power generation which is driven towards the neighbouring systems through the slack bus. The solution of the wind curtailment can be applied to achieve:

1) Limitation of excessive power flows in the transmission system, reducing the risk of overloading
2) Reduction of the variability of the power flow distributions caused by wind power
3) Increase of the potential for further wind energy development

Hence, wind curtailment could be a solution for the improvement of power system operation with large-scale wind power.

References

[1] L. Soder, L. Hofmann, A. Orths, H. Holttinen, Y. Wan, and A. Tuohy, "Experience from wind integration in some high penetration areas," *IEEE transactions on energy conversion*, vol. 22, March 2007.

[2] European Wind Energy Association (EWEA), "Powering Change: EWEA annual report 2006," Available: http://www.ewea.org, 2006.

[3] B. C. Ummels, M. Gibescu, W. L. Kling, and G. C. Paap, "Integration of wind power in the liberalized dutch energy market," *Wind Energy*, vol. 9, Issue 6, pp. 579–590, July 2006.

[4] P. Gardner, S. McGoldrick, T. Higgins, and B. O'Gallachoir, "The effect of increasing wind penetration on the electricity systems of the republic of ireland and north ireland," *proceedings of the European Wind Energy Conference*, vol. 12(2), June 2003.

[5] B. C. Ummels, M. Gibescu, E. Pelgrum, W. L. Kling, and A. J. Brand, "Impacts of Wind Power on Thermal Generation Unit Commitment and Dispatch," *IEEE Transactions on Energy Conversion*, vol. 22, no. 1, pp. 44–51, March 2007.

[6] M. C. Caramanis, "Analysis of non-dispatchable options in the generation expansion plan," *IEEE Transactions on Power Apparatus & Systems*, vol. PAS-102, no. 7, pp. 2098–2103, July 1983.

[7] G. Papaefthymiou and B. Klöckl, "Mcmc for wind power simulation," *approved for publication in IEEE Transactions on Energy Conversion*.

[8] G. Papaefthymiou, "Integration of stochastic generation in power systems," Ph.D. dissertation, Delft University of Technology, Delft, the Netherlands.

[9] G. J. Anders, *Probability Concepts in Electric Power Systems*. Wiley Interscience, 1990.

[10] G. Papaefthymiou, A. Tsanakas, D. Kurowicka, P. H. Schavemaker, and L. van der Sluis, "Probabilistic power flow methodology for the modeling of horizontally-operated power systems," *submitted to the International Conference on Future Power Systems, 2005*.

[11] A. Papoulis and S. U. Pillai, *Probability, Random Variables and Stochastic Processes*, 4th ed., ser. Electrical and Computer Engineering. McGraw-Hill, 2002.

[12] G. Papaefthymiou, J. Verboomen, and L. van der Sluis, "Estimation of power system variability due to wind power," in *submitted to PowerTech 2007 Conference, Lausanne, Switzerland*, July 1-5 2007.

[13] J. Grainger and W. D. Jr. Stevenson, *Power Systems Analysis*, ser. Electrical Engineering. McGraw-Hill International Editions, 1994.

Allocation of System Reserve Based on Standard Deviation of Wind Forecast Error

Aidan Tuohy*, Eleanor Denny, Mark O'Malley
Electricity Research Centre, University College Dublin, Dublin 4, Ireland.
* Ph +353 1 7161857, email: atuohy@ee.ucd.ie

***Abstract*— As wind power penetration grows on a system, the unit commitment problem changes, due to the increased uncertainty of wind power forecasts. Unit commitment aims to schedule generation to meet demand at the lowest cost to the system. Reserve is also carried to cater for outage of units, and system demand forecast errors. However, with large amounts of wind power, there is greater uncertainty on the system. This causes the amount of reserve carried on the system to increase. The method of calculating the required level of this extra reserve is normally based on a multiple of the standard deviation of wind power forecast errors. By using a higher multiple of standard deviations, the reliability of the system increases. However, the costs incurred by the system also increase, causing a trade-off between system reliability and costs. This paper examines the relationship between cost of operating the system and the amount of reserve being carried on the system.**

***Index Terms*— Wind power generation, Costs, Power system economics, Power generation dispatch, Unit Commitment, Wind Forecasting, Reliability.**

I. Introduction

Unit commitment aims to schedule generation to meet system demand at the lowest cost. This is usually carried out every 24 hours. Reserve is carried on the system, to cater for the loss of generation and demand forecast errors. The reserve is scheduled while carrying out unit commitment. The methods used for unit commitment without significant wind power capacity installed on the system are well established [1], [2]. However, wind power adds a stochastic element to a previously deterministic problem [3]. This means that extra reserve needs to be carried on the system, to cater for the increased uncertainty that wind power brings. Much improvement has been made in wind forecasting, but there still remains an error, which has to be catered for using reserve. The amount of extra reserve needed obviously relies somewhat on the error of the wind power forecasts. Reserve is also needed to cater for unit outages and demand error, and this can still be calculated using methods used previously.

However, measuring reliability of a system with high amounts of wind power is not a simple task. It is normally assumed that increasing the extra reserve carried for wind increases reliability. One method to calculate the amount of extra reserve needed is to multiply the forecasted wind power by the standard deviation of forecast error. As increased reliability on a system is desirable, usually two or three times the standard deviation of wind forecast error is used to calculate additional reserve for wind power [4]. In addition to this, reserve is also carried to cater for the loss of the largest unit on the system.

This paper examines the costs incurred by increasing the wind reserve being carried. The number of standard deviations of wind forecast error is varied, between zero and 5 deviations, and the total costs of system operation are examined. It is shown that, even though the number of standard deviations increases linearly, the costs of operating the system do not increase linearly.

II. Methodology

A. Wind forecast error

The standard deviation of wind forecast error versus forecast horizon is shown in Figure 1. This was obtained from historical data on the Irish system. It can be seen that, as forecast horizon increases, the error increases, which is as expected. When operating the system in this study, the forecasted wind power is multiplied by the standard deviation in forecast error. This means that for those hours nearest the start of the day, the reserve is smaller than for those hours nearer the end of the day, if the same amount of wind is forecast. The standard deviation of error when persistence forecasting is used is shown as a comparison. Persistence forecasting assumes that the wind power over the forecast horizon will be the same as the current wind power. This can be seen as a worst case scenario, and current methods can be seen to be an improvement on this.

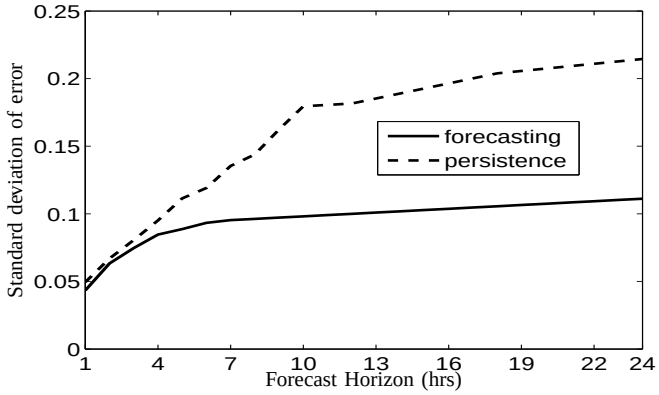

Fig. 1. Standard deviation of forecast error versus time

B. Model used for study

To study the effect of increased reserve on the system, a model based on for previous work, [5], was used to simulate the scheduling of the power system. This code was a simplified version of unit commitment which aims to find the least cost for each hour of operation, ensuring that plant is kept within its operating limits. However, it does not take into account startup costs or ramp rates and does not try to

reduce costs over the whole 24 hour period, rather it treats each hour separately.

This model first schedules units to be on or off so that the system can meet the load minus the forecasted wind. If the forecasted wind is different than the actual wind power output, this is then put into the model, and the operational levels of the units scheduled to be on are optimized with respect to the updated wind profile. This corresponds to real time operation of the system, so units are not allowed to turn on or off during this second run -only those units scheduled, plus some open cycle gas units, are allowed to meet the demand. As the demand less wind has changed from that expected, this means units operating levels will need to be changed, and those which were supplying reserve may need to be called upon. In extreme cases, where, the wind is far greater than forecasted, wind may need to be curtailed. However, this is not examined in this study. A flow chart showing the operation of the model is shown in Figure 2. Here, pumped storage and hydro schedule are taken from a unit commitment solution obtained from previous work [6], as this model is not able to schedule these types of plant.

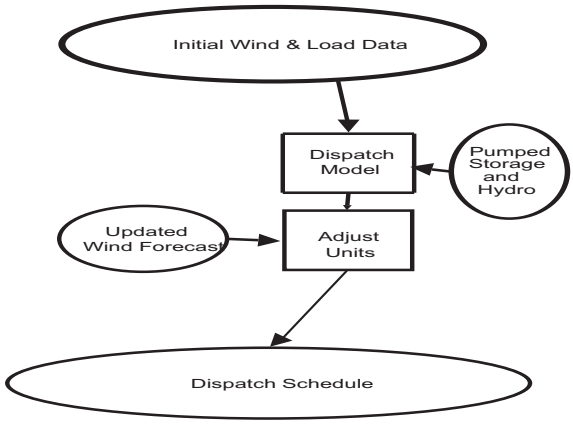

Fig. 2. Flowchart showing operation of model

The model was compared to rolling unit commitment in previous work and found to give dispatch schedules very close to the results obtained when rolling commitment was used on the Irish power system [6]. Here, rolling unit commitment was carried out using the Plexos unit commitment and dispatch software [7]. Rolling unit commitment involved doing 24-hour unit commitment more frequently, i.e. every 3 hours. The system is committed, then time rolled forward 3 hours, and the initial data is changed to reflect the system in the third hour of operation. The system is then re committed for the next 24 hours. By committing more frequently, the system has to carry less reserve to cater for wind uncertainty. This is due to the fact that the forecast error increases as forecast horizon lengthens, as shown in Figure 1. This would be expected to lead to a reduction in system costs. This method of rolling commitment using unit commitment software was compare to the code described above, and the results showed that the code can be taken as a good approximation of unit commitment.

C. All Island electricity system

The all Ireland electricity system consists of two systems, the Northern Ireland and Republic of Ireland. These are interconnected using a 400MW ac link. At present, plans are being finalised for the Single Electricity Market (SEM), which will operate what was until now two separate systems as one system, which is what this paper examines. The SEM will be a gross pool market with centralized commitment [8]. This centrally committed market is something many electricity markets are moving away from, but it has been shown in [9] and [10] that centralized unit commitment is almost identical to a model which allows generators to bid incrementally and self-commit. Centralized unit commitment can be used for predicting operating decisions in decentralised markets [9]. This model could therefore represent alternative market designs as well as the centralised gross pool market used in this model [5].

The installed capacity for the single Irish system is approximately 7500MW. There is currently approximately 800-900MW of wind power installed, with plans to increase this in the next decade. There is currently just one 500MW HVDC interconnector to Scotland. Historical data is used in this paper for interconnector exchanges. Most of the other units on the system are conventional units - coal, OCGTs, CCGTs, oil and peat. There is also a small amount of hydro power, and a pumped storage plant. As mentioned in II-B, these cannot be optimised in the model, as they involve optimising over the whole day. Therefore, the schedules for these are taken from previous work.

For this study, one week's load and wind data was used, corresponding to a week in March, which would be expected to be somewhere between the peak load in winter and minimum load in summer. Fuel costs and wind profiles were obtained from [11]. The wind profile was then scaled so that it reflects a wind series for 1500MW of installed capacity, which is a reasonable estimate of the amount of wind power that would be expected on the system within then next 5 years. The rest of the power system is based on the current (2007) power system. Data for the other units was taken from [11]. For this study 75MW of error was assumed in the load forecast for the Irish electricity system, with a largest unit size of 400MW.

III. Results and Discussion

The test system described in II-C was examined using the model described in II-B. The total system costs, including costs for startup of units, were then calculated for different values of standard deviation between zero (i.e. no extra reserve) and six times the standard deviation. The total amount of reserve scheduled over the week is shown Figure 3.

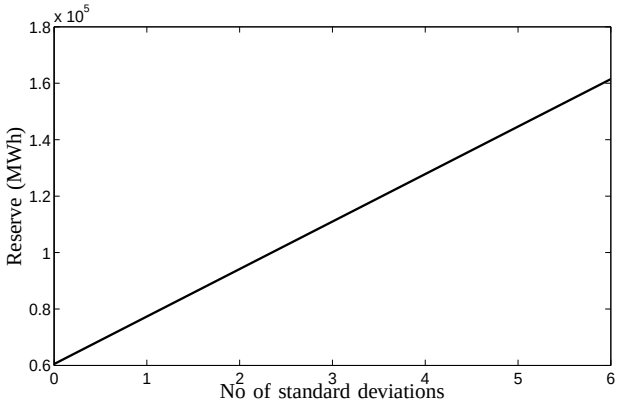

Fig. 3. Standard deviations of forecast error in reserve versus total reserve

It can be seen that the reserve increases linearly, and that the amount of reserve scheduled when 6 times the standard

deviation of error is used to calculate reserve is approximately double the reserve scheduled for the week when one standard deviation is used. This is as expected, as increasing the amount of standard deviations in a linear fashion has the effect of increasing reserve in a linear fashion.

The total cost for the week examined is shown in Figure 4, versus the number of standard deviations of wind forecast error used in calculating reserve. Unlike the amount of reserve scheduled, this relationship is not linear. This result is significant, as it shows that, for what would be expected to be a linear increase in reliability, the increase in operating the costs is nonlinear, with the rate of increase in costs increasing as number of standard deviations increases. This means that, for example, if the amount of reserve on the system doubles, the extra cost due to this reserve is not doubled, but more than doubled. The likely reason for this is that more units are being switched on, to cater for reserve and this increases both startup and fuel costs, as units are being operated less efficiently. It can be seen that, by doubling the amount of extra reserve carried to cater for wind from twice the standard deviation of forecast error to four times the standard deviation, the total system operating cost for the week increases by an average of approximately €400000, or approx 2.5%. While this is not a very large increase, it should taken into account that this is an increase in total system operating costs, of which the cost of providing reserve is only a small part. This shows that an increase in reserve can cause a significant increase in cost for the system.

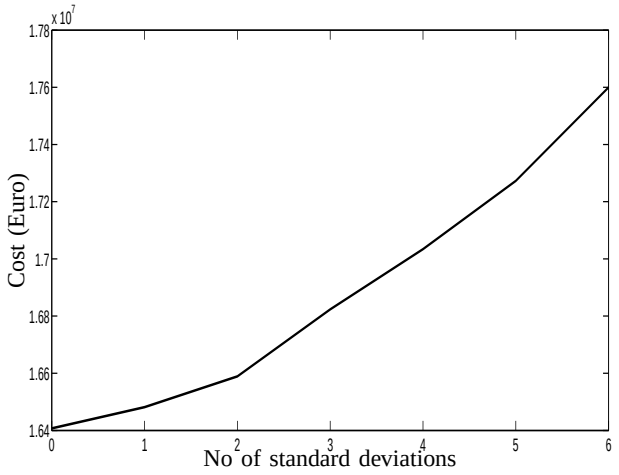

Fig. 4. Number of standard deviations of forecast error in reserve versus total system costs

It is assumed that the reason for the extra cost when providing extra reserve is due to the additional number of units being turned on. To examine this, the startup costs of the system were found for the week examined, and are shown in Figure 5.

It can be seen that there is a different shape here, with the rate of increase getting smaller at around four standard deviations of error. This is most likely due to the fact that at this point, many extra units have been turned on to provide reserve, and therefore less units need to be turned on as reserve demand increases. However, by this stage, the units being turned on would be more expensive units, and so the cost of providing the reserve would continue to increase. It can also be seen that, out of the extra €400000 cost when using four standard deviations instead of two, approximately €250000 of this can be attributed to additional startup costs. It is expected that the rest of the additional cost would be due to using more expensive units to meet load so that enough spare capacity is available to meet the reserve target. As the amount of reserve grows, the share of additional cost due to using expensive units to meet load, as opposed to due to startups, will also grow, as shown by the shape of Figure5.

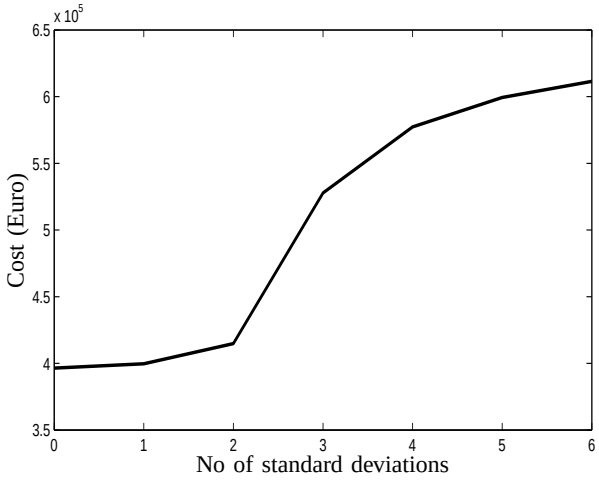

Fig. 5. Number of standard deviations of forecast error in reserve versus startup costs

IV. Conclusions and further work

This was an initial study in the area of reliability of a power system with significant installed wind. Rather than look immediately at defining reliability, it was decided to examine a method currently used, that is basing reserve on wind power uncertainty, specifically, the standard deviation of forecast error. The costs associated with this were examined,and it was found that there is a non-linear relationship between increasing the amount of reserve and the extra cost incurred by doing this. it was shown that much of this increase was due to larger startup costs

This work will be extended by quantifying the system reliability associated with the different levels of reserve, in a familiar format, e.g. Loss of load probability. This will then show how many standard deviations of forecast error should be used in order to meet desired reliability, keeping in mind the additional cost. A stochastic model, Wilmar, [12], will be used to examine the unit commitment problem when wind is on the system, and the method of setting reserve targets based on standard deviation of forecast error compared to other methods. By running the system with a full years data, the results would be more conclusive, as they would take into account winter peak, summer valley, as well as extreme wind scenarios.

V. Acknowledgements

This work has been conducted in the Electricity Research Centre, University College Dublin which is supported by Electricity Supply Board (ESB) Networks, ESB Power Generation, ESB National Grid, Commission for Energy Regulation, Cylon, Airtricity and Enterprise Ireland.

REFERENCES

[1] A. J. Wood and B. Wollenberg, *Power Generation, Operation and Control*, 2nd ed. Wiley-Interscience, 1996.

[2] R. Baldick, "The generalized unit commitment problem," *IEEE Transactions on Power Systems*, vol. 10, no. 1, pp. 465–475, 1995.

[3] P. Meibom, H. Ravn, L. Sder, and C. Weber, "Market integration of wind power," in *EWEA 2004*, Dec. 2004.

[4] Hirst E, Kirby B. , "Ancillary-service details: dynamic scheduling," *Oak Ridge National Laboratory*, 1997.

[5] E. Denny and M. O'Malley, "A quantitative analysis of the net benefits of grid integrated wind," *IEEE Transacions on Power Systems*, vol. 22, no. 2, 2007.

[6] A.Tuohy, E.Denny, and M.O'Malley, "Rolling unit commitment for systems with significant installed wind capacity," *Proc. IEEE Lausanne Power Tech Conf*, no. 1, 2007.

[7] PLEXOS for Power Systems - Electricity Market Simulation, *www.draytonanalytics.com*.

[8] The Single Electricity Market, "High level design decision paper - AIP/SEM/42/05," *Available: www.allislandproject.org*, June 2005.

[9] J. Xu and R. Christie, "Decentralised unit commitment in competitive energy markets,," *in DIMAC Conference on Unit Commitment, Rutgers, New Jersey. Also published as a chapter in Hobbs, Rothkopf, O'Neill and Chao, eds., The Next Generation of Electric Power Unit Commitment Models, Kluwer.*, 1999.

[10] S. Ede, R. Zimmerman, T. Mount, R. Thomas, and W. Schulze, "An economic analysis of the self commitment of thermal units." in *Proc. 33rd Hawaii International Conference on System Sciences*, 2000.

[11] All Island Project, "Wind series 2006-2010," *Available from www.allislandproject.org*.

[12] W. P. I. in Liberalised Electricity Markets (WILMAR) project, *www.wilmar.risoe.dk*.

Aidan Tuohy received a B.E. degree in Electrical and Electronic Engineering from University College Cork. He is currently studying for a Ph. D. degree in the Electricity Research Centre, University College Dublin with research interests in the integration of wind energy in power systems

Eleanor Denny received a B.A. degree in Economics and Mathematics and a M.B.S. degree in Quantitative Finance from University College Dublin. She has just completed a Ph. D. degree in the Electricity Research Centre, University College Dublin on the costs and benefits of the grid integration of wind generation.

Mark O'Malley received B.E. and Ph. D. degrees from University College Dublin in 1983 and 1987, respectively. He is the professor of Electrical Engineering in University College Dublin and is director of the Electricity Research Centre with research interests in power systems, control theory and biomedical engineering. He is a fellow of the IEEE.

State-of-the-art of design and operation of power systems with large amounts of wind power, summary of IEA Wind collaboration

Hannele Holttinen[1*)], Bettina Lemström[1)], Peter Meibom[2)], Cornel Ensslin[3)], Aidan Tuohy[4)], John Olav Tande[5)], Ana Estanqueiro[6)], Emilio Gomez[7)], Lennar Söder[8)], Anser Shakoor[9)], J. Charles Smith[10)], Brian Parsons[11)], Frans van Hulle[12)]
[1)] VTT, Vuorimiehentie 3, Espoo, P.O. Box 1000, FI-02044 VTT, Finland. [*)] tlf. +358 20 722 5798, e-mail hannele.holttinen@vtt.fi
[2)] Risø DTU, Denmark; [3)] Ecofys, Germany; [4)]UCD, Ireland; [5)]SINTEF, Norway; [6)]INETI, Portugal; [7)]University Castilla la Mancha, Spain; [8)] KTH, Sweden; [9)]Centre of Distributed Generation and Sustainable Electrical Energy, UK; [10)]UWIG, USA; [11)]NREL, USA; [12)]EWEA

Abstract — An international forum for exchange of knowledge of power system impacts of wind power has been formed under the IEA Implementing Agreement on Wind Energy. The task "Design and Operation of Power Systems with Large Amounts of Wind Power" is analysing existing case studies from different power systems.There are a multitude of studies made and ongoing related to cost of wind integration. However, the results are not easy to compare. This paper summarises the results from 15 case studies with discussion on the differences in the methodology as well as issues that have been identified to help wind integration.

Index Terms — grid integration, wind power, power system operation.

1. Introduction

The existing targets for wind power anticipate a quite high penetration of wind power in many countries. It is technically possible to integrate very large amounts of wind capacity in power systems, the limits arising from how much can be integrated at socially and economically acceptable costs. So far the integration of wind power into regional power systems has mainly been studied on a theoretical basis, as wind power penetration is still rather limited in most countries and power systems. However, already some regions (e.g. West Denmark, North of Germany and Galicia in Spain) show a high penetration and have first practical experience from wind integration.

Wind power production introduces more uncertainty in operating a power system: it is continuously variable and difficult to predict. To enable a proper management of the uncertainty, there will be need for more flexibility in the power system: either in generation, demand or transmission between areas. How much extra flexibility is needed depends on the one hand on how much wind power there is and on the other hand on how much flexibility already exists in the power system.

In recent years, several reports have been published in many countries investigating the power system impacts of wind generation. However, the results on the costs of integration differ and comparisons are difficult to make due to different methodology, data and tools used, as well as terminology and metrics in representing the results. An R&D Task titled "Design and Operation of Power Systems with Large Amounts of Wind Power Production" has been formed within the "IEA Implementing Agreement on the Co-operation in the Research, Development and Deployment of Wind Turbine Systems" [1] in 2006 and will continue for three years. The objective is to analyse and further develop the methodology to assess the impact of wind power on power systems. This R&D task will collect and share information on the experience gained and the studies made, with analyses and guidelines on methodologies. The Task has started by producing a state-of-the-art report on the knowledge and results obtained so far and will end with developing guidelines on the recommended methodologies when estimating the system impacts and the costs of wind power integration. When possible, best practice recommendations will be formulated on system operation practices and planning methodologies for high wind penetration.

2. Power system impacts of wind power

Wind power has impacts on power system reliability and efficiency. The studies address different impacts and the different time scales involved usually mean different models (and data) used in impact studies. The case studies for the system wide impacts have been divided to three focus areas: Balancing, Adequacy of power and Grid (Fig 1). In this international collaboration (IEA WIND Task 25), more system related issues are addressed, as opposed to local issues of grid connection like power quality. Primary reserve is here denoted for reserves activated in seconds (frequency activated reserve; regulation) and Secondary reserve for reserves activated in 10...15 minutes (minute reserve; load following reserve).

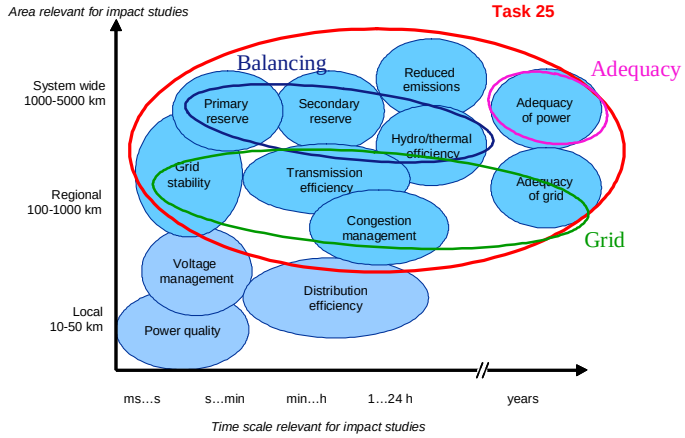

Figure 1 Impacts of wind power on power systems, divided in different time scales and width of area relevant for the studies.

Balancing: increases needed in allocation and use of short term reserves (time-scale minute…half an hour) and the impact of wind variability and prediction errors on efficiency and unit commitment of existing power capacity (time scale: hours…days). Unpredicted part of the variations of large area wind power should be combined with any other unpredicted

variations the power system sees, like unpredicted variations in load. General conclusions on increase in balancing requirement will depend on region size relevant for balancing, initial load variations and how concentrated/distributed wind power is sited. The added costs of balancing due to wind power will depend on the marginal costs for providing regulation or mitigation methods used in the power system for dealing with increased variability, generation mix and the transmission system spatial structure (e.g. radial vs meshed). Market rules will also have an impact, so technical costs can be different from market costs. Variability of wind power impacts also on how the conventional capacity is run and how the variations and prediction errors of wind power change the unit commitment. Analysing and developing methods of incorporating wind power into existing planning tools is important in order to take into account wind power uncertainties and existing flexibilities in the system correctly. The simulation results give insight into the technical impacts of wind power, and also the (technical) costs involved.

Adequacy of power: This is about total supply available during peak load situations (time scale: several years). System adequacy is associated with static conditions of the system. The estimation of the required generation capacity needs includes the system load demand and the maintenance needs of production units (reliability data). The criteria that are used for the adequacy evaluation include the loss of load expectation (LOLE), the loss of load probability (LOLP) and the loss of energy expectation (LOEE), for instance. The issue is the proper assessment of wind power's aggregate capacity credit in the relevant peak load situations – taking into account the effect of geographical dispersion and interconnection.

Grid: Transmission adequacy, efficiency and system stability: The impacts of wind power on transmission depend on the location of wind power plants relative to the load, and the correlation between wind power production and load consumption. Wind power affects the power flow in the network. It may change the power flow direction, reduce or increase power losses and bottleneck situations. There are a variety of means to maximise the use of existing transmission lines like use of online information (temperature, loads), FACTS and wind power plant output control. However, grid reinforcement may be necessary to maintain transmission adequacy and security. When determining adequacy of the grid, both steady-state load flow and dynamic system stability analysis are needed. Different wind turbine types have different control characteristics and consequently also different possibilities to support the system in normal and system fault situations. For system stability reasons operation and control properties similar to central power plants are required for wind plants at some stage depending on penetration and power system robustness.

3. SUMMARY OF CASE STUDIES REVIEWED

For the case studies reviewed in this paper, the emphasis is on more recent studies and especially on those that have tried to quantify the power system impacts of wind power. Further case studies will also be made during the 3 years of the IEA collaboration. A short list of on-going research is given in [2]. A summary table for the power systems and largest wind penetration studied is presented in Table 1. A short description of the studies is given here, a more detailed description is provided in [3] and [4].

Greennet-EU27 [5] estimated increases in system operation costs as a result of increased shares of wind power for a 2010 power system case covering Denmark, Finland, Germany, Norway and Sweden combined with three wind cases. The integration costs of wind is calculated as the difference between the system operation costs in a model run (WILMAR) with stochastic wind power forecasts and the system operation costs in a model run where the wind power production is converted into an equivalent predictable,

Table 1. Data for power systems and wind power in case studies. The use of interconnection capacity is not taken into account in studies marked with *. In Nordic 2004 study the interconnection capacity between the Nordic countries is taken into account, not the interconnection to outside Nordic area.

	Load			Inter-connect. capacity	Wind power					
					2006	Highest studied		Highest penetration level		
Region / case study	Peak MW	Min MW	TWh/a	MW	MW	MW	TWh /a	% of peak load	% of gross demand	% of (min load + interconn)
Nordic 2004	67000	24000	385	3000*	4108	18000	46	27 %	12 %	67 %
Nordic+Germany/Greennet	155500	65600	977	6600	24730	57500	115	37 %	12 %	80 %
Finland 2004	14000	3600	90	1850*	86	4000	8	29 %	9 %	73 %
Germany 2015 / dena	77955	41000	552.3	10000*	20622	36000	77.2	46 %	14 %	71 %
Ireland / ESBNG	5000	1800	29	0	754	2000	4.6	40 %	16 %	111 %
Ireland / ESBNG	6500	2500	38.5	0	754	3500	10.5	54 %	27 %	140 %
Ireland / SEI	6127	2192	35.5	500	754	1950	5.1	32 %	14 %	72 %
Ireland / SEI	6900	2455	39.7	900	754	1950	5.1	28 %	13 %	58 %
Netherlands	15500		100	12930*	1560	6000	20	39 %	20 %	46 %
Mid Norway /Sintef	3780		21			1062	3.2	28 %	15 %	
Portugal	8800	4560	49.2	1000	1697	5100	12.8	58 %	26 %	92 %
Spain 2011	53400	21500	246.2	2400*	11615	17500		33 %	19 %	73 %
Sweden	26000	13000	140	9730*	572	8000	20	31 %	14 %	35 %
UK	76000	24	427	2000*	1963	38000	115	50 %	27 %	146 %
US Minnesota 2004	9933	3400	48.1	1500*	895	1500	5.8	15 %	12 %	31 %
US Minnesota 2006	20000	8800	85	5000	895	5700	21	30 %	25 %	41 %
US New York	33000	12000	170	7000	430	3300	9.9	10 %	6 %	17 %
US Colorado	7000		36.3			1400	3.6	20 %	10 %	

constant wind power production during the week. The following conclusions could be drawn from the study: a) Wind power integration costs are lower in hydro dominated countries (especially Norway) compared to thermal production dominated countries (Germany, Denmark). The reason is that hydropower production has very low costs connected to part-load operation and start-up and that hydro-dominated systems are generally not constrained in regulating capacity. b) Wind power integration costs increase when a neighbouring country gets more wind power. c) Germany has the highest integration costs because the wind power capacity in Germany is very unevenly distributed with North-western Germany having a high share of wind power relatively to the electricity demand and the export possibilities out of the region.

In Finland the operating reserve requirement due to wind power in the Nordic countries has been estimated in 2004 [6]. The estimate is made from hourly time series for load and wind power, 4 times standard deviation of the variations time series is used as confidence level when looking at the increase in hourly variations from load to net load. The effect of prediction errors day-ahead has not been taken into account; this is only for the real-time hour to hour variations. Existing reserves for disturbances have not been considered; the impact is only estimated on operating reserves used for load following. The increase in reserve requirements for Finland was twice as much as for the Nordic region, due to lower smoothing of wind power variations in one country compared to larger area and the relatively small load variations in Finland. The cost was estimated assuming new natural gas capacity was built for this purpose, and the investment costs was allocated to wind power production. The increase in use of reserves was also estimated and a cost estimate was made at existing regulating market prices of 5-15 €/MWh for imbalances.

A study of 4000 MW wind power in Sweden was published in 2005 [7].The Swedish additional reserve requirements were estimated based on probability and forecast approach, using several years of wind data and load forecast error data. It has been concluded that decisive parameters for the additional requirements are the wind power penetration level and the consumption variations. In power systems with large consumption variations, like the Swedish, lower additional reserves are required compared with power systems with lower consumption variations, like the Finnish. The study indicates that the requirement of additional regulating/reserve capacity is comparatively small, at least for the time horizon 1 hour and with an approach including probability and forecasts. In many cases these extra requirements may also already be available which means that no extra investments are needed.

The main existing study covering wind integration in Germany is German Energy Agency's (dena) study "Planning of the integration of wind energy into the German grids ashore and offshore regarding the economy of energy supply", 2005 [8]. The study ascertained that based on the assessed regional distribution and identified grid reinforcement and extension, the integration of a total of 36 GW of wind power capacity into the German transmission system in 2015 will be possible. Up to the time horizon 2015 approximately 850 km of 380-kV-transmission routes as well as reinforcement of 390 km of existing power lines will be needed. In addition, numerous 380-kV-installations will need to be fitted with new components for active power flow control (e. g. Quadrature Regulators) and reactive power compensation (approximately 7,350 Mvar till 2015). According to this study, a modification of the existing German Grid Code for connection and operation of wind power plants in the high voltage grid will be necessary, for instance in view of fault-ride-through and grid voltage control. Capacity credit of wind power was estimated as well as the additional requirement for reserves. The regulating and reserve power capacity required for the following day was determined in relation to the forecasted wind infeed level. The additionally required regulating energy could be provided by the existing conventional power stations.

Irish TSO ESBNG report 2004 [9]: the wind input assessment methodology used was direct scaling of output data from existing wind power production combined with some planned site wind data to create a power time series. The system assessment methodology was generating system simulation using a unit commitment and dispatch simulator. The study found that a high wind energy penetration greatly increased the number of start ups and ramping for gas turbine generation in the system and that the cost of using wind power for CO2 abatement in the Irish electricity system is €120/Tonne. Capacity credit of wind power was estimated by assessing the amount of conventional plant that is displaced, while keeping generation adequacy at the desired level.

Ireland SEI report from 2004: "Operating Reserve Requirements as Wind Power Penetration Increases in the Irish Electricity System" [10] the wind input assessment methodology was to use a time series generated from statistical manipulation of historic wind power plant data. The system assessment methodology was generating system simulation using a proprietary system dynamic model. The study findings were that fuel cost and CO2 savings up to a 1500MW wind power penetration in the Republic of Ireland (ROI) system were directly proportional to the wind energy penetration. It found that while wind did reduce overall system operation costs it could lead to a small increase in operating reserve costs: 0.2 €/MWh for 1300 MW wind and 0.5 €/MWh for 1950 MW of wind.

Two case studies from UK were taken in review: the ILEX/Strbac report from 2004 [11] and Strbac et al 2007 [12]. Regarding reserve requirements, extra plant may be needed if the existing capacity is insufficient, but the amounts involved are very modest – around 5% of the wind plant capacity, at the 20% penetration level (% of gross demand). Estimates of extra reserve costs from [13] used market costs, which may be expected implicitly to include a capital recovery element. A value of £2.38 per MWh of wind produced for 10% wind penetration is used, rising to £2.65/MWh at 15% and £2.85/MWh at 20% penetration. Historically, transmission costs have been driven by a north-south flow from thermal generators located predominantly in the north, to demand in the south. With significant wind resources in Scotland and off the North West and North East of England and North Wales coasts, it is possible to envisage scenarios where this pattern of flows endures, increasing the requirement for transmission reinforcement and the level of transmission losses. Alternatively, if onshore wind generation were developed across Great Britain and included the offshore wind resources around the England and Wales coast, then transmission reinforcement costs could be significantly smaller. In [13] costs of between £275m and

£615m to accommodate 8 GW of wind, i.e. between £35/kW and £77/kW, were found. In [11] the effects of connecting wind power plants at various locations across the country on the transmission reinforcement cost were considered. This included the impact of the locations of new conventional plant and decommissioning of existing generation. The range of cost was found to be between £1.7b and £3.3b for 26 GW wind (£65/kW to £125/kW of wind capacity). Lower values correspond to scenarios with dispersed wind generation connections, with significant proportions of offshore wind around the England and Wales coast, while the higher values correspond to the scenarios with considerable amount of wind being installed in Scotland and North of England. For a small level of wind penetration the capacity value of wind is roughly equal to its load factor, approximately 35%. But as the capacity of wind generation increases, the marginal contribution declines. For the level of wind penetration of 26 GW, about 5GW of conventional capacity could be displaced, giving a capacity credit of about 20% (for a future UK system 70GW peak load and a 400TWh energy demand, and a 35% load factor of wind).

Consequences of 6000 MW offshore wind power for the 150/380 kV grid of the Netherlands were determined by a load flow study. This showed that additional voltage control equipment is required and that a limited number of lines have to be upgraded. Investment costs to the grid were estimated at 344-660 ME, depending on location/scenario (about 4% of est. total investment for 6 GW wind) [14].

For Portugal, in the overall period 2005 – 2010, the investment directly attributable to renewables, mostly for wind parks, will total 200 Million €. These numbers do not consider the investment of the wind park main substation nor the direct line to the transmission network connection point, which are built by the promoter. A study carried out in 2004 by the Portuguese TSO (REN) showed a danger of instability in Portugal + Spain following a short circuit in certain locations of the transmission network. At this moment, REN and its Spanish counterpart REE are completing a second and more detailed joint study with higher wind targets (5100 MW in Portugal and 20000 MW in Spain) that shows also that possibility. The new grid codes with fault ride through were proved to be required, at least at certain parts of the grid.

Different studies, [15-16], were carried out by Spanish and Portuguese TSOs REE and REN to determine the maximum wind power capacity that the Iberian grid could handle. Specifically, the integration of existing wind turbine technologies and future modifications were studied under different scenarios (demand, wind energy production and different degrees of adaptations of new wind turbine and wind power plant technologies). Two scenarios were studied with 17500 MW of installed wind power. Its major conclusions were that with 75% of wind power technically adapted, transient stability was supported for 14000 MW wind power production in a peak demand scenario and 10000 MW wind power production in a valley one. The importance of future 400 KV D/C interconnection line with France was highlighted. In the Spanish case, wind power development has imposed new connecting and operating rules, being the connection and reinforcement costs paid by wind power plants (from the wind power plant to the electrical substation). On the other hand, this has provoked an updating in connecting requirements, protection equipment, remote metering and control, resolution of constraints or wind power plant clustering. Obviously, transmission network must be updated as well; the investment 2200 Million €, not only attributable to renewable, has been estimated by REE for the overall period 2006 – 2010. In terms of investments due to wind energy, it is difficult to obtain the figures for the Spanish case, since grid reinforcements and new lines are needed for wind power plants and other clients (electrical demand growing rates have been high in the last years).

The impact of wind power on system adequacy for one region in Norway was reported in [17]. The impact is assessed using data from a real life regional hydro-based power system with a predicted need for new generation and/or reinforcement of interconnections to meet future demand. Wind power will have a positive effect on system adequacy. Wind power contributes to reducing the LOLP and to improving the energy balance. Adding 3 TWh of wind or 3 TWh of gas generation are found to contribute equally to the energy balance, both on a weekly and annual basis. Both wind and gas improve the power balance. The capacity value of gas is found to be about 95 % of rated, and the capacity value of wind about 30 % at low wind energy penetration and about 14 % at 15 % penetration. The smoothing effect due to geographical distribution of wind power has a significant impact on the wind capacity value at high penetration.

The first Minnesota Dept. of Commerce/Enernex Study (2004) [18], estimated the impact of wind in a 2010 scenario of 1500 MW of wind in a 10 GW peak load system. Three year data sets of 10-minute power profiles from atmospheric modeling were used to capture geographic diversity. Wind plant output forecasting was incorporated into the next day schedule for unit commitment. Extensive time-synchronized historic utility load and generator data was available. A monopoly market structure, with no operating practice modification or change in conventional generation expansion plan, was assumed. Incremental regulation due to wind was found to be 8 MW (at 3σ confidence level). Incremental intra-hour load following burden increased 1-2 MW/min. (negligible cost). Hourly to daily wind variation and forecasting error impacts are the largest cost items. A total integration cost of $4.60/MWh was found, with $0.23/MWh representing increased regulation costs, and $4.37 due to increased costs in the unit commitment time frame. A capacity credit of 26%-34% was found with a range of assumptions using the ELCC method.

The second Minnesota Dept. of Commerce/EnerNerx study (2006) [19] took as a subject power system a consolidation of four main balancing areas into a single balancing area for control performance purposes. Simulations investigating 15%, 20%, and 25% wind energy penetration of the Minnesota balancing area retail load in 2020 were conducted. The 2020 system peak load is estimated at 20,000 MW, and the installed wind capacity is 5700 MW for the 25% wind energy case. Three years of high resolution wind and load data were used in the study. The cost of wind integration ranged from a low of $2.11/MWh of wind generation for 15% wind penetration in one year to a high of $4.41/MWh of wind generation for 25% wind penetration in another year, compared to the same energy delivered in firm, flat blocks on a daily basis. These are total costs and include both the cost of additional reserves, and cost of variability and day-ahead forecast error associated with the wind generation. The cost of the additional reserves attributable to wind generation is

included in the wind integration cost. Special hourly runs were made to isolate this cost, which was found to be about $.11/MWh of wind energy at the 20% penetration level. The remainder of the cost is related to how the variability and uncertainty of the wind generation affects the unit commitment and market operation. In the study, the Minnesota balancing authority was assigned responsibility for all the reserves and intra-hour resources for balancing. At the hourly level, the day-ahead markets and in-the-day re-dispatch at the hourly level were administered by MISO for the entire footprint, with an assumed 2020 peak load in excess of 120 GW. Since the real-time market actually operates on five-minute increments, further efficiencies could be obtained if it were assumed that out-of-state resources were available to balance within the hour. Capacity values were investigated and ranged between 5% and 20% for the scenarios studied.

The NYSERDA/GE Energy Study for the New York ISO was completed in 2005 [20]. It estimated the impact of wind in a 2008 scenario of 3300 MW of wind in a 33-GW peak load system. Wind power profiles from atmospheric modeling were used to capture statewide diversity. The study used the competitive market structure of the NYISO for ancillary services, which allows determination of generator and consumer payment impacts. For transmission, only limited delivery issues were found. Post-fault grid stability improved with modern turbines using doubly-fed induction generators with vector controls. Incremental regulation due to wind was found to be 36 MW. No additional spinning reserve was needed. Incremental intra-hour load following burden increased 1-2 MW/ 5 min. Hourly ramp increased from 858 MW to 910 MW. All increased needs can be met by existing NY resources and market processes. Capacity credit was 10% average onshore and 36% offshore. Significant system cost savings of $335- $455 million for assumed 2008 natural gas prices of $6.50-$6.80/MMBTU were found.

The Xcel Colorado/Enernex Study (2006) [21] examined 10% and 15% penetration cases (wind nameplate to peak load) in detail for ~7 GW peak load system. Regulation impact was $0.20/MWh and hourly analysis gave a cost range of $2.20-$3.30/MWh. This study also examined the impact of variability and uncertainty on the dispatch of the gas system, which supplies fuel to more than 50% of the system capacity. Additional costs of $1.25-$1.45/MWh were found for the 10% and 15% cases, bring the total integration costs to the $3.70-$5.00/MWh range for the 10% and 15% penetration cases.

The CA RPS Integration Cost Project examined impacts of existing installed renewables (wind 4% on a capacity basis). Regulation cost for wind was $0.46/MWh. Load following had minimal impact. A wind capacity credit of 23%-25% of a benchmark gas unit was found.

4. SUMMARY OF RESULTS ON INCREASED BALANCING REQUIREMENTS

Summaries for the results for balancing requirements presented in section 3 are presented in Fig 2 and 3.

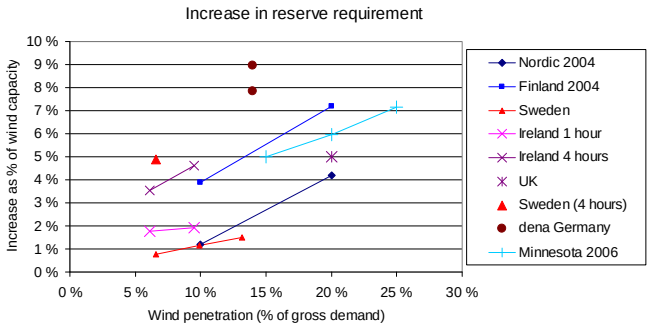

Figure 2. Results for the increase in reserve requirement due to wind power. German dena estimates are taking into account the day-ahead uncertainty (for up and down reserves separately). In Minnesota, day ahead uncertainty has been included in the forecast. For the others the effect of variations during the operating hour is considered. For UK, Ireland and Sweden the 4 hour-ahead uncertainty has been evaluated separately.

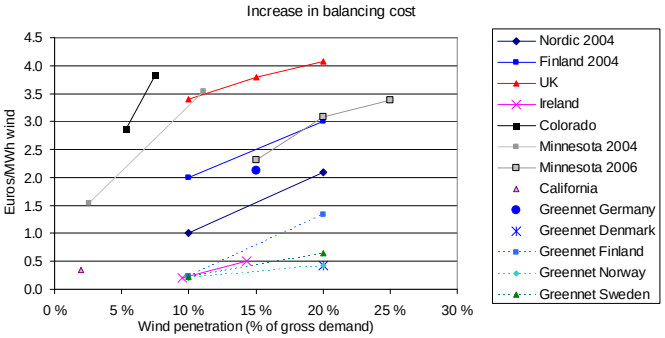

Figure 3. Results from estimates for the increase in balancing and operating costs due to wind power. The currency conversion used here is *1 € = 0.7 £ and 1 € = 1.3 US$.*

The increase in reserve requirement is mostly estimated by statistical methods combining the variability of wind power to that of load. In some studies also the sudden outages of production is combined to reserve requirements (disturbance or contingency reserve). For the impact on operation of power systems, model runs are made and most results are based on comparing costs of system operation without wind and adding different amounts of wind. The costs of variability are also addressed by comparing simulations with flat wind energy to varying wind energy (for example in US Minnesota and Greennet Nordic+Germany).

At wind penetrations of up to 30% of system peak demand, system operating cost increases arising from wind variability and uncertainty amounted to about 1-4 €/MWh. This is 10% or less of the wholesale value of the wind energy. It can be seen that there is considerable scatter in results for different countries and regions. The following differences have been remarked:

- Different time scales used for estimating – For UK, the increased variability to 4 hours ahead has been taken into account. For US studies also the unit commitment impact for day-ahead scheduling is incorporated. For the Nordic countries and Ireland only the increased variability during the operating hour has been estimated. For the Greennet study, the unit commitment and reserve allocation are done according to wind forecasts but the system makes use of updated forecasts 3 hours before delivery for adjusting the production levels.

- Costs for new reserve capacity investment – For the Greennet and SEI Ireland studies only incremental increase in operating costs has been estimated whereas also investments for new reserves are included in some results (Nordic 2004)
- Larger balancing areas – The Greennet, Minnesota 2006 and Nordic 2004 studies incorporate the possibilities for reducing operation costs through power exchange to neighbouring countries, whereas Colorado, California, German dena study, Sweden, UK and Ireland studies analyse the country in question without taking transmission possibilities into account. The two studies for Minnesota, US show the benefit of larger markets in providing balancing. The same can be seen from the Nordic 2004 results compared with results calculated for Finland alone. Dealing with large wind output variations and steep ramps over a short period of time could be challenging for smaller balancing areas. Larger power systems make it possible for smoothing of the wind variability.

As shown in table 1 the interconnection capacity to neighbouring system is often significant. For the balancing costs it is then essential in the study setup whether the interconnection capacity can be used for balancing purposes or not. A general conclusion is that if interconnection capacity is allowed to be used also for balancing purposes, then the balancing costs are lower compared to if they are not allowed to be used. From first review of methodology the other important factors identified as reducing integration costs were aggregating wind plant output over large geographical regions, and operating the power system closer to the delivery hour.

5. SUMMARY OF GRID RESULTS

With current technology, wind power plants can be designed to meet industry expectations such as riding through voltage dips, supplying reactive power to the system, controlling terminal voltage, and participating in SCADA system operation with output and ramp rate control. In areas with limited penetration, system stability studies have shown that modern wind plants equipped with power electronic controls and dynamic voltage support capability can improve system performance by damping power swings and supporting post-fault voltage recovery. The results of the studies performed in Spain and Portugal suggest that at higher penetration levels, requiring sufficient fault ride through capability for large wind power plants would be economically efficient.

Grid reinforcements may be needed for handling larger power flows and maintaining a stable voltage, and is commonly needed if new generation is installed in weak grids far from load centers. The issue is generally the same be it modern wind power plants or any other power plants. The cost of grid reinforcements due to wind power is therefore very depending on where the wind power plants are located relatively to load and grid infrastructure, and one must expect numbers to vary from country to country. It is also important to note that grid reinforcements in general should be held up against the option of curtailing wind or altering operation of other generation, and these latter options may in some cases prove to be very cost efficient.

For the grid reinforcement, the reported results in the national case studies are:

- UK: £65-125 / kW (85-162 €/kW) for 26 GW wind (20 % energy penetration) and £35/kW- £77/kW for 8 GW of wind
- Netherlands: 60-110 €/kW for 6000 MW offshore wind
- Portugal: from 53 €/kW (only summing the proportion related to the wind program of total cost of each grid development or reinforcement) to around 100 €/kW (adding total costs of all grid development items) for 5100 MW of wind.
- German dena study results are about 100 €/kW for 36 000 MW wind.

The costs of grid reinforcement needs due to wind power cannot be directly compared, they will vary from country to country much depending on location of the wind power plants relative to load centers. The grid reinforcement costs are not continuous; there can be single very high cost reinforcements. Also there can be differences in how the costs are allocated to wind power – for example, in Portugal it has been evaluated how much of the new lines are due to wind power, and only that part of the costs have been allocated to wind.

6. SUMMARY OF ADEQUACY/CAPACITY CREDIT RESULTS

The capacity credit of wind power answers questions like: Can wind substitute other generation in the system and to which extent? Is the system capable of meeting a higher (peak) demand if wind power is added to the system?

Wind generation will provide some additional load carrying capability to meet expected, projected increases in system demand. This contribution can be up to 40% of installed wind power capacity (in situations with low penetration and high capacity factor at times of peak load), and down to 5 % in higher penetrations or if regional wind power output profiles correlate negatively with the system load profile.

Results for the capacity credit of wind power are summarised in Fig 4. Results of capacity credit calculations show a considerable spread. One reason for different resulting levels arises from the wind regime at the wind power plant sites and the dimensioning of wind turbines. For zero penetration level, all capacity credit values are in the range of the capacity *factor* of the evaluated wind power plant installations. This is one explanation for low German capacity credit results shown in Fig. 4. The correlation of wind and load is very beneficial, as can be seen in Fig. 4 in the case of US New York offshore capacity credit being 40 %.

The wind capacity credit in percent of installed wind capacity is reduced at higher wind penetration, but depends also much on the geographical smoothing. This is demonstrated comparing the cases of Mid Norway with 1 and 3 wind power plants. In essence, it means that the wind capacity credit of all installed wind in Europe or the US is likely to be higher than those of the individual countries or regions, even if the total penetration level is as in the individual countries or regions. Indeed, this is true only when assuming that the grid is not limiting the use of the wind capacity, i.e. just as available grid capacity is a precondition for allocating capacity credit to other generation.

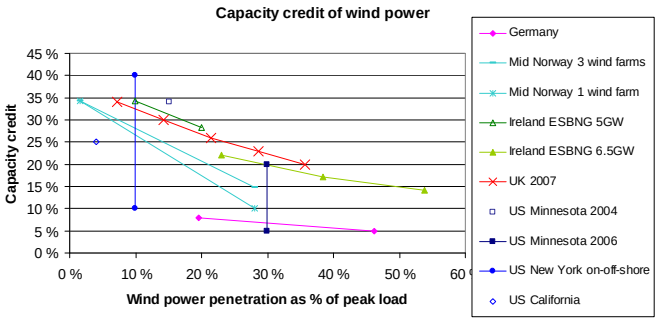

Figure 4. Capacity credit of wind power, results from national studies.

7. CONCLUSIONS AND DISCUSSION

Integration cost can be divided into different components arising from the increase in the operational balancing cost and grid expansion cost. The value of the capacity credit of wind power can also be stated. The case studies summarized in this paper are not easy to compare due to different methodology and data used, as well as different assumptions on the availability of interconnection capacity.

Wind generation may require system operators to carry additional operating reserves. Wind's variability cannot be treated in isolation from the load variability inherent in the system. From the investigated studies it follows that at wind penetrations of up to 20% of gross demand (energy), system operating cost increases arising from wind variability and uncertainty amounted to about 1-4 €/MWh. This is 10% or less of the wholesale value of the wind energy. The actual impact of adding wind generation in different balancing areas can vary depending on local factors. From first review of methodology some important factors were identified to reduce integration costs, such as aggregating wind plant output over large geographical regions, larger balancing areas, and operating the power system closer to the delivery hour.

With current technology, wind power plants can be designed to meet industry expectations such as riding through voltage dips, supplying reactive power to the system, controlling terminal voltage, and participating in SCADA system operation with output and ramp rate control. Grid reinforcements may be needed for handling larger power flows and maintaining a stable voltage, and is commonly needed if new generation is installed in weak grids far from load centers. The cost of grid reinforcements due to wind power is therefore very depending on where the wind power plants are located relatively to load and grid infrastructure, and one must expect numbers to vary from country to country. It is also important to note that grid reinforcements in general should be held up against the option of curtailing wind or altering operation of other generation, and these latter options may in some cases prove to be very cost efficient. The results from studies in this paper vary from 50 €/kW to 160 €/kW. The grid reinforcement costs are not continuous; there can be single very high cost reinforcements. Also there can be differences in how the costs are allocated to wind power.

Wind generation will also provide some additional load carrying capability to meet forecasted increases in system demand. This contribution can be up to 40% of installed capacity, and down to 5 % in higher penetrations or if local wind characteristics correlate negatively with the system load profile. Aggregating larger areas benefits the capacity credit of wind power.

Wind resources have impacts that have to be managed through proper plant interconnection, integration, transmission planning, and system and market operations. The issues that impact on the amount of wind power that can be integrated are: aggregation benefits of large areas which mean using transmission possibilities between countries and regions as well as large balancing areas; working electricity markets at less than day-ahead time scales; using and improving wind forecasting. Transmission is the key to aggregation benefits, electricity markets and consolidating balancing areas.

Integration costs of wind power need to be compared to something, like the production costs or market value of wind power, or integration cost of other production forms. It is important to note whether a market cost has been estimated or whether the results refer to technical cost for the power system. There is also benefit when adding wind power to power systems: it reduces the total operating costs and emissions as wind replaces fossil fuels. In this summary only the cost component has been analysed. For high penetration levels of wind power, the optimisation of the integrated system should be explored. Modifications to system configuration and operation practices to accommodate high wind penetration may be required. Not all current system operation techniques are designed to correctly incorporate the characteristics of wind generation and surely were not developed with that objective in mind. For high penetrations also the surplus wind power needs to be dealt with, e.g. by increased system flexibility, transmission to neighbouring areas, storage (e.g. pumping hydro or thermal) or demand side management. There is a need to assess wind power integration at the international level, for example to identify the needs and benefits of interconnection of national power systems.

REFERENCES

1 http://www.ieawind.org/

2 Holttinen, H, Meibom, P, Orths, A, Van Hulle, F, Ensslin, C, Hofmann, L, McCann, J, Pierik, J, Tande, J O, Estanqueiro, A, Söder, L, Strbac, G, Parsons, P. Smith, J C, Lemström, B. Design and Operation of Power Systems with Large Amounts of Wind Power, IEA collaboration. In Proceedings of European Wind Energy Conference EWEC2007, 27th February-2nd March, 2006, Athens, Greece.

3 Holttinen, H, Meibom, P, Orths, A, Van Hulle, F, Ensslin, C, Hofmann, L, McCann, J, Pierik, J, Tande, J O, Estanqueiro, A, Söder, L, Strbac, G, Parsons, P. Smith, J C, Lemström, B. Design and Operation of Power Systems with Large Amounts of Wind Power, first results of IEA collaboration. In Proceedings of 6th International workshop on Large Scale Integration of Wind Power, 23-25th October, 2006, Delft, Netherlands.

4 Holttinen, H, et al. Design and operation of power systems with large amounts of wind power. State-of-the-art report. VTT Working papers 82. Espoo, Finland, 2007. http://www.vtt.fi/inf/pdf/workingpapers/2007/W82.pdf

5 Meibom, P., Weber, C., Barth, R.,Brand, H., Operational costs induced by fluctuating wind power production in Germany and Scandinavia, pp 133-154, In: Swider, D., Voss, A. (Eds), Deliverable D5b – Disaggregated system operation cost and grid extension cost caused by intermittent RES-E grid integration, GreenNet-EU27, 2006. http://greennet.i-generation.at/

6 Holttinen, H, 2005. Impact of hourly wind power variations on the system operation in the Nordic countries. Wind Energy, vol. 8, 2, ss. 197 – 218.

7 Axelsson U, Murray R, Neimane V, 4000 MW wind power in Sweden - Impact on regulation and reserve requirements. Elforsk Report 05:19, Stockholm, 2005. http://www.elforsk.se

8 DENA : Planning of the grid integration of wind energy in Germany onshore and offshore up to the year 2020 (dena Grid study). Deutsche Energie-Agentur Dena, March 2005.

9 ESB National Grid, Impact of wind power generation in Ireland on the operation of conventional plant and the economic implications, February 2004.

10 SEI: Operating reserve requirements as wind power penetration increases in the Irish electricity system. Sustainable Energy Ireland, 2004.

11 Ilex Energy, Strbac, G, 2002. Quantifying the system costs of additional renewables in 2020. DTI, 2002. http://www.dti.gov.uk/energy/developep/080scar_report_v2_0.pdf

12 G Strbac, Anser Shakoor, M Black, Danny Pudjianto, Thomas Bopp. Impact of wind generation on operation and development of the future UK electricity systems, Electric Power Systems Research, Volume 77, Issue 9, Pages 1143-1238, Elsevier, July 2007

13 National Grid submission for the UK energy white paper, 2003.

14 H.F. Eleveld, J.H.R. Enslin, J.F. Groema, K.J. van Oeveren, M.A.W. van Schaik: Connect 6000 MW-II, Elektrische infrastructuur op Zee. 2005, Kema 40510025-TDC-05-48500

15 Estudio de Estabilidad Eólica de la Península Ibérica - Síntesis de Criterios y Metodologías, REE / REN. May, 2005.

16 Rodríguez-Bobada, F; Reis Rodriguez, A; Ceña, A; Giraut, E, Study of wind energy penetration in the Iberian peninsula. European Wind Energy Conference (EWEC), 27 February – 2 March, 2006, Athens, Greece

17 Tande J O, Korpås M, Impact of large scale wind power on system adequacy in a regional hydro-based power system with weak interconnections. Nordic Wind Power Conference Hanasaari, Finland, 22-23rd May, 2006.

18 Xcel North sudy (Minnesota Department of Commerce), EnerNex/Windlogics. http://www.state.mn.us/cgi-bin/portal/mn/jsp/ content.do?contentid=536904447 &contenttype=EDITORIAL&hpage=true&agency=Commerce

19 Enernex, 2006. Final Report - 2006 Minnesota Wind Integration Study. Available at http://www.uwig.org/opimpactsdocs.html

20 General Electric and AWS Scientific/TrueWind solutions: New York State ERDA study. http://www.nyserda.org/rps/draftwindreport.pdf

21 Zavadil, R, 2006. "Wind Integration Study for Public Service Company of Colorado", May 22, 2006. available at http://www.xcelenergy.com/XLWEB/CDA/0,3080,1-1-1_1875_15056_15473-13518-2_171_258-0,00.html

Towards Smart Integration of Wind Generation.

G. Giebel[a], P. Meibom[a], P. Pinson[b], and G. Kariniotakis[c] for the ANEMOS.plus Team.

a - Risø National Laboratory, The Technical University of Denmark, Denmark, Gregor.Giebel@risoe.dk
b – Informatics and Mathematical Modelling, The Technical University of Denmark
c – ARMINES, Ecole des Mines de Paris, France

Summary

This paper presents current and future challenges for the integration of wind power into the grid using short-term predictions. This includes the currently running virtual laboratories of the EU project POW'WOW as well as the research methodology of the soon-to-start EU projects ANEMOS.PLUS and SafeWind, which aim to develop advanced tools for the management of electricity grids with large-scale wind generation and to get a better handle on extreme events. Focus in ANEMOS.PLUS is given to functions such as optimal scheduling, reserves estimation, bottleneck management, storage management and also optimal trading in electricity markets. For all of them, short-term forecasting as well as uncertainty estimation plays a major role. However, this information is not yet fully integrated in daily practices. The aim is thus to propose advanced tools for the above functions that integrate the full information on the expected wind generation. In order to demonstrate the value of these tools for end-users, demonstration projects in eight European countries including Denmark are defined. SafeWind on the other hand is a project more focussed on research, especially research in extreme events. Those can be extreme winds, but also extreme forecast errors, requiring an extraordinary amount of reserve capacity. In order to help forecasters to estimate their models against the state-of-the-art models, a Virtual Laboratory for short-term prediction has been instantiated under the POW'WOW project.

Introduction

Wind energy high penetration grids

Nowadays, wind power has an increasing share in the electricity generation mix in several European countries with Germany, Denmark and Spain witnessing already a high wind-energy penetration. Due to the fluctuating nature of the wind resource, the large-scale integration of wind power causes several difficulties in the operation and management of a power system. This paper focuses on larger time scales ranging from few minutes to hours or days. When it comes to large-scale wind integration one has to consider as given the different wind turbine technologies already connected to the grid. Wind integration can then be enhanced by bringing Information and Communication Technologies and Intelligence in the decision processes related to the power system management.

Often, a high level of reserves is allocated to account for the variability in wind production, thus reducing the benefits from the use of wind energy. Today it is widely recognized by end-users such as Transmission System Operators (TSOs), independent power producers, utilities a.o. that forecasts of the power output of wind farms a few hours up to few days ahead contribute to a secure and economic power system operation. Increasing the value of wind generation through the improvement of prediction systems' performance is one of the priorities in wind energy research needs in the last years and is expected also to be one in the future[1,2,3]. This is especially true for the reduction of extreme errors, which can bring down the entire system. In March 2005, the UTCE[1] published recommendations for "Seven Actions for a Successful Integration of Wind Power into European Electricity Systems". Among them, the necessity is stressed for further research in the area of improved forecasting tools for wind generation.

The ANEMOS.plus Project Team contains members

- from research institutes: ARMINES/Ecole des Mines de Paris, Danish Technical University, CENER, ICCS/NTUA, INESC Porto, RISOE, University Carlos III of Madrid, University College of Dublin, University of Antilles,
- and industrial partners: Overspeed, Energy & Meteo Systems, Enfor, ACCIONA, EDF, EIRGRID, DONG EWE, PPC, REE, REN, SONI, Vattenfall.

From weather prediction to end-use at client

Producing and using wind power forecasts operationally is a complex issue. The whole chain contains

- the data acquisition and transmission process,
- the production of numerical weather predictions by meteorological models,
- the production of forecasts and uncertainty estimates for the power output of wind farms,
- the use of these forecasts in the decision making process of the operators,
- the application of these decisions in practice and the evaluation of their impact on the power system economics and security.

[1] *The "Union for the Co-ordination of Transmission of Electricity" (UCTE) is the association of transmission system operators in continental Europe, providing a reliable market base by efficient and secure electric "power highways".*

It is not obvious how to apply and integrate the forecasting information into the day-to-day operation of power systems. The integration of wind generation itself in a power system is highly dependent on how system operators will be able to adapt their management practices to account for the intermittent nature of wind. Traditionally, system operators manage the power system based on forecasts of the electricity demand. Demand is highly predictable due to periodicities related to the human activity and to high smoothing effects from individual consumptions (typical errors in predicting demand in interconnected systems are less than 5%). For this reason, power system management tools (i.e. unit commitment, economic dispatch etc) are in general based on deterministic approaches and thus not appropriate when high amount of intermittent resources are considered in the process. Applying wind power prediction results in the daily work of TSOs, energy suppliers and traders is far from straightforward. It requires the development of a stochastic optimization paradigm, which is technically challenging and will require a change of operators' attitudes and practices.

By integrating advanced wind power forecasts and information on their uncertainty in the power system key management functions, the ANEMOS.PLUS project aims to provide new intelligent management tools for addressing the variability of wind power. The objective is to demonstrate the applicability of such management tools at an operational level for managing wind generation in power systems and for participating in the electricity markets.

State of the Art

The "Anemos" Wind Power Prediction System

A number of leading institutes in the area of wind power forecasting have launched in 2002 the 4-year EU Research and Development (R &D) project ANEMOS, which aimed at improving the available technology. Forecasting solutions were developed to meet a variety of end-user requirements (i.e. different time and geographical scales, reliability and robustness of operational tools, uncertainty estimation etc) and types of applications (management of the power system, bidding in an electricity market).

The project has produced an advanced pilot wind power forecasting system, called ANEMOS, able to run operationally for predicting wind power at single wind farm scale as well as on a regional/national scale. A major contribution of the ANEMOS project in the area of wind forecasting was the development of the first operational approaches for on-line uncertainty estimation of wind predictions and also the so-called risk indices explained below. The prediction models together with the uncertainty tools provide the necessary information (but not yet the tools) needed for advanced decision making procedures for the optimal integration of wind power.

The ANEMOS wind forecasting technology makes extensive use of Information and Communication Technology since the various wind power prediction models, the meteorological forecasting models, the data acquisition systems data bases, the user interfaces can be distributed. Communication capabilities are enabled through internet.

Wind Power Forecasting and Uncertainty

The state of the art in wind power forecasting has been pushed forward during the EU funded ANEMOS project (see *www.anemos-project.eu*). Usually, the forecast starts with Numerical Weather Prediction (NWP) from a meteorological institute and online data from the targeted wind farm. Then, either using physical considerations or statistical adaptive tools, a horizon-dependent connection is made between the NWP wind speed and direction input on the one hand, and the measured power output on the other hand. The estimated power curve is used to forecast up to the horizon of the NWP model output. ANEMOS contributed to the state of the art with improved statistical estimation methods, improved physical parameterisations and downscaling, dedicated models for offshore use, and better upscaling algorithms for regional forecasts.

The ANEMOS project has also provided appropriate approaches to estimate on-line the uncertainty of wind forecasts. The adapted resampling approach based on statistics and fuzzy logic provides an estimation of the whole distribution of wind generation in the next hours as shown in Figure 1. Moreover, the project proposed new tools, such as risk indices based on ensemble weather predictions, able to predict the level of error for the next hours. The wind power uncertainty is also assessed using an optimal combination of various short-term prediction models or models fed by different NWP models. Direct quantile forecasts were developed[4] that directly (based on either a simple NWP input or an ensemble of NWP inputs) estimate the quantiles of the likely wind power distribution. The use of ensemble predictions has also been used to yield direct estimation of the quantiles of the predicted wind power[5]. Although the probabilistic approaches open up for an alternative to wind power forecasts, they have not been fully utilised by end-users yet.

ANEMOS has also developed an industrial strength plug-in architecture and platform allowing the integration with existing Energy Management Systems installed at utilities.

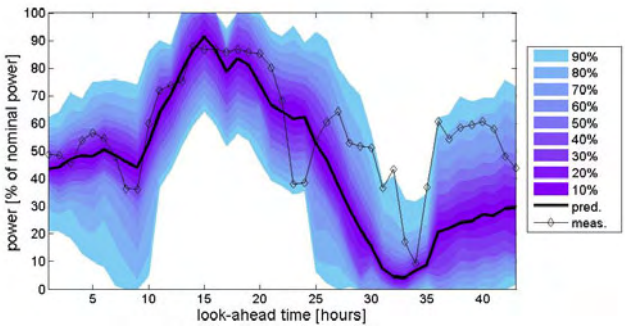

Figure 1: Example of forecasts for the next 48 hours compared to measured values. Prediction intervals for various levels of confidence are displayed. Intervals are estimated with the adapted resampling approach.

Management of Power Systems

Power systems are traditionally operated on a deterministic way. For instance, Economic Dispatch and Unit Commitment are based on accurate load forecasts considered to be perfect. Reserves are carried in case of a loss of generation. In spite of great advances in wind forecasting there are relatively large forecast errors that need to be managed. As wind penetration levels rise, these errors would dominate other error sources (i.e. load forecasting errors). Therefore it will be necessary to account for them inside the unit commitment and economic dispatch algorithms. Wind penetration levels at this time are only starting to have a major impact and the state of the art is to simply carry additional reserves. Quantifying these additional reserves is not trivial and considerable research work has been recently done in this field[6]. The challenge now is to integrate wind farm output forecasts and information on their uncertainty into the unit commitment and economic dispatch algorithms.

The use of storage capabilities provides an interesting approach to increase the profits of wind generation plants in electricity markets. The definition of the combined wind-hydro-pumping strategy leading to the maximization of trading profits needs wind power forecasts and market prices for the next hours as well as grid restriction information. Research work has already been developed in this field by using optimised approaches and techniques able to identify the operational pumping, wind-hydro generation strategy for each hour in a daily time horizon[9, 7]. This approach has been initially designed for a single cluster of wind parks together with a hydro pumping station and has latter been extended to several clusters of wind parks and several hydro pumping power stations in a network area.

The combined wind energy storage techniques can also be used to solve operational restriction related with congestion management in some network areas or to allow the integration of large amounts of wind generation in isolated grids, by storing wind energy during the valley hours and delivering it back to the grid during peak hours. Such a management always requires a wind forecast to deal properly with the available storage limits.

The assessment of the uncertainty in these forecasts plays here also an important role. Research works have also been developed to identify robust operational strategies regarding this issue. Namely Monte Carlo techniques have been used so far to deal with this problem. Results from the ANEMOS project have shown that uncertainties in wind predictions depend on several factors such as the terrain complexity, the meteorological conditions, the time of the year, the spatial and temporal resolution of the NWP system considered, the level of predicted power, the spatial smoothing effect of wind farms etc. By developing a synergy with the area of wind power forecasting in the frame of the ANEMOS.PLUS and SafeWind projects it will be possible to consider realistic information in these functions. This is a necessary condition to evolve towards operational tools.

A Virtual Laboratory to establish the state of the art

As development and operational use of forecasting solutions take more and more importance in the wind energy sector, the consortium of the European Coordination Action 'Prediction of Wakes, Waves and Offshore Wind' (POW'WOW) has taken the initiative of setting up a Virtual Laboratory (ViLab)[8]. The related objectives are to stimulate research efforts in this field, to tighten the collaboration between forecasters and forecast users, as well as to follow and communicate the state of the art in short term prediction of wind generation.

More and more research organizations and companies invest efforts in the development of operational tools for the short-term prediction of wind power production. The relevant and common forecast length of these tools is up to 48- or 72-hour ahead, corresponding to the needs of forecast users for management or trading purposes. A state of the art on wind power forecasting has been published by Giebel et al[9]. Such forecasting systems are fully recognized as a cost effective solution for an optimal integration of wind generation into power systems. TSOs, wind farm operators, and traders among others, usually rely on a unique or on several forecasting systems for making optimal decisions.

In the frame of the European Coordination Action 'Prediction of Waves, Wakes and Offshore Wind' (POW'WOW, see *powwow.risoe.dk*) an initiative is undertaken consisting of setting up a Virtual Laboratory (ViLab) for the evaluation of state-of-the-art prediction methods and systems, in addition to stimulating collaborative research in the field of wind power forecasting. It can be seen as a follow-up of the benchmarking exercise carried out in the frame of the European project ANEMOS, in which more than 10 prediction systems have been evaluated on a variety of test cases with different terrain characteristics and wind climatologies, see eg. [10].

By setting up the ViLab, the main scientific and technological objective is to promote the evaluation of operational methods and systems for the short-term prediction of wind generation in order to follow and stimulate the advances in this area. Since wind predictions provided by meteorological offices are the principal input used by the various prediction methods, it is also crucial to evaluate the quality of the wind forecasts used as input. A second objective is to disseminate results that can help the wind energy sector to have a better appraisal of the state of the art in short term forecasting. Through the ViLab, forecasters will have the opportunity to test their models on wind farms representing a set of representative environments and forecasting conditions, for which a large quantity of high quality data would be made available. They can also compare the performance of their prediction models against other participants. This will permit to identify advantages and drawbacks of rival methodologies and to point towards the necessary scientific and technological developments in the field. Another advantage for these participants is to be included in the dissemination actions

of the POW'WOW project eg. web page, presentations, workshops, etc.

The essential dates for the ViLab benchmarking exercise are the 1st June 2007 for its starting data, and the 30th April 2008 as the deadline for the forecasters participating in the ViLab to provide their final results. A commitment of the POW'WOW consortium will finally be to compile, analyse and communicate these results, in parallel to defining directions for further research in wind power forecasting.

Scientific and technical objectives of ANEMOS.PLUS

The ANEMOS.PLUS project aims to bring to the day-to-day practice of key end-users (such as TSOs, Utilities, Independent Power Producers, Energy traders) advanced tools in order to help them managing wind power in an optimal way. Demonstration cases with already high wind penetration are selected in order to have a realistic environment to prove the viability of the proposed new technology. The scientific and technical objectives of the project are described hereafter:

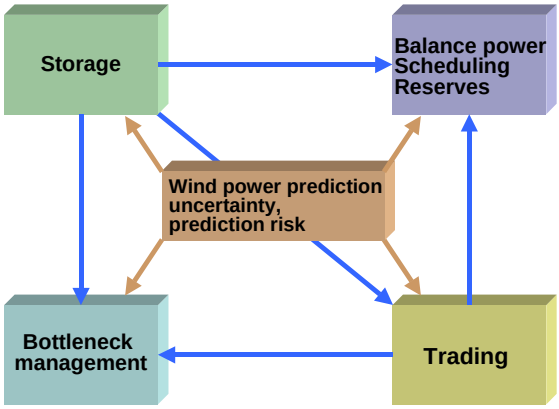

Figure 2: *The ANEMOS.PLUS project aims to enhance the synergy between wind power forecasting and power system management functions.*

1. **Reliability, Ergonomy and Monitoring in Wind Power Forecasting. Embedding into the energy data management and the planning procedures used by grid operators, power plant operators and energy traders.**

Experience with the operation of hybrid wind power prediction systems shows that end-users require:

- Highly accurate forecasts
- 100% reliable delivery of forecasts
- full compatibility with energy management systems
- smooth embedding into decision procedures

The first item has been thoroughly addressed by the FP5 ANEMOS project where a considerable research effort has been put into the improvement of wind power predictions. The remaining items are of equal importance to meet the high standards of operational availability commonly used in the energy industry. Especially reliability is compromised by various factors such as the availability of communication with SCADA systems providing input measurements, the availability of NWP provided by weather services, the reliability of the computing infrastructure etc. The ANEMOS.PLUS project will focus on the development of techniques permitting to detect such situations and restore missing information using rule-based intelligent approaches. The ergonomy and the transferability of the prediction systems in general, and of the ANEMOS pilot system in particular, will be studied in collaboration with end-users and the graphical user interfaces will be adapted accordingly.

2. **Operational probabilistic wind power forecasts and prediction risk for use in decisional processes.**

In the frame of the FP5 ANEMOS project various wind power prediction models were developed covering a wide range of end-user requirements. In the ANEMOS.PLUS project, the Anemos platform will be extended to integrate probabilistic models like models based on Numerical Weather Predictions ensembles. A priority is to extend uncertainty estimation tools for the case of regional forecasting for which no models exist today (uncertainty estimation focus on single wind farm predictions). This is a major requirement by end-users such as TSOs that manage regional/national grids.

The ANEMOS.PLUS project aims to provide operational modules for the "prediction risk indices" developed and evaluated in the frame of Anemos. These indices permit, together with power predictions and their intervals, to develop decision support tools to manage or trade wind power.

3. **Demonstration of new operational tools for intelligent power system management**

As mentioned above, the available deterministic software tools for the optimal scheduling of conventional power plants are not appropriate when considering an energy mix with high share of intermittent sources. Current Unit Commitment or Economic Dispatch algorithms consider wind as a "negative load" and foresee usually a fixed margin to account for wind variability. In cases of high penetration, operators often consider high reserve margins leading to a less economic operation of the power system. This reduces the benefits from wind energy.

The ANEMOS.PLUS project aims to develop and demonstrate new operational tools appropriate for the case of large-scale wind penetration for key power system management functions like unit commitment and economic dispatch. As mentioned above, the challenge now is to integrate wind forecasts and their uncertainty into these functions; to switch from wind "variability" towards wind "predictability". This will require a reframing of the objective. The state of the art is to maximise social welfare subject to the constraints, where a deterministic approach is taken. With large levels of wind power a more pertinent question will be to

maximise the expected social welfare subject to the constraints both deterministic and stochastic. It is this last question that will require careful consideration in ANEMOS.PLUS.

In the demonstration case studies considered in the project, the developed tools will run operationally at the control centres and in parallel to the existing Energy Management Systems (EMS). The management tools of ANEMOS.PLUS will provide their output in a "consultative" way to the operators. It would be unrealistic to propose to replace the existing management functions in the existing EMSs. This can be potentially an objective after the demonstration phase of the ANEMOS.PLUS project. The monitoring of the ANEMOS.PLUS tools during the demonstration phase will permit to quantify the advantages of the new methods compared to the existing ones on a set of predefined criteria (robustness, cost of system operation, CO2 savings etc). The aim of the project is to improve the operational costs, fuel savings and CO2 savings by at least 10% compared to the actual EMS technology.

In this project emphasis is given in autonomous systems or systems with weak interconnection. In the first case belong the systems of islands where wind generation contributes to fuel displacement. In several European islands like in Greek ones (Crete, Cyclades etc), French (Guadeloupe, Corsica etc), Portuguese (e.g. Azores) and others, wind energy appears to be an attractive alternative to conventional generation. However, when it comes to large shares of wind penetration, which can be quickly attained in a small grid, it is necessary to assist operators in their management task through advanced prediction and scheduling tools. The case of the grids of Republic of Ireland and Northern Ireland-UK is also examined here. Both systems face increasing wind integration and the need for operational solutions to manage the combined system.

4. Advanced tools for managing secondary and tertiary reserves

In large interconnected grids with high wind penetration it is of primary importance to use wind power forecasts to estimate the necessary reserves required to operate safely the system and to meet demand. In practice operators apply the UCTE criteria for defining reserves. However, these are deterministic ones and do not take necessarily into account situations with large penetration from intermittent sources.

The work on the estimation of reserves and on wind predictability in the frame of this project is expected to provide useful input in the development of efficient balancing mechanisms by TSOs. The integration of large shares of wind generation requires an increase in the amount of reserves that are needed to balance generation and consumption according to the different time frames defined by the UCTE criteria.

Developing new techniques for the on-line definition of the reserve needs within each control area, taking into account the risk indices of the forecasts for each time horizon of interest, will be one the tasks of the project. A minimization of the reserve amounts needs to be developed taking into account the mentioned forecast risk indices. This will allow a decrease in the balancing costs that result from the integration of wind generation. Fuzzy techniques can be applied to deal with this problem.

A decision making tool able to deal with different risk strategies and risk aversion levels that the system operators may adopt, will be developed for the management of secondary and tertiary reserves. Hydro storage capabilities will be exploited for this purpose. It will be tested and demonstrated during the project in control areas characterized by large amounts of wind energy penetration (cases of Portugal / Spain).

5. Congestion management in large power systems as well as local grids

Areas with high wind potential are often areas with very low energy consumption. The medium voltage grids are not built for the transport of these enormous wind capacities. In high wind situations the limit of the grid capacity can be reached so that at certain grid points congestions can occur. Today wind power predictions are not used in load flow calculations or daily congestion forecasts. The standard practice is to enforce the grid by building new power lines and connectors based on the worst-case scenarios of maximum wind power production combined with low power consumption.

Often the erection of new grid lines is not realized due to high costs and, primarily, time-consuming building permits with planning periods of up to 10 years. This leads to curtailment of wind power production by shutting down wind farms on demand to ensure grid stability restricted connection of new wind farms to the grid in areas with frequent congestions

Connecting the wind power forecast to the load flow calculations will be the major task for an improved integration of wind power at this grid level. This will allow more realistic load flow predictions and increase the capacity of the grid.

The grid can be used more efficiently with a higher penetration of wind energy while at the same time the high security standard of the grid is kept. Consequently, grid enforcements and extensions can be minimised or even avoided. In addition, the assumption of a maximum wind power production together with a minimum load is unrealistic, e.g. storms occur mainly in winter where the load is typically higher than average.

Hence, the integration of intermittent wind power into grid management leads to:

- reduced curtailments of wind power
- allows for new wind farm installations (or repowering) in areas with high penetration

6. **Decision making tools for optimal trading of wind power in electricity markets with advanced strategies based on forecasts and prediction risk.**

A major application of wind power forecasts concerns the electricity trading by wind power producers participating in a liberalised market. Together with information on the uncertainty of the forecasts, strategies can be developed to reduce financial risks from imbalances induced by forecast errors. Imbalance costs reduce the revenues of wind farm owners, having a direct impact on the economic efficiency of their investment. Understanding the behaviour of wind energy actors in liberalised markets is also a key point important for TSOs. In fact, TSOs may conceive wind farms bids as forecasts for the next hours. However, such forecasts might be biased whether motivated by economic criteria and do not necessarily represent the best objective guess such as provided by weather forecasts.

The use of storage capability provides an interesting tool for trading wind energy in electricity markets, allowing the displacement of wind energy from low-load hours to peak hours where energy is more expensive. The definition of the optimum combined wind-hydro-pumping strategy needs forecasts about wind power generation and market prices for the next hours.

This project proposes to use an operational tool input by wind power forecasts and the electricity costs. It will provide to the power producers trading scenarios for the energy market (daily and intra-daily markets) based on alternative bidding strategies. These strategies will account for the uncertainty, prediction risk and storage options. The efficiency of each alternative strategy will be monitored as a function of the effective wind production, prediction errors, electricity prices and imbalance penalties.

7. **Implement tools for optimal management coordination of storage and wind power forecasting technology in managing wind intermittency.**

In grids with storage potential, wind power forecasts could be used for optimizing the assignment of different storage devices like hydro dams or pump-storages. In conventional systems, utilities perform storage coordination and planning (e.g. for dams) taking into account forecasts of the demand and of water inflows. Nowadays it is necessary to demonstrate how wind energy can be integrated in the process.

8. **An efficient methodology and advanced monitoring tools to quantify the benefits from large-scale wind integration.**

Wind energy is criticised at various levels. As an example it is mentioned that additional reserves, required to compensate intermittency, may result to higher CO_2 emissions. When it comes to large-scale wind integration and one has to modify well-established operation practices, there are impacts at different levels that are difficult to evaluate. The project aims to develop a detailed evaluation methodology to quantify the impact of wind integration in the various demonstration cases, i.e. in terms of CO_2 emissions, power system security, monetary benefits from fuel saving etc.

9. **Standardization of wind power output forecasting technology.**

Further standardization of the emerging wind power forecasting technology has to be carried out. Benefits for TSOs from using a standardized forecasting system output in view of exchanging information about wind production at a European level have to be evaluated (for example in the frame of UCTE).

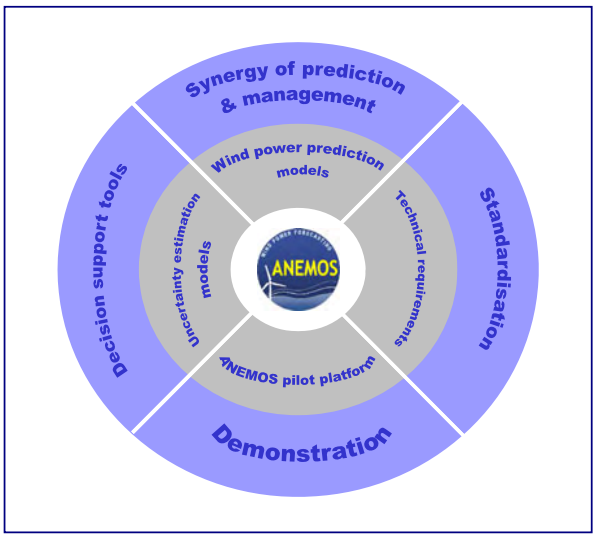

Figure 3: Added value of the ANEMOS.PLUS project.

The added value of the project compared to the current state of the art is shown pictorially in Figure 3. The project will contribute in maximizing the benefits of modern power systems from the use of wind power forecasts and appropriate management tools accounting for the wind intermittency. An advanced forecasting system will be fully integrated into the energy data management process of different utilities and optimized for practical use under the specific requirements of grid operation, power plant scheduling, and energy trading.

Two types of tools are designed: the wind power forecasting system and the management tools on a highly integrated approach welding together the worlds of fluctuating wind power and traditional energy systems. For reaching this goal, technical demonstrations are not sufficient. The use and integration of the needs and knowledge of daily users like operators and traders are key parts of this project.

SafeWind

While ANEMOS.PLUS is a project with a large demonstration and development part, SafeWind will go further into new fields of research. As already mentioned above, the integration of wind generation into power systems is affected by uncertainties in the forecasting of expected power output. Misestimating of meteorological conditions or large forecasting errors (phase errors, near

cut-off speeds etc), is very costly for infrastructures (both the turbines themselves and the electricity grid as a whole) and reduce the value of wind energy for end-users. The state of the art in wind power forecasting focused so far on the "usual" operating conditions rather than on extreme events. Thus, the current wind forecasting technology presents several strong bottlenecks. End-users urge for dedicated approaches to reduce large prediction errors or predict extremes at local scale (gusts, shears) up to a European scale as extremes and forecast errors may propagate in space and time. Similar concerns arise from the areas of external conditions and resource assessment where the aim is to minimize project failure. The aim of SafeWind project is to substantially improve wind power predictability in challenging or extreme situations and at different temporal and spatial scales.

The project concentrates on: using new measuring devices for a more detailed knowledge of the wind speed and energy available at local level; develop strong synergy with research in meteorology; develop new operational methods for warning/alerting that use coherently collected meteorological and wind power data distributed over Europe to early detect and forecast extreme events; develop models to improve medium term wind predictability; develop a European vision of wind forecasting taking advantage of existing operational forecasting installations at various European end-users. Finally, the new models will be implemented into pilot operational tools for evaluation by the end-users in the project.

Conclusions

Wind energy industry is a success story in Europe. This is to a large extent thanks to ambitious research programs undertaken in the last decades aiming to provide a reliable wind turbines technology and solutions for optimising wind integration in power systems. As wind penetration increases, new problems arise and require new solutions. This is highly recognised by the European Commission that supports actively projects such as ANEMOS, POW'WOW, ANEMOS.plus and SafeWind mentioned here. These projects deal with integration of wind energy in power systems and focus on improving wind predictability and increasing the value of wind energy. They try to put together researchers from various disciplines and countries in order to exploit synergies and move ahead the state of the art. Tightly integrated with the research is the exchange of knowledge with the industry through demonstration projects that aim to quantify the benefits of the innovations proposed.

Acknowledgements

The European Commission is acknowledged for funding in part the projects POW'WOW (Contract Number 019898), ANEMOS.PLUS (Contract No 038692) and SafeWind.(Proposal No 213740).

References

[1] European Commission, "*European Wind Energy at the dawn of the 21st century*, *Research funded under the Fifth Framework Programme"*, EUR 21351, Publication iof the European Commission, 2005. Available on-line at http://europa.eu.int/comm/research/energy/nn/nn_pu/article_1078_en.htm#wind.

[2] EWEA, "Prioritizing Wind Energy Research Strategic Research Agenda of the Wind Energy Sector", Publication of the European Wind Energy Association 2005, available on-line at www.ewea.org/documents/projects/WEN/SRA_final.pdf.

[3] EUREC Agency, "FP7 Research Priorities for the Renewable Energy Sector", Publication of the EUREC Agency, March2005. Available online at http://www.eurec.be/FP7Priorities_Renewable_Energy.pdf.

[4] P. Pinson, H. Aa. Nielsen, H. Madsen, M. Lange, G. Kariniotakis: *Methods for the estimation of the uncertainty of wind power forecasts.* Anemos EU project, Deliverable Report D3.1b, March 2007

[5] Giebel, G. (ed.), J. Badger, L. Landberg, H.Aa. Nielsen, T.S. Nielsen, H. Madsen, K. Sattler, H. Feddersen, H. Vedel, J. Tøfting, L. Kruse, L. Voulund, L.: *Wind power prediction using ensembles.* Risø-R-1527(EN) (2005) 43 p.

[6] Doherty, R. and O'Malley, M.J., "New approach to quantify reserve demand in systems with significant installed wind capacity", IEEE Transactions on Power Systems", Vol. 20, pp. 587 -595, 2005

[7] J. Matevosyan, L. Söder: *Short-term hydropower planning coordinated with wind power in areas with congestion problems.* Wind Energy **10**(3): pp. 195-208, May/June 2007

[8] P. Pinson, S. Lozano, I. Marti, G. Kariniotakis, G. Giebel & the POW'WOW consortium (2007). *ViLab: a Virtual Laboratory for collaborative research on wind power forecasting.* Wind Engineering **31**(2), pp. 117-121.

[9] Giebel, G., R. Brownsword, G. Karioniotakis: *The State-Of-The-Art in Short-Term Prediction of Wind Power - A Literature Overview*. Project report for the Anemos project, downloadable from anemos.cma.fr (40 p., 2003)

[10] Kariniotakis G., et al : *What Performance Can Be Expected by Short-term Wind Power Prediction Models Depending on Site Characteristics?*, in: Proceedings of the European Wind Energy Conference EWEC 2004 (CD-Rom proceedings), London, UK, 2004

[9] Castronuovo, E.D., Pecas Lopes J.A.: *Optimal operation and hydro storage sizing of a wind–hydro power plant.* International Journal of Electrical Power & Energy Systems, Volume 26, Issue 10, December 2004, Pages 771-778

50 pct. Wind Power in Denmark and Power Market Integration

Jesper Werling, Lars Bregnbæk
Ea Energy Analyses, Frederiksholms Kanal 1, 1., DK-1220 København K.

Abstract — This paper presents the results of an extensive analysis of how to incorporate 50 pct. wind power in the Danish electricity system and what the welfare economic costs and benefits will be for Denmark as well as for the North European Region.

To estimate the consequences for the development of the power system and the costs and benefits of the increased wind power, model analysis has been carried out using the electricity market model, Balmorel. For this analysis the model covers the Nordic countries and Germany. Two scenarios have been analysed. In the first scenario, the reference scenario, all investments in production capacity including wind power is based on market mechanisms. In the second scenario, the 50 pct. wind scenario, the investments in wind power in Denmark are governed by a target of establishing 50 pct. wind power in Denmark in 2025. In the second scenario 3500 MW wind power is established on land and by 2025 Denmark will have 2900 MW wind power off shore.

The calculations result in a welfare economic benefit for Denmark of approximately 20 million DKK pr. year on average. For the Nordic countries and Germany as a whole, the benefit is 660 million DKK pr. year on average. This benefit is dependent on a welfare economic discount rate of 3%. The welfare gain takes into account costs of additional infrastructure, trade effects, savings on fuel consumption, investment and operating costs on plants as well as reduced consumption of CO_2 quotas, and the damaging effects of NO_x and SO_2 emissions.

Index Terms — Mathematical market modelling, System analysis, Wind power integration.

1. Introduction

In January 2007 the Danish Government published its proposal for an energy policy for Denmark "A visionary Danish energy policy". The long term goal is to make Denmark independent on fossil fuels and the proposal includes an aim for 2025 of doubling the share of renewable energy in the energy supply to 30 pct. In the proposal it is mentioned that an important contribution could come from doubling the wind power capacity to 6.000 MW in 2025 thus covering 50 pct. of the Danish power demand.

According to the Danish policy proposal essential contributions could come from:

- A doubling of wind power capacity from approx. 3,000 MW to 6,000 MW.
- Approx. 50% of electricity demand in Denmark supplied by wind turbines in 2025.
- 500 – 1,000 offshore wind turbines producing electricity equivalent to consumption in Denmark's residential sector.

A number of questions arise on the future increase in wind power capacity in Denmark:

- How is it possible to technically integrate a greater amount of wind power into the Danish electricity system?
- What are the consequences for the North European electricity market and for security of supply?
- Which drivers and barriers do investors in Denmark encounter compared to the investment climate in other countries?
- What are the costs and benefits of a target of 50% wind power in 2025?

In this paper, emphasis is given to the final question, i.e. determining the costs and benefits of 50 pct. wind power in Denmark in 2025. Additionally, scenarios with 30% and 40% have been analyzed for comparison.

The model assumptions and simulations are also used to discus the value of wind power capacity in the Nordic electricity system, and the cost of wind power integration.

The results presented in this paper should be viewed in conjunction with results presented in the conference paper "50 pct. Wind Power in Denmark – Establishing the Necessary Infrastructure" at the Nordic Wind Power Conference 2007. This second conference paper details suggested steps towards securing adequate infrastructure to realize the 50 pct. vision for Danish wind power.

2. Definitions and clarifications

To be precise, by "50 pct. wind power in Denmark" it should be understood that wind power generation in Denmark, should annually equate to 50 pct. of the Danish gross consumption (prior to network losses). Denmark is a part of an international power market with connections to the Nordel power region and to the UTCE system. Power flows across Danish are different in each individual hour. The quantity of imports and exports are extensively influenced by the amount of precipitation to which falls in the Norway and Sweden as well as by fuel prices, and temperature variations.

By costs and benefits it is understood to be costs and benefits for society as a whole. This implies costs and benefits for consumers, generators, system operators and to a lesser extent public finances. This includes environmental costs which are not priced in the market (externalities).

3. General methodology

In order to quantify the costs and benefits of a 50 pct. wind power vision for Denmark a number of model simulations were performed using the Balmorel model.

3.1. Socio-economic quantification

In the analyses, the socio-economic costs and benefits of the 50 pct. wind power target, as well as the distributional

effects, are quantified by comparing a model simulation with and without the wind power target.

The socio-economic effects considered are the total costs in the electricity and district heating systems from procurement of fuels, operation and maintenance, investments etc. Other implications for society are not considered and as such this is a partial analysis of the electricity and district heating sectors, where the relevant agents are producers, consumers, system operators and public finances.

For each year in the calculations, the total costs of the system are accounted. Specifically, calculations were made on the years 2010, 2015, 2020 and 2025. The yearly costs and revenues in the years in-between are interpolated. An annual socio-economic discount rate of 3 pct. is employed, and the average yearly costs are determined.

It is important to note, that although in general, perfect markets are assumed, with respect to risk premiums and required investment returns, a perceived value the market demands is used namely 11.75 pct, rather than a socio-economic interest rate. With respect to risk, a balanced investment climate is assumed, which does not favour one technology over another. This assumption favours investments in risk prone technologies such as technologies with a relatively high cost burden from capital costs over variable costs.

In spite of the required annual return on investment being just below 12 pct, investment costs are quantified using the social discount rate of 3 pct. Investments in generation technologies are annualised over an assumed lifetime of 20 years and then, each annuity value is discounted with the 3 pct. This implies that if the entire lifetime of the technology was represented, the impact on the social accounting issue would be the investment cost discounted to the year 2006. However, since investments are made which have a positive economic benefit beyond the model horizon, the annuity values of these years are not included in the social accounting.

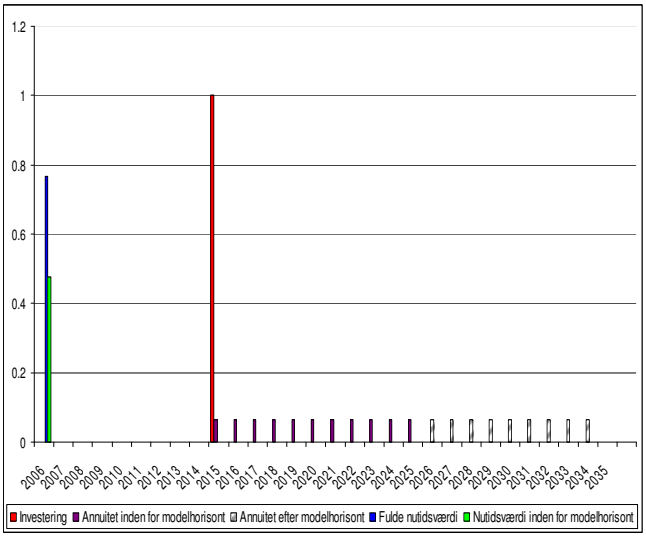

Figure 1: Method of accounting investment costs with short-term costs. If 1 Euro is invested in 2015 (red), an annuity equivalent is made over 20 years. The "annuity payments" which fall within the model horizon are included in the overall value calculation (purple), whereas payments after the horizon are assumed to be matched by revenues after the horizon (grey). The full net-present value (NPV) of the investment (blue) is therefore not included, but the perceived NPV within the model horizon is (green).

Figure 1 illustrates how investments are accounted for in the socio-economic problem. The virtue of this method is that scrap-values issues are resolved implicitly.

Investments are made on the basis of profitability in an average year of precipitation and electricity consumption. Therefore investments in peak load capacity may have been overlooked in the optimisation, as the effect of precipitation levels in the Nordic region is defining for the level of the electricity price.

4. THE BALMOREL MODEL

The Balmorel model is a partial equilibrium model covering the electricity and combined heat and power (CHP) sectors. The model is a linear programming model which by interpretation assumes perfect competition. The objective function maximizes the social-surplus, subject to technology constraints and policy (i.e. taxation) distortions. This corresponds to the social-planner minimizing total costs of satisfying demand when end-user demands are assumed to be unresponsive to prices. Costs for generation units in the model are fuel costs, fixed and variable O&M costs, capital costs, emissions and energy taxes, CO_2-quota prices and balancing costs of wind power.

The model is multi-regional consisting of a number of electricity regions with limited transmission capacity between regions. Balance of supply, demand and net exports are maintained in each region and in each subordinate district heating system. Balances from heat storages and hydropower with reservoirs ensure chronology and a temporal equilibrium between marginal costs, which are interpreted as market prices under perfect competition.

The model has the capacity to generate optimal investment decisions, on the basis of a given investment climate (i.e. required return on investments). Investment decisions are myopic beyond one year of full foresight. In addition the model simulates optimal operation in a climate of perfect competition and full foresight. This generates outputs such as generation on specific or aggregated plants, consumption of fuels, emissions from generation, losses, international transmission, etc. Relevant taxes are included and the CO_2 emissions trading system is represent through a price on CO_2 emissions.

The model is fitted with data for nominal annual projections and temporal variations for electricity and district heating demand, technical parameters for generating units (efficiencies, capacities, emission factors etc.), variations in water inflow for hydropower and wind power variations as well. Central assumptions are presented in section 5.

In the calculations performed for this project, a time resolution with 8 representative time steps in 52 weeks has been used. The precise time aggregation is optimized to represent variations in Danish electricity demand and variations in wind power generation.

For further information on the Balmorel model, please refer to [1] or the website www.balmorel.com.

4.1. Implementing a political target for wind power

In order to analyse a target for wind power share of consumption, such a target was incorporated in the Balmorel model as a new constraint. When this constraint is active, the model finds the best solution which satisfies this constraint. Since electricity demand is exogenously given in the model,

the amount of wind power which must be generated each year is known to the model a priori.

The use of electricity in the production of district heating is however endogenous, but assumed negligible in Denmark, and as such is not included in the target. However, this could easily be modified.

The Balmorel model uses a generic optimization algorithm to find the best solution for the system as a whole, subject to specified assumptions. This makes it possible to interpret the impact on and incentives for different agent groups in the market by evaluating dual variables to the different constraints. Each agent group demonstrates price-taking and profit maximising behaviour.

A target for wind power generation, implemented as a model constraint, thus has a dual variable which can be interpreted as the marginal subsidy required for achieving the wind power target. However, it says nothing about how such a subsidy package is composed, only that on the margin, the subsidy is equal to the dual price from the model.

The simplest form of interpretation is the price a *wind power generation certificate* would attain in a market. However, a fixed predefined production subsidy per energy unit would give the same result. An efficient tendering process would give the same result on the margin, but with different wealth distributional consequences.

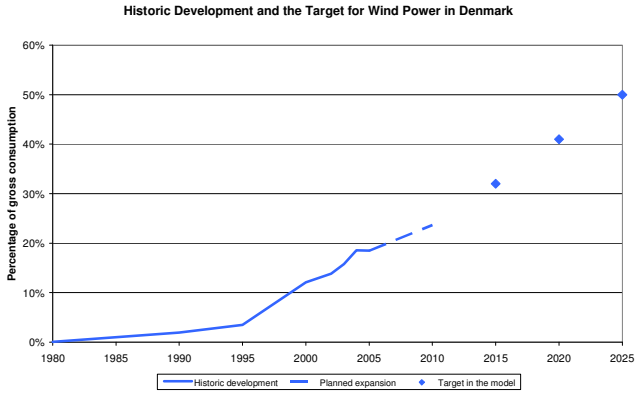

Figure 2: The wind power penetration targets assume 32 pct. in 2015, 41 pct. in 2020 and 50 pct. in 2025. The figure also shows the historic development of wind power generation as ratio of total capacity.

5. CENTRAL ASSUMPTIONS

5.1. Geography and transmission constraints

The model used for this study covers the Nordic and the German electricity and district heating systems. In Balmorel the system is divided in regions to represent capacity constraints in the power system. The Nordic system is divided in 10 regions and the German system in 3 regions. The figure below illustrates the modelled capacity constraints between the different regions.

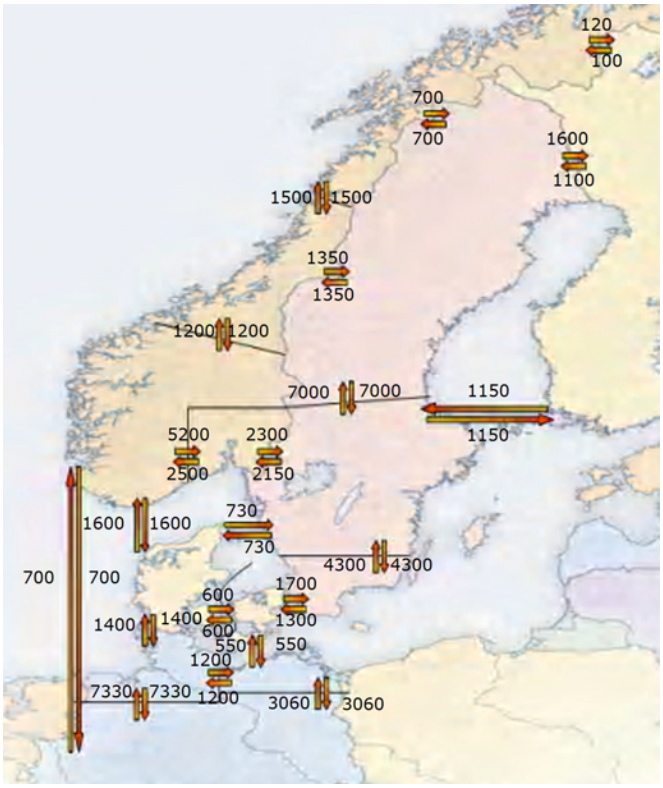

Figure 3: Transmission capacities between regions in the model. It is assumed that the 5 Nordic prioritized cross-sections are established. Also, a 4000 MW expansion of capacity over the German "Elben snit" is assumed to go along with the German windpower expansion. In Norway, Capacities between Northern and Central Norway, as well as Central and Southern Norway are assumed expand by 500 MW. 90% availability of transmission capacity is assumed at all times.

5.2. Electricity demand

The assumptions on electricity consumption are based on the most recent projections from the Danish Energy Authority [7].

Table 1: Projections of electricity consumption in the analysis (TWh/year).

TWh	Denmark	Finland	Norway	Sweden	Germany
2005	35,7	85,0	125,9	147,3	533,8
2015	37,2	98,1	134,9	156,1	585,8
2025	39,4	104,3	138,7	159,7	646,6

5.3. Fuel prices and CO_2 costs

The fuel price projections are also based on the latest projections from the Danish Energy Authority. These are again based on IEA's World Energy Outlook 2006. The prices used are shown in the table below.

Table 2: Fuel prices used in the analysis.

DKK06/GJ	Light oil	Fuel oil	Coal	Natural gas	Straw	Wood
2005	67,0	37,5	15,4	36,6	33,8	33,1
2015	67,2	37,6	13,7	37,8	33,8	33,1
2025	69,4	38,9	14,3	39,7	33,8	33,1

The price for CO_2 is assumed to be 150 DKK/ton throughout the analyzed period of time.

To represent balancing costs for wind power an extra cost of 20 DKK/MWh is added in the beginning of the period rising to 40 DKK/MWh in 2025. This is discussed further in section 7.

5.4. New investments in production capacity

Only known investments in new production capacity are included as exogenous investments in the model. This includes the new 1.600 MW nuclear plant in Finland. An exception is the expansion of wind power in Norway, Sweden, Finland and Germany. It is expected that this expansion is partly politically driven and therefore the current plans for wind power expansion have been included based on the EWIS study and the DENA Grid Study [9], [11], [12].

Table 3: Projections of wind capacity in the countries around Denmark (MW).

Capacity (MW)	Finland total	Norway total	Sweden total	Germany onshore	Germany offshore
2010	410	1275	2000	22.248	5.400
2015	610	3250	4000	26.200	9.800
2020	860	6000	6000	27.900	20.400
2025	860	6000	6000	27.900	20.400

All other new investments are determined by the model calculations. The investment data for new technologies are based on the Danish Technology Catalogue [4] except the data for new wind power investments. During the project it was estimated that the investment cost for wind power in the Catalogue were too optimistic. Therefore, for wind power the investment data has been adjusted according to data from IEA and BTM-Consult ([7] and [8]). The figure below shows the assumed development investment costs for wind power, on shore and off shore.

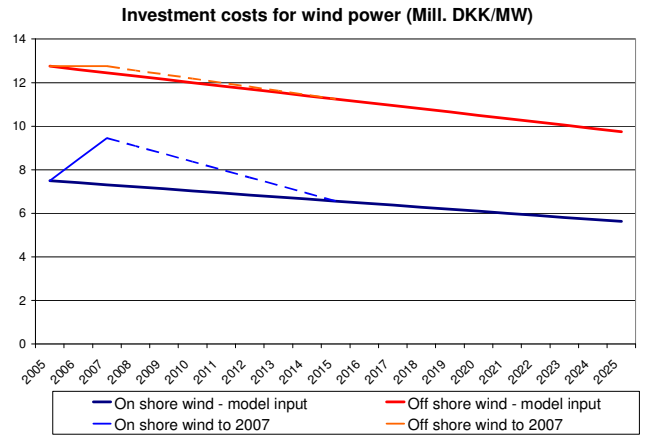

Figure 4: Investment data for wind power. A linear decrease from the price level to a estimated price level in 2025 has been assumed. The 2025 estimate is based on Danish Technology Catalogue [4] and IEA [7]. The figure also shows the increase in prices that has been experienced from 2005 to 2007.

An upper limit for the number of wind turbines installed in Denmark was set for on shore and off shore wind power in Eastern and Western Denmark respectively. Furthermore a maximum number of new wind power investments was set at 500 MW/year.

5.5. Environmental externalities

In this project, the approach was to include environmental externalities in the socio-economic accounting.

Results from European research project ExternE show that climate change and air pollution are the most important environmental externalities linked to energy production. Because of the significant uncertainties related to climate models ExternE recommends using an "avoidance cost"-principle to set the cost of CO_2. In this study a price of 150 DKK/ton is used and the cost of CO_2 is internalised in the power market through the market for CO_2.

Except for CO_2 the externalities are not included in the model optimisation. In the optimisation any existing tax rates on emissions are included, so in principle, if these tax rates were the same as the social values of the externalities, the optimal market incentives with respect to externalities would be included.

Considering air pollution the ExternE analyses demonstrate that the emission of classic pollutants such as SO_2, NO_x and particles are much more serious than other pollutants such as CO, dioxins and furans. Therefore only SO_2, NO_x and particles were considered in these analyses.

Air pollutants have a number of negative impacts on the environment such as increased corrosion of buildings, reduces crop yields, damage to ecosystems and human health effects. Of these health effects have the largest economic impact.

Making an accurate assessment of the socio-economic consequences of air pollutants from specific plants is rendered complex by a number of scientific and methodological issues. Most pressing and controversial is the value set on lost human lives or life years. Two competing approaches are found relevant. The VSL approach (Value of Statistical Life attributes the same value to any human life. The VLYL approach (Value of Life Years Lost) attributes a lower value on older people's lives, as they loose less life years upon premature death. There is no consensus among environmental economists as to which approach is correct. For this reason, results from both methods have been employed and weighted equally in these calculations.

Table 4: External cost of emissions according to the CAFE (Clean Air For Europe program under the EU.

External cost (DKK/kg)	CAFE 2005 Low est. (VLYL)	CAFE 2005 High est. (VSL)
Particles	120	360
NO_x/nitrate	33	91
SO_2/sulphate	39	113

In this study the environmental benefits of wind power are estimated with the Balmorel model. The installation of additional wind power can be seen to push out more polluting existing capacity. In reality, the net-effects are difficult to quantify in general terms, however, with a solid representation of existing power generation options, alternative investment options, the net effects can be quantified by use of a sector model such as the Balmorel model.

6. Model results

As part of the study modelling and cost analysis have been carried out in detail for a reference scenario and a 50 pct. Wind power scenario for Denmark in 2025. Furthermore sensitivity analyses for lower penetration of wind power as well as for different fuel prices and CO_2 allowance prices have been undertaken.

6.1. Investments in the reference and the 50 pct. Wind scenarios

Two scenarios have been analysed. In the first scenario, the reference scenario, all endogenous investments in production capacity including wind power is based on the market mechanism. In the second scenario, the 50 pct. wind scenario, the investments in wind power in Denmark is governed by a target of establishing 50 pct. wind power in Denmark in 2025. In the second scenario 3500 MW wind power is established on land and by 2025 Denmark will have 2900 MW wind power off shore. The investments in electricity generation capacity in Denmark determined by the model are shown in the figure below.

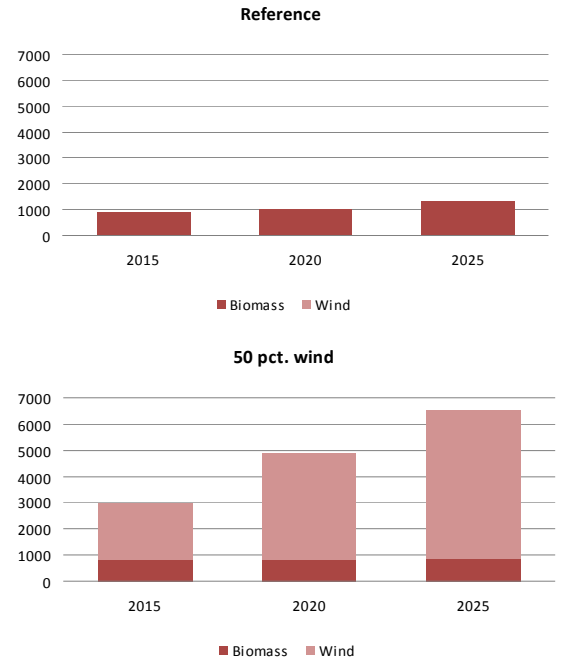

Figure 5: Increase of power plant capacity in Denmark in the two scenarios. In the reference scenario, biomass-fired power plants are established, especially at the beginning of the period. In the 50 pct. wind power scenario, wind power is increased steadily as a consequence of the 50 pct. objective. In addition to this, new thermal plants are established.

The figure below shows endogenous investments in electricity production capacity in the countries around Denmark in the reference and in the 50 pct. wind scenarios. It has been assumed in the model calculations that there is no allocation of free CO_2 allowances to new plants.

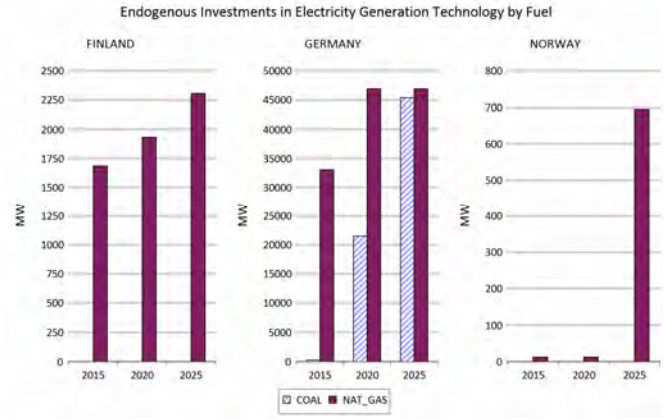

Figure 6: Investments in power production capacities in the two scenarios in other countries than Denmark. Note that the Y-axes are of different scale.

No new investments are undertaken in Sweden according to the model results.

According to the model all new investments in electricity production capacity are coal or gas fired plants. The main part of the investments is situated in Germany. As a consequence of the Danish target for expansion with wind power the investments in thermal capacity is reduced in the wind power scenario compared with the reference scenario. In Norway a new gas fired condensing plant is not established in the wind power scenario and in Finland the number of investments in gas fired capacity is also somewhat reduced. In total the investments in new thermal capacity are reduced by 1.460 MW because of the accelerated Danish wind power expansion. Of this reduction 420 MW is reduced in Denmark and the remaining 1.040 MW are in the other countries. This is later used to asses the capacity value in section 7.1.

Note that both scenarios have extensive wind power expansions in the other countries.

6.2. International Trade

In the 50 pct. scenario there is a larger export of electricity from Denmark than in the reference scenario.

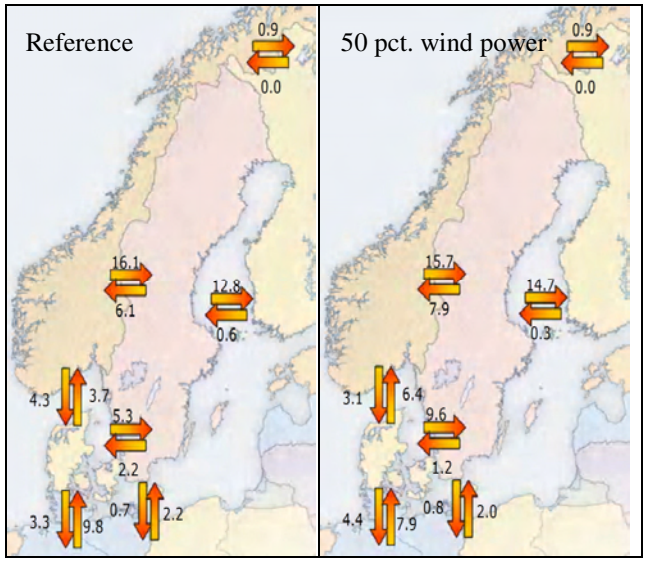

Figure 7: Yearly electricity transmission between countries in the two scenarios in 2025.

The transit flows on Figure 7 demonstrate how electricity is transmitted between countries on an annual basis. In both scenarios Denmark is a transit country for German wind power and Nordic hydropower, but the transit is reduced in the 50 pct. wind power scenario. The fact that additional wind power in Denmark results in increased net annual exports is not surprising. In the wind power scenario, more capacity was established in Denmark and less elsewhere. Again, recall that progressive wind power expansions in neighboring countries are assumed in both scenarios.

International electricity trade ensures that the expansion of generation capacity (e.g. wind power capacity) pushes the most inefficient capacity out of the market irrespective of geography, as long as transmissions capacity is sufficient. Progressive wind power scenarios can thus be motivator to expand international electricity transmission capacity. Also, in scenarios with plentiful wind power, the advantage of

electricity transmission capacity is extensive, since wind generates power at different times with respect to geography.

6.3. Impact on electricity prices

The development of electricity prices in the two scenarios can be seen in the figure below.

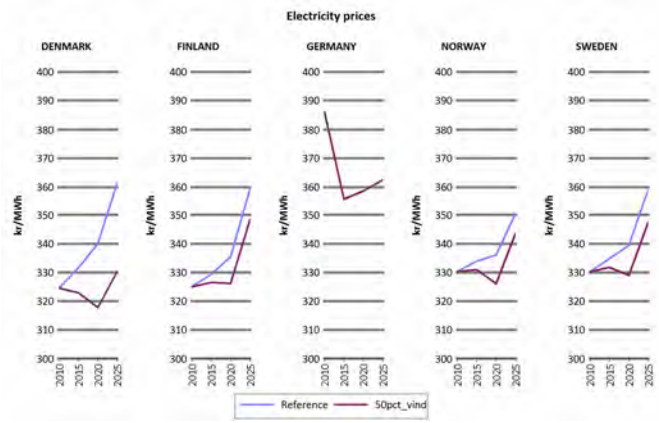

Figure 8: Electricity price development in the two scenarios 2010 - 2025.

The consequence of the increased wind power capacity in Denmark is that the price of electricity in Denmark in 2025 decreases from 361 DKK/MWh to 330 DKK/MWh.

A more detailed illustration of the electricity prices is shown in the figure below. The figure shows the electricity price duration curve for 2010, for 2025 in the reference scenario and in the wind power scenario.

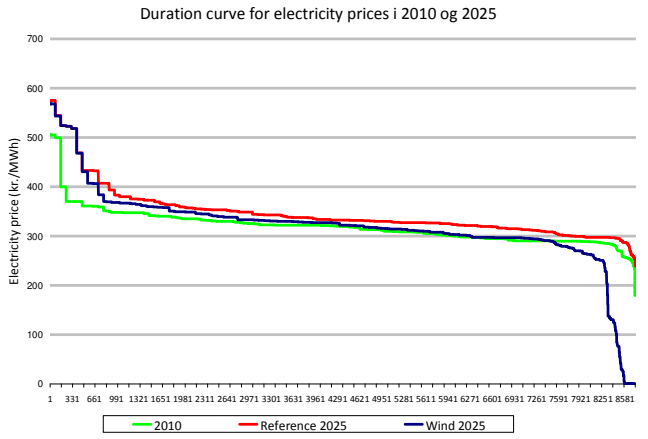

Figure 9: Duration curve for the electricity price in 2010 and 2025.

The increasing wind capacity gives a larger quantity of low electricity prices in 2025. The number of low electricity prices increases compared to the reference scenario where the wind power expansion is lower. An interesting observation is, that the peak electricity prices, i.e. when the electricity capacity balance is most strained, is not higher in the 50 pct. wind power scenario. This implies that although the prices are under pressure from wind power investments, there is still sufficient incentive to ensure available capacity, without having extreme peaks form in the market.

The necessary investments to achieve the 50 pct. wind target will not be realized under free market conditions. With the assumed fuel prices and technology data a subsidy is needed to make investors invest in wind power instead of conventional capacity. This can be seen from the figure below that shows the necessary marginal subsidy needed in 2015, 2020 and 2025 to make the model invest in the necessary wind capacity to realize the targets.

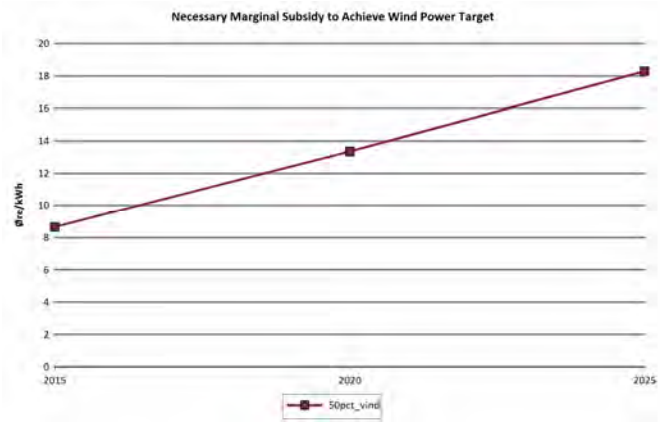

Figure 10: Necessary marginal subsidy to achieve the wind power targets in 2015, 2020 and 2025.

From the figure it can be seen that the necessary subsidy is 80-90 DKK/MWh i 2015. This target can be achieved by on shore wind alone and therefore the subsidy is equivalent to the necessary subsidy to on shore wind power with the expected technology development to 2015. In 2020 the marginal subsidy is 130 DKK/MWh and in 2025 it increases to 180 DKK/MWh. The reason for the increasing subsidy is that different types of wind turbines and locations are marginal in the different years. In 2015 only on shore wind is established and the marginal location is Eastern Denmark. In 2020 more on shore wind power is established in Eastern Denmark and some off shore wind power in Western Denmark where the wind conditions are better than in Eastern Denmark. The off shore wind sets the level of the marginal subsidy. In 2025 the maximum level of off shore wind power in Western Denmark is reached and the wind power expansion continues in Eastern Denmark. In this case the offshore wind power in Eastern Denmark determines the level of the marginal subsidy.

This can be compared with the current subsidy levels where power from turbines established after January 1st 2005 is remunerated according to the market price plus a 100 DKK/MWh production subsidy during the first 20 life years of the turbine.[1]

6.4. Socio economic consequences

By comparing the two scenarios, the economic consequences of the Danish 50 pct. objective can be assessed. In the analyses, these costs have been assessed both for Denmark alone and for the entire area (Denmark, Norway, Sweden, Finland and Germany). An important result of the model calculations are the overall annual energy costs of meeting the needs for electricity and heat in the five countries included in the model area. The costs comprise capital costs for new plants, fuel costs, operation and maintenance as well as balancing costs for wind power.

1 Additionally a 120 DKK/MWh subsidy is awarded for the first 12.000 full load hours, if decommissioning certificates were used in the establishment. Turbines connected between January 1st 2005 and December 31st 2009 are thus entitled. (DEA 2007: www.ens.dk)

The emission of CO_2 is not the same in the two scenarios, and one economic advantage of the 50 pct. scenario is lower costs for purchase of CO_2 quotas.

The additional expenses for grid infrastructure are due to investments in installations to connect the offshore wind farms to the main grid and the necessary grid reinforcements. The overall costs of the infrastructure elements are estimated at well over DKK 8.0bn over 16 years, equivalent to well over DKK 3.6m per MW offshore wind farm. This investment makes it possible to set up 2,250 MW new offshore wind turbines and ensures a cable solution without constructing any new overhead lines for achieving this.

The reduction in the cost of environmental impact is a result of reduced emissions of SO_2 and NO_x as production from thermal plants is replaced by emission-free wind power.

In the basic calculation, a socio-economic discount rate of 3% is used. The table shows that calculated as an average over the years 2010 – 2025, the 50% objective would produce a socioeconomic profit compared to the reference. Our analysis shows that the profit will be around 20 million DKK per year for Denmark and approx. DKK 660m per year for the area as a whole. Alternatively, at a discount rate of 6%, Denmark would get a deficit of DKK 215m while there would be a profit of approx. DKK 240m per year for the entire model area.

Table 5: Socio-economy of 50% wind power in Denmark expressed as the average cost in the period 2010 – 2025, at a 3% discount rate.

Million DKK per year	Denmark	The whole area
Fall in energy costs	27	- 287
Less consumption of CO_2 quotas	97	406
Grid infrastructure	- 236	- 236
Reduction in cost of environmental impact (SO2 and NOx)	132	777
Total gain	20	660

6.5. Sensitivity analyses

A number a sensitivity analyses have been carried out in order to test the robustness of the economic conclusions. The sensitivity analyses are carried out after two different principles. In the first type of sensitivity analysis the total investment pattern in the electricity system is recalculated with the new assumptions in the reference and in the wind power scenarios. This principle has been used in an analysis of the consequences of a development where the expected price decrease on the investment price of new wind power is not realised. In the other sensitivity analyses a new investment pattern is not calculated with the model. The reference and the wind power scenario have just been recalculated with other assumptions on fuel prices and CO_2 prices. In this way the robustness of the economy of the 50 pct. wind power scenario is tested.

Table 6: Socio-economy of 50% wind power in Denmark expressed as the average cost in the period 2010 – 2025, at a 3% discount rate.

Million DKK per year	Denmark	The whole area
50 pct. wind power – base calculation	20	660
No price decrease for wind power	-161	479
Higher fuel prices (75 $/barrel)	246	806
Lower CO_2 price (75 DKK/ton)	-158	161
Higher CO_2 price (300 DKK/ton)	590	1,259

The sensitivity analyses show that the socio economic consequences for Denmark are dependent on the development of fuel prices, CO_2 prices and investment prices for wind power. Rising fuel prices and CO_2 prices will make the economy better whereas lower CO_2 prices and higher investment costs will worsen the economy for Denmark and for the total model area. In some case the wind power investments have a negative impact on the socio-economic results for Denmark whereas the wind power investments in all cases have a positive socio-economic impact for the total model area.

7. MARKET INTEGRATION OF WIND POWER

Three main issues with regard to wind power integration are:

- Generation intermittency
- Production gradient
- Uncertainty

Intermittency is covered in the model as historic profiles for wind power generations are represented with a reasonable level of detail. The time resolution is optimized with respect to intermittency and variations in demand in the Danish market. The supply and demand balance is enforced strictly during each time step, ensuring that intermittent capacity is complemented by dispatchable capacity. Thus in a free market, capacity balances become an economic issue rather than a technical issue.

Production gradient refers to the notion that wind power can change the level of production from one hour to the next on a large scale. This would instil the need for quickly regulating power plants to complement wind power. We do not explicitly consider constraints on production gradients of the power system in the model. The frequency of large changes in wind power generation from one hour to the next is low historically (see Figure 11). The presence of large numbers of decentralized generation units, international transmission capacity, and Nordic hydropower, makes changes on this scale appear insignificant.

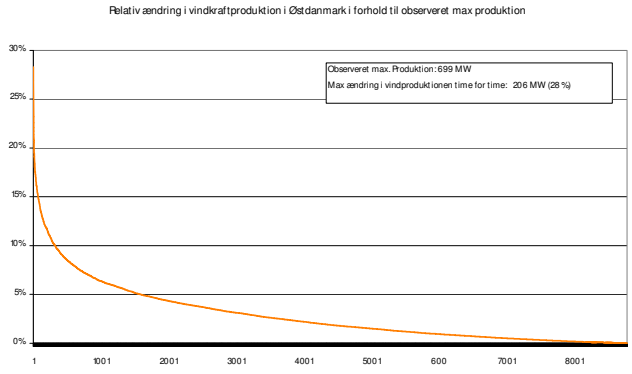

Figure 11: Relative hourly change in wind power generation in relation to observed maximum generation. Data from Eastern Denmark (1.12.2004-30.11.2004).

The Balmorel model is a deterministic model and therefore does not shed light on the cost of wind power uncertainty. The methodology is therefore to define balancing costs a priori.

Currently in the Danish system, there are two options to ensure balancing with respect to this uncertainty. The balancing task can be left to the system operator, Energinet.dk, or it can be handled privately. Energinet.dk charge a balancing tariff, currently 23 DKK/MWh fed into the system. This is used to finance the purchase of balancing power from other generators in the system. This price is driven by the average price on balancing power and the average prediction error of wind power between submitting bids to the spot market and the hour of operation. The level of the balancing costs in 2005-2006 was 30 DKK/MWh for Eastern Denmark [2] and the average prediction error has been estimated to be 35% when the bid is given 13-36 hours before the hour of operation as it is today in the Nordpool market [2].

Since wind power is increased from now until 2025 in the simulation it has been chosen to use an increasing cost of balancing from 20 DKK/MWh to 40 DKK/MWh in 2025. This is founded on a number of assumptions.

- Market development, especially the active use of the Nordic intraday market Elbas, will increase until 2025, hence put pressure on the price of regulating power.
- Balancing power trade will expand internationally. Balancing Danish wind power with Nordic hydro power for instance.
- Improvements in wind power forecasting methods and or changes in market design to better accommodate wind power (i.e. by moving spot bids closer to the hour of operation). It is assumed that the average error in prediction will decrease to 25%. (This assumption means that the cost of balancing in general is assumed to increase to 160 DKK/MWh in 2025, thus giving a cost for balancing wind power of 40 DKK/MWh).

With respect to wind power generation forecasts it is also important to note that with increased wind power competition between forecasting methods is intensified. This adds robustness to the forecasts as different wind power generators will use different forecasting methods, thus diversifying the effects of unavoidable systemic errors in forecast methods.

7.1. Evaluating the capacity value of wind power

As mentioned above the intermittent nature of wind power is implicitly included in the model calculations. The capacity value of wind power can be evaluated from the model results.

The term capacity value is used to express the value of generation to the electricity system. Basically this is a question of timing: plants which are able to adjust their production according to the system demand have a high value whereas intermittent technologies such as wind power would usually have a lower value.

There are several ways to assess the capacity value of an electricity production technology. In a well developed electricity market, the value of the electricity production can be assessed as the price a technology may obtain in the electricity market. In the Nordic market there is no separate capacity value payment and it can thus be assumed that the spot price in the mature electricity market reflects the real value of electricity production (energy and capacity value) hour by hour. In other studies, the capacity value has been assessed in different ways – for instance for wind power, it has been estimated what the extra investment will be for sufficient backup capacity for periods without wind.

Based on an evaluation of the value of wind power electricity in the market Ea Energy Analyses have previously estimated the capacity value of wind power to be 20 DKK/MWh [16].

A UKERC [17] report estimates the costs to maintain system reliability to be 37 – 60 DKK/MWh under British conditions. IEA [6] refers to the ILEX [18] study and the Green-net study [19] and estimates the capacity costs of wind power to be between 22 and 50 DKK/MWh.

The capacity value is not a constant technology parameter. The value of wind power for the system is very dependent on the incumbent capacity of the system. In a system with high penetration of hydropower with reservoirs or with many fast regulating gas turbines, the capacity value for wind power will be high, compared to a system with an abundance of slowly regulating nuclear or coal power.

As explained earlier the Balmorel model was used to calculate a reference scenario based on market driven investments and a scenario where a target of 50 pct. wind power was implemented. Furthermore, two scenarios with a target of 30 pct. and 40 pct. wind power have been calculated. In order to analyze the capacity value of wind power the table below shows the installed new wind power capacity in the 3 scenarios as well as the quantity of thermal capacity replaced by the new wind power capacity.

Table 7: Investments in thermal and wind power capacity in the 30 pct., 40 pct. and 50 pct wind power scenarios compared to the reference scenario.

	30 pct. wind	40 pct. wind	50 pct. wind
New investments in wind power capacity (MW)	3,589	4,539	5,670
Reduced investment in thermal capacity compared to the reference scenario (MW)	943	1,132	1,459
Replaced thermal capacity / new wind power	0.263	0.249	0.257

The model results show that for each MW of wind power the investments in thermal plants are reduced by 0.25-0.26 MW. In other terms for each MW of wind power 0.75 MW of thermal capacity is required according to the model. In the case that all this extra capacity is built only to handle the intermittent nature of wind power and ensure that power can be supplied in every hour also when the wind does not produce the extra costs can be calculated by calculating the extra capacity costs of the needed thermal capacity. Assuming that the 0.75 MW pr. MW wind is established as single cycle gas turbines at 3.5 million DKK/MW the yearly capacity cost of 1 MW off shore wind power will be 73 DKK/MWh. However, this will be an upper limit of the capacity cost related to the wind power since the extra gas turbine capacity can also be used for other purposes in the electricity market.

Another indicator of capacity value is the average MWh-price awarded to wind power in the market, in comparison with the average electricity price and other technologies.

This is a more relevant indicator in the Nordic market since the capacity value is included in the market price (there is no separate capacity market). The figure below shows the results of the model calculations. The figure shows the difference between the yearly average electricity price and the average price in the market for an efficient existing coal fired plant, an efficient existing biomass fired plant, and land and sea based wind power where the years represent the level of technological development. Model results for 2025 are shown for the 30%, 40% and 50% wind scenarios.

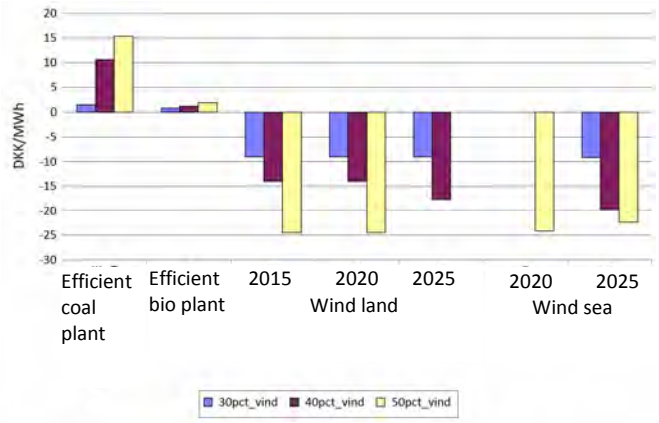

Figure 12: Model results for 2025. Capacity value of an efficient existing coal fired plant, an efficient existing biomass fired plant which is similar to the technology in which is invested, and land and sea based wind power where the years represent the level of technological development (see Figure 4).

It can be seen that the coal plant gets a price in the market that is higher than the average yearly electricity price and thus has a positive capacity value. The average price for the wind power units is lower than the average yearly electricity price and they therefore have a negative capacity value. The capacity value for wind decreases with increasing quantity of wind in the system.

With the coal fired plant as reference the capacity value of wind power is 10 DKK/MWh in the 30% scenario, 25 DKK/MWh in the 40% scenario and 40 DKK/MWh in the 50% scenario.

8. Conclusion

It is technically feasible to incorporate 50 pct. wind power in the Danish electricity without reducing the security of supply in the electricity system. The prerequisite for reaching the target with good economy for society is establishment of the necessary infrastructure, development of a more dynamic electricity system and an efficient, international market where also the regulation and operational reserves can be handled internationally.

Three aspects of wind power integration have been discussed. Although many values can be presented, even from the same simulation results, for the capacity value of wind power, we propose that capacity value of wind power must be seen in context with the flexibility of the electricity system. Methods which relying on calculating "necessary" quantities of back-up capacity, tend to grossly overestimate the cost of integrating wind power. So called backup capacity can have multiple sources of revenue. Also, the presence of well functioning international power markets, sufficient quantities of international transmission capacities, ensure that the cost of integrating wind power is lowered. Geographical spacing of wind power diminishes intermittency issues in well connected systems.

Acknowledgement

This paper is a result of several projects undertaken by Ea Energy Analyses during the spring of 2007. The Projects were financed by the Danish Wind Industry Association and the Danish Environmental Assessment Institute (now under the Secretariat of the Danish Economic Council). Individual project publications are referenced below.

References

[1] Ravn H et al. Balmorel: a model for analyses of the electricity CHP markets in the Baltic Sea Region, 2001. www.balmorel.com
[2] Ea Energy Analyses: "50 pct. vindkraft i Danmark i 2025 - en teknisk-økonomisk analyse", 2007.
[3] Ea Energy Analyses: "Vindkraftens systemomkostninger", 2007.
[4] Risø: "WILMAR - Wind Power Integration in a Liberalised Electricity Market", Risø 2006
[5] Danish Energy Authority: "Basisfremskrivningen til CO_2-kvoteallokeringsplanen for 2008-12 og regeringens energistrategi: En visionær dansk energipolitik", January 2007.
[6] IEA: "Projected costs of generating electricity – 2005 update", 2005.
[7] BTM-Consult: "International Wind Energy Development – World Market Up-date 2006 – Forecast 2007-2011", March 2007
[8] Deutsche Energie-Agentur (DENA): "Planning of the Grid Integration of Wind Energy in Germany Onshore and Offshore up to the Year 2020 (DENA Grid study)", 2005.
[9] Danish Energy Authority: "Forudsætninger for samfundsøkonomiske analyser på energiområdet, Appendiks", January, 2007.
[10] Nordel: "Wind power in Nordel – system impact for the year 2008", January 2007.
[11] ETSO: "European Wind Integration Study (EWIS) Towards a Successful Integration of Wind Power into European Electricity Grids", 2007.
[12] AEA Technology Environment (2005). Methodology for the Cost-Benefit analysis for CAFE. February 2005.
[13] AEA Technology Environment (2005). Damages per tonne emission of PM2.5, NH3, SO2, NOx and VOCs from each EU25 Member State (excluding Cyprus) and surrounding seas. March 2005.
[14] ExternE (2005). Externalities of Energy Methodology, 2005 Update
[15] ExternE (1999). National Implementation.Energistyrelsen, Elkraft System og Eltra (2005): "Technology Data for Electricity and Heat Generating Plants (Teknologikataloget)", March 2005.
[16] Ea Energy Analyses: "Elproduktionsomkostninger for nye, danske anlæg", 2006
[17] UKERC: "The costs and impacts of intermittency: An assessment of the evidence on the costs and impacts of intermittent generation on the British electricity network". UK Energy Research Centre, 2006.
[18] ILEX: "Quantifying the System Costs of Additional Renewables in 2020". ILEX Energy Consulting & Goran Strbac, Manchester Center of Electrical Energy, 2002.
[19] Green-net: "Guiding a least cost grid integration of RES-electricity in an extended Europe". Green-net Europe. Hans Auer et al, Energy Economics Group, Vienna University of Technology, 2007.

2GW of wind and rising fast – Grid Code compliance of large wind farms in the Great Britain transmission system

There is more to Grid Code compliance than Fault Ride Through.

Wind farms - just like any other power station from a Grid Code perspective.

Helge Urdal & Jonathan Horne
National Grid Electricity Transmission, Generation Dynamic Performance, National Grid House, Warwick, CV34 6DA. UK
Helge.Urdal@uk.ngrid.com , Jonathan.Horne@uk.ngrid.com

Abstract - The Great Britain (GB) Grid Code has many challenging requirements which are applied to all forms of generation, including wind. These have been developed to meet the needs of the relatively small islanded GB system. This paper discusses compliance against the 6 main Grid Code requirements. These include Fault Ride Through (FRT), Reactive Range, Voltage Control, Frequency Range, Frequency Response and Modelling with details of what they are, where they have come from and how they are applied in GB.

Index Terms - Grid Code, Great Britain, Wind, Frequency Response

1. Introduction

National Grid is one of the world's largest utilities, aiming to be a global leader in energy networks. It is focused on Gas & Electricity, in Great Britain (GB) (where it is the largest utility), and the United States (where it is the 2nd largest). National Grid Electricity Transmission (NGET) is the Transmission Owner (TO) in England & Wales. and the System Operator (SO) for the whole of GB (England, Wales and Scotland).

NGET through its transmission license has responsibilities relating to safety, security and quality of supply and to facilitate competition in the generation and supply of electricity. A major part of NGET's activity is dealing with a large number of participants in the electricity markets, both for wholesale energy as well as for the balancing services that are required in operational timescales. A variety of these services are provided by all generation plant on the system (beyond a certain size) to maintain a secure and stable system over a range of timescales. These are traded services with multiple GB wide market mechanisms optimised for the individual type of service they provide. The GB electricity market ethos is based on unconstrained access for all generation (assuming it has a connection that meets the planning standards).

The focus of this paper is to show the early experience of evaluating the technical capabilities of wind farms to maintain security of supply and to provide balancing services for trading. This includes the new developments of fast acting voltage and frequency controllers. Wind farms are covered by the terminology of "Power Parks". This term is in GB given to a collection of any generating units powered by any intermittent power source [6] including wind, wave and solar. In this paper however the focus is on wind, hence the term "wind farms" will be used. While the requirements discussed apply to all Power Parks the content of this paper references only wind powered generation as this is the dominant technology at present. The main technical requirements are defined in the Grid Code. In addition, these requirements are supplemented for each project by a set of site specific requirements which are defined in a Bilateral Connection Agreement (BCA).

2. GB System, Wind Resources & Developments

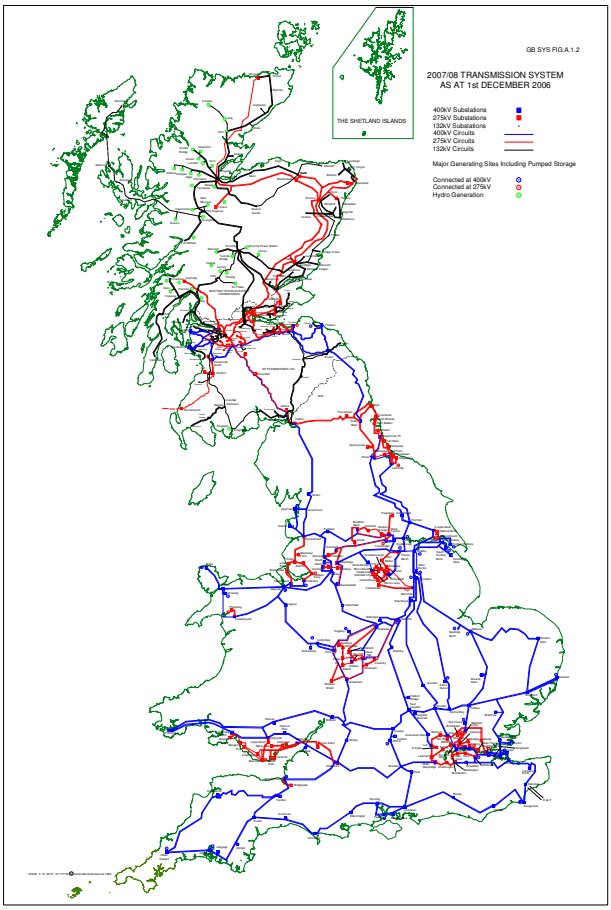

Figure 1 Overview of the GB Transmission System
Peak demand = 60GW; Minimum demand = 23GW

The bulk of the GB transmission system is operated at 400kV, with smaller parts at 275kV and in Scotland substantial parts at 132kV (Figure 1). The GB system is a stand alone ac system, although it is connected via France to the UCTE ac system by a 2GW HVDC link and to the Irish ac system via a 0.5GW HVDC link. These links currently

represent less than 5% of the peak GB demand which is approximately 60GW, although further links are currently under consideration.

In terms of wind resource, GB is well placed both onshore and offshore. The largest onshore wind resource is concentrated in Scotland, while offshore the majority of developments have been around the English & Welsh coasts, in the Irish and North Sea. A typical load factor for wind in GB is about 30%, compared to typically 20% elsewhere in Europe [1]. Considering the volume and quality of this wind resource, the level of installed capacity of 2.2 GW (as of August 2007 [2]) is moderate when compared with countries such as Germany, Spain and Denmark. Figure 2 shows current and future transmission contracted wind capacity in GB up to 2012.

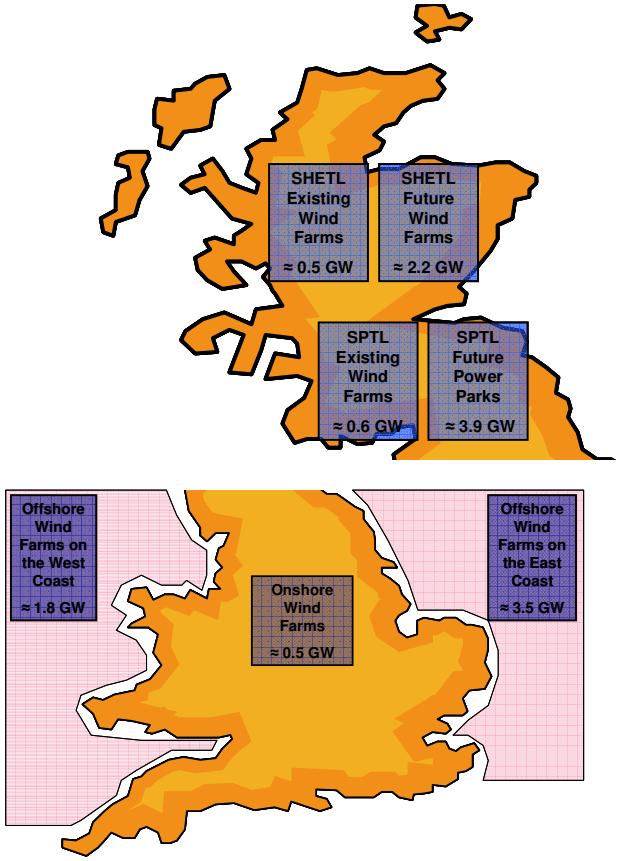

Figure 2 GB wind farms totals for existing and future sites up to 2012. SHETL is the TO in North Scotland and SPTL is the TO in South Scotland

3. Performance Requirements

The GB Grid Code requirements for Power Parks, including wind farms, were issued in the summer of 2005. This three year development process and the need for such requirements from a Transmission perspective have previously been reported by NGET in [3]. By contrast, the focus of this paper is on the practical implementation of the technical requirements in a process called generator compliance or sometimes referred to as Grid Code compliance.

The Transmission Licence requires NGET to apply the Grid Code, without undue discrimination, to all types of generation. This has resulted in similar requirements for wind farms as for conventional synchronous generation with the exception of moving the technical compliance evaluation from the generator terminals to the wind farm point of connection. The reason for this difference is to provide the freedom for the wind farm developer to optimise the internal design. The Grid Code requirements endeavour to avoid any future limitations on the level of penetration of renewable generation [3].

A review of the early experience of applying the Grid Code to wind farms is in progress. This work is close to completion with consultation already having taken place for the proposed fine tuning, [4]. The requirements described in this paper are based on these latest G06 Grid Code proposals.

The Grid Code requirements apply to large and medium but not small power stations. The MW boundaries of these 3 classes vary depending upon geography to reflect the strength of the system. In England & Wales (E&W) large is defined as greater than 100MW and small is less than 50MW, with medium in between. In Scotland there is no medium class. The boundary between large and small is 30MW in South Scotland and only 10MW in North of Scotland where the transmission system is weaker.

3.1. Fault Ride Through (FRT)

The FRT requirement in GB is similar to that of many utilities around the world. The principle is to ensure that large amounts of generation do not disconnect for 'credible' network faults. A distribution system fault will only tend to affect the generation connected at this voltage level and below. Conversely, a transmission system fault can disturb larger areas with the risk of affecting greater amounts of generation and hence risk of generation losses exceeding 1320MW, the largest planned for loss. Figure 4 demonstrates the extent of the voltage depression for a three phase fault at 400kV in GB [3].

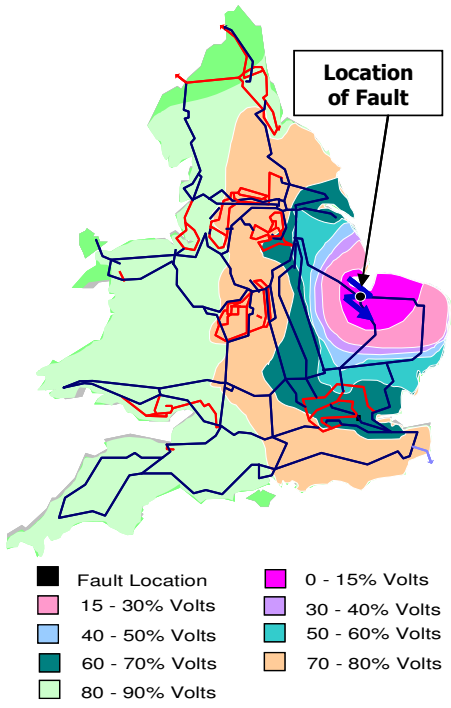

Figure 4 Diagram demonstrating effect of a 3 phase 400kV fault on transmission system voltage in England & Wales

The majority of the country can therefore be affected by a significant decrease in voltage for a single transmission system fault. The FRT requirement in GB is for a fault at the nearest transmission system location and not at the generator terminals.

The majority of transmission system faults are cleared within 140ms. Occasionally voltage depressions in excess of 140ms can occur and there is a corresponding voltage duration curve illustrating the minimum FRT requirement. More details can be found in [3], [5] & [6].

3.2. Reactive Capability Requirement

Wind farms in GB should be capable of 0.95 power factor lead and lag at the point of connection. The developer and manufacturer are free to choose their preferred method of delivery. NGET has had experience of many different methods of reactive power provision including turbines, central compensation, or a combination of both. Additional Mvar sources have included STATCOMs, Thyristor Switched Capacitors (TSCs), switched capacitors and inductors and combinations of these.

To make better use of wind farm assets during periods of low power resource, National Grid is encouraging reactive support even when the turbines are not operating. In many cases this is already available where central compensation is installed (STATCOM etc), while in others it may require some minor modification to the turbines to allow grid side converters (for example with DFIGs or Full Converter (FC) machines) to function independently like a STATCOM.

3.3. Voltage Control Requirement

The voltage control requirements for Power Parks differ slightly from those for synchronous plant. Where conventional stations must control terminal voltage to a target value, the wind farm must control to a voltage slope with a predefined 'droop' value – similar to frequency control. The slope can be considered equivalent to the reactance of the generator transformer.

Two types of voltage control methodology have developed by the wind turbine manufacturers and developers to meet the requirements in GB. Some choose to measure the voltage at the point of connection and control the turbines and/or central reactive sources from a central controller. Others prefer to use a fast local target based control on the turbines and then a slower central controller to provide a reference to the required voltage slope. Both methodologies are acceptable. As a consequence the G06 Grid Code consultation [4] has modified the voltage control requirement to take account of this by defining a 1 second (dynamic) and 5 second (steady state) requirement. Provided that the system can get a reasonable dynamic injection of reactive power within 1 second (G/06 states 90% of the full reactive power to be delivered in 1 second, with an initial delay of no more than 200ms) then voltage collapse can be avoided. The importance of a minimal initial delay can be demonstrated by computer simulation. The following example (Figure 4) includes typical large wind farm layout where reactive support is provided by Thyristor Switched Capacitors (TSC). In each of the three cases a 100ms fault is applied at transmission system voltage relatively close to the point of connection. In Case 1 the TSC controller has ultra fast response times of 20ms, Case 2 has a response time of 200ms (the maximum permitted in the Grid Code) and Case 3 has a response time of 300ms.

These plots demonstrate that as the delay in response increases, more control effort is required to stabilise the voltage. See reactive power in Case 2 compared with Case 1. Once the delay has increased to 300ms (Case 3) the voltage collapses. This is an undesirable situation for both the wind farm owner and the utility.

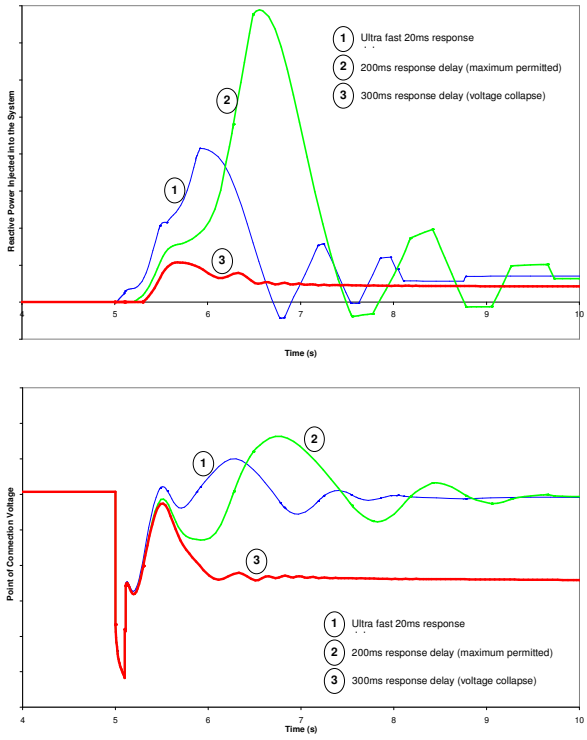

Figure 4 Plots of reactive output for TSC controllers with different delays (20ms, 200ms and 300ms) for a 100ms fault, and the consequence on transmission system voltage.

Following the 1 second transient response there are a further 4 seconds for the control system to reach the required steady state point on the slope which is normally set at around 4% (a 4% decrease in voltage from nominal at the point of connection will cause the wind farm increase reactive injection from zero to maximum (0.95 power factor)).

3.4. Frequency Range Requirement

In GB plant must be capable of continual and stable operation within the system frequency range of 47.5 – 52Hz and 47 – 47.5Hz for 20 seconds. Due to the relatively small size of the GB system, the movement of system frequency with changes in load and generation is much greater than the European UCTE system.

The GB System is designed and operated against a loss of up to 1320MW of generation. Following such a loss, the frequency is expected to drop no further than to 49.2Hz from 50Hz. For this reason it is essential that all generating plant can withstand large deviations in frequency to avoid cascading generation loss and frequency instability.

Figure 5 is a typical example of how the GB system frequency varies over the period of 1 hour. Although

relatively active the frequency remains within operational limits (50Hz ± 0.2).

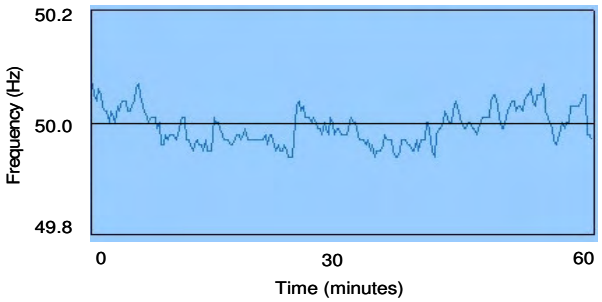

Figure 5 Typical system frequency trace

3.5. Frequency Control Requirement

Fast and accurate frequency control is essential for maintaining a stable system. Every new power station including wind farms greater than 50MW in GB must be capable of providing at least 10% (of MW capacity) frequency response for a 0.5Hz deviation and must always be in one of two frequency control 'modes'. The first of these is Frequency Sensitive Mode (FSM) where the plant should respond to deviations in system frequency from 50Hz (±0.015Hz) at a predefined droop in the range of 3 – 5%. It is not economical to keep all generators in this particular mode as this is a paid for service. The amount of plant selected to be frequency sensitive is calculated at the NGET control centre for securing the system against the largest credible losses of generation and demand. The individual selection of plant depends on the prices submitted into the market. All plant expected to contribute upward regulation for frequency falls has to be de-loaded. In GB this de-load value is a constant MW target, even for generation with a variable power source. The plant should then provide regulation in both directions when system frequency changes occur.

If the plant is not selected to be in Frequency Sensitive Mode, then it should always be in Limited Frequency Sensitive Mode (LFSM) where it will only provide downward regulation if the frequency exceeds 50.4Hz. Should an extreme excess of generation cause this to happen, then all plant, not just those in FSM, will reduce output.

In order for deloaded plant in FSM to be able to halt any frequency deviation it is essential that the response is available quickly. The impact of a two second delay can extend the frequency deviation for a 1320MW loss from 0.8 to 1.0Hz. This can be demonstrated by considering the simulation results shown in Figure 6 where a 1320MW load is switched in (identical to tripping a unit without the loss in system inertia, voltage support etc) on a simplified GB system model.

A 2 second delay would erode the frequency margin allowed before general consumer load shedding. Going beyond this is unacceptable.

These requirements for frequency response are applied equally to all forms of generating plant. It is essential for system frequency stability that the response is accurate, predictable and fast. These factors are as important as the actual volume of response provided.

Wind farms are likely to have a high cost of deloading. It is therefore possible that operation in FSM without deloading becomes the most competitive response service from wind. In this arrangement clearly only high frequency regulation (above 50.0Hz) is available, but the loss of renewable energy is drastically reduced.

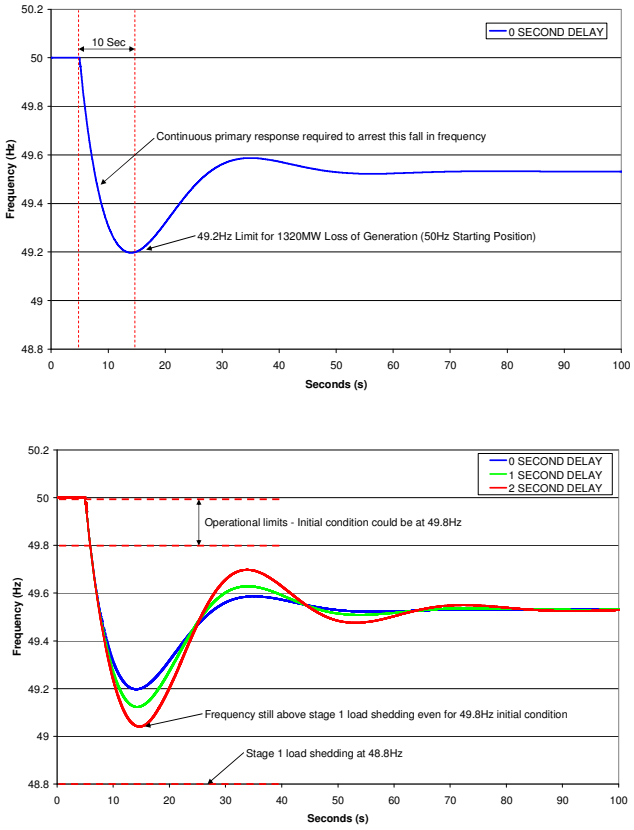

Figure 6 – Plots showing the possible effect of governor delay in excess of 2 seconds.

3.6. Models & Model Validation Requirement

NGET requires full & open descriptions of mathematical models in block diagram format (using the Laplace Operator) for all plant on the system. So called 'black box' models are not accepted as the model users need to have a full understanding of its limitations, and be able to diagnose numerical problems, particularly when used in full system studies. This is not possible when dealing with encrypted models. NGET will generally code the models in-house in the chosen software platform, currently DIgSILENT Power Factory. For more information on modelling by NGET and other TSO partners please see [7].

3.7. Quality of Supply Requirement

In GB the responsibility for Quality of Supply rests with the network owner. Where wind farms are small scale with small numbers of turbines connected at each point, usually at low voltages close to consumers, Quality of Supply is a substantial issue. In Denmark and Germany this has been the case. Wind developments in GB have benefited from the hard work already done in Denmark and Germany where these markets have delivered wind turbines with good Quality of Supply performance. Typical transmission connected wind farms in GB, particularly at 132kV and above, have more modest Quality of Supply challenges,

often linked to the effects of the cable capacitance rather than the power electronics.

4. Grid Code Compliance – Why and How

While the User is responsible for complying, the industry rules allocate the responsibility for overseeing compliance to the GB SO (NGET) for all large Power Stations. This applies even if the Power Station is embedded in a DNO network.

Most medium embedded wind farms in England & Wales, fall into a category know as 'LEEMPS' (Licence Exempt Embedded Medium Power Station). This form of Licence exemption makes the DNO responsible for overseeing the Grid Code compliance.

NGET as the GB SO issues two guidance notes for the purpose of explaining the main Grid Code compliance requirements. In context of wind, the relevant document is called "Guidance Notes for Power Park Developers"[5]. The main purpose of the guidance notes is to explain how to demonstrate compliance. Additionally, for convenience of the developers and their contractors they also collate the information about the performance requirements. The guidance notes describe the practical steps in the process towards compliance of a new wind farm. The compliance activity helps to ensure that the wind farms are prepared for dealing with abnormal as well as routine system conditions and hence make the required contribution to security and quality of supply. The practical content of the guidance notes contain a lot of experience, but as guidance it remains optional, unlike the Grid Code itself.

The GB experience with compliance has been built up over the last 15 years in which the dominant type of new generation has been large Combined Cycle Gas Turbines (CCGTs) with typical installations of 400 to 1200MW. For these large projects, operating individual project based compliance processes has been appropriate. Initially the same approach was applied to Power Parks with installed capacities as low as 10MW. The main stages of the compliance process are:

- NGET review of the design via the data submission
- Interim Operational Notification (ION) to allow the site to be energised and followed by commissioning in stages.
- Performance testing, witnessed by NGET in some cases
- Review of results, determination of Grid Code compliance and mathematical model verification
- Final Operational Notification (FON) to allow normal operation

The project based compliance process illustrated on the right of Figure 7 has been successful. However, for large numbers of projects utilising a small number of wind turbine generator types, this process is not necessarily fully optimised for the TO/SO, the Developer and the Consultants/Contractors/Manufacturers. Following a review of the objectives, a proposal was presented by NGET in the autumn of 2005 to the main manufacturers for a more streamlined approach. This generic process (on the left of Figure 7) involves type registration of performance issues of individual WTGs including model data & verification, control systems performance and Fault Ride Through type test data. The main aims are to minimise the costly on-site activity, to provide timely management of risks for all concerned including uncertainty for owners / investors and to reduce the overall resource needed for the process. Once, a wind turbine type has gone through the type registration process, the project focus is limited to farm level issues and simple confirmation that the plant is delivered as designed. After a slow start, this process is now gathering momentum for the most popular WTG types.

For both of these compliance methods, 3 key deliverables have to be achieved:

- Confirmation of compliance with requirements
- Explicit data defining the capability to deliver Balancing Services
- Verified models including control systems for use in transmission system security assessment studies including dynamic studies.

Model verification is achieved by comparing the model simulation results with test results from either single turbines or whole power parks, either at sites in GB or at a manufacturer test site [7].

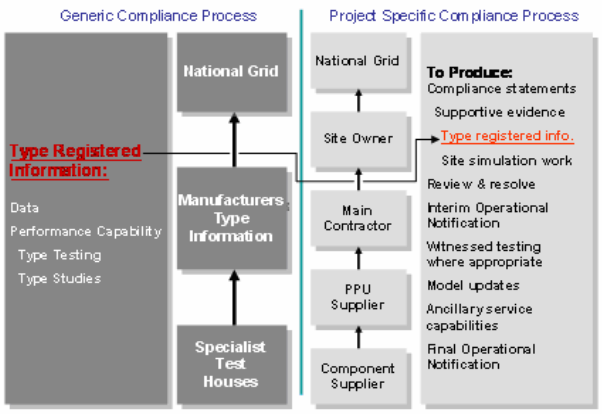

Figure 7 Grid Code compliance process – generic vs. project specific.

5. How NGET Determine if a Site is Compliant with the Grid Code

5.1. The Stages of the Process

On each project there are several stages that NGET and the developer / manufacturer must work through to achieve a successful and compliant wind farm. This begins with a NGET explaining the process to all parties involved, followed by the developer designing the installation and then providing documentary evidence of compliance. NGET then performs the design review to ensure that the plant will meet the requirements on paper before construction begins. Once a single turbine has been installed the developer can proceed with the first of the site tests known as the 20% test. This involves verifying that the voltage control system is functioning correctly with anywhere between 1 turbine and 20% of the turbines installed. This keeps the risk to the system of something going wrong to a minimum, while providing the flexibility to retain the momentum of the project. There is a similar test between 50% and 70%, again for the voltage control system, but also for the frequency control system (if the total registered capacity of the power park will be above 50MW). Finally once all turbines are installed NGET will witness a full set of tests covering reactive range, voltage control and frequency control. These tests will be used both for judging compliance, determining

contract values and for model validation. The details of these tests are covered in the sections below.

For each of the witnessed tests on site NGET provide a range of recording and analysis equipment. This equipment is specially designed for the purpose and leads to rapid interpretation of results in real time on site. Major problems can usually be rectified immediately, provided the proper personnel are available at the wind farm, avoiding the need for expensive repeat testing at a later date. The signals available should be direct from a transducer and normally in the range ±10V dc. Sample rates should be at least 10Hz for frequency response recording and at least 100Hz for all other tests.

5.2. Fault Ride Through (FRT) Verification

Demonstrating FRT by testing is not practical on a project basis. NGET has stated that it can accept the risk of up to 200MW of one particular type of turbine to be connected to the system without it being fully type tested and registered against FRT. Until this point NGET is content with simulation studies to demonstrate compliance. Most manufacturers are using either specific test sites with back-to-back HVDC, or portable FRT test equipment to complete the FRT type tests that the majority of utilities are now asking for. In all cases the equipment can control the terminal voltage of the test turbine to a preset level. The effect of the 'fault' on the rest of the system is usually buffered by either the back-to-back HVDC, or a large inductor.

5.3. Reactive Capability Verification

This is a relatively simple test where the voltage set-point is increased or decreased to a point where either 0.95 power factor lead / lag is achieved, or the voltage limit at the point of connection is reached. In each case the limits must be maintained for at least 60 minutes at full (or near full) MW output. The tests are repeated at lower MW output to ensure that the full range as specified in the Grid Code [6] can be met.

5.4. Voltage Control System Testing & Verification

The best method for determining voltage control performance varies depending on the type of control used in the wind farm. For sites with one voltage sensing point, signal injection, similar to that performed during synchronous machine AVR and governor testing, is the best method. In this case a series of 1% and 2% positive and negative steps are superimposed onto the actual measured voltage signal. This allows verification of both the 1 second dynamic and 5 second slope performance characteristics. If the wind farm has inner local turbine control coupled with central outer control then this type of verification is difficult as simultaneous injection on all turbines and the central controller is logistically impossible. Instead a combination of injections in the local control system of one turbine and again in the central controller can be judged individually, combined with results from upstream transformer tapping where available.

An example of the type of result from transformer tapping on a site in GB is shown in Figure 8. The pass criteria is that 90% of the steady state requirement is achieved within 1 second (for a large enough step), and the correct slope (droop) value of MVAr is achieved within 5 seconds (steady state component) [4] and [5].

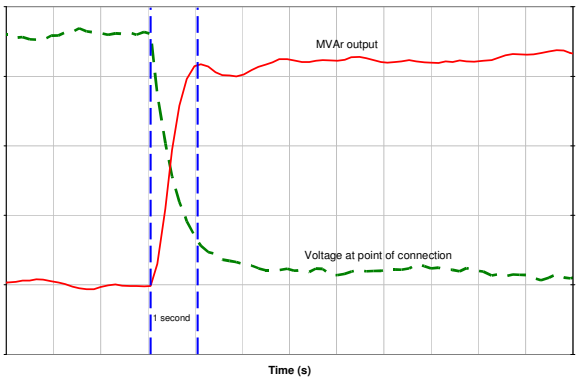

Figure 8 – Example of an upstream transformer tap test for determining voltage control performance

5.5. Frequency Range Verification

This is another parameter that is impossible to test on site. Generally a manufacturer, via the developer will state that the equipment can meet the 47.5 – 52Hz frequency range requirement. Operational monitoring during normal frequency excursions will determine if the plant meets a proportion of this requirement, however the overall responsibility for the turbines and all critical subsystems lies with the developer.

5.6. Frequency Response System Testing & Verification

The frequency response tests that are conducted have a number of purposes. The first is to populate the contractual frequency response matrix. This contains the values that the electricity control room uses to calculate the amount of frequency response available. The procedure involves injecting numerous 10 second ramps into the control system that are either superimposed onto real system frequency, or pure injections isolated from real system speed. There are a number of different sizes of injection to cover the majority of frequency deviations experienced during normal system operation (±0.1Hz, ±0.2Hz, ±0.5Hz). Primary, secondary (both for low frequency) and high frequency response values are taken as the minimum value of response achieved between 10 and 30 seconds, the minimum value of response achieved between 30 seconds and 30 minutes, and the minimum value of response achieved after 10 seconds respectively. In practice the tests are not conducted for 30 minutes or more and a degree of engineering judgement determines the end of the test. All tests are repeated at a number of different load levels to highlight any differences in response across the operating range.

In addition to the ramps, a number of frequency profiles are injected to determine the response of the plant to a typical system frequency event comprising a frequency decrease followed by a partial recovery. The most onerous of these is a 0.8Hz fall in frequency over 10 seconds, followed by a 0.5Hz rise from this value at 30 seconds. An example of this test on a wind farm in GB is shown in Figure 9. The first plot shows the injected frequency and the change in power from the turbine. The second plot has a repeat of the MW trace but also includes the available power during the test. Note how the MW output holds a constant value even though the available power is changing.

The next purpose of the tests is to determine control system robustness. This is achieved by injecting a range of frequency steps (±0.2Hz and ±0.5Hz) to ensure a stable response, in particular to islanding or system split scenarios.

If a repeatable, fast acting, stable and robust performance is achieved, with at least 10% (of rating) primary, secondary and high frequency response, then the test will have met the main pass criteria.

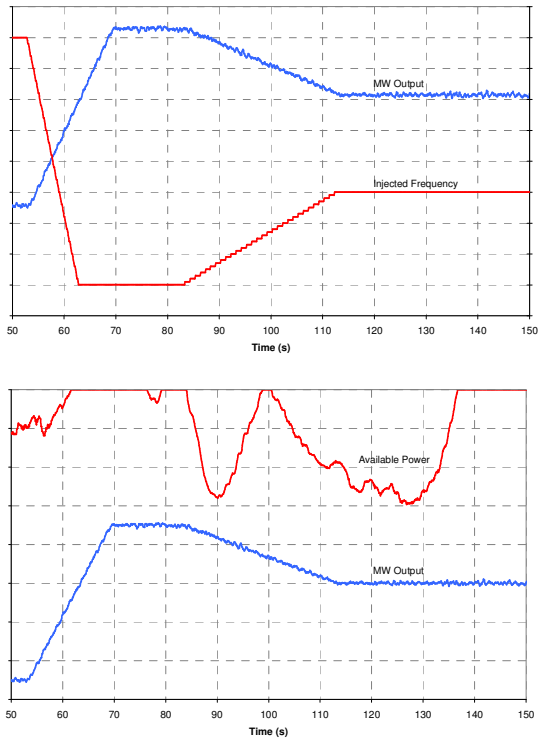

Figure 9 A frequency response test example.

6. Experience of Wind Farms in the GB System to Date

The introduction of large amounts of wind powered generation is a relatively new challenge for most utilities. Previously they have only had to manage well understood, predictable conventional synchronous generation. The result is a steep learning curve for utilities, developers and wind turbine manufacturers as the various teething problems are discovered and resolved. From NGET's perspective this had to be achieved in a manner that does not adversely affect the system, is sympathetic to developers and the capabilities of the new technology without creating undue discrimination for existing forms of generation. Some of the main experiences / problems / solutions encountered by National Grid to date are outlined below.

- Compliance with the GB Grid Code is a complex task particularly for a relatively new technology and for participants not familiar with the problems of operating an island system, in particular requiring fast acting voltage & frequency control. Understanding and coping with the multiple requirements is further complicated by the numerous individuals and companies involved, often from countries with a different focus.
- Synchronous and asynchronous plant have to be treated equally as far is as possible to avoid unfair market advantages, or adverse effects on the system.
- The learning curve for all parties, including NGET, is steep. Inevitably all processes and actions have not been perfect from day one and misunderstandings have inevitably occurred. Generally these challenges have been overcome resulting in better, more robust equipment for the manufacturer, an enhanced product for the developer and a desired response for the system. This can particularly be seen with the development of manufacturers' new products.
- Good communication, usually face to face with all relevant parties, is the key to delivering a successful project that is compliant with the Grid Code.
- The "Guidance Notes for Power Park Developers" [5] is the main NGET point of reference for understanding the methods of demonstrating compliance with the Grid Code.
- The GB system has benefited from the international work on Fault Ride Through (FRT) requirements. NGET believe that while still an exceptionally important part of Grid Code compliance, FRT is yesterdays problem with the major technologies / manufacturers largely now able to cope with the demanding requirements.
- NGET is leading the way by encouraging manufacturers to develop methods of providing frequency response from wind turbines. Frequency response must be provided in a similar way to conventional synchronous generation.
- The system need and market based self dispatch of generation on the GB system generates the requirement for all new plant to have similar voltage control response times as the synchronous plant it is replacing. Delivering fast acting voltage control, although this again appears to be a first, has not proven to be quite as technically demanding as the frequency response issues encountered.
- NGET are making preparations to incorporate as much 'type' testing and registration as possible to reduce workload for all parties.
- Problems with wind turbine modelling are beginning to get resolved. NGET wants to gain a deep understanding of the modelling techniques and operation of the turbines rather than including 'black boxes' in the system simulations. More information can be found in [7]
- The variation in the resource (wind) with time is a well known challenge, but one unforeseen issue was the variation of wind within a wind farm. The wind speed at one part of the wind farm can be significantly different to that at another. This can cause problems for providing repeatable predictable frequency response as the turbines operate with different loading and hence different capability for de-loading.
- Delays in the communications between central controllers and individual turbines can have significant detrimental effects in the fast response required for voltage and frequency control. Rather than using traditional slow SCADA systems high speed dedicated communication links are essential. This had not previously been a problem on conventional synchronous plant as all systems are relatively close together.
- Due to the geographic spread of the equipment with multiple voltage / frequency sensing points, National Grid has had to develop new methods of site testing. New conventional synchronous plant is now well prepared for easy injection of test signals and monitoring of the effects. This is not currently the case with the majority of wind

turbine plants. However, National Grid is encouraging improvements for the future.

7. Future Compliance Developments

Currently, work is in progress to define responsibilities and ownership for the offshore transmission networks, covering all 132kV & above. It is proposed that all offshore transmission connected installations above 10MW will be defined as large Power Stations. This low MW value will make the Grid Code apply in most cases.

After 2009 the offshore transmission network will be owned by Offshore TOs. The voltage related Grid Code requirements including reactive capability will be imposed on the Offshore Transmission Owners (OTO) at the onshore connection point. The OTOs may choose to deliver this from reactive compensation on the boundary or from the wind turbines or from a combination. The frequency control will be implemented offshore, at the boundary between the OTO and the wind farm. Hence, this part of compliance has to be delivered by the wind farm itself. This is also the case for fault ride through, where Offshore Generators will have the option to meet the requirements based on the existing requirements with faults at the Onshore / Offshore TO interface point or with faults at the offshore Grid Entry Point The latter simplifying evaluation of compliance.

It is expected that NGET will be appointed as the SO for the offshore transmission systems. NGET is also likely to be the responsible party to evaluate compliance at the new ownership boundaries. The draft proposals include provision for the option of HVDC offshore transmission of both conventional type (current commutated) as well as voltage source type HVDC connections. These may be introduced for large wind farms situated far from the coast. System design of the offshore network is expected to be allocated to the GBSO (NGET).

The massive wind resource in GB combined with the EU June 2007 decision to implement a binding renewable requirement for 20% of all energy by 2020, has lead to increased interest in scenarios of very high levels of wind penetration. 20% of renewable energy across all energy sectors may result in legally binding electricity sector requirement for 30 or even 40% renewable energy. If this is going to be delivered in the main by wind, it would require installations of 30 to 50GW, probably extensively from offshore. Such capacity would substantially exceed the GB minimum demand of 23GW. This in turn would increase the prospects for interconnections and or access to high volume energy storage, if this can be made economical. These possible future developments reinforce NGET's view that all the generation components connected to the electricity system, notably the wind farms, must be designed with full flexibility in mind. Technical capability including dynamic performance across the range of generation technologies is an important feature for the deregulated whole sale and balancing market, with its absence of central generation dispatch.,

The possible vast wind developments reinforce the drivers for greater use of open markets for electricity and associated balancing services throughout the EU. A single weather system is geographically greater than each nation, making the logical case for greater sharing of use of the resource and for delivering the solutions to the associated balancing challenges, notably delivery of reserve capacity. Greater EU wide connectivity may also lead to increased activity to harmonise Grid Codes as well as market mechanisms. Some exploratory work is in progress in these respects in the EU backed TSO R&D programme called European Wind Integration Study (EWIS). 16 TSOs, including NGET are engaged on transmission and market R&D focused on requirements in 2015. This work is expected to conclude in summer 2009.

8. Conclusions

Successful implementation of compliance against challenging technical requirements defined in the GB Grid Code has been described for a range of the most common wind turbine technologies. This process has involved new requirements for fast acting voltage and frequency control systems, which are at the leading edge worldwide. This success story has demonstrated the practicality of broadly equal treatment of wind farms compared with other traditional generation technologies. Wind turbine technologies have now been proven as mature.

NGET believes that wind turbine technologies are more than capable of meeting, and in some cases exceeding, the demanding requirements in the GB Grid Code, provided that they are fully understood and the control systems are well designed to take account of them.

The route to success has been challenging for all involved and has been critically dependent upon good communications. Refinements of the compliance process have been defined and initiated to provide a better fit process for all stakeholders. Wind is now ready to be considered for scaling up from the existing low GW level in GB to 10s of GW, to implement the UK and EU ambitions for renewable energy and as such deliver a substantial contribution towards the move from a high carbon economy towards a low carbon economy.

Acknowledgement

The authors would like to extend their thanks to Neil Rowley & Antony Johnson, both of NGET, for their help in preparation of this paper.

References

[1] Oxford University Environmental Change Institute report. Wind power and the UK wind resource available at www.eci.ox.ac.uk/publications/downloads/sinden05-dtiwindreport.pdf

[2] British Wind Energy Association website, www.bwea.com/statistics/

[3] A. Johnson and N. Tleis The development of Grid Code requirements for new and renewable forms of generation in Great Britain Wind Engineering, Volume 29, No3 2005, pp 201-215.

[4] G / 06 GB Grid Code consultation on Power Park Modules and Synchronous Generating Units, available at https://www.nationalgrid.com/uk/Electricity/Codes/gridcode/consultationpapers/2006/

[5] Guidance Notes for Power Park Developers, issue 2 draft 1 February 2007, available at https://www.nationalgrid.com/uk/Electricity/Codes/gridcode/associateddocs

[6] The Great Britain Grid Code, available at http://www.nationalgrid.com/uk/Electricity/Codes/gridcode/gridcodedocs/

[7] J. Toal, H. Urdal, J. Horne, Y. Coughlan, C. Brozio et al. Building Confidence in Computer Models of Wind Turbine Generators from a Utility Perspective. NWPC2007 – to be published.

A Survey of Interconnection Requirements for Wind Power

Florin Iov[1*], Anca D. Hansen[2], Nicolaos A. Cutululis[2], Poul Soerensen[2]
[1] Institute of Energy Technology, Aalborg University, Pontoppidanstraede 101, DK-9220 Aalborg East, Denmark
[*] tlf. +45 9635 9266, e-mail fi@iet.aau.dk
[2] Risø DTU, VEA-118, P.O. Box 49, DK-4000 Roskilde, Denmark

Abstract — Currently, more wind power is expected to enter into the electrical network all over the world. Therefore the power system becomes more vulnerable and dependent on the wind energy production. The European countries with already grid connection requirements for wind power have revised them in the last two years while other countries have started to address these requirements. In all cases the grid codes reflect the penetration of the wind power into the electrical network both at distribution and transmission levels or a future development is prepared with these demands. Issues as power controllability, power quality, fault ride-through and grid support capability during network disturbances are addressed through these demands. The present paper provides a world wide overview of the existing grid codes for wind power.

Index Terms — Wind power, Interconnection requirements.

1. Introduction

The World Energy Council predicts that by 2050, the global energy mix will be made up of different energy sources in which renewables will have an important share. On the same time the European Union has a target of 22% electricity generation from renewables by 2010 and recognizes that wind power will be the main contributor for meeting this goal [1]. A study from European Wind Energy Association [3] estimates that wind is capable of delivering 12% by 2020 and in excess of 20% by 2030. According with International Energy Agency in the last decade wind power had one of the highest average annual growth rates among renewable sources [2]. On the same time in the last decade the wind turbines become bigger and bigger and currently single units up to 5 MW are commercially available. Europe seems to lead at this moment the penetration of the wind power into the electrical network, Denmark and the northern Germany having the highest level of penetration. In 2006 more than 20% from the total electricity consumption in Denmark was provided by the wind power. Spain and Ireland as well as Great Britain will install more wind power in the near future. The future development of wind power is also expected in Canada, Australia and Japan.

Modern MW wind turbines currently replace a large number of small wind turbines and there is a significant attention to offshore wind parks/farms, mainly because of higher average wind speed and no space limitations. Large wind farms like Horns Rev (160 MW) or Nysted (170 MW) in Denmark are in operation and more large wind farms are in construction or in the planning stage all over Europe.

However, in order to achieve objectives as continuity and security of the supply a high level of wind power into electrical network posses new challenges as well as new approaches in operation of the power system. Therefore some countries have issued dedicated grid codes for connecting the wind turbines/farms to the electrical network addressed to transmission and/or distributed system. In most of the cases, e.g. in Denmark, Germany, Ireland, these requirements have focus on power controllability, power quality, and fault ride-through capability. Moreover, some grid codes require grid support during network disturbances e.g. Germany and Spain. Denmark has the most demanding requirements regarding the controllability of the produced power. Wind farms connected at the transmission level shall act as a conventional power plant providing a wide range of controlling the output power based on Transmission Network Operators demands and also participation in primary and secondary control. The power quality requirements are very demanding in respect with flicker emission as well as the harmonic compatibility levels for voltages especially at Distribution System level comparing with relevant standards. All existing grid codes require fault ride-through capabilities for wind turbines. Voltage profiles are given specifying the depth of the voltage dip and the clearance time as well. However, in some of the grid codes the calculation of the voltage during all types of unsymmetrical faults is very well defined e.g. Ireland, while others do not define clearly this procedure.

Many references e.g. [3], [5] and [7] consider that the present grid codes often contain costly and demanding requirements e.g. fault ride-through capability and primary control which are not reflecting the real penetration of the wind power in a given area.

Moreover, according to [3] “grid codes and other technical requirements should reflect the true technical needs for system operation and should be developed in cooperation between Transmission System Operators, the wind energy sector and government bodies”.

The present paper presents a survey of the existing grid codes for wind power both at distribution and transmission system levels in different countries. Comparisons between the main points of concern are made as well as remarks about the sensitive issues within these requirements.

2. Overview of Wind Turbine Concepts

The most commonly applied wind turbine designs can be categorized into four wind turbine concepts [4] and [7].

The main differences between these concepts are the generating system and the way in which the aerodynamic efficiency of the rotor is limited during above the rated value in order to prevent overloading. These concepts are presented in detail in the following paragraphs.

2.1. Fixed Speed Wind Turbines (Type A)

This configuration corresponds to the so called Danish concept that was very popular in 80’s. This wind turbine is fixed speed controlled machine, with asynchronous squirrel cage induction generator (SCIG) directly connected to the grid via a transformer as shown in Figure 1.

This concept needs a reactive power compensator to reduce (almost eliminate) the reactive power demand from the turbine generators to the grid.

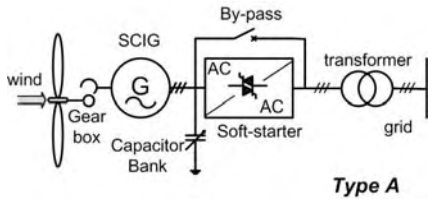

Figure 1. Fixed speed wind turbine with directly grid connected squirrel-cage induction generator.

It is usually done by continuously switching capacitor banks following the production variation (5-25 steps) Smoother grid connection occurs by incorporating a soft-starter. Regardless the power control principle in a fixed speed wind turbine, the wind fluctuations are converted into mechanical fluctuations and further into electrical power fluctuations. These can yield to voltage fluctuations at the point of connection in the case of a weak grid. Because of these voltage fluctuations, the fixed speed wind turbine draws varying amounts of reactive power from the utility grid (in the case of no capacitor bank), which increases both the voltage fluctuations and the line losses.

Thus, the main drawbacks of this concept are: does not support any speed control, requires a stiff grid and its mechanical construction must be able to support high mechanical stress caused by wind gusts.

2.2. Partial Variable Speed Wind Turbine with Variable Rotor Resistance (Type B)

This configuration corresponds to the limited variable speed controlled wind turbine with variable rotor resistance, known as OptiSlip (Vestas^{TM}) as shown in Figure 2.

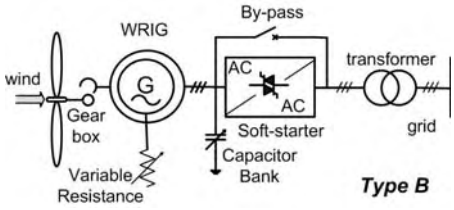

Figure 2. Partial variable speed wind turbine with variable rotor resistance.

It uses a wound rotor induction generator (WRIG) and it has been used by the Danish manufacturer Vestas Wind Systems since the mid 1990's.

The generator is directly connected to the grid. The rotor winding of the generator is connected in series with a controlled resistance, whose size defines the range of the variable speed (typically 0-10% above synchronous speed). A capacitor bank performs the reactive power compensation and smooth grid connection occurs by means of a soft-starter. An extra resistance is added in the rotor circuit, which can be controlled by power electronics. Thus, the total rotor resistance is controllable; the slip and thus the power output in the system are controlled. The dynamic speed control range depends on the size of the variable rotor resistance. Typically the speed range is 0-10% above synchronous speed. The energy coming from the external power conversion unit is dumped as heat loss. In [9] an alternative concept using passive component instead of a power electronic converter is described. This concept achieves 10% slip, but it does not support controllable slip.

The stator is directly connected to the grid, while a partial-scale power converter controls the rotor frequency and thus the rotor speed.

2.3. Variable Speed WT with partial-scale frequency converter (Type C)

This configuration, known as the Doubly-Fed Induction Generator (DFIG) concept, corresponds to the variable speed controlled wind turbine with a wound rotor induction generator (WRIG) and partial-scale frequency converter (rated to approx. 30% of nominal generator power) on the rotor circuit as shown in Figure 3.

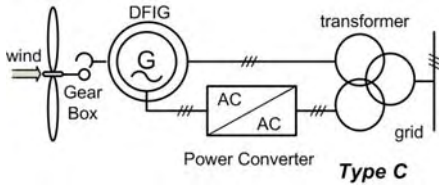

Figure 3. Variable speed wind turbine with partial scale power converter.

The power rating of this partial-scale frequency converter defines the speed range (typically ±30% around synchronous speed). Moreover, this converter performs the reactive power compensation and a smooth grid connection. The control range of the rotor speed is wide compared to that of OptiSlip. Moreover, it captures the energy, which in the OptiSlip concept is burned off in the controllable rotor resistance. The smaller frequency converter makes this concept attractive from an economical point of view. Moreover, the power electronics is enabling the wind turbine to act as a more dynamic power source to the grid. However, its main drawbacks are the use of slip-rings and the protection schemes in the case of grid faults.

2.4. Variable Speed Wind Turbine with Full-scale Power Converter (Type D)

This configuration corresponds to the full variable speed controlled wind turbine, with the generator connected to the grid through a full-scale frequency converter as shown in Figure 4.

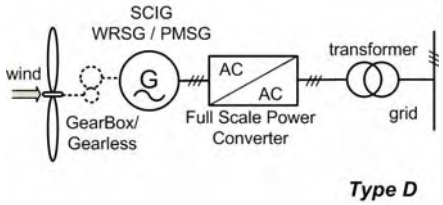

Figure 4. Variable speed wind turbine with full-scale power converter.

The frequency converter performs the reactive power compensation and a smooth grid connection for the entire speed range [4], [6] - [16]. The generator can be electrically excited (wound rotor synchronous generator WRSG) or permanent magnet excited type (permanent magnet synchronous generator PMSG). The stator windings are connected to the grid through a full-scale power converter.

Some full variable speed wind turbines systems are gearless – see dotted gearbox in Figure 4. In these cases, a bulky direct driven multi-pole generator is used.

A two stage conversion is usually used for the power converter; a AC to DC stage on the generator side and a DC to AC one on the grid side. An extra DC to DC conversion stage may be used e.g. permanent magnet synchronous generator based wind turbines as shown in Figure 5.

Most of these power converters are based on the two-level voltage source inverter topology [4]. However, there is an increasing interest in multilevel power converters especially

for medium to high-power, high-voltage wind turbine applications [17]-[19].

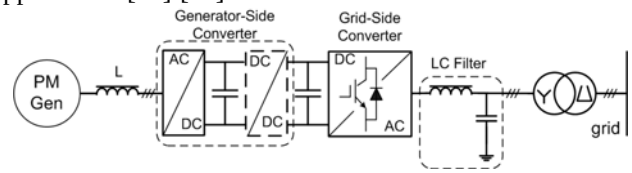

Figure 5. Permanent magnet synchronous generator based wind turbine with bidirectional power converter [4].

2.5. System comparison of wind turbines

Comparing the different wind turbine topologies in respect to their performances will reveal a contradiction between cost and the performance to the grid [4], [17]. A technical comparison of the main wind turbine concepts, where issues on grid control, cost, maintenance, internal turbine performance is given in Table 1.

Table 1. System comparison of wind turbine configurations [4].

System	Type A	Type B	Type C	Type D
Variable speed	No	No	Yes	Yes
Control active power	Limited	Limited	Yes	Yes
Control reactive power	No	No	Yes	Yes
Short circuit (fault-active)	No	No	No/Yes	Yes
Short circuit power	contribute	contribute	contribute	limit
Control bandwidth	1-10 s	100 ms	1 ms	0.5-1 ms
Standby function	No	No	Yes +	Yes ++
Flicker (sensitive)	Yes	Yes	No	No
Softstarter needed	Yes	Yes	No	No
Rolling capacity on grid	Yes, partly	Yes, partly	Yes	Yes
Reactive compensator (C)	Yes	Yes	No	No
Island operation	No	No	Yes/No	Yes
Investment	++	++	+	0
Maintenance	++	++	0	+

3. Grid Connection Requirements for Wind Power

Few countries worldwide have at this moment dedicated grid codes addressed to interconnection requirements of Renewable Energy Sources (RES). However, Europe is leading in this area. In most of the cases, these requirements reflect the penetration of renewable sources into the electrical network or that a future development is prepared with these demands. Among all kinds of renewable sources the wind power has specific requirements.

The requirements for wind power cover a wide range of voltage levels from medium voltage to very high voltage. The grid codes for wind power address issues that make the wind farms to act as a conventional power plant into the electrical network. These requirements have focus on power controllability, power quality, fault ride-through capability and grid support during network disturbances. According to several references [5], [7], [20] and [21] in some of the cases these requirements are very difficult to fulfil.

3.1. Design voltages and frequencies

Some grid codes specify the voltage and frequency design charts in the Point of Common Coupling (PCC). Typical charts for the design voltages and frequencies in the Danish grid codes for Distribution and Transmission networks are given in Figure 6 and Figure 7 respectively.

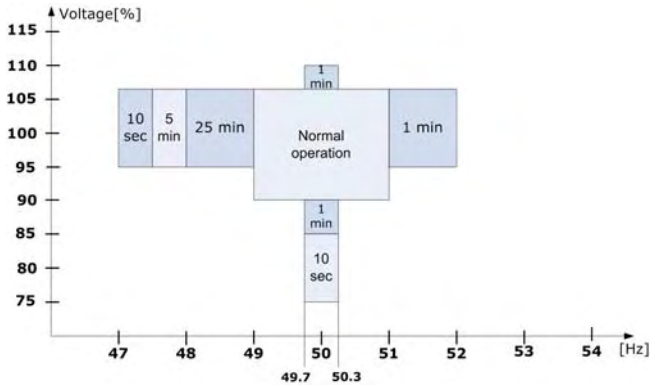

Figure 6. Voltages and frequencies used for design of a wind turbine connected to Medium Voltage networks [22].

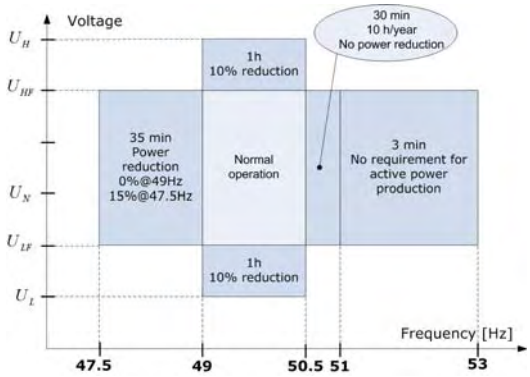

Figure 7. Operational range of wind farms connected to the Danish transmission networks [23].

Other transmission grid codes e.g. the German one are more restrictive than the Danish one for the entire range of voltages and frequencies, as shown in Figure 8.

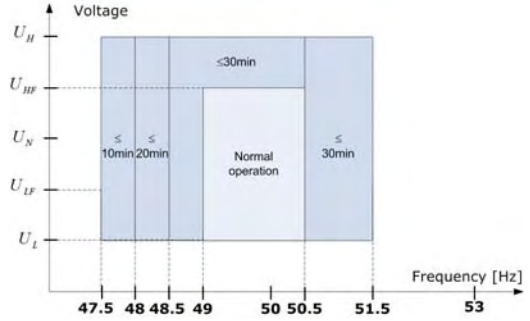

Figure 8. Operational range of wind farms connected to the transmission networks in the German grid [26], [27].

3.2. Active power control

The wind turbines must be able to control the active power in the Point-of-Common-Coupling (PCC) in a given range. The active power is typically controlled based on the system frequency. In Denmark, Ireland, Germany [22]-[28] the power delivered to the grid is decreased when the grid frequency rises above 50 Hz.

A typical characteristic for the frequency control in the Danish grid code is shown in Figure 9.

Other grid codes, e.g. Great Britain [29] specifies that the active power output must be kept constant for the frequency range 49.5 to 50.5 Hz, and a drop of maximum 5% in the delivered power is allowed when the frequency drops to 47 Hz as shown in Figure 10.

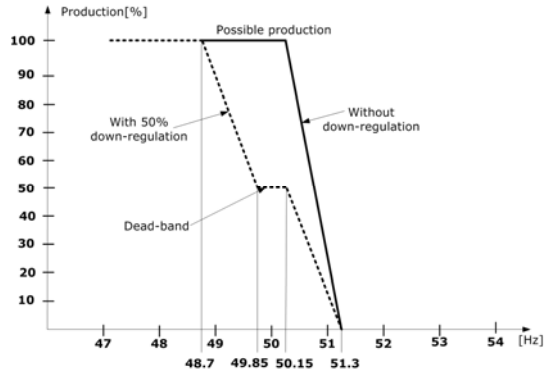

Figure 9. Frequency control characteristic for the wind turbines connected to the Danish grid [22], [23].

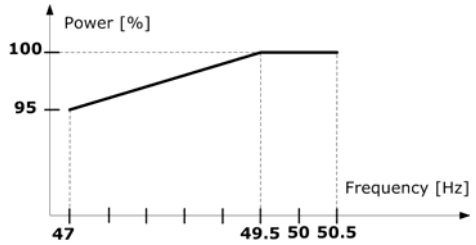

Figure 10. Frequency control characteristic in the Great Britain's grid code.

In the Italian grid code for wind turbines [34], it is specified that the produced active power shall be controlled with a maximum positive ramp rate of 20% from the rated power per minute for wind farms with a rated power over 25 MW. Wind turbines can not operate if the grid frequency is greater than 50.3 Hz.

In the Canadian grid codes the "requirements to control power output are generally absent, implied or very loosely defined" [37].

Curtailment of produced power based on system operator demands is mandatory in Denmark, Ireland, Germany and Great Britain [22]-[29].

Currently, Denmark has the most demanding requirements regarding the controllability of the produced power. Wind farms connected at the transmission level shall act as a conventional power plant providing a wide range of controlling the output power based on Transmission System Operator's (TSO) demands and also participation in primary and secondary control [23]. Seven regulation functions are required in the wind farm control. Among these control functions the following must be mentioned: delta control, balance control, absolute production and system protection as shown in Figure 11.

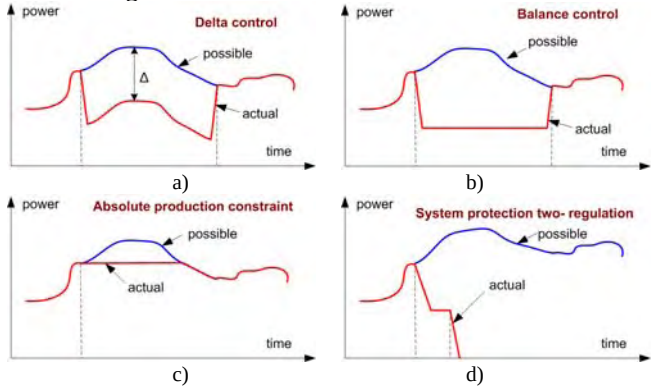

Figure 11. Regulation function for active power implemented in the wind farm controller required by the Danish grid code: a) delta control, b) balance control, c) absolute production constraint and d) system protection [23].

3.3. Reactive power control and voltage stability

Reactive power is typically controlled in a given range. The grid codes specify in different ways this control capability. The Denmark's grid code for both Distribution and Transmission networks gives a band for controlling the reactive power based on the active power output as shown in Figure 12.

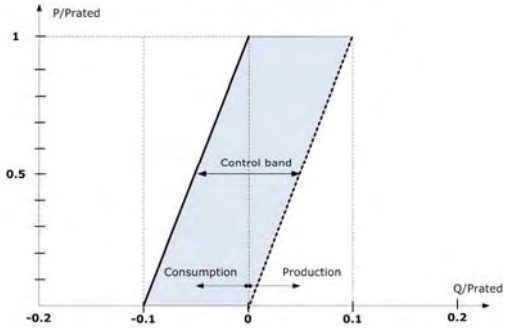

Figure 12. Danish grid code demands for the reactive power exchange in the PCC.

The Irish grid code specifies e.g. the reactive power capability in terms of power factor as shown in Figure 13.

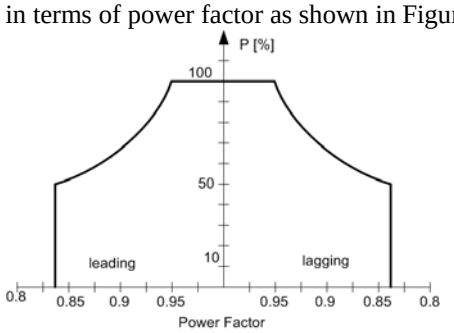

Figure 13. Requirements for reactive power control in the Irish grid code for wind turbines

The German transmission grid code for wind power specifies that these units must provide reactive power provision in the connection point without limiting the active power output the range as shown in Figure 14.

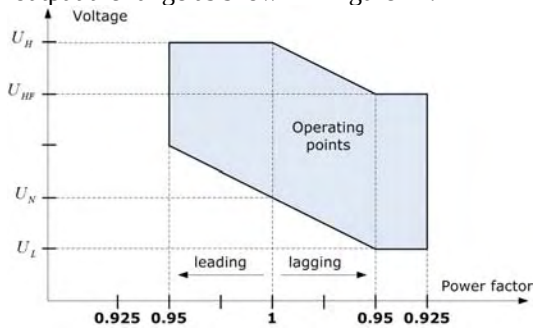

Figure 14. Requirements for reactive power provision of generating units without limiting the active power output in the German transmission grid code [26], [27].

3.4. Power quality

Power quality issues are addressed especially for wind turbines connected to the medium voltage networks. However, some grid codes, e.g. in Denmark and Ireland have also requirements at the transmission level.

Mainly two standards are used for defining the power quality parameters namely: IEC 61000 and EN 50160. Specific values are given for fast variations in voltage, short term flicker severity, long term flicker severity and the total harmonic distortion. An example of these requirements is

given in Table 2 for the wind turbines connected to the High Voltage networks in Denmark [23].

Table 2. Power quality parameters for wind turbines connected to transmission networks in Denmark [23].

Parameter	Value	Based on
Fast variations	< 3%	IEC 61000-3-7
Short term flicker severity (10 min)	< 0.3	
Long term flicker severity (2 h)	< 0.2	
Total Harmonic Distortion	< 1.5 %	-

A schedule of individual harmonics distortion limits for voltage are also given based on standards or in some cases e.g. Denmark custom harmonic compatibility levels are defined [22]. Interharmonics may also be considered as in the Danish grid codes [22].

3.5. Low voltage ride-through capability

All considered grid codes for wind power require Low-Voltage Ride-Through (LVRT) capabilities for wind turbines [22]-[33]. Voltage profiles are given specifying the depth of the voltage dip and the clearance time as well (see Appendix 1).

A voltage profile for ride-through capabilities of wind turbines as specified in the Danish grid code for wind turbines connected to Distribution networks is shown in Figure 15.

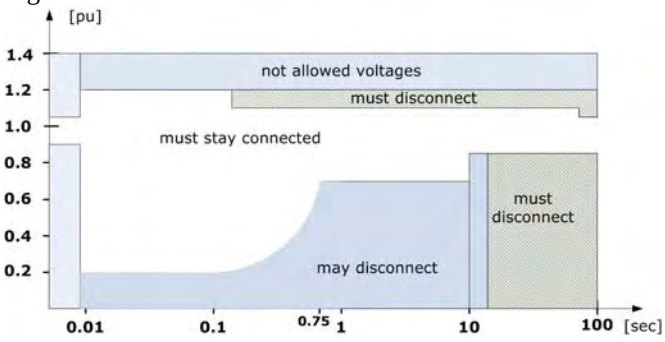

Figure 15. Danish requirements for disconnection of wind turbines in the event of deviations in voltage [22].

One of the problems is that the calculation of the voltage during all types of unsymmetrical faults is not very well defined in some grid codes. The Danish requirements specifies the voltage profiles for symmetrical and asymmetrical faults [22], [23], while the German requirements for Transmission networks [26] define very clear the voltage limits for disconnection only for three-phase symmetrical faults as shown in Figure 16.

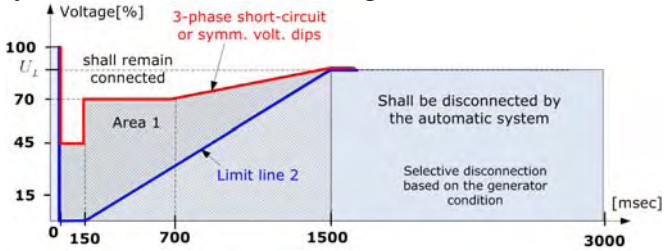

Figure 16. Voltage limits for disconnection of wind turbines in the case of faults in the German transmission networks [26].

According to [26] special requirements are applied in Area 1 in Figure 16.

In United States the interconnection requirements for wind energy connected to the transmission networks are defined by Federal Energy Regulatory Commission (FERC) [38]. According to this document the wind power plants "shall be able to remain online during voltage disturbances up to the time periods and associated voltage levels" as shown in Figure 17.

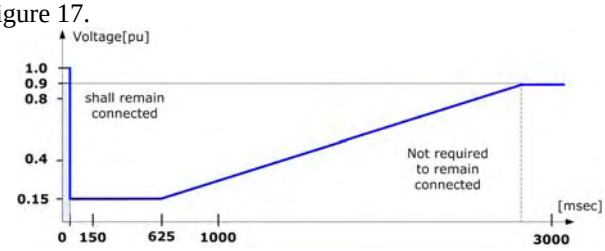

Figure 17. Minimum required wind plant response to emergency low voltages in United States [38].

This voltage profile is similar to that issued by the transmission operator in the Canadian province Alberta (AESO).

In Canada Hydro-Quebec's requirement is defined for "the positive sequence voltage on the high-voltage side of the switchyard" [35] as given in Figure 18. According to [35] the wind generators must remain to the transmission system without tripping during symmetrical and asymmetrical faults.

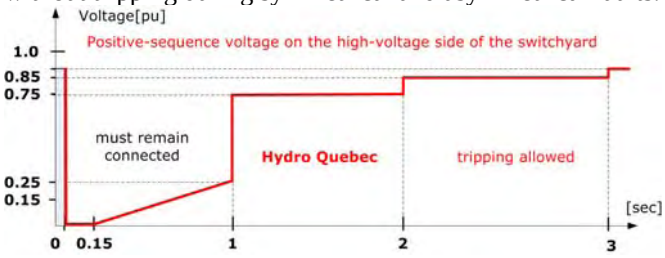

Figure 18. LVRT requirement from Hydro-Quebec for wind generators during faults.

In a study made by Garrad Hassan for Canadian Wind Energy Association [37] is stated that "the Quebec LVRT requirement is likely to become standard across many Canadian provinces and that Alberta and other grid codes will cede to this".

Ireland's grid code[24], [25] is very demanding in respect with the fault duration – up to 1 sec - while Denmark has the lowest short circuit time duration with only 100 msec. However, Denmark's grid code requires that the wind turbine shall remain connected to the electrical network during successive unsymmetrical faults [22] as shown in Figure 19.

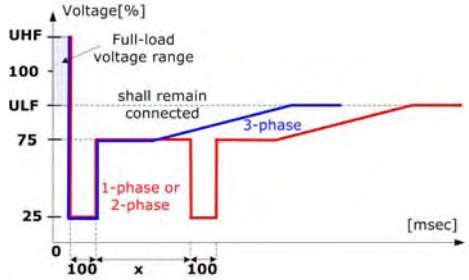

Figure 19. Fault ride-through capabilities of WTs connected to the Danish Distribution networks [22].

On the other hand Germany and Spain requires grid support during faults by reactive current injection up to 100% from the rated current [26], [30] as shown in Figure 20. and Figure 21.

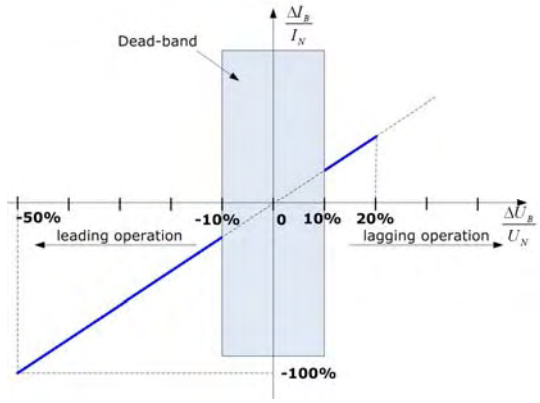

Figure 20. Grid support during faults by reactive current injection as specified in the German grid code for wind power [26], [27].

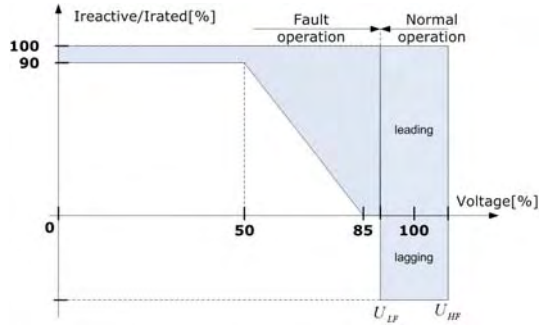

Figure 21. Grid support during faults by reactive current injection as specified in the Spanish grid code for wind power [30].

This demand is relative difficult to meet by some of the wind turbine concepts e.g. active stall wind turbine with directly grid connected squirrel cage induction generator (Type A).

Based on the existing grid codes for wind power the voltage profile for ride-through capability can be summarized as shown in Appendix 2.

A summary regarding the main parameters for the interconnection requirements for wind power in Europe is given in detail in Appendix 3.

4. Grid Compliance of Wind Power

It is obviously that today, there are very hard grid connection requirements [20]-[39] which require MW-size wind turbines concentrated in large wind farms connected to the transmission networks to support the grid actively and to remain connected during grid events (i.e. voltage sags), otherwise it could cause a grid blackout. The main role for such technical demands of the grid operators is played today by the power electronics within the wind turbines and wind farms.

Analyzing the wind turbine concepts presented in §2 as well as the grid connection requirements given in §3 some general conclusions and also trends for future can be drawn.

One off-shore wind farm equipped with power electronic converters can perform both active and reactive power control and also operate the wind turbines in variable speed to maximize the energy captured as well as reduce the mechanical stress and noise. This solution is shown in Figure 22 and it is in operation in Denmark as a 160 MW off-shore wind power station.

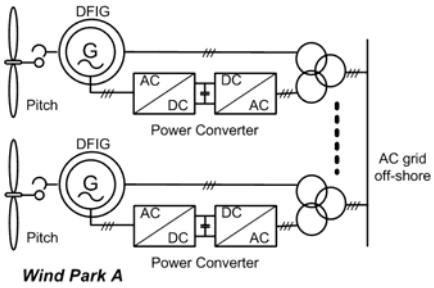

Figure 22. Doubly Fed Induction Generator based wind farm with an AC grid connection.

Still, the doubly-fed concept is sensitive to grid faults and requires special protection schemes inserted in the rotor side. Moreover, since the power converter is rated to 30% from the wind turbine power, it is not capable to deliver too much reactive current in case of a grid fault.

The wind turbine concept based on directly grid connected squirrel-cage induction generator (Type A) itself cannot fulfill most of the interconnection requirements. However, concentrating these wind turbines in off-shore wind farms and providing reactive power compensation in the PCC e.g. using a Static VAR Compensator as shown in Figure 23 may be a solution for most of these requirements.

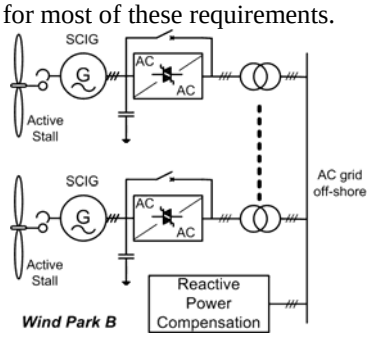

Figure 23. Active stall wind farm with an AC grid connection.

One of the remaining problems in this case is the reactive current injection in case of faults. This solution depends also strongly on the ratings of the compensation unit.

For long distance power transmission from off-shore wind farm, HVDC may be an interesting option. In an HVDC transmission system, the low or medium AC voltage at the wind farm is converted into a high dc voltage on the transmission side and the dc power is transferred to the on-shore system where the DC voltage is converted back into AC voltage as shown in Figure 24.

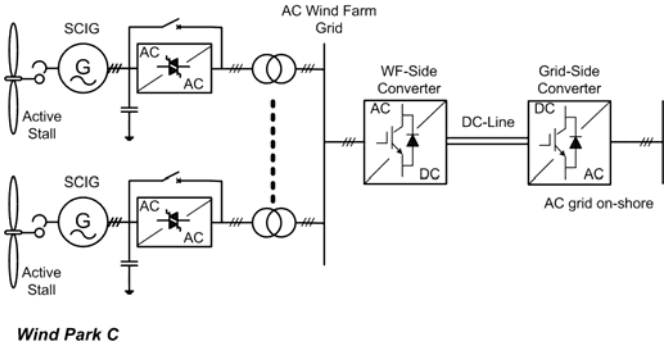

Figure 24. Active stall wind farm with a HVDC-link grid connection.

In this way a complete decoupling of active and reactive power between wind farm and grid is achieved. Also, the grid side converter can inject up to 100% reactive current into the power system. This configuration may even be able

to vary the speed on the wind turbines inside the wind farm [40], [41].

Another possible DC transmission system configuration is shown in Figure 25, where each wind turbine has its own power electronic converter, so it is possible to operate each wind turbine at an individual optimum speed. A common DC grid is present on the wind farm while a full scale power converter is used for the on-shore grid connection.

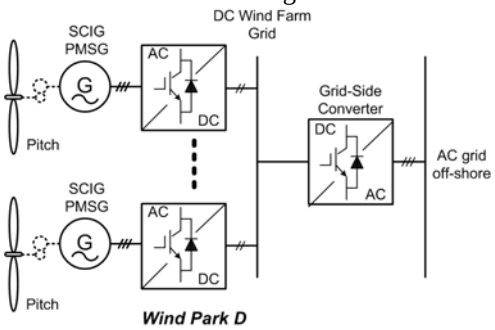

Figure 25. Wind farm with common DC grid based on variable speed wind turbines with full scale power converter.

The wind farm topologies based on a full scale power converter on the grid side (see Figure 24 and Figure 25) can fulfill all the interconnection requirements for normal operation as well as during the grid faults. Extra features can also be provided e.g. harmonic compensation, black start capability, etc. Moreover, using multilevel power converter topologies the transformer can be eliminated.

A comparison of these possible wind farm topologies in terms of control abilities, response to grid faults as well as economical aspects is shown in Table 3 [4].

Table 3. Comparison of wind farm topologies

	Wind Park A	Wind Park B	Wind Park C	Wind Park D
Individual speed control	Yes	No	Yes	No
Control active power electronically	Yes	No	Yes	Yes
Control reactive power	Yes	Centralized	Yes	Yes
Short circuit (active)	Partly	Partly	Yes	Yes
Short circuit power	Contribute	Contribute	No	No
Control bandwidth	10-100 ms	200ms - 2s	10 -100 ms	10 ms – 10 s
Stand by-function	Yes	No	Yes	Yes
Soft-starter needed	No	Yes	No	No
Rolling capacity on grid	Yes	Partly	Yes	Yes
Redundancy	Yes	Yes	No	No
Investment	+	++	+	+
Maintenance	+	++	+	+

5. CONCLUSIONS

Since more wind power is expected to enter into the grid, more changes are also expected in the existing grid codes. The variety of requirements within these codes makes difficult a benchmarking and a fair comparison. Thus, more challenges are posed for researchers as well as for the wind turbine industry regarding the grid integration of wind power.

The response of the present wind turbine concepts to the interconnection requirements is different. Some of these concepts can fulfil partially the requirements e.g. power controllability and reactive power control, while other concepts can comply with the worst case scenario e.g. grid support by reactive current injection and black-start capability. Thus, full-scale power converter based solutions are very promising especially in terms of ride-through and grid support capabilities. Currently, most of the interconnection requirements address ride-through capabilities only for the transmission level. However, this may be changed in the near future because one of the targets for Distributed Generation is to make these relatively small units to act as conventional power plants. An example in this sense is the Danish grid code for wind turbines connected to distribution networks [22].

Moving to large wind farms connected at the transmission level there is an increasing trend in all grid codes over the world to require wind farms to behave more and more as conventional power plants in the power system. This means that, sooner or later, they will have to share some of the duties carried out today by the conventional power plants. Thus, power converter based solutions for grid interfacing seems to be to only promising technology that can cope with all interconnection requirements.

Consequently, it is obvious that power electronics is the key-enabling technology in the grid integration of wind power. Using power converters for grid interfacing not only the current requirements can be fulfilled but also some extra features as harmonic cancellation capabilities, black-start and complete grid support during grid events can be provided. These solutions are already available e.g. the HVDC concept and new topologies are in the research stage such as the UNIFLEX-PM system [42]. The only remaining question is how fast these solutions will be adopted on large scale.

ACKNOWLEDGEMENTS

The authors acknowledge the support from the Energinet.dk through Contract PSO FU-6319 and from the European Commission through Contract no. 019794 SES6 (UNIFLEX-PM).

REFERENCES

[1] European Commission – New ERA for electricity in Europe. Distributed Generation: Key Issues, Challenges and Proposed Solutions, EUR 20901, 2003, ISBN 92-894-6262-0;

[2] IEA - Variability of wind power and other renewables. Management options and strategies. IEA, www.iea.org ;

[3] EWEA Large scale integration of wind energy in the European Power Suply; December 2005;

[4] F. Iov, F. Blaabjerg - *UNIFLEX-PM. Advanced power converters for universal and flexible power management in future electricity network – Converter applications in future European electricity network.* Deliverable D2.1, EC Contract no. 019794(SES6), February 2007, p. 171, (available www.eee.nott.ac.uk/uniflex/Deliverables.htm);

[5] D. Milborrow, "Going mainstream at the grid face. Examining grid codes for wind", *Windpower Monthly*, September 2005, ISSN 109-7318;

[6] A.D. Hansen, P. Sørensen, F. Iov, F. Blaabjerg – Centralised power control of wind farms with doubly-fed induction generators, Journal of Renewable Energy, Elsevier Science, Oxford, Vol. 31, No. 7, 2006, pp. 935-951, ISSN 0960-14811;

[7] A.D. Hansen, F. Iov, F. Blaabjerg, L.H. Hansen, "Review of contemporary wind turbine concepts and their market penetration", *Journal of Wind Engineering*, 28(3), 2004, pp. 247-263

[8] F. Iov, Z. Chen, F. Blaabjerg, A. Hansen, P. Sorensen, "A New Simulation Platform to Model, Optimize and Design Wind Turbine", *Proc. of IECON '02*, Vol. 1, pp. 561-566

[9] K. Wallace, J.A. Oliver, "Variable-Speed Generation Controlled by Passive Elements", *Proc. of ICEM '98*, 1998.

[10] L.H. Helle, F. Blaabjerg, E. Ritchie, S. Munk-Nielsen, H. Bindner, P. Sørensen, B. Bak-Jensen, *Conceptual survey of Generators and Power Electronics for Wind Turbines*, Risø-R-1205(EN)

[11] L.H. Hansen, P.H. Madsen, F. Blaabjerg, H.C. Christensen, U. Lindhard, K. Eskildsen, "Generators and power electronics technology for wind turbines", *Proc. of IECON '01*, Vol. 3, 2001, pp. 2000 – 2005
[12] T. A. Lipo, "Variable Speed Generator Technology Options for Wind Turbine Generators", *NASA Workshop on HAWTT Technology*, May 1984, pp. 214-220
[13] O. Carlson, J. Hylander, S. Tsiolis, "Variable Speed AC-Generators Applied in WECS", *European Wind Energy Association Conference and Exhibition*, October 1986, pp. 685-690.
[14] K. Thorborg, *"Asynchronous Machine with Variable Speed"*, Appendix G, Power Electronics, 1988, ISBN 0-13-686593-3, pp. 61
[15] O. Carlson, J. Hylander, K. Thorborg, "Survey of variable speed operation of wind turbines", *Proc. of European Union Wind Energy Conference*, Sweden, 1996, pp. 406-409.
[16] E.N. Hinrichsen, "Controls for variable pitch wind turbine generators", *IEEE Trans. on Power Apparatus and Systems*, Vol. 103, No. 4, 1984, pp. 886-892.
[17] J.M. Carrasco, E. Galvan, R. Portillo, L.G. Franquelo, J.T. Bialasiewicz, "Power Electronics System for the Grid Integration of Wind Turbines", *in Proc. of IECON '06 Conference*, November 2006, pp. 4182 – 4188.
[18] R. Portillo, M. Prats, J.I. Leon, J.A. Sanchez, J.M. Carrasco, E. Galvan, L.G. Franquelo, "Modelling Strategy for Back-to-Back Three-Level Convertres Applied to High-Power Wind Turbines", *IEEE Trans. on Industrial Electronics*, vol. 53, no. 5, October 2006 pp. 1483-1491.
[19] F. Blaabjerg, F. Iov, R. Teodorescu, Z. Chen, "Power Electronics in Renewable Energy Systems", *keynote paper in Proc of EPE-PEMC 2006 Conference*, Portoroz, Slovenia, p. 17
[20] P. Sørensen, B. Bak-Jensen, J. Kristian, A.D. Hansen, L. Janosi, J. Bech, " Power Plant Characteristics of Wind Farms", *Proc. of the Int. Conf. in Wind Power for the 21st Century*, 2000.
[21] S. Bolik, "Grid Requirements Challenges for Wind Turbines", *Proc. of Fourth International Workshop on Large-Scale Integration of Wind Power and Transmission Networks for Offshore Windfarms*, 2003.
[22] EnergiNet, *Grid connection of wind turbines to networks with voltages below 100 kV*, Regulation TF 3.2.6, May 2004, p. 29, Denmark
[23] EnergiNet, *Grid connection of wind turbines to networks with voltages above 100 kV*, Regulation TF 3.2.5, December 2004, p. 25, Denmark.
[24] ESB Networks, *Distribution Code*, version 1.4, February 2005, Ireland
[25] CER, *Wind Farm Transmission Grid Code Provisions*, July 2004, Ireland.
[26] E.ON-Netz, *Grid Code. High and extra high voltage*, April 2006, Germany.
[27] VDN, *Transmission Code 2003*. Network and System Rules of the German Transmission System Operators, August 2003, Germany.
[28] VDN, *Distribution Code 2003*. Rules on access to distribution networks, August 2003, Germany.
[29] National Grid Electricity Transmission plc, *The grid code*, Issue 3, Revision 17, September 2006, Great Britain.
[30] REE, *Requisitos de respuesta frente a huecos de tension de las instalaciones de produccion de regimen especial*, PO 12.3, November 2005, Spain.
[31] ENEL, *DK 5400 - Criteri di allacciamento di clienti alla rete AT della distribuzione*, October 200, Italy.
[32] ENEL, *DK 5740 - Criteri di allacciamento di impianti di produzione alla rete MT di ENEL distribuzione*, February 2005, Italy.
[33] TERNA, *Codice di trasmissione, dispacciamento, sviluppo e sicurezza della rete*, 2006, Italy.
[34] CEI 11/32, Appendice N.6, *Normativa impianti di produzione eolica*, February 2006 (draft), Italy.
[35] Hydro-Québec TransÉnergie – Transmission Provider Technical Requirements for the connection of power plants to the Hydro-Québec Transmission System, March 2006.
[36] Alberta Electric System Operator – Wind Power Facility. Technical Requirements, Revision 0, November 2004.
[37] CanWEA - Canadian Grid Code for Wind Development Review and Recommendations, Document no. 11163/OR/01 B, 2005 Garrad Hassan Canada Inc.
[38] FERC – Interconnection of Wind Energy, 18 CFR Part 35, Docket No. RM05-4-001; Order No. 661-A December 12, 2005.
[39] F. Iov, A.D. Hansen, P. Soerensen, N.A. Cutululis, *Mapping of grid faults and grid codes*. Risø-R-1617(EN) (2007) p. 41 (available on line: www.risoe.dk).
[40] F. Iov, P. Soerensen, A.D. Hansen, F. Blaabjerg – Modelling, Analysis and Control of DC-connected Wind Farms to Grid, *International Review of Electrical Engineering*, Praise Worthy Prize, February 2006, pp.10, ISSN 1827- 6600.
[41] F. Iov, P. Soerensen, A.D. Hansen, F. Blaabjerg - Modelling and Control of VSC based DC Connection for Active Stall Wind Farms to Grid, *IEE Japan Trans. on Industry Applications*, Vol. 126-D, No. 5, April 2006.
[42] UNIFLEX-PM – project web page: www.eee.nott.ac.uk/uniflex/

Appendix 1. Summary regarding fault ride through capability of wind turbines/farms in National Grid Codes [39].

Country	**Voltage Level**	**Fault ride-through capability**				
		Fault duration	Voltage drop level	Recovery time	Voltage profile	Reactive current injection
Denmark	DS	100 msec	25%U_r	1 sec	2, 3-ph	no
	TS	100 msec	25%U_r	1 sec	1, 2, 3-ph	no
Ireland	DS/TS	625 msec	15%U_r	3 sec	1, 2, 3- ph	no
Germany	DS/TS	150 msec	0%U_r	1.5 sec	generic	Up to 100%
Great Britain	DS/TS	140 msec	15%U_r	1.2 sec	generic	no
Spain	TS	500 msec	20%U_r	1 sec	generic	Up to 100%
Italy	> 35 kV	500 msec	20%U_r	0.3 sec	generic	no
USA	TS	625 msec	15%U_r	2.3 sec	generic	no
Ontario/Canada	TS	625 msec	15%Ur	-	-	no
Quebec/Canada	TS	150 msec	0%U_r	0.18 sec	Positive-sequence	no

Appendix 2. Voltage profiles for fault ride through capability of wind turbines/farms in National Grid Codes.

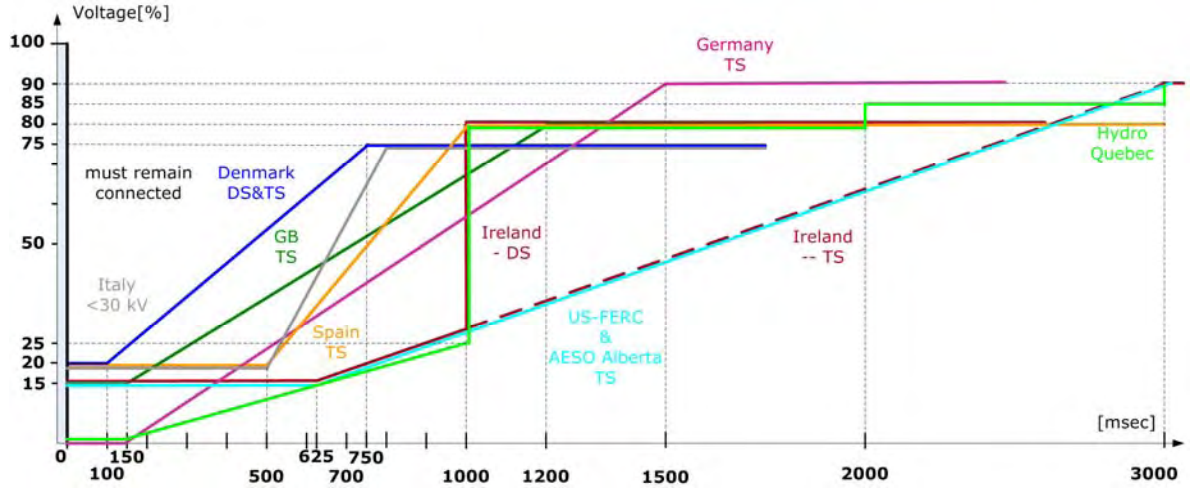

Appendix 3. Review of connection requirements for wind power in European grid codes [4]

		Denmark		Ireland	Germany	Great Britain	Spain	Italy (draft)
Voltage Level		DS	TS	DS(TS)	TS(DS)	TS(DS)	TS	> 35 kV
Power Level		all	all	≥5MW	all	all	all	> 10 MW
Tolerance over frequency range		yes	yes	yes	yes	yes	-	yes
Frequency	**Frequency control**	all	all	all	all	all	-	> 25 MW
	MW Curtailment	20-100% P_r	20-100% P_r	yes	yes	-	-	-
	Maximum Ramp Rates	10-100% P_r/min	10-100% P_r/min	1-30 MW/min	yes	-	-	<20% P_r/min
Voltage	**Voltage Control**	no	no	yes	no	no	-	no
	Reactive Power Control	yes	yes	yes	yes	yes	-	yes
Voltage quality	**Fast voltage variations**	≤ 3%	≤ 3%	-	≤ 2%	≤ 3%-	-	EN 50160
	Short Term Flicker Severity	-	≤ 0.3	≤ 0.35	-	≤0.8	-	EN 50160
	Long Term Flicker Severity	≤ 0.35	≤ 0.2	≤ 0.35	≤ 0.46	≤0.6	-	EN 50160
	Harmonic Compatibility Levels	Specific levels	-	Specific Levels[1)]	EN 50160	IEC 61000-3-2	-	EN 50160
	THD	-	≤ 1.5%	≤ 1.5%	≤ 8%	N/A	-	EN 50160
Fault ride-through	**Fault duration**	100 msec	100 msec	625 msec	150 msec	140 msec	500 msec	500 msec
	Min voltage	25%U_r	25%U_r	15%U_r	0%U_r	15%U_r	20%U_r	20% U_r
	Recovery time	1 sec	1 sec	3 sec	1.5 sec	1.2 sec	1 sec	0.3 sec
	Voltage profile	2, 3-ph	1, 2, 3- ph	1, 2, 3- ph	generic	generic	generic	generic
	Reactive current injection	no	no	no	Up to 100%	no	Up to 100%	no
Island operation		not required	not required	not required	not required	not required	not required	not required
Black start capability		not required	not required	may	if required	not required	not required	not required
Signals, Communication and Control	**Availability**	yes	yes	yes	yes	yes	-	yes
	Active power output	yes	yes	yes	yes	yes	-	yes
	Reactive power output	yes	yes	yes	yes	yes	-	yes
	MW Curtailment	yes	yes	yes	yes	yes	-	-
	Frequency control	yes	yes	yes	yes	yes	-	-
	Circuit breaker status	yes	yes	yes	yes	yes	-	yes
	Meteorological data: Wind speed, wind direction, air pressure and temperature	yes	yes	yes	-	-	-	yes

1) Harmonic compatibility levels are given in general for loads and installations. DSO shall provide a schedule of individual limits where appropriate.

Comparing the Fault Response Between a Wind Farm Complying With the E.ON Netz Code and That of Classical Generators

Nayeem Rahmat Ullah[1)], Jörgen Svensson[2)] and Andy Karlsson[3)]
[1)]Chalmers University of Technology, Göteborg-412 96, Sweden, email: nayeem.ullah@chalmers.se
[2)]E.ON Vind AB, Malmö-205 09, Sweden
[3)]E.ON Elnät AB, Malmö-205 09, Sweden

***Abstract*— This paper investigates and compares the response of a wind farm (WF) during network faults, while complying with an example grid code (E.ON Netz code), with that of a conventional synchronous generator (SG). The impact of the response of a WF during network faults while complying with an example grid code, on the performance of the nearby grid is also quantified and compared with the case when the WF is replaced with a SG with the same capacity. The Cigré 32-bus test system is used to perform a case study. For the studied case, it is found that, the rotor angle stability of a nearby conventional generating unit is improved when the WF complies with the E.ON code (34^o) compared to cases when the WF operates at unity pf during the fault or when the WF is replaced with a SG (40^o).**

***Index Terms*— variable speed wind turbine, grid code, frequency converter, synchronous generator (SG).**

I. Introduction

In the past, requirements for wind turbines were focused mainly on protection of the turbines themselves and did not consider the effect on the power system operation since the penetration level of wind energy was fairly low. As the integration level of wind energy is increasing, concerns regarding the stability of the already existing power system are becoming of utmost importance and for a reliable and secure power system operation, the loss of a considerable part of the wind generators due to network disturbances cannot be accepted any more [1].

A comment on the conclusion drawn in [2] is that today wind turbines of variable speed type have become more common than traditional fixed-speed turbines. The variable speed wind turbines are either of the doubly-fed induction generator (DFIG) type or of the full power converter type [3]. In particular the full power converter type turbines already contains the needed hardware set-up for making the turbine to act as a static synchronous compensator (STATCOM, with limited capability). This means that a controlled response of wind farms (WF) during faults can be achieved with minor additional costs, and this feature should accordingly be utilized if it leads to grid stability improvements.

Technical regulations for WFs to be connected to a power system vary considerably from country to country. The differences in requirements depend on the wind power penetration level and on the robustness of the power network besides local traditional practices [2]. Usually fault ride-through (FRT) for temporary under-voltages is nowadays required by system operators, see for example [4]–[8].

In a previous paper, it is shown that the stability of a grid is improved during network disturbances if a nearby WF responds according to the E.ON code, compared to the traditional unity power factor operation of the WF [9]. It is also shown in [9] that the stability of the nearby grid can be enhanced further when the response of the WF follows a slightly modified E.ON code compared to the E.ON case, as well as when wind turbines of the WF are equipped with larger converters than required. It will be quite easy to modify the response of a variable speed wind turbine during faults as flexible power electronic converters are already included in the design, as mentioned earlier. A real life example in this regard is reported in [10] where the control of the voltage source converter (VSC) of an existing HVDC light installation was modified to incorporate an additional voltage stability function.

Conventional synchronous generators (SGs) are usually responsible for supporting the grid. An interesting topic is accordingly to compare the response of a WF complying with the E.ON code during network faults with that of a conventional SG with the same capacity and also to quantify and compare the improvements they can have on the stability of the nearby grid. Such a study could be interesting in the sense that it can demonstrate whether we are demanding *excess contributions* from a WF regarding grid supports than what the already existing SGs are contributing. The study can also identify opportunities, if any, for a WF to get benefited for the *excess contributions* it makes towards the grid stability improvement compared to that of a conventional SG.

The goal of the paper is to compare the response of a WF complying with an example grid code (E.ON Netz code) during network faults with that of a conventional SG. Moreover, a purpose of the paper is to compare the improvements a WF can have on the nearby grid while complying with an example grid code with that of base case values where the WF is replaced with a SG with the same capacity.

II. E.ON Netz Fault Response Code for WFs

The FRT requirement for E.ON Netz is shown in Fig. 1. It requires a WF to be grid connected as long as the voltage at the grid connection point is above the solid line of Fig. 1(a).

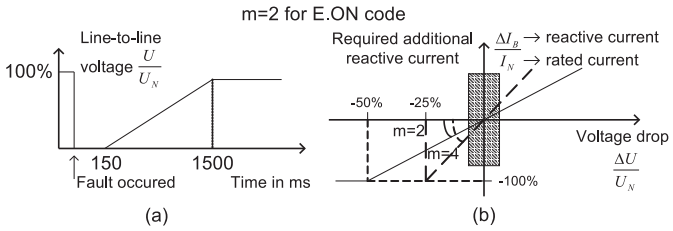

Fig. 1. The E.ON (a) voltage limit curve at the grid connection point during a fault and (b) the reactive power support required during a network fault.

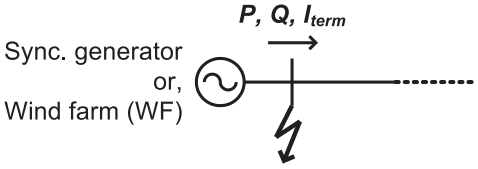

Fig. 2. SG or WF exposed to network faults.

Reactive current support should be provided on the low voltage side of the generator transformer following the characteristic shown in Fig. 1(b). It specifies the reactive current output from the WF to increase 2% (on a pu base) for a 1% voltage decrease, to have the 100% rated capacity of the converter utilized at 50% voltage at the wind turbine terminal. Accordingly, the slope of the reactive current support line, m, is 2. The E.ON regulation requires WFs to provide this reactive current support within 20 ms after a fault detection. The regulation also states that if the generators are too far away from the grid connection point resulting in an ineffective voltage support, then the measurement of the voltage dip should be done at the grid connection point and the voltage support should be provided at this point as a function of this measured value [6].

III. Modeling

A. WF modeling

In this work, a variable speed wind turbine with a power electronic interface (a full-power converter system) is considered. It is assumed that the wind turbines are equipped with a voltage dip ride-through facility and have a rapid current controller. Based on these assumptions, the WF is modeled as an user written model in PSS/E which is a current injection source with current limitation determined by the converter capacity constraint. As a very fast response can be achieved from a power electronic converter, the WF can thus be modeled as a controlled current source with a small time constant (20 ms). Ottersten *et al*. [11] experimentally demonstrated that a PWM voltage source converter can respond very quickly to a voltage disturbance. Similar results were also shown in [12] and in [13]. The results from these researches justify the assumption of modeling a WF as a very fast controlled current injection source. A similar approach of modeling a WF was also adopted in [10] and in [14]. The reference current is generated in accordance with the E.ON grid code which is then injected into the grid.

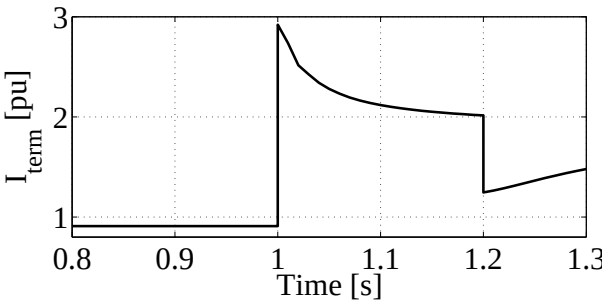

Fig. 3. Terminal current of a synchronous generator during a bolted three-phase fault.

B. SG modeling

A round rotor SG is modeled by the PSS/E library model GENROU which represents solid rotor generators at the subtransient level. The voltage regulator of this generator is modeled by the PSS/E library model SEXS which represents the general characteristic of a wide variety of properly tuned excitation systems. The power system stabilizer model used is the PSS/E library model STAB2A which is a representation of a specific type of supplementary stabilizing unit [15]. The values of different parameters of these models are based on [16] and are given in the Appendix.

IV. WFs vis-à-vis SGs during Network Faults

To compare the response of a WF complying with the E.ON code with that of a SG during network faults, a SG and an aggregated WF with the same capacity of the SG are exposed to network faults resulting in different remaining voltages at the terminal (see Fig. 2). It is made sure that the initial active and reactive power from the WF and the SG are the same.

A. Terminal current

The armature current of a synchronous generator during network faults becomes very high compared to the steady-state value. The rate at which the subtransient and the transient current decays are determined by the associated time constants [17]. Fig. 3 shows the terminal current of a SG during a network fault. The magnitude of the fault current also depends on the fault impedance, apart from the SG parameters. However, in the case of a wind turbine with a full scale power electronic converter, the fault current is limited to the maximum current rating of the converter due to the sensitive power electronic equipment [18].

B. Active and reactive power

The active and reactive power from a SG during network faults of different magnitudes – leading to different remaining voltages – are calculated and shown in Fig. 4. The values shown in the figure are the active and reactive power from the SG at the instance of the fault occurance. At the instance of the fault clearance, the reactive power are lower than these values as the air-gap flux will diminish. It can be seen from the figure that the reactive power output from the SG is maximum

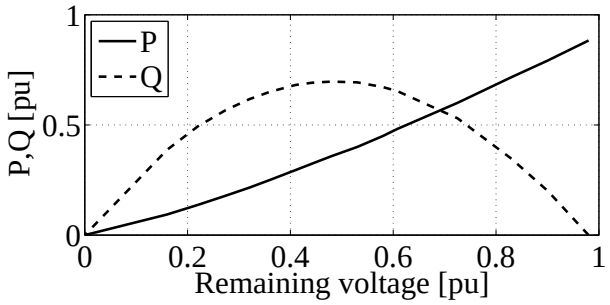

Fig. 4. Active (P) and reactive (Q) power from a SG during network faults of different magnitudes.

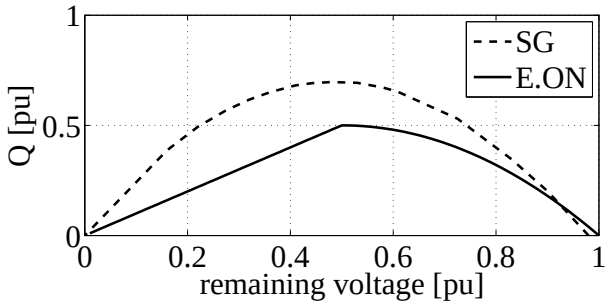

Fig. 5. Comparison of the reactive power during network faults with different severity form a SG and a WF complying with the E.ON Netz code.

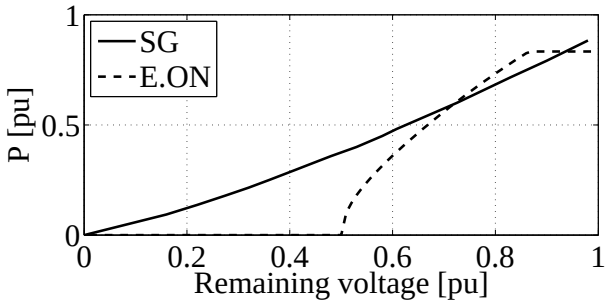

Fig. 6. Comparison of the active power during network faults with different severity form a SG and a WF complying with the E.ON Netz code.

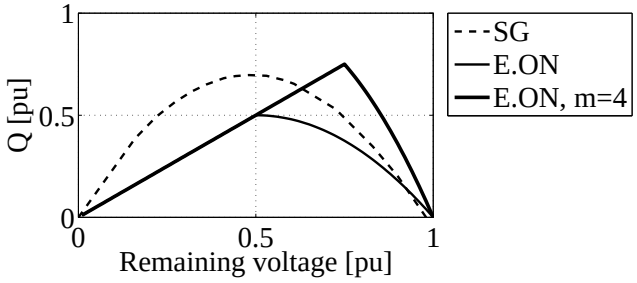

Fig. 7. Reactive power during network disturbances from a SG, a WF complying with the E.ON Netz code and a WF complying with the modified E.ON code (m=4).

when a network fault leads to a 0.5 pu remaining voltage at the bus. Also, note the almost linear decay of the active power of the SG with increasing fault severity.

In a previous paper, the active and reactive power from a WF complying with the E.ON Netz code, during network faults, were presented [9]. Fig. 5 and Fig. 6 show the WF reactive and active power during network faults with different fault severities together with that of a SG. It can be seen that the reactive power from a typical SG during network faults are higher compared to that of a WF complying with the E.ON Netz code. The reactive power from the WF decreases linearly due to the converter current limitation for fault severities leading the point of common coupling (pcc) remaining voltage below 0.5 pu. On the other hand, the active power from the WF decreases rapidly compared to the SG and reaches to zero at 0.5 pu remaining voltage. Note that the value of the remaining voltage where the converter current limitation occurs depends on the rating of the converter and also on the control strategy of the WF during the fault (see [9] for further details on this regard).

The reactive power from the WF during network faults are also calculated following a different control strategy other that the E.ON recommended one, where a higher value of m is chosen (m=4) (see Fig. 7). In Fig. 7, the reactive power from the WF during network faults with the modified E.ON code is presented together with the original E.ON case and the SG case. As can be seen from the figure, the reactive power from the WF is higher when it complies with the modified E.ON code compared to the other two cases for less severe faults (when the pcc remaining voltage is higher than 06 pu). For severe faults (when the remaining voltage is lower than 0.6 pu) the reactive power contribution from a SG is higher than a WF.

C. Field forcing capability (FFC)

The ceiling voltage of an excitation system is the maximum dc voltage that the excitation system can supply under specified conditions [17]. The field forcing capability (FFC) of a SG is associated with the excitation system ceiling voltage. With an excitation system with high FFC, the reactive power capability from a SG during network faults is increased compared to a low FFC excitation system. However, no change in the reactive power at the time of fault occurance is noticed. The reactive power at the instant of fault clearance is higher when a high FFC excitation system is utilized. Fig. 8 shows the field current (I_{fd}) with a high and low FFC excitation system. The corresponding pcc voltage and the reactive power from the SG is shown in Fig. 9.

In the case of a wind turbine with a full-power converter system, the converter output voltage has to be reduced to limit the converter current, so that the current capacity of the converter does not violate. So, to increase the reactive power (current) from a wind turbine during network faults, by increasing the converter output voltage (like the high FFC excitation system of a SG), will not be possible unless the converter is made over-rated.

D. Active and reactive power control flexibility

Note that the active and reactive power from a SG during network faults are not controllable. They are determined by the machines' pre-fault conditions. However, the reactive power of a SG is controlled by the excitation system and the power

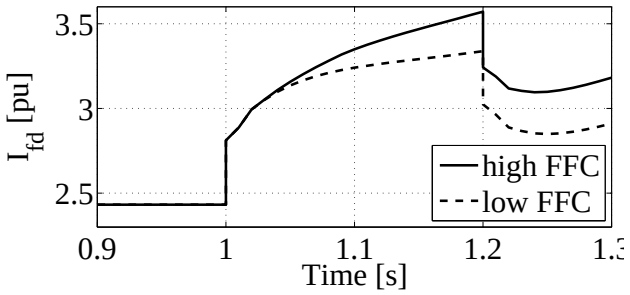

Fig. 8. SG field current with a high and low FFC excitation system.

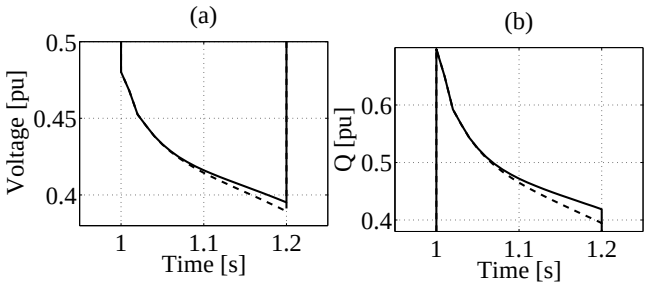

Fig. 9. (a) PCC voltage and (b) reactive power from a SG excitation system with two different FFC (legends are same as Fig. 8).

system stabilizer (pss) to control voltage and damp power oscillations in the range of 0.2–2 Hz [17]. In the case of a wind turbine with power electronic converter, the active and reactive power is controllable during network faults [18]. It is reported in [18] that a very fast response in terms of active and reactive power from a wind turbine with full power converter system and from a WF with this type of turbines can be achieved which is in the range of 0.5–100 ms.

V. Case Study Results

A. Example power system

The Cigre Nordic32 test network is used in this paper. A detailed description of this network can be found in [16], [19]. The original Nordic32 model was modified and is shown in Fig. 10. The main modifications made are: 1) splitting the existing transmission lines between buses 1044 and 1042 into three parallel lines and 2) addition of a 100 MW offshore WF at bus 1042 with two sea cables and two transformers. For the purpose of comparison, the WF is also replaced with a traditional SG with the same capacity as the WF (see the Appendix for different parameters of the SG).

The portion representing the WF and the closest grid, from Fig. 10, is redrawn here and is shown in Fig. 11.

B. Comparing the impact on the nearby grid

To illustrate the effect of the response of a WF operating according to the E.ON code during network disturbances, on different power system stability aspects like voltage stability and transient stability, a grid fault near bus 1042 is applied. The fault is applied on one of the parallel lines between buses 1042 and 1044 near bus 1042 and the faulted line is disconnected after 200 ms.

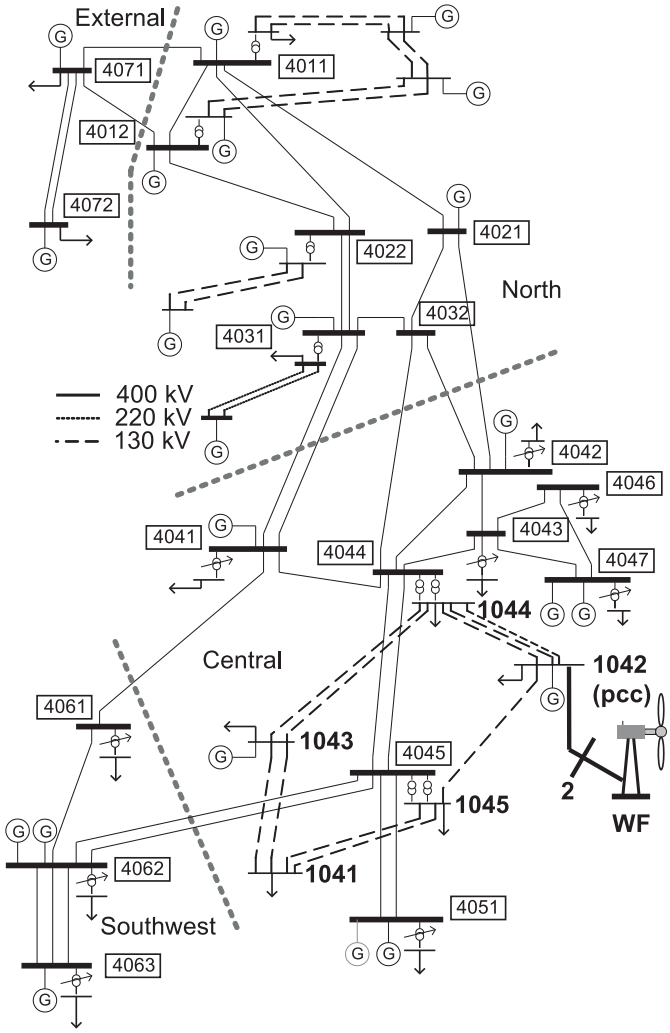

Fig. 10. Slightly modified Cigre Nordic32 grid augmented with a WF.

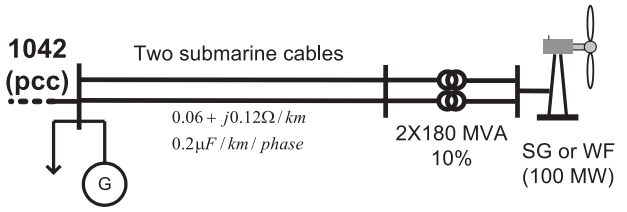

Fig. 11. Investigated WF layout.

Three different WF control strategies are investigated. They are: a WF complying with the E.ON NEtz code during network disturbances (case-1), a WF complying with the modified E.ON code (case-2) and a WF operating at unity power factor (pf) during disturbances (case-3). For the purpose of comparison the WF is replaced with a SG of the same capacity (case-4).

Fig. 12 shows the rotor angle of the machine at bus 1042 (pcc bus) and the pcc voltage when a moderate fault is applied at the pcc bus (remaining voltage 0.8 pu) in the presence of a WF with different control strategies and a SG. Note that for this less severe fault, the reactive power from the WF when complying with the modified E.ON code, is higher compared

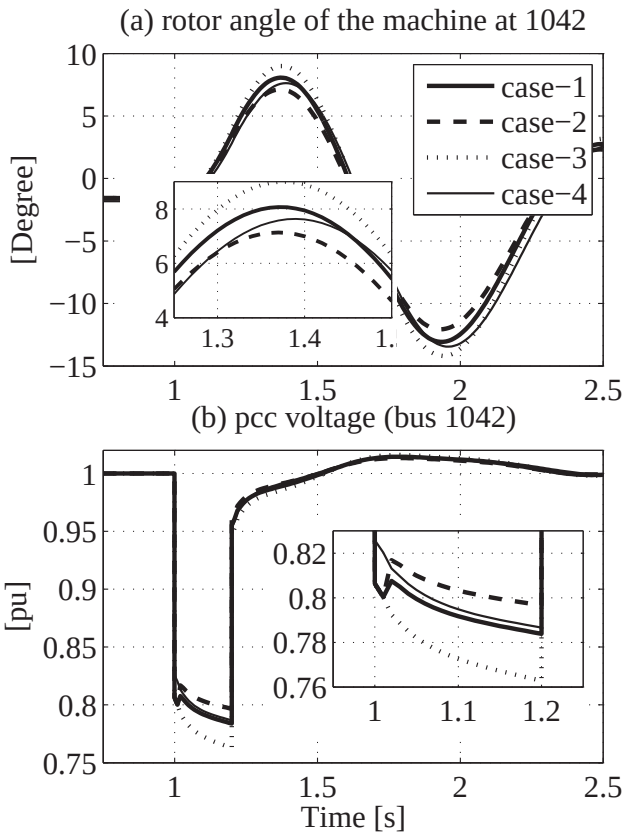

Fig. 12. Rotor angle of the machine at bus 1042 and the pcc voltage in the presence of a WF with different control strategies during network faults (less severe fault scenario).

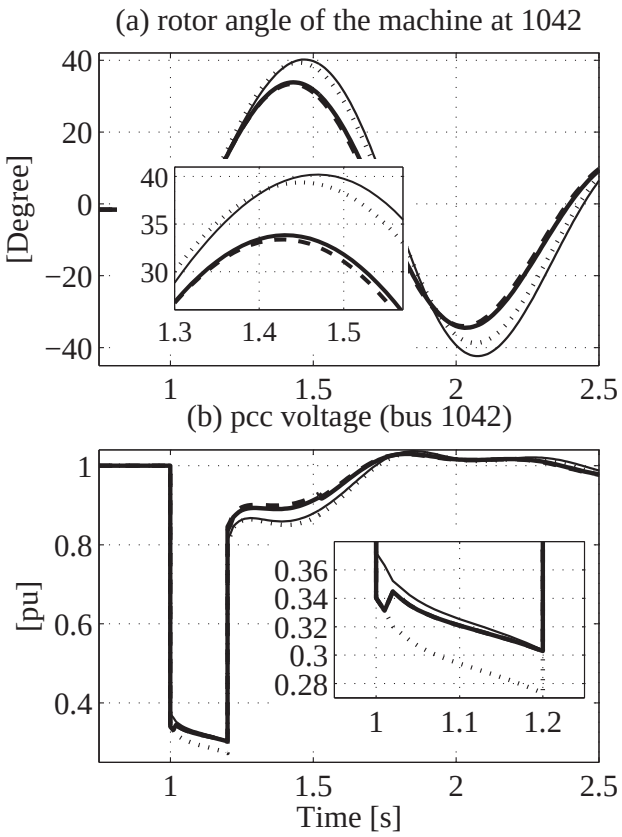

Fig. 13. Rotor angle of the machine at bus 1042 and the pcc voltage in the presence of a WF with different control strategies during network faults (severe fault scenario). Legends same as Fig. 12.

to other three cases (see Fig. 7). The maximum rotor angle swing of the machine at bus 1042, following the disturbance, is 8^o when the WF complies with the E.ON code (case-1). The rotor angle swing reduces to 7^o when the WF complies with the modified E.ON code (case-2). The rotor angle swing of the machine at bus 1042 is the maximum when the WF maintains unity pf during the disturbance (case-3). When the WF is replaced with a SG, the rotor angle swing of the machine at bus 1042 becomes 7.5^o. It is noted that the remaining voltage at the pcc during the fault is highest for case-2 (modified E.ON code compliance). As expected, the remaining voltage at the pcc during the fault is minimum for case-3 (unity pf operation of the WF).

A severe fault scenario is also considered and the results are shown in Fig. 13. It can bee seen from the figure that the maximum rotor angle swing of the machine at bus 1042 is around 34^o when the WF comply with the E.ON code and the modified E.ON code during the fault. The rotor angle swing of the machine at bus 1042 increases to around 40^o when the WF maintains unity pf or the WF is replaced with a SG. The remaining voltage at pcc bus during the fault is the minimum when the WF maintains unity pf (case-3). The remaining voltage at the pcc during the fault for other three cases are higher than case-1, as can be seen from the figure.

VI. Conclusion

This paper compares the response of a WF equipped wind turbines with full power converters while complying with the E.ON Netz fault response code with the fault response of a conventional SG. It is found that the reactive power from a SG during network faults is higher than from a WF equipped with turbines with full power converters and complying with the E.ON Netz fault response code. However, if the slope of the reactive power support line (m) is increased compared to the E.ON defined value, the reactive power from the WF is higher than the SG for less severe network faults. But, for severe network faults, the reactive power from a SG is much higher than a WF complying with the E.ON code. For the studied system, it is noticed that the active power from a SG during network faults decreases almost linearly with increasing fault severity leading to lower remaining voltages at the pcc bus, while the active power from the WF decreases more sharply and becomes zero during faults leaving the remaining pcc voltage below 0.5 pu.

During severe network faults, it is found that, the rotor angle stability of a nearby conventional generating unit is improved when the WF complies with the E.ON code (34^o) compared to cases when the WF operates at unity pf during the fault or when the WF is replaced with a SG (40^o). The remaining voltage at the pcc during severe network faults are higher when the WF is replaced with SG.

ACKNOWLEDGMENT

The first author acknowledges the financial support from E.ON Sverige AB's Research Foundation.

APPENDIX

Generator data: $T_{do}^{'}$=7.0s, $T_{do}^{''}$=0.05s, $T_{qo}^{'}$=1.5s, $T_{qo}^{''}$=0.05s, H=6s, D=0, X_d=2.20pu, X_q=2.00pu, $X_d^{'}$=0.30pu, $X_q^{'}$=0.40pu, $X_d^{''}$=$X_q^{''}$=0.20pu, X_l=0.15pu, S(1.0)=0.1, S(1.2)=0.3 (pu on machine MVA base).

Exciter data: T_A/T_B=0.10, T_B=50s, K=120, T_E=0.10s, E_{MIN}=0.0pu, E_{MAX}=5.0pu (pu on E_{FD} base).

REFERENCES

[1] I. Erlich and U. Bachmann, "Grid code requirements concerning connection and operation of wind turbines in Germany," in *IEEE PES general meeting*, June 2005, pp. 2230–2234.

[2] Frans Van Hulle (principal author), "Large scale integration of wind energy in the European power supply: analysis, issues and recommendations," european wind energy association (EWEA), Tech. Rep., December 2005.

[3] T. Ackermann (editor), *Wind Power in Power Systems*. West Sussex: John Wiley and Sons Ltd., 2005.

[4] Svenska Kraftnät, Tech. Rep. SvKFS 2005:2. Affärsverket svenska kraftnäts föreskrifter och allmänna råd om driftsäkerhetsteknik utformning av produktionsanläggningar. (in Swedish).

[5] "Wind Turbines Connected to Grids with Voltages above 100 kV - Technical regulation for the properties and the regulation of wind turbines," Elkraft System and Eltra Regulation, Draft version TF 3.2.5, Dec. 2004.

[6] "Grid Code: High and extra high voltage," E.ON Netz GmbH, Tech. Rep., April 2006 (Status:1).

[7] "Technical requirements for the connection of generation facvilities to the Hydro-Québec transmission system: Supplementary requirements for wind generation," Hydro-Québec, Tech. Rep., May 2003 (Revised 2005).

[8] "Wind Power Facility Technical Requirements," Alberta electric system operator, Tech. Rep., Nov. 2004 (Revision 0).

[9] N. R. Ullah, T. Thiringer and D. Karlsson, "Voltage and transient stability support by wind farms complying with the E.ON Netz grid code," *IEEE Trans. Power. Syst.*, vol. 22, no. 4, pp. –, Nov. 2007.

[10] N. R. Ullah and T. Thiringer, "Variable speed wind turbines for power system stability enhancement," *IEEE Trans. Energy Conv.*, vol. 22, no. 1, pp. 52–60, March 2007.

[11] R. Ottersten, A. Petersson, K. Pietiläinen, "Voltage sag response of pwm rectifiers for variable speed wind turbines," in *Proc. Nordic Workshop on Power and Industrial Electronics (NORpie 2004)*, Trondheim, Norway, June 2004.

[12] M. Chinchilla, S. Arnaltes and J. C. Burgos, "Control of permanent-magnet generators applied to variable-speed wind-energy systems connected to the grid," *IEEE Trans. Energy Conv.*, vol. 21, no. 1, pp. 130–135, March 2006.

[13] A. Yazdani, R. Iravani, "A neutral-point clamped converter system for direct-drive variable-speed wind power unit," *IEEE Trans. Energy Conv.*, vol. 21, no. 2, pp. 596–607, June 2006.

[14] Å. Larsson, A. Petersson, N. R. Ullah, O. Carlsson, "Krieger's Flak Wind Farm," in *Nordic Wind Power Conference NWPC 2006*, Helsinki, Finland, May 2006.

[15] "PSS/E 29 Program Application Guide Volume II," Oct. 2002, Power Technologies, INC.

[16] K. Walve, "Nordic32-A CIGRÉ Test System for Simulation of Transient Stability and Long Term Dynamics," Svenska Kraftnat, Sweden, Tech. Rep., 1993.

[17] P. Kundur, *Power System Stability and Control*. New York: McGraw-Hill Inc., 1993.

[18] F. Blaabjerg, Z. Chen, R. Teodorescu and F. Iov, "Power electronics in wind turbine systems," in *IEEE power electronics and motion control conference, IPEMC'06*, vol. 1, Aug. 2006, pp. 1–11.

[19] CIGRÉ TF 38.02.08, "Long term dynamics, Phase II, final report," CE/SC 38 GT/WG 02, Ref. No. 102, Tech. Rep., 1995.

Ride-through methods for wind farms connected to the grid via a VSC-HVDC transmission

Lennart Harnefors[1)*], Ying Jiang-Häfner[1)], Mats Hyttinen[1)] and Tomas Jonsson[2)]
[1)]ABB, Power Systems/HVDC, SE-771 80 Ludvika, Sweden
[*)]Ph. +46 240 783361, e-mail lennart.harnefors@se.abb.com
[2)]ABB, Corporate Research, SE-721 78 Västerås, Sweden

Abstract — In this paper, seven candidate ride-through methods for wind farms connected to the main grid via a VSC-HVDC transmission are evaluated. The most critical fault case is considered: a severe three-phase dip in the main-grid voltage. It is found that, unless very high demands regarding the speed of output-power reduction are placed on the wind-turbine generators (WTGs), a small braking resistor (with limited energy dissipation capability, controlled by a chopper) should be installed in the HVDC transmission. This also has the advantage that the mechanical stress on the WTGs will be reduced. Furthermore, it is shown that a large braking resistor, which is able to dissipate the rated power of the wind farm for the duration of the fault event, is not needed for good performance.

Index Terms — HVDC, ride-through, VSC, wind farm.

I. Introduction

Voltage-source converter high-voltage direct-current (VSC-HVDC) transmissions are attractive for connecting remotely located (e.g., offshore) wind farms to the main grid. This is partly because the high capacitance per length unit makes an ac cable impractical for cable lengths above 50–100 km: a significant amount of reactive power is generated, and low-frequency resonances may result in instability phenomena. Moreover, classical line-commutated thyristor-based HVDC transmissions are less attractive, since a synchronous compensator or a static synchronous compensator (STATCOM) may be required at the wind farm in order to maintain a smooth line voltage for the thyristors to commutate against. This problem does not exist for VSC-HVDC transmissions, which use pulsewidth-modulated transistor VSCs with inherent voltage control capability.

Grid codes for wind-turbine generators (WTGs) have lately become more strict. Ride-through of voltage dips down to 15% of the nominal voltage—or even zero voltage—for up to 150 ms is today often required [1], [2]. It is also anticipated that requirements for frequency response, i.e., that the wind-farm output power should be increased as the grid frequency decreases and vice versa, will be imposed [3].

Frequency response can be introduced in a wind farm connected via a VSC-HVDC transmission by maintaining a telecommunication link between the main-grid-side and wind-farm-side terminals, where, among other variables, the instantaneous main-grid frequency is transmitted, see Figure 1. Since the voltage at the wind-farm bus is fully controllable (to its amplitude, frequency, and phase) by the rectifying VSC, the grid frequency can be "mirrored" to the wind-farm grid without significant delay. Of the three fundamental WTG types: fixed-speed induction generators (FSIGs), doubly-fed induction generators (DFIGs), and full-converter generators (FCGs)—the latter which are normally equipped with a synchronous machine—only FSIGs have a natural frequency response. For DFIGs and FCGs, frequency response must be introduced by adding a loop in the control system, which feeds the deviation between the instantaneous grid frequency and its nominal value (50 or 60 Hz) to the active-output-power reference [4]. We shall in this paper assume that such a loop is included.

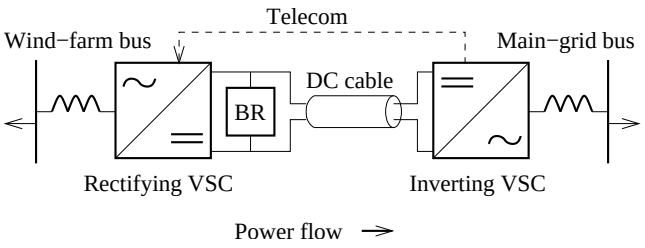

Figure 1. VSC-HVDC transmission connecting a wind farm to the main grid. "BR" is a braking resistor, normally controlled by a chopper.

A. Problem Description

Ride-through of voltage dips due to faults at the rectifying VSC, i.e., in the wind-farm grid, is not particularly difficult. By closed-loop control, the converter current is kept within its prescribed limits, which allows the VSC-HVDC transmission to remain on-line until the fault is cleared, while ride-through capability of the WTGs is already specified by grid codes.

Ride-through of voltage dips at the inverting VSC, i.e., in the main grid, is, on the other hand, more troublesome. A reduced main-grid voltage implies that the power transmission capability is reduced by a similar proportion, due to the current limit of the inverting VSC. For example, for a dip down to 15% of the nominal voltage, only 15% of the rated transmission capability remains. In a VSC-HVDC transmission connecting two utility grids, a similar scenario is solved by quickly reducing the input power to the rectifying VSC through closed-loop current control. In a strong grid

with an amount of generation that is much greater than the rated HVDC transmission capability, this will occur without a significant variation in the voltage.

The characteristics of a wind farm are, however, different. The wind-farm network is much smaller than the typical utility grid, and consequently weaker. Its rated generation normally matches the rated HVDC transmission capability. A fast reduction of the input power of the rectifying VSC may therefore lead to a significant increase of the wind-farm grid voltage (due to the capacitance in the circuit), resulting in overvoltage tripping of the VSC and/or the WTGs. In principle, there are two methods to overcome this problem:

1) Signal to the WTGs, by varying suitably the wind-farm grid voltage, that their output power should be reduced as quickly as possible.
2) Use a braking resistor ("BR" in Figure 1)—normally controlled by a chopper—to dissipate the excess energy that cannot be transmitted by the inverting VSC.

The second solution is robust, and leaves the wind farm unaffected during main-grid faults. Unfortunately, it is costly, since extra equipment has to be installed.

Complicating the first solution are two facts.

First, the total dc capacitance (sum of the capacitances installed in the VSCs and the cable capacitance) is normally fairly small; if power transmission is interrupted, the dc voltage may reach an unacceptably high level (typically, the VSC-HVDC protection action level is set at an overvoltage of about 30%) within a period of only 5 to 10 ms. The WTGs must therefore be able both to detect that a power reduction should be made, *and* reduce the output power (possibly from rated to zero), within this time frame, which may be quite demanding.

Second, the response of WTGs to a varying voltage is generally not the same for the three main WTG types (FSIGs, DFIGs, and FCGs). Yet, as it is possible that several different WTG types may be used side-by-side in a wind farm, it is desirable that the ride-through strategy should be general for all WTG types.

In the remainder of this paper, a number of feasible ride-through methods will be evaluated, and recommendations given.

II. Evaluation of Ride-Through Methods

Seven methods (A–G) for ride-through of voltage dips in the main grid are evaluated in this section. The first six involve signaling to the WTGs that their output power should be reduced:

- AC-voltage magnitude reduction, without (A) and with (B) a small braking resistor.
- AC-voltage frequency increase, without (C) and with (D) a small braking resistor.
- Fast reduction of the input power to the rectifying VSC, without (E) and with (F) a small braking resistor.
- A large braking resistor (G).

By a large braking resistor it is, as previously mentioned, implied that the braking resistor should be able to dissipate the full wind-farm output power the duration of the fault. A small braking resistor should be able to dissipate the excess power during a limited time period, in the neighborhood of 50 ms.

To give an illustration of a fault ride-thorugh event, simulation results for method A are presented in the Appendix.

A. Fast ac-voltage magnitude reduction

This method works as follows. As soon as the retifying VSC identifies that the power transmission capability is reduced (either by telecommunication or by detection of an elevated dc voltage), it quickly reduces the magnitude of the ac voltage at the wind-farm bus. The natural response of the WTGs will lead to an appropriate reduction of power generation, since the maximum output power is proportional to the ac-voltage magnitude.

The advantages of this solution are as follows:

- No additional requirements are needed for the WTGs, except ride-through capability as specified in grid codes.
- The solution is general for all WTG types.
- No additional apparatus is needed in the HVDC transmission.
- If the magnitude of the voltage dip is transmitted by telecommunication to the rectifying VSC, the fault can be "mirrored" from the main-grid side to the wind-farm side. This allows partial continued power transmission during the disturbance, up to capability of the inverting VSC.
- The solution is very reliable for ac faults that tend to occur frequently, i.e., single-phase faults and distant three-phase faults.

The disadvantages are as follows.

- A sudden ac-voltage reduction will lead to a very fast change in the electrical torque of the WTGs, resulting in high mechanical stress.
- The crowbar in DFIGs may be triggered.
- Particularly for severe dips, a fast enough reduction of the ac voltage may not be possible to achieve, since the VSC's current limit may be reached. This is dependent on the inductance in series between each generator and the VSC-HVDC terminal, i.e., the sum of the generator's leakage inductance, the leakage inductances of all transformers in the circuit, and the line inductance. A fairly large inductance is required to avoid overcurrent. If the reduction of the ac voltage must be slowed down in order to prevent overcurrent, the VSC output power is not reduced fast enough. Thus, unacceptably high transient dc overvoltage cannot be prevented, implying ride-through failure.

B. AC-voltage magnitude reduction with a small braking resistor

Equipping the HVDC transmission with a small braking resistor allows the rectifying VSC to reduce the ac voltage magnitude slowly enough, so that transient overcurrent is avoided. Meanwhile, the braking resistor is activated, so that the dc voltage is kept below the protection action level.

This method shares the same benefits as method A, with the addition that

- the mechanical stress on the WTGs is reduced, as the torque reduction is slower, due to the slower ac-voltage magnitude reduction.

The disadvantages are

- the extra cost of the braking resistor, and that
- the crowbar in DFIGs may be triggered.

As mentioned, the small braking resistor need only be active during 50 ms at most, during which the input power to the rectifying VSC gradually decreases. Hence, while the maximum current capability of the chopper (which controls the braking resistor) must be the same as for a large braking resistor, the total energy-dissipation capability can be much lower.

C. Fast ac-voltage frequency increase

In this method, the rectifying VSC will quickly increase the frequency of the wind-farm-grid voltage as soon as reduced power transmission capability is detected. For FSIGs, the natural machine response will result in a reduction of power generation, since the slip quickly decreases. As the rated slip of a FSIG may be a couple of percents, i.e., the rated slip frequency may be between 1 and 2 Hz for a base frequency of 50 Hz, the required frequency increase to achieve a reduction from rated to zero power may be as large as 1–2 Hz.

It is assumed that, for DFIGs and FCGs, the control system is equipped with a frequency-response loop (as discussed in the Introduction). This loop may have fairly low dynamics, since the grid frequency normally varies slowly. Hence, the frequency-response loop must be enhanced in order to allow fast—within a few ms—detection of a frequency increase. It might nevertheless be difficult to achieve satisfactory performance in many cases, due to the obvious difficulty of detecting a frequency increase within a fraction of one period (i.e., 20 ms for a base frequency of 50 Hz). Furthermore, the response to a power-reference change must also be quick (response time of a few ms at most).

The advantages of this solution are that

- no additional apparatus is needed for the HVDC transmission, and that
- the crowbar in DFIGs will not be triggered.

The disadvantages are as follows.

- As discussed above, the requirements on dynamic performance of DFIGs and FCGs are high, and may well be impossible to fulfill for some WTGs. Hence, the method may not be reliable.
- A quick reduction of the WTG output power will lead to a very fast change in the electrical torque, resulting in high mechanical stress (as for method A).
- Grid codes do not generally allow a large enough frequency increase to signal an output power reduction from rated to zero.

D. AC-voltage frequency increase with a small braking resistor

If a small braking resistor is installed, the requirements for fast detection of a frequency increase and fast reduction of the WTG output power can be relaxed. It is possible that the already existing frequency-response loop may be relied upon without modification. Consequently, the advantages of this solution are that

- no additional apparatus is needed for the HVDC transmission;
- the crowbar in DFIGs will not be triggered; and that
- the mechanical stresses will be lower compared to method C, as the output power is reduced slower.

The disadvantages are that

- there is the additional cost of a braking resistor; and that
- (as for method C) grid codes may not allow a large enough frequency increase to signal an output power reduction from rated to zero.

E. Fast reduction of the input power to the rectifying VSC

If the input power to the rectifying VSC is reduced quickly when a fault is detected, the voltage magnitude on the wind-farm bus will increase fairly quickly, since the energy produced by the WTGs will partly be stored in the capacitances of the wind-farm grid. The control system of DFIGs and FCGs can be equipped with an algorithm that reduces the output power as the ac-voltage magnitude reaches a predetermined protection action level.

The advantages of this solution are that

- no additional apparatus or algorithms (besides active power control) are needed for the HVDC transmission, and that
- the crowbar of a DFIG will not be triggered.

The disadvantages are that

- a quick reduction of the WTG output power will lead to a very fast change in the electrical torque, resulting in high mechanical stress (cf. methods A and C);
- the method may not be reliable, since it in practice may be difficult to achieve a fast enough power reduction;
- additional algorithms are needed in the control system for DFIGs and FCGs (as for method C); and
- the method cannot be used for FSIGs.

F. Fast reduction of the input power to the rectifying VSC with a small braking resistor

Equipping the HVDC transmission with a small braking resistor the first two disadvantages of method E vanish, but the obvious disadvantage of extra cost for the braking resistor is added.

G. A large braking resistor

Already briefly discussed in the Introduciton, the advantages of this method are as follows:

- The wind farm is not affected by any fault in the main grid.

- All fault types can be handled reliably.

The obvious disadvantage is that

- the large braking resistor (with chopper) is costly and consumes significant space.

III. Conclusions

The table below summarizes the properties of the methods evaluated.

Method	*Ride-through failure risk*	*Cost*	*Stress on WTG*	*Applicable to all WTG types*
A	High	Low	High	Yes
B	Low	Medium	Medium	Yes
C	High	Low	High	Yes*
D	Medium	Medium	Low	Yes
E	Medium	Low	High	No*
F	Low	Medium	Low	No*
G	Low	High	Low	Yes

*Requires modified or extra algorithms in the control system for DFIGs and FCGs.

The following conclusions can be drawn:

- Installation of a large braking resistor is not necessary for satisfactory performance.
- Unless a small braking resistor is installed, the WTGs will be affected by increased mechanical stress during fault events main the main grid. (Note that the stress is obviously yet not higher than if the wind farm were connected directly to the main grid, i.e., without an intermediate HVDC transmission.)
- Unless a small braking resistor is installed, only WTGs that are able to reduce their output power from rated to zero very quickly (within a couple of ms) may be employed in the wind farm.
- The most general method is *B: AC-voltage magnitude reduction with a small braking resistor*, since it can be used for all WTG types and does not require extra functions to be added to the WTG control system.
- Methods that rely on signaling a power reduction by an increase of the wind-farm grid frequency can be used only in cases where grid codes permit a large frequency increase (1–2 Hz). If so, the best method available is *D: AC-voltage frequency increase with a small braking resistor*.

Appendix: Simulation results

Even though methods B and D were found to be preferable in general, we have elected to present simulation results for method A, in order to show that ride-through in some cases indeed can be accomplished without a braking resistor.

At a rated power transmission of 400 MW, a 150-ms dip to 15% remaining voltage in the main-grid voltage occurs at $t = 0.1$ ms. Figure 2 shows a successful ride-through event. The series inductance is large enough to prevent overcurrent when the wind-farm grid voltage is reduced.

References

[1] J. Morren and S. W. H. de Haan, "Ridethrough of wind turbines with doubly-fed induction generator during a voltage dip," *IEEE Trans. Energy Convers.*, vol. 20, no. 5, pp. 435–441, June 2005.

[2] I. Erlich and U. Bachmann, "Grid code requirements concerning connection and operation of wind turbines in Germany," in *Proc. IEEE Power Eng. Soc. Gen. Meeting*, vol. 2, pp. 1253–1257, June 2005.

[3] P. B. Eriksen, T. Ackermann, H. Abildgaard, P. Smith, W. Winter, and J. R. Rodríguez García, "System operation with high wind penetration," *IEEE Power and Energy Magazine*, pp. 65–74, Nov./Dec. 2005.

[4] J. Morren, S. W. H. de Haan, W. L. Kling, and J. A. Ferreira, "Wind turbines emulating inertia and supporting primary frequency control," *IEEE Trans. Power Syst.*, vol. 21, no. 1, pp. 433–434, Feb. 2006.

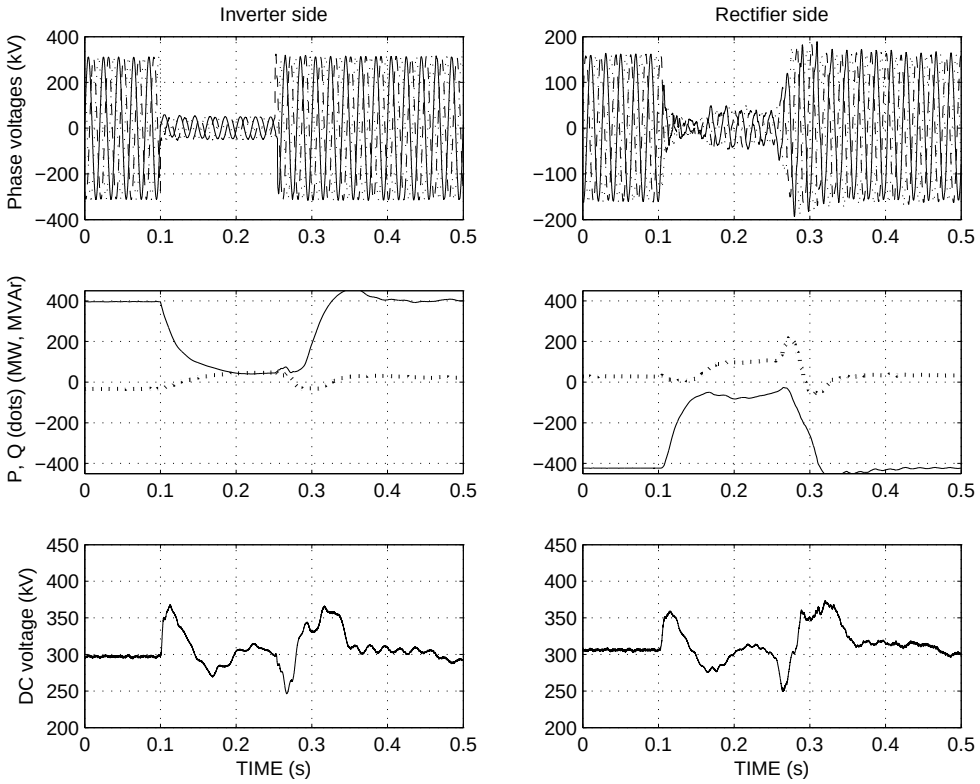

Figure 2. Method A, Fast ac-voltage magnitude reduction: successful ride-through. P and Q are the converter active and reactive output powers, respectively.

Real Time Estimation of Possible Power for Wind Plant Control

Stephane Eisen[1*)], Poul Sørensen [2)], Martin H. Donovan[3)] , Kurt S. Hansen[1)]
[1)] Technical University of Denmark(DTU), Dept of Mech. Eng., Building 403 - Nils Koppels Alle, DK-2800 Lyngby, Denmark
[*)] tlf. +45 26 57 18 66, e-mail stephane.eisen@gmail.com
[2)] Risø DTU, VEA-118, P.O. Box 49, DK-4000 Roskilde, Denmark
[3)] DONG Energy, A.C. Meyers Vaenge 9, DK-2450 Copenhagen, Denmark

Abstract — This paper proposes a model for real time estimation of possible production at the Nysted Wind Plant. The model employs the nacelle wind speed measurements and a power curve with an empirical correction for local flow effects about the nacelle anemometer and a dynamic wake model to account for changes in individual turbine wakes during plant regulation. An alternative model employing power rather than the nacelle wind speed measurements which requires no corrections is also presented.

Index Terms — Wake Modelling, Wind Plant Simulation, Wind Plant Control.

1. Introduction

Real time estimation of possible plant production is important for successful control of wind power plants which participate actively in power system control. Estimation of a wind power plant's maximum possible production depends not only on the current wind conditions but also on the operational state of the wind plant. In this present work 2 different strategies are investigated for estimation of the possible plant production during wind plant control regulation.

The first method, denoted the power curve method, is an extension of current practice at Nysted which employs NWS (Nacelle Wind Speed) measurements and a power curve to estimate possible production. To extend the method to provide better performance during wind plant down-regulation, a NWS correction is proposed to account for the changes in local flow effects in the vicinity of the NWS anemometer. A dynamic wake model is also proposed to account for changes in turbine wakes between normal and down-regulated operation. Attention is also given to the power curve, to improve its performance in different ambient wind conditions.

The power curve method is also compared to an alternative control strategy, denoted the grid method, that requires no wind speed measurement error correction or wake model development. The grid method essentially splits the wind plant into two separate grids; one grid is used to estimate the total plant production from power measurements while the other is down-regulated to meet the desired control objectives.

2. Power Curve Method

2.1. Nacelle Wind Speed Correction

Estimation of the possible production based on the power curve method employs the NWS measurement of each turbine in the wind plant as primary input. The measurement consists of a nacelle mounted cup anemometer located approximately 5 meters above the rotor axis and 15 meters downwind of the rotor plane. The NWS correction accounts for changes in local flow conditions due to near wake effects generated by the rotor. Previously, near wake effects at Nysted were investigated by [1]. The NWS measurement was found to "speed up" relative to a reference wind speed measurement as the blade pitch moves increasingly negative (Nysted turbines are stall regulated) during down-regulation. The "speed up" effect, caused predominantly by changes in the near rotor wake are accounted for to accurately estimate the possible production during down-regulation. The NWS correction is intended to correlate the NWS measurement to an equivalent rotor wind speed, U_{EWRS}, representing the mean wind speed of entire rotor disk immediately upwind of the rotor. U_{EWRS} is then used as input to a power curve to subsequently estimate the possible production. Determination of U_{EWRS} is depicted graphically in Figure 2-1 where U_{NWS} is the NWS measurement and θ_{blade} is the blade pitch angle of one blade (Nysted turbines are collectively pitched).

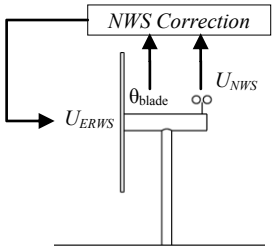

Figure 2-1: Determination of the Equivalent Rotor Wind Speed

In this present work, the NWS correction is determined from analysis of approximately 21000 unique turbine shut-down events recorded over approximately 500 days. During a turbine shutdown the blade pitch angle is ramped towards the negative pitch limit to reduce the rotor power to zero and subsequently generate adequate negative rotor torque to absorb the rotational energy of the rotor. The initial pitching action during shut-down is similar to a down-regulation event except that in this case the blade pitch continues beyond the maximum down-regulation point of approximately -15.0 degrees. The initial part of the shut-down, where the power is ramped to zero is a transient event, lasting no more than 10-15 seconds, compared to down-regulation which can last orders of magnitude longer (hours time scale). Extending the dynamic response of the NWS measurement to conditions during down-regulation is a significant assumption of this approach requiring further investigation. During the initial part of the shut-down, the NWS correction (NWS_{cor}) for varying pitch angles is determined as:

$$NWS_{cor}(\theta, U_{NWS\,Ref}) = U(\theta)_{NWS}/U_{NWS\,Ref} \quad (1)$$

Where $U_{NWS\,Ref}$ corresponds to the NWS measurement at the initiation of shut-down and $U(\theta)_{NWS}$ is the NWS measurement for varying pitch angles during the shut-down. To ensure that $U_{NWS\,Ref}$ corresponds to the initiation of shut-down the NWS measurement data are time shifted 2 second to approximate the transport time of the wind parcel affected by the pitch angle change. A two second time shift corresponds to the wind parcel traveling 15 meters at 7.5 meters per second. The approach is depicted graphically in Figure 2-2. Variable transport will be considered in future work.

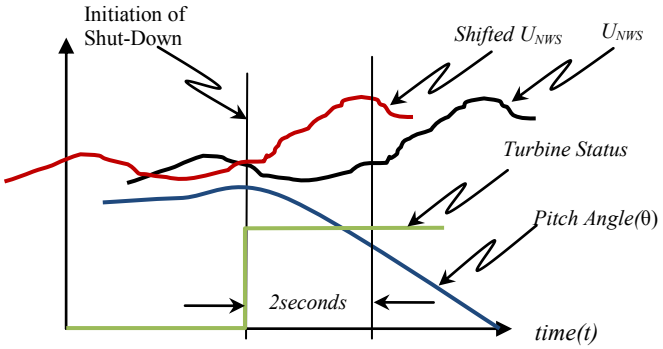

Figure 2-2: Determination of NWS Correction

During the shut-down event the stochastic ambient wind inflow results in a corresponding stochastic response of the NWS measurement to pitch angle changes relative to $U_{NWS\ Ref}$. Assuming the NWS measurements are normally distributed in the local vicinity of $U_{NWS\ Ref}$, the NWS correction corresponds to the bias in the calculated NWS ratios for varying pitch angles. Figure 2-3 depicts the resulting NWS correction ratios, as a function of pitch angle from processing of approximately 21000 unique shut-down events at Nysted.

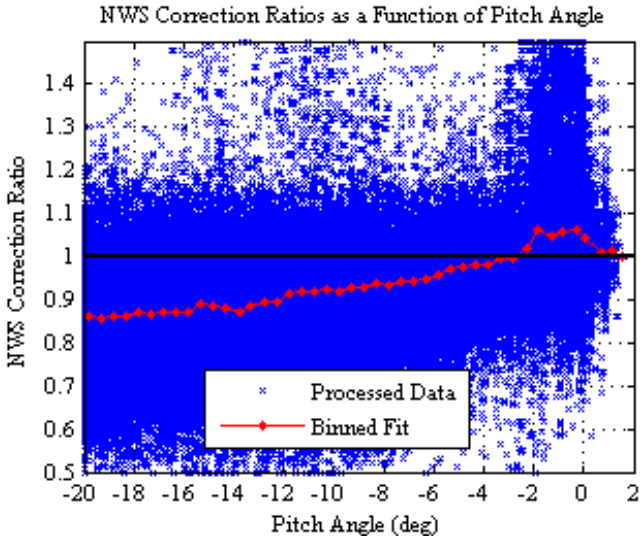

Figure 2-3: NWS Correction Ratios as a Function of Pitch Angle

The resulting data set is also processed as function of pitch angle and wind speed, resulting in NWS correction ratios depicted in Figure 2-4 as color intensity values according to the colorbar legend at the bottom of the figure. Additionally, ISO Coefficient of Thrust (C_T) contour lines, derived from blade element momentum (BEM) calculations for the Nysted turbines, are overlaid in the figure. The NWS correction ratios roughly follow the ISO C_T contour lines; where greater "speed up" of the NWS measurement corresponds to higher rotor C_T.

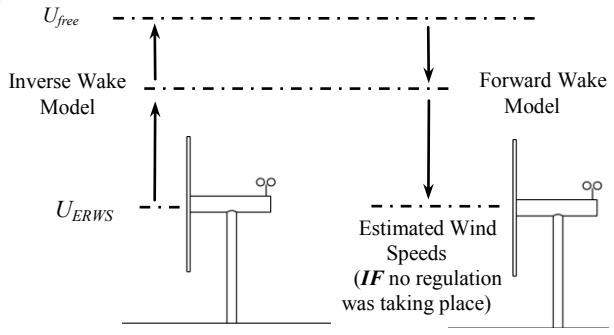

Figure 2-5: Overview of the Dynamic Plant Wake Model

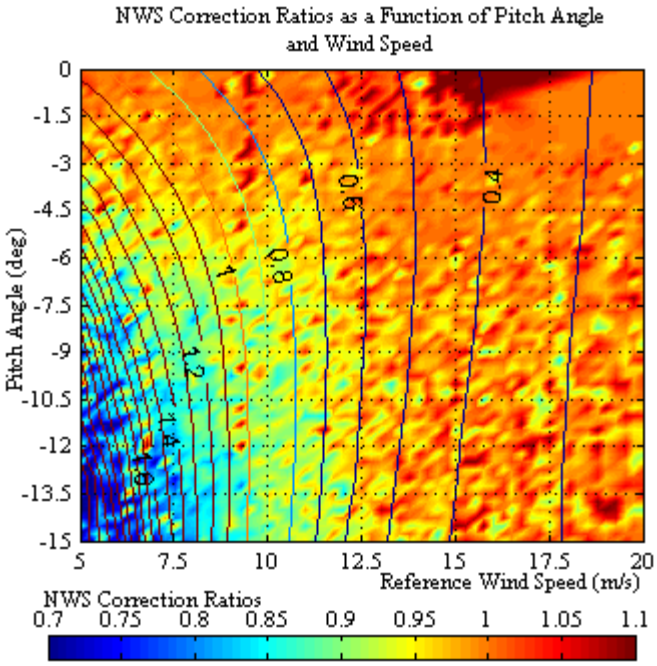

Figure 2-4: NWS correction Ratios as a Function of Pitch Angle and Wind Speed

2.2. Dynamic Plant Wake Model

The dynamic plant wake model (DWM) accounts for changes in individual turbine wakes in real time during down-regulated operation to estimate the wind speeds that would exist if no down-regulation had occurred. It is based on application of the simple wake model originally proposed by [2] and later expanded by [3]. The dynamic plant wake model applies the simple wake model in both inverse and forward directions. The inverse direction removes the wind speed deficits caused by the wakes of down-regulated turbines and estimates U_{free}. U_{free} represents the wind speed that would exist at each turbine location if no turbines (and their subsequent wakes) where actually there. U_{free} is then used as input to the forward application of the wake model which adds the wind speed deficits that would exist during normal operation. An graphical overview of the DWM is depicted in Figure 2-5.

In brief, the simple wake model is based on the description of the conservation of momentum of a single wake, employing the initial wake wind speed deficit and a linear wake decay model to describe the wake down-wind of the rotor. At a given distance down-wind of the rotor the wind speed deficit is assumed to be constant across the wake. Interacting wakes are treated by a simple area overlap model. The resulting wind speed ratio (WSR) of each turbine's wake acting at every other turbine in the wind plant is given as:

$$WSR_{i,j} = 1 - \frac{V_{i,j}}{U_{free}} = (1 - \sqrt{1 - C_T}) \left(\frac{D}{D + 2kX}\right)^2 \frac{A_{i,j\ overlap}}{A_{rotor}} \qquad (2)$$

Where V is the reduced wind speed in the wake, D is the rotor diameter, k is the wake decay constant (determined from fitting the simple wake model with measurements from Nysted), $X_{i,j}$ is the down-wind distance between the ith and jth turbines, $A_{i,j\ overlap}$ is the area overlap of the ith turbine's wake on the jth turbine and A_{rotor} is the area of the turbine rotor. The WSRs are summed energetically as proposed by [3] and include reflected wakes, denoted V_r, to account for wake-ground interaction. The total wind speed deficits, denoted V_t, and subsequent total wind speed ratios WSR_t at each turbine throughout the wind plant are given as:

$$\begin{bmatrix} \mathrm{WSR_{t,1}} \\ \vdots \\ \mathrm{WSR_{t,N}} \end{bmatrix} = \begin{bmatrix} 1 - \frac{V_{t,1}}{U} \\ \vdots \\ 1 - \frac{V_{t,N}}{U} \end{bmatrix} \begin{bmatrix} \sqrt{\sum_{i=1}^{N} \left(1 - \frac{V_{1,i}}{U}\right)^2 + \sum_{i=1}^{N} \left(1 - \frac{V_{r,1,i}}{U}\right)^2} \\ \vdots \\ \sqrt{\sum_{i=1}^{N} \left(1 - \frac{V_{1,N}}{U}\right)^2 + \sum_{i=1}^{N} \left(1 - \frac{V_{r,1,N}}{U}\right)^2} \end{bmatrix} \qquad (3)$$

Where N is the total number of turbines in the plant. In summary the wind speed ratio at each turbine, for a given wind plant layout

and turbine configuration, is a function of C_T and wind direction (φ):

$$WSR_{t,i} = f(C_{T,i}, \varphi) \quad (4)$$

In the present model configuration the wind direction is assumed to be single valued throughout the wind plant and is derived from yaw angle measurements of online (power producing) turbines. Online turbines are assumed to have prefect alignment with the inflow, i.e. no yaw error resulting in the yaw angle and wind direction being equal.

The C_T values employed in the wake model are derived from steady state BEM calculations. For a rotor operating in steady wind with constant angular velocity and given structural and aerodynamic properties the C_T is a function of blade pitch angle, and wind speed. The C_T is determined by table lookup using individual pitch angle and wind speed measurement data from each turbine in real time. For a stall regulated turbine operating at reduced power the C_T values exceed 1.0 for certain combinations of wind speed and pitch angle (see overlaid C_T values in Figure 2-4). For C_T values greater than 1, the momentum theory on which the wake model is based is no longer valid. and the relationship between C_T and the wind speed deficit in the wake is ill defined. In this present work the wind speed deficit in the wake is assumed to remain constant for C_T values greater than 1 (C_T values greater than 1 are set to 1 in the model). This may be a reasonable assumption since unstable flow caused by large changes in momentum at the rotor plane for high C_T values may entrain fresh momentum from flow outside the rotor area [4]. This fresh momentum may help to stabilize the wind speed deficit so that further increases in C_T do not result in increased wind speed deficits. This is a significant assumption for application of the wake model to a heavily stalled rotor. An extend measurement campaign at Nysted is planned to gain insight into this relationship.

2.2.1. Dynamic Plant Wake Model Implementation

Implementation of the dynamic plant wake model consists of a sub-model which applies the inverse wake model to determine the "free" wind speed throughout the wind plant and a second sub-model which applies the normal wake model to determined the wind speed that would exist at each turbine if no down-regulation was taking place. Block diagrams of both sub-models are depicted in Figure 2-6 and Figure 2-7.

For application of the inverse wake model real time pitch angles and wind speed measurements at each turbine are first used to determine U_{ERWS}. Subsequently, C_T values at each turbine are determined from table lookup of the pitch angle measurements and U_{free}, where U_{free} is determined by iteration of U_{ERWS} divided by WSR. Determination of the C_T values employ U_{free}, since the wake model is based on estimation of the WSRs from the free stream wind speed and not U_{ERWS} which includes wake effects from surrounding turbines.

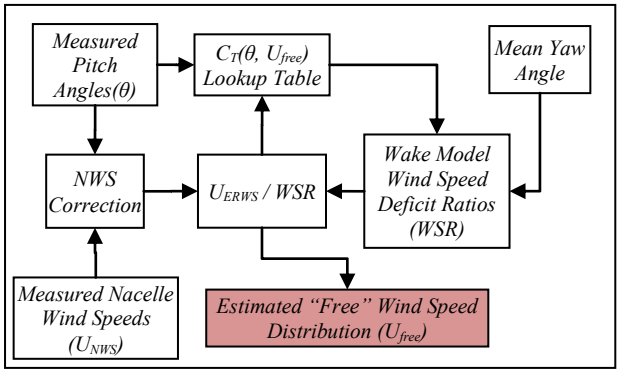

Figure 2-5: Inverse Application of the Wake Model

Application of the normal wake model requires knowledge of the pitch angle trajectory for normal operation and U_{free} to calculate the C_T values that would exist if no down-regulation was taking place. The pitch angle trajectory for normal operation is based on a simple binned fit of historic pitch angle data over the range of operating wind speeds. The C_T values and the mean wind direction are then used to determine the wake model WSRs and are subsequently multiplied by U_{free} to determine the wind speed distribution at each turbine for normal operation.

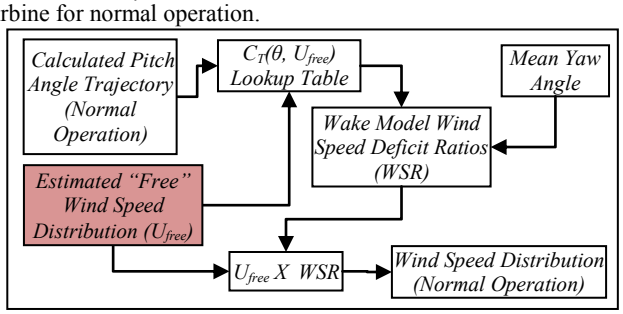

Figure 2-7: Normal Application of the Wake Model

2.3. Power Curve

The power curves employed in the estimation of possible production with the power curve method are derived from one turbine at Nysted. The intent was to initially follow IEC 61400-12 [5] to calculate a single standard power curve. However, this approach gives unsatisfactory results for use in real time estimation of the turbine production since it is intended to capture long term statistical behavior of the wind turbine and does not account for real time changes in ambient wind conditions. Additionally [5] is intended for comparing different wind turbine configurations and as such requires a reference wind speed measurement from which comparisons can be made. The reference wind speed measurement is not the measurement employed in the estimation of the possible production. A power curve based on the NWS measurement gives better correlation than a reference wind speed measurement located some distance from the turbine.

In this present work the turbulence intensity is taken as a measure of the ambient wind conditions and is included in the calculation of the power curve. The turbulence intensity is calculated directly from each NWS measurement to give an indication of the local ambient wind conditions. Subsequently, a family of power curves based on turbulence intensity, derived from the method of bins and corrected to an ISO standard atmosphere as outlined in [5] gives improved performance for estimating the possible plant production. An example of the turbulence intensity (TI) based power curves is depicted in Figure 2-8.

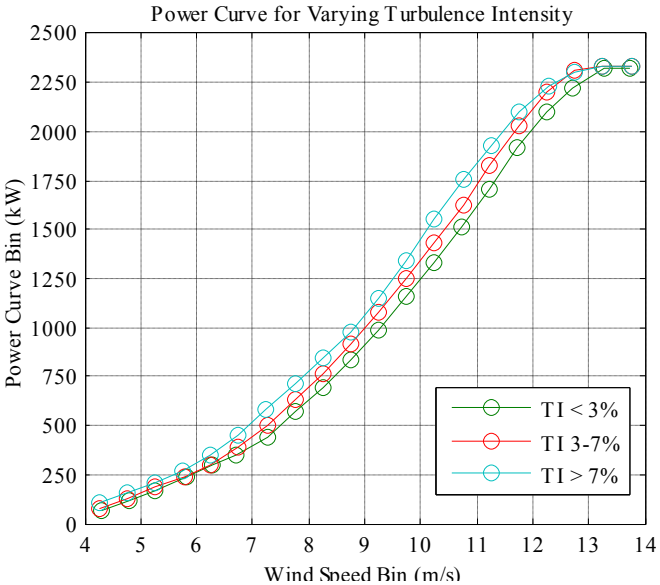

Figure 2-8: Example Turbulence Intensity Based Power Curves

2.4. Performance Analysis

The power curve method is implemented in Matlab® Simulink® to evaluate its performance against approximately 1 year of Nysted measurement data. Performance is defined as the ability of the

power curve method to accurately estimate the possible plant production. This is a straight forward analysis regarding normal operation, where the estimated production can be directly compared to the measured production. However, during down-regulation the possible production estimate can only be evaluated qualitatively since there are no control measurements available for comparison. Additionally, very limited down-regulation has occurred at Nysted (approximately 12 hours out of 2 years of measurements available in this present work). A statistical analysis is performed to ensure that the power curve method effectively predicts the plant production in normal operation; a condition for good performance but not sufficient to ensure that the method will perform during down regulation. The statistical analysis of normal operation provides at a minimum the best case performance of the power curve since the uncertainty of the estimate during down-regulation will increase.

2.4.1. Statistical Analysis

The statistical analysis of the power curve method's overall performance applied to normal operating data with NWS and DWM corrections and the TI based family of power curves, indicates that the absolute estimate error is 4%, 90% of the total operating time analyzed. This compares to 5.3%, 90% of the total operating time analyzed for the estimate derived from a single power curve, based on the method outlined in [5], and no corrections. This is essentially the configuration currently in place at Nysted. The estimate based on the TI based family of power curves and employing only the NWS correction gives the minimum absolute error of 3.4%, 90% of the total operating time analyzed. Note that the corrections should not change the estimate error during normal operation since they should only be active during down-regulation. All the methods employ the air density correction according to [5]. Figure 2-9 depicts duration curves of the estimate error for the different variations.

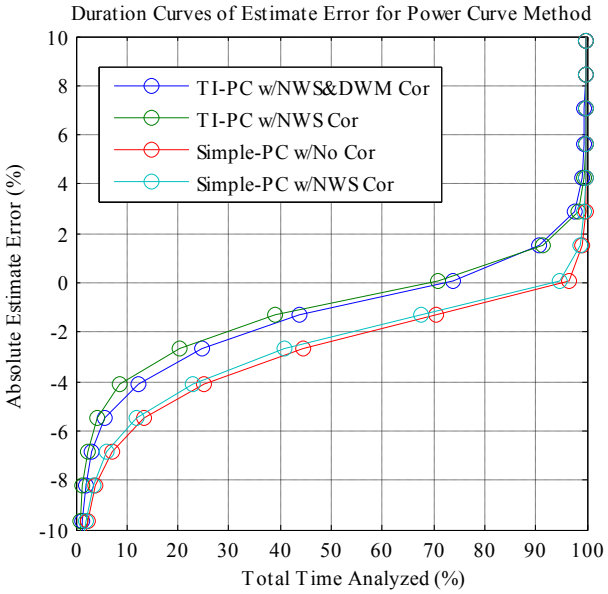

Figure 2-9: Duration Curves of Power Curve Estimate Error in Normal Operation (Measurement Data)

2.4.2. Qualitative Analysis

The power curve method applied to 2 regualtion events are depicted in Figure 2-10 (shown on next page). Both plots include the measured production, commanded setpoint, and three different estimations of possible produciton as indicated in the plot legend. The left plot in Figure 2-10 depicts an absolute limit regualtion at approximately 545 minutes that lasts for 10 minutes. At 560 minutes a delta regulation is then requested and lasts for 15 minutes. During the regualtion events the estimate of possible production with no corrections increases sharply while the estimates based on only the NWS correction and both the NWS and DWM corrections follow a constant slope similar to that of the actual production slope before and after the regualtion. This indicates that the corrections are qualitatively doing the right thing. However, the NWS corrrection and the NWS/DWM corrections give almost the same results indicating that the DWM does not contribute much to the overall correction. Actually, the DWM is increasing the estimate of the possible production. From this observation of the regualtion data it can be concluded that the NWS correction provides the greatest improvement in the possible production estimate currently employed at Nysted.

The second regualtion event, depicted in the right plot of Figure 2-10 features a absolute limitation command of approximately 93 MW at time 625 minutes. At that time the estimate with no corrections jumps approximate 15 MW; where as the estimates employing the NWS correction and the NWS and DWM correction appear not to respond to the down-regulation. At time 675 minutes the plant reaches the maximum possible production of 157 MW (less than the rated plant power of 168 MW due to offline turbines) and all 3 of the estimates converge as the turbines enter power limiation mode. Another interesting observation is at 725 minutes the actual power drops slightly below the plant set-point. At this point the estimates which employ the corrections converge with the actual power as expected. However the estimate with no corrections indicates a possible production of 100MW and therefore if this estimate was correct, the actual production would remain at the set-point level.

2.4.3. Simulation of Power Curve Method

Simulations of the Power Curve Method for both normal and down-regulated operation were preformed to investigate the performance of the DWM using 574 hours of 1 Hertz simulated stochastic wind speed and wind direction input data for each turbine. In the case of down-regulated operation, the estimated production was compared directly to the production during normal operation to determine an estimate error. This being possible because the wind direction and wind speed input for both cases are identical.

The simulation model is based on the Nysted Wind Plant, incorporating the as-built wind plant controller and representation of the 72 individual wind turbines. The turbines are based on a Cp-lookup map, derived from BEM code calculations, and include individual turbine controllers to provide closed loop blade pitch control and start-up and shut-down functionality. A wake model is also included to simulate the wind speed deficits throughout the wind plant due to individual turbine wakes. The wind speed input data are generated by Risø's model for simulation of power fluctuations [6].

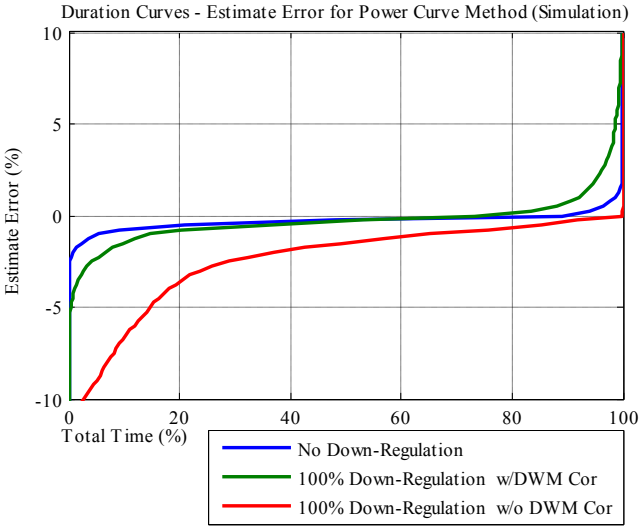

Figure 2-11: Duration Curves of Power Curve Estimate Error in All Modes of Operation (Simulation Data)

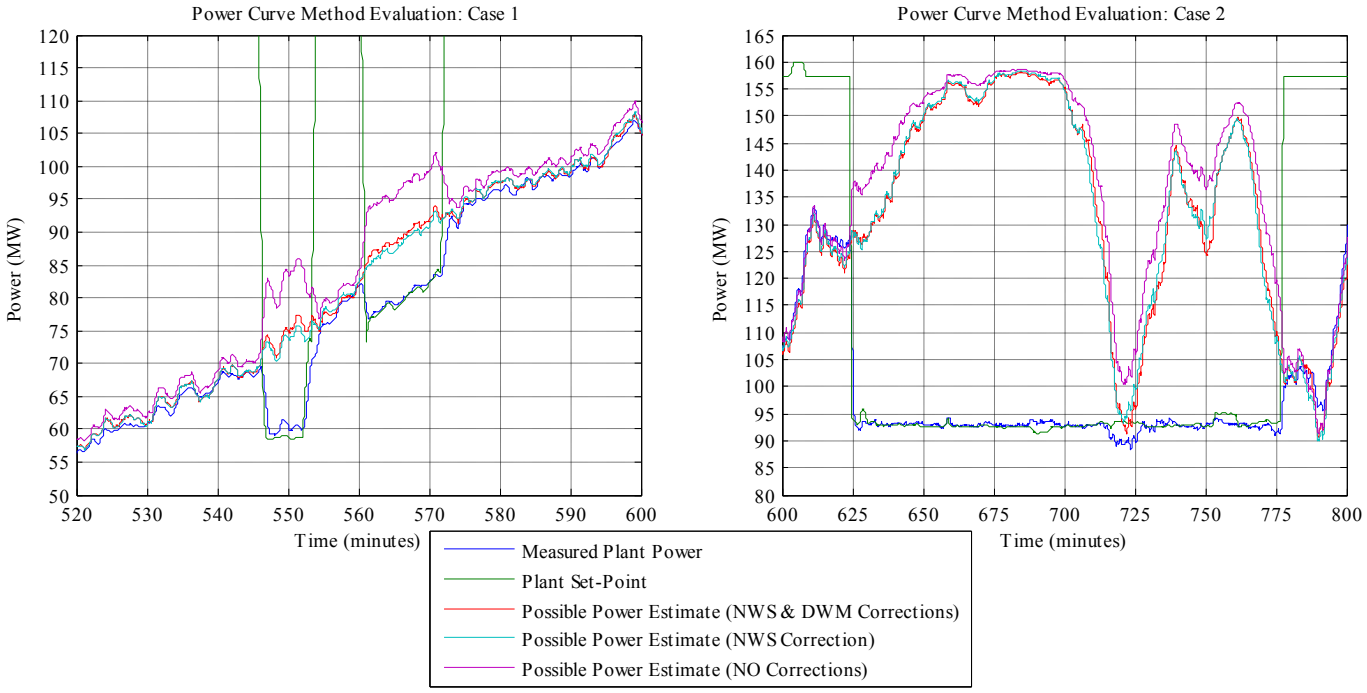

Figure 2-10: Qualitative Analysis of the Power Curve Method During Down-Regulation

The results indicate that the DWM performs as expected. During normal operation, the DWM makes essentially no correction since no down-regulation occurs. A duration curve of the estimate error for normal operation is depicted in Figure 2-11 as the blue trace. The duration curve of the estimate error for simulated normal operation is significantly less than that from measurements since the model employs both a "perfect" power curve and identical wind speed inputs for the power curve estimate and wind turbine models. In actual operation the rotor power is related to the mean wind speed across the entire rotor disk in contrast to the single point value measured at the NWS anemometer. For the case of 100% down regulation, i.e. all turbines down-regulated to zero power, the estimate error without the DWM under predicts the possible production since down-regulation decreases the wind speed in each turbine's wake. Inclusion of the DWM returns the mean estimate error to approximately zero but includes increased scatter compared to the no down-regulation case.

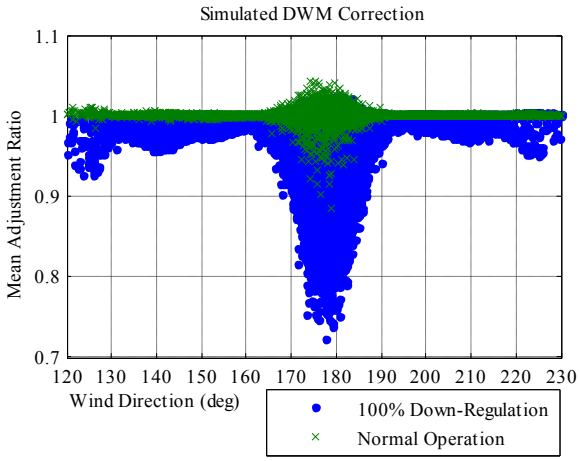

Figure 2-12: Simulated DWM correction for Normal Operation and 100% Down-Regulation

The mean DWM adjustment of all turbines, for normal and down-regulated operation versus wind direction are depicted in Figure 2-12. During normal operation the DWM should provide no correction. The corrections visible in Figure 2-12 during normal operation are due to discrepancies between the pitch angle trajectory for normal operation employed in the simulations and the commanded pitch angles of the individual wind turbine model controllers. The discrepancies are exacerbated when the wind direction corresponds to a principle alignment direction (in this case 178 degrees) in which the turbines are perfectly aligned in rows. During down-regulation the DWM provides a varying level of correction that is also heavily dependent on wind direction. The correction ratios are less than 1 during down regulation since wind speed deficits increase for stall regulated turbines during down regulation.

3. Grid Method

The grid method is an alternative control strategy for estimation of the possible wind plant production during regulation requiring no wake model development, wind speed measurement error correction or power curve. This strategy splits the wind plant into two separate grids; one grid is used to estimate the total plant production while the other is down regulated to meet the desired plant control objectives. This approach is advantageous in its simplicity, which is an important factor for successful implementation of a real time controller. Additionally, it employs the power measurement directly rather than inferring it from other measurement quantities. An obvious drawback however, is that only 50% of the possible plant production can be down-regulated or possibly less depending on the limitations of each turbine. The underlying assumption for employing either grid method is that the average wind conditions throughout both grids are the same during both normal and down-regulated operation. In this case one grid serves as the measurement grid, where these turbines are maintained at their maximum production and represent one half of the total possible production. The second grid is a control grid that is down-regulated to meet the desired wind plant control objective.

Two grid layouts are investigated. The split grid layout which employs 2 grids based on a mean plant wind direction determined from the average yaw angles of all online turbines. The wind plant controller maintains the grid layout within a +/-45 deg window about the split direction. If the wind direction changes outside this window the wind plant controller switches the split grid layout to match the mean plant wind direction with adequate hysteresis to avoid oscillation between different grid layouts. Three split grid layouts, for are varying wind directions are depicted in Figure 3-1. The second layout, denoted the interlaced grid and also depicted in

Figure 3-1 is a static layout that does not change with wind direction.

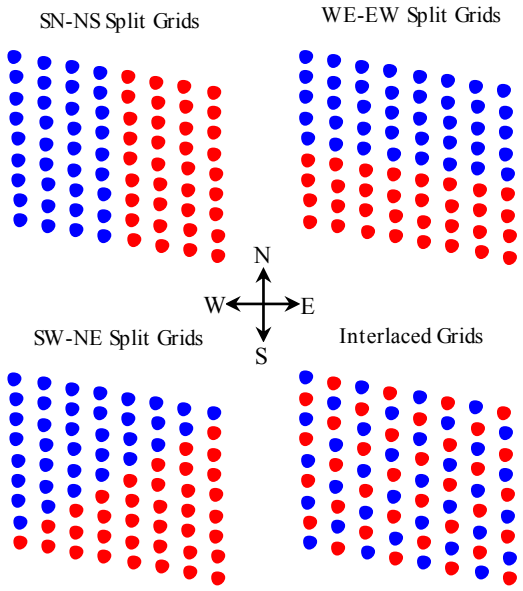

Figure 3-1: Split Grid and Interlaced Grid Layouts

For both layouts, approximately 1 year of measurement data from Nysted are used to compare the power output between the NS split grids and the interlaced grids during normal operation. The results of the comparison are depicted in Figure 3-2 as duration curves of the difference between the grids as a percentage of rated production. For the split grid layout, the measurement data were limited to +/-45 degree window about the NS direction.

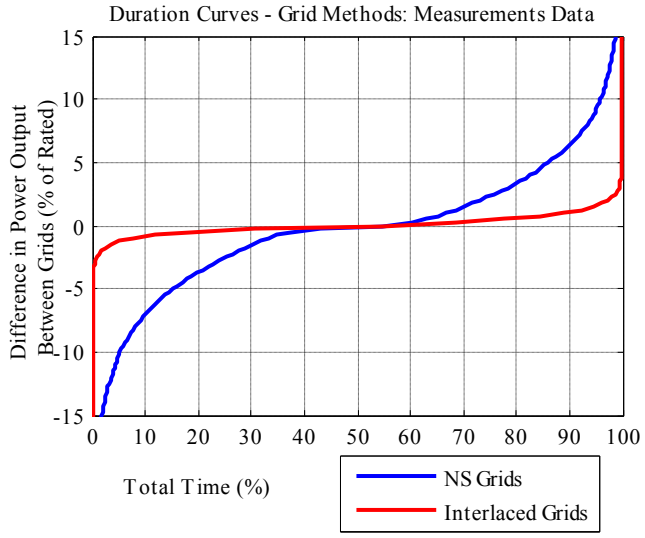

Figure 3-2: Duration Curves of the Difference Between Grids for Normal Operation: Measurement Data

The results indicate that for both layouts the mean difference in power between grids is close to zero (indicated by the symmetry of the duration curves) but the NS layout has significantly more scatter than the interlaced layout. These results however, do not include any down-regulated operation which will induce errors in the "true" value of the measurement grid due to altered wake effects of the down-regulated (control) grid. For the split grid case the error is significant for unfavorable wind directions where the measurement grid is down-wind of the control grid. For the interlaced grid altered wake effect always induce an error since certain measurement turbines will always be down-wind of down-regulated control turbines.

Simulations of split and interlaced grid layout were preformed for both normal and down-regulated operation. The normal operating case provides a base line to validate the model against measurement data while the down-regulated case provides an estimation of the performance of the grid methods during down-regulation. In the case of down-regulation, the estimated production was compared to the production during normal operation to determine the estimate error. This being possible because the wind direction and wind speed input for both cases are identical. For simulations of down-regulated operation the control turbines were down-regulated 100% to ensure the worst case change in wake effects of the down-regulated turbines.

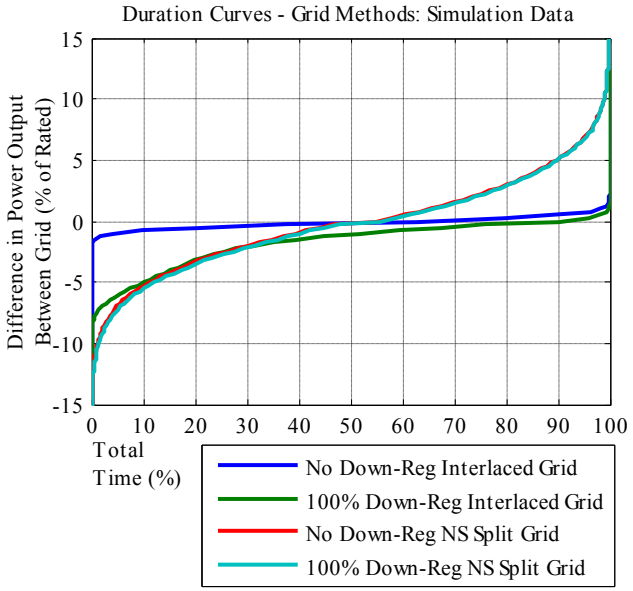

Figure 3-3: Duration Curves of the Difference Between Grids for Normal and Down-Regulated Operation: Simulation Data

Duration curves for simulation of the grid methods are depicted in Figure 3-3. Results for the split grid layout indicate that the difference between the grids does not change significantly during down regulation (the curve are almost indistinguishable), implying that the interaction of the altered wake effects between grids tends to average out for even wind direction distributions about the principle split direction (which is the case in this present work). However the difference between the grids during down-regulation with the interlaced grid layout becomes increasingly negative as a result of wakes from control (down-regulated) turbines affecting measurement turbines.

4. Comparison of Wake Effects for Different Wind Plant Configurations

The error in the plant production estimate, if wake effects are not accounted for at Nysted is depicted in Figure 4-1. The plot depicts the relative change in the plant production at 9.4 m/s for varying levels of down-regulation over all wind directions. This wind speed corresponds to the maximum possible change in the rotor C_T between normal and maximum down-regulated operation. These conditions represent the worst case error in the plant production estimate due to altered wake effect during down-regulation. The plot indicates that during down regulation at Nysted the overall change in the plant production estimate between normal and down-regulated operating does not exceed 5% for most wind directions. The worst case, where the overall change approaches 10% is for a narrow yaw sector about the North-South(358deg) / South-North(178deg) direction, corresponding to the smallest turbine spacing of 5.7D. This indicates that overall the wake effects between normal and down-regulated operation contribute a relatively small amount to the error in the estimation of possible power at Nysted.

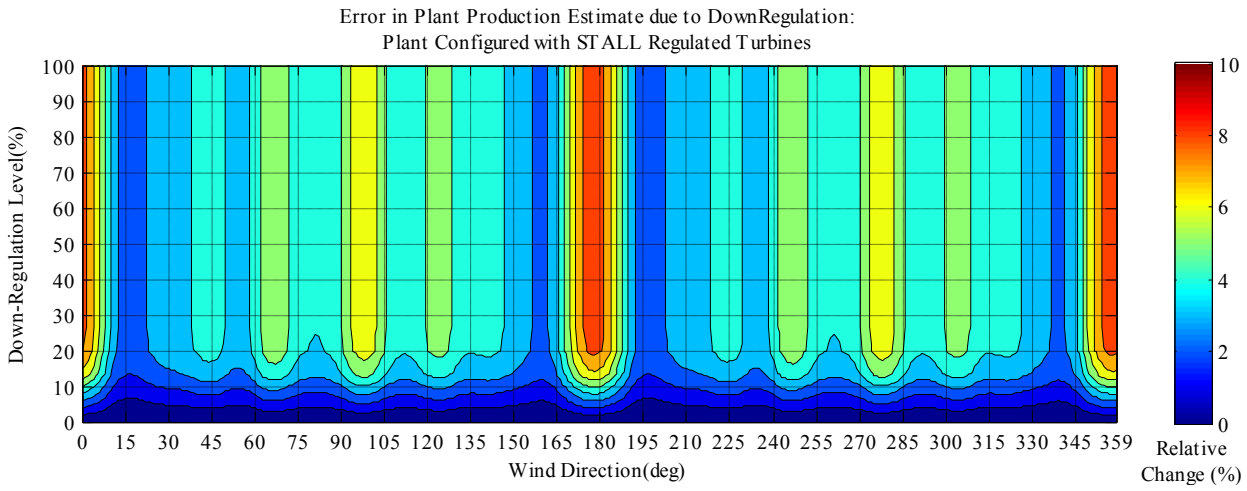

Figure 4-1: Error in Plant Production Estimate due to Down Regulation with a Wind Plant Configured with Stall Regulated Turbines

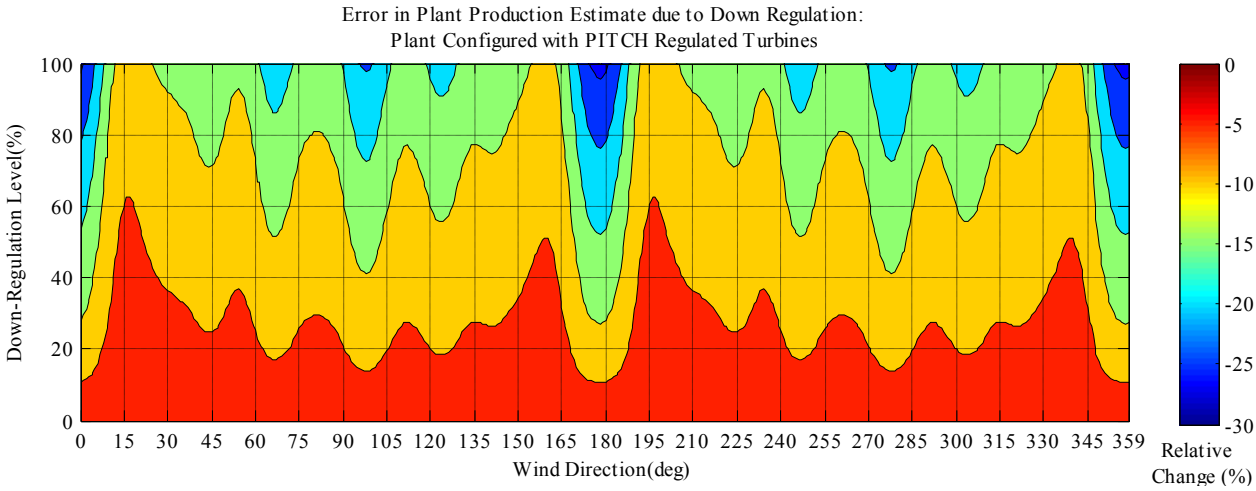

Figure 4-2:Error in Plant Production Estimate due to Down Regulation with a Wind Plant Configured with Pitch Regulated Turbines

Figure 4-2 depicts the error in the plant production estimate, at 6.5 m/s for varying levels of down-regulation over all wind directions for the Nysted wind plant configured with a pitch regulated turbine. In this example the historic Tjaereborg turbine is used as a representative pitch regulated machine. The chosen wind speed corresponds to the maximum possible change in the rotor C_T between normal and maximum down-regulated operation. For down-regulation of a wind plant incorporating pitch regulated turbines the wind speed reduction decreases in contrast to a wind plant with stall-regulated turbines. Additionally, the wake changes continually for increasing levels of regulation for the pitch regulated turbines rather the reaching a plateau at approximately a 25% down regulation. This indicates that the changes in the wake effects between normal and down-regulated operation are more significant for a wind plant configured with pitch-regulated turbines

5. Conclusion

Results from modeling and simulation of the Power Curve Method indicate an improvement in the estimate of possible production during down-regulation over the currently employed method at Nysted. The largest improvement is gained from correction of the wind speed measurement error; whereas the dynamic wake correction contributes relatively little.

Simulation results indicate that the alternative control strategy successfully estimates the possible plant production. However, the overall down-regulation capability is limited to 50% since only half the turbines participate in down-regulation.. A clear benefit to this method is that it deals directly with the measurement of interest (power) rather than inferring it from other measurement quantities.

A comparison of the DWM applied to a wind plants configured with stall regulated turbines indicate that overall the wake effects between normal and down-regulated operation contribute a relatively small amount to the error in the estimation of possible power at Nysted. In contrast the wake effects between normal and down-regulated operation are more significant for a wind plant configured with pitch-regulated turbines.

References

[1] Hansen & Henneberg. "Notat vedr. undersøgelse af indflydelse af mølleregulering på målinger fra nacelleanemometer, 3908not006, Rev. 0.26.07.2005." Hansen & Henneberg, 2005.

[2] Jensen, N.O. A note on wind generator interaction. Roskilde, DK: Risoe National Laboratory, 1983.

[3] Katic, I., J. Højstrup and N.O. Jensen. "A simple model for cluster efficiency." Proc. European Wind Energy Conference and Exhibition. Rome, Italy, 1986. pp407-410.

[4] Hansen, M. O. L. Aerodynamics of wind turbines. London: James and James, 2000.

[5] IEC. "Wind turbine generator systems part 12: wind turbine power performance testing." (IEC) 1998.

[6] Sørensen, P., Hansen, A.D., Carvalho Rosas, P.E.,. "Wind models for simulation of power fluctuations from wind farms." Journal of Wind Engineering and Industrial Aerodynamics, no. 90: (2002): pp1381–1402.

Power Fluctuations from Offshore Wind Farms; Model Validation

Nicolaos A. Cutululis[1*)], Poul Sørensen[1)], Stephane Eisen[2)], Martin Donovan[3)], Leo Jensen[3)], Jesper Kristoffersen[4)]
[1)] Risø DTU, VEA-118, P.O. Box 49, DK-4000 Roskilde, Denmark
[*)] tlf. +45 4677 5075, e-mail poul.e.soerensen@risoe.dk
[2)] DTU, Anker Engelundsvej 1, Lyngby, DK-2800, Denmark
[3)]DONG Energy, Kraftværksvej 53, Skærbæk, DK-7000 Fredericia, Denmark
[4)]Vattenfall A/S, Oldenborggade 25-31, DK-7000 Fredericia, Denmark

Abstract — This paper aims at validating the model of power fluctuations from large wind farms. The validation is done against measured data from Horns Rev and Nysted wind farms. The model time scale is from one minute to a couple of hours, where significant power fluctuations have been observed. The comparison between measured and simulated time series focuses on the ramping characteristics of the wind farm at different power levels and on the need for system generation reserves due to the fluctuations. The comparison shows a reasonable good match between measurements and simulations.

Index Terms — power fluctuation, wind farms, model validation, ramping and reserves requirements.

1. Introduction

The electrical power system, due to the increasing importance of power produced by wind turbines, becomes more vulnerable and dependent on the wind power generation. Therefore, a fundamental issue in the operation and control of power systems, namely to maintain the balance between generated and demanded power, is becoming more and more influenced by wind power.

Scheduling of generation ensures that sufficient generation power is available to follow the forecasted load, hour by hour during the day [1]. Besides, sufficient reserves with response times from seconds to minutes must be available to balance the inevitable deviations from the schedules caused by failures and forecast errors.

In the Nordic power system the generation is scheduled on the NORDPOOL spot market [2] on the day ahead spot market, while the reserve capacities are agreed in the Nordel cooperation between the Nordic transmission system operators [3]. Those reserves include a "fast active disturbance reserve", which is regulating power that must be available 15 minutes after allocation. The purpose of the regulating power is to restore the frequency controlled reserves, which are activated due to frequency deviations from the nominal value. The frequency controlled reserves are much faster than the regulating power, with required response times from a few minutes down to a few seconds, depending on the frequency error.

The wind power development influences the power balancing on all time scales. An example of this is the experience of the Danish transmission system operator, Energinet.dk, with the operation of the West Danish power system. According to Akhmatov et. al. [4], Energinet.dk has found that the active power supplied from the first large 160 MW offshore wind farm in this system, Horns Rev, is characterized by more intense fluctuations in the minute range than previously observed form the dispersed wind turbines on land, even though the installed power in Horns Rev is relatively small compared to the total 2400 MW wind power installation in the system.

Generally, the onshore wind power fluctuates much less than the Horns Rev wind farm, first of all because the offshore turbines are concentrated in a very small area where the wind speed fluctuations are much more correlated than the wind speeds at the turbines dispersed over a much bigger area. Another reason which may increase the fluctuations from Horns Rev is that the meteorological conditions are different offshore than onshore.

The West Danish power system is DC connected to the Nordic synchronous power system, and it is a part of the Nordel cooperation. At the same time, the system is interconnected to the Central European UCTE system through the German AC connection. Therefore, the West Danish system also has obligations to the UCTE system, including the responsibility to keep the agreed power flow in this interconnection within acceptable limits.

With the present wind power capacity, the power flow in the interconnection can be kept within the agreed limits. However, a second neighbouring wind farm, the 200 MW Horns Rev B is already scheduled for 2008, and Energinet.dk is concerned how this will influence the future demand for regulating power in the system.

This paper will compare the measured and simulated power fluctuations for both Horns Rev and Nysted wind farm. Section 2 briefly presents the simulation model, section 3 describes the sites and data acquisition on Horns Rev and Nysted wind farms, and section 4 presents the analyses and the comparisons. Finally, the paper ends with conclusions in section 5.

2. Wind farm power simulation model

The wind farm power simulation model uses a statistical description of the wind speed characteristics given in the frequency domain and outputs the time series of the power produced by the wind farm. The model is based on the wind speed fluctuation model developed by Sørensen *et al* [5]. The focus in these studies has been on the slower wind speed variations and on the coherences between wind speeds measured over horizontal distances.

A detailed description of the model is given in [6]. In this section only a brief presentation of the model is provided to support the analyses and conclusions.

The basic structure of the simulation model is shown in Figure 1. The wind farm consists of N wind turbines, indexed with i between 1 and N.

The inputs to the model is the N power spectral densities (PSD's) $S_{u[i]}(f)$ of wind speeds $u_{[i]}(t)$ in hub height of the

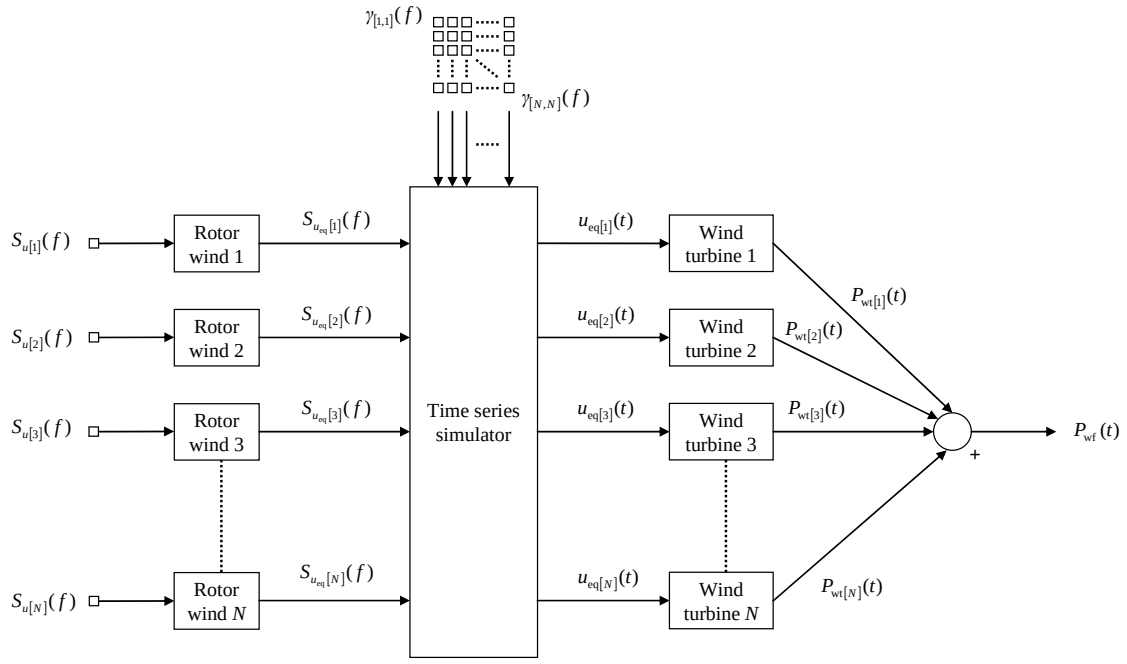

Figure 1. Basic structure of model for simulation of power fluctuation from wind farm.

wind turbines, and the $N \times N$ coherence functions $\gamma_{[r,c]}(f)$ between $u_{[r]}(t)$ and $u_{[c]}(t)$. The output from the model is simply time series of the total wind farm output power $P_{wf}(t)$.

The PSD's quantify the average energy in the wind speed variability, distributed on frequencies. The PSD $S_{u[i]}(f)$ of $u_{[i]}(t)$ is defined according to

$$S_{u[i]}(f) \cdot \Delta f = \left\langle U_{[i]}(f) \cdot U_{[i]}^{*}(f) \right\rangle \tag{1}$$

$U_{[i]}(f)$ is the Fourier transform of $u_{[i]}(t)$ and Δf is the frequency step between adjacent Fourier coefficients, i.e. $\Delta f = 1/T_{seg}$. The * operator denotes complex conjugation and the $\langle\rangle$ operator denotes the mean value of results from an ensemble of periods of length T_{seg}.

The simulation results are highly dependent on the specification of the wind speed PSD's. The PSD's depend on the average wind speed in the included segments, the surface roughness which generates turbulence, meteorological stability and other external conditions. However, structural engineers use standard wind PSD's for design of buildings, bridges and wind turbines.

For relatively high frequencies $f > 0.01$ Hz, the variability of the ambient wind speed is described by the turbulence PSD's, which are available from literature, e.g. Kaimal [7], and in codes of practice for structural engineering, e.g. the wind turbine standard IEC 61400-1 [8].

As it is seen in Figure 1, the power fluctuation model uses individual PSD's for the individual wind turbines. This way, the added turbulence to wind speeds inside the wind farm is taken into account for the wind turbines inside the wind farm.

The added turbulence inside the wind farm is significant compared to the low ambient turbulence offshore, and for that reason it is included in the structural design of wind turbines. The standard deviation of the added wind farm turbulence is included in the power fluctuation model, quantified according to specifications in IEC 61400-1.

The added turbulence in the wind farm is on an even shorter time scale than the ambient turbulence. The main reason why Rosas simulations underestimated the power fluctuations was that the low frequency variability for frequencies $f < 0.01$ Hz was not included. There are no standards specifying the PSD's for those low frequencies. The studies of wind speed measurements from Risøs test site for large wind turbines proposed a low frequency PSD term, which is used in the present simulations.

Thus, the PSD's applied in the present model is the sum of PSD's for ambient turbulence, added wind farm turbulence, and low frequency fluctuations.

The coherence functions quantify the correlation between the wind speeds at the individual wind turbines. The definition of the coherence function $\gamma_{u[r,c]}$ between $u_{[r]}(t)$ and $u_{[c]}(t)$ is given by

$$\gamma_{u[r,c]}(f) = \frac{S_{u[r,c]}(f)}{\sqrt{S_{u[r]}(f) \cdot S_{u[c]}(f)}} \tag{2}$$

$S_{u[r,c]}(f)$ is the cross power spectral density (CPSD) between $u_{[r]}(t)$ and $u_{[c]}(t)$, defined according to

$$S_{u[r,c]}(f) \cdot \Delta f = \left\langle U_{[r]}(f) \cdot U_{[c]}^{*}(f) \right\rangle \tag{3}$$

The simulation results are also quite sensitive to the specification of the coherence functions. There are no standards specifying the horizontal coherence between wind speeds over a large distances corresponding to a wind farm. In the literature, Schlez and Infield [9] have proposed a model based on measurements in distances up to 100 m in 18 m height in Rutherford Appleton Laboratory test site, U.K., and Nanahara [10] has used measurements in distances up to 1700 m in 40 m height in Japan Sea.

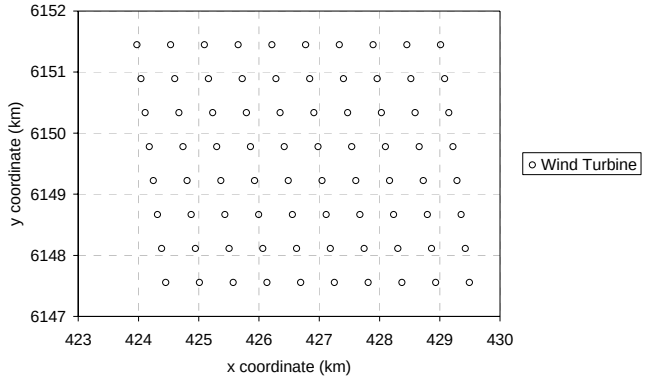

Figure 2. Horns Rev wind farm.

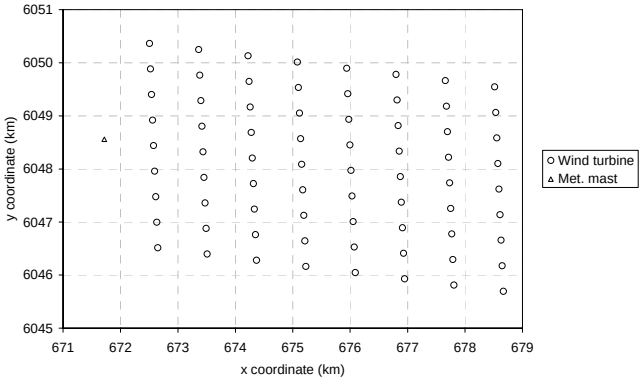

Figure 3. Nysted wind farm.

There is, however, a significant difference in the conclusions of Schlez and Nanahara. In the present simulations, the results of studies in Risø National Laboratory's test site in 80 m height over 1.2 km distances are applied.

The estimation of coherence based on measurements is relatively uncertain, because coherence of wind speeds in two points strongly depends on the inflow angle, i.e. on the wind direction. Therefore, even more data is required to estimate the coherence functions than to estimate the PSD's. Thus, the assumed horizontal coherence functions are still a point with possible improvement.

The kernel of the model in Figure 1 is the time series simulator, which converts a set of PSD's and coherence functions to a set of time series. The time series simulation can be divided into two steps. The first step is to generate a random set of Fourier coefficients fulfilling (1), (2) and (3). When this is done, the second step is simply to apply a reverse Fourier transform to provide the time series.

The random generation of Fourier coefficients ensures that the time series simulation can generate different sets of time series, depending on a seed which initializes a random generator. The generation of Fourier coefficients ensures that an ensemble of time series generated with different seeds gets the specified PSD's and coherence functions.

A detailed mathematical description of the time series simulator is given in reference [5], where it is used directly on the set $S_{u[i]}(f)$ of PSD's of the hub height wind speeds. In the present model, the time series simulator is used on PSD's $S_{ueq[i]}(f)$ of equivalent wind speeds $u_{eq[i]}(t)$.

The equivalent wind speed $u_{eq[i]}(t)$ takes into account that the wind speed is not the same over the whole wind turbine rotor. The equivalent wind speed is defined as the wind speed, which can be used in a simple aerodynamic model to calculate the aerodynamic torque on the rotor shaft as if the wind speed was equal to $u_{eq[i]}(t)$ over the whole rotor. Thus, the equivalent wind speed can be obtained as a weighted average of the wind speed field in the rotor disk.

The equivalent wind speed defined in [5] includes fast periodic components which are harmonics of the rotor speed, but they are omitted in the present model because they are outside the time scale of interest for this model.

Omitting the periodic components, the equivalent wind speed $u_{eq[i]}(t)$ fluctuates less than the fixed point wind speed $u_{[i]}(t)$. According to reference [6], the PSD of the equivalent wind speed can be found by the PSD of the fixed point wind speed, which is done by the rotor wind blocks in Figure 1.

Finally, the wind turbine models in Figure 1 specify the relation between the equivalent wind speed and the output power. In the present model, a simple power curve is applied, i.e. a purely steady state model of the wind turbine. The reason for this choice is that the dynamics of the mechanical and electrical systems of the wind turbine are in a much faster time scale than the time scale of interest for the power fluctuation model.

3. Wind Farms and Data Acquisition

The modelling of the power fluctuation is validated using wind speed and power measurements from the two large offshore wind farms in Denmark, namely Horns Rev and Nysted.

Horns Rev wind farm consists of 80 Vestas V80 variable speed wind turbines, using doubly-fed induction generators. The rated power of the V80 turbines is 2 MW, and the rotor diameter is 80 m.

Figure 2 shows the layout of Horns Rev wind farm. The distance between the turbines is 560 m in the rows as well as columns, corresponding to 7 rotor diameters.

The measured data is acquired by the SCADA system used by the wind farm main controller, which off course has the first priority. The acquired data originates from the wind turbine control systems. The wind speed is measured on the nacelle of each wind turbine with ultrasonic sensors. The power is measured by the control system on the low voltage terminals as a sum of rotor and stator power. Finally, the yaw position registered in the wind turbine is used to indicate the wind direction. Wind speed, power, power setpoint and yaw position is logged with 1 Hz sampling frequency.

Data acquired from February 2005 to January 2006 are used in this paper. In some periods, the data acquisition was not working, e.g. the SCADA system had other tasks, with high priority, to do, or the wind turbines operation status was not on "normal". For validating the model, 2-h segments with continuous data and normal operation status from at least 72 wind turbines were used.

The result is 1110 segments, which corresponds to 92.5 days, representing wind speeds from 1 to 19 m/s.

Nysted wind farm consists of 72 Siemens SWT-2.3-82 fixed speed wind turbines, with a rated power of 2,3MW and with the rotor diameter of 82 m.

Figure 3 shows the layout of Nysted wind farm. The distance between the turbines in a column is 481 m corresponding to 5.9 rotor diameters, while the distance

between the turbines in a row is 867 m corresponding to 10.6 rotor diameters.

Like in Horns Rev, the measured data is acquired by the SCADA system used by the wind farm main controller with 1 Hz sampling frequency. The acquired data originates from the wind turbine control systems and from a meteorology mast indicated in Figure 3. The measurements from the wind turbine control systems are the wind speed measured on the nacelle of each wind turbine with cup anemometer, the power measured by the control system on the low voltage terminals, the power setpoint and the yaw position.

Data acquired from January 2006 to May 2007 are used in this paper. In some periods, the data acquisition was not working, e.g. the SCADA system had other tasks, with high priority, to do, or the wind turbines operation status was not on "normal". For validating the model, 2-h segments with continuous data and normal operation status from at least 62 wind turbines were used.

The result is 1989 segments, which corresponds to 165.75 days, representing wind speeds from 1 to 24 m/s.

4. Analyses and comparisons

The analyses are done in terms of ramp rates and reserves requirements, defined for the wind farm power. Duration curves are used to compare measured and simulated power fluctuations.

In Sørensen *et al* [12] the analyses and the comparisons between the simulated and measured power series, for Horns Rev wind farm, are presented in details. In this paper, the same analyses are made for Nysted wind farms and the results are presented for both wind farms.

The definitions of ramp rates and reserve requirements are involving a statistical period time T_{per}, which reflects the time scale of interest. The time scales of interest will depend on the power system size, load behavior and specific requirements to response times of reserves in the system. In order to study the wind variability and model performance in different time scales, the analysis of Nysted data is performed with one minute, ten minute and thirty minute period times.

For the present analysis, the measured wind farm power is calculated in p.u. as the average power of the available turbines in each 2 hour segment. Thus, the reduction of the wind farm power due to non availability of wind turbines is removed. This choice is justified because missing data from a turbine is not necessarily indicating that the turbine is not producing power, but can also be because of failures in the SCADA system.

For each measured 2 hour segment, the average wind speed and wind direction is calculated, and a 2 hour wind farm power time series is simulated. The simulations are performed with the complete model including low frequency fluctuations and wind farm generated turbulence.

4.1. Ramp rates

The definition of ramp rates applied in this paper is quite similar to the definition of load following applied by Parson et. al. [11]. The intention is to quantify the changes in mean values from one period T_{per} to another, which specifies the ramp rate requirement that the wind farm power fluctuation causes to other power plants.

The definition of ramp rates is illustrated for period time T_{per} = 600 s in Figure 4.

The instantaneous time series of power can be either measured or simulated, in our case both are with on second time steps. Then the mean value of the power is calculated at the end of each period, although it is illustrated for all time steps in Figure 4. The ramp rate is simply the change in mean value from one period to the next, i.e.

$$P_{\text{ramp}}(n) = P_{\text{mean}}(n+1) - P_{\text{mean}}(n) \tag{4}$$

Note that this definition specifies the ramping of the wind farm power. Thus, negative ramp rate means decreasing wind power, which requires positive ramping of other power plants.

When the ramp rates have been calculated for each set of neighbour periods n and n+1 for all segments, the ramp rates are binned according the corresponding initial power $P_{\text{mean}}(n)$. This is because the statistics of the ramping will depend strongly on the initial power. For instance, the power is not likely to increase very much when it is already close to rated. A power bins size 0.1 p.u. has been selected.

The ramping is sorted in each power bin, and a duration curve is obtained. This is done for the measurements and for the simulations. As an example, the duration curves for ten minute ramp rates in the initial power range between 0.8 p.u. and 0.9 p.u. is shown in Figure 5. There is a good agreement between the simulated and the measured duration curves.

The same good agreement, with differences no bigger than 0.02 p.u., is observed in all power ranges.

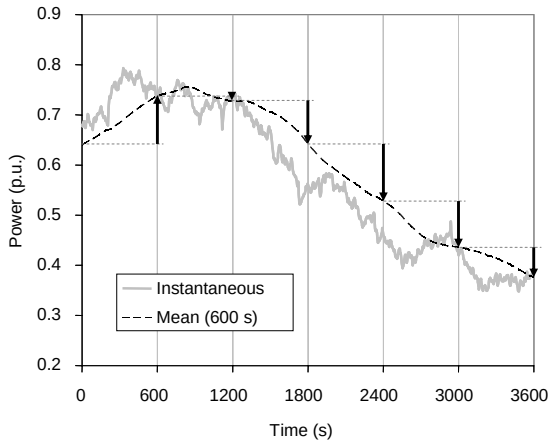

Figure 4. Definition of ramp rated for period time Tper = 10 min. The ramp rates are indicated with arrows.

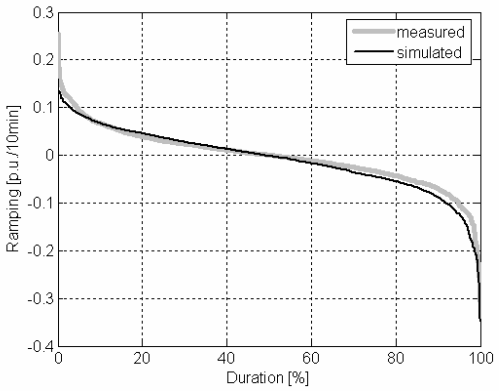

Figure 5. Duration curves of 10-min ramp rates in the initial power range from 0.8 p.u. to 0.9 p.u.

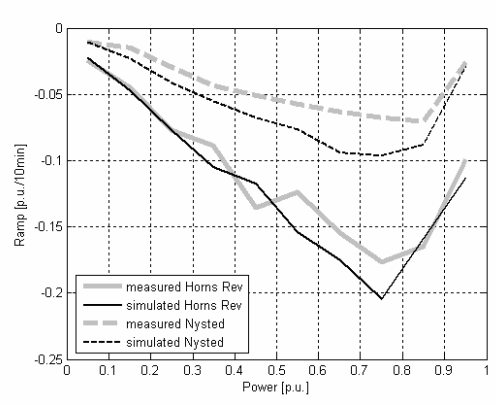

Figure 6. The 99% percentiles of 10-min ramp rates in all power ranges for Horns Rev and Nysted wind farm

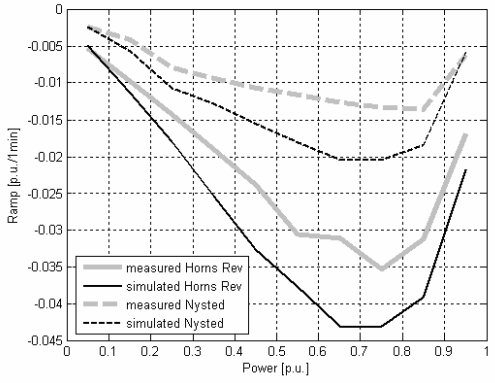

Figure 7. The 99% percentiles of 1-min ramp rates in all power ranges for Horns Rev and Nysted wind farm

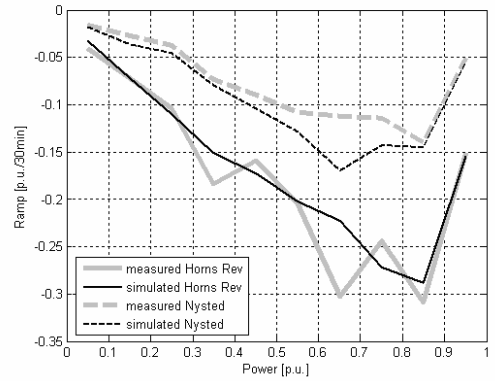

Figure 8. The 99% percentiles of 30-min ramp rates in all power ranges for Horns Rev and Nysted wind farm

The most interesting point of the duration curves is the highest wind farm negative ramp rate, i.e. around 100% on the duration curve, because this quantifies the highest requirement to the ramp rates of other power plants. The wind farm positive ramp rates are not so interesting here because they can be limited directly by the wind farm main controller.

In Figure 6 the 99% percentile of the 10-min ramp rates duration curve for all power ranges is shown. In order to assess the model performances, both Horns Rev and Nysted simulated and measured ramp rates are plotted.

There is an acceptably good match, with differences generally less than 0.03 p.u./10 min for both Horns Rev and Nysted, although Nysted simulated ramp rates are systematically bigger the measured ones.

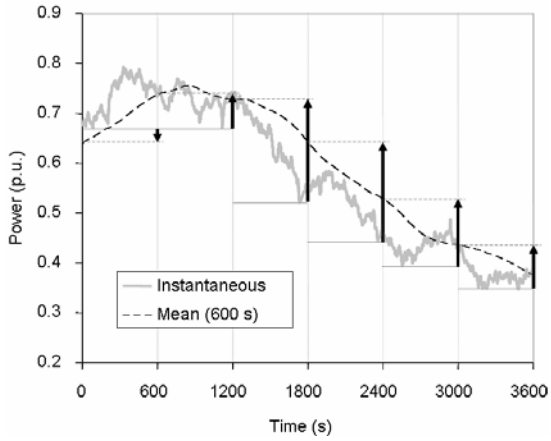

Figure 9. Definition of reserve requirements for period time Tper = 10 min. The reserves are indicated with arrows

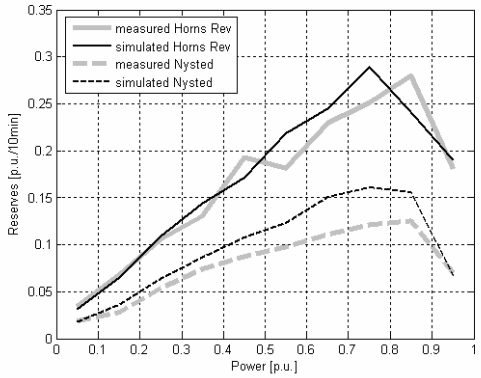

Figure 10. 1 % percentiles of 10 minutes reserve requirements in Horns Rev and Nysted wind farm

The 99% percentile for 1 min and 30-min period is shown in Figure 7 and Figure 8, respectively. The match between simulated and measured power fluctuations is similar to the 10-min periods, with the simulated power fluctuations still being systematically bigger than the measured ones. For the 1-min period, Although the difference between simulated and measured looks significant, it is less than 0.01 p.u./1min.

Summarizing, the ramping analyses, for Nysted wind farm, show a good match between simulated and measured time series. The systematic overestimation of the simulated power fluctuations time series should be further analysed.

4.2. Reserve requirements

The intention is to quantify the difference between the instantaneous power and the mean value which are dealt with as ramping. Since the reserves must be allocated in advance, the positive reserve requirement is defined as the difference between the initial mean value and the minimum value in the next period.

This definition of reserve requirements is illustrated for period time T_{per} = 600 s in Figure 9. Formally, the reserve requirements are defined as

$$P_{res}(n) = P_{mean}(n) - P_{min}(n+1) \quad (5)$$

Note that with this definition, positive reserves means decreasing wind power that requires positive reserves form other power plants.

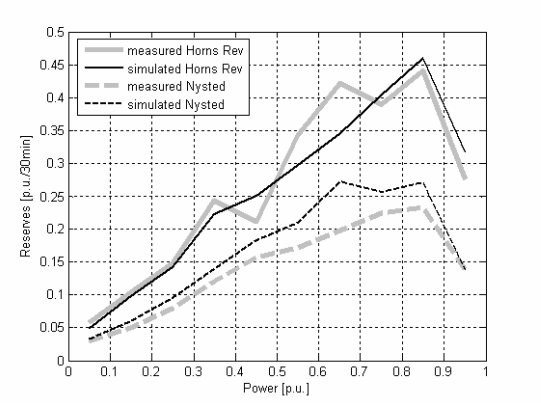

Figure 11. 1 % percentiles of 30 minutes reserve requirements in Horns Rev and Nysted wind farm

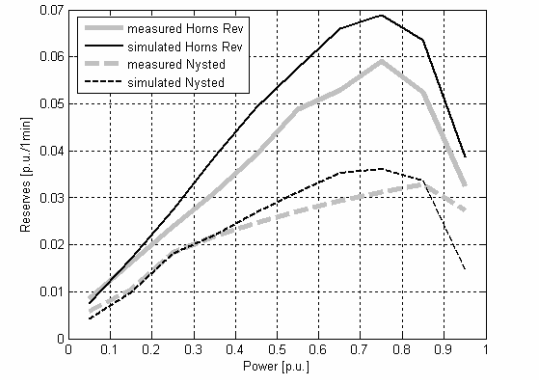

Figure 12. 1 % percentiles of 1 minute reserve requirements in Horns Rev and Nysted wind farm

The duration curves are then calculated for the reserves in all power bins, and the 1 % percentiles are found in each power bin.

The resulting 1 % percentiles with 10 min, 30 min and 1 min period times are shown in Figure 10, Figure 11 and Figure 12, respectively.

It is concluded that the simulated time series agree quite well with the measured in the prediction of the reserves. As expected, the reserve requirement decreases in the highest power bin because the wind speed is above rated.

As expected, the reserve requirements in Nysted wind farm are smaller than ones in Horns Rev. The same conclusion can be drawn when 30-min and 1-min periods are considered, as shown in Figure 11 and Figure 12, respectively.

5. CONCLUSIONS

The balance between generated and demanded power is more and more influenced by wind power. Large wind farms contribute with more power fluctuations to the system than a similar capacity of distributed wind power. This is because a large wind farm, geographically concentrated in a small area, experience strongly correlated slow wind fluctuations, while this correlation is decreasing with the distance.

The simulation model predicts the PSDs of the power series very well. Duration curves for ramp rates and reserve requirements are generally simulated to slightly higher values than measured. The extreme values though obtained from simulations agree well with the measured ones.

The presented power fluctuation model simulates the power fluctuation of wind power on an area up to several km and for time scales up to a couple of hours.

ACKNOWLEDGEMENT

The work presented in this paper is done in the research project "Power fluctuations from large offshore wind farms" financed by the Danish Transmission System Operator Energinet.dk as PSO 2004 project number 6506.

REFERENCES

[1] B. M. Weedy, B.J. Cory, *Electric power systems*, Chichester, United Kingdom: John Wiley & Son, Fourth Edition 1998, ch. 4

[2] http://www.nordpool.com

[3] Nordic grid code: Nordel, June 2004

[4] V. Akhmatov, H. Abildgaard, J. Pedersen, P. B. Eriksen, "Integration of Offshore Wind Power into the Western Danish Power System," in *Proc. Copenhagen Offshore Wind 2005*, CD.

[5] P. Sørensen, A. D. Hansen, P. A. C. Rosas, "Wind models for simulation of power fluctuations from wind farms," *J. Wind Eng. Ind. Aerodyn*, vol. 90, Dec. 2002, pp. 1381-1402.

[6] P. Sørensen, N. A. Cutululis, A. Vigueras-Rodríguez, H. Madsen, P. Pinson, L. E. Jensen, J. Hjerrild, M. Donovan, "Modelling of Power Fluctuations from Large Offshore Wind Farms," invited paper submitted to special issue of *Wind Energy*.

[7] J. C. Kaimal, J. C. Wyngaard, Y. Izumi, O. R. Cote, "Spectral characteristics of surface-layer turbulence," *Q. J. R. Meteorol. Soc.* vol. 98, 1972, pp 563-598.

[8] International standard IEC 61400-1, "Wind turbines – Part 1: Design requirements," Third edition 2005-08.

[9] W. Schlez, D. Infield, "Horizontal, two point coherence for separations greater than the measurement height," *Boundary-Layer Meteorology*, vol. 87, 1998, pp.459-480.

[10] T. Nanahara, M. Asari, T. Sato, K. Yamaguchi, M. Shibata, T. Maejima, "Smoothing effects of distributed wind turbines. Part 1. Coherence and smoothing effects at a wind farm," *Wind Energy* , vol. 7, Apr./Jun. 2004, pp 61-74.

[11] B. Parson, M. Milligan, B. Zavadil, D. Brooks, B. Kirby, K. Dragoon, J. Caldwell, "Grid Impacts of Wind Power: A summary of recent studies in the United States," *Wind Energy* , vol. 7, Apr./Jun. 2004, pp 87-108.

[12] P. Soerensen N.A.Cutululis, A. Vigueras-Rodríguez, L.E. Jensen, J. Hjerrild, M.H. Donovan, H. Madsen, Power Fluctuations from Large Wind Farms, IEEE Trans. on Power Systems, **22**(3): 958-965, 2007

System grounding of wind farm medium voltage cable grids

Peter Hansen[1)], Jacob Østergaard[2)], Jan S. Christiansen[3)]
[1)] Danish Energy Association R&D (DEFU), Rosenørns Allé 9, DK-1970 Frederiksberg, Denmark
[2)] Centre of Electric Technology (CET), Ørsted•DTU, DK-2800 Kgs. Lyngby, Denmark
[3)] DELPRO A/S, Dam Holme 1, DK-3660 Stenløse, Denmark

Abstract — Wind farms are often connected to the interconnected power system through a medium voltage cable grid and a central park transformer. Different methods of system grounding can be applied for the medium voltage cable grid. This paper outlines and analyses different system grounding methods. The different grounding methods have been evaluated for two representative wind farms with different size. Special emphasis is put on analysis of isolated system grounding, which has been used in some real wind farm medium voltage cable grids. Dynamic simulations of earth faults have been carried out. The paper demonstrates for grids with isolated system grounding how the phase voltage can build up to a level of several times the system voltage due to re-ignition of the arc at the fault location. Based on the analysis it is recommended to use low-resistance grounding as the best compromise to avoid destructive transient over voltages and at the same time limit the earth fault currents in the wind farm grid to an acceptable level.

Index Terms — System grounding, wind farms, voltage rise, single-phase earth faults.

1. BACKGROUND

In Denmark wind farms has according to the traditional practice used in distribution systems often been established with isolated system grounding medium voltage cable grids. Abroad wind farms instead according to the traditional practice often have been established with (low) resistance grounding.

Within the last couple of years the first generation of "wind power plants" has been exposed to different kinds of faults. In the *Middelgrunden* wind farm several step-up transformers have faulted caused by switching voltage transients. Following several step-up transformers at the *Horn Rev* wind farm also have faulted, which lead to a replacement of all 80 wind turbine step-up transformers. At the same time the system grounding was changed from an isolated system to a kind of reactance grounding (via the wind farm auxiliary-supply transformer, designed with appropriate zero-sequence impedance).

The establishment of the first generation of wind farms (larger than 40 MW) in Denmark has in other words been exposed to different faults cases, which to a certain extent is believed to be influenced by the choice of the wind farm system grounding method.

2. SYSTEM GROUNDING METHODS

Different methods of system grounding in medium voltage networks are well-known. Basically the aim of choosing system grounding method is to find the best compromise between the different technical properties and the associated costs related to the specific system application. This should be judged case by case. Important technical properties to consider include fault current levels and over voltages.

This paper will focus on earth fault currents, fault re-ignition and reducing transient over voltages in case of single-phase to ground faults for different methods of system grounding.

Five different methods of system grounding have been analysed:

2.1. Isolated system

In the isolated system the network is without direct connection to ground. The only connections to ground are through the large zero sequence capacitance of the cables.

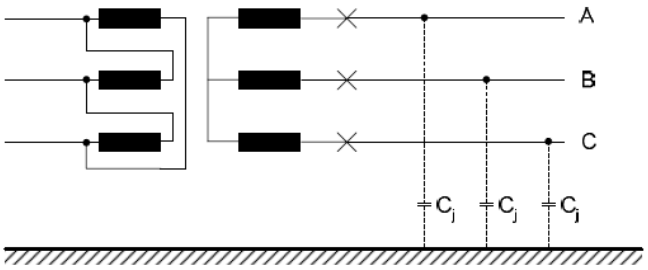

Figure 1. Isolated system grounding

The network zero-sequence impedance is approximately a pure capacitive impedance, which is much larger than the short circuit positive-sequence impedance. As a consequence single-phase earth fault currents are much smaller than short circuit fault currents, and depend on the cables and the length of the cable grid. Usually for wind farms single-phase to ground fault currents are smaller than load currents.

With respect to over voltages the isolated system has some major disadvantages, discussed further in section 3 and 4.

2.2. Direct (effective) grounded system

With direct grounded systems is meant systems with a direct connection via the transformer neutral to ground. Direct grounding is well-known and normally used in low voltage distribution networks. In transmission networks (above 100 kV) effective grounding – a special version of direct grounding, is well-known.

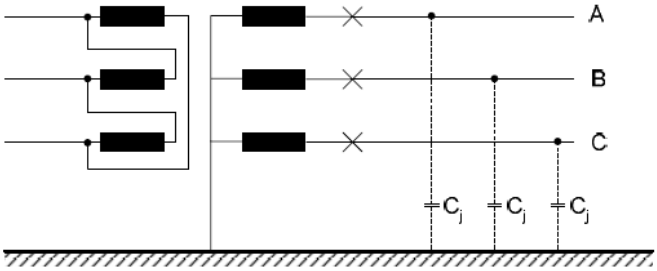

Figure 2. Direct (effective) grounded system

In direct (and effective) grounded systems single-phase earth fault currents is of the same size as short circuit currents. In other words single-phase earth fault currents will be relatively large (typically many kA). Cables, circuit breakers etc. must be designed for these large fault currents.

The effective grounded system is – as mentioned before, a special version of the direct grounded system. By grounding not all transformer neutrals in the network and by keeping impedance ratios within defined values (everywhere in the network, see table 2), the voltage rise on the healthy phases is said not to exceed 0.8 pu of the phase-to-phase voltage. Further single-phase earth fault currents is said to be approx. 0.6 pu of the three-phase short circuit fault current.

2.3. Reactance and resonance grounded systems

In reactance grounded systems the transformer neutral is connected to ground through a reactance.

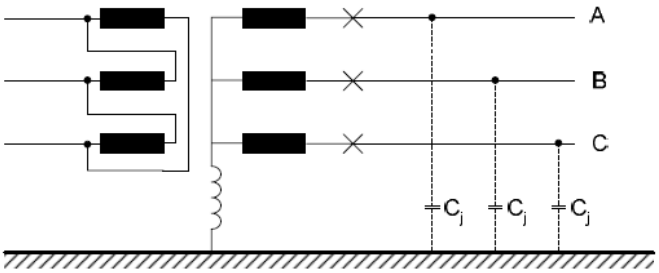

Figure 3. Reactance and resonance grounded system

By connecting the system to ground (through a reactance) it is possible to reduce the single-phase earth fault currents. To avoid destructive transient over voltages earth fault currents must be in the range of 0.25-0.6 pu of the network three-phase short circuit fault current. This is possible to achieve if impedance ratios is kept within defined values (see table 2).

A special case of reactance system grounding is when the reactance (inductance) is designed to exactly compensate the capacitive earth fault current; for this case, single-phase to ground fault current can be almost eliminated (reduced to a very small resistive current). If done, system grounding is said to be resonance grounded.

2.4. Resistance grounded system

In resistance grounded systems the transformer neutral is connected to ground through a resistance. Within resistance grounded systems two different methods are well-known; High-resistance grounding and low-resistance grounding.

High-resistance grounding has some similarities with isolated networks. The most characteristic relation is small single-phase earth fault currents (a few A), but properly designed the severe transient over voltages associated with isolated systems can be avoided. The high-resistance grounding method has not been treated in the latter analysis.

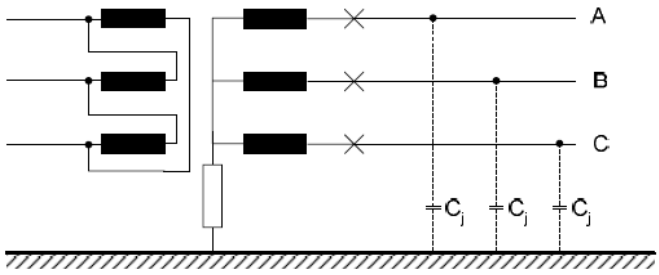

Figure 4. Resistance grounded system

Low-resistance grounding has the ability to reduce earth fault currents. By keeping impedance ratios within defined values (see table 2) earth fault currents is said to be within 200-1000 A.

As stated above the method of system grounding has significant impact on the magnitude of earth fault currents and the ability to reduce transient over voltages in case of earth faults. One consideration when selecting system grounding is therefore to try to achieve the best compromise between reducing earth fault currents and reducing possible destructive transient over voltages.

Table 1 shows typical level of fault currents and voltage rises on healthy phases (50Hz) for different methods of system grounding in networks [1]-[4]. The level in table 1 is determined by the network impedance characteristics shown in table 2 [1]-[4].

Table 1, Characteristic fault currents and voltage rises of system grounding methods

Grounding method	Earth fault current [pu of 3-phase fault current]	Phase-earth voltage [pu of phase voltage]
Isolated	-	1.73 pu
Effective	> 0.6 pu	< 1.4 pu
Reactance	0.25-0.6 pu	<1.73 pu
Resonance	-	1.73 pu
Resistance	200-1000 A	<1.73 pu

Table 2, Impedance characteristics of system grounding types

Grounding method	X_0/X_1	R_0/X_1	R_0/X_0	R_0/X_{C0}
Isolated	(∞) - (- 40)	-	-	-
Effective	0 – 3	0 – 1	-	-
Reactance	3 – 10	0 – 1	-	-
Resonance	-	-	-	-
Resistance	0 – 10	30-60	≥ 2	≤ 1

3. THEORY FOR VOLTAGE RISE DUE TO SINGLE-PHASE TO EARTH FAULTS (ARCING GROUND) IN ISOLATED SYSTEMS

In a symmetrical, three-phase circuit the symmetrical components will be represented by three uncoupled equivalents for the positive sequence, negative sequence and zero sequence component.

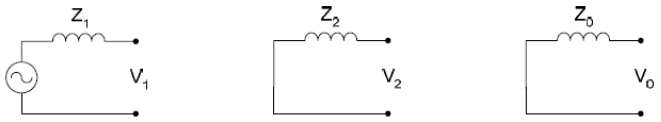

Figure 5. Symmetrical components, positive-, negative and zero sequence components

In short, in case of unsymmetrical faults e.g. single-phase earth faults, the three symmetrical components will be coupled and be represented by the equivalent shown fig. 6.

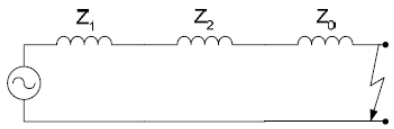

Figure 6. Equivalent for single-phase to ground fault

If the resistance in the network is ignored, the network zero sequence impedance will be mainly capacitive (as a consequence of the network capacitance to ground) and the positive and negative sequence impedances will be inductive (as a consequence of inductance in cables and transformers). If the fault impedance is assumed to be $Z_F = 0\ \Omega$, then the equivalent in figure 6 can be reduced to figure 7 in case of a single-phase to ground fault, where the fault arc is replaced by a circuit breaker.

It is seen, that the network positive- and negative sequence voltages now is represented by the voltages across the network reactance X_{1+2} and the zero sequence voltage V_0 is represented by the capacitance voltage.

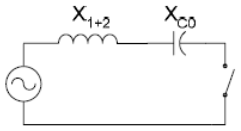

Figure 7. Simplified equivalent for single-phase to ground faults

Further the network zero sequence capacitance X_{co} will be much larger than the network inductance X_{1+2}. The earth fault current will therefore mainly be capacitive and lead the voltage by approx. 90°.

The non-linear circuit shown in figure 7 will do, that the zero sequence voltage and the phase-to-ground voltages at the two healthy phases will oscillate up to ±1 pu around the new 50Hz voltage (see figure 8, no. 1) until the transient oscillation is damped out. Within the first couple of ms after the fault has occurred the phase voltage on the two healthy phases can rise up to 2.73 pu. This phenomenon is verified by dynamic computer simulations later in section 4.

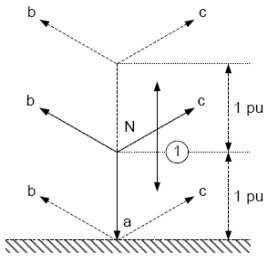

Figure 8. Transient oscillation in case of a single-phase to ground fault

When the arc current passes the natural current zero, the arc may extinguish, and the insulation potentially can re-establish the voltage withstand (the breaker at figure 7 will open). At the same time the zero sequence voltage is lagging the current by 90° and is at its maximum, i.e..up to 1 pu. The zero sequence voltage (the voltage across the capacitance in figure 7) – which actually means the isolated system is now "locked" with a new zero reference at 1 pu.

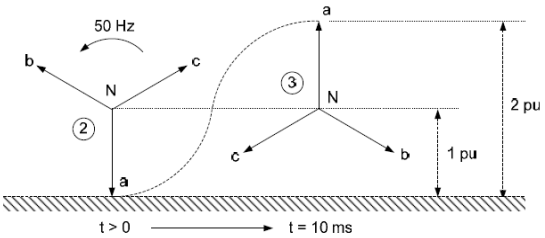

Figure 9. Voltage rise as a consequence of "locked" zero voltage

Within the next ½ period (10 ms) the faulted phase voltage will rise again – now up to 2 pu (see figure 9, no. 3).

If again assumed a fault re-ignition happens at voltage maximum ($V_a = 2$ pu), another transient oscillation can occur – now with a ± 2 pu oscillation for the zero sequence voltage and for the voltage at the healthy phases. This can result in very high transient oscillation on the healthy phases – theoretically now up to more than 3.5 pu.

These three steps (1-3) could theoretically go on forever. In practise the insulation in cables or transformers will break down at some point, creating a fault on a second phase which causes a protective CB trip and stop the ongoing voltage rise.

It appears above that if the zero sequence voltage can be discharged then the severe transient over voltages cannot build-up. This discharge must take place in the time span from the arc extinguish till the next voltage maximum on the (pre-) faulty phase (i.e. the time for risk of re-ignition). To ensure discharging an adequately resistance in the zero sequence system must be present. The decay of the zero sequence voltage will then be according to the below formula (1), where V_a is the phase to ground voltage before fault occurrence:

$$V_0(t) = V_a \cdot e^{\left(\frac{-t}{R_0 \cdot C_0}\right)} \qquad (1)$$

It can be seen that the lower the resistance the faster decay of the zero sequence voltage and subsequently the lower the transient over voltages. Obviously this is one of the important properties of a resistance grounded network.

4. SIMULATION OF VOLTAGE RISE AT SINGLE-PHASE TO GROUND FAULT IN ISOLATED SYSTEM

To verify the transient voltage oscillations described in section 3, dynamic simulations of single-phase to ground faults and re-ignition of single-phase to ground faults have been carried out (see figure 10).

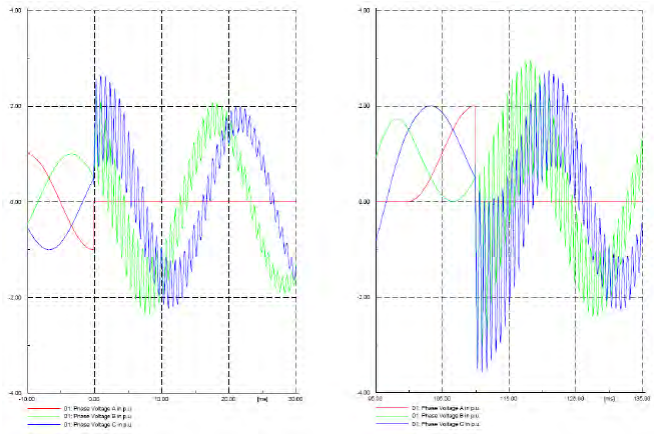

Figure 10. Simulation of transient voltage oscillations in case of single-phase to ground faults (left) and re-ignition of single-phase to ground faults (right).

The simulations show that the theoretical description of the voltage rise at single-phase earth faults is verified.

5. System Grounding in Wind Farms

Two different wind farms have been analysed – *A* and *B* [5]. The purpose of the analysis has been to analyse fault currents and transient voltage rises at single-phase earth faults. For each wind farm five different grounding methods has been analysed.

Dynamic simulations have been carried out using the DigSilent Power Factory computer simulation program.

5.1. Wind farm A (2 WT, 7.2 MW)

Wind farm *A* contains of two wind turbines of 3.6 MW each. The wind turbines are interconnected to a 1.5 km medium voltage cable grid.

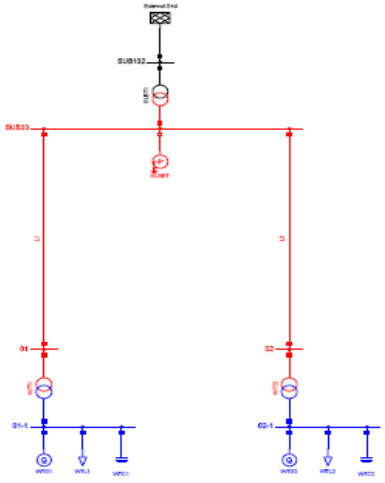

Figure 11. Wind farm A

Table 3 sums up the simulation impedance input values for the wind farm A substation earthing transformer (SUBET) and the impedance from transformer neutral to ground.

Table 3. Impedance characteristics of wind farm A

Grounding method	SUBET		Neutral impedance	
	R_0	X_0	R_N	X_N
Isolated	-	-	-	-
Effective	15 Ω	30 Ω	0 Ω	0 Ω
Reactance	15 Ω	300 Ω	0 Ω	0 Ω
Resonance	15 Ω	30 Ω	370 Ω	3.7k Ω
Resistance	15 Ω	30 Ω	95 Ω	0 Ω

Table 4 and table 5 sums up the impedance characteristics and earth fault currents and max transient phase voltage on the healthy phases in wind farm *A*. All values are measured at the wind farm substation medium voltage busbar.

Table 4. Impedance characteristics of wind farm A

Grounding method	X_0/X_1	R_0/X_1	R_0/X_0	R_0/X_{C0}
Isolated	(1.3 k)	-	-	-
Effective	3.6	1.8	-	-
Reactance	37	1.9	-	-
Resonance	(2.5 k)	(13 k)	(5.2)	(9.7)
Resistance	2.6	36	13.8	0.03

Table 5. Fault currents and transient over voltages of wind farm A

Grounding method	Earth fault current [faulted phase]	Max. phase voltage [healthy phase voltage]	
		Earth fault	Fault re-ignition
Isolated	6 A	2.7 pu	3.7 pu
Effective	1.3 kA	2.1 pu	2.0 pu
Reactance	0.2 kA	2.5 pu	3.5 pu
Resonance	0 A	2.6 pu	2.6 pu
Resistance	0.2 kA	2.1 pu	2.1 pu

In case of earth faults in wind farm A fault currents is found to be within the characteristic fault current values shown in table 1. Further transient over voltages is found to be up to 1 pu higher than the characteristic values.

In case of re-ignited earth faults transient over voltages for the effective-, resonance- and resistance grounding method is found to be at the level as the initial earth fault. For the isolated and reactance grounding method transient over voltages is found be in the range of 3.5-3.7 pu if an earth fault re-ignites. (It is known that 'fault re-ignition' in case of effective-, reactance- or resistance grounded systems may be somewhat hypothetically partly because of the size of the earth fault current (the arc will not extinguish) partly because protective relays usually will trip the faulty string instantaneous thereby preventing arcing faults. This comment applies also for case 5.2 below).

5.2. Wind farm B (20 WT, 72 MW)

Wind farm *B* contains of 20 wind turbines of 3.6 MW each. The wind turbines are interconnected to a 4.5 km medium voltage cable grid.

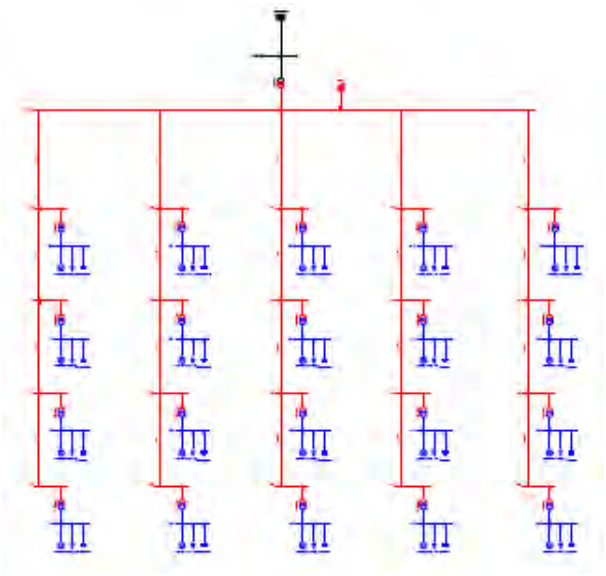

Figure 12. Wind farm B

Table 6 sums up the simulation impedance input values for the wind farm B substation earthing transformer (SUBET) and the impedance from transformer neutral to ground.

Table 6. Impedance characteristics of wind farm B

Grounding method	SUBET		Neutral impedance	
	R_0	X_0	R_N	X_N
Isolated	-	-	-	-
Effective	1 Ω	3 Ω	0 Ω	0 Ω
Reactance	1 Ω	3 Ω	0 Ω	0 Ω
Resonance	1 Ω	3 Ω	12 Ω	120 Ω
Resistance	15 Ω	30 Ω	15 Ω	0 Ω

Table 7 and table 8 sums up the impedance characteristics and earth fault currents and max transient phase voltage on the healthy phases in wind farm *B*. All values are measured at the wind farm substation medium voltage busbar.

Table 7. Impedance characteristics of wind farm B

Grounding method	X_0/X_1	R_0/X_1	R_0/X_0	R_0/X_{C0}
Isolated	(0.3 k)	-	-	-
Effective	2.7	0.9	-	-
Reactance	8.3	0.9	-	-
Resonance	-	-	-	-
Resistance	-	54	3.5	0.2

Table 8. Fault currents and transient over voltages of wind farm B

Grounding method	Earth fault current [faulted phase]	Max. phase voltage [healthy phase voltage]	
		Earth fault	Fault re-ignition
Isolated	0.2 kA	2.3 pu	3.7 pu
Effective	9.9 kA	1.7 pu	2.1 pu
Reactance	5.1 kA	2.1 pu	3.1 pu
Resonance	19 A	2.4 pu	2.7 pu
Resistance	0.8 kA	2.3 pu	2.4 pu

In case of earth faults in wind farm B fault currents is also found to be within the characteristic fault current values shown in table 1. Further transient over voltages is still found to be higher than the characteristic values in table 1.

Transient over voltages in the resistance grounded system caused by re-ignited earth faults only show a small increase compared to transient over voltages at the initial earth fault. For other grounding methods increases between 0.3-1 pu in case of earth fault re-ignition are observed.

In the isolated grounded system transient over voltages as high as 3.7 pu is possible in case of earth fault and earth fault re-ignition.

6. Conclusion

Throughout dynamic simulations two different wind farms have been analysed with respect to system grounding. For both wind farms it has been shown, that the best compromise for reducing earth fault currents and transient over voltages is obtained by low-resistance grounding of the internal medium voltage cable grid. Therefore low-resistance system grounding is recommended to be applied in wind farms with an internal medium voltage cable grid. The design must be in accordance with the impedance characteristic in table 2.

For the rare case where possibility of continuous operation of the wind turbines despite an earth fault has priority another grounding method like the high-resistance grounding method may be considered.

Even though resonance grounding from the perspective of the issue of this paper seems attractive this method has other disadvantages (risk of Ferro-resonance, more complex, and more expensive) which usually makes it not recommendable for wind farm collection grids.

Isolated system grounding is not recommendable due to risk of very high transient over voltages in case of single-phase earth faults followed by single-phase earth fault re-ignition.

References

[1] IEEE (Kelly, L. J. et al.), Recommended Practice for Grounding of Industrial and Commercial Power Systems, IEEE Green Book, IEEE std-142-1991

[2] IEEE, Guide for the Application of Neutral Grounding in Electrical Utility Systems – Part 1: Introduction, IEEE Std C62.92.1-2000, IEEE, 2001.

[3] ABB, Switchgear Manual, 10th Edition, 1999/2001

[4] S. Vørts, Elektriske fordelingsanlæg, 4. udgave, 1968

[5] P. Hansen. Valg af systemjording i vindmølleparker (System grounding i wind farms, report only in Danish), May 2006

Modeling of the energizing of a wind park radial

Tarik Abdulahović [1*)], Torbjörn Thiringer [1**)]
[1)] Division of Electric Power Engineering, Department of Energy and Environment,
Chalmers University of Technology, 412 96 Gothenburg, Sweden
[*)] e-mail tarik.abdulahovic@chalmers.se
[**)] e-mail torbjorn.thiringer@chalmers.se

***Abstract*— This paper presents measurement and modeling of the energizing of a wind park radial. The measurements in this paper are taken from the Utgrunden wind park that consists of seven wind turbines each of $1.5\ MW$ rated power. This park is connected to the Öland $55\ kV$ grid at the Degerhamn station. The wind turbines in the Utgrunden wind park are of the pitch-regulated doubly-fed induction generator (DFIG) type.**

The transient voltage and the energizing current graphs are presented and both active and reactive powers are analyzed as the radials to the wind park is connected.

Furthermore, the model of the Utgrunden wind park radial is built using PSCAD/EMTDC software. For the cable model, the frequency-dependent (phase) model built in model is used. A built-in model with the saturation modeling is simulated for the purpose of the transients analysis and the results are compared with measurements.

The results show that the measured resonance frequency agrees well with the measurements while the damping is underestimated in the simulations.

***Index Terms*— wind turbine, transient, cable energizing, transformer energizing**

I. Introduction - Utgrunden wind park

The Utgrunden wind park (WP) is a wind park located in southern Kalmarsund in Sweden with a rated power production of $10\ MVA$. The WP is connected to the $55\ kV$ grid on Öland at the Degerhamn substation. The Utgrunden WP consists of 7 wind turbines (WT) each rated at $1.5\ MVA$. The Utgrunden WP is placed $8\ km$ west of Öland and the power is transported using the sea cable. A simplified presentation of the Utgrunden WP can be observed in Figure 1.

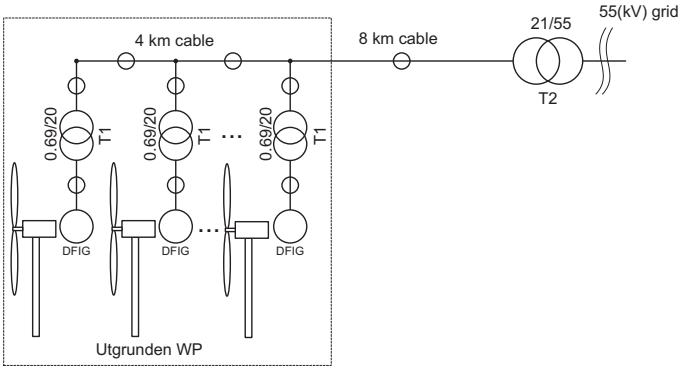

Fig. 1. Utgrunden WP, sea cable and 21/55 kV/kV substation

The WTs used at Utgrunden are of doubly-fed induction generator (DFIG) type.

The cable used in the Utgrunden WP is a $24\ kV$ XLPE cable. The length of the cable from the WP to the $21/55\ kV$ transformer in the Degerhamn substation is $8\ km$ and the park is about $4\ km$ long. The sea cable has a rated current of $275\ A$. The other important parameters of the cable such as the capacitance, inductance and resistance per unit length are:

$$\begin{array}{lcl} C_{km} & = & 0.281\ \mu F/km \\ L_{km} & = & 0.352\ mH/km \\ R_{km} & = & 0.14\ \Omega/km. \end{array}$$

In order to use these parameters in the advanced PSCAD/EMTDC cable model, the dimensions of the cable have to be determined. Observing the data sheets in ABB's "XLPE Cable Systems - User's guide" a perfect match could not be found. The cable with electrical parameters that is the closest match, is a $24\ kV$ cable with $240\ mm^2$ cross-section of the conductor. The outer diameter of this cable matches to the outer diameter of the cable used in the Utgrunden WP. The parameters of this cable such as the capacitance and inductance per unit length are:

$$\begin{array}{lcl} C_{km} & = & 0.31\ \mu F/km \\ L_{km} & = & 0.35\ mH/km. \end{array}$$

For the cable length of $12\ km$ the total cable capacitance, inductance and reactances are calculated to be:

$$\begin{array}{lcl} C_{12km} & = & 3.72\ \mu F \\ L_{12km} & = & 4.2\ mH \\ X_C & = & 855\ \Omega \\ X_L & = & 1.32\ \Omega. \end{array}$$

In the WTs, the $24\ kV$ XLPE cable is connected to the local WT transformer which transforms the $21\ kV$ voltage level to $690\ V$ which is appropriate for the induction generators. The rating of the transformer is $1.6\ MVA$ with an assumed short-circuit impedance of $6\ \%$. A calculation of the base impedance at the $20\ kV$ bus gives the value of $Z_{bT1} = 250\ \Omega$ and the reactance and inductance of the transformer seen from the $20\ kV$ bus are $X_{T1} = 15\ \Omega$ and $L_{T1} = 47\ mH$.

The transformer in the Degerhamn substation has a Y/Y winding connection with a $21kV/55kV$ ratio and a rated power of $12\ MVA$. On the high-voltage side of the transformer, there is a tap changer used for the adjustment of the transformer ratio with steps of $\pm 1.67\ \%$. The primary voltage can be adjusted in 8 steps. The base impedance referred to the $21\ kV$ side of the transformer is $Z_{bT2} = 36.75\ \Omega$. The short circuit impedance is $Z_{T2\ pu} = 0.4 + j6\ \%$ or $Z_{T2} = 0.147 + j2.2\ \Omega$

$$\begin{array}{lcl} X_{T2} & = & 2.2\ \Omega \\ R_{T2} & = & 0.147\ \Omega. \end{array}$$

The inductance of the transformer seen from the low-voltage side is $L_{T2} = 7\ mH$.

The 55 kV grid has a short-circuit power of 126 MVA with a grid impedance angle of 73°. The short-circuit impedance referred to the 55 kV grid side is $Z_{gr} = 24\ \Omega$. Taking into account the value of the impedance angle, the short circuit reactance and resistance of the 55 kV grid connected in the Degerhamn substation is:

$$\begin{aligned} X_{gr} &= 23\ \Omega \\ R_{gr} &= 7.02\ \Omega. \end{aligned}$$

This gives the inductance and resistance of the 55 kV grid to be $L_{gr} = 73\ mH$ and $R_{gr} = 7\ \Omega$. Referred to the 21 kV voltage level, the inductance of the grid is $L_{gr(21)} = 10.6\ mH$ and the resistance is $R_{gr(21)} = 1.02\ \Omega$

II. Resonance in the Utgrunden wind park

The Utgrunden WP presented in a single-line diagram can be seen in the Figure 2.

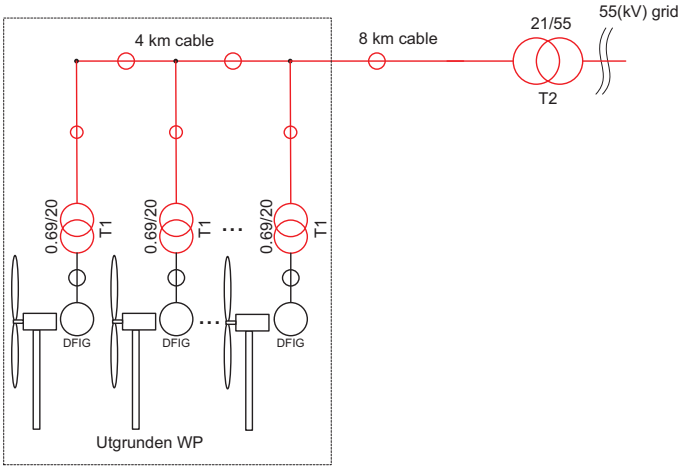

Fig. 2. Simplified single phase diagram

As the switch of the transformer T2 is closed (on the 21 kV side) the cable and the WT transformers are energized. The capacitance of the cable is dominating in the system and the other capacitances are neglected. The calculated resonance frequency, taking into account the total inductance of the system consisting of the T2 transformer inductance L_{T2}, the cable inductance $L_{12\ km}$, the inductance of the 55 kV grid referred to the 21 kV level and the total system capacitance consisting of the cable capacitance $C_{12\ km}$ is :

$$f_{res} = \frac{1}{2\pi\sqrt{C_{12km}(L_{12km} + L_{T2} + L_{gr(21)})}} = 559\ Hz \tag{1}$$

III. Measurements and analysis of cable energizing in Utgrunden

In Figure 3 and Figure 4 the voltage and current of T2 is presented.

After the cable has been energized, the voltage rises slightly due to the reactive power generated by the cable capacitance. The amount of the injected reactive power and the rise of the voltage can be seen on Figure 5 and Figure 6

A zoom of the voltages and currents are shown in Figure 7 and Figure 8

In these figures the resonance frequency of approximately 794 Hz can be observed. The calculated resonance frequency

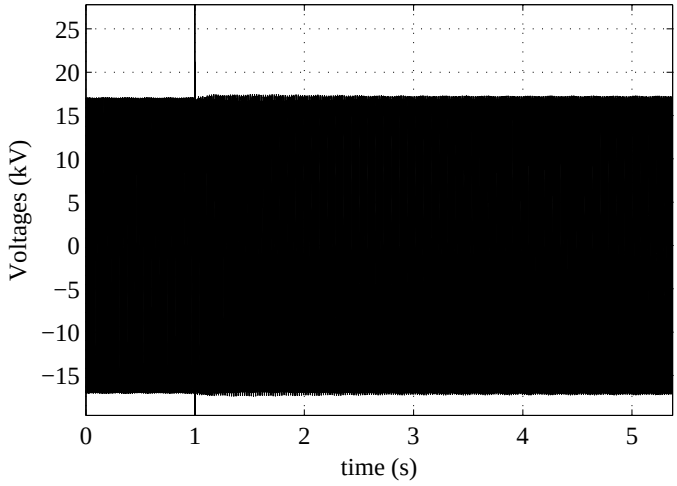

Fig. 3. Phase volgates during energizing

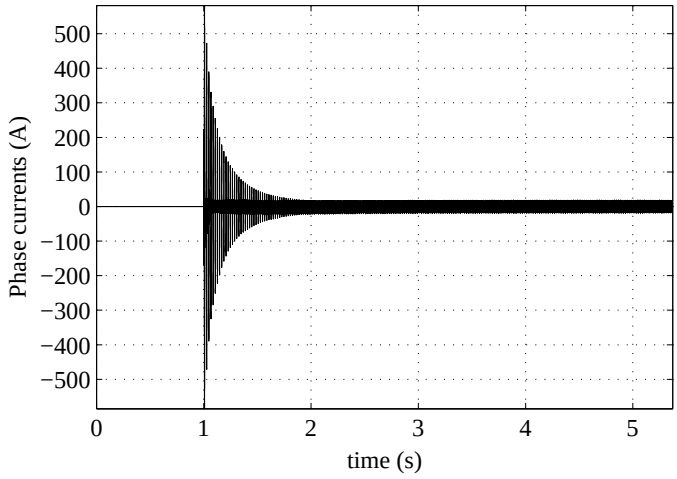

Fig. 4. Phase currents during energizing

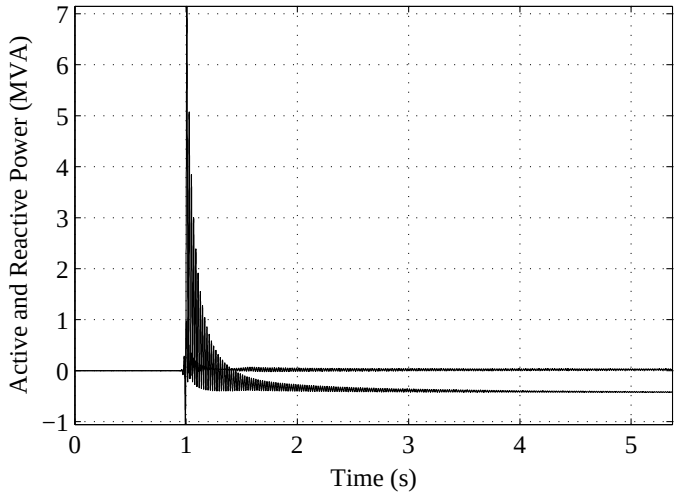

Fig. 5. Active and reactive power when cable is energized

differs from the measured frequency for 235 Hz. The calculation of the resonance frequency is quite sensitive to small deviation of capacitances and inductances present in the system and such deviation was expected given the difficulties in defining cable parameters.

In the very beginning of the transient, between the time instants of $t = 0.0065\ s$ and $t = 0.012\ s$, the current transient

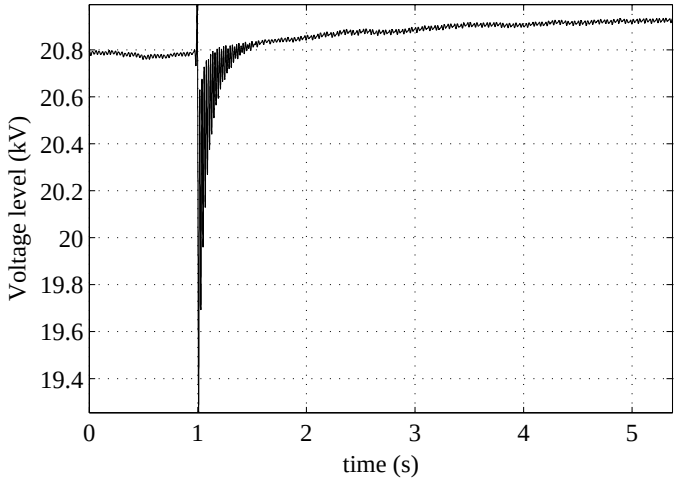

Fig. 6. Voltage level when cable is energized

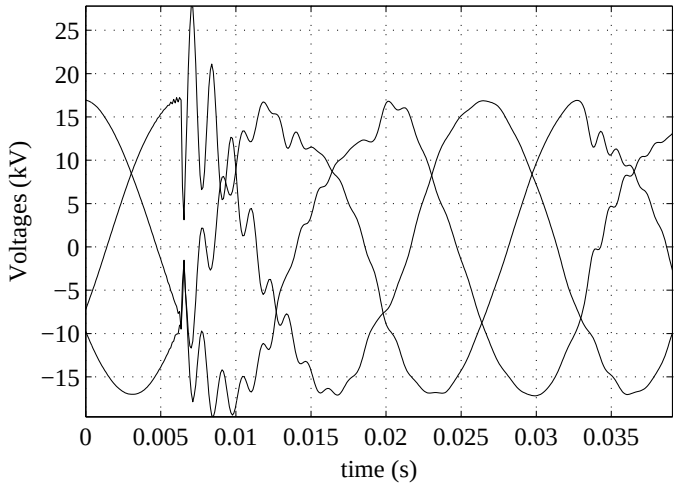

Fig. 7. Phase voltages during transient

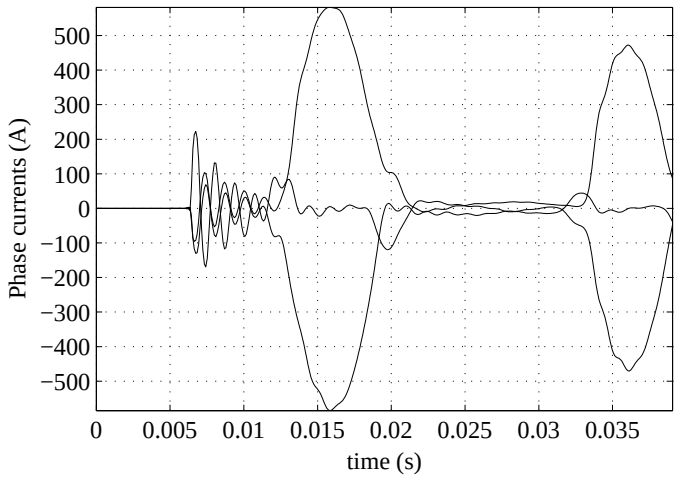

Fig. 8. Phase currents during transient

caused by the cable energizing can be seen in Figure 8. After the cable is energized, the transformer becomes heavily saturated drawing strongly distorted currents with the peak value of $580\ A$. The current caused by the T2 transformer energizing is shown more in detail in Figure 9.

After a time period of $1\ s$ the current transient has ceased and only the no-load capacitive current caused by the

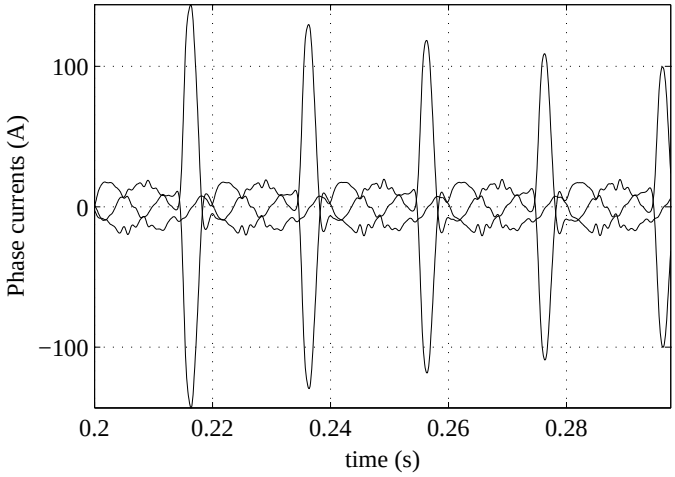

Fig. 9. Phase currents during the transformer energizing transient

cable capacitance remains in the system, which is shown in Figure 10.

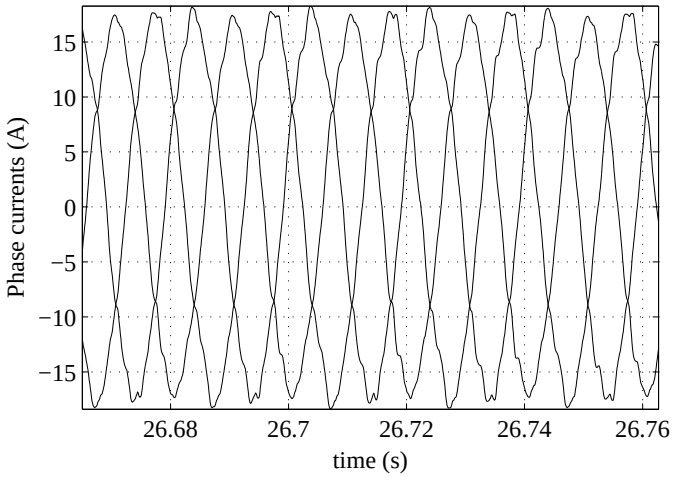

Fig. 10. Steady-state phase currents - no-load current

Now, the cable and transformer energizing of the Utgrunden WP is simulated using PSCAD/EMTDC. The system is modeled using master library components. The test is performed by closing the breaker on the $21\ kV$ side of the T2 transformer. By closing the breaker, the energizing of the cable and of the transformers in the WT's is initiated.

In Figure 11 and Figure 12 the voltage and current of T2 is presented.

During the energizing of the cable and the transformers the positive sequence voltage drops. After the cable has been energized, the voltage rises slightly due to the reactive power generated by the cable capacitance. The initial voltage drop of the positive sequence voltage and the voltage rise after the cable is energized can be seen on Figure 13

A zoom of the voltages and currents are shown in Figure 14 and Figure 15

In these figures the resonance frequency is $600Hz$ and matches the calculated resonance frequency.

In the very beginning of the transient, between the time instants of $t = 0.0065\ s$ and $t = 0.012\ s$, the current transient caused by the cable energizing can be seen in Figure 15. After the cable is energized the transformer becomes heavily saturated producing strongly distorted and very high currents

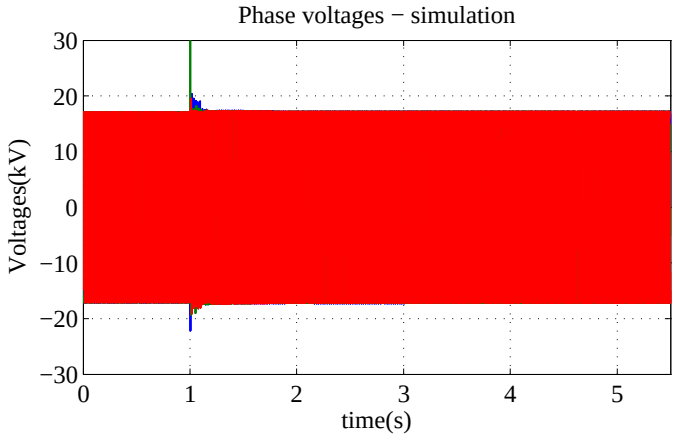

Fig. 11. Phase volgates during energizing - simulation

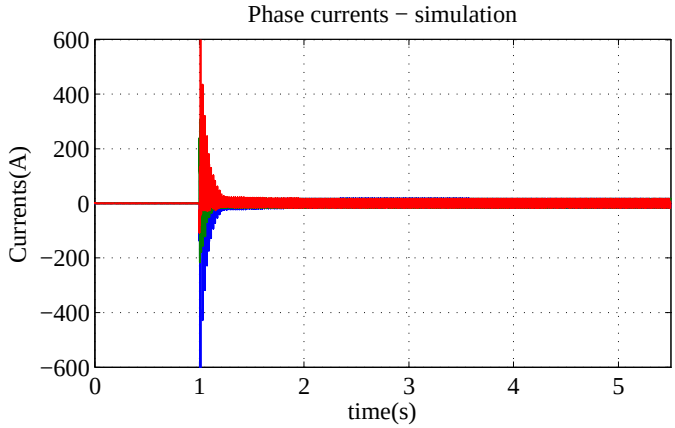

Fig. 12. Phase currents during energizing - simulation

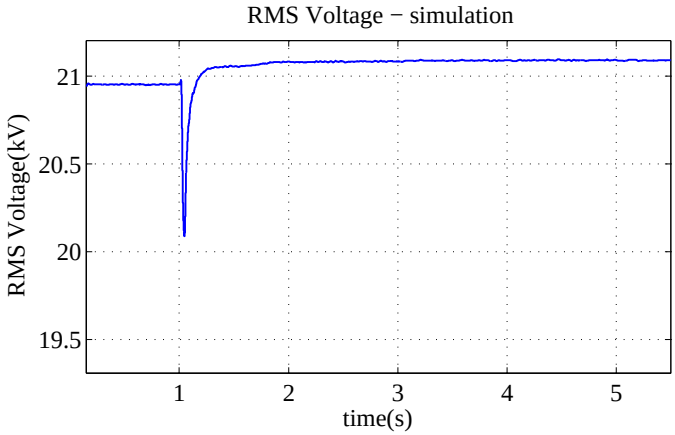

Fig. 13. Voltage level when cable is energized - simulation

with the peak value about $600\ A$.

Measured resonance frequency in the PSCAD/EMTDC simulations varies between $555\ Hz$ and $593\ Hz$ depending on the cable model. This is in agreement with the calculated resonance frequency given by (1).

There is a difference in damping between the simulated and measured results. Since the frequency of the transient is much higher than the power frequency, the damping is effected by skin effect. The increased damping due to the skin effect is modeled only for the cable model, while for the transformers and the grid the skin effect is neglected. Improvement in the simulations might be made by more accurate modeling of the skin effect leading to a better agreement between the measurements and simulations.

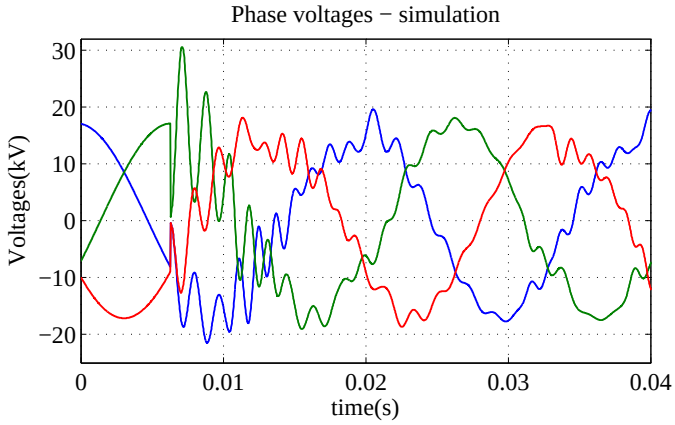

Fig. 14. Phase voltages during transient - simulation

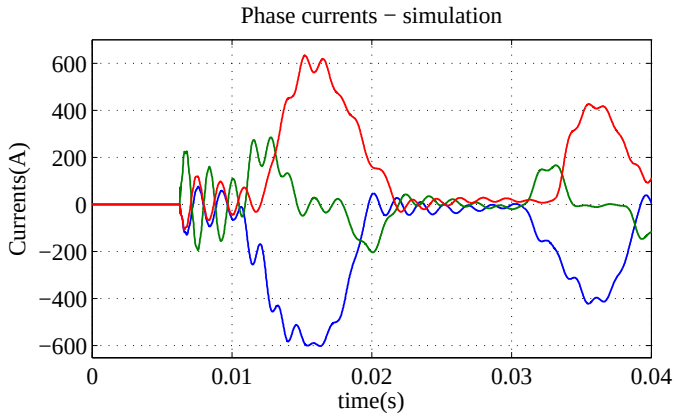

Fig. 15. Phase currents during transient - simulation

ACKNOWLEDGEMENT

The financial support provided by the Swedish National Energy Administration, GE Wind, Energimyndigheten and Vindforsk is gratefully acknowledged.

REFERENCES

[1] *Research program of the Utgrunden demonstration offshore wind farm, Final Report: Part3, WP2*, Technical Report, Chalmers University of Technology/Statens energimyndighet P11518-2, 2005

Bulk Energy Transport Assessment on Wind Power

Muhamad Reza[1*)], Alexandre Oudalov[2**)]
[1)] ABB AB, Corporate Research, Forskargränd 7, SE-721 78, Västerås, Sweden
[*)] phone +46 21 324 274, e-mail muhamad.reza@se.abb.com
[2)] ABB Switzerland Ltd., Corporate Research, Segelhof 1, Dättwil
[**)] phone +41 58 586 8031, e-mail alexandre.oudalov@ch.abb.com

Abstract — Bulk energy transport possibility for wind energy sources is only either by means of wire technology (HVAC or HVDC transmission) or pipeline using hydrogen (H2) as the transport media. This paper compares these transport alternatives. A straightforward cost model ("BET model") is used to address the relevant combinations of problem scenarios and technologies, and embraces common practice techniques for life cycle cost analysis. Taking into account overall energy efficiency and technology maturity, wire transmission with HVDC technology demonstrate a significant improvement over the hydrogen transport for bulk energy transport of wind power.

Index Terms — Bulk Energy Transport (BET), Hydrogen, Life Cycle Cost Analysis, Wire Technologies.

1. Introduction

1.1. Bulk Energy Transport

Bulk Energy Transport (BET) is a move of large raw/electric energy quantity (>500 MW equivalent) over long distances (>100 km). Table 1 illustrates a variety and applicability of different alternative bulk energy transportation scenarios, which have different levels of efficiency, reliability, and environmental safety.

Classical primary energy resources such as coal and – to some extent – gas can be moved directly by railroad, truck, pipeline, barge, vessel or conveyor. A remark should be made that oil is not widely used for electricity generation. Otherwise, energy obtained from primary resources can be transported as a liquid or gaseous fuel or as electricity.

For the classical primary energy sources, the transport mode used depends upon the amount to be moved, haul distance, capital and operating costs for the transport system, plus flexibility, reliability, and responsiveness to changes in end-user demand [1], [2]. An additional factor affecting the selection of a transportation mode is the resulting environmental impact: air pollution, water pollution, solid waste, noise levels, traffic congestion, and safety aspects [3].

For renewable energy sources such as wind, solar, hydro and geothermal, the transport possibility is only either by means of wire technology (HVAC or HVDC transmission) or pipeline using hydrogen (H2) as the transport media [4].

The illustration of the alternative technologies of bulk energy transportation is shown in Table 1.

1.2. Bulk Wind Energy Transport

Nowadays, many wind power plants (parks) are built or planned to generate hundreds of MWs up to GWs of electricity power. Tens or even hundreds of wind turbines with 1-5 MW capacity per turbine will be required in such wind park located in areas with strong wind potential [5]. Considering the size and the number of the required wind turbines, such wind park must be built in areas with no (or very low) population. Globally, locations that are fulfilling the characteristics of having strong wind potential and no (or very low population) may be found offshore or at remote areas on-land. The first potential wind park location, the offshore, will be the case e.g. in Europe. In this case, the wind parks will be located at a distance of a couple of tens or some hundreds of km from the load centers. The other potential wind park location, at remote areas on-land, will be the case e.g. in North America, China or India. In this case, the wind parks can be located at a distance of hundreds or even thousands of km from the load centers. Figure 1 illustrates some of the potential locations in the world, for building the wind parks with hundreds of MWs or GWs power capacity.

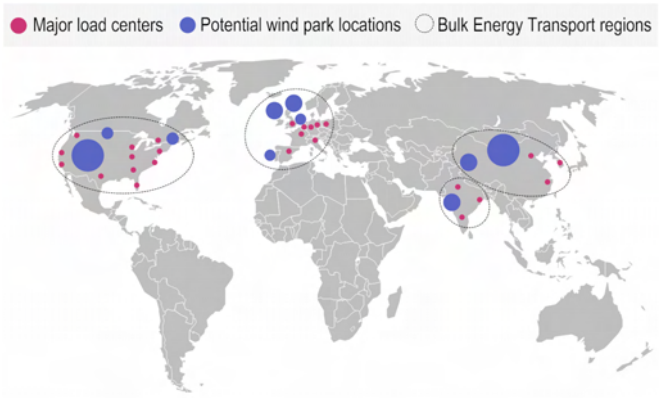

Figure 1. Some potential locations for bulk wind energy transport (Red ovals/circles = load centers, blue circles = areas with strong wind population and low population, black ovals = potential areas for bulk wind energy transport).

When the wind parks are built offshore, there is only one alternative technology to transport the electricity to the load center that is by using wire technology (submarine cables). However, when the wind parks are built at remote areas on-land there may be other alternative to transport the generated electricity, for example, by using pipeline with hydrogen (H_2) as the transport media, provided that there are sufficient water resources close to the wind parks. In this paper, alternative technologies for bulk wind energy transport from wind parks built at remote areas on-land will be assessed. Two basic technologies will be compared, namely: transporting bulk wind energy by means of wire technology (overhead lines HVAC or HVDC) or by means of pipeline using hydrogen (H_2) as the transport media.

A hypothetical case of a wind park built at remote area on-land will be defined. The assessments will be performed by using the "Bulk Energy Transport (BET) Model" that was constructed to address all relevant combination of problem scenarios and technologies of bulk energy transport (Table 1) including the particular case (bulk wind energy transport) defined in this paper [6].

Table 1. Alternative Technologies of Bulk Energy Transportation

Symbol	Wire	Rail	Barge	Vessel	Pipe	Truck	Conveyor
Coal	HVAC, HVDC	Unit trains	Tows	Coal vessel	Slurry, coal, logs, synthetic gas	Impractical for distances > 100 km	Impractical for distances > 50 km
Gas		Uneconomical		LNG	Overland, underground		Physically impossible
Oil	Not widely used for electricity generation						
Renewable Energy Sources		Physically impossible			H_2	Physically impossible	

2. BULK ENERGY TRANSPORT (BET) MODEL

A Bulk Energy Transport Model ("BET Model") is constructed to address all relevant combinations of problem scenarios and technologies (All alternative primary energy sources and the transport technologies listed in Table 1), and embraces common practice techniques for life cycle cost analysis with monetization of externalities and supporting sensitivity analysis [6].

The "BET Model" is implemented as a spreadsheet simulation tool for a comparative analysis of different bulk energy transport scenarios. It can be used in the context of existing planning and decision making instruments, such as integrated resource planning, technology assessment, power plant sitting, etc. In this paper, we examine the options for a bulk wind energy transport using this "BET Model" by providing parameters and assumptions that correspond to the bulk wind energy transport.

Figure 2 shows the main block of the BET Model. As it basically design to assess all relevant combinations of bulk energy transport scenarios, a considered bulk energy transport analysis framework consists of two major options, namely: electric energy transmission and primary energy resource transport (see Figure 2).

For the case of bulk wind energy transport on-land, the primary energy resource (wind) cannot be transported. Thus, the first option will be to transport the bulk wind energy as electric energy transmission. However, by using hydrogen (H_2) as the transport media, bulk wind energy assessment can be done by using the second option of BET Model "primary energy resource transport" with some adjustments. Please note that these adjustments have been equipped within the BET Model. Therefore, assessing a scenario of bulk wind energy transport by means of hydrogen via pipelines can be done by providing parameters and assumptions of the scenario as input to the BET Model.

The detail of the cost calculation within the BET Model can be found in Appendix A. A remark should be made that BET Model enables the calculation of externality cost. The externality cost is all costs that can be potentially applied to any BET option in the future. In this paper however, the externality implication is not take into account. The assessment for the bulk wind energy transport options are based only on the annualized total cost that consists of the capital cost and the operating cost.

3. TEST CASE

3.1. Scenarios

This section illustrates results of a comparative analysis of bulk wind energy transport scenarios defined according to state of the art technology and typical use on-land (Figure 3). The selected scenarios are related to a transportation of energy from a wind park built in a remote are on-land to the load center and as following:

- Wind energy by wire technology AC.
- Wind energy by wire technology DC.
- Wind energy by hydrogen and pipeline.

A remark should be made that in the scenario of wind energy by hydrogen and pipeline, a sufficient water resource (to be converted into hydrogen with electrolysis process) is assumed to be available close to the wind park.

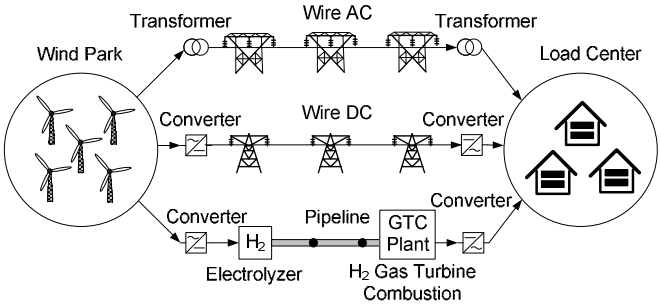

Figure 3. Bulk wind energy transport scenarios

In this test case a functional unit of the analysis is to transport an average of 1000 MW electricity received at the load center (***BET_P*** = 1000 in the BET Model, see Appendices A and B) over 1000 km (***BET_D*** = 1000 in the BET Model, see Appendices A and B) in distance. We also assume that:

- All required data on capital and operating costs are available (Appendix B)
- Electric transmission and pipeline do not exist and must be built.
- Externality cost is not implied.

Considering the average power of the wind park, the following assumptions are taken:

- The wind park has a capacity factor of 25%.
- No energy storage system is installed at any of the scenario. Therefore, the transport infrastructure for each option is designed for the maximum installed capacity of the wind park.

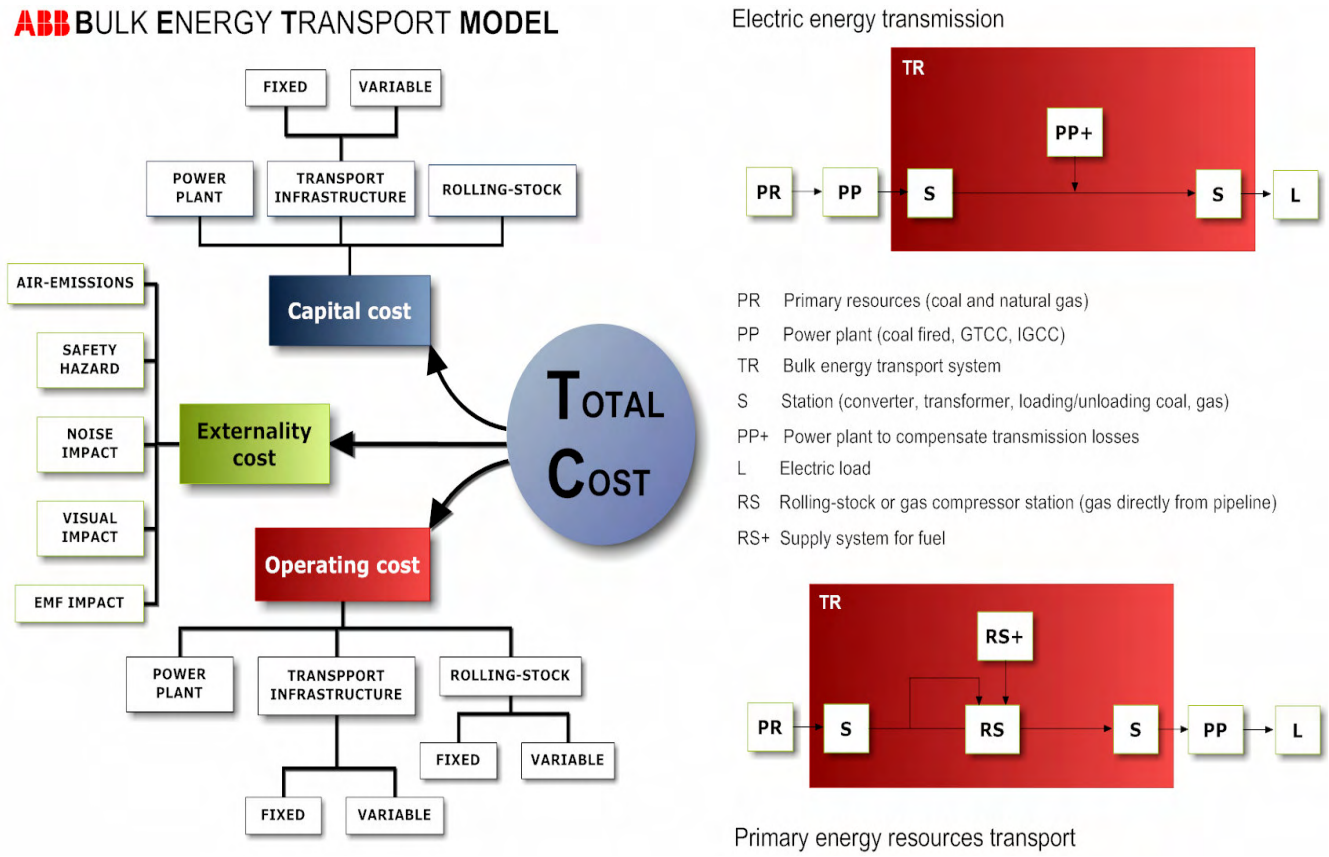

Figure 2. Main blocks of the BET Model

We consider a capital cost of both power plant and transport infrastructure as annualized capital cost. To accommodate the fluctuation in power generated by the wind park, the transmission lines (in scenarios using wire technologies) are rated at the maximum power. For the Wind energy by hydrogen and pipeline scenario we assume that the pipeline can flatten the power fluctuation and therefore the gas turbine power plant is rated at the received power at the load center (1000 MW).

3.2. Results

Simulation results are reported in Figure 3 to Figure 5. Figure 3 shows a summary of annual costs for different wind energy transport options in the test case, with:

- "AC OH 750 kV" refers to the scenario of transporting wind energy by wire technology with 750 kV AC overhead transmission lines.
- "DC OH 600 kV" refers to the scenario of transporting wind energy by wire technology with 600 kV DC overhead transmission lines.
- "Pipe H_2" refers to the scenario of transporting wind energy by hydrogen pipeline. Here, hydrogen (H_2) is produced from water with electrolyzer using electricity generated by the wind farms. The hydrogen is then transmitted via pipeline and finally it is converted into electricity by means of a gas turbine power plant close to the load center.

Pleas note that fFor better observation, the annual operating and maintenance cost from Figure 3 is shown separately in Figure 4. Figure 5 illustrates the electricity cost at the load center including generation and energy transport.

As shown in Figure 3, annual capital cost is the most dominant element in the total annual cost of each bulk wind energy transport option while the annual operating and maintenance cost is insignificant (very low). This is because the annual operating and maintenance cost include only the maintenance cost while no operation cost is considered (no fuel cost is considered). Any auxiliary energy consumption of power plant or transport infrastructure (e.g. compressors in the wind energy by hydrogen and pipeline scenario) will result as an increase in the installed (nominal) capacity of the wind park. Therefore, the cost for the auxiliary energy consumption will appear in the power plant capital cost instead of in the annual operating and maintenance cost.

3.3. Analysis

The annualized capital cost for transporting wind energy by hydrogen pipeline is the most expensive among all options. The capital cost for power plant for transporting wind energy by hydrogen pipeline is much higher than the wire technology option because of two reasons.

Firstly, in addition to the wind power plant, transporting wind energy by hydrogen pipeline requires extra electrolyzer and gas turbine power plants. Secondly, the overall energy efficiency of converting electricity (generated by the wind park) into hydrogen (by means of water electrolysis) and then again into electricity (by means of gas turbine power plant) is very low, i.e. around 30%. Therefore, after overrating the wind park to accommodate power fluctuations, the wind park must be overrated more to accommodate this low energy efficiency. On the other hand, wire technologies (especially in case of DC) can easily reach energy efficiency of more than 90% from the electricity generated by the wind

park, since there is no conversion of electricity into other form of energy until it is delivered to the load center and the total losses in the converters (in case of DC), the transformer (in case of AC) and the lines for 1000 km are less than 10%.

Moreover, the extra plants needed for transporting wind energy by hydrogen pipeline (i.e. electrolyzer and gas turbine power plants) require more maintenance hence operating and maintenance cost (see Figure 4).

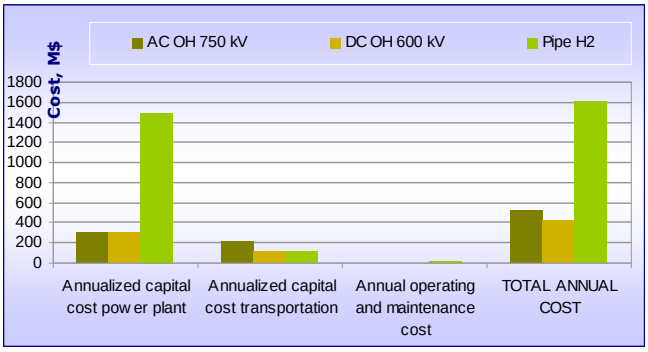

Figure 3. Summary of annual costs

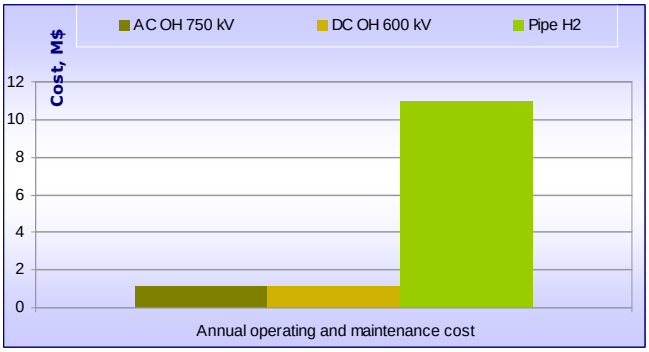

Figure 4. Annual operating and maintenance cost

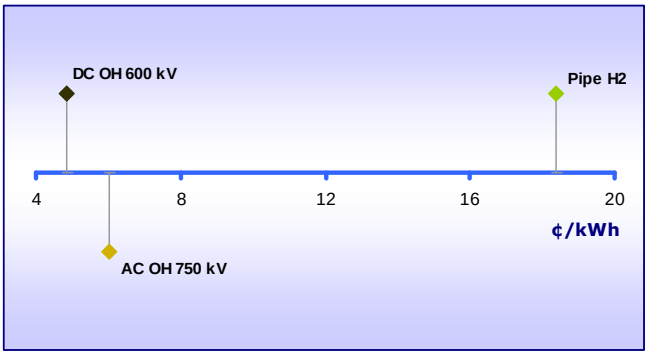

Figure 5. Electricity cost at the load center

4. Conclusion

The results in the test case show that bulk wind energy transport with HVDC overhead transmission line is more advantageous than transporting the bulk wind energy with HVAC overhead transmission line or with pipeline using hydrogen as the transport media.

Moreover, the results lead to the following main conclusions:

- Ranking of the bulk wind energy transport systems mainly depends on the annualized capital cost of the power plant.
- Overhead DC line offers the cheapest electricity cost.
- Transporting bulk wind energy by hydrogen pipeline results in the most expensive capital and operating costs hence the electricity cost.

A. Appendix A: Bulk Energy Transfer (BET) Tool

An annualized total cost of each transport option TC and cost of electricity delivered to the load centre ELC are calculated as (1) and (2) correspondingly.

$$TC = CC + OC + EC \quad (1)$$

$$ELC = \frac{TC}{BET\_P * 8760} \quad (2)$$

A.1. Capital cost

Capital cost is needed to bring a facility to commercially operable status and is one time expense, although payment may be spread out over many years. It includes all costs linked to production, construction and decommissioning of energy transport infrastructure.

A.1.1. Generation

The power plant capital cost is proportional to the power plant capacity which differs for each energy transport scenario due to the plant characteristics and the additional power required to compensate losses. The amount of additional capacity and primary energy resources is obtained from the loss calculation. The total energy transport system efficiency has fixed and variable parts with regard to the transport distance BET_D. The fixed part is measured in percent and includes either losses of primary energy resources during loading/unloading of rolling-stock or electric losses in converter and transformer stations at both ends of energy transport route. The variable part is measured in percent per 1000 km of energy transport route and includes energy losses during transportation such as coal lost due to car shaking, gas taken from a pipeline to run compressors, electric losses in conductors, etc.

A.1.2. Transport infrastructure

The capital cost of the energy transport infrastructure consists of fixed and variable parts with regard to the energy transport distance BET_D. The fixed part corresponds to the cost of primary energy resource loading/unloading facilities or converter and transformer stations at both ends of energy transport route. The variable part corresponds to the cost of transport route such as rail track, pipeline or high voltage overhead line or cable. The economy of scale in energy transport systems lowers the costs if the transport systems use the full capacity, especially for railroad, i.e. spreading the capital cost of transport infrastructure over more shipments of primary energy resources would decrease the cost of electricity delivered to the load centre.

A.1.3. Rolling-stock

The capital cost of rolling-stock can be a significant part of the total capital cost of energy transport systems based on railroad and ship transportation. It depends upon the number of circulating rolling-stock to satisfy uninterruptible delivery of primary energy resources from their location to the power plant in the vicinity of the load centre to generate BET_P, The number of circulating rolling-stock depends upon the number of movers (e.g. a number of locomotives per unit train, tow boats per tow, etc.) and units (e.g. the number of

hopper cars per unit train, barges per tow, etc.) in a single rolling-stock.

A.2. Operating cost

Operating cost is the recurring expenses needed to operate the energy transport facility. It includes all costs linked to primary energy resources production and transportation, power generation and transmission, compensation of losses, land use taxes, etc.

A.2.1. Generation

The power plant operating cost is the cost required to produce BET_P. Additional operating cost which is linked to a generation needed to cover electric losses is added to the transport infrastructure operating cost.

A.2.2. Transport infrastructure

The operating cost of energy transport infrastructure consists of fixed and variable parts with regard to the energy transport distance BET_D. The fixed part is mainly depends on the amount of transported energy BET_P and includes both: 1) cost which is required to cover the electric losses in converter and transformer stations or the lost primary energy resources during loading and unloading of rolling-stock; 2) maintenance cost of the fixed transport infrastructure. The variable part is the function of the energy transport distance BET_D. It consists of both: 1) cost of generating an additional electric power which is required to cover the electric losses in conductors or lost of primary energy resources during transportation; 2) maintenance cost of the variable transport infrastructure.

A.2.3. Rolling stock

The operating cost of rolling-stock also consists of fixed and variable parts with regard to the energy transport distance BET_D. The fixed operating cost is related to maintenance of rolling-stock. The variable operating cost is mainly depends on the price of diesel fuel consumed by locomotives and ships. An analysis of different studies shows that, on the average, water carriers consume 6.8 liters and rail transport 6.4 liters of diesel fuel per ton of primary energy resources moved over 1000 km [7].

B. APPENDIX B: NOMENCLATURE

All the data have been collected from scientific publications, data bases, etc. and publicly available on internet. Detail data are listed in Table B.1.

REFERENCES

[1] I. Knoepfl. A Framework for Environmental Impact Assessment of Long-distance Energy Transport Systems. International Journal on Energy vol. 21, No. 7/8 1996, pp. 693-702.

[2] A. Clerici, A. Longhi. Competitive Electricity Transmission System as an Alternative to Pipeline Gas Transport for Electricity Delivery. In Proc. 17th World Energy Congress. Houston, Texas, 1998.

[3] J. Bergerson, L. Lave. Should We Transport Coal, Gas, or Electricity: Cost, Efficiency, and Environmental Implications. Environmental Science & Technology vol. 39, No. 16 2005 pp. 5905-5910.

[4] F. Trieb. Trans-Mediterranean Interconnection for Concentrating Solar Power. Final Report Federal Ministry for the Environment, Nature Conservation and Nuclear Safety Germany, June 2006.

[5] Global Wind Energy Council. Global Wind Energy Outlook 2006, September 2006.

[6] A. Oudalov, M. Reza. Externality Implication on Bulk Energy Transport. In Proc. 27th United States Association of Energy Economics Conference. Houston, Texas, September 16-19, 2007.

[7] S. C. Davis. Transportation Energy Databook, Edition 19. Center for Transportation Analysis, Oak Ridge National Laboratory, U.S. Department of Energy, 1999.

Table B.1. Alternative Technologies of Bulk Energy Transportation

Parameter	Unit	Description	Value
BET_D	Km	Transport distance between a location of primary resources and load center	1000
BET_P	MW	Power delivered to the load center	1000
CC_PP_total	$/KW	Total capital cost factor of power plant	1000 (wind power plant), 500 (gas turbine power plant), 700 (electrolyzer)
CC_TR_fix_total	$/MW	Total capital cost factor of fixed transport infrastructure	50000 (AC-OH), 170000 (DC-OH), 5000 (Pipeline)
CC_TR_var_total	$/MW	Total capital cost factor of variable transport infrastructure	3000000 (AC-OH), 1500000 (DC-OH), 1500000 (Pipeline)
CRF		Capital recovery factor	0.073
dRate	%	Discount rate	6
η_{pp}	%	Power plant efficiency	65 (electrolyzer), 60 (gas turbine power plant)
η_{TRfix}	%	Fixed transport system efficiency	1 (AC-OH), 1.7 (DC-OH), 0 (Pipeline)
η_{TRvar}	%/1000 km	Variable transport system efficiency	5 (AC-OH), 4 (DC-OH), 1.9 (Pipeline)
OC_PP_total	$/MWh	Operating cost power plant total	0.5 (wind park), 1.5 (electrolyzer), 3 (gas turbine power plant)
OC_TR_fix_total	$/MWh	Fixed operating and maintenance cost factor of transport infrastructure	0.053 (AC-OH), 0.077 (DC-OH), 0 (Pipeline)
OC_TR_var_total	$/MWh/km	Variable operating and maintenance cost factor of transport infrastructure	20e-5 (AC-OH), 12.4e-5 (DC-OH), 10.3e-5 (Pipeline)
PP_eff	%	Power plant capacity factor	25
PR_ED	MJ/kg	Hydrogen energy density	120
t	years	Life cycle of the project	30

Case Study on utilizing Wind Power as a part of Intended Island Operation

Kari Mäki, Anna Kulmala, Sami Repo and Pertti Järventausta
Tampere University of Technology, Institute of Power Engineering
P.O. Box 692, FI-33101 Tampere, Finland
e-mail: kari.maki@tut.fi

Abstract — The increasing amount of distributed generation enables new possibilities on the area of network reliability through intended islanded operation of the network. The durations of interruptions could be reduced. Among different energy resources used in distributed generation applications, wind power is seldom suitable for maintaining a network island alone. However, it can be exploited in cases in which another generator unit maintains the state of the island stable enough. This paper presents case studies in a network which is occasionally used in islanded mode. During the islanded operation, the network is fed by diesel back-up power. The existing wind power units could possibly be used to reduce the running costs of the diesel units. This possibility is studied.

Index Terms — Distributed generation, islanded operation, wind power

1. Introduction

The progress of distributed generation (DG) has directed an increasing amount of interest on the possibility of using the distribution network in islanded mode during longer interruptions. This would enable enhancement of network power quality by reducing the duration of service interruptions experienced by the customer. [1], [2] However, the actual number of interruptions is not reduced. [1] At the present situation, this improvement has been striven in the case of particularly important customers with back-up generation units located directly at the customer's network. Due to the propagation of DG, this back-up generation feature could be expanded to cover also larger areas than separate customers.

Islanded operation means a situation, during which a network or, more commonly, a part of it is fed by one or multiple generator units without a connection to the main public system. All DG techniques are not suitable for the operation in islanded mode. For instance wind power or similar intermittent energy resource is typically not capable of maintaining the island alone.

It is important to differentiate between intended and unintended islandings. An intended islanding represents totally new possibilities, whereas detecting unintended islandings is the most problematic issue at the moment in the area of DG protection. Islanding detection problems have been covered by the authors earlier in [3] and [4].

Where islanded operated is intended to be applied during interruptions, it is still often necessary to detect the forming of the island reliably. This can be needed in order to adjust the control mode of the generator unit for stand-alone use. [5] Thus the islanding detection problems relate closely to the intended islanded operation as well.

2. Operating the distribution network in an islanded mode

There are certain challenges related to operating the distribution system as an island. The most important of these is managing the voltage and the frequency of the system. In other words, this means managing the balance of active and reactive power. The control systems of the DG units affect the stability of the island. Modern converter applications can be very useful in this sense as their control system can be efficiently adjusted. [6] Also the availability and adjustability of the primary energy resource are essential factors. Increasing the number of DG units typically improves the possibility of islanded operation, however problems related to the co-operation of units' control systems may occur as well.

Another significant challenge is the protection of the islanded network. The safety of the network must be assured similarly to the normal situation. On the other hand, the protection should not be too sensitive in order to allow the islanded operation. Thus the great challenge will be in coordinating the protection so that safety is assured but the formation of the island as well as normal disturbances during the island are tolerated. Protection of the island is not considered further in this paper.

3. The case studied

The studies performed consider the possibility of exploiting wind power units as a part of islanded operation. In other words, wind power is not assumed to maintain the island alone, but the impacts of wind power on the stability of the island are considered.

The studies were performed in dynamical PSCAD simulation environment. The modelling of the network was based on actual network data. The wind power units as well as diesel generators were also modelled with actual data available. The protection device models applied in the wind power units' connection points have been created by the authors. HElib Model Library created by VTT and University of Vaasa was also used in the simulations.

The part of the network operated islanded is located also geographically on an island at the Finnish coast. Same case has been studied earlier regarding network protection impacts [7]. The loading located on the island is normally fed with a sea cable connection from the mainland. The island is also equipped with two diesel-operated back-up power units for cable failure and service purposes. These back-up units have been rated for feeding the maximum loading of the island together. During lower loads it is also possible to run only one of the diesel units. The network is presented in figure 1.

Four small-scale wind power units are installed on the island. At the present situation, these units are kept disconnected from the network while operating in islanded mode. This practice has been chosen as the wind power units have not been designed for operation during islanded operation and their impact on system stability is therefore unsure. However, using the wind power as a part of the island could present significant benefits in the form of reduced costs of running diesel units. Fuel could definitely be saved and maintenance costs might also be decreased if the operation times of diesel units could be decreased by the contribution of wind power. In a more wide perspective, it can be said that the already existing wind power units should always be exploited when it is possible. This can be stated according to the environmental and economical aspects of wind power.

The data of the wind power units and the main transformers are given in table 1. The wind power units are equipped with typical protection devices as presented in table 2.

It is evident that wind power is not the most reliable form of energy for such a system. However, it could be used as a "negative loading" for decreasing the power generated by the diesel units. Due to the intermittent nature of wind energy, control systems of the diesel units play an essential role regarding the stability of the island.

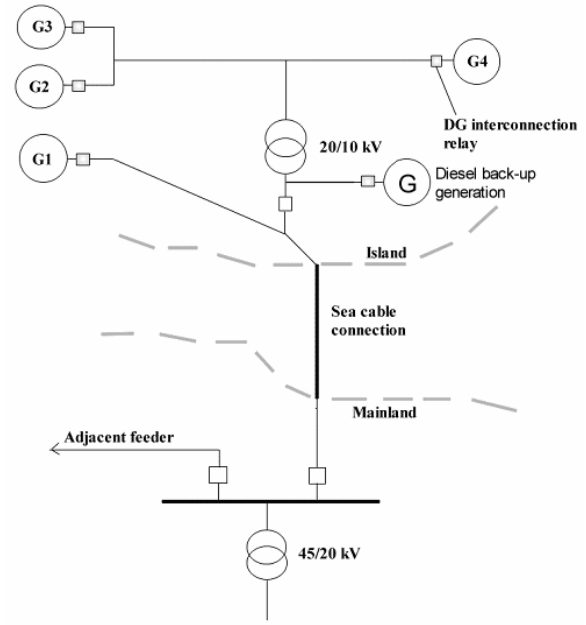

Figure 1. The studied network.

Table 1. Technical data of the equipment

Main transformers	45/20 kV	20/10 kV
Sn	6.3 MVA	5 MVA
Pk	48 kW	37 kW
Zk	7.0 %	10.8 %
Winding	Ynd11	YNyn0
Wind power units	G1, G4	G2, G3
Rated power	500 kW	300 kW
Voltage	690 V	400 V
Hub height	35 m	31.5 m
Power regulation	Stall	Stall
Generator	Induction	Induction
Block transformer	Dyn	Dyn
- Sn	0.63 MVA	0.8 MVA*
- Zk	4.0 %	5.3 %

* One transformer for two 300 kW generators

Table 2. Wind power units' protection settings

	G1	G2 & G3	G4
Overvoltage >>			
- Setting	110 %	110 %	110 %
- Operation time	50 ms	50 ms	50 ms
Overvoltage >			
- Setting	108.5 %	104.5 %	108.5 %
- Operation time	60 s	60 s	60 s
Undervoltage <<			
- Setting	50 %	50 %	50 %
- Operation time	100 ms	100 ms	100 ms
Undervoltage <			
- Setting	85.5 %	82 %	85.5 %
- Operation time	10 s	10 s	10 s
Frequency			
- Range	± 1.5 Hz	± 1 Hz	± 1.5 Hz
- Operation time	200 ms	200 ms	200 ms
Overcurrent >>			
- Setting	3150 A	3150 A	3150 A
- Operation time	0.1 s	0.1 s	0.1 s
Overcurrent >			
- Setting	630 A	630 A	630 A
- Operation time	0.6 s	0.6 s	0.6 s

4. SIMULATIONS

A situation, during which the islanded operation could be used, is typically initiated with a fault or other failure resulting in interruption. In the case studied, the most likely cause is the failure of the sea cable. While starting up the network, the wind power units must remain disconnected from the network. As the islanded network is stable enough, the wind power units can be connected one by one. Connecting several units at the same moment could result in oscillations that would further trip the wind power immediately.

4.1. Connecting wind power units to the islanded network

In the simulations, the wind power units were connected to the network with certain sequence, first connecting the 500 kW units (G1 and G4) on the 20 kV level and then the 300 kW units (G2 and G3) on the 10 kV level. The operation of DG units' protection devices plays an essential role while forming the island. If voltage or frequency is driven outside the protection limits, the DG unit will be tripped. As the protection is based on local measurements in the DG connection point, this can also be considered as one kind of control method. During an intended islanding it could be reasonable to apply more allowable protection limits. On the other hand, the protection settings are also intended for assuring the safety of the DG unit itself.

In similar studies, for instance [8], it is often assumed that the protection system becomes automatically readjusted when transforming to the islanded mode. This could solve problems described, but the actual implementation could easily be too expensive for the small-scale DG units.

4.1.1. Operation during maximum loading

The maximum loading situation is the easiest one regarding the interconnection of DG units as the deviations of voltage and frequency are easier to manage. The maximum loading of the network is about 1800 kW, during which it is possible to connect all four wind power units to the network. Figures 2 and 3 show the situation during the wind power connecting sequence. Figure 4 shows the output power of the diesel generator during the sequence.

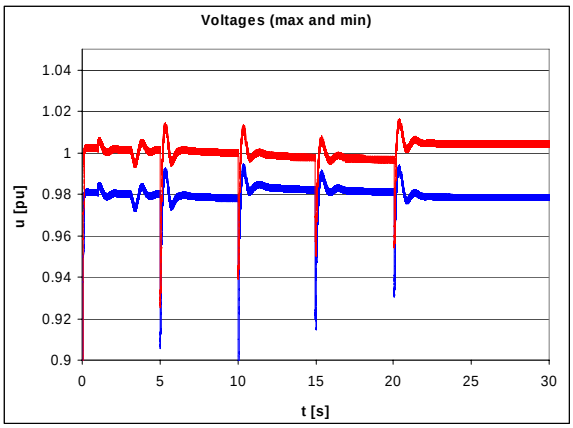

Figure 2. Maximum and minimum voltages in the studied network while connecting the wind power units.

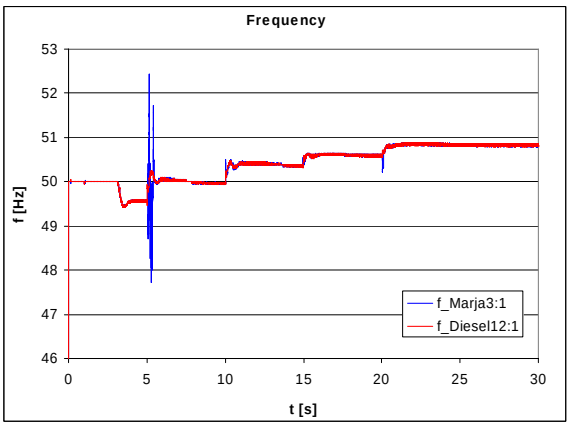

Figure 3. Frequencies in the studied network while connecting the wind power units.

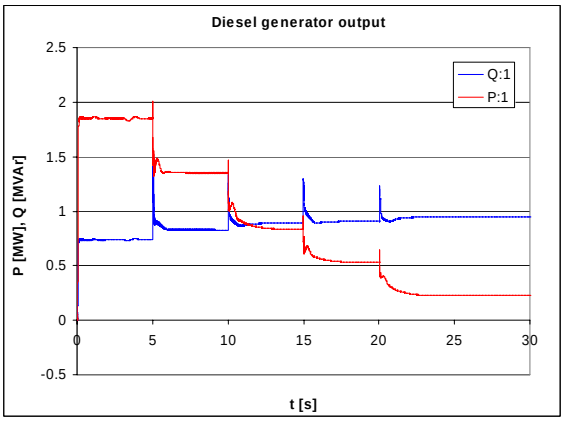

Figure 4. Output of the diesel generator. Generated real power decreases according to the increase of wind power. Generated reactive power increases due to the need of magnetizing.

4.1.2. *Operation during minimum loading*

During minimum loading, the circumstances for running wind power units are evidently difficult. As the minimum loading of the network can be as low as 400 kW, it is practically not possible to interconnect the larger 500 kW units. Also the smaller 300 kW units can not be used as the interconnection results in frequency deviations that will trip the unit immediately. This is shown in figure 5.

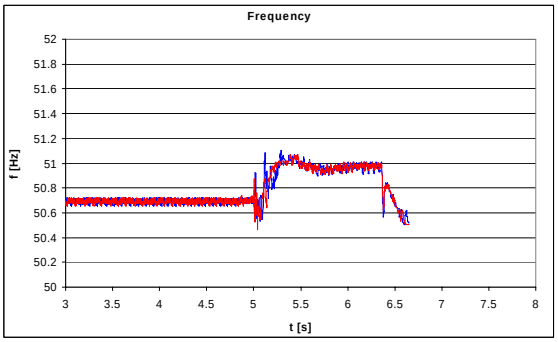

Figure 5. Connecting the smallest unit during low loading is likely to result in too great frequency deviations.

4.1.3. *Operation during average loading*

As a third case, a situation with a loading of 50 % of the maximum loading was studied. This means a network loading of approximately 950 kW. This kind of situation is the most realistic one to be considered as the maximum and minimum situations are more or less theoretical.

It is possible to connect one 500 kW unit to the network during this situation. However, connecting another similar will evidently result in too high frequencies and tripping of the units. This is shown in figure 6.

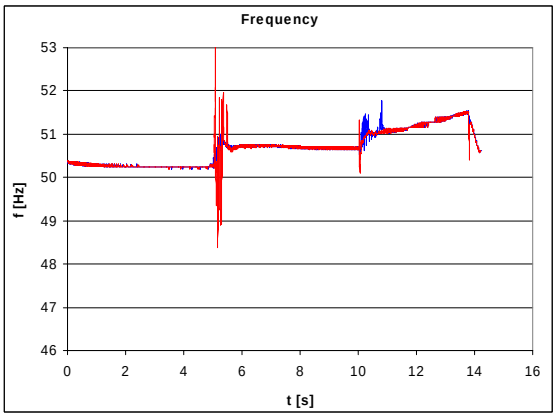

Figure 6. Connecting two 500 kW wind power units results in too high frequency.

The average loading situation allows the connection of one 500 kW unit and one smaller 300 kW unit. With this combination the frequency remains within its limits. This is shown in figure 7. With this combination, the output of the diesel generator decreases significantly.

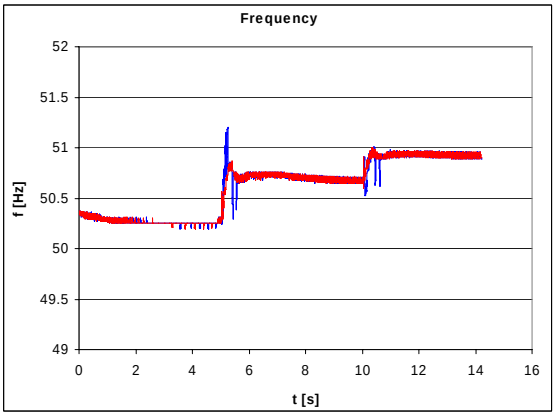

Figure 7. The situation allows the connection of one 500 kW unit together with another 300 kW unit.

4.2. The impact of varying wind speed

In the previous simulations the wind speed was assumed to be constant when studying the interconnection moment. Separate simulations were performed in order to study the impact of varying wind speed. The wind speed signal applied is presented in figure 8. The signal is formed with dedicated component in the PSCAD simulation environment. The average loading situation described in previous chapter is used during these studies.

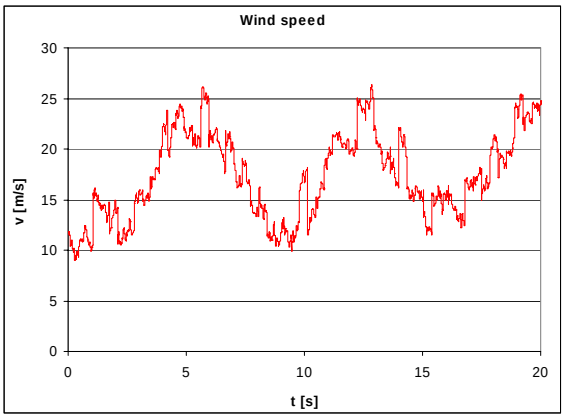

Figure 8. The wind speed signal used.

The wind speed naturally affects the generated power of the units. These impacts show with certain delay due to the inertia of the turbine. During higher wind speed peaks, the stall control applied in the turbine results in dips in the output power as shown in figure 9.

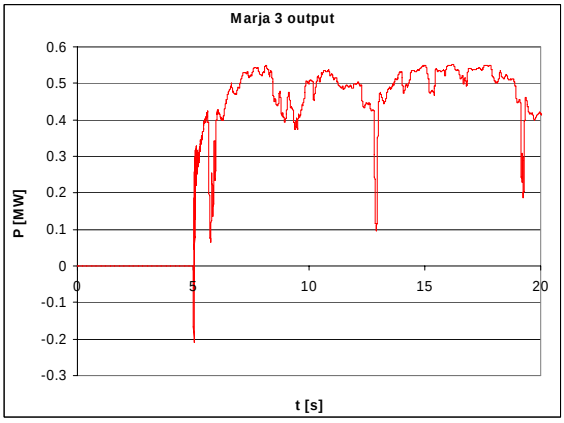

Figure 9. The generated real power of a 500 kW wind power unit G1 during varying wind speed. The power is measured from the connection point. The unit is connected at 5 seconds.

The variation of one 500 kW generator output does not affect the state of the network essentially. Frequencies and voltages in the network remain within normal operation limits. The diesel generator was observed to be able to follow the wind generation variations and to maintain the stability of the island. Figure 10 presents the operation of the diesel unit.

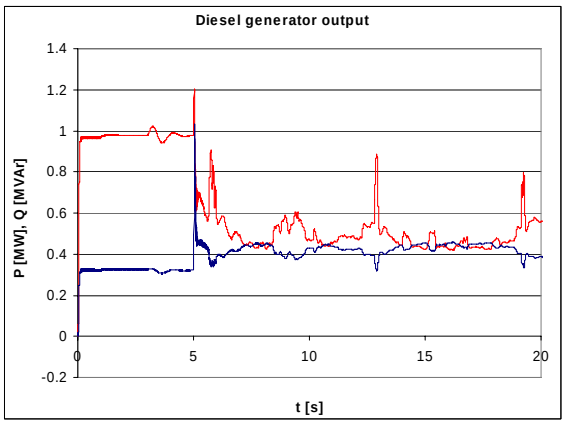

Figure 10. The output of the diesel generator.

In the previous studies it was observed that two wind power units with a combined generation of 800 kW can be connected to the network during the average loading situation. It was also studied, how the wind speed variation affects this generation-loading combination. It was observed that the smaller 300 kW unit is likely to become repetitive tripped due to high frequency when the wind speed varies rapidly. Thus it seems to be impossible to connect more than one wind power unit to the network during strongly varying wind speeds. On the other hand, a loading greater than the average can allow adding of the smaller unit. Figure 11 shows the frequency for the varying wind speed in the case of two wind power units.

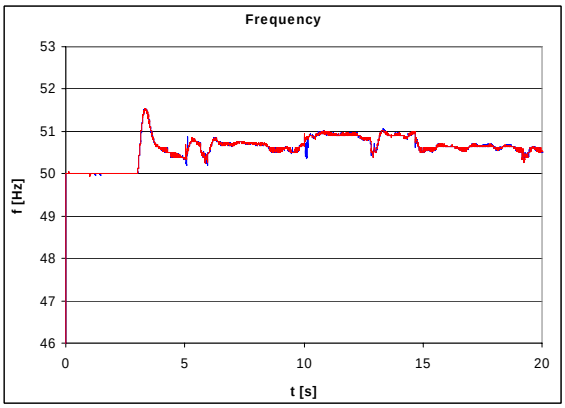

Figure 11. Frequency rises momentarily above tripping limits at t=14.6 s. The smaller 300 kW unit is tripped faster and the 500 kW unit remains in the network.

4.3. The impact of varying loading

In the previous studies the significance of varying wind speed was considered. The varying loading of the network has similar impacts on the situation. Thereby a factor for load variation was added to the simulations. The wind speed varies similarly to previous chapter during following studies.

The load factor was set to vary between values 0.25…0.7. Factor 1 equals to the maximum loading of the network whereas factor 0.2 equals to the minimum loading. Thus relatively wide-ranging variance was considered, although the most extreme situations were excluded. Figure 12 shows the variation of loading.

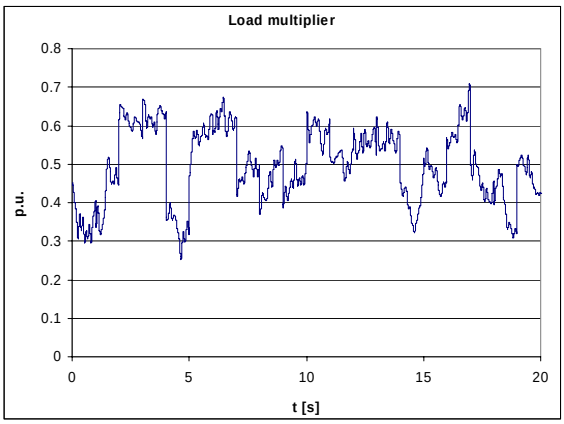

Fig.12. Variance of the load factor during the simulation.

The behavior observed in the simulations was similar to the previous situation in which the load was constant. With one 500 kW wind power unit no problems were faced, but adding a 300 kW unit resulted in high frequencies. In this case, the moment at which the smaller unit was tripped was slightly shifted, but the behavior was otherwise similar.

At the same, a simulation in which the mechanical moment of the units was kept constant was conducted. It was observed that the variance of the loading does not result in significant oscillations. It seems that the varying wind speed has much greater impact on network state in comparison to the varying loading. This conclusion is explicable as the protection devices are located at the wind power units' connection points, where variations of generation are experienced without damping impact of the network.

In the practical situation both wind speed and loading vary, which can make the situation different to manage and may result in additional trippings of the wind power units.

4.4. Comparison to normal operation

The situation during the intended operation was also compared to the usual one, during which the sea cable connection is in use, wind power units are connected to the network and diesel generator is not used. As it can be expected, the sea cable connection to the network on mainland stabilizes the studied network significantly. Figures 13, 14 and 15 show the differences in frequency and voltages. During these simulations, both wind speed and network loading varied similarly to the previous chapter.

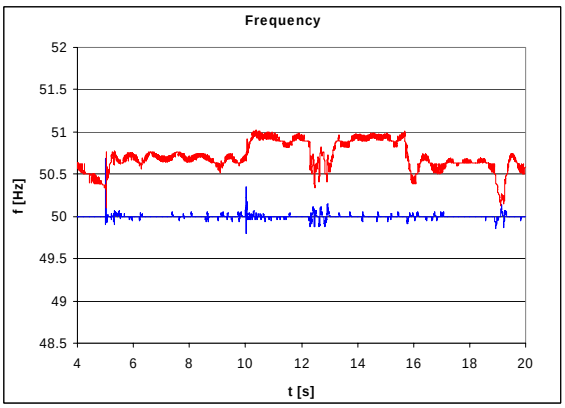

Figure 13. Frequency of the studied network during normal operation and islanded mode. The upper line shows the behavior during islanded operation.

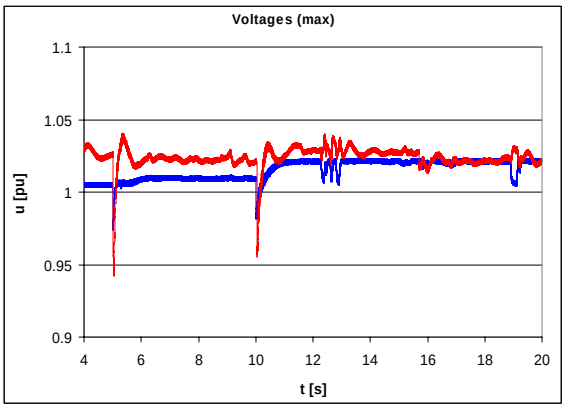

Figure 14. Maximum voltages in the network during normal and islanded operation. The upper line shows the behavior during the island.

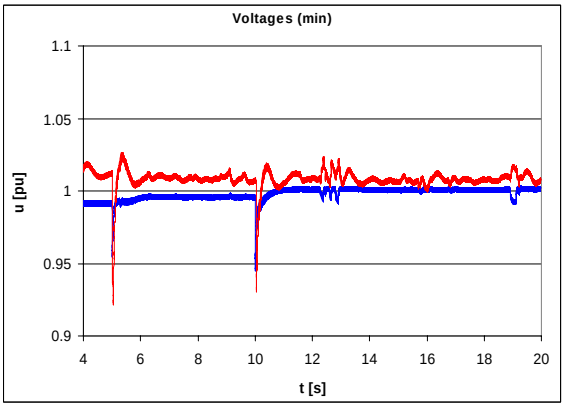

Figure 15. Minimum voltages in the network during normal and islanded operation. The upper line shows the behavior during the island.

5. CONCLUSIONS AND DISCUSSION

The purpose of the simulations was to study the possibility of exploiting the wind power units during intended islanded operation. Presently the island is fed by diesel generators while the wind power units are kept disconnected. The generators used in the wind power units are traditional induction generators, which are typically not able to maintain a voltage in the island alone. However, they could be used during the islanded operation to reduce the power generated by the diesel generators.

In islanded operation the network is much more prone to various oscillations and disturbances as the connection to the larger system is missing. The control system of the back-up generators seeks to maintain the state of the network within certain limits. As the proportion of wind power generation of the total network loading increases, the network gets more unstable during different transients. Thereby the network loading has an essential role in the amount of connectable wind power.

It was observed that all four wind power units can be connected to the network during maximum loading situation. On the other hand, during a minimum loading it was not possible to connect even one unit. Other loading situations were also studied and it was observed that the allowable amount of wind power increases in proportion to the network loading. Figure 16 presents the loading of the network during one year calculated according to the modeled load curves. As it can be seen, the loading of the network depends strongly on the season. It can be deduced that possibilities for using the wind power units during islanded operation are better

during winter months as the loading is higher. During summer, it may be difficult to use even one smaller unit while in islanded operation mode. The maximum loading situation used in the simulations is very rare. Table 3 presents also the division of hourly loadings. Most of the hours allow connection of one or two wind power units assuming a nominal output power from the units. Wind speed statistics should also be included in order to increase the accuracy of the analysis.

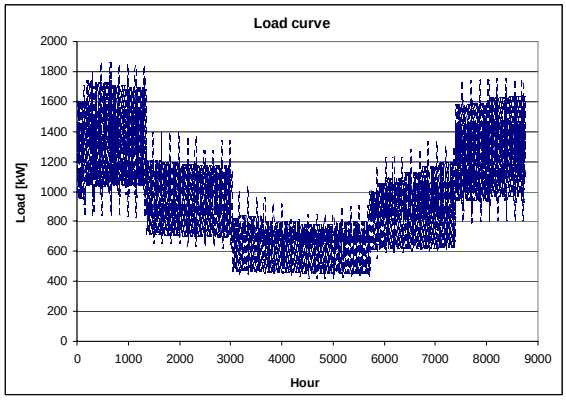

Figure 16. Loading of the network calculated by using the modeled load curves.

Table 3. Hourly division of one year's loading

Load [kW]	Hours per year
0-500	398
500-1000	5223
1000-1500	2848
1500-	291

In the studied network the main problem seems to lie in frequency rise instead of typical voltage rise problems. Among others, this is due to the consumption of reactive power by the induction generators and the structure of the network. The protection settings applied for the wind power units are quite strict regarding islanded operation. On the other hand, they seem to be suitable during the normal operation with the sea cable connection in use. It could be beneficial to reassess the protection settings if the wind power is wanted to be included in the islanded operation.

The impacts of varying wind speed and network loading were also analyzed. Both aspects affect the stability of the island. The impact of wind speed was observed to be more significant. Generally, the impacts were minor. However, in a case with extreme amount of wind power, they can easily result in exceeding the protection limits.

The studies presented focused on the operation of small-scale wind power units as a part of intended island operation. Thus it is important to notice that the operation of the intended island was not endangered in the cases where the wind power units were disconnected. The wind power unit is disconnected according to the local measurement. This also operates as one kind of control system which maintains the state of the network within desired limits.

Low voltages or frequencies are improbable as the diesel generators are able to feed the maximum loading alone. In this sense, disconnecting the wind power units is not problematic.

It could be possible to improve the control system of the diesel generators in order to respond faster to the deviations of wind power generation. However, the studies conducted focused on the possibilities of the present system and the development ideas where thereby not processed further. It is also evident that the proportion of wind power can not be increased much as certain margin must be maintained to the network loading and at least one diesel unit must be kept running as a backup for fast wind speed variations.

The results should be gathered so that it is always reasonable to include as much wind power in the islanded operation as it is technically possible, if the resource is otherwise available. However, it is not reasonable to connect wind power units repeatedly to the island where no prerequisites for longer online periods exist.

REFERENCES

[1] G. Celli, E. Ghiani, S. Mocci, F. Pilo. Distributed Generation and Intended Islanding: Effects on Reliability in Active Networks. CIRED International Conference on Electricity Distribution. Turin, Italy, June 2005

[2] K.A. Nigim, Y.G. Hegazy. Intention Islanding of Distributed Generation for Reliability Enhancement. International Symposium on Quality and Security of Electric Power Delivery Systems, October 2003

[3] K. Mäki, S. Repo, P. Järventausta. Impacts of distributed generation on earth fault protection in distribution systems with isolated neutral. CIRED 19th International Conference on Electricity Distribution, Vienna, Austria, May 2007

[4] K. Mäki, A. Kulmala, S. Repo, P. Järventausta. Problems related to islanding protection of distributed generation in distribution network. PowerTech'07 Conference, Lausanne, Switzerland, July 2007

[5] H. Zeineldin, E.F. El-Saadany, M.M.A Salama. Intentional Islanding of Distributed Generation. IEEE Power Engineering Society General Meeting, June 2005

[6] H. Zeineldin, M.I. Marei, E.F. El-Saadany, M.M.A Salama. Safe Controlled Islanding of Inverter Based Distributed Generation. IEEE Power Electronics Specialists Conference, Aachen, Germany, 2004

[7] K. Mäki, S. Repo, P. Järventausta. Network protection impacts of distributed generation – a case study on wind power integration. Nordic Wind Power Conference 2006, Espoo, Finland, May 2006

[8] P. Fuangfoo, W-J. Lee, M-T. Kuo. Impact Study on Intentional Islanding of Distributed Generation Connected to Radial Subtransmission System in Thailand's Electric Power System. Industry Applications Conference, Tampa, USA, October 2006

The transport sectors potential contribution to the flexibility in the power sector required by large-scale wind power integration

Per Nørgaard[1*], H. Lund[2], B. V. Mathiesen[2]
[1] Risø DTU, P.O. Box 49, DK-4000 Roskilde, Denmark
[*]phone +45 4677 5068, e-mail per.norgaard@risoe.dk
[2]Aalborg University, Aalborg, Denmark

Abstract — In 2006, the Danish Society of Engineers developed a visionary plan for the Danish energy system in 2030. The paper presents and qualifies selected part of the analyses, illustrating the transport sectors potential to contribute to the flexibility in the power sector, necessary for large-scale integration of renewable energy in the power system – in specific wind power. In the plan, 20 % of the road transport is based on electricity and 20 % on bio-fuels. This, together with other initiatives allows for up to 55-60 % wind power penetration in the power system. A fleet of 0.5 mio electrical vehicles in Denmark in 2030 connected to the grid 50 % of the time represents an aggregated flexible power capacity of 1-1.5 GW and an energy capacity of 10-150 GWh.

Index Terms — Energy system, energy plan, electrical transport, renewable energy, wind energy, sustainable development.

1. Introduction

The IDA Energy Plan 2030[i] – a visionary energy plan for the Danish energy system – was developed as part of The Danish Society of Engineers' (IDA) project 'Energy Year 2006' – a project involving more than 1600 professionals at 40 workshops during 2006 (Ref [1], [2], [3]).

The aim of the IDA Energy Plan 2030 was threefold:

- to maintain the security of energy supply;
- to reduce the CO2-emission; and
- to extend the energy technology business opportunities.

The analysis results indicate that the Danish society can meet all three targets even with a positive economic result (Figure 1, Figure 2, Figure 3, Figure 4). The targets can however only be met by long-term investments in energy savings, energy efficiencies and new energy technologies – investments that are paid back over time. The IDA-results are compared to a 'business-as-usual' 2030 reference scenario based on a scenario developed by the Danish Energy Authory (Ref [5]).

The Danish energy system has been modelled and analysed using the computer model for energy system analysis, EnergyPLAN[ii], developed at Aalborg University, Denmark (Ref [9]). The energy system has been analysed on hourly basis for power and energy balance analyses, however with no indication of potential distribution bottlenecks.

The robustness of the results has been tested by sensitivity analyses on the investment costs (including the discount rate used) and the energy market prices. The robustness of the recommendations for the system development has been tested by a projection of the system development to 100 % renewable energy based (in year 2050)

1.1. CO2 emission

One of the aims of the IDA study was to identify solutions to reduce the energy sectors CO2 emission by 50 %, without reducing the service levels. All means in all sectors were investigated, evaluated and utilised – including increasing the energy efficiency, decreasing the energy needs and shifting towards renewable energy resources. The recommended

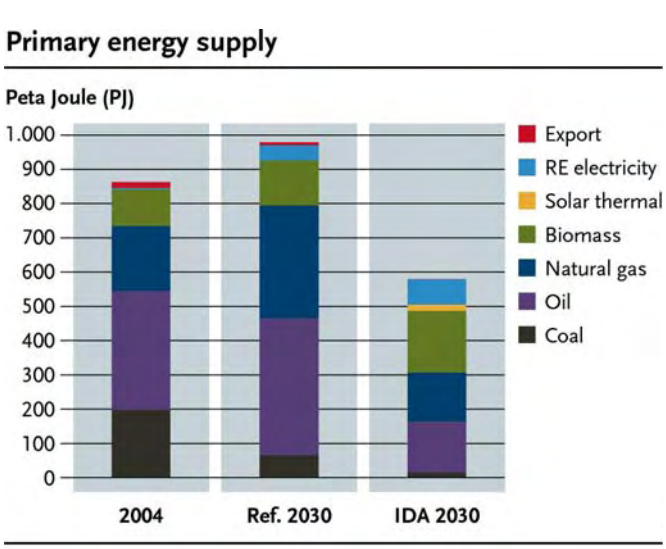

Figure 1: The primary energy supply for the Danish energy system in 2004, for the 2030 reference scenario and for the IDA 2030 scenario. (Source: Ref [1])

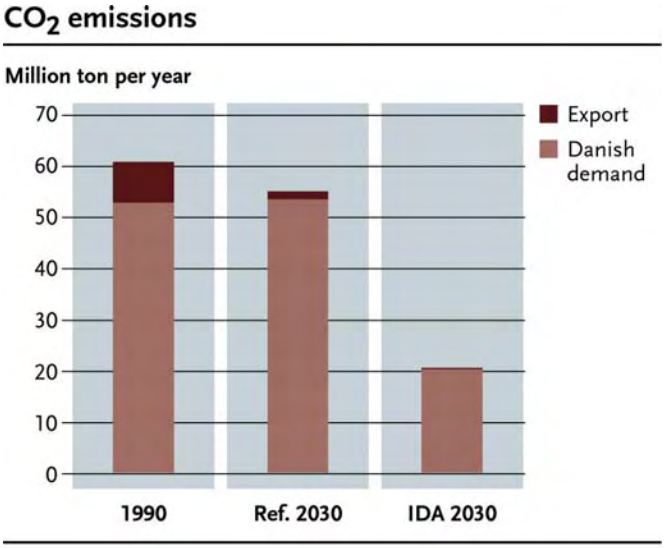

Figure 2: The CO2 emission from the Danish energy sector in 1990 (the Kyoto reference year), for the 2030 reference scenario and for the 2030 IDA scenario. (Source: Ref [1])

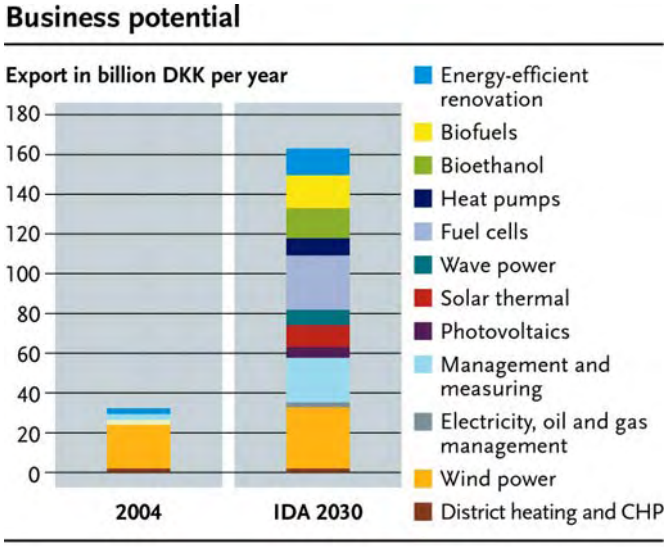

Figure 3: The estimated business potential in the Danish energy sector in 2004 and for the 2030 IDA scenario. (Source: Ref [1])

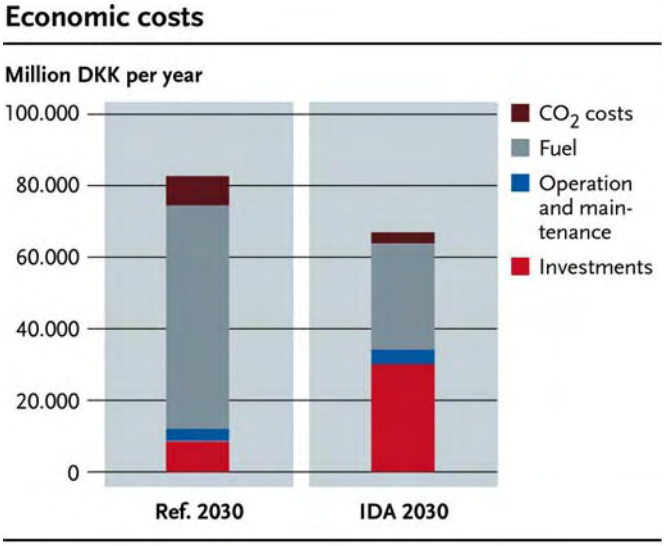

Figure 4: The estimated additional economic cost for the 2030 reference scenario and for the 2030 IDA scenario. (Source: Ref [1])

solution requires a large share of wind power in the power system, which again requires a high degree of flexibility in the power system in order to be able to optimise the system operation and the wind power integration. Several means were introduced to provide the necessary flexibility – including flexible bio-refineries producing bio fuels and the flexible power buffering provided by electrical vehicles, while connected to the grid.

In the IDA Energy Plan 2030, 20 % of the energy for road transport is based on electricity and 20 % is based on bio-fuels. This, together with other initiatives to increase the flexibility in the power system, allows for up to 55-60 % of the electricity consumption covered by wind power. The present paper qualifies these numbers.

The batteries in the electrical driven vehicles act as intelligent electrical buffers, whenever connected to the grid – charging the batteries when abundant generation capacity in the power system (and thus low electricity prices), and supplying power and other system services to the power system when needed by the system (expressed by high market prices). The vehicles intelligent controllers ensure that the vehicles are able to provide the requested transport work when needed by the user – specified by the user when connecting the vehicle to the grid in terms of required operating distance at specified time.

The bio-fuels for the transport sector are produced at flexible, multi-product bio-refineries, e.g. producing a mix of syngas, transport fuels, power plant fuels, power, heat (for district heating), animal feed, fertilization, fibre materials and other chemical products – with a flexibility of adjusting the actual product mix depending on the varying market prices. These multi-product plants are able to switch between e.g. production of power and production of liquid fuels (based on the syngas) for the transport sector.

2. Sustainable transport development

In the IDA Energy Plan, a wide range of measures towards a sustainable transport development has been proposed and analysed. The measures are different from other suggestions related to transport policy because the plan involves a wide range of technologies and includes both the demand and supply side. Also, it differs from other analyses as its measures have been analysed both in the context of the surrounding energy system and in relation to economics.

The following proposals have been used in the analysis as part of the transport theme for Denmark:

- Passenger transport work (person km) in 2030 in vehicles, trains and bicycles is stabilised at the 2004 level.
- The rate of increase in passenger air transport is limited to 30 % (instead of 50 %) in the period from 2004 to 2030.
- 20 % of the passenger road transport is transferred to trains, ships and bicycles in 2030:
- 5 % transport of goods (ton km) transferred from roads to trains and 5 % to ships
- 5 % passenger transport is transferred to trains and 5 % to bicycles.
- 30 % more energy efficiency in the transport sector compared to the reference situation in 2030 with stable passenger transport at the 2004 level and with a lower increase in air transport.
- 20 % biofuels and 20 % battery electric vehicles in road transport in 2030.

Some of the results of the analysis are shown in Table 1 and in Figure 5.

2.1. Electrical vehicles

Although electrical vehicles have been on the market for

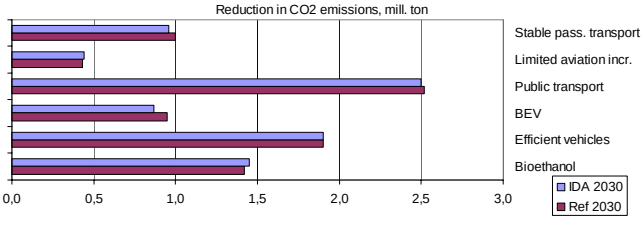

Figure 5: The estimated CO2 emission reduction for the 2030 reference scenario and the 2030 IDA scenario. (Source: Ref [7])

TWh/year	Reference 2030	IDA 2030
JP4 (for aviation)	13,25	11,63
Diesel	27,50	18,82
Petrol	28,46	6,33
Biomass for ethanol		7,98
Electricity	0,24	2,10
Sum	69,45	46,85

Table 1: The estimated fuel consumption for the transport work in Denmark. (Source: Ref [7])

	CO2/km	Reference
Standard gasoline car	160 g	Danish Transport Agency
Hybrid car	100 g	Toyota
Electrical car	70 g	Danish Energy Association
Electrical car on renewable power	0 g	

Table 2: Typical CO2-emission figures for various vehicle concepts. (Ref [11])

decades, they have never real materialised. The weak part has been the lack of sufficiently robust, energy compact and cheap batteries (Ref [10]).

However, the recent and the expected development in battery technology, power electronic and electrical drives in terms of robustness, energy efficiency, energy density, reliability, long life and low cost provides new potentials for the deployment of electrical driven vehicles.

The state-of-the-art capacities of the Lithium-based battery types are 0.2 kWh/kg. The Lithium-type batteries allows extended dynamic operation with many, rapid and heavy charging/discharging cycles, while preserving their high energy efficiency and long lifetime. Electrical vehicles typical have an energy consumption of 0.15 kWh/km (compared to typically 0.5 kWh/km for traditional, efficient internal combustion engine based vehicles and 0.4 kWh/km for hybrid vehicles). A battery package of 200 kg with an energy capacity of 40 kWh corresponds thus to a driving range of up to 250 km.

The deployment of electrical driven vehicles is supported by the potential step-by-step development from the presently introduced 'hybrid vehicle concept' (already mass-produced by several of the large car manufactures) over the so called 'plug-in hybrid' to the dedicated electrical vehicles. The hybrid concept consists of a combination of an internal combustion engine (ICE), an electrical motor/generator and a battery, and provides only increased fuel efficiency by a combination of picking-up and utilising the braking energy and optimising the operation of the ICE. The plug-in concept has typically a larger battery capacity, can drive solely on the electrical drive for short distances and has the option of charging the battery from the grid – while parked and connected to the grid. The dedicated electrical vehicle concept has a pure electrical drive train, but the operation range may be extended by an on-board fuel based battery charger – e.g. based on fuel cell technology.

The ultimate electrical vehicle concept is the so called 'vehicle-to-grid' (V2G), enabling the power between the grid and the battery to flow in both directions, and with the potential through intelligent control of the inverter for the vehicle to provide system services to the power grid. The concept requires a fully controllable bi-directional inverter between the grid and the battery, an possibility for on-line power trading with the power distribution company while connected to the grid and an intelligent controller that can optimise both the system services and the battery charging. The system services provided by the grid connected electrical vehicles may contribute to the flexibility in the power system needed for the optimisation of large-scale wind power integration. The concept is not expected to materialise within the first 5-10 years, but the concept forms the basis for the analyses of the 2030-potential presented in the present paper.

In addition, the development of electrical drive platforms for vehicles is further pushed by their potentials for reducing the transport sectors dependency of fossil fuels, CO2-emission (Table 2), local air pollution and noise emission, as well as their potentials for 'smart' drives with the electrical engines integrated in the wheels, providing true all-wheels-drive, turning support etc.

2.2. The Danish transport sector

The transport sector in Denmark (as well as in EU) is 98 % (2006) dependant on fossil oil products (gasoline and diesel). The annual grow in number of person vehicles in Denmark is 3-5 %, with 2 mio in 2006, in average driving 15-20 000 km annually and in average in use less than 90 % of the time.

A fleet of 0.5 mio electrical vehicles (corresponding to 20 % of the expected vehicles in 2030 with the present grow rate), each having a battery capacity of 50 kWh and a 5 kW inverter, and in average connected to the grid in 50 % of the time represents a power capacity of 1.2 GW and an energy capacity of 12 GWh – corresponding to the maximum power generation from 250×5 MW wind turbines in 10 hours. 50 kWh battery capacity is expected to be realistic for vehicles within the next 10 years. The price and size of 5 kW inverters expects to be pressed by the competition on the expected increasing PV market, also within the next 10 years. The development of a market for trading of large number of small-scale system services is driven by the household's potentials for power demand response and other power system services, and is also expected to materialise within the next 10 years.

The implementation of the necessary infrastructure for grid connection of the vehicles is highly dependent of standardisation of power level, communication between grid and vehicle, and the control of the power flow, of registration of the power trading and of the development power system

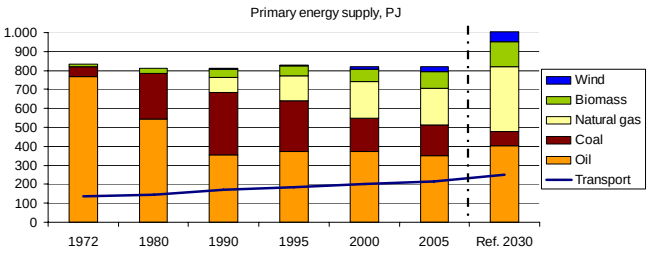

Figure 6: The Danish primary energy supply and fuel supply for transport from 1972 to 2005 and for the 2030 reference scenario. (Source: Ref [7])

service markets. It is therefore important to initiate pilot project that can test, demonstrate and characterise these topics, and thereby form the basis for standardisations. The infrastructure is not expected to materialise until standards has been established.

3. CONCLUSION

The technologies required for the manufacturing of electrical vehicles (especially the battery technology) have developed at lot during the last years in terms of reliability, performance and price, and the developments are expected to continue. The electrical vehicle concepts provide interesting and valuable potentials regarding environmental impact, fossil fuel dependency, energy system flexibility, and driving characteristics. And the electrical vehicles may be introduced through a step-by-step development from the present hybrid vehicles, over plug-in to the vehicle-to-grid, providing the full potential. This in combination leads to an expected deployment of electrical vehicles within the next 10 years.

In a visionary energy plan for the Danish energy system in 2030, developed by the Danish Society of Engineers in 2006, 20 % of the road transport is based on electricity and 20 % is based on bio-fuels. This, together with other initiatives to increase the flexibility in the power system, allows for up to 55-60 % of the electricity consumption covered by wind power.

A fleet of 0.5 mio electrical vehicles (corresponding to 20 % of the expected vehicles in 2030 with the present grow rate), each having a battery capacity of 50 kWh and a 5 kW inverter, and in average connected to the grid in 50 % of the time represents a power capacity of 1.2 GW and an energy capacity of 12 GWh – corresponding to the maximum power generation from 250 × 5 MW wind turbines in 10 hours.

ACKNOWLEDGEMENT

Acknowledgment is made to the Danish Society of Engineers.

REFERENCES

[1] Ingeniørforeningens Energiplan 2030 - Hovedrapport. Danish Society of Engineers, IDA, Copenhagen, 2006.
[2] The Danish Society of Engineers' Energy Plan 2030 – Summary. Danish Society of Engineers, IDA, Copenhagen, 2006.
[3] H. Lund and B. V. Mathiesen., Ingeniørforeningens Energiplan 2030 - Tekniske energisystemanalyser, samfundsøkonomisk konsekvensvurdering og kvantificering af erhvervspotentialer. Baggrundsrapport (Danish Society of Engineers' Energy Plan 2030). Danish Society of Engineers, IDA, Copenhagen, 2006.
[4] Det fremtidige danske energisystem – Teknologiscenarier. Danish Board of Technology (Teknologirådet), 2007.
[5] Energy Strategy 2025 - Perspectives to 2025 and Draft action plan for the future electricity infrastructure. The Danish Ministry of Transport and Energy, Copenhagen, 2005.
[6] P. Nørgaard, H. Lund, B.V. Mathiesen. Perspectives of the IDA Energy Year 2006 project. Presentation: Risø International Energy Conference, 2007.
[7] B.V. Mathiesen, H. Lund, P. Nørgaard. Integrated transport and renewable energy systems. Conference paper: Dubrovnik Conference on Sustainable Development of Energy, Water and Environment Systems, 2007.
[8] H. Lund, B.V. Mathiesen. Energy System Analysis of 100 per cent Renewable Energy Systems. Conference paper: Dubrovnik Conference on Sustainable Development of Energy, Water and Environment Systems, 2007.
[9] H. Lund. EnergyPLAN - Advanced Energy Systems Analysis Computer Model - Documentation Version 7.0. Aalborg Univerity, Aalborg, Denmark, 2007.
[10] Jørgen Horstmann. Elbiler i Danmark – sammenfattende rapport. Miljøstyrelsen, Denmark, 2005.
[11] Klaus Illum. Personbiltransporten i Danmark – ved vendepunktet. Notat, 2007.

[i] IDA Energy Year 2006 web: http://ida.dk/Netvaerk/Energiaar+2006
[ii] EnergyPLAN web: www.energyplan.eu

Analysis of electric networks in island operation with a large penetration of wind power

Adrián García [1)], Jacob Østergaard [2)]
[1)]Centro Técnico de Automatismos e Investigación. Parque Científico Tecnológico de Gijón. Edificio CTAI. 33203 Gijón Principado de Asturias. Spain
[2)] Center for Electric Technology (CET), Ørsted•DTU, Technical University of Denmark (DTU), Elektrovej 325, DK-2800 Kgs. Lyngby, Denmark

Abstract — The percentages of wind power penetration in some areas of the electric distribution system are reaching rather high levels. Due to the intermittent nature of wind power, the voltage and frequency quality could be seriously compromised especially in case of island operation of such an area of the grid. In this paper the impact of wind power in island distribution systems has been analysed with respect to voltage and frequency. Possible measures for controlling both voltage and frequency are suggested and have been analysed. The suggested measures are static voltage controller (SVC), dump loads, kinetic energy storage systems, and load shedding. It is shown that the measures effectively can bring voltage and frequency quality within the normal operation range.

Index Terms — Dump load, Flicker, Island operation, Kinetic energy storage system, Load shedding, SVC, Wind power.

1. INTRODUCTION

For many years the power consumption has relied on the production of centralized power plants interconnected through transmission lines and thereby accomplishing a rather stable power system. Nowadays this philosophy is changing due to the increase of the embedded generation of small combined heat and power (CHP) plants and wind farms. This configuration leads to some drawbacks but also to advantages. Considering the fact that the electric power has to flow through distribution lines instead of transmission lines, the losses will be increased in many cases. In addition, in the case of wind turbines, the nature of the energy source and the use of power electronics in the generation process can affect the power quality. Nevertheless, wherever the embedded generation capability is able to fulfil the consumption, in cases of e.g. disturbances in the grid or imminent blackout, the network could be split in autonomous grid cells working independent from each other as shown in Figure 1.

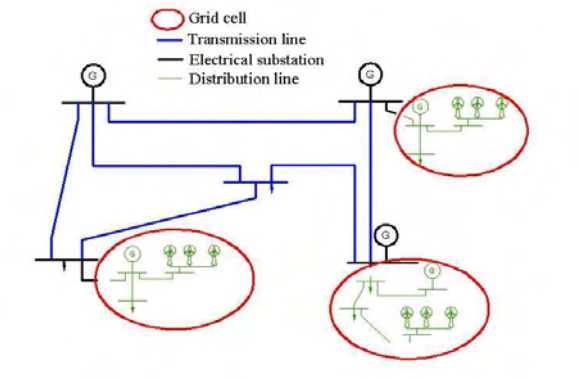

Figure 1. Split network.

The arising problem is the possible instability in terms of voltage and frequency due to the weakness of such a small electric network operated in island. Regarding the frequency, the problems are caused mainly because of the rather low inertia (*H*) of the system. As it is shown in the network electromechanical equation (1) a mismatch between produced power (P_{mech}) and consumed power (P_{elec}) generates variations in the angular frequency ω of the generators and thereby the frequency of the system. These variations are dumped by the inertia of the system, and since the inertia, in this case, is much smaller than in non isolated operation, the frequency will be more affected.

$$\omega \frac{\partial \omega}{\partial t} = \frac{P_{mech} - P_{elec}}{2H} \quad (1)$$

In the case of the voltage, the reactive power variations of the demand and wind generation have a more significant impact on the total reactive power balance of the system compared with interconnected operation. Considering that the excitation systems of the synchronous generators are not fast enough to compensate such variations, the voltage will be affected.

Considering the objections of the isolated operation, this paper presents the results of a study on the dynamic behaviour of a typical Danish electric distribution network in island operation. The study has been realized by use of the power systems simulation program *PowerFactory* by *DigSilent* based on a quite simple grid. The considered power system includes a variable demand, a CHP plant and a wind farm with variable production.

The wind power is going to be considered as wind turbines of the *Danish concept* type and without any power control capability, i.e. they are fixed speed wind turbines and do not have active stall or pitching systems for controlling the power output. Under these conditions, the power output of the wind turbine will depend mainly on the wind speed; hence the wind power production is an uncontrollable energy source which, as in the case of the variable demand, might generate disturbances in the grid.

The fluctuating wind power and its penetration percentage present a key issue in a grid cell. In order to outbalance the frequency disturbances from the wind power in a grid cell, the use of dump loads, kinetic energy storage systems and load shedding is considered, and in the case of the voltage, the application of a SVC is considered.

2. STUDIED MODEL

The analyzed model is representative of a grid cell. It consists of three nodes interconnected through a distribution line in the level of 60 kV. In one node there is a gas engine based CHP plant, in another node there is a wind farm which rated power will be modified to study different cases, and in the third node variable consumption is located.

In order to get a good approximation to the real network behaviour in the studied conditions, the grid components models must be as accurate as possible and real data has to be used whenever possible.

The CHP have four groups of 3.5 MW each and is modelled considering real data provided by the Danish transmission system operator *Energinet.dk*. The model includes a voltage controller, a power controller (speed controller), a primary mover unit model and the electric generator. The models for both the voltage controller and the primary mover unit are realised with the actual values of the CHP model. However, since in normal operation this plant is not requested to control the frequency, the speed controller which was basically a proportional controller was replaced by a PID controller which should be able to perform a good frequency control since it has no steady state error.

The wind farm considered consists of 8 wind turbines with a rated power of 500 kW each. Since there was not enough data available to realise an aggregated model for the wind farm, the 8 wind turbines have been modelled separately. The model of the wind turbines is done with data from a 500 kW Nordtank wind turbine [4]. This model uses the mechanical power as input along the simulation time, and considers the soft coupling of the low speed shaft and the electric generator, both with the actual values for the parameters. The data used as input for the wind turbine models is a key issue. It would not be a real case if all the wind turbines had the same input, because the smoothing effect, which takes place in the power output of the wind farm with respect to a single wind turbine, would be neglected [4]. To overcome this problem, 8 measurement files of the Nordtank wind turbine were taken in which the average wind speed and turbulent value were similar to simulate the real behaviour in a wind farm.

The consumption values used to simulate the dynamic behaviour of the load are based on measured values from *DONG Energy*, one of the Danish distribution companies in four of its 10 kV feeders. The average active and reactive consumption is 7 MW and 4 Mvar, respectively. The measurement of active and reactive power was with one second resolution which permits to simulate faithfully the load profile. In the node where the load is located, the corrective measures proposed to help with the frequency and voltage control will be placed.

In the simulations the impact of wind power in both, frequency and voltage is analysed. The impact of wind power in the grid cell depends on one hand on the wind behaviour, as previously mentioned, and on the other hand on the penetration percentage of wind power in the network. Hence, the influence of five different penetration percentages of wind power between 0% (if there is no wind turbine connected) and 52% (if all the wind turbines are connected) of the total mean demand in the network is going to be discussed.

To analyze the frequency and voltage it is necessary to set up the quality standards taken into account. According to the Nordic grid code [1] the maximum frequency deviations in normal operation must not exceed ±0.1 Hz. The frequency data from the simulation results will be presented into histogram pictures and tables. By using these tools it is easier to evaluate the frequency quality.

Concerning voltage, the limit considered in this study is set by the maximum short term flicker power (P_{st}) which has to be below one according to IEC [3]. In this case, an algorithm is applied to the voltage rms values obtained in the simulations to compute the P_{st}. This algorithm is developed according to [2].

3. CORRECTIVE MEASURES PROPOSED

Due to the reasons explained previously, this paper proposes measures to deal with frequency and voltage instability. These are, in the case of the frequency dump loads, load shedding and systems of kinetic energy storage. On the other hand, the use of an SVC will be discussed for the voltage control. Hereafter are presented thoroughly these proposals and in the appendix are shown the developed models used in the simulations.

3.1. Dump Load

A dump load is basically a type of load which consumption can be controlled quite fast to perform frequency control. Dump load is widely used in hybrid wind-diesel systems because the diesel engine is not capable to perform a good frequency control. In the early days the energy of the dump load was wasted in a resistors bank, but now it can be used to charge batteries or heating up water. Normally, the dump loads are specifically designed for working as such, which is an important drawback in this case because most of the time they would not be necessary as the network would not normally be in island operation.

A possible solution for this problem would be to use some normal consumers as dump loads. The requested power could be modified without causing big problems. Some of those peculiar consumers could be:

- Desalination plants. The change on requested power in this kind of industry would be realised by controlling pumps and would only affect the water flow.
- Heaters. In big installations in which electric energy is used for heating up e.g. fluids.
- Pumping stations. This is a similar case to the desalination plant..
- Ice making factories. The power consumption changes would affect to the time needed to make the ice.

If the power of these loads is momentarily changed, either increased (if it is possible) or decreased, the troubles caused would be hardly noticeable whenever the averaged power consumption stays constant. A so called dynamic grid interface could manage these loads to meet the requirements of frequency control. In this study, a dump load of 600 kW is considered. It is assumed that the dump load has a normal operational power of 400 kW and an up-and-down regulating capability of ±200 kW.

3.2. Kinetic energy storage system (KESS).

A kinetic energy storage system is a device which stores energy in kinetic form in a flywheel. This device can either release or absorb energy according to the requirements. It is considered to be a useful device in the studied case because it could help to the balance between demand and supply due to its fast response capability.

For storing energy another device such as batteries could be used, however they would not be so suitable due to the operating conditions needed. Since the frequency may flicker very fast, the energy storage system has to be charged and discharged as well very fast. This cyclic loads upon batteries, would lead in the real life to a decrease in their lifetime. Nevertheless, a flywheel can stand much better these cyclic loads without a big impact on its durability.

The model made in *PowerFactory* does not consider the interface between the system and the grid, i.e. the power converter is not taken into account. This consideration can be assumed in this dissertation because the scope is only analyzing the frequency control capability of this system and not how the power controller works. The data for the model was obtained from the characteristics of a real KESS [13], which in this case is able to store 18 MWs with a maximum power of 300 kW.

3.3. Load Shedding

Load shedding consists of load which in cases of under frequencies, is disconnected to reach a new balance between production and consumption. All major electric power systems have certain amount of load able to be shed under extreme low frequencies. These loads are typically complete distribution feeders including all connected customers. This load shedding philosophy has a major impact on consumers and it is not supposed to help to the frequency control in small deviations.

In recent years another sort of load shedding philosophy [9] has been proposed. It consists of making automatic load shedding and is formed by a large number of small loads instead of few large loads. These small loads would belong to the household and residential consumption in such a manner that their partial disconnection from the grid would not affect the consumers comfort. Examples of this sort of loads are:

- Refrigeration. For short periods of time it is disconnected from the compressor, meanwhile the lights are on.
- Clothes dryers. The heating element is interrupted and the rotating drum is not stopped.
- Water heating. The thermostat is set back temporarily.
- Cookers. The heating devices of the cookers can be intermittently disconnected hardly affecting the cooking time.
- Other heat sources, as i.e. those used for keeping the coffee warm once it is made, could also be temporarily disconnected.

In the simulation program, this has been modelled as a load which connects or disconnects itself according to the requirements of the frequency. Since the frequency is permitted to be in the range between 49.9 Hz and 50.1 Hz, the load shedding is activated when the frequency goes under 49.9 Hz and it is not reconnected until the frequency is totally recovered to 50 Hz. As the size of the load shedding has a major impact on the frequency, results with several quantities of load shedding will be presented.

3.4. Static Var Compensator (SVC)

Since the only reactive power source in the network is the CHP generators which excitation systems are not fast enough to perform a rapid control of the voltage, a system with capability to deal with the sudden reactive power variations is needed. That is provided by an SVC; it consists of a three-phase capacitor directly connected to the network in parallel with a three-phase reactor connected through thyristors. This configuration leads to a fixed reactive power injection caused by the capacitor bank and a controllable reactive power consumption by the reactor. The reactive power control is performed by setting the appropriate firing angle for the thyristors which is the reason for its fast control.

PowerFactory itself contains a model for this device, so it was only needed to setup its governor. The work philosophy of the SVC, in this case, consists of keeping the rms value of the voltage in the consumers node constant to avoid the flicker problems.

4. NETWORK OPERATION WITHOUT CORRECTIVE MEASURES

The frequency histogram is depicted in Figure 2. Each colour corresponds to a wind power penetration percentage in the network which varies from 0% to 52% in 13 % steps of the total average power consumption of 7 MW.

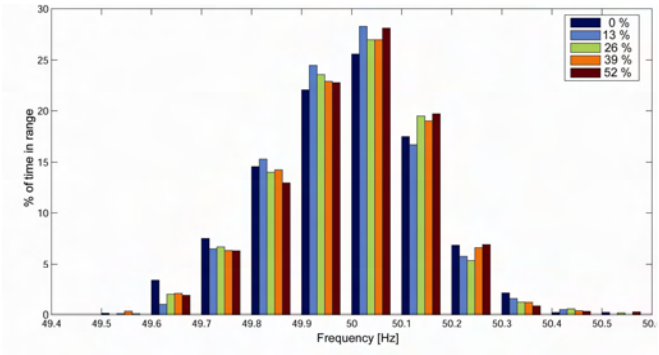

Figure 2. Frequency histogram for different wind power percentages.

Table 1. Impact on frequency and voltage with several percentages of wind power penetration

% of wind power	% time inside limits	P_{st}
0	47	3.73
13	53	2.91
26	51	3.01
39	50	3.1
52	51	3.28

Reminding the normal operation limits of 50 ± 0.1 Hz, it is possible to notice in Figure 2 that the frequency goes out of its normal operation limits under all wind power penetration levels. The frequency deviations are quite remarkable and for rather big percentages of time. In almost all the cases, the frequency is out of limits for approximately the half of the simulation period as it is shown in Table 1. Carrying out a deeper look into the results for the different wind power

percentages, the case with no wind power in the network leads to the worst frequency results. The reason for this can be explained by (1) which links the balance between produced and consumed power with the system frequency. When a mismatch between produced and consumed power takes place, the system frequency is affected. Since the system inertia (H) is dividing the power mismatch, the bigger the inertia is, the smaller is the influence in the frequency. Due to their really big rotors, wind turbines have a big inertia meaning an important part of the total inertia in isolated systems as is the case. Nevertheless, there is not a linear link between the inertia increase caused by wind turbines and the frequency improvement. In fact, increasing the wind power percentage level makes the frequency worse. The reason why this happen is because on one hand, wind turbines increase the inertia of the system which helps the frequency, but on the other hand, due to the variable nature of the wind and to the types of wind turbines used, the wind fluctuations are transformed into power fluctuations and generating power imbalances. In short, in terms of frequency, the wind power in the grid cell has a positive effect due to the inertia increase but also a negative one due to the power perturbations it generates.

To study the voltage quality a flicker analysis, which results are shown in Table 1, is performed. Considering that the limit for short term flicker power (P_{st}) is set to 1 by the IEC standard [3], the results are rather poor in all the cases. These flicker levels would result in being annoying for the consumers.

5. NETWORK OPERATION WITH CORRECTIVE MEASURES

Next the simulation results will be presented and analysed considering the different measures proposed. Since those taken to improve the frequency can hardly improve the voltage, the SVC system will be used in all cases studied.

5.1. Dump load and SVC

The use of the dump load together with the SVC should improve respectively the frequency and the voltage in the network. In addition to the frequency and the voltage study, it will be discussed how the dump load will be operated along the simulation to get an idea of how the end use of the load would be affected.

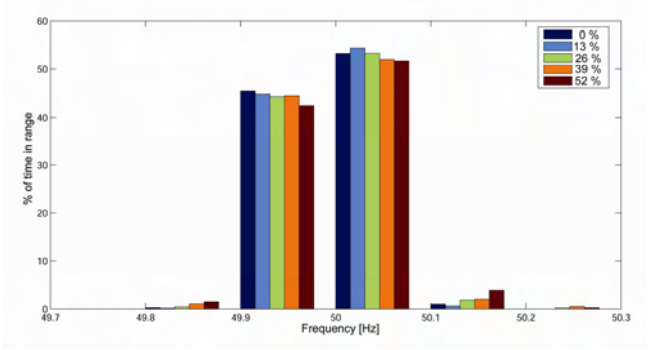

Figure 3. Frequency histogram with the use of the dump load and the SVC.

The results of the frequency are shown in Figure 3. The improvement with regard to the case of no corrective measures is very large. The frequency still goes out of the limits, but just for very small percentages of time. It seems that the deviations are bigger when the wind power penetration is increased, this is more clearly shown in Table 2. In all the different wind power penetration percentages the frequency is within the permitted range more than the 90% of the time, reaching values as high as 99% in the case of 13% of wind power penetration in the grid. The reason for this great improvement is that the fast and relatively small power changes are dumped by the dump load, meanwhile the CHP only has to deal with the long term power changes which are usually quite slow and not causing big problems. Since the consumption range of the dump load is between 200-600 kW, the total amount of power able to be dumped is 400kW which means less than the 6% of the average consumption in the simulated situation. This is a very good advantage, because with a few percentage of power dumping capability the improvement in the frequency is very high. In Table 2 the mean values of the power consumption of the dump load are shown, P_{dl}. These values increase slightly with the percentage of wind power penetration in the grid cell.

In Table 2 the values of the short term flicker power (P_{st}) are shown. For all cases the flicker levels are below the limit set by the standard at Pst = 1, but with the maximum wind power penetration considered (52%) the value is quite close to the limit. Under these conditions, the addition of more wind power to the grid would probably lead to annoying flicker levels.

Table 2. Impact on frequency and voltage with the use of the dump load and the SVC.

% of wind power	% time inside limits	P_{st}	P_{dl}[MW]
0	98.7	0.53	0.41
13	99.2	0.62	0.43
26	97.5	0.69	0.44
39	96.5	0.77	0.45
52	94.2	0.91	0.47

5.2. Kinetic energy storage system and SVC

The kinetic energy storage system can supply or consume either active power or reactive power. The active power is absorbed or released by a flywheel according to the requirements set to control the frequency. The reactive power can be controlled by the power electronics which connect the flywheel with the grid, however, in these simulations, that task is performed by an SVC.

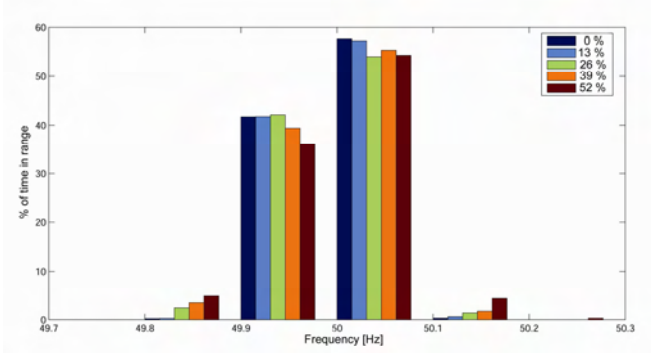

Figure 4. Frequency histogram with the use of the KESS and the SVC.

In Figure 4 the frequency histogram for different wind power percentages penetration is illustrated. It seems that the frequency is quite well controlled, and stays within the limits

most of the time. The deviations in the case of no wind power in the grid are almost completely eliminated. In the histogram it is also possible to notice that the higher the percentage of wind power in the network is, the higher are the deviations from the permitted range. However, comparing this result with the case of no corrective measures taken, the over and under frequencies are much attenuated. The values of the percentage of time, in which the frequency is within the permitted range, and the short term flicker power values are presented in the Table 3. Here it is possible to note that in all the cases of wind power penetration studied, the kinetic energy storage system is able to keep the frequency within the range of 49.9-50.1 Hz for more than 90% of the time. It is even reaching values as high as 99% for the cases of no wind power in the network and 13% of wind power penetration.

Table 3. Impact on frequency and voltage with the use of the KESS and the SVC.

% of wind power	% time inside limits	P_{st}
0	99.4	0.47
13	99.2	0.55
26	96.2	0.65
39	94.7	0.74
52	90.7	0.87

In terms of voltage, the improvement is very remarkable. All the values of short term flicker power are below one, which is the maximum permitted level. It can as well be noticed that the values in this case are smaller than the values with the dump load. The reason for this could be related to the different response from the KESS and the dump load. While the KESS simply modify its active power exchange with the grid, the dump load changes both, active and reactive power. These reactive power changes are another source of voltage disturbances which the SVC system has to deal with.

5.3. Load shedding and SVC

Since the load shedding only has been set up to be able to help with the under frequency problems, it is more interesting to examine the percentage of time where the frequency drops below 49.9Hz. The possible impact in the consumers comfort due to the load shedding is discussed as well by mean of computing the percentage of time that the load is connected.

Table 4. Underfrequency percentages with different amounts of load shedding.

% of wind power	0 kW	50 kW	100 kW	150 kW
0	25.5	17.2	11.4	4.1
13	22.9	16.2	9.8	3.4
26	22.2	16.8	12	6
39	21.9	17.2	11.7	6.4
52	20.8	17.4	13.3	8.5

In the Table 4 the values of percentage of time in which the frequency is below 49.9Hz are shown. Cases of 0kW, 50kW, 100kW, 150kW of load shedding are shown. The average power consumption is 7MW, so the cases of load shedding correspond to 0%, 0.71%, 1.4% and 2.1% of the total consumption. Those percentages are quite small in comparison with the very noticeable improvement they generate in terms of under frequencies. The improvement is illustrated by comparing the column for 0% load shedding with the following, in which the load shedding is applied. As it could be expected, the higher the load shedding amount is, the smaller is the percentage of time with under frequencies. With 150kW of load shedding capability the under-frequencies are highly reduced leading the frequency to go below the limit for small percentages of time.

Table 5. Percentages of time that the load is connected.

% of wind power	50 kW	100 kW	150 kW
0	71	76	77
13	72	75	78
26	72	75	77
39	72	75	77
52	73	75	76

To check the impact in the consumers comfort it is necessary to look at the percentage of time along the simulation in which the load is connected. In Table 5 such percentages are shown. The percentage of time each load shedding capability is connected does not change much by rows. It can be approximated that with 50kW the load is consuming 72% of the time, with 100kW it is consuming 75% of the time, and with 150kW it is consuming 77% of the time. In all the cases, there would be some impact on the customers. The consequence of this could for some loads concern the time needed for carrying out their task (e.g. water heaters), or slightly affect their duty cycles (refrigerators, space heating or freezers

Table 6. Impact on frequency and voltage (% time inside frequency limts and P_{st}, respectively) with the use of different amounts of load shedding and the SVC.

% of wind power	50 kW		100 kW		150 kW	
0	64	0.65	73	0.68	83	0.70
13	65	0.67	42	0.70	83	0.73
26	62	0.75	71	0.77	79	0.79
39	62	0.83	72	0.87	79	0.86
52	57	0.89	67	0.93	74	0.95

In Table 6 it is possible to take a general view of the improvements in frequency and voltage in the conditions discussed in this section. In terms of frequency, the improvement is not as noticeable as with the dump load or the KESS. This is, as mentioned before, due to the fact that the load shedding is only able to overcome problems with under frequencies and not able to react to over frequencies. Regarding voltage, the SVC manages to keep the voltage quite stable and all the flicker power values are below the limit of one.

6. CONCLUSION

The operation of a grid cell (average load: 7 MW) separated from the interconnected power system has been analysed under several different scenarios of wind power percentage

penetration from 0% to 52%. The grid cell is representative for a Danish distribution system with respect to characteristics for local CHP, wind turbines and consumption. Without introduction of any specific measures simulation results unveiled that the variable load is able to cause considerable deviations in frequency (49.5-50.5 Hz) and very wide variations in the voltage; leading to annoying flicker levels (P_{st}=3.73). The normal consumption variations in active and reactive power cannot be compensated fast enough by the local CHP. With 13% of wind power in the network a slightly improvement in the frequency quality takes place. The reason for this is the system inertia increase with the addition of wind turbines. The higher the inertia of the system is, the smaller the frequency deviations are.

For improving the frequency control the use of a dump load and a kinetic energy storage system has been examined. Testing these devices gave very satisfactory results and the frequency deviations were highly reduced. With 400 kW of dumping load capability the frequency is kept within limits more than 94% of time, and with a 300 kW KESS more than 90%. This kind of devices are very helpful for controlling short term frequency deviations, but the long term deviations have to be controlled by other means.

The effect of different amounts of automatic load shedding has also been considered. This operation is useful for cases of under frequencies, and the results were quite good. The under frequencies were reduced, and the frequency improvement increased with increasing amount of load shed. The possible impact on the customers was also analyzed by calculating the percentage of time the loads would be connected.

For improving the poor voltage quality, the use of a Static Var Reactor (SVC) has been considered. This device is able to control the voltage in the consumers' node eliminating the flicker problems due to its capability of controlling the reactive power very fast.

7. DISCUSSION

Even though it might seem like the use of these devices are not feasible to apply in the actual grid, due to the need of a large amount of such devices spread along the whole network, the application could be feasible if the following considerations are taken into account:

- There are a lot of loads spread in the electric grid which potentially can be used as dump loads. For becoming a dump load a Dynamic Grid Interface (DGI) is needed, which would control the power according to requirements for frequency. The DGI could also be used in a cost-effective operating philosophy in non isolated operation. In that operation mode, the dump load would be controlled for example to avoid the penalty fares of large power peaks in the consumption of a large factory. This could encourage the use of these devices.
- The kinetic energy storage systems could have two different purposes, on one hand they could perform the task exposed here, but nowadays they are already being used as Uninterrupted Power Supply (UPS). These two possible applications of the KESS could make their use in the electric grid suitable.
- The SVC is a quite expensive system and large scale use would probably not be affordable. However, the task realised by this system could be done by other devices. For example, the power converters of the KESS or DGI could perform the task of a SVC in a small scale. In fact, in the datasheet for the used KESS model, its capability for voltage support by reactive power control is explained.

APPENDIX

Dump load model in *PowerFactory*

In Figure 5 the blocks diagram of the model is depicted and the values used for the parameters are shown in Table 7.

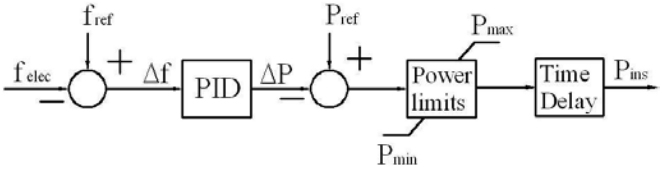

Figure 5. Blocks diagram of the dump load model built in *PowerFactory.*

Table 7. Parameter values of the dump load model.

Definition	Parameter	Value
Frequency reference	f_{ref}	1 [pu]
PID Gain	K	80
PID integral constant	T_i	0.005
PID differential constant	[α, T_D]	[0.5, 2]
Power reference	P_{ref}	0.4 [MW]
Maximum power	P_{max}	0.6 [MW]
Minimum power	P_{min}	0.2 [MW]
Time delay constant	T_r	1.5 [s]

KEES model in *PowerFactory*

The model used for the kinetic energy storage system is depicted in Figure 6. That figure does not show the PID controller which transform the frequency deviation in the signal a_t, but in the Table 8 the values of its parameters are shown.

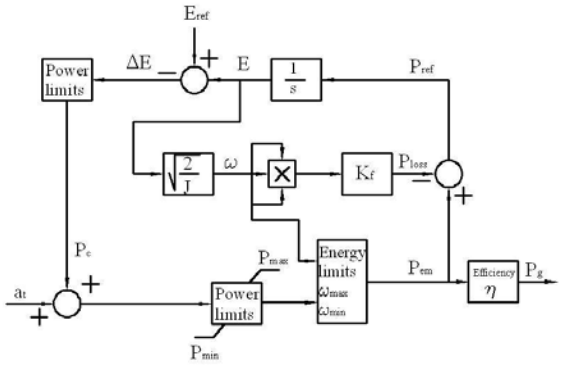

Figure 6. Blocks diagram of the kinetic energy storage system.in *PowerFactory.*

Table 8. Parameter values of the energy storage system model.

Definition	Parameter	Value
Frequency reference	f_{ref}	1 [pu]
PID Gain	K	$-50 \cdot 10^6$
PID integral constant	T_i	0.01
PID differential constant	[α, T_D]	[0.25, 4]
Energy reference	E_{ref}	13.7 [MJ]
Charge-Discharge power	P_c	$\pm 20 \cdot 10^3$ [W]
Friction constant	K_f	$2.9 \cdot 10^{-4}$ [W(s/Rad)^3]
Efficiency	η	0.94
Max. power absorption	P_{max}	300 [kW]
Max. power supply	P_{min}	-300 [kW]
Max. rotational speed	ω_{max}	345 [Rad/s]
Min. rotational speed	ω_{min}	188.5 [Rad/s]

ACKNOWLEDGEMENT

The authors would like to thank the people of *WindData*, *Energinet.dk* and *DONG Energy* for their inestimable collaboration for building the models.

REFERENCES

[1] Nordic grid code. Nordel, January 2007.
[2] Flickermeter standard IEC 868. IEC, 1990.
[3] Limitation of voltage changes, voltage fluctuations and flicker in public low-voltage supply systems, for equipment with rated current <=16 A per phase and not subject to conditional connection IEC 61000-3-3. IEC, October 2005.
[4] P. Rosas. Dynamic influences of wind power on the power systems. Risø National Laboratory. PhD-thesis, March 2003.
[5] V. Akhmatov. Analysis of dynamic behaviour of electric power systems with large amount of wind power. Ørsted·DTU, Electric Power Engineering. PhD-thesis, June 2003.
[6] J. Schlabbach, D. Blume, T. Stephanblome. Voltage quality in electrical power systems. December 2001.
[7] P. von Brug, J. Allmeling. Flywheel based power quality improvement in a medium voltage grid. Chester International Conference 1998. June 1998.
[8] S. M. Drouilhet. Power flow management in a high penetration wind-diesel hybrid power system with short-term energy storage. U.S. National renewable energy laboratory, June 1999.
[9] Z. Zu, J. Østergaard, M. Togeby, C. Marcus-Møller. Design and modelling of thermostatically controlled loads as frequency controlled reserve, IEEE Power Engineering Society 2007 General Meeting (IEEE-PES 2007), 24-28 June, 2007 Tampa, FL, USA.
[10] D. Trudnowski. Power-system frequency and stability control using decentralized intelligent loads. IEEE Power Engineering Society T & D Conference and Expo. 2005.
[11] R. Guttromson, M. Kintner-Meyer, D. Oedingen, S. Lang. Final report for California energy commission: Smart load control and grid friendly appliances. Architecture Energy Corporation and Battelle Memorial Institute. October 2003.
[12] DigSilent. PowerFactory user manual. 2006.
[13] Power store 500 wind/diesel. Powercorp powerstore brochure. Exports drive, Darwin Business park, Berrimah, northern territory, Australia 0828.

Load flow analysis considering wind turbine generator power uncertainties

Divya K.C., *Member, IEEE*

***Abstract*— In this paper the effect of wind turbine generator (WG) output uncertainties on the distribution system node voltages has been investigated. For this purpose a new approach viz., interval method of analysis has been proposed. In this method, the wind speed variations are represented as intervals and the WG output uncertainties are computed. Further, an interval load flow method has been proposed to compute the effect of this WG output uncertainties on the distribution system node voltages. The performance of the proposed interval method has been compared with the Monte Carlo method.**

***Index Terms*— Distributed generation, Load flow analysis, Uncertainty, Wind turbine**

NOMENCLATURE

$[\underline{a}, \overline{a}]$: Indicates that a is an interval and $\underline{a}$ is the minimum value/lower bound, $\overline{a}$ is the maximum value/upper bound.
P_{WG}: Active power output of WG
Q_{WG}: Reactive power of WG
u_w: Wind speed
V: Voltage magnitude
$u_{w_{nominal}}$: Nominal wind speed (Minimum wind speed at which the power output of the wind turbine is equal to its rated value)
P_p: Active power at bus p (subscripts p, q have been used to indicate the bus number)
Q_p: Reactive power at bus p
V_p: Voltage magnitude at bus p
θ_p: Voltage angle at bus p
$Y_{pq} = G_{pq} + \jmath B_{pq}$, G_{pq} and B_{pq} are the real and imaginary parts of the pq^{th} element of the admittance matrix.
$V_{p_0}, \theta_{p_0}, P_{p_0}, Q_{p_0}$: Mid point of voltage magnitude, voltage angle, active and reactive power intervals at bus p. These are deterministic scalar values and calculated as the average of their respective interval upper and lower bound values.
R_1: Induction generator stator resistance
X_{l1}: Induction generator stator leakage reactance
R_2: Induction generator rotor resistance
X_{l2}: Induction generator rotor leakage reactance
X_m: Induction generator magnetizing reactance
X_c: Reactance of shunt capacitor compensation
N: Number of poles (Induction generator)
$u_{w_{CI}}$: Cut-in wind speed (Lowest wind speed at which the WG starts generating power)
$u_{w_{CO}}$: Cut-out wind speed (Wind speed at beyond the WG is shutdown)

K.C. Divya is with Center for Electrical Technology, Oersted DTU, Kgs. Lyngby 2800, Denmark (email: dkc@oersted.dtu.dk).

I. INTRODUCTION

In the last decade generation of electricity from wind energy has gained world wide attention. At present large number of wind turbine generating units (WG) are being connected to the distribution systems. Due to intermittency in the WG output, the connection of these sources could effect the voltages, power flows and losses of the distribution systems. Quantification of these effects is important in determining the maximum allowable wind power penetration in a distribution network.

In an attempt to quantify the effects of WG output uncertainties on the distribution system node voltages the use of probabilistic load flow methods has been suggested in [1], [2] while in [3] a sequence of deterministic load flow simulations have been carried out.

In the context of load flow analysis considering uncertainties, the probabilistic approach has been suggested by many investigators. The probabilistic methods used in [1], [2], [4]–[10], requires probability distribution function(PDF) of powers at each node, which is difficult to obtain [2]. Further, in most of these investigations [1], [5], [9], [10] the linearized load flow equations are used. In some of the investigations [2], [7], [8], where in the linearity assumption is not made, sequence of deterministic load flow solutions are used to compute the node voltage statistics (mean/standard deviation/PDF). However, the node voltage statistics obtained using these methods depends either on the quantization step of the nodal power PDF [2], [7] or on the manner in which the node voltage ranges are chosen [2], [8]. Further, the methods suggested in [2], [7], [8] require considerable computational effort.

In this paper, a new method of analyzing the effect of WG power output uncertainties on the power system network steady state voltage has been proposed. This method is based on interval method of analysis, wherein the uncertainties are represented by intervals. Since this method requires the uncertainty in the inputs to be specified as interval range (WG active and reactive powers), first a method has been presented here to calculate interval range for the power output of the WG. In order to determine the upper and lower bound (interval range) for the voltage at each node of the network an interval load flow algorithm has been suggested here. Simulation studies have been presented to demonstrate the effect of WG output uncertainties on the distribution system node voltages. Further, the results obtained using the proposed interval method have been compared with the one obtained using the Monte Carlo method suggested in [8].

II. Interval model for WG power output

For a given/obtained wind speed range the WG power output range is computed by modifying the steady state WG models developed in [11], [12]. In [11] a steady state model has been developed for each type of WG i.e., stall regulated fixed speed, pitch regulated fixed speed, semi-variable and variable speed WG. However, these steady state models can not be directly used here since it requires a deterministic value for wind speed, voltage and computes a (deterministic) value for the WG power output. In order to quantify the WG power output uncertainty by intervals, some modifications have been proposed here to the steady state WG models suggested in [11]. In particular, the method suggested here is based on the sensitivity of the power output of different types of WG (fixed-stall and pitch regulated, semi variable and variable speed) to the wind speed and voltage. In the following sections, the procedure for calculating the active and reactive power intervals of each of the four types of WG has been discussed.

A. Determination of interval range for a given wind speed variation

The wind speed range is generally obtained from the wind speed measurement data at a given WG site. The wind speed measurements or recording (at a wind site) could correspond to either instantaneous or the average values of wind speed. If average wind speed data is available then it would not contain the high frequency components (few milliseconds) of wind speed variation. Hence, the wind speed range can be obtained directly i.e., maximum and minimum values of the average wind speed data. In cases where the instantaneous values of wind speed data is available it is necessary to eliminate the high frequency components. This is because the high frequency wind speed variations may not affect the WG power output [13]. Hence, the high frequency components present in the wind speed data is first filtered out using a low pass filter (the method is illustrated later in simulation studies) and from this the wind speed range is obtained.

B. Stall regulated fixed speed WG

From the study carried out in [11] it is evident that the active power output increases with wind speed up to the nominal wind speed. However, beyond nominal wind speed, increase in wind speed decreases the power output of the WG. Further, it has been shown that voltage variation has little impact on the active power output of the stall regulated fixed speed WG and hence can be neglected.

The reactive power demand varies with voltage as well as wind speed and it increases with increase in wind speed (up to nominal) and beyond nominal it decreases. However, with increase in voltage the reactive power demand decreases and vice-versa.

For the given wind speed interval, the maximum as well as minimum values of the power output are computed using the WG models developed in [11] and the following procedure:

Method of computing stall regulated fixed speed WG power output range ($[\underline{P_{WG}}, \overline{P_{WG}}]$ and $[\underline{Q_{WG}}, \overline{Q_{WG}}]$)

Given intervals for wind speed $[\underline{u_w}, \overline{u_w}]$ and voltage $[\underline{V}, \overline{V}]$
If $u_{w_{nominal}} \in [\underline{u_w}, \overline{u_w}]$ then

a) Minimum value of the active and reactive power ($\underline{P_{WG}}$, $\underline{Q_{WG}}$):
Compute the active and reactive power using the method suggested in [11] for the following cases:
   i) Minimum wind speed and maximum voltage
   ii) Maximum wind speed and minimum voltage
Minimum value of active and reactive powers are

$$\underline{P_{WG}} = \min(P_{WG}(\underline{u_w}, \overline{V}), P_{WG}(\overline{u_w}, \underline{V})) \quad (1)$$
$$\underline{Q_{WG}} = \min(Q_{WG}(\underline{u_w}, \overline{V}), Q_{WG}(\overline{u_w}, \underline{V})) \quad (2)$$

b) Maximum value of active and reactive power ($\overline{P_{WG}}$, $\overline{Q_{WG}}$):
Compute the active and reactive power, for nominal wind speed and minimum voltage, i.e.,

$$\overline{P_{WG}} = P_{WG}(u_{w_{nominal}}, \underline{V}) \quad (3)$$
$$\overline{Q_{WG}} = Q_{WG}(u_{w_{nominal}}, \underline{V}) \quad (4)$$

Else

a) Minimum value of active and reactive power ($\underline{P_{WG}}$, $\underline{Q_{WG}}$):
Compute the active and reactive power, for minimum wind speed and maximum voltage, viz.,

$$\underline{P_{WG}} = P_{WG}(\underline{u_w}, \overline{V}) \quad (5)$$
$$\underline{Q_{WG}} = Q_{WG}(\underline{u_w}, \overline{V}) \quad (6)$$

b) Maximum value of active and reactive power ($\overline{P_{WG}}$, $\overline{Q_{WG}}$):
Compute the active and reactive power, for maximum wind speed and minimum voltage, viz.,

$$\overline{P_{WG}} = P_{WG}(\overline{u_w}, \underline{V}) \quad (7)$$
$$\overline{Q_{WG}} = Q_{WG}(\overline{u_w}, \underline{V}) \quad (8)$$

C. Pitch regulated fixed speed and Semi-variable speed WG

The active and reactive power of these two types of WG increases with increase in wind speed up to nominal wind speed. For wind speeds greater that nominal, the active power output of this WG remains constant. Further, the active power output does not vary appreciably with voltage. However, the variation of reactive power with voltage needs to be considered. The reactive power demand increases with decrease in voltage and vice-versa.

The procedure used to compute the active and reactive power output range for this WG has been given below:
Method of computing pitch regulated fixed speed WG power output interval ($[\underline{P_{WG}}, \overline{P_{WG}}]$ and $[\underline{Q_{WG}}, \overline{Q_{WG}}]$)
Given wind speed $[\underline{u_w}, \overline{u_w}]$ and voltage $[\underline{V}, \overline{V}]$ intervals
If $u_{w_{nominal}} \in [\underline{u_w}, \overline{u_w}]$

a) Minimum value of the active and reactive power ($\underline{P_{WG}}$, $\underline{Q_{WG}}$):
Compute the active and reactive power, for minimum

wind speed and maximum voltage, using the method suggested in [11] i.e.,

$$\underline{P_{WG}} = P_{WG}(\underline{u_w}, \overline{V}) \quad (9)$$

$$\underline{Q_{WG}} = Q_{WG}(\underline{u_w}, \overline{V}) \quad (10)$$

b) Maximum value of active and reactive power ($\overline{P_{WG}}, \overline{Q_{WG}}$):
Compute the active and reactive power for nominal wind speed and minimum voltage i.e.,

$$\overline{P_{WG}} = P_{WG}(u_{w_{nominal}}, \underline{V}) \quad (11)$$

$$\overline{Q_{WG}} = Q_{WG}(u_{w_{nominal}}, \underline{V}) \quad (12)$$

Else

a) Minimum value of the active and reactive power ($\underline{P_{WG}}$, $\underline{Q_{WG}}$):
Compute the active and reactive power, for minimum wind speed and maximum voltage i.e.,

$$\underline{P_{WG}} = P_{WG}(\underline{u_w}, \overline{V}) \quad (13)$$

$$\underline{Q_{WG}} = Q_{WG}(\underline{u_w}, \overline{V}) \quad (14)$$

b) Maximum value of active and reactive power ($\overline{P_{WG}}, \overline{Q_{WG}}$):
Compute the active and reactive power for maximum wind speed and minimum voltage i.e.,

$$\overline{P_{WG}} = P_{WG}(\overline{u_w}, \underline{V}) \quad (15)$$

$$\overline{Q_{WG}} = Q_{WG}(\overline{u_w}, \underline{V}) \quad (16)$$

D. Variable speed WG

In the case of variable speed WG it has been shown in [11] that for normal range of voltage variations, the active as well as reactive power do not vary. Further, the reactive power either remains constant at the specified value (irrespective of the wind speed variations) or corresponds to the one required to maintain the specified power factor. Hence, in the normal operating range, the active power output depends on the wind speed alone and reactive power is constant or depends on the active power output of the WG. Hence, the maximum and minimum value of the active power output corresponds to the one at maximum and minimum wind speeds respectively.

III. Interval Load flow method

The interval load flow method essentially means a procedure to find a solution for the following interval load flow equations i.e., solving (17),(18) for $[\underline{V_p}, \overline{V_p}]$ ($p \in$PQ buses) and $[\underline{\theta_p}, \overline{\theta_p}]$ ($p \neq$slack) for given $[\underline{P_p}, \overline{P_p}]$ ($p \neq$slack), $[\underline{Q_p}, \overline{Q_p}]$ ($p \in$PQ buses) and $[\underline{V_p}, \overline{V_p}]$ ($p \in$PV buses).

$$[\underline{P_p}, \overline{P_p}] = [\underline{V_p}, \overline{V_p}] \sum_{q=1}^{n} \{[\underline{V_q}, \overline{V_q}](G_{pq} \cos[\underline{\theta_{pq}}, \overline{\theta_{pq}}] + B_{pq} \sin[\underline{\theta_{pq}}, \overline{\theta_{pq}}])\}, p = 1, ..., n; p \neq Slack \quad (17)$$

$$[\underline{Q_p}, \overline{Q_p}] = [\underline{V_p}, \overline{V_p}] \sum_{q=1}^{n} \{[\underline{V_q}, \overline{V_q}](G_{pq} \sin[\underline{\theta_{pq}}, \overline{\theta_{pq}}] - B_{pq} \cos[\underline{\theta_{pq}}, \overline{\theta_{pq}}])\}, p = 1, ..., n; p \neq PV, p \neq Slack \quad (18)$$

where,
n is the number of buses
$[\underline{\theta_{pq}}, \overline{\theta_{pq}}] = [\underline{\theta_p}, \overline{\theta_p}] - [\underline{\theta_q}, \overline{\theta_q}]$
It must be noted here that (17),(18) differs from the standard load flow equations in polar coordinates [14] since the active and reactive power at all the PQ buses and active power and voltage magnitude at all the PV buses are intervals.

The procedure for solving the non-linear interval load flow equations (17),(18) involves two main steps [12]. The first step is to find the load flow solution (voltage magnitude/angle, say V_{p_0}/θ_{p_0}) at the mid points of the intervals for $[\underline{P_p}, \overline{P_p}]$ and $[\underline{Q_p}, \overline{Q_p}]$ i.e., at $P_{p_0} = (\underline{P_p} + \overline{P_p})/2$ and $Q_{p_0} = (\underline{Q_p} + \overline{Q_p})/2$. The next step is to calculate the elements of the standard load flow Jacobian in polar coordinates are computed at V_{p_0} and θ_{p_0}. From this, the interval for voltage magnitude and angle are obtained. The procedure for computing the intervals for voltage magnitude and angle is given below:

Algorithm for solving interval load flow equations

Given intervals for $[\underline{P_p}, \overline{P_p}]$, $[\underline{Q_p}, \overline{Q_p}]$ at all PQ buses and $[\underline{P_p}, \overline{P_p}]$, $[\underline{V_p}, \overline{V_p}]$ at all PV buses, the interval for $[\underline{V_p}, \overline{V_p}]$ at all PQ buses and $[\underline{\theta_p}, \overline{\theta_p}]$ at all PQ and PV buses are computed in the following way:

i) Obtain the load flow solution at (P_{p_0}, Q_{p_0} and V_{p_0}) the mid points of each of the intervals.
Let the solution be V_{p_0} and θ_{p_0} ($p = 1, 2, ..., n+m+1$).

ii) Let $[\underline{V_p}, \overline{V_p}] = [V_{p_0}, V_{p_0}]$ and $[\underline{\theta_p}, \overline{\theta_p}] = [0, 0]$. At the slack bus the voltage magnitude and angle are point intervals and are deterministic values equal to V_{p_0} and zero respectively.

iii) Compute the elements of the load flow Jacobian matrix (J_{Polar}) at V_{p_0} and θ_{p_0}.

iv) Solve the following equations for $[\underline{\triangle V}, \overline{\triangle V}], [\underline{\triangle \theta}, \overline{\triangle \theta}]$

$$[\underline{\triangle S}, \overline{\triangle S}] = (J_{Polar}) \begin{pmatrix} [\underline{\triangle \theta}, \overline{\triangle \theta}] \\ [\underline{\triangle V}, \overline{\triangle V}] \end{pmatrix} \quad (19)$$

where

$$[\underline{\triangle S}, \overline{\triangle S}] = \begin{pmatrix} [\underline{P_p} - P_{p_0}, \overline{P_p} - P_{p_0}] \\ [\underline{Q_p} - Q_{p_0}, \overline{Q_p} - Q_{p_0}] \end{pmatrix} \quad (20)$$

and J_{Polar} is the standard [14] load flow Jacobian matrix ie.,

$$J_{Polar} = \begin{pmatrix} \frac{\partial P}{\partial \theta} & \frac{\partial P}{\partial V} \\ \frac{\partial Q}{\partial \theta} & \frac{\partial Q}{\partial V} \end{pmatrix} \quad (21)$$

where, $\frac{\partial P}{\partial \theta}, \frac{\partial P}{\partial V}, \frac{\partial Q}{\partial \theta}, \frac{\partial Q}{\partial V}$ are the elements of the standard load flow Jacobian matrix in polar coordinates [14] and these elements are calculated at V_{p_0} and θ_{p_0}.

In order to solve the above equation, first the inverse of the Jacobian matrix (${J_{Polar}}^{-1}$) is computed. Later interval arithmetic [15] is used to compute the product ${J_{Polar}}^{-1}[\underline{\triangle S}, \overline{\triangle S}]$. It must be noted here that interval addition and multiplication is quiet different from the usual addition and multiplication [15].

v) $[\underline{V_p}, \overline{V_p}] = [V_0 + \underline{\triangle V}, V_0 + \overline{\triangle V}]$ and $[\underline{\theta_p}, \overline{\theta_p}] = [\theta_0 + \underline{\triangle \theta}, \theta_0 + \overline{\triangle \theta}]$

IV. Interval Load flow algorithm with WG output uncertainty

For the interval load flow analysis suggested here, the WG are modeled as PQ buses. However, the interval load flow algorithm described in the previous section can not be directly used because the interval range for P,Q of the WG can be calculated only if the node voltage interval is known at the WG bus (Section II). However, the node voltage interval is not known till the load flow solution is obtained. In order to account for this interdependency, a two step procedure (interval load flow equations are solved twice) has been suggested here.

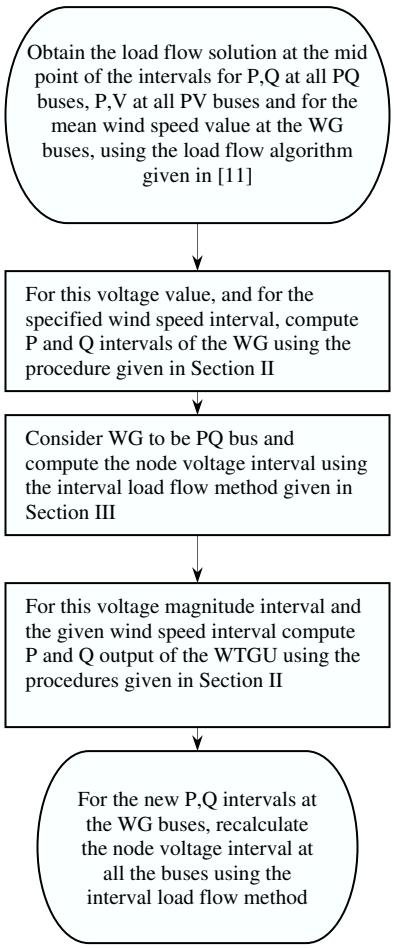

Fig. 1. Flow chart : Load flow analysis with WG (considering wind speed variation)

A flowchart giving all the steps involved in computing the node voltage intervals at all the buses in a power system network considering the WG output uncertainties is shown in Fig. 1. Here, the WG bus is considered as a PQ bus and at the beginning of each iteration, for a given voltage magnitude and wind speed interval, the interval range for active as well as the reactive power output of the WG ($[\underline{P_{WG}}, \overline{P_{WG}}]$ and $[\underline{Q_{WG}}, \overline{Q_{WG}}]$) is obtained using one of the methods (depending on the type of WG) given in the Section II. For these interval ranges of power at the WG bus, the interval range at all the buses is calculated using the interval load flow algorithm given in the previous section. Further, if there is uncertainty in power/voltage magnitude at the other buses (load/generator bus) then these can also be considered by representing them as intervals. However, if there is no uncertainty then the power/voltage magnitude are deterministic values and in the interval load flow flowchart shown in Fig. 1 i.e., they are considered to be point intervals. For example if the active power at bus q is a deterministic value (say 0.1pu) then the interval for the active power at bus is $[\underline{P_q}, \overline{P_q}] = [0.1, 0.1]$, i.e., $\underline{P_q} = \overline{P_q}$ (this type of interval is called as point interval).

Further, it may be seen from the interval load flow algorithm (Fig. 1) that the node voltage at all the buses will be intervals if there is uncertainty in power/voltage magnitude at even one bus. For example if the active power only at bus-p is an interval (not point interval) then the voltage magnitude (at all PQ buses) and angle (at all PV, PQ buses) are intervals.

V. Simulation study

For the simulation study a 33 bus radial distribution system [16] with all the four types of WG and a set of actual measured wind speed data have been considered. Each WG is of 900kW capacity and the data for these types of WG have been given in Table I.

TABLE I
WG DATA

Parameter [12]	Types of WG			
	Stall	Pitch	Semi-variable	Variable
MW	0.9	0.9	0.9	0.9
kV	0.69	0.69	0.69	0.69
R_1 (pu)	0.00643	0.0051	0.0051	0.0051
X_{l1} (pu)	0.10397	0.04726	0.04726	0.04726
R_2 (pu)	0.00567	0.00416	0.00416	0.00416
X_{l2} (pu)	0.0794	0.08696	0.08696	0.08696
X_m (pu)	3.0246	2.6087	2.6087	2.6087
X_c (pu)	3.0246	2.6087	2.6087	2.6087
N	4	4	4	4
$u_{w_{CI}}$	4	4	4	4
$u_{w_{CO}}$	25	25	25	25

System base = 0.9MVA,0.69kV

In order to assess the impact of wind speed variation on WG output and the distribution system voltage profile, the wind speed variation is needed in addition to the WG and system data. The wind speed interval is obtained from the measured wind speed data at a typical wind site. Three different measured wind speed variation have been considered and these measurements have been made over a period of 10 min. Since the sampling frequency used in all these measurements is 35Hz, the measured wind speed data captures some fast wind variations too. In [13] it has been stated that the high frequency wind speed variations are very local and will not cause power output variations. In order to eliminate the high frequency components present in the wind speed measurements, it has been suggested that the measured wind speed data should be passed through a low pass filter.

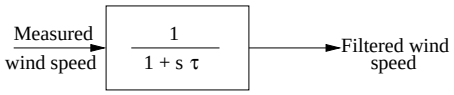

Fig. 2. Wind speed filter: Block diagram

1) Computing wind speed interval/range: Fig. 2 shows the block diagram of the low pass filter.

The raw data (measured wind speed) is first passed through the low pass filter (Fig. 2). Later the filtered wind speed data is used to find the minimum and maximum values. This has been illustrated below for one of the wind speed measurements considered here. For the study carried out here the time constant of the low pass filter is taken to be $\tau = 4$sec. The filtered output as well as the raw (measured) wind speed data have been shown in Fig. 3.

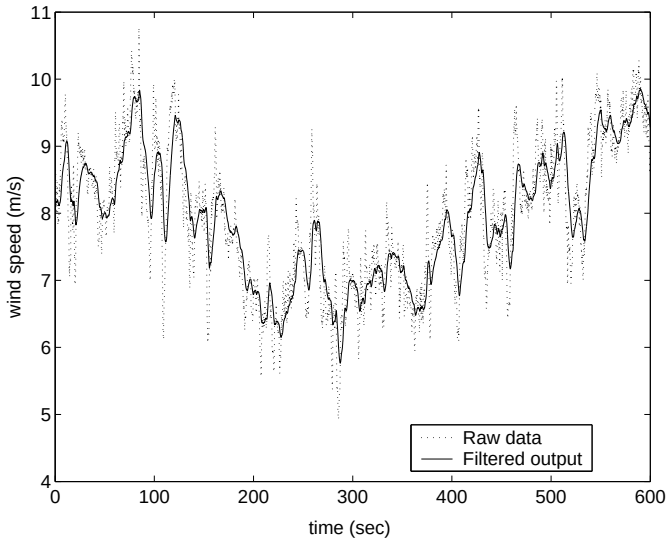

Fig. 3. Wind speed variation with time

From Fig 3 it may be seen that the maximum and minimum values of the filtered wind speed output are 5.7m/s and 9.8m/s respectively while that of the measured wind speed data are 4.9m/s and 10.7m/s respectively. The same procedure has been followed to obtain the wind speed interval for all the wind speed data at the other three WG and these are given in Table II.

TABLE II
WIND SPEED INTERVALS CONSIDERED AT EACH WG

Wind speed details		WG details	
$[\underline{u_w}, \overline{u_w}]$ (m/s)	Mean wind speed	WG type	Location Bus No.
$[5.7, 9.8]$	7.8	Fixed speed (stall)	33
$[5.3, 7.5]$	6.4	Semi-variable speed	6
$[5.5, 9.2]$	7.3	Fixed speed (pitch)	18
$[5.3, 7.5]$	6.4	Variable speed	25

For this case, the WG power output and the node voltage intervals have been obtained using the interval method suggested here and the Monte Carlo simulation. A summary of the load flow results obtained using the proposed interval method and using the Monte Carlo method are given in Table III. From this table it may be seen that, even for the same WG output intervals, the node voltage intervals obtained using the interval method and the Monte Carlo method [8] are different. It may be observed that the intervals obtained using the Monte Carlo method is a subset of that obtained using the proposed interval method. Further, it must be noted here that the Monte Carlo method used in practice does not always guarantee that the bounds obtained will correspond to the worst case. This is because in reality, it is generally difficult to ensure that the entire sample space is covered. However, the interval method does not have this limitation and the manner in which the interval arithmetic is carried out ensures that the upper and lower bounds obtained correspond to the worst case. Hence, for a given uncertainty in nodal power/wind speed, this method always guarantees that the node voltage magnitude can never be outside the computed interval. However, one of the limitations of the interval method is that it is very difficult to use it for large nodal power uncertainties (interval range is broad). This is because, the interval method could compute a voltage interval range which is so broad that it may have little practical significance. Hence, the proposed interval method could be effectively used to analyze the impact of small nodal power uncertainties on the power system nodal voltages.

TABLE III
SUMMARY OF LOAD FLOW RESULTS-DISTRIBUTION SYSTEM

Bus No.	WG power output		Voltage Magnitude
	$[P_{WG}]$	$[Q_{WG}]$	$[V]$
Interval Method			
33	[0.1190 0.5577]	[-0.0097 0.1345]	[0.8819 0.9208]
6	[0.0847 0.2770]	[-0.0150 0.0077]	[0.9352 0.9559]
18	[0.0331 0.4920]	[-0.0163 0.1118]	[0.8957 0.9499]
25	[0.0960 0.3106]	[0.0000 0.0000]	[0.9668 0.9763]
Monte Carlo Method			
33	[0.1190 0.5577]	[-0.0081 0.1219]	[0.8877 0.9142]
6	[0.0847 0.2770]	[-0.015 0.0076]	[0.9379 0.9533]
18	[0.0331 0.4920]	[-0.0163 0.1117]	[0.9037 0.9413]
25	[0.0960 0.3106]	[0.0000 0.0000]	[0.9678 0.9759]

VI. CONCLUSION

In this paper a new approach has been used to quantify the effect of WG output uncertainties on the distribution system node voltages. This approach is based on the interval method of analysis. In this method for a given wind speed interval the WG output uncertainties are computed. To compute the effect of these uncertainties on the distribution system node voltages an interval load method has been proposed. A comparison of the results obtained from the proposed method with Monte Carlo method has shown that the Monte Carlo method could under-estimate the effect of WG output uncertainties on the distribution system nodal voltages.

ACKNOWLEDGMENT

The author would like to thank Prof. Jacob Østergaard for his valuable suggestions on this paper and also for his constant support and encouragement.

REFERENCES

[1] N. Hatziargyriou, T. Karakatsanis, and M. Papadopoulos, "Probabilistic load flow in distribution systems containing dispersed wind power generation," *IEEE Transactions on Power Systems*, vol. 8, no. 1, pp. 159 – 165, 1993.

[2] N. G. Boulaxis, S. A. Papathanassiou, and M. P. Papadopoulos, "Wind turbine effect on the voltage profile of distribution networks," *Renewable Energy*, vol. 25, no. 3, pp. 401–415, 2002.

[3] C. Masters, J. Mutale, G. Strbac, S. Curcic, and N. Jenkins, "Statistical evaluation of voltages in distribution systems with embedded wind generation," *IEE Proceedings-Generation, Transmission and Distribution*, vol. 147, no. 4, pp. 207 – 212, 2000.

[4] B. Borkowska, "Probabilistic load flow," *IEEE Transactions on Power Apparatus Systems*, vol. PAS-93, no. Apr, pp. 752–759, 1974.

[5] J. F. Dopazo, O. A. Klitin, and A. M. Sasson, "Stochastic load flow," *IEEE Transactions on Power Apparatus Systems*, vol. PAS-94, no. Mar/Apr, pp. 299–309, 1975.

[6] A. Dimitrovski and K. Tomsovic, "Boundary load flow solutions," *IEEE Transactions on Power Systems*, vol. 19, no. 1, pp. 348– 355, 2004.

[7] A. Leite da Silva and V. Arienti, "Probabilistic load flow by a multilinear simulation algorithm," *IEE Proceedings-Generation, Transmission and Distribution*, vol. 137, no. 4, pp. 276 – 282, 1990.

[8] D. McQueen, P. Hyland, and S. Watson, "Application of a monte carlo simulation method for predicting voltage regulation on low-voltage networks," *IEEE Transactions on Power Systems*, vol. 20, no. 1, pp. 279 – 285, 2005.

[9] A. Schellenberg, W. Rosehart, and J. Aguado, "Cumulant-based probabilistic optimal power flow (p-opf) with gaussian and gamma distributions," *IEEE Transactions on Power Systems*, vol. 20, no. 2, pp. 773 – 781, 2005.

[10] ——, "Introduction to cumulant-based probabilistic optimal power flow (p-opf)," *IEEE Transactions on Power Systems*, vol. 20, no. 2, pp. 1184 – 1186, 2005.

[11] K. C. Divya and P. S. N. Rao, "Models for wind turbine generating systems and their application in load flow studies," *Electric Power Systems Research*, In Press, Available online 28 December 2005.

[12] K. C. Divya, "Wind based distributed generation and grid interaction : Modelling and analysis," Ph.D. dissertation, Dept. of Electrical Engg.,, 2006.

[13] J. Slootweg, H. Polinder, and W. Kling, "Representing wind turbine electrical generating systems in fundamental frequency simulations," *IEEE Transactions on Energy Conversion*, vol. 18, no. 4, pp. 516–524, 2003.

[14] G. W. Stagg and A. H. El-Abiad, *Computer Methods in Power System Analysis*. McGraw Hill, 1968.

[15] L. Jaulin, M. Kieffer, O. Didrit, and E. Walter, *Applied interval analysis*. Springer, 2001.

[16] M. E. Baran and F. F. Wu, "Network reconfiguration in distribution systems for loss reduction and load balancing," *IEEE Transactions on Power Delivery*, vol. 4, no. 2, pp. 1401–1407, 1989.

Increasing Wind Power Penetration by Advanced Control of Cold Store Temperatures

Tom Cronin[1*)], Henrik Bindner[1)], Carsten Hansen[1)], Oliver Gehrke[1)], Mikel Iribas Latour (CNER), Monica Aguado (CNER), David Rivas Ascaso (CNER), Kostadin Fikiin (TU Sofia), Mathijs van Dijk (NEKOVRI), René Reinders (ESSENT), Bram Hage (PAL), Sietze van der Sluis (TNO – MEP, Project Coordinator)
[1)] Risø DTU, VEA-118, P.O. Box 49, DK-4000 Roskilde, Denmark
[*)] tlf. +45 4677 5961, e-mail tom.cronin@risoe.dk

Abstract — By adjusting the control of cold store compressors so that, in times of high wind energy availability cold store temperatures are reduced, energy can be absorbed which otherwise would be considered excess and therefore lower the price of electricity. In turn, this increases the value of wind energy paving the way for market forces to drive a higher penetration. The proposal is that the integration of renewable energy resources into the European electricity grid can be assisted by providing new facilities for energy storage, through the use of existing hardware and thus relatively little capital investment.

Index Terms — cold store, control, energy storage, wind power.

1. Introduction

As part of an EU-funded project – NightWind – Risø is simulating electrical systems that enable the investigation of the interaction between cold stores and production from wind turbines. The simulation environment is Risø's in-house software package, IPSYS, which is designed for assessing networks with multiple sources of energy.

The Night Wind concept combines wind energy and refrigerated warehouses in an innovative way, in order to address some of the problems associated with high wind penetration. The warehouses are effectively used as energy storage devices by providing an additional means to help match demand and fluctuating supply. The Night Wind project aims to store wind power in the form of thermal energy by influencing the temperature control in refrigerated warehouses. In times of high wind supply the temperature can be lowered, using the "excess energy" and, additionally, decreasing future cooling demand. When wind power availability is low, the storage can be "discharged" by allowing the temperature to rise again. This has the effect of adding a "virtual battery" to the power system with relatively little investment in new hardware.

Cold stores currently schedule their ability to store thermal energy with the control signal being the electricity price but this is derived purely from the traditional demand-supply pattern which simply results in cold stores using most energy at night time. The challenges are, then, to:

- Simulate the co-ordination of cold store energy use with wind power generation to assess the impact on the amount of wind capacity in a system.
- Implement a controller that by some means of forecasting can decide when energy can be "stored" or when energy should be "released" because there is a higher value in having the ability to store energy at some future point in time. Fundamentally, the controller always has the food safety temperatures as overriding limits.
- Assess the means by which this co-ordination can be done, i.e. can a price signal be used which indicates the correlation of the amount of wind energy production with the electricity price, in a system with high wind penetration?
- Consider how the enabling of cold stores to provide energy storage services to the grid can increase their competitiveness.
- Investigate the extent to which temperature ranges in cold stores can be extended so that their storage of thermal energy can be increased.

There are two main stages in the simulations:

1) Simulation of a single cold store, some local wind turbines and a grid connection – this enables the fundamentals of the control system to be worked out, together with some degree of verification using data from an actual cold store belonging to one of the project partners.

2) Representative simulation of a larger network to assess the impact of the Night Wind concept on a wider scale. It is intended that this should implement a more advanced development of the control system to include the influence of wind power availability and the electricity price.

This paper further describes the concept, giving the background to the problems of increasing wind energy penetration in the European network. The simulation models together with the controllers being developed will be explained and the results of the investigation so far will be presented and conclusions drawn that serve to guide the continuation of the work.

2. Cold Store Operation and Temperature Control

Cold stores are major users of electrical energy. The cold store which makes up the demonstration element in the Night Wind project consumes around 12 million kWh per year. Whilst it is one of the largest in Europe, the fundamental principles of operation are common with other cold stores. (Note that the focus here is on cold stores with an upper temperature limit of -18°C and not chilled stores where goods are maintained above freezing.) The major power consumption comes from the compressors within the

refrigeration units, whose main loads are the heat transfer from the external environment and from the goods coming into the store at around -7°C. The control system at present attempts to use cheaper night-time electricity, but invariably the compressors also need to run at times during the day to keep the temperature below the upper limit.

2.1. Benefits of a new control scheme

A new control schemes that takes account of the availability has potential attractions from a number of points of view:

The cold store owner may be able to:

- get added return for his investment (i.e. owning a cold store) if he becomes a wind turbine operator as well :
  - when the price of wind power is low, use it for own consumption
  - when the price of wind power is high, sell it
- reduce operating costs by taking advantage of "excess" wind power.
- sell the ability to defer load as an ancillary service to the power system operator.

The power system operator may be able to:

- increase the value of wind power.
- achieve a increased ability to match actual and predicted generation.

The European network may be able to:

- increase the penetration of wind power as a whole.

Above all, there is the potential to increase wind power integration at a low cost.

In order to make these models match, the power price would have to reflect the supply of wind power (which it does at a high enough penetration, in a functioning market)

2.2. Requirements for a new controller

Traditional cold stores employ a simple thermostatic control with a certain hysteresis. The thermostat measures the temperature of the cold store air but the temperature of the product is not being taken into account. Since the air temperature is constant (within the hysteresis band of the thermostat), the product temperature will approach it asymptotically and stay almost constant as well.

This situation does not hold anymore if the goal of storage of energy is considered. The economical and technical value of any energy storage device depends on its storage capacity and power rating. The latter is linked to the speed of energy conversion, i.e. the speed at which the device can be charged and discharged.

The energy storage capacity of a cold store depends on the heat capacities of the stored products and the surrounding air. However, the volumetric heat capacity of products with a high water content – as most foods have – is more than 1000 times that of air. Even if a cold store is almost empty, almost all of the potential for energy storage lies in small variations of the product temperature. From this perspective, the cold store air is just a transmission medium and small interim buffer.

The charging and discharging rates are linked to the speed of heat transfer between the stored product and the air in the cold store. This speed is proportional to the temperature difference between the two. When the refrigeration machines (compressors) are operating, the air temperature quickly reaches a lower equilibrium T_{LE} some degrees below product temperature T_P, where the available cooling power equals the heat transfer from product to air plus the heat transferred from the outside. This equilibrium point will then slowly move towards lower temperatures as the product itself becomes colder. Once the refrigerators are turned off, the air temperature quickly rises towards a second equilibrium T_{HE} – this time above product temperature - where the heat transfer into the product equals the heat transferred from outside the cold store. As the product temperature slowly rises, this equilibrium moves towards higher temperatures as well.

In order to achieve the highest possible charge rate, the lower setpoint of the thermostat must be set equal to, or below, the lower equilibrium point T_{LE}, in order for the compressor to continuously stay on (maximum charge, 100% duty cycle). Lower charge rates can be achieved using setpoints between T_{LE} and T_P. Similarly, for the highest possible discharge rate, the upper setpoint of the thermostat has to be equal to or above the upper equilibrium T_{HE} (maximum discharge, 0% duty cycle). Note that the location of the equilibria depends on product temperature, and that a duty cycle of 50% does not necessarily correspond to charge-neutral behaviour.

The use of food as a storage medium for thermal energy is quite demanding. Its temperature may vary only within well-defined limits; too low temperatures cause damage, while too high temperatures have a detrimental effect on food safety. To address these concerns, and to get an idea of the current state of charge, the absolute food temperature needs to be known. However, direct measurement of food temperature is not common practise as it may vary slightly within the product and is dependent on where the product is in the cold store. Contractually, cold stores are obliged only to measure the air temperature so the challenge will be to estimate the product temperature using product heat capacities, product throughput and historical air temperatures.

The goal of the new controller then, is to be able to use the high availability of wind power to lower the temperature of the product, whilst ensuring the food-safety limits of the food are not breached.

3. THE SIMULATION MODEL

The simulation has been implemented in IPSYS [1], a simulation engine developed by Risø. IPSYS focuses on the discrete control of distributed energy systems and the interaction between different system balances, such as electricity, heat, water etc. It is built in a modular way and consists of a core framework and a collection of system components, controllers and energy domains which can be plugged into the core. New types of components and controllers can be added to the simulation with relatively little effort.

The two main parts of the simulation built for the NightWind project are a representation of the grid connection and a cold store model. The grid representation (Figure 1) is modelled as a distribution feeder with connections to a wind turbine, the cold store and additional, lumped load. The focus of interest in the grid simulation lies with the interchange of power between the distribution feeder and upper voltage levels.

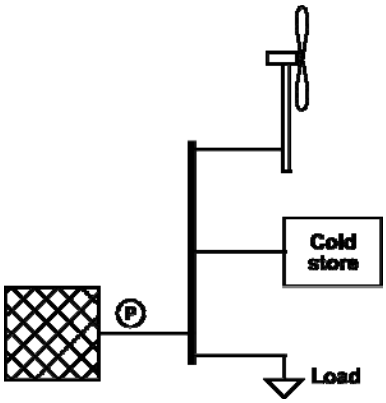

Figure 1. Simplified components of the simulation system.

The cold store model, shown in Figure 2, describes the heat exchange between three bodies – stored product, air inside the cold store and the environment. The refrigeration machinery consists of several identical units which can be switched on or off independent of each other. This enables operation under partial load. The product is represented not as a solid body, but as a loose stack of smaller bodies, yielding a relatively high ratio of surface to volume. The outside temperature is being read from timeseries data.

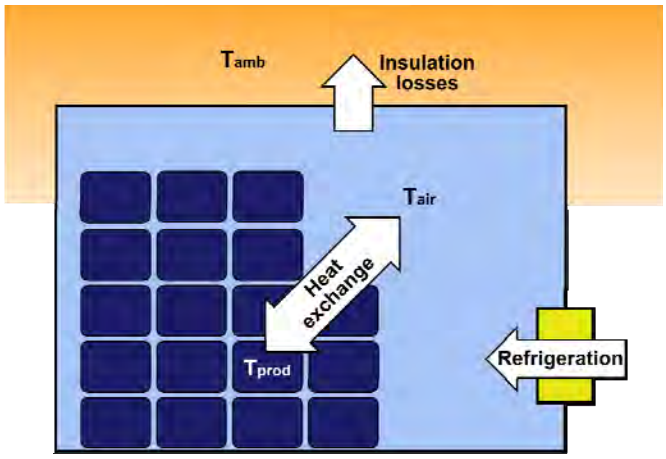

Figure 2. Heat transfer paths in the cold store model.

Even though it is believed this model to be realistic enough to support the initial development of controllers, it is still incomplete and has a number of shortcomings. As the modelling work progresses, some of them will be addressed.

- The model of the refrigeration unit is very simple. In a real-world refrigeration system, both the energetic efficiency (COP – coefficient of performance) and the cooling capacity depend on the temperature difference between evaporator and condenser. The present model assumes constant (fixed) COP and output, which is a reasonable first-order approximation if neither the outside temperature nor the store temperature are allowed to vary by more than a few degrees °C.
- The simulation does not yet include the product flow in and out of the store. Because the heat capacity of food is much larger than that of the air in the cold store, almost the whole potential for energy storage is in changing the temperature of the product. "Leaks" in the storage system occur due to products being shipped off immediately after having been "charged", i.e. cooled below the required temperature. These are inevitable to some degree, but can possibly be reduced if the control strategy considers product flow.
- The heat flow model currently assumes perfect heat exchanges between product surface, cold store air and outer walls, as well as a homogenic air temperature throughout the whole volume. Because of forced convection present in the cold store, this is a reasonable first-order approximation, but the simulation can be expected to slightly exaggerate the amount of heat exchange between product and air.
- The cold store is modelled as a single contiguous volume, representing the main storage area. In practice, cold stores have separate sections for initial (fast) refrigeration, intermediate storage and loading/unloading. These other sections operate at different temperature levels, and may not be able to participate in any load-shifting control scheme applied to the main area: Fast refrigeration of incoming products, for example, cannot be deferred, even if the main area is "discharging", i.e. the temperature rises.

4. SIMULATIONS USING SIMPLE THERMOSTATIC CONTROL

The first simulations were done using purely thermostatic control, i.e. it was only the temperature of the air that switched the compressors on or off.

4.1. Cold store performance and response in the simulation

The first very noticeable result in cold store performance from the simulations was the sensitivity of compressor cycling times to the temperature limits that were set for the air temperature. The cycling of the compressors predicted in the simulations is shown in Figure 3. Clearly, the tighter the required temperature band, the more frequently the compressors have to switch on and off.

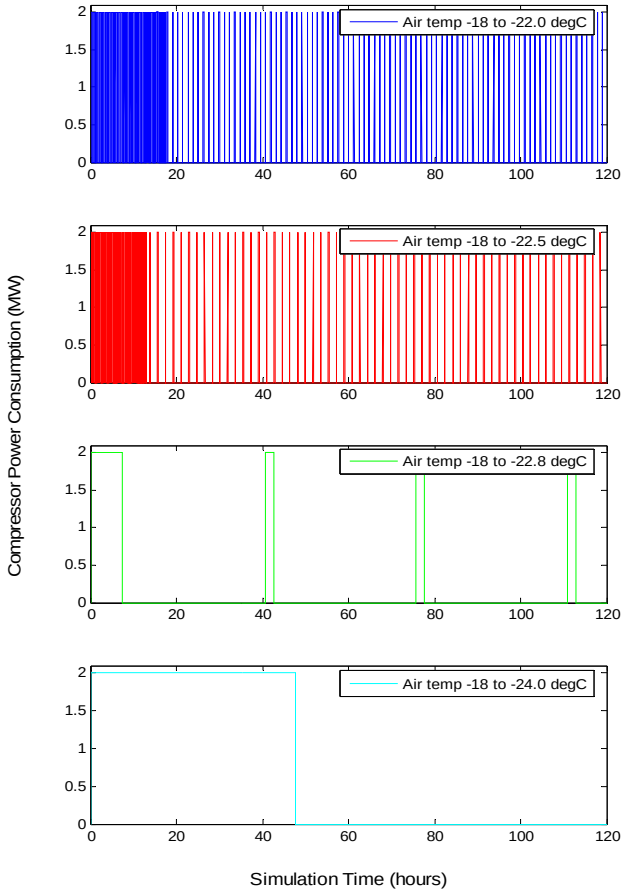

Figure 3. Comparison of simulated compressor cycling with varying air temperature limits.

A closer look at the temperature profiles that are predicted by the simulations (Figure 4) reveals an explanation of what is going on. Please note the very different scales for the air and product temperatures. From the time beginning at the timestamp of 30 hours, it can be seen that product temperature is steadily rising as the warmer air transfers heat to the colder product. The air temperature is also steadily rising (but does not show up on the scale shown) because, despite losing heat to the product, it is gaining heat from the much warmer outside environment.

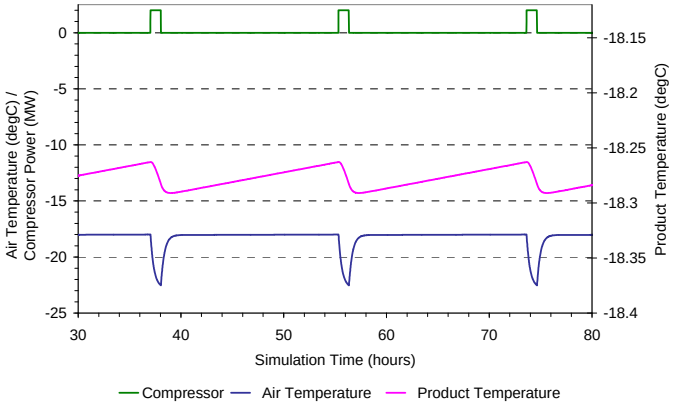

Figure 4. Profiles of temperatures and compressor cycling for air temperature limits of -18 to -22.5 °C.

Just before the 37th hour timestamp, the air temperature reaches -18°C and the compressors switch on. The air temperature quickly drops as the heat transfer to the compressors is much higher than from the outside or the product. When it reaches the lower temperature limit (set at -22.5°C but due to the time step of the simulation, there is a slight overshoot) the compressors are switched off. Shortly after the compressors were switched on, the temperature of the air fell below the product and the heat transfer reversed direction (heat flowing from the product to the air) and thus the product temperature reduces. The product temperature continues to fall once the compressors are turned off again but not for long because the heat flow to the air from outside starts to increase the air temperature again. The air temperature rises again quite quickly until it reaches the same temperature as the product, at which point the rate of increase slows because the heat transfer from outside is somewhat counteracted by the heat transfer to the cooler product. The cycle then repeats itself.

Salient points arising from these observations:

- The simulations shown that, as predicted, the air temperature varies quickly whilst the product temperature varies slowly. This is dues to the very different heat capacities and means that, in order to act as a store of energy, the temperature of the product must be varied further than at present. The air mass stores very little energy itself.
- The compressor cycling depends on the temperature range set for three reasons:
  a) The mass of air takes longer to cool because more heat transfer is required
  b) The cooler the air becomes the more heat transfer in from the outside (there would, in fact, come a stage at a low enough temperature at which the heat inflow from the outside would balance the heat transfer to the compressors and the air temperature could not be lowered any further.)
  c) The product average temperature lowers and thus is able to absorb more heat transfer when the compressors are off.
  (In reality there is also the additional reason that the compressor efficiency drops off the colder the air temperature becomes.)

- There is an intricate interplay between the relative temperatures of the three bodies (the outside, the air, and the product) and their heat capacities (outside – infinite, the air – small, the product – large).

Observations concerning the simulation model:

- The heat transfer depends not only on the temperature difference but also on the surface area in contact between the two bodies. In this model, each cubic metre of product is assumed to have six square metres of surface area.
- The heat transfer coefficient and heat capacities are taken as constant, i.e. it is assumed that there is no temperature gradient within the bodies and that the whole of the surface area is in contact with the core temperature of the other body.

5. Simulations using the wind-noticing controller

Following on from the relatively simple simulations above, the next progression was to look at how the availability of wind power would affect the compressor cycling if there was an attempt to run the compressors when there was sufficient wind power – in effect to "store" the wind energy. The aspect that was to be observed was the change in the use of energy from the electricity supply grid and electricity delivered to the grid depending on the wind turbine capacity installed.

For these simulations, the thermostatic limits were kept the same, namely -18 to -22.5°C, which the normal controller would work to. A base case was run without any wind input and then the number of 300kW wind turbines was increased step by step to see the effect on the energy exchange with the grid. The switch-on and switch-off percentages for the wind-noticing controller (i.e. the threshold at which the controller considered there was "sufficient" wind power) were also varied in a further set of simulations to see the impact this had.

The wind-noticing controller also has the ability to switch on and off individual compressors. In the preceding simple simulations, there was only one compressor modelled. In the simulations that follow there are three compressors with the same combined power consumption as all three in the simple simulations.

Since it was seen in the simple simulations that little energy could be store in the air – the density of the air has been increased by a factor of ten to try to represent some manner of energy storage capability. Whilst it is acknowledged that this is wholly unrepresentative of real physical conditions, it means that the objective of the controller (i.e. to control the air temperature) was not changed.

5.1. Wind-noticing controller simulation results

An output of one of the simulations is shown in Figure 5. This shows examples of incidences of the compressors being switched on by the thermostatic controller overriding the wind-noticing controller when the air temperature has reached the upper limit. It also shows instances of the wind-noticing controller switching on the compressor when there was sufficient wind and switching it off when there was a lack of sufficient wind.

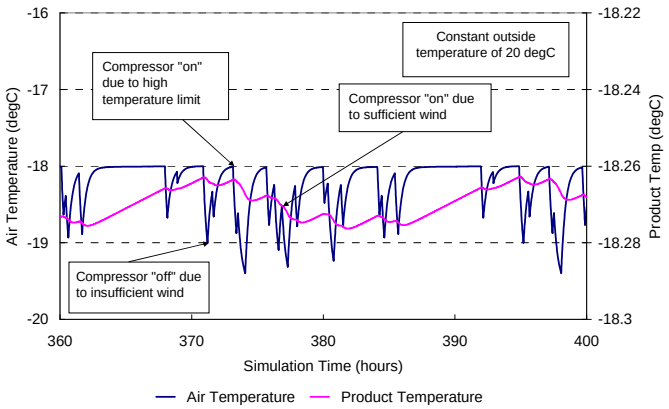

Figure 5. Compressor actions in response to controller signals.

Figure 6 shows the various power flows during a selected period of one of the simulations. The periods when a compressor is off show that the wind power generated is being fed to the grid. Conversely, when a compressor is on the wind power being produced is used with the deficit being made up from the grid up to the power of the compressor.

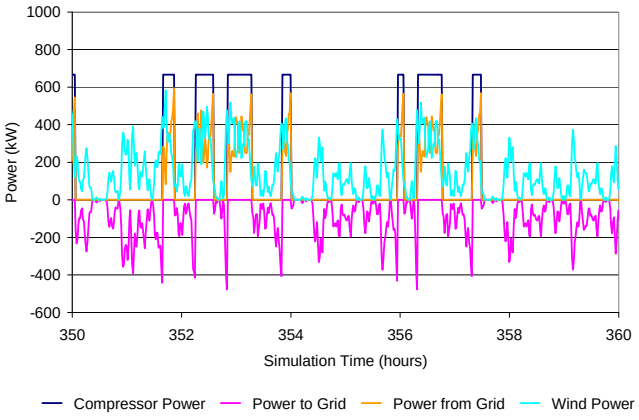

Figure 6. Power flows: to/from grid, wind power generation and compressor consumption.

A summary of the results of the two sets of simulations is shown in Figure 7, which shows that the wind-noticing controller is acting as expected, that is, as more wind capacity is added more is being "stored" in the cold store and less energy is being required from the grid. A lowering of the switch-on threshold also shows that the fall in energy being taken from the grid is more rapid.

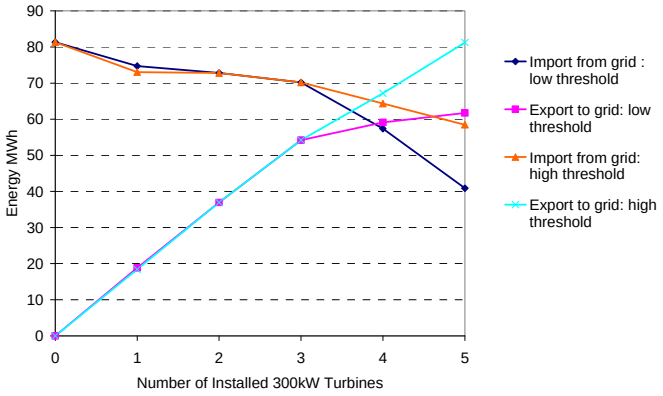

Figure 7. Impact of installed wind capacity on the energy exchange with the grid

6. CONCLUSION AND FURTHER WORK

Initial results from the first simulations that have been done with a controller that aims to minimise the exchange of energy with the grid show that, indeed, controller parameters can be adjusted so that the cold store can make use of the availability of wind energy.

Work will continue on refining the cold store model, particularly with respect to the efficiency of the compressors but also with a verification exercise that will ensure that the energy consumption of the simulated cold store with a traditional controller is in line with the actual energy use of the project's demonstration cold store.

The simulation model will be expanded to represent a larger system, so that the advanced development of the control system to include the influence of wind power availability and the electricity price can be incorporated.

ACKNOWLEDGEMENT

The NightWind project is a Specific Targeted Research Project under the European Commission 6th Framework Programme. Full title, "Grid Architecture for Wind Power Production with Energy Storage through load shifting in Refrigerated Warehouses"

REFERENCES

[1] Bindner, H. et al., IPSYS – "A Simulation Tool for Performance Assessment and Controller Development of Integrated Power System Distributed Renewable Energy Generated and Storage", WREC VIII, Denver, Colorado.

Implementation of a load management research facility in a distributed power system

Yi Zong[1*)], Anton Andersson[1)], Oliver Gehrke[1)], Francesco Sottini[2)], Henrik Bindner[1)], Per Nørgård[1)]
[1)] Risø DTU, VEA-118, P.O. Box 49, DK-4000 Roskilde, Denmark
[*)] tlf. +45 4677 5045, e-mail yi.zong@risoe.dk
[2)] DTU, Informatics and Mathematical Modelling Department, DK-2800 Kgs. Lyngby, Denmark

Abstract — To investigate active load management in distributed power systems, the FlexHouse research facility has been created. The objectives of this project, the system requirements and the discussion on software design are presented in detail, followed by the implementation of the hardware module with LabVIEW in this paper. The control of the FlexHouse ensures that studies can be performed on the reaction of this intelligent house to a hybrid power grid.

Index Terms — Distributed power system, load-management research facility, LabVIEW.

1. Introduction

In many places of the world, power systems are in a state of rapid transformation. This affects business models and company structures as well as a whole range of technical aspects, from the choice of generation technologies to the practices of system operation and control. An important aspect of this development is a change in the energy mix and the location of generation facilities. Transmission and distribution grids, once designed for a small number of large fossil-fueled power plants, have to cope with an increasing share of production from small power plants.

In recent years, some countries have gained a high penetration of generation from grid-connected renewables, most prominently from wind power. Due to the intermittency of the new energy sources, these systems require additional operational flexibility to ensure the stability of the grid as penetration levels rise.

Active management of the consumption side, i.e. the load in a power grid is widely seen as one of the keys to achieving this flexibility. However, efficient use of load management demands tight integration with the power grid's control system.

This paper introduces FlexHouse, a new experimental facility for exploring the technical potential of actively controlled buildings in power grids with a high penetration of renewable energy. A description of the facility is followed by a discussion of the requirements for the software platform on which building controllers can be executed. The implementation of the platform is described together with some initial controllers.

2. Integration of Wind Power, System Flexibility and SYSLAB

In power systems with an increasing level of wind power, the task of controlling the system is becoming increasingly demanding. The fluctuations of the wind power put large requirements for flexibility on the rest of the system to ensure the balance between generation and consumption. Figure 1 shows power demand and wind power generation in a power system, over a period of two days. It is clearly seen that the load has a daily pattern with some stochastic variations on top of it and that the wind power varies stochastically as well, while having no correlation with the load. It is also seen that the variations in wind power can be very large even in rather short timescales, i.e. from minutes to hours. Both the lack of correlation and the stochastic nature of the wind power put very strong requirements for flexibility on the rest of the system.

Traditionally, there has been a separation between production and consumption of electricity: Consumption has been regarded a passive part of the system with respect to control, and therefore any generation mismatch causes by variations in wind power production has to be compensated by other generating units. It has been realised in recent years that there is a large potential for additional flexibility in the control of power systems by enabling active participation of the consumption side in the balancing of power. This potential mainly comes from the ability to defer consumption in cases where the exact time of power use is not critical for the application.

Load management can be used in certain large industrial applications such as the refrigeration of cold stores or the lighting in greenhouses. Residential buildings offer possibilities as well; examples for such cases include many heating and cooling applications – space heaters, heat pumps, refrigerators, water heaters etc. – where thermal energy can be stored in the heat capacitances of buildings, water or food. Many automated household appliances, such as washing machines or dish washers, can defer the start of their operation by some time without a drop in perceived comfort level.

The current development of information and communication technologies makes it possible to exploit this potential. It is, however, uncertain how it can be realised.

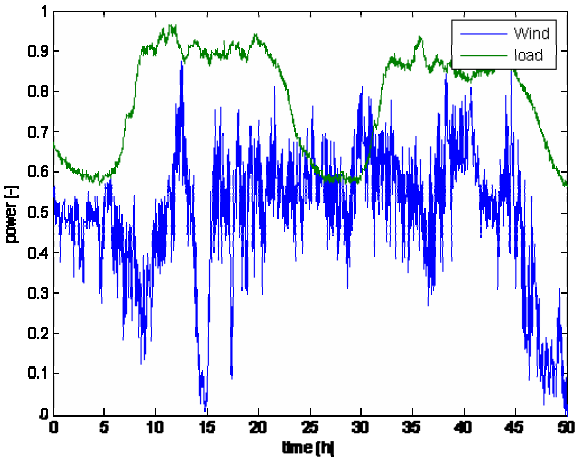

Figure 1. Load and wind power variations

Figure 2. Components in SYSLAB

There is a large need to investigate how flexible consumption should be implemented, seen from the perspective of power system control as well as from that of a consumer. Any such system will have to be integrated with the rest of the power grid's control system – likely by means of a market for system services and an aggregation mechanism. In order to gain acceptance, the user's needs have to be fulfilled without much noticeable compromise on perceived comfort. Ideally, the user stays in control while providing flexibility to the grid.

3. The FlexHouse facility

During the last years, Risø DTU has established SYSLAB, a new laboratory for intelligent distributed control of power systems [1]. SYSLAB is built around a small power grid with renewable (wind, solar) and conventional (diesel) power generation, battery storage, and various types of consumers (See Figure 2). All components in the grid are remotely controllable and locally supervised by a "node" computer collocated with each unit. A high-speed data network connects all these nodes; together they form a distributed platform for testing new concepts for system controllers.

One of the loads on the SYSLAB grid is a small, free-standing office building, FlexHouse, which has been designed as a research facility for active load management. The building contains seven offices, a meeting room and a kitchen. The electrical load of the building consists of heating, lighting, air-conditioning, a hot-water supply and various household appliances, such as a refrigerator and a coffee machine. The combined peak load of the building is close to 20kW and dominated by ohmic loads, with the exception of fluorescent-tube lighting.

All individual loads in the building are remote-controllable from a central building controller. The same controller is able to receive input from a multitude of indoors and outdoors sensors (see Figure 3): Each room is equipped with a motion detector, temperature and light sensors, window and door contacts. A meteorology mast on the outside of the building supplies local measurements of temperature, wind speed, wind direction and solar irradiation. These environmental measurements can be used for obtaining precise estimates of the heat flux in and out of the building.

The building controller is able to communicate with the SYSLAB grid through its own node computer. This interface can be used to provide the controller with power system information, either as raw data or processed into e.g. a price signal. Information may also flow in the other direction, for example providing the power system controller with the expected near-future behaviour of the building loads.

Comfort settings can be adjusted individually for each room of the building, by means of small touch-screen user interfaces. This approach allows the adaptation of the user interface depending on the chosen control strategy, and a comparison of user acceptance between different types of user interface.

The main purpose of the FlexHouse facility is to serve as a test bench for comparing various strategies for active and passive load management.

4. Technology and system requirements

To realize the operation of the FlexHouse as a flexible load for the SYSLAB, there are general requirements for the FlexHouse software design. Firstly, it should interact successfully as a SYSLAB component and negotiate electrical demand with the SYSLAB environment. Secondly, the events and conditions in and around the FlexHouse should be collected and preserved into a database in order to provide information for the controller to make decisions and display the history records in some user interfaces. Thirdly, the controller can perform some automatic control algorithm to make the FlexHouse react to the external power grid (SYSLAB). Finally, user-visualization via TouchScreen and user-interaction via PDA should be supplied in the house.

Considering the FlexHouse system carefully and deeply, we put forward the following technical requirements for the software design to fulfil the whole system's general requirements:

- Flexibility of the software architecture to provide a dynamic research environment. For example, the system allows the hardware structure, control algorithms and provided functionalities to be changed.
- Reliability and robustness of the software architecture.
- Allowing the system architecture to be distributed over a network.
- Real time response of the system to the house events.
- Possibility to change the software architecture at running time. For example, it is possible for us to change an algorithm inside the controller without shutdown the whole system.
- User interfaces easy to be used and understood.
- User identification

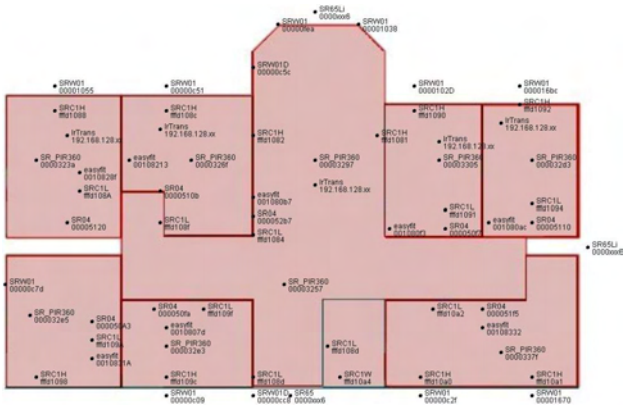

Figure 3. Sensors and actuators in FlexHouse

5. DISCUSSION ON SOFTWRE DESIGN

According to the above requirements for the whole software design, we divided the whole system into different domains. The architecture of the software can be looked as a network where each node is an independent and autonomous module (See Figure 4). Each of them has different functionalities and can be developed individually. They can all provide an interface to communicate with the other entities through standard network technologies. A client/server architecture was used to carry out the communication and collaboration among the different modules.

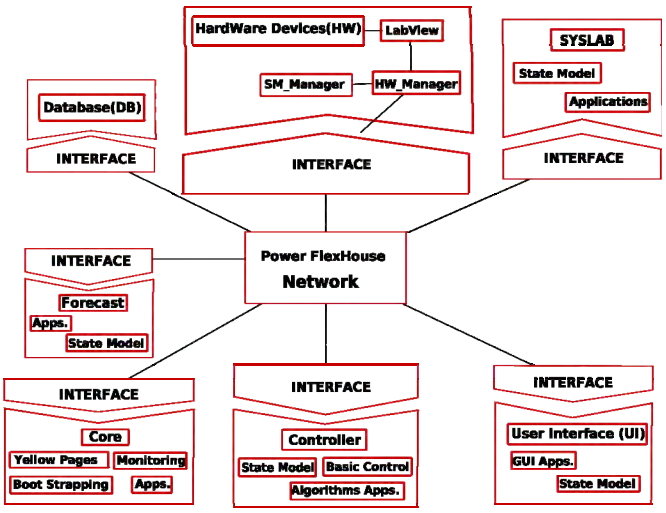

Figure 4. Architecture of the Flexhouse software design

The Hardware module (HW) is dedicated to the management of all the EnOcean devices that are in or around the house. There are motion sensors, temperature sensors, window/door sensors, light switches, radiators and light actuator for collecting information or control. First of all, this module should achieve the wireless communication between sensors and a transceiver connected to the RS232 port of an embedded PC. At the same time, this embedded PC is connected to the power FlexHouse node unit and thereby interfaces with the rest of SYSLAB's network. So it is possible for us to take the SYSLAB status like available power, wind speed and diesel load into account for controlling the house. Next, when there are new measurement data received from sensors, the HW module raises events and sends them to the other modules. Meanwhile, the HW module also receives commands from the Controller module. In addition, it should manage a state model for all the hardware devices.

The Controller module processes the information provided by the HW, User Interface (UI), SYSLAB and Forecast modules in order that it makes control decisions on how to manage the house. Control command from the controller should be send out to control the different loads in the FlexHouse. To develop the first version of the system, at the beginning, we designed a basic controller which manages the real time temperature in the house without applying any particular policies to the behaviour of the house. In the future, with the purpose to optimize the behaviour of the house via the developed control algorithms, the evolution of the controller will need to collect information from SYSLAB environment, Database (DB), UI module, events from the HW module and energy model from the Forecast module.

The CORE module involves all the necessary functionalities to start and manage the applications for the FlexHouse system (Application Server). This module permits to build an architecture based on publishing/requesting of services from the other different modules. The core will provide, in fact, something like a Yellow Pages service in the system. In this way we can obtain a system that can be distributed on a network and give the maximum independence to each domain.

The UI module permits the user to interact with the FlexHouse system via PDA. There is one PDA for each room in FlexHouse and a Touch Screen in the meeting room. The user not only can observe all kinds of information, such as, wind power capacity, electricity price and the status of the room in which he is, but also he can set some parameters to require a different behaviour for his room. At the same time, the user interface can show the real time measurement of the sensors and the energy information coming from the SYSLAB module. Web technologies have been chosen to develop this part.

In the first place, the DB module is dedicated to the storage of the information on the happened events, measurement data, configuration messages, executed commands, state models and the logs of actions and decisions coming from the UI and Controller modules. In the second place, it provides history records as a reference for the Controller and Forecast module to create control strategy and for the UI module to display historic data.

The SYSLAB and Forecast module are responsible for providing information about electricity price, electricity production, weather and energy forecast for the FlexHouse. SYSLAB and Forecast interact continuously to build an energy model for the house. For example, once SYSLAB receives a detailed weather forecast for Roskilde, it transmits this information to the Forecast module. The Forecast module deducts the loads it must serve and does some modelling work to predict how much solar and wind power will be available over the coming 24 hours. It provides this information for SYSLAB system to answer via an interface, where the price of electricity varies over time and consumption. Basing its elaboration on the past, present and future data about the energy management, the Forecast module can provide the best behaviour for the FlexHouse. There is a tentative plan to integrate the house users' Outlook calendars into the Forecast module in order that we can obtain a better forecast for the future energy consumption.

The different modules are maintained in a lightweight application server and can be started and stopped individually from a web interface (Figure 5).

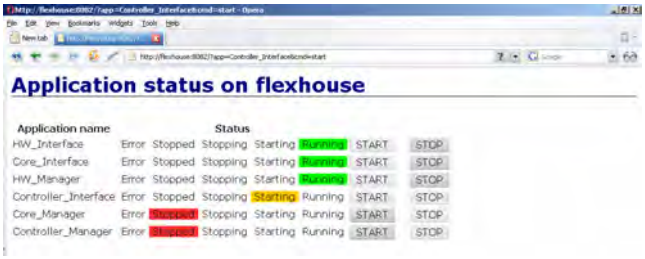

Figure 5. FlexHouse application server

6. IMPLEMENTATION OF HARDWARE MODULE WITH LABVIEW

A LabVIEW (*Lab*oratory *V*irtual *I*nstrumentation *E*ngineering *W*orkbench) application can simply be moved from Windows machine to a Linux machine without modification as long as it dose not call any platform specific functions, i.e. Windows ActiveX components and Windows dll, etc. It also displays strong power when we use LabVIEW to implement the measurement and automation task. We can use NI-VISA to communicate with most instrumentation buses including GPIB, USB, Serial, and Ethernet. In addition, VIs (Virtual Instruments) built using LabVIEW are the easiest to control and share over the Internet since LabVIEW has a number of VIs, such as VI Server, Datasocket technology and general TCP/IP communication protocol that can be used to design and develop Internet-enabled virtual instruments [2][3]. These are the reasons why we selected LabVIEW for the software implementation of the HW module in this project. It has shortened the development time and gained accuracy of measurement and control.

The LabVIEW section in the HW module is responsible to interact directly with the hardware devices. It receives notification events from the event sensor and it gives commands to the actuators. This module represents as a stand-alone application and interacts with the rest of the HW Module. It communicates with the HW_Manager application through TCP/IP (Transmission Control Protocol)/ (Internet Protocol) mechanism. The HW_Manager is in charge of management of all the information that related to the FlexHouse. With its own IP address, the HW_Manager communicates with the HW_Interface via RMI (Remote Method Invocation) mechanism; meanwhile, it obtains the house information from the LabVIEW application and sends command from the Controller module to the LabVIEW side by the Java TCP/IP Socket, based on the LabVIEW default TCP/IP port 6340.

6.1. RS232 program with NI-VISA

We chose to use the EnOcean wireless products to realize the control tasks of the FlexHouse. Figure 6 illustrates a room in the FlexHouse equipped with EnOcean devices. There are motion sensors, temperature sensors, light sensors, window sensors, door sensors, radiators, light switches, and light actuators for control. In order to transform energy fluctuations into usable electrical energy, piezo-generators, solar cells, thermocouples, and other energy converters are used in these batteryless and wireless radio sensors and radio switches that need no maintenance during their whole lifetime. The signals of these sensors and switches can be transmitted across a distance up to 300 meters. The EnOcean transceiver (TCM120) is powered through a 5V DC USB supply. Communication is performed with RS-232 [4][5].

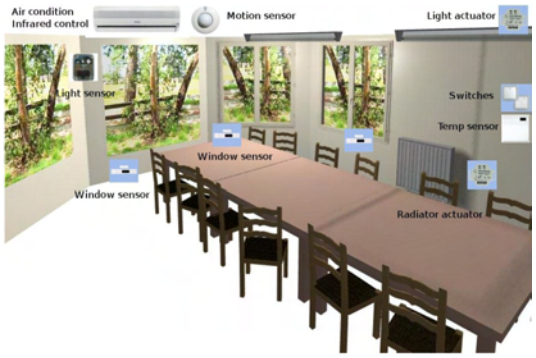

Figure 6. Schematic rendering of equipment in FlexHouse

To obtain the transmitted/received message from the sensors and actuators, the local embedded PC was connected to the transceiver via serial communication port (RS232) and USB power supply. NI-VISA gives us the ability to easily create code to communicate with the EnOcean sensors and actuators. Our program written using VISA function calls is easily portable from Windows platform, to Linux system (Gentoo) without any modifications. (See Figure 7):

6.2. Communication

Although DataSocket (The National Instruments has developed an own version of Datasocket that simplifies data exchange between different computers and applications) can be used on Linux, Solaris and Macintosh, however, the DataSocket Server application is built on Windows-based ActiveX technology and so is only available for Windows environments. In our situation, the whole system is operated on Linux machine; therefore, we chose the classical TCP/IP communication protocols with LabVIEW supported on all platforms to achieve the communication between the LabVIEW application and HW_Manager.

TCP/IP communication provides a simple user interface

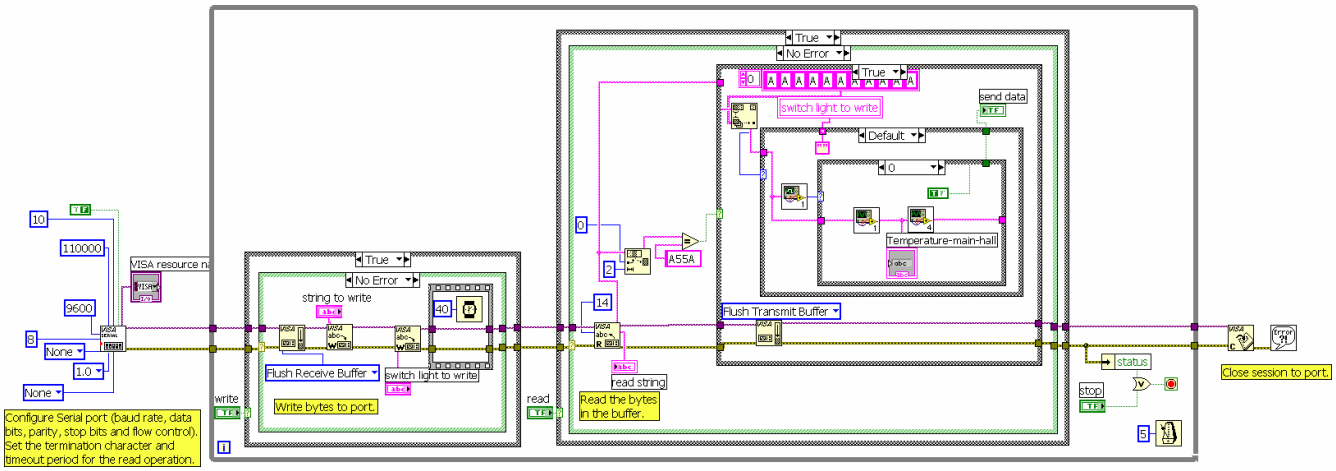

Figure 7. RS232 configuration and NI-VISA

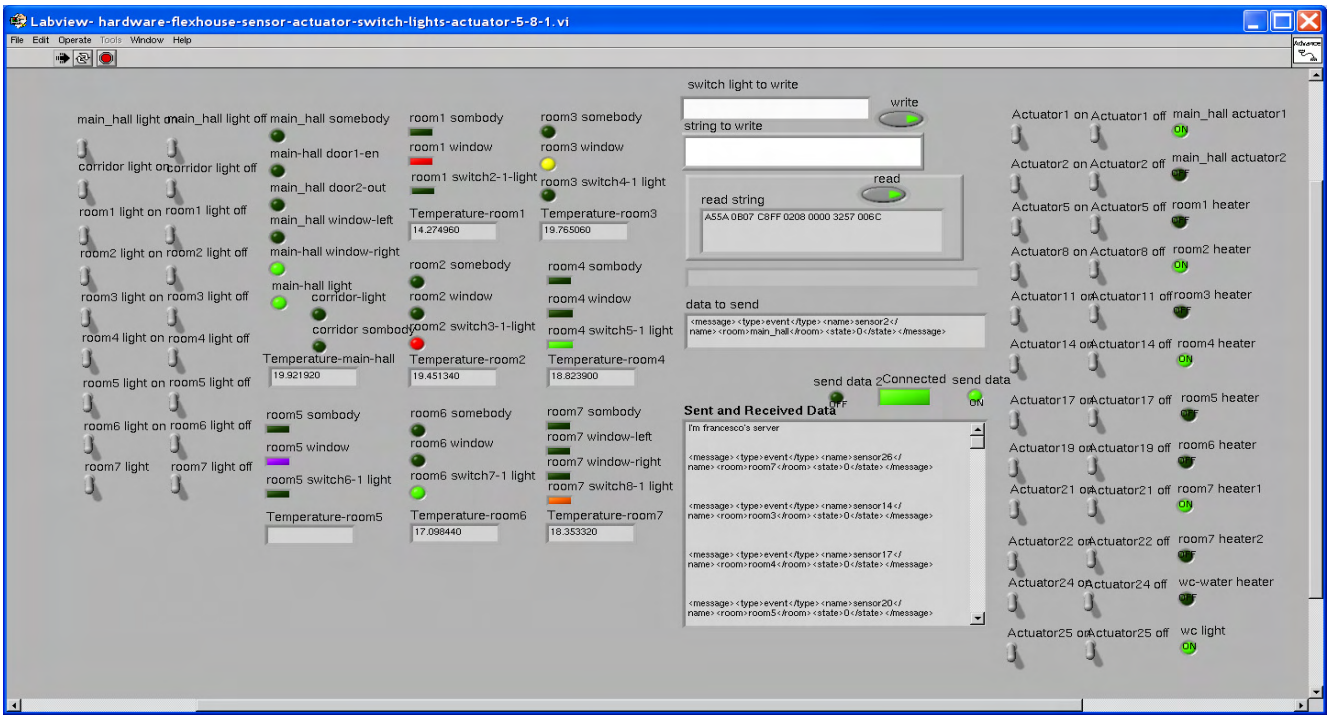

Figure 8. LabVIEW front panel in the HW module

that conceals the complexities of ensuring reliable network communications [6]. In our case, we only need to develop the Client using LabVIEW TCP/IP functions and the Server is implemented in Java language. The process involves opening the connection, reading and writing the information, and closing the connection.

6.3. Optimization of VI performance

LabVIEW handles many of the details that we must handle in a text-based programming language. One of the main challenges of a text-based language is memory usage. In LabVIEW, we do not allocate variables, nor assign values to and from them. Instead, we create a block diagram with connections representing the transition of data. Functions that generate data take care of allocating the storage for those data. When data are no longer being used, the associated memory is deallocated. When we add new information to an array or a string, enough memory is automatically allocated to manage the new information. This automatic memory handling is one of the chief benefits of LabVIEW. However, because it is automatic, we have less control of when it happens. Since we work with large sets of data in this project, it is important to have some understanding of when memory allocation takes place. Also, an understanding of how to minimize memory usage can also help to increase VI execution speeds, because memory allocation and copying data will take a considerable amount of time. In our case, some useful rules helped us to create VIs and use memory efficiently, see the reference [7].

On the other hand, other factors, such as using local variable overhead and subVI call overhead, usually have minimal effects on execution speed, hence, when we designed the front panel, the best solutions were to reduce the number of front panel objects and kept the front panel displays as simple as possible. In addition, what we did to minimize subVI overhead was to turn subVIs into subroutines. The in-situ state of the FlexHouse can be observed through the LabVIEW front panel. (See Figure 8).

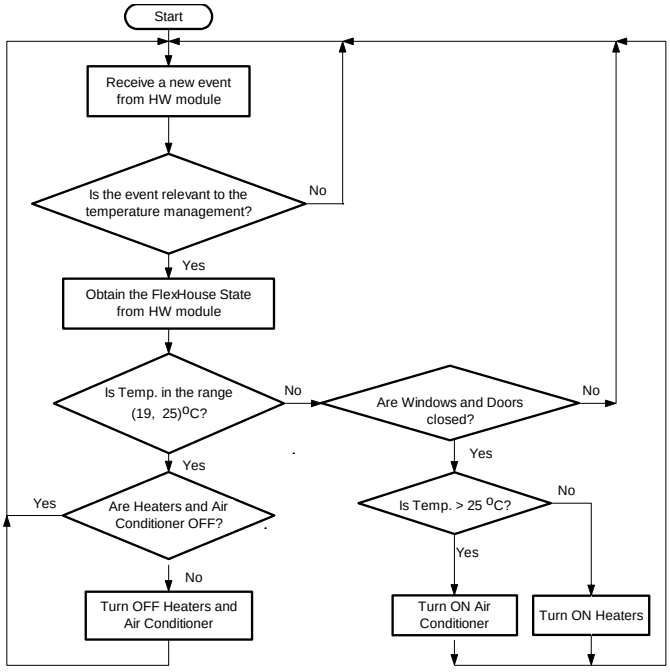

Figure 9. FlexHouse temperature control diagram

7. CONTROL STRATEGY (FIRST VERSION)

To verify the behaviour of the HW module and the communication ideas (RMI and TCP/IP communication) of the software design for the rest modules, such as the Core and Controller module. (See Figure 4), we used some simple control strategies (e.g. Bang-bang control) for the Controller to control the house's temperature. The control objective is to maintain the temperature of the different rooms in the house at 22 ±3°C. Figure 9 is the control diagram. Utilizing this simple control algorithm, it proves that the system can work

smoothly and what we did on the software design is feasible in the whole distributed system.

8. FUTURE WORK

At this moment, we are using an XML file to describe the state model of the house. Lately, a local or remote database should be built to store the historic records on the house state, configuration messages and control commands from the User Interface and Controller module, etc. Next, we must enforce the program's security and stability for a long time. Finally, we should propose better control ideas on the load management of the FlexHouse in order to react to fluctuations in wind, and to perform power peaking-shaving.

9. CONCLUSION

Different communication methods (TCP/IP and RMI) have been applied successfully among the different modules in the whole system's software design. With the help of LabVIEW, firstly, we performed the communication between EnOcean sensors or actuators and an embedded PC in the FlexHouse via NI-VISA. Secondly, the HW module could implement the communication based on TCP/IP with HW_Manager. The whole VIs program was portable from Windows machine to Linux platform. Finally, to test the basic functionality of the system, we designed a simple temperature control strategy and it performed successfully. It proves that various control strategies and theories can be investigated on how this intelligent house is used to stabilize fluctuations in the power grid with high penetration of renewable energy, in comparison with the actual power system presented within the SYSLAB.

REFERENCES

[1] http://risoe-staged.risoe.dk/Research/sustainable_energy/wind_energy/projects/SYSLAB
[2] Nikunja K. Swain, James A. Anderson, Ajit Singh. Remote data acquisition, control and analysis using LabVIEW's front panel and real time engine. Proceeding IEEE SouthestCon, 2003. pp.1-6
[3] NI Corp LabVIEW User Manual，USA，2006
[4] EnOcean Company, TCM120 Transceiver Module User Manual V1.5, March,2006
[5] http://www.thermokon.de/index.php?showMenu=37&contentID=61
[6] NI Corp Application Note 160, Using LabVIEW with TCP/IP and UDP，USA，2003
[7] NI Corp Application Note 168, LabVIEW™ performance and memory management，USA，2004

Modelling of wind turbine cut outs in a power system region

P. Sørensen*), X.G. Larsén, J. Mann, N. A. Cutululis
Risø DTU, VEA-118, P.O. Box 49, DK-4000 Roskilde, Denmark
*) tlf. +45 4677 5075, e-mail poul.e.soerensen@risoe.dk

Abstract — This paper outlines the structure of a simulation model to quantify the times and volumes of lost generation due to wind turbine cut outs at high wind speeds in a power system region. To deal with this issue, the paper will analyse the wind variability in a region with typical dimensions of hundreds of kilometres, considering time scales from seconds to hours. This time scale is selected to include the fast variability which may influence the response of the wind turbine controller, as well as the slow variability corresponding to the time it takes a weather system to pass a region. The idea is to develop a generic wind model, which combines the slow variability provided by large climate models using low resolution in time and space with a stochastic simulation model which adds the higher resolution in time as well as location.

Index Terms —cut-out, high wind speeds, wind power variability.

1. INTRODUCTION

This paper outlines the structure of a simulation model to quantify the times and volumes of lost generation due to wind turbine cut outs at high wind speeds in a power system region.

In power system regions with large scale wind power, the TSO's and power producers with balancing responsibility have increased concern about wind turbine cut outs due to high wind speeds. This issue was pointed out in the UCTE position paper on Integrating wind power in the European power systems [1], and has been justified by the practical experience from the power system region in West Denmark. The passages of storm systems have caused loss of significant generation, which must be accounted for by the power balancing in the system.

The concern about storm passages has a similar background as the concern about the response of wind turbines in the cases of faults in the transmission system. In both cases, the key problem is about loss of significant generation in the system. But there are also significant differences between the impact of storm passages and transmission system faults.

First of all, transmission system faults are seen simultaneously by the wind turbines in the system, i.e. within time differences of maximum a few milliseconds, whereas a storm passage will take several hours.

Another significant difference is that wind power predictions give a warning to the operator in advance of a storm passage, whereas faults in the transmission system are unpredictable. Although there is an uncertainty in prediction of the timing and strength of the storm front passage, the prediction makes in possible to ensure that the necessary reserves are online in due time.

These differences clearly indicate that the grid fault issue is normally more critical to the system stability than the storm front passage. This is also hinted by the fact that wind turbine response to grid faults has been included in grid codes as requirements to wind turbines for several years, while there are not similar requirements to operation at high wind speeds.

However, the experience with storms in the operation of the present Danish system, combined with the plans for doubling the installed wind power capacity from approximately 3000 MW today to approximately 6000 MW in 2025 [2] has caused increased focus on the issue.

The cut-out of a wind turbine at high wind speeds depends on the wind speed measured on the nacelle and on the control algorithm implemented in the wind turbine. Most modern wind turbines cut out at 25 m/s, although several of the older wind turbines in the Danish power system cut-out at lower wind speeds.

The wind turbine control system averages the measured wind speed before the wind turbine is cut out, and applies some hysteresis in the control before it cuts in again when the wind speed decreases. This ensures that the turbine is not stopped and started unnecessarily many times at high wind speed. The cut-out is done to protect the mechanical structure of the wind turbine, but the shut down and start up itself at high wind speed stresses the wind turbine mechanically.

Enercon has introduced a storm control [3] to mitigate the effect of a storm passage on the power system balancing. The idea is to modify the power curve of the wind turbine so that it does not drop directly from rated power to zero when the cut-out wind speed is reached. Instead, the power curve decreases gradually towards zero power for high wind speeds. This approach is patented by Enercon, but many other control strategies can be developed to mitigate the storm effect.

Obviously, Enercon has taken the storm control into account in the mechanical design of the wind turbine, and a Danish research project [4] is also studying the effect on the mechanical loads when the wind turbine is operated at higher wind speeds. The idea of the present paper is to develop a tool that can be used to study the effect of new wind turbine control strategies on the power balancing task.

In order to be generally useful, not only for the present wind power installations but also to study possible future wind power development scenarios, and also not only for Denmark but also for other power systems, such a tool should be able to simulate the wind speed simultaneously at wind turbines with specified geographical locations. And the time scale of the simulation should be from approximately one minute to several hours, to cover the fast response in the wind turbine control system as well as the relatively slow passage of a storm front over a region. As an indication, a 25 m/s storm front will approximately take 8 hours to pass 200 km through a region.

This paper presents the idea of developing such a tool as a combination of climate models with relatively low resolution in time and geographical position with stochastic simulation model which can simulate with much higher resolution. Climate models are based on historical data, while the stochastic model simulates variability dependent on the selection of a random seed. Thus, the amount of data time

series available from the climate models is limited to the historic period that it is based on, while the stochastic model in principle can simulate an infinite number of data time series.

In the following chapters, the climate models and the stochastic model are first presented. Then the approach for combining the models is described and analysed, and finally conclusions are drawn.

2. CLIMATE MODELS

There are several climate models that provide data time series for longer historic periods. They are mainly characterised by the geographic area that they cover, the resolution in time and space, and the historic period which is included.

Figure 1 shows the resolution for a number of selected climate models. The models are described in a little more details below. The NCEP/NCAR and the ERA models are global, while the MPI models are regional.

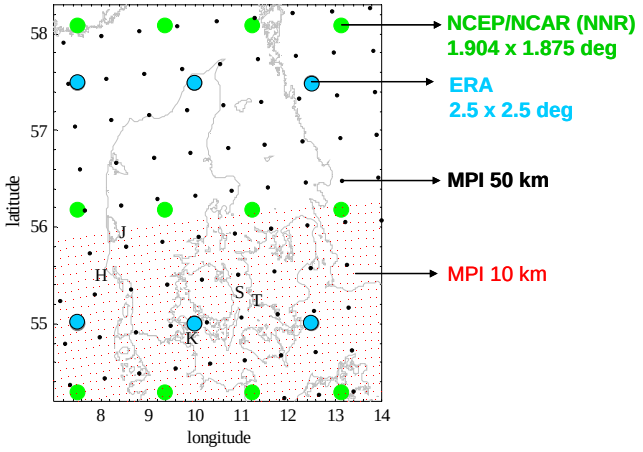

Figure 1. Climate models.

National Centers for Environmental Prediction / National Center for Atmospheric Research (NCEP/NCAR) [5] provide 59 years (1948 – 2006) of data with a resolution 1.875º × ~1.9º and 2.5º × 2.5º, every 6 hours.

European Center for Medium range Weather Forecasting (ECMWF) [6] provide the Re-Analysis data (ERA) for 45 years (1958 – 2001) in total, with the resolution 2.5º × 2.5º, every 6 hours.

The German Max Planck Institute for Meteorology provides regional data driven by ECMWF 15 years Re-Analysis data (ERA-15) for 1979 – 1993, supplemented with ECMWF analysis data for 1994 – 2003. Data is available for all Europe with a resolution of 50 km × 50 km, 1 hour, and for Germany+ with a resolution of 10 km × 10 km, 1 hour.

For the present purpose, if all Denmark should be covered by highest possible resolution, the MPI 50 Reanalysis data is applied.

3. STOCHASTIC SIMULATION MODEL

The stochastic model applied was published in the first version under the name PARKWIND [7]. The first version included a standard turbulence model as the source of wind variability to simulate the wind speeds at a number of wind turbines with specified geographical location. The turbulence mainly specifies the variability within a few minutes. Since this model underestimated the variability on a little longer term, a new version of the model has been implemented [8], including slower variability of the wind speed (typically variability within one hour).

The basic idea of the stochastic simulation model is based on the power spectral densities (PSD's) of the wind speed at each location where a wind turbine is operating, and the coherence function between these wind speeds. With these input functions given in the frequency domain, the simulation model simulates random time series with the specified PSD's and mutual coherence functions.

The stochastic simulation model has been verified by measurements from the 160 MW offshore wind farm Horns Rev [9]. For the present purpose, the intension is to use it in a full power system region, possibly West Denmark or all Denmark.

Figure 2 shows the location of wind turbines in Denmark. The source data for this is available on the Wind Turbine Master data register [10]. Besides the location of each wind turbine, this data register contains information about the hub height, rated power and commissioning date of the turbines. Thus, the data register can be used as basis for simulation of the wind power in the present and future systems.

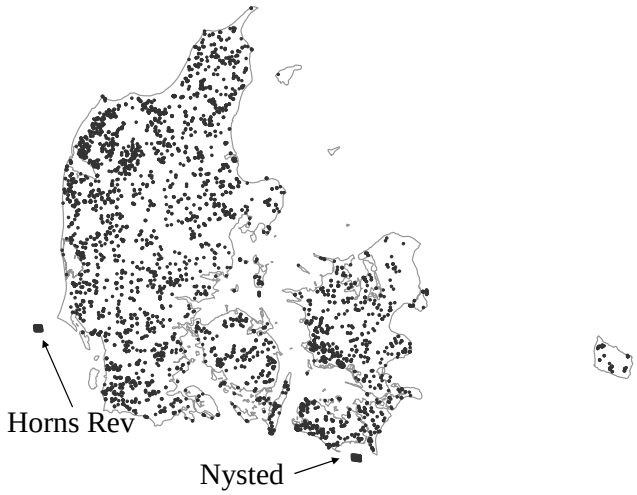

Figure 2. Wind turbine locations in Denmark.

4. COMBINATION OF MODELS

The simplest, and probably most operational way of combining the models is to simulate the wind speed $u_{[x,y]}(t)$ in a position (x,y) as the sum of the climate model contribution $u_{CM[x,y]}(t)$ and the stochastic simulation contribution $u_{SS[x,y]}(t)$, i.e.

$$u_{[x,y]}(t) = u_{CM[x,y]}(t) + u_{SS[x,y]}(t) \quad (1)$$

With this approach, the PSD of the stochastic simulation contribution is needed. Since the added variability from the stochastic simulation is random, we can assume it is not correlated with the climate model contribution. Thus the relation between the PSD's $S_{[x,y]}(f)$ of $u_{[x,y]}(t)$, $S_{CM[x,y]}(f)$ of $u_{CM[x,y]}(t)$ and $S_{SS[x,y]}(f)$ of $u_{SS[x,y]}(t)$ is

$$S_{[x,y]}(f) = S_{CM[x,y]}(f) + S_{SS[x,y]}(f) \quad (2)$$

Now, the unknown PSD $S_{SS[x,y]}(f)$ to be applied in the stochastic simulation can be found from PSD $S_{[x,y]}(f)$ of the actual wind speed and the PSD $S_{CM[x,y]}(f)$ of the climate model data. For this purpose, the PSDs $S_{[x,y]}(f)$ and $S_{CM[x,y]}(f)$ have been calculated on the locations shown in Figure 3, where 10 min mean values of wind speeds have been measured during several years.

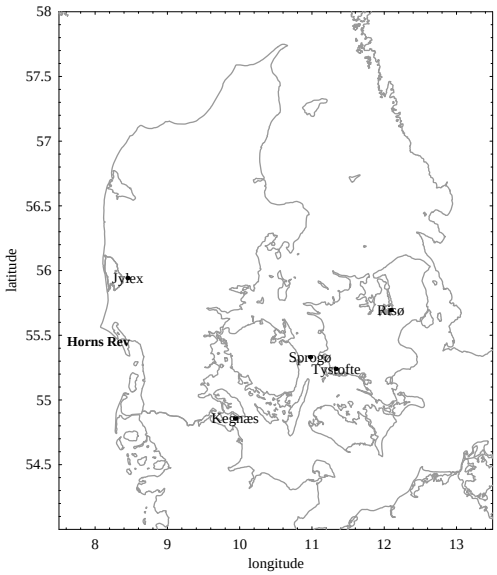

Figure 3. Measurement sites.

Figure 4 shows the PSD's for the Horns Rev location. Since the MPI 50 and MPI 10 climate models provides the wind speed in 10 m height, the model data is compared to measurements in 10 m height. The MPI data points of the 50 km grid and 10 km grid closest to the Horns Rev location has been selected.

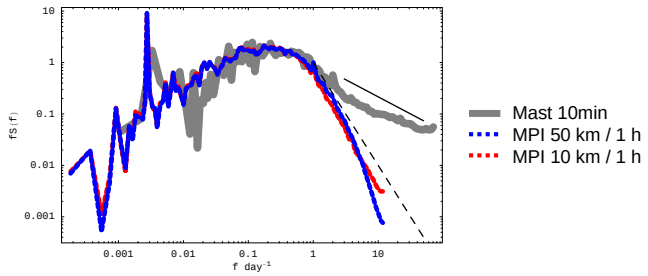

Figure 4. Measured (10m mast) PSD $S_{[x,y]}(f)$ compared to climate model (MPI) PSD's $S_{CM[x,y]}(f)$ for the Horns Rev site.

Figure 4 shows a good agreement between measured and climate model data for frequencies $f < 1$ day^{-1}. This indicates that the model wind speeds are scaled correctly regarding roughness and height. However, already for frequencies $f > 3$ day^{-1}, i.e. for period times less than 1/3 day = 8 hours, the PSD's of climate models are only half of the measured PSD, indicating that only half of the fluctuation energy is present in the climate model. For frequencies $f > 4$ day^{-1}, i.e. for period times less than 6 hours, the PSD's of climate models are only a quarter of the measured PSD, indicating that the amplitudes of the climate model waves at that frequency have only half the size of the measured amplitudes.

Another interesting observation is that the 50 km and the 10 km climate models are quite similar for frequencies $f > 8$ day^{-1}, i.e. for period times less than 3 hours.

Figure 5 shows the corresponding PSD's for the Kegnæs site, where the measurements are also done in 10 m height. It is seen that there is a small difference between the energy for frequencies $f < 1$ day^{-1}. Since the measurements are in 10 m height as are the climate model results, this indicates that the terrain roughness is a little less on the Kegnæs site than it has been assumed for the selected grid points in the climate models.

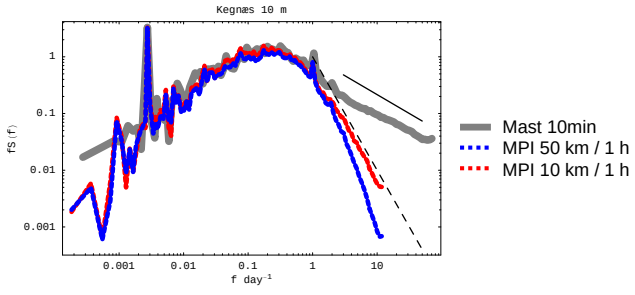

Figure 5. Measured (10m mast) PSD $S_{[x,y]}(f)$ compared to climate model (MPI) PSD's $S_{CM[x,y]}(f)$ for the Kegnæs site.

Figure 6 shows the comparison for the Risø site, where the measurements were done in 44 m height. The measured PSD is here higher than the climate model PSD's for frequencies $f < 1$ day^{-1}, which is expected because of the height difference. It is also noted that the 50 km grid PSD is much closer than the 10 km grid PSD to the measured PSD, which is probably because the roughness length assumed in the climate model is greater for the nearest 10 km grid point than for the nearest 50 km grid point.

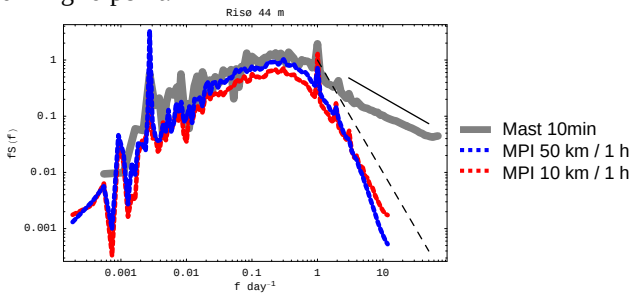

Figure 6. Measured (44 m mast) PSD $S_{[x,y]}(f)$ compared to climate model (MPI) PSD's $S_{CM[x,y]}(f)$ for the Risø site.

Finally PSD's are shown for the Sprogø and Tystofte sites in Figure 7 and Figure 8. These sites are interesting because they are relatively close to each other, and the Sprogø site is almost offshore while the Tystofte site is on land. The sites has similar PSD's for the 50 km grid, but the PSD's for the 10 km grid capture some of the difference between offshore and onshore.

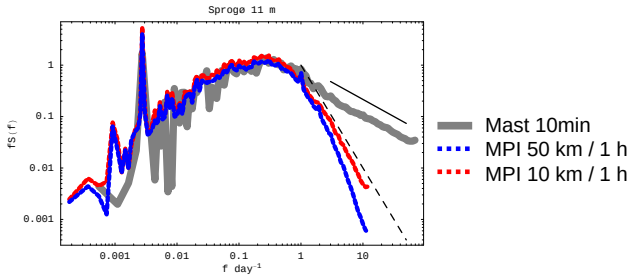

Figure 7. Measured (11m mast) PSD $S_{[x,y]}(f)$ compared to climate model (MPI) PSD's $S_{CM[x,y]}(f)$ for the Sprogø site.

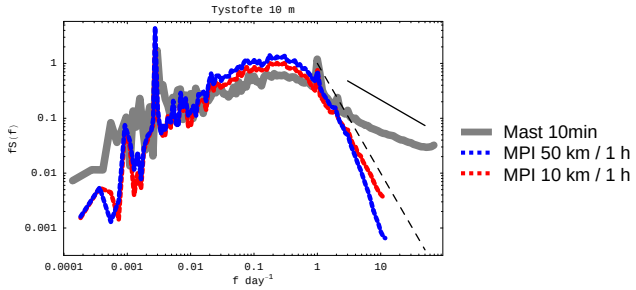

Figure 8. Measured (10m mast) PSD $S_{[x,y]}(f)$ compared to climate model (MPI) PSD's $S_{CM[x,y]}(f)$ for the Thystofte site.

The conclusion of this is that data should be corrected for the difference in roughness length and measurement height. Further research has indicated that better results can be obtained using the pressure gradient data of the climate models rather than the wind speed data. The idea is to first simulate the geostropic wind speed based on the pressure gradient, and then apply the local roughness at each wind turbine location to provide the local wind speed. It is expected that this will reduce significantly the gap between the PSD's for frequencies $f < 1$ day^{-1}.

After those corrections have been made, the work can proceed with estimating the gap in the PSD's for frequencies $f < 1$ day^{-1}, which will define the PSD $S_{SS[x,y]}(f)$ which should be applied in the stochastic simulation.

5. Wind turbine model

The wind turbine model should output a power time series based on the input wind speed time series. A steady state power curve is considered a sufficient basis for such a model, neglecting the aeroelastic and control dynamics, except for the control algorithm applied for cut-out or power reduction at high wind speeds.

The actual control algorithm applied for cut-out at high wind speeds is not known, and it will vary from one type of wind turbines to another. For a model of the state-of-the-art, it can be assumed that the wind turbine will cut-out the wind turbine when the average (e.g. 10 minute) wind speed reaches 25 m/s. It can further be assumed that the wind turbine will restart when the wind speed again decreases to below a certain value. Some hysteresis should be included, e.g. applying a restart wind speed of 20 m/s.

6. Conclusion

The model proposed in this paper has not been implemented, and as a consequence, it is also not validated. Still, initial data analysis look promising, and the following conclusions can be made at this state:

The climate model data seems to reproduce the measured wind speed variability for frequencies $f < 1$ day^{-1} quite well for an offshore site, where the roughness assumed in the climate model is close to the roughness on the measurement site.

For measurements on land sites, the model must correct for the difference between the assumed roughness in the climate models and at the measurement site Further research has indicated that better results can be obtained using the pressure gradient from the data of the climate models rather than the surface wind speeds for this purpose.

Finally, the model must correct for the difference between the assumed height above ground in the climate models and at the measurement site.

Acknowledgement

The present work is part of the research project "Offshore wind power – research related bottlenecks", contract No 2104-04-0005 funded by The Danish Agency for Science, Technology and Innovation under the Danish Ministry for Science, Technology and Innovation.

References

[1] UCTE Position Paper on Integrating wind power in the European power systems – prerequisites for successful and organic growth. Union for the co-ordination of Transmission of Electricity (UCTE). May 2004.

[2] En visionær dansk energipolitik 2025. Faktaark – Vedvarende energi. http://www.ens.dk/graphics/Energipolitik/dansk_energipolitik/Energistrategi2025/Faktaark_VE_190107Endelig.pdf. 19. januar 2007.

[3] Enercon wind turbines. Product overview. http://www.4energia.ee/files/File/Enclosure%201.1%20Product%20overview.pdf. . .

[4] Research project "Grid fault and design-basis for wind turbines". Energinet.dk contract number PSO-F&U 2006-1-6319.

[5] www.cdc.noaa.gov

[6] www.ecmwf.int

[7] P. Sørensen, A. D. Hansen, P. A. C. Rosas. Wind models for simulation of power fluctuations from wind farms. J. Wind Eng. Ind. Aerodyn. (2002) (no.90) , 1381-1402.

[8] P. Sørensen, N. A. Cutululis, A. Vigueras-Rodriguez, H. Madsen, P. Pinson, L. E. Jensen, J. Hjerrild, M. H. Donovan. Modelling of Power Fluctuations from Large Offshore Wind Farms. Wind Energy (published online 2007)

[9] P. Sørensen, N. A. Cutululis, A. Vigueras-Rodriguez, L. E. Jensen, J. Hjerrild, M. H. Donovan, H. Madsen. Power fluctuations from large wind farms. IEEE Trans. Power Systems (2007) 22 , 958-965

[10] Danish Energy Authority. Wind Turbine Master data register. http://www.ens.dk/sw34512.asp.

State Space Averaging Modeling and Analysis of Disturbance Injection Method of Maximum Power Point Tracking for Small Wind Turbine Generating Systems

Shengtie Wang, Tore Undeland
ELKRAFT NTNU, O.S. Bragstads Plass 2E, 7491 Trondheim, Norway
tlf. +47 7359 4280, e-mail Wang.Shengtie@elkraft.ntnu.no

Abstract — Based on a configuration with low cost and high reliability, disturbance injection method is employed to achieve the maximum power point tracking (MPPT) for the small wind turbine generating systems(SWTGS) in this paper. State space averaging method is used to model the whole system, and its nonlinear and linearization model are given. The choosing principle of two crucial parameters of disturbance magnitude d_m and angular frequency ω are proposed by the frequency response analysis of the system. Experiment results show that the disturbance injection method of MPPT, system modeling and theoretical analysis are correct and practical. Results obtained in the paper lay the foundation for the application of disturbance injection method of MPPT to SWTGS, and have theoretical significance and practical value in engineering

Index Terms — disturbance injection method, maximum power point tracking(MPPT), small wind turbine generating systems (SWTGS), state space averaging modeling

1. INTRODUCTION

The small wind power is one of the promising research and development fields in using the wind energy. The small wind turbine generating systems (SWTGS) of 1-10 kW, which can operate alone or connect with the power grid, can be installed in some areas of hills, grasslands, islands and even cities due to its flexibility. Though there are some 160 thousand sets of small wind power systems operating at present in China, its potential market is huge throughout the world[1].

Because of its small capacity and geographic location, it is important and essential for SWTGS to have low cost, high reliability as well as high efficiency. To meet these requirements, various system configurations and maximum power point tracking (MPPT) strategies have been reported [2]-[11]. The scheme proposed in [4] has the characteristics of simple structure and inexpensive hardware, for no position or speed sensors and complicated digital controllers are employed to realize MPPT control strategy or capture as much energy as possible from wind, and some analysis for the system performance has been done by means of both transfer function method and experiment. In this paper, state space averaging method is used to model the proposed SWTGS and its theoretical analysis of disturbance injection method of MPPT is carried out. As a result, the choosing principle of two crucial parameters of disturbance magnitude d_m and angular frequency ω are given. Finally experiment verifies the correctness of system modeling and theoretical analysis for SWTGS.

2. DISTURBANCE INJECTION METHOD OF MPPT[4]

The configuration of SWTGS shown in Figure 1 has the advantage of low cost and high reliability because it consists of permanent magnet synchronous generator, diode rectifier and chopper, and no speed sensors are needed to track the maximum output power of wind turbine. Output power or current of chopper is adjusted by controlling its duty due to almost constant voltage across the battery.

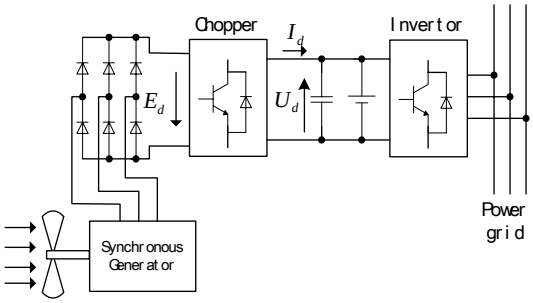

Figure 1. Configuration of SWTGS

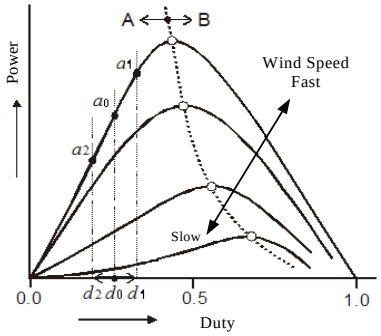

Figure 2. Relationship between output power and duty

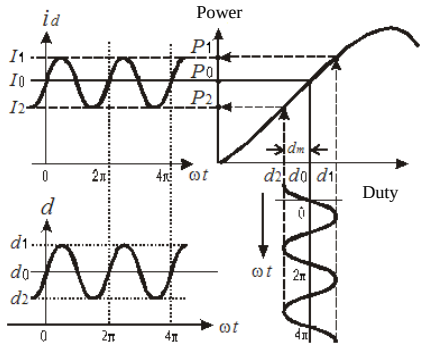

Figure 3. Principle of disturbance injection method

A disturbance injection method of MPPT for SWTGS is shown in Figure 2 and 3. A sine disturbance signal with certain magnitude and frequency is injected to the chopper, and output current is sampled at the time of $\pi/2$ and $3\pi/2$ each cycle, respectively I_1 and I_2. The control law can be described by the following equations

$$d = d_0 + d_m \sin \omega t$$
$$d_0 = K \int (I_1 - I_2) dt \quad (1)$$

Suppose that the phase lag between output current and injected disturbance signal is φ. Because of the sampling time of output current, $\varphi=(2n+1)\pi/2$ when the system gets the maximum output power point, where n is integral. The precondition for (1) is that: $\varphi \in (-\pi/2+2n\pi, \pi/2+2n\pi)$ if the system is operating at area A; $\varphi \in (\pi/2+2n\pi, 3\pi/2+2n\pi)$ if operating at area B. When this condition is not satisfied, d_0 in (1) will change into

$$d_0 = -K \int (I_1 - I_2) dt \quad (2)$$

Disturbance magnitude dm and angular frequency ω are two critical parameters of the disturbance injection method of MPPT for SWTGS. If d_m is too big, large current fluctuation will occur in the system; If d_m is too small, it will be not easy to detect the current difference at sample times, and not beneficial to get better control performance. If ω is too big, the phase lag of system will increase, and system realization will become difficult; If ω is too small, the dynamic response of the system is slow and control performance gets bad. The choosing of d_m and ω will be discussed in the following sections.

3. State Space Averaging Modeling of SWTGS

3.1. Electrical circuit model

For simplicity, the following assumptions are made for the system: 1) the property of wind turbine is simulated by a DC motor; 2) the property of synchronous generator and rectifying bridge with diodes is approached by a DC generator; 3) Boost chopper is employed; 4) the battery property is equivalent to an ideal voltage source in series with a resistor; 5) the property of inverter and load is similar to a resistor. Based on the assumptions above, the equivalent circuit of SWTGS is shown in Figure 4.

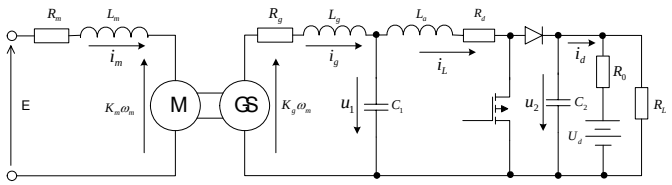

Figure 4. Equivalent circuit of SWTGS

3.2. Mathematic model

Since it is difficult for the conventional method to be used to model the electrical circuit with switching devices, state space averaging method is employed here to model it [12]. Two main steps of state space averaging method are: 1) the individual state equations which correspond to 'on' or 'off' state of the system are obtained respectively; 2) the total state equation is acquired by weighing these individual state equations.

Assume that switching device and diodes have the same voltage drop V_d when they are 'on' state, and the current of inductor of chopper is continuous (duty is d). If current of inductors, voltage of capacitors and angular speed of generator are chosen as state variables, the state equation of the whole system is obtained by state space averaging method

$$\dot{X} = \begin{bmatrix} -\frac{R_m}{L_m} & -\frac{K_m}{L_m} & 0 & 0 & 0 & 0 \\ \frac{K_m}{J} & 0 & -\frac{K_g}{J} & 0 & 0 & 0 \\ 0 & \frac{K_g}{L_g} & -\frac{R_g}{L_g} & -\frac{1}{L_g} & 0 & 0 \\ 0 & 0 & \frac{1}{C_1} & 0 & -\frac{1}{C_1} & 0 \\ 0 & 0 & 0 & \frac{1}{L_a} & -\frac{R_d}{L_a} & -\frac{1-d}{L_a} \\ 0 & 0 & 0 & 0 & \frac{1-d}{C_2} & -\frac{1}{C_2}\left(\frac{1}{R_0}+\frac{1}{R_L}\right) \end{bmatrix} X + \begin{bmatrix} \frac{1}{L_m} & 0 & 0 \\ 0 & 0 & 0 \\ 0 & 0 & 0 \\ 0 & 0 & 0 \\ 0 & 0 & -\frac{1}{L_a} \\ 0 & \frac{1}{R_0 C_2} & 0 \end{bmatrix} U$$

$$i_d = \begin{bmatrix} 0 & 0 & 0 & 0 & 0 & \left(\frac{1}{R_0}+\frac{1}{R_L}\right) \end{bmatrix} X + \begin{bmatrix} 0 & -\frac{1}{R_0} & 0 \end{bmatrix} U \quad (3)$$

where, $X = [i_m \quad \omega_m \quad i_g \quad u_1 \quad i_L \quad u_2]^T$, $U = [E \quad U_d \quad V_d]^T$

When the system gets into steady state, its output current is

$$i_d(\infty) = \frac{(1-d)\frac{K_g}{K_m} E - (1-d)^2 \frac{R_l}{R_0+R_L} U_d - (1-d) V_d}{R_g + \left(\frac{K_g}{K_m}\right)^2 R_m + (1-d)^2 \frac{R_0 R_L}{R_0+R_L} + R_d} \quad (4)$$

3.3. Linearization model

The system described by (3) is a nonlinear one, for it contains the product of variables. Equation (3) is linearized near its equilibrium point for dynamic analysis. Suppose that the system is on equilibrium state, we have $d=d_0$, $x=x_0$, $i_d=i_{d0}$ $A(d)=A(d_0)$. If a small disturbance Δd near equilibrium point is injected into the system, then $d=d_0+\Delta d$, $x=x_0+\Delta x$, $i_d=i_{d0}+\Delta i_d$, $A(d)=A(d_0)+A(\Delta d)$. Substitute them into (3), and use Δd and Δi_d as input and output respectively, we get linearization model of the system by rearranging them

$$\Delta\dot{X} = \begin{bmatrix} -\frac{R_m}{L_m} & -\frac{K_m}{L_m} & 0 & 0 & 0 & 0 \\ \frac{K_m}{J} & 0 & -\frac{K_g}{J} & 0 & 0 & 0 \\ 0 & \frac{K_g}{L_g} & -\frac{R_g}{L_g} & -\frac{1}{L_g} & 0 & 0 \\ 0 & 0 & \frac{1}{C_1} & 0 & -\frac{1}{C_1} & 0 \\ 0 & 0 & 0 & \frac{1}{L_a} & -\frac{R_d}{L_a} & -\frac{1-d_0}{L_a} \\ 0 & 0 & 0 & 0 & \frac{1-d_0}{C_2} & -\frac{1}{C_2}\left(\frac{1}{R_0}+\frac{1}{R_L}\right) \end{bmatrix} \Delta X + \begin{bmatrix} 0 \\ 0 \\ 0 \\ 0 \\ \frac{u_{20}}{L_a} \\ -\frac{i_{L0}}{C_2} \end{bmatrix} \Delta d$$

$$\Delta i_d = \begin{bmatrix} 0 & 0 & 0 & 0 & 0 & \left(\frac{1}{R_0}+\frac{1}{R_L}\right) \end{bmatrix} \Delta X \quad (5)$$

its transfer function is

$$\frac{\Delta i_d(s)}{\Delta d(s)} = \frac{b_1 s^5 + b_2 s^4 + b_3 s^3 + b_4 s^2 + b_5 s + b_6}{a_0 s^6 + a_1 s^5 + a_2 s^4 + a_3 s^3 + a_4 s^2 + a_5 s + a_6} \quad (6)$$

where, coefficients in (6) are the function of system parameters, and not listed here due to its complication.

4. CHARACTERISTICS ANALYSIS

4.1. Steady state analysis

Since equation (4) is a second order function of d, its maximum output current i_d^* exists and is unique. Neglect of $(1-d)^2$ term in denominator, optimal $d^*$and maximum output current i_d^* are obtained respectively

$$d^* = 1 - \frac{\frac{K_g}{K_m}E - V_d}{2\frac{R_L}{(R_0+R_L)}U_d} \approx 1 - \frac{K_g E}{2K_m U_d} \tag{7}$$

$$i_d^* = \frac{\frac{\left(\frac{K_g}{K_m}E - V_d\right)^2}{4U_d}}{\left[R_g + \left(\frac{K_g}{K_m}\right)^2 R_m + R_d\right]\frac{R_L}{R_0+R_L} + \frac{\left(\frac{K_g}{K_m}E - V_d\right)^2}{4U_d{}^2}R_0} \approx \frac{\frac{E^2}{4U_d}}{R_m + \left(\frac{K_m}{K_g}\right)^2 (R_g + R_d)} \tag{8}$$

It can be seen from (7) that d^* mainly depends on four parameters of E, U_d, K_g and K_m. If E increases or decreases, d^* will decrease or increase, i.e., d^* varies with the wind speed. Equation (8) shows that i_d^* has something to do with not only the four parameters mentioned above, but R_m, R_g and R_d as well. In a word, equation (7) and (8) can be conveniently used for the system analysis and design.

4.2. Frequency response analysis

When parameters of the experimental system are used and E=100V, bode diagram of linearization model is shown in Figure 5. Similar bode diagrams can be obtained for different E.

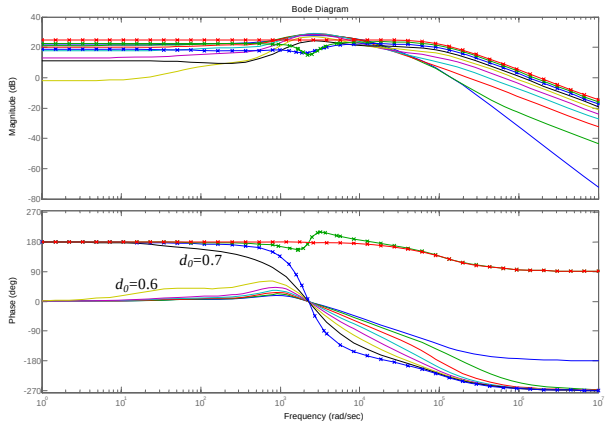

Figure 5. Bode diagram of linearization model

It can be seen from Figure 5 that: 1) when d_0 changes from 0.6 to 0.7, notable change happens in bode diagram, i.e., d_0^* is in between 0.6 and 0.7; 2) when φ=±90°, the system gets into equilibrium state. Equilibrium point is usually different from optimal point, and the difference between them relies on ω. 3) When ω is relatively small, if initial d_0<0.6, d_0 will increase and approach to d_0^* under the direction of controller, because 0°≤ φ <90°; if initial d_0>0.7, d_0 will gradually approach to d_0^*, because 90°<φ ≤180°; 4) when ω is relatively large, d_0 will approach to certain equilibrium point. Because bode diagrams are very near, the equilibrium point is usually far from optimal point. 5) magnitude response is relatively smooth in lower frequency.

In summary, considering together the dynamic performance of the system, the choosing principle of disturbance magnitude d_m and angular frequency ω is: 1) ω is as large as possible when it is guaranteed that the system will acquire or approach to d_0^*; 2) d_m depends on magnitude response and allowed fluctuation of system.

4.3. Phase lag analysis

If there exists phase lag in the system, its phase response will move down. If angular frequency ω is given, d_0 will go away from d_0^*, and output current will drop. Phase lag in the system comes from system itself and current detection circuit. Low pass filter (LPF) is introduced in current detection circuit to suppress current fluctuation. When angular frequency ω is given, phase lag of LPF can be calculated. Phase lag compensation of LPF can be carried out by changing the sampling time of output current.

5. EXPERIMENT RESULTS

In experimental system, DC motor with additional exciting current is used to simulate the wind turbine; permanent magnet synchronous generator from wind mill is employed; switching device is MOSFET and its switching frequency is 40 kHz; DSP acts as controller; triangle waveform generating circuit is used to modulate pulse width; battery group consists of 4 single batteries of 12V. Parameters of the experimental system are listed in Table 1.

Table 1. Parameters of the experimental system

name	value	name	value	name	value
J (Kg·m·m)	0.0047	R_g (Ω)	1.386	U_d (V)	47.6
R_m (Ω)	2.0	L_g (mH)	1.1	R_0 (Ω)	1.51
L_m (mH)	1.8	L_a (mH)	0.167	R_L (Ω)	30
K_m (V·s/rad)	0.81	C_1 (μF)	1300	V_d (V)	1.25
K_g (V·s/rad)	0.32	C_2 (μF)	6.8	R_d (Ω)	0.005

5.1. Steady state characteristics

When E is given, and d changes from 0.1 to 0.8 with the interval of 0.1, output current for each d forms a curve of steady state characteristics for system. Different curves for different E as well as those for analytic model are shown in Figure 6. It reaches a conclusion from Figure 6 that analytic model matches the experiment result apart from small d. In fact, the chopper usually works at the duty d of above 0.3.

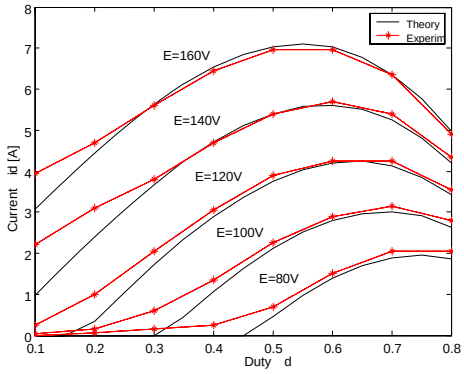

Figure 6. Steady state relationship between output current and duty

5.2. Maximum power point tracking

According to the choosing principle of disturbance parameters, ω=10×2π rad, d_m=0.05 and K=10. Steady state d and i_d are shown in Figure 7 , where E=160V. It shows that the closed loop control system achieves the maximum power control, where d_0^* and i_{d0}^* are 0.60 and 6.4A respectively. When E has a sudden change from 160V to 80V, d_0^* gradually converges to a new optimal duty of 0.75, where new optimal output current is 1.7A. Waveforms of variables are shown in Figure 8. This shows that the controller is able to search optimal point 'on line' and make the system generate the maximum power all the time even when wind speed changes.

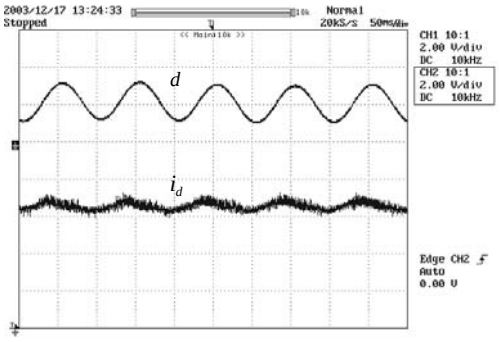

Figure 7. Waveforms of MPPT (E=160V)

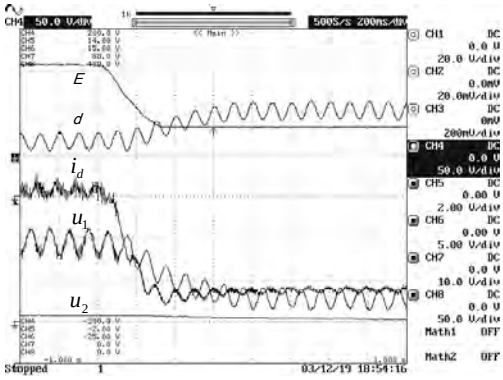

Figure 8. Waveforms of MPPT (E=160V drop to 80V)

5.3. Performance improvement

When compensation phase matches the phase lag from current detection device, the maximum output current can be obtained. The optimal compensation phase is about 30º, the maximum output current is shown in Figure 9. In fact, when E=160V, more current of 0.5A (power 24W) is obtained, i.e., the efficiency of electricity generation is improved by 7.7%.

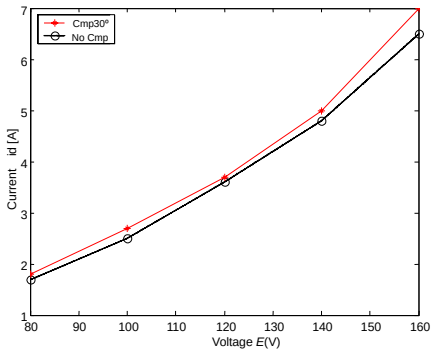

Figure 9. Performance improvement of phase lag compensation

6. CONCLUSION

Small wind turbine generating systems(SWTGS) has found certain applications and has a large potential development all over the world. Because of the geographic locations and working conditions, its property of low cost, high reliability and high efficiency has been paid much attention.

Based on a simple structure of SWTGS, disturbance injection method of maximum power point tracking (MPPT) is employed to capture as much energy as possible from wind. State space averaging method is used to model the entire system, and its nonlinear and linearization models are given. Dynamic and steady analysis of the system model sheds the light on the nature of disturbance injection method of MPPT. As a result, the choosing principle of two crucial parameters of disturbance magnitude dm and angular frequency ω are proposed. Experiment results prove that the disturbance injection method of MPPT, system modeling and theoretical analysis are correct and practical.

Results obtained in the paper can play the guidance role in analysis, design and application of disturbance injection method of MPPT to SWTGS.

REFERENCES

[1] Staff Editor. China's Wind Power in Rapid Progressing. Electricity-CSEE, Vol.12, No.2, 2001, pp.42-45.

[2] M. D. Simoes, B. K. Bose, R. J. Spiegel. Design and performance evaluation of a fuzzy-logic-based variable-speed wind generation system. IEEE Trans. on Ind. Applications, Vol.33, No.4, July/August 1997, pp.956-965.

[3] N. Yamamura, M. Ishida, T. Hori. A Simple Wind Power Generating System with Permanent Magnet Type Synchronous Generator. PEDS'99, IEEE 1999 International Conference on Power Electronics and Drive Systems, Vol.2, July 27-29, 1999, Hong Kong, pp.849-854.

[4] Y. Higuchi, N. Yamamura, M Ishida. An improvement of performance for small-scaled wind power generating system with permanent magnet type synchronous generator. IEEE IECON 2000, Vol.2, Oct. 22-28, 2000, Nagoya, Japan, pp.1037-1043.

[5] Y. Q. Jia, Z. Q. Yang, B. G. Cao. A new maximum power point tracking control scheme for wind generation. POWERCON 2002, Proceedings of International Conference on Power System Technology, Vol.1, Oct.13-17, 2002, Kunming, China, pp.144-148.

[6] T. Nakamura, S. Morimoto, M. Sanada. Optimum control of IPMSG for wind generation system. PCC Osaka 2002, Proceedings of Power Conversion Conference 2002, Vol.3, April 2-5, 2002, Osaka, Japan, pp.1435-1440.

[7] Q. Wang, L. C. Chang. An Intelligent maximum power extraction algorithm for inverter-based variable speed wind turbine systems. IEEE Trans. on Power Electronics, Vol.19, No.5, Sept. 2004, pp.1242-1249.

[8] E. Koutroulis, K. Kalaitzkis. Design of a maximum power tracking system for wind-energy-conversion applications. IEEE Trans. on Ind. Electronics, Vol.53, No.2, April 2006, pp.486-494.

[9] M. Arifujjaman, M. T. Iqbal, J. E. Quaicoe. Maximum Power Extraction from a Small Wind Turbine Emulator using a DC - DC Converter Controlled by a Microcontroller. ICECE '06, International Conference on Electrical and Computer Engineering, Dec. 2006, Dhaka, Bangladesh, pp.213 – 216.

[10] N. Mutoh, A. Nagasawa. A Maximum Power Point Tracking Control Method Suitable for Compact Wind Power Generators. PESC '06, 37th IEEE Power Electronics Specialists Conference, June 18-22, 2006, pp.1-7.

[11] R. J. Wai, C. Y. Lin, Y. R. Chang. Novel maximum-power-extraction algorithm for PMSG wind generation system. IET Electric Power Applications, Vol.1,No.2, March 2007, pp.275-283.

[12] S. Ang, A. Oliva. Power Switching Converters. Taylor & Francis Group, New York, 2005, pp.247-276.

Modelling of floating wind turbine platforms for controller design

Thomas Fuglseth[*)], Tore Undeland
Dept. of Electrical Power Engineering, NTNU, O.S. Bragstads plass 2E, N-7491 Trondheim, Norway
[*)] tlf. +47 73 59 42 29, e-mail Thomas.Fuglseth@elkraft.ntnu.no

Abstract — This paper presents an ongoing project to construct a computer modelling tool based on MATLAB/Simulink and the wind turbine simulation code FAST for simulating wind turbines on a floating foundation. It summarises how hydrodynamic forces can be modelled in a computationally efficient way using linearization techniques, and shows how these techniques are applied to a specific floating foundation design.

Index Terms — Computer modelling, Floating offshore wind energy, System identification.

1. Introduction

In many parts of Europe and other areas of the world, desirable onshore space for wind energy development is becoming scarce, and developments are stopped by public demand as property owners resent having wind turbines in their view. Even offshore installations are having trouble with protests because they are too close to the shore. And so, development is moving towards even greater sea depths and distance to shore, which eventually requires a floating foundation.

A floating foundation presents different conditions for a wind turbine than a foundation firmly fixed into the ground or seafloor. A floating structure is subjected to wave excitation forces and forces that depend on the movement of the structure. In order to properly control a wind turbine mounted on a non-fixed foundation, it is important to be able to predict how the platform will respond to the forces it is subjected to by the wind turbine mounted on it.

This paper presents a continuation of the work presented in [1]. The purpose is to provide an overview of the work that has gone into creating modelling tools that can be used for simulating floating wind turbines, and the future plans for the project. The modelling approach consists of modifying the existing wind turbine simulation code FAST to accept input from a linearised model of the hydrodynamic forces implemented in Simulink. This gives us a computationally efficient simulation tool that allows us to model the complete system of a floating wind turbine, including aero- and hydrodynamics as well as electrical and electromechanical components. This can then be used for designing and testing control systems for the full system.

2. Modelling basics

This section treats some of the basic elements of modelling the dynamics of floating structures in general and the modelling of floating wind turbines in particular.

2.1. General representation of floating structures

The *j*-th equation of motion for a body moving in six degrees of freedom can be written as:

$$\sum_{k=1}^{6}(m_{jk}+\alpha_{jk}(\omega))\ddot{q}_k+\sum_{k=1}^{6}\beta_{jk}(\omega)\dot{q}_k+\sum_{k=1}^{6}c_{jk}q_k=\tau_j^D+\tau_j^A+\tau_j^E \quad (1)$$

where $\alpha_{jk}(\omega)$ is the frequency-dependent added mass, $\beta_{jk}(\omega)$ is the frequency-dependent potential damping, and c_{jk} is the restoring coefficient. τ_j^D are diffraction forces, caused by waves breaking against the body. τ_j^A are actuator forces and τ_j^E are other external forces. These last two elements typically represent wind forces and, in the case of a floating wind energy converter, the forces from the turbine itself.

2.2. FAST wind turbine simulation code

FAST is an aeroelastic wind turbine simulation code developed at NREL in Colorado, USA. It is written in Fortran, and can be interfaced with Simulink for use in controller design and development. As FAST is an open source program, it can be modified by users to suit their needs.

2.3. Platform and WAMIT model

The simulation tool which is being developed is intended to be useable for modelling a multitude of platform designs. However, this research is based on a specific design consisting of a ballasted, tubular buoy with a relatively conventional horizontal axis wind turbine mounted on the platform. This is similar to concepts which are being developed in Norway today [2]. The floating platform, as illustrated in figure 1, is a cylindrical concrete platform. The cylindrical section is 9.4 meters in diameter and 108 meters long. The wind turbine itself is attached to a coned section that adds a further 12

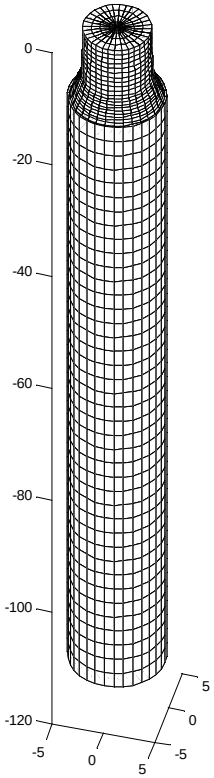

figure 1: geometry of the platform

meters to the height of the platform, so the total draught from the water surface is 120 meters.

To get the frequency-dependent hydrodynamic coefficients $\alpha_{jk}(\omega)$ and $\beta_{jk}(\omega)$ we use the program WAMIT. The illustration in figure 1 shows a graphical representation of the panel data used when calculating hydrodynamic data for the platform in WAMIT

The geometry file that is shown in the illustration is generated with a MATLAB script, but for more complex geometries a modelling program such as Multisurf would be preferable.

With WAMIT, a total of 52 frequency samples are generated for each of the 36 components of the frequency dependent added mass and radiation damping matrices.

3. LINEARIZATION OF RADIATION FORCES

The frequency-dependent hydrodynamic coefficients found with WAMIT can be used to identify linear state-space systems that can be solved in simulations to approximate the time-dependent hydrodynamic forces. These approximations can be used both in simulations and as a basis for model-based controllers. There are multiple available methods for finding linear representations of the radiation force convolution integral, and several of these have been examined as part of this work.

The hydrodynamic forces in (1) can be represented in a convolution integral form, which gives the following formulation of the equation of motion:

$$\begin{aligned}&\sum_{k=1}^{6}(m_{jk}+a_{jk})\ddot{q}_k+\sum_{k=1}^{6}b_{jk}\dot{q}_k+\sum_{k=1}^{6}c_{jk}q_k\\&+\sum_{k=1}^{6}\int_{-\infty}^{t}K_{jk}(t-\sigma)\dot{q}_k(\sigma)d\sigma\\&=\tau_j^D+\tau_j^A+\tau_j^E\end{aligned}\qquad(2)$$

where $a_{jk}=\alpha_{jk}(\infty)$ and $b_{jk}=\beta_{jk}(\infty)$ are frequency-independent added mass and potential damping coefficients, and the frequency-dependence of the radiation forces are represented by the convolution integral. The constant added mass term a_{jk} is usually nonzero. For a body that is holding station, i.e. not experiencing any continual motion through the fluid, the parameter $\beta_{jk}(\omega)\to 0$ as $\omega\to\infty$ [4]. For the purpose of this work we therefore assume that $b_{jk}=0$.

To get to a linear model, we start out with the tables of $\alpha_{jk}(\omega)$ and $\beta_{jk}(\omega)$ generated with WAMIT and try to find a good approximation to the transfer function $K_{jk}(\omega)$. This is the frequency domain representation of the convolution integral:

$$\mu_{jk}=\int_{-\infty}^{t}K_{jk}(t-\sigma)\dot{q}_k(\sigma)d\sigma\qquad(3)$$

We can find $K_{jk}(\omega)$ directly in the frequency domain through the following equation as explained in [5]:

$$K_{jk}(\omega)=(\beta_{jk}(\omega)-b_{jk})+j\omega\cdot(\alpha_{jk}(\omega)-a_{jk})\qquad(4)$$

Alternatively, we can find the time-domain impulse response representation $K_{jk}(t)$ by numerically solving one of the following equations [3]:

$$K_{jk}(t)=-\frac{2}{\pi}\int_0^{\infty}\omega\cdot\left(\alpha_{jk}(\omega)-a_{jk}\right)\cdot\sin\omega t d\omega\qquad(5)$$

$$K_{jk}(t)=\frac{2}{\pi}\int_0^{\infty}\omega\cdot\left(\beta_{jk}(\omega)-b_{jk}\right)\cdot\cos\omega t d\omega\qquad(6)$$

Using (6) is generally preferable to (5), as the former converges faster.

Finally, we wish to represent the solution to the convolution integral (3) as the output of a linear state space system:

$$\begin{aligned}\dot{\xi}_{jk}&=\mathbf{A}_{jk}\xi_{jk}+\mathbf{B}_{jk}\dot{q}_k\\\mu_{jk}&=\mathbf{C}_{jk}\xi_{jk}+\mathrm{D}_{jk}\dot{q}_k\end{aligned}\qquad(7)$$

The system in (7) is easily implemented in software such as MATLAB/Simulink. Calculating the output of a state space system is also very computationally efficient compared to solving (3) for each time step of a simulation. The linearization result can also be used as a basis for model-based controller structures.

3.1. Kristiansen's method

This method is detailed in [3], but will be summarized here. Kristiansen's approach consists of constructing an impulse response from the available frequency domain data by numerically solving equation (6), and then using a time domain system identification algorithm to find a linear state space system that represents this impulse response. Kristiansen uses Kung's SVD algorithm, as implemented in the MATLAB function IMP2SS.

IMP2SS yields high order models, with the model order sometimes going as high as 280. To get a model that is more computationally efficient, a square root balanced truncation model reduction is performed, using the function BALMR from MATLAB Robust Control Toolbox.

3.2. Least squares fit to frequency response

This approach is treated in more detail in [4]. With this method, a state-space representation is found directly from the frequency domain data, rather than going via a time-domain impulse response.

We start out by noting that the transfer function K_{jk} can be expressed as the ratio of two polynomials:

$$K_{jk}(s) = \frac{B_{jk}(s)}{A_{jk}(s)} \tag{8}$$

Furthermore, $K_{jk}(j\omega)$ is a complex valued function, and it can be seen from (4) that:

$$\mathrm{Re}\left[\frac{B_{jk}(j\omega)}{A_{jk}(j\omega)}\right] = \beta_{jk}(\omega) - b_{jk} = \beta_{jk} \tag{9}$$

$$\mathrm{Im}\left[\frac{B_{jk}(j\omega)}{A_{jk}(j\omega)}\right] = \omega \cdot \left(\alpha_{jk}(\omega) - a_{jk}\right) \tag{10}$$

By converting the frequency dependent added mass and potential damping into a vector of complex values, we can use a least squares fitting method to find a linear system that gives approximately the same frequency response. McCabe et. al. [4] use the commercially available INVFREQS function in MATLAB.

3.3. Subspace methods

Subspace methods are a family of model identification routines that use a subspace approximation to find state space models. Tests have shown them to be both fast and to give good results. Subspace methods are well suited for finding state space models based on data in the form of samples of the frequency spectrum of the input $U_k = U(\omega_k)$ and output $Y_k = Y(\omega_k)$ at a set of *M* frequencies ω_k. Subspace methods usually involve representing the measured input and output data in vector-matrix form

$$\mathbf{Y} = \mathrm{O}\mathbf{X} + \Gamma\mathbf{U} \tag{11}$$

where O is the extended observability matrix and Γ is a lower block-triangular Toeplitz matrix. It should be noted that only **U** and **Y** are known. The challenge is then to remove the influence of the Γ**U**-term, estimate the range space of the O**X**-term and calculate the state space system's A and C matrices from the estimated observability matrix. Finally, the B and D matrices are estimated from A and C. [6] treats this subject in more detail.

The method that is used in this work is implemented in the function N4SID in MATLAB System Identification Toolbox. The algorithm itself is described in section 10.6 of [7].

4. LINEARIZATION RESULTS

All three linearization methods mentioned in the previous chapter were tested with the data generated in WAMIT and the results compared.

The time it took to calculate the finished state space models when using the three methods was noticeably different, Kristiansen's method being particularly CPU intensive. Calculating the state space representation of $K_{11}(\omega)$ took more than half an hour with Kristiansen's method, while the two other methods computed a solution within a matter of seconds. All computations were performed on a 2.4 GHz Pentium 4 CPU with 1 GB main memory. As the calculations only have to be performed once, solution time is not a factor in selecting a method.

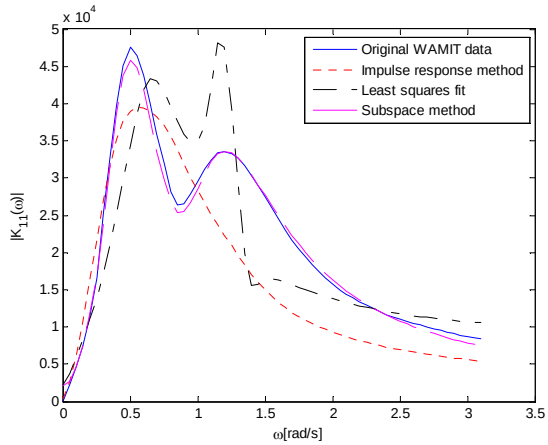

figure 2: amplitude of $K_{11}(\omega)$

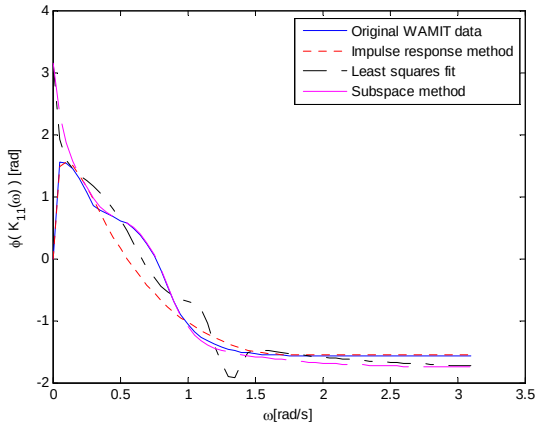

figure 3: phase angle of $K_{11}(\omega)$

The results when using the different methods were noticeably different, however. Figures 2 and 3 show a comparison between the transfer function $K_{11}(\omega)$ computed from the WAMIT data and the result from the different linear approximations. Please note that this single example does not give anywhere near the full picture. The various methods were tried out on all 36 elements of the radiation force, and linear systems with orders ranging from third to 20th were generated and compared. However, this example is very representative of the observed behaviour of the different linearization techniques. In this example, we have used 8th order linear systems.

The impulse response method required long calculation times, but provided fairly good results. However, it had a hard time capturing some phenomena, such as the twin-peaked frequency spectrum shown in figure 2. It generally gave a good result for the phase angle.

Least squares fit proved to be somewhat difficult to get good results with. Very often it would come down to a choice between good amplitude results or good phase angle results.

A configuration that gave good amplitude matching would tend to yield phase angle spikes, where the phase angle was drastically different from the original data over a short frequency interval. Alternately, a configuration that gave good phase angle results would yield poor amplitude matching. Overall, getting good all round results with the least squares fit method was often a case of time-consuming testing of many different settings.

The subspace method was the one that proved to give a linearization that most accurately match the original data. As can be seen from figure 2, the subspace method follows the amplitude curve of the original data very well, and this was a general tendency. Phase angle also matches very well, except for the lowest frequencies where it for some cases tended to go towards π radians rather than 0.

For the moment, the subspace method is the one that yields the best results, and will be used in simulations. Hopefully it is possible to improve the low frequency phase response, but if not care will simply have to be taken when simulating to avoid very low frequency excitation of the system.

5. Building a simulation model

As mentioned in section 4, the subspace linearization method implemented in MATLAB System Identification Toolbox proved to be a very good tool for providing a linear model that can be used in simulations for calculating the radiation forces. Another advantage is that the toolbox also includes Simulink blocks that make it simple to implement state space models found with linearization tools in Simulink.

The next stage in modeling is the wind turbine itself. For this we have, as mentioned earlier, chosen to use the software FAST, available from National Renewable Energy Laboratory (NREL) in the USA [8]. The program is available with source code, and both a standalone implementation and a Simulink S-Function implementation are available.

FAST solves both the aeroelastic equations for the aerodynamics of the blades and rotor, and the equations of motion for the wind turbine as a whole. Therefore, it is possible to model a wind turbine on a floating foundation simply by adding the hydrodynamic forces to the equation of motion. The chosen method involves dividing the hydrodynamics into two components. The constant added mass matrix $[a_{jk}]$ is made part FAST's platform configuration file and simply added to the mass matrix of the turbine when solving the equations of motion. The frequency dependent component is modeled using the subspace linearization approach detailed in the previous section, and the 36 state space systems are implemented using the idmodel Simulink block that is part of the System Identification Toolbox.

Doing this required adding six new inputs to the FAST S-function, as well as modifications to the routine for loading the platform configuration file. While the programming job is done, there has unfortunately not been time to test the system by the time of writing.

6. Conclusion

In this paper we have summarized how linearization can be used to provide a computationally efficient tool for simulating the hydrodynamic forces on a floating platform. While this project concerns the modelling of floating wind energy converters, the same approach is useful in simulating other offshore structures such as wave energy converters.

Several different methods for generating linearized representations of the hydrodynamic forces have been compared to each other, and the conclusion is that subspace linearization provides the overall best results.

With the tools available in MATLAB/Simulink, we can connect a hydrodynamic model with a modified implementation of the wind turbine simulation code FAST. Simulink also provides us with many options for simulating the electrical and electromechanical components of the wind turbine. In other words, this will provide us with a flexible tool that can simulate all major aspects of a floating wind energy converter.

The finished model can then be used to simulate existing and proposed designs for floating wind energy converters. It can be used for design and testing of control strategies aimed at optimizing the power production and reducing structural stresses.

References

[1] T Fuglseth, T Undeland.. Modelling of floating wind turbines for simulation and design of axial thrust and power control strategies, Renewable Energy 2006, Chiba, Japan.

[2] F G Nielsen, T D Hanson, B Skaare. Integrated dynamic analysis of floating offshore wind turbines, Proceedings of 25TH International Conference on Offshore Mechanics and Arctic Engineering, OMAE 2006.

[3] E Kristiansen, Å Hjulstad, O Egeland. State-space representation of radiation forces in time-domain vessel models, Ocean Engineering 32, 2005, pp. 2195-2216.

[4] A P McCabe, A Bradshaw, M B Widden. A time-domain model of a floating body using transforms, 6th European Wave and Tidal Energy Conference, Glasgow, Scotland.

[5] Ø Lande, "Application of System Identification Methods to Time-domain Models of Marine Structures based on Frequency-domain Data", MSc. thesis from the Dept. of Marine Technology, Norwegian University of Science and Technology, 2006

[6] T McKelvey. Subspace methods for frequency domain data, Proceedings of the 2004 American Control Conference, 2004, pp. 673-678

[7] L Ljung. System Identification: theory for the user, 2nd edition, Prentice Hall, 1999

[8] NREL FAST homepage: http://wind.nrel.gov/designcodes/simulators/fast/

Capacity Credit of Wind Power in Germany

M. Sperling, A. Pamfensie, T. Hartkopf
Institute for Renewable Energies, TU-Darmstad
Landgraf-Georg-Str. 4, 64283 Darmstadt, Germany

Abstract — Covering the peak loads with a reliable safety margin is a task that becomes more difficult in the moment that base load power plants are exchanged by renewable energy resources. This is an issue that might affect Germany in the next years. This paper analyses the power plant mix in Germany and calculates the wind power capacity credit for different scenarios. The contribution of the wind power on covering the peak loads in discussed.

Index Terms — Balancing wind power, capacity credit, power plant park.

1. Introduction

The German power plant mix will suffer strong changes in the next decades. On the one hand, the renewable energies will keep their growth tendency. On the other hand nuclear power plants will be shutdown. To assure the energy supply, gas turbines will be installed.

How many conventional power plants can be shutdown after installing a certain amount of wind turbines, keeping the same security of supply as before? This question is the issue of this paper, considering the situation of Germany now and in the future.

The main idea of calculating the capacity credit is to make a verification to which extent the wind power is capable to substitute conventional generating plants.

2. Power Plant Mix

The 3 main types of power plant in the German power generation park are the nuclear, the hard coal and brown coal power plant, each of them contributing approximately with one quarter of the total generated electricity. The rest is distributed in water, wind, gas, oil and other types with small share on the total generation.

2.1. General Situation

There are 18 nuclear power plants in operation in Germany and no concession is planned to be given to new ones. The last nuclear plant is planned to be shutdown in 2020. Today there is a big discussion about the prolongation of the operation licences of some nuclear power plants. An example is the block Biblis A, which is supposed to stop operating in 2008, and there has been a renegotiation of its shutdown for 2011.

The hard coal power plants, working as medium load, will still be constructed in the future, but not as much as others will go out of operation. The power plants running on natural gas, typically working as peak load, will gain importance and assume a part of the generation in the middle load region. The brown coal power plants, working on base load, will still be active, but will reduce their participation on the total power generation.

The water power, including pump storage stations, does not have a good potential for growing, since there are almost no more sites to place such power plants in Germany.

The other renewable energies, such as biomass, photovoltaic and geothermal have been experiencing a fast growth in the last years, but are still in an early stage of development. The same is valid to the CHP (combined heat and power), that receives incentives through the CHP law (KWK-Gesetz).

2.2. Wind Power

Today, the wind capacity in Germany amounts to 20621 MW corresponding to 5.7% of the generated electricity in Germany according to BWE (Bundesverband Windenergie), stand of January 2007 [1]. According to DEWI (Deutsches Windenergie-Institut), the expected capacity for 2014 amounts 30811 MW [2]. The further development of the wind will be given specially on the construction of offshore wind parks and repowering of onshore old unities.

2.3. Prognosis

The most relevant study to make a prognosis of the German power plant park has been done by the institutes EWI and Prognos called "Energy Scenarios for the Energy Forum 2007" [3]. It forecasts the development of the energy resources for electricity generation until 2020 in 3 different scenarios, based on the energy policies of the 2 biggest political parties. Table 1 shows the resulting installed capacity of various types of power plant in 2005 and the expectation for 2020. Scenario *RE (renewable energies)* represents a favourable conjunction to the renewable energies while scenario *NP (nuclear power)* is favourable to the extension of the operation licence of the nuclear power plants.

Table 1. Installed capacity and participation on electricity generation of various types of power plants. 1: Installed capacity in MW, 2: participation on electricity generation in %. [3]

Types of Power plants	2005		Scenario RE 2020		Scenario NP 2020	
	MW[1]	%[2]	MW	%	MW	%
Water	12.1	4.6	12.5	5.7	12.5	5.5
Nuclear	21.5	26.3	7.1	8.4	21.5	29.1
Hard coal	29.4	21.6	25.0	14.8	19.2	9.3
Brown coal	22.0	24.8	15.7	21.3	15.7	17.1
Natural gas	23.3	11.4	29.3	20.8	24.9	16.1
Oil	5.5	1.9	3.2	0.9	3.2	0.9
Others	6.0	4.7	199	11.2	14.2	9.3
Wind	18.4	4.4	37.7	14.9	32.7	11.5
Photovoltaic	2.1	0.3	12.5	2.0	8.2	1.2
Total	140.3	100	162.8	100	152.1	100

According to this study, in the scenario *RE* the wider use of fluctuating renewable energy will, on the one hand, stimulate the use of gas fired power plants, due to its flexibility. On the other hand, the shutdown of nuclear power plants would stimulate the use of coal power plants, to cover the base load. On scenario *NP*, the coal fired plants lose the full load hours

to the nuclear plants. The renewable energies would decelerate the growth, and so the natural gas fired plants.

3. PEAK LOAD

One of the main arguments against wind energy is its small contribution to the assured power needed to cover the peak loads. It is generally assumed that between 5 and 10 % of the installed wind power can be counted as sure for the moments of high load.

The total net capacity in Germany is estimated in 124,3 GW by the VDN [4]. The net capacity is the gross capacity subtracted from the consumption of auxiliaries in the generation plants. The assured power at the year peak load in 2006 was 86.2 GW, being the load 77.8 GW. The resulting free load was 8.4 GW. According to [5] Germany is the UCTE country with the percental lowest free power and should make sure to not let it fall below unacceptable levels.

Table 2 shows the status of the power capacities during the peak load. The *reserve for system operational services* constitutes the primary and secondary control reserves, which can not be used for covering the load. Some capacities were under *revision* and *outage*. The *not available power* represents limitations of the power plants like low water level in water power plants, low wind speed, lack of fuel, lack of licence to operate, etc.

Table 2. Power balance of the electric power supply in Germany at the moment of the year peak load in 2006. [4]

Power status	Net-Power [GW]
Load	77.8
Free Power	8.4
Assured Power (Subtotal)	*86.2*
Reserve for system operational services	7.9
Revision	2.4
Outage	4.0
Not available power	23.8
Total power inland	*124.3*

4. INTEGRATING WIND POWER

The DENA-Study [6] is in Germany the main Study about the integration of the wind energy into the network. Basically, it proposes the construction of new transmission lines, which will carry the power from the windy coastal region in the north to the industrialised regions in the south. Furthermore, it adverts to the need of increased acquisition of regulation power by the transmission system operators, to balance the wind forecast errors, and the maintenance of long term reserves for covering the peak loads.

The actions described in the DENA-Study can be seen as the natural solution for the problem of integrating the wind energy. Nevertheless, there are other possibilities under research that could become economically feasible in the future, reducing the need of constructing new transmission lines and contracting energy reserves. A very promising technology is the demand-side management, which could adapt the user to the conditions of the energy system, helping to balance the wind power. Another alternative solution is making the use of storage systems in vicinity to wind power generation. In the case of Germany, the air compressed energy storage seems to be a good possibility, since it has favourable geographical conditions for being installed in the north of the country. The balancing of the wind power by decentralised small power plants operating as a virtual power plant is also not discarded. The communication technologies will be in the future connected to the generating system, enabling them to work on a coordinated way.

5. CAPACITY CREDIT

5.1. Definition of capacity credit

The capacity credit is a measure of the ability of the energy resource to statistically produce an ensured available power. This term is normally related to the intermittent renewable energies. The availability of the system becomes specially critical during the periods of peak load and unexpected outages of big power plants. In those moments, the installed wind capacity is able to contribute with the energy supply. The amount of power of the wind turbines that can be considered sure is the capacity credit of the wind power. Normally it is given in percent of the installed power.

The capacity credit is the gain on assured power. The power can be considered sure according to a reference called security of supply level. In this work, a security level of 99 % was chosen, the same used in the DENA-Study. This represents the probability in which the power will be available in a certain moment. In other words, the power supply is not 100 % sure.

5.2. Calculating capacity credit

To calculate the capacity credit of wind power, it is necessary first to determine the ensured power of the conventional power plants in the electrical system. This is done with the method of the *recursive convolution.* The probability distribution of the sum of two independent random variables is equal the convolution of their individual distributions. So, to have the distribution function of the whole power plant mix, the convolution of the functions of all the power plants is done.

An example of an available power distribution function of a single generation plant with rated power 500 MW is described in the picture below. The power plants have normally only 2 status: available with rated power and not available. Only the unplanned disconnections of power plants are considered as unavailable, since planed repairs, for example, are done in the moments of light load. The probability of an outage is according to the DENA-Study between 1.8 % and 3.8 %, corresponding to the type of power plant.

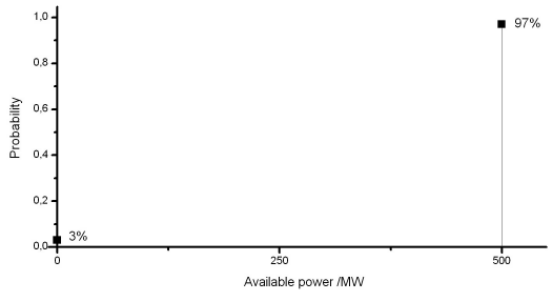

Figure 1. Available power distribution function of a conventional thermal power plant with a 3% probability of outage.

The recursive convolution of each function results on the available power distribution function of the power plant mix. Finally, the resulting function is convoluted with the distribution function of the wind power.

The integration of the distribution function of available power results in the diagram that is shown below. There, it is made possible to read to which probability a certain capacity will be available on a determined moment. By plotting this curve with and without considering the wind power it is possible to read to which extent the wind power contributes to the security of supply. The difference of the two points marked on the curve is the gain on ensured power, called capacity credit.

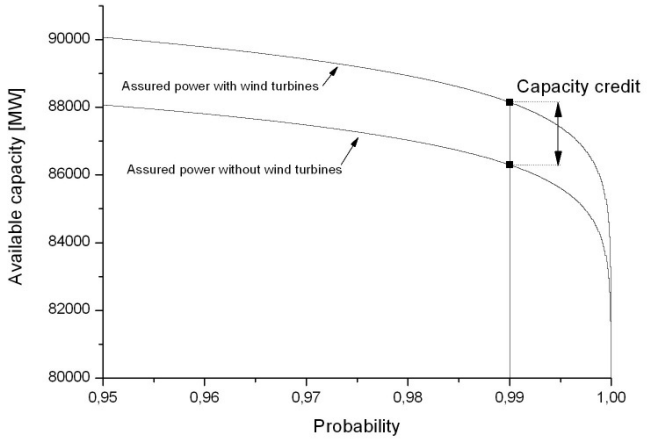

Figure 1. Wind power capacity credit with a security level of 99 %.

A list of different methods for calculating the capacity credit is given in [7]. In [8] the history of this subject is reviewed and a large number of sources is given.

6. RESULTS

The capacity credit of wind power was calculated for the scenarios of the power plant park showed on table 1. The recursive convolutions were made based on a list of the German power plants containing the information of rated power and probability of outage. The power distribution of the wind turbines was generated based on the time series of the total wind power fed into the network in Germany in the year of 2006. If the scenario being calculated has a different installed wind power than from 2006, it is assumed that the time series of wind power change linearly according to the difference.

The values in table 1 represent gross power capacities in the power system. These values were transformed to net values, based on the [3]. The number of power plants under revision is estimated in being equivalent to 2 % of the total capacity in winter, according to the forecast of power balance done by VDN (Verband der Netzbetreiber) for the years of 2005 until 2015 [5]. In summer this number goes to 10% of the total capacity, because the load is significantly lower than in winter. The reserves for operational services are estimated in ca. 10 % of the load. For the German case this is equivalent to ca. 7 GW. The estimation of not available power was taken from the same study. Considering only the conventional energy sources it amounts ca. 4 % of the total net capacity.

After the values from the scenarios in table 1 were transformed to net capacities, and the *system reserves*, *power plant under revision* and *not available power* were subtracted from them, the resulting list is compared to the data base of power plants. The data base is completed with power plants having typical values, until it reaches the number of power plants that represent the scenario that is being calculated. Finally, the recursive convolutions are done, including the power distribution function of the wind turbines, and the capacity credit is calculated.

Table 3 shows the capacity credit of wind power for scenarios *RE* and *NP* in percent of wind capacity. For the year of 2006, the resulting value was 7.98 %.

Table 3. Capacity credit of the scenarios RE (renewable energies) and NP (nuclear power) in percent of the total installed capacity of wind turbines.

Scenario / Year	RE	NP
2010	7.14	7.39
2015	6.49	6.85
2020	5.94	6.39

It is concluded that the assumed changes in the power plant park does not significantly affect the capacity credit. The dominating factor for the capacity credit is the amount of wind energy in the electrical network. The figure 2 illustrates this by showing the calculated capacity credits as a function of the installed wind capacity.

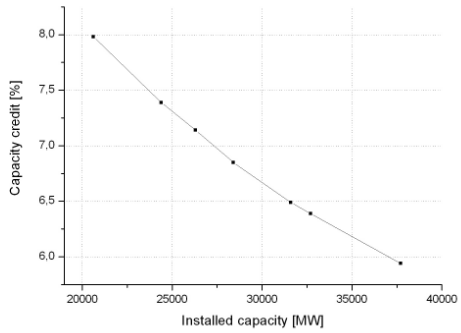

Figure 2. Capacity credit as a function of the installed capacity of wind turbines.

The measured values of wind power used as basis for this calculation could cause uncertainties on the prediction of the power distribution in the next years. It is acceptable that the average wind speed on the turbines might increase in the future. The main reasons are the construction of higher towers by repowering inland wind turbines and the location of turbines on offshore sites, with more favourable wind conditions.

7. SUMMARY AND FURTHER RESEARCH

This paper analysed the power plant mix in Germany and discussed the tendencies for the near future. It showed the conditions of the power plant park during the moment of peak load, that is the situation in which the concept of capacity credit is applied. The topic integration of wind power was reviewed, discussing shortly the conventional and the alternative solutions. A definition of wind power capacity credit was given, as well as a description of how to calculate it.

The wind power capacity credit was calculated based on the example of the scenarios *RE* (renewable energies) and *NP* (nuclear power). The constitution of the power plant park did not affect significantly the results. The total installed wind power was the most important factor.

As an issue for further research, the author considers of relevance the analysis of the effect on the ensured power the mentioned possible solutions for balancing the wind energy, such as demand-side management and storage systems.

REFERENCES

[1] BWE. http://www.wind-energie.de/.

[2] DEWI. WindEnergieStudy 2006 – Market Assesment of the Wind Energy Industry up to the year 2014.

[3] EWI/Prognos. "Energy Scenarios for the Energy Forum 2007"

[4] VDN. Jahresbericht 2006.

[5] VDN. Leistungsbilanz der allgemeinen Stromversorgung in Deutschland. Vorschau 2005 – 2015.

[6] DENA. Energiewirtschaftliche Planung für die Netzintegration von Windenergie in Deutschland an Land und Offshore bis zum Jahr 2020.

[7] C. Ensslin, A. Badelin, Y. M. Saint-Drenan. The Influence of Modelling Accuracy on the Determination of Wind Power Capacity Effects.

[8] G. Giebel. Wind Power has a Capacity Credit – A Cataloge of 50+ Suporting Studies.

Wind Farm Repowering: A Case of Study

Luis Selva
Renewable Energy Engineer
Albacete (SPAIN)
Email: luisselva83@hotmail.com

Miguel Cañas and Emilio Gómez and Antonio Pujante
Renewable Energy Research Institute
Dept. of Electrical, Electronic
and Control Eng. EPSA
Universidad de Castilla-La Mancha
02071 Albacete (SPAIN)
Email: emilio.gomez@uclm.es

***Abstract*— Wind farm repowering involves the replacement of smaller and middle sized wind turbines with state-of-the-art multi-megawatt turbines. In this paper, a detailed study of the repowering of a wind farm is presented, by computing the generated active power from existing wind turbines and the new ones. The active power generated with the wind turbines are totalized to obtain the yearly generated energy, analyzing so economic studies, taking into account the repowering costs too.**

I. Introduction

Wind power has developed dramatically in recent years; indeed, over the past few years, new installations of wind power have surpassed new nuclear plants. This growth is even more impressive in Europe as it is shown in Table I, where appears Europe's wind energy generating capacity by December 2006. Taking these growths into account, it is clear that wind power has become a competitive technology for clean energy production, and will provide in the near future two digit percentages in many country energy supply. Two are the reasons justifying these figures: the technology employed —mainly in the wind power turbines— and the policies and incentives offered in these countries.

In Europe, Germany headed the list with 20 622 MW connected to the electrical network, followed by Spain — 11 615 MW— and Denmark —3 136 MW—. These three countries alone accounted for 74% of the wind power capacity installed in European Union by end of 2006, Table I. Figure 1 shows in detail the evolution of the installed wind power capacity, in absolute terms per year —figure 1(a)—, the accumulated value —figure 1(b)—, and the average electrical rated power of the installed wind turbines per year —figure 1(c)—.

Obviously, the first wind farms installed in Spain, or other countries, were located in sites where the highest wind resource was found. These wind farms are already paid off, and could be replaced with multi-megawatt turbines.

On the other hand, in some countries — as Denmark and Germany— there is no much more suitable sites to place a productive wind farm. In Spain the situation will be the same in a few years. For investors, it is more efficient to replace smaller and middle sized wind turbines on highly productive sites with new larger ones, instead of just building the new ones on less productive sites, process known as repowering. For example, up to 1200 used turbines in the

TABLE I
EUROPE WIND ENERGY GENERATING CAPACITY BY END OF 2006

Country	Capacity(MW)
Germany	20.622
Spain	11.615
Denmark	3.136
Italy	2.123
UK	1983
Netherlands	1.560
Portugal	1.716
Austria	965
France	1.567
Greece	746
Sweden	572
Ireland	745
Belgium	193
Finland	86
Poland	152.5
Luxembourg	35
Estonia	32
Czech Republic	50
Latvia	27
Hungary	61
Lithuania	55.5
Slovakia	5
EU-25 total	48.027
Accesion Countries	68
EFTA Countries	325.6

Source: European Wind Energy Association (EWEA)

TABLE II
CHARACTERIZATION OF GAMESA WIND TURBINES G47 AND G80

Technical data	G47	G80
Generator type	DFIG	DFIG
Rated power (kW)	660	2000
Voltage (V)	690	690
Frequency (Hz)	50/60	50/60
Rotor diameter (m)	47	80
Swept area (m2)	1.735	5.027
Rotational speed (r.p.m.)	23-31	9-19
Towers Height (m)	40/45/55	60/67/78/100
Number of blades	3	3
Length of blades (m)	23	39
Blade weigth (kg)	4500	6500

Source: Gamesa

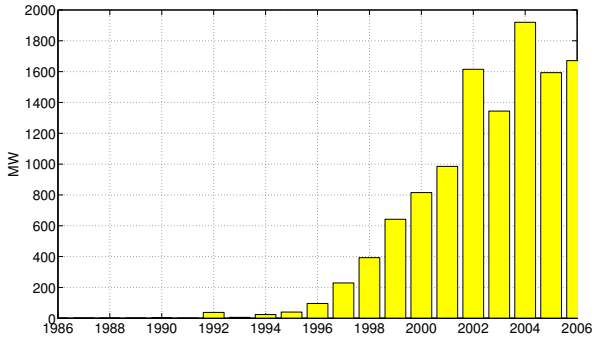

(a) Installed wind power capacity. Data obtained from "Instituto para la diversificación y el ahorro de la energía —IDAE—"

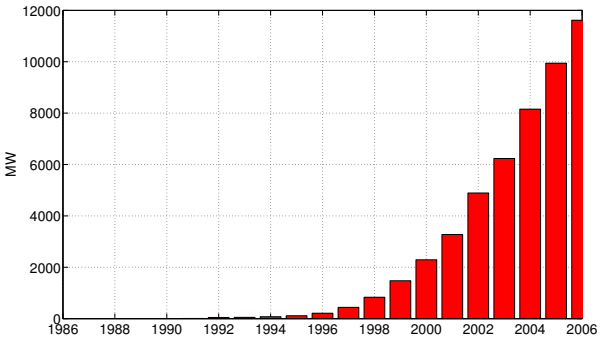

(b) Accumulated installed wind power capacity. Data obtained from "Instituto para la diversificación y el ahorro de la energía —IDAE—"

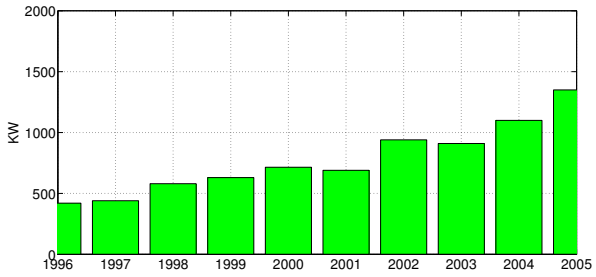

(c) Evolution in size of installed wind turbines. Data obtained from the Spanish Wind Energy Association

Fig. 1. Evolution of wind power in Spain

range of 150 to 600 kW in Germany will be available on the international market within the forthcoming 10 years, [1]. Denmark will replace over 900 old wind turbines with 150-200 new ones around 2 MW of rated power at least [2]. One destiny to these turbines are developing countries. This is due to, in many cases, wind farms with multi-megawatt turbines can not be developed, since it is necessary a sophisticated infrastructure and specialists to carry out the construction, operation and maintenance of the wind farm. Currently, second hand wind turbines are mainly being demanded in Poland, Russia, Romania, Morocco, Bulgaria and Turkey. In most of these countries renewable energy laws have recently passed the legislation to initiate project planning.

For the the transmission system operators, new generation wind turbines offer an improvement of network stability due to better grid integration, by using connection methods similar to conventional power plants, and also achieving a higher utilization degree, [3]. Other aspect is related with the visual impact, being improved due to less wind turbines in the landscape and a more quiet visual impression as the rotational speed of larger turbines is lower, [4].

The advantage for developing countries is the establishment of their own wind energy industries thanks to the experience acquired in working with renewable energy sources. By this way, they can train qualified personnel, [1].

Repowering has some disadvantages too, since it could be hard to find a second-hand wind turbine that could be adapted to the requirements of a specific project because wind turbines and their equipment are designed for a specific location. So, a turbine designed to be placed in north of Germany, could be not suitable to be used in the desert of Morocco. Also, the procurement of spare parts might become an obstacle, as the usual technical support of manufacturers expires after 20 years. Other disadvantages include the costs of second-hand equipment and the real state of the wind turbine, paying special attention to the blades and the gearbox, the most expensive elements to transport [1].

II. Data

The repowering of a wind farm has been studied. The existing wind farm consists in 50 wind turbines with a rated power of 660 kW, totalizing 33 MW. The re-powered wind farm owns 25 wind turbines with a rated power of 2 MW, totalizing 50 MW of installed power generating capacity. These wind turbines generators (WTG) are made by Gamesa, a Spanish manufacturer with experience in the wind turbine sector. Specifically, the models studied are G47 (660 kW) and G80 (2MW) both equipped with double fed induction generator, DIFG.

The characteristics of the wind turbines are indicated in the Table II. In figure 2 there is shown a comparison between power characteristic curves of both wind turbines. It can be observed that the G80 WTG needs lower wind speed to start generating higher power, whereas the G47 WTG needs a higher wind speed to achieve the same initial power output. It should be noted that in the curves the maximal wind speed is limited to 20 m/s although the wind turbines can operate up to 25 m/s.

The energy generated in the two cases has been studied, figure 7, taking into account the wind speed data obtained from the existing wind turbines, and measured with a time interval of ten minutes during an entire year. A total of 2.628.000 data have been handled in the wind farm equipped with 50 G47 WTG, while that the fictitious farm composed for 25 G80 WTG only the half of the wind data have been used. Figure 7 also shows that better energy values are generated during the initial and the latter months in the year.

From the figure 7 can be deduced that the greater difference of power generated is found among the registrations of the

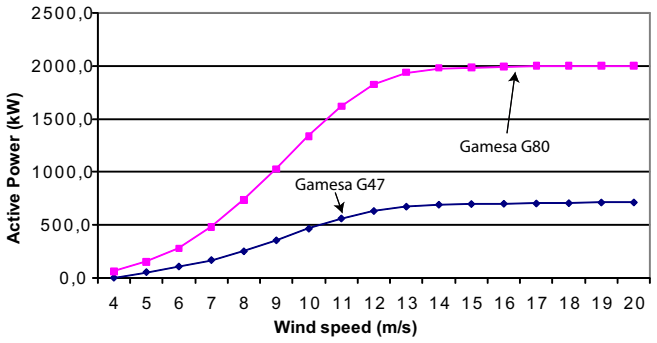

Fig. 2. Power curve of Gamesa G47 and G90

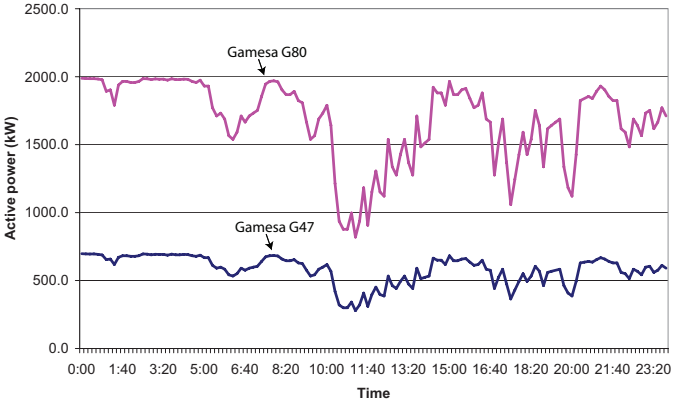

Fig. 3. Generated active power in January, 1

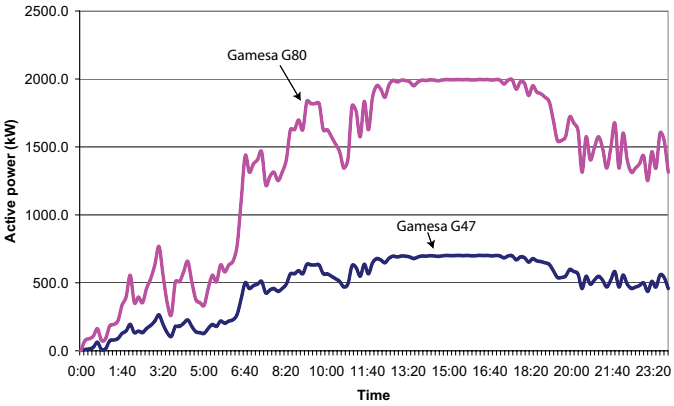

Fig. 4. Generated active power in July, 1

winter season (December) and of the summer season (August), since in the first and last months of the year the highest values of wind are registered. The annual generated energy is obtained by totalizing the generated active power computed by the active power vs wind speed curves provided by the manufacturer in time interval of ten minutes.

Analyzing the annual power data of each wind turbine, it is interesting to observe the graphics where it is reflected the monthly production comparative in real-time representation, as well as the daily production comparative graphic, which can be analyzed thanks to the time interval applied for the data recorded. Figures 3, 4, 5 and 6 present the variation of compared active power productions in terms of a day or a month, showing for example intervals where the rated power in both turbines are achieved.

As can be seen in the figure 3, the two generated energy curves present a similar waveform and the lower output energy occurs approximately from 10:00 to 12:30 hours, although there are two significant drops at 17:30 and 20:00 hours respectively. Finally, when evening came and during the night the energy production is higher than the rest of the day, because the wind speed is also affected by the solar radiation, even though this variation depends on the site.

In the figure 4, the higher output energy occurs approximately from 12:00 to 19:00 hours in the two power curves, although there also is peak production at 9:30 hour. In the first hours the energy generation is lower and the instant power growth is more pronounced, but in the rest of the day this curve is steadier because the atmospheric conditions in July (summer) are more stable than in January (winter), figure 3, in this location of Spain.

Figures 5 and 6 show the temporal progress of generated energy curves in the January and July of the same year, taking into account a data pair for every day in such months. As can be remarked the two wind turbine curves are similar waveforms like it occurs in figure 3 and 6. It should be noted that during the first January fortnight some zero generating days appear, while at second fortnight the number of such days is considerably reduced, thence the average generating value to the end of January is recovered. However, during the whole July the energy generation presents a great variability, in this case there are a few days where the rated power is achieved, therefore the average generating value to the end of July is one of the lower value during the year, like the rest of the months of summer season.

III. Economic Evaluation

The economic study is based firstly by the economic balance carried out from the generating data obtained for both wind turbines G47 and G80. On the one hand, it is necessary to assign a rate final price that depends on the location and the wind plant sort. On the other hand is needed to obtain an average price estimation by power unit installed. The references used are the following: the year in which they began to install the first wind farms compounding by G47 wind turbines was 1998, the proposed date for the beginning of the installation in the wind farm with G80 wind turbines is 2006 and the Real Decreto 436/2004 that describes the Spanish grid requirements for wind farms. An useful life of 20 years is considered for both wind farms.

Knowing these data a comparative among the two wind plants can be carried out to analyze the cost of each one as well as to determine the most minimum repayment time as function of the reference rate and the average price by MW power installed. In this case, the reference or average electric rate for the year 2005, defined in the corresponding law has a value of

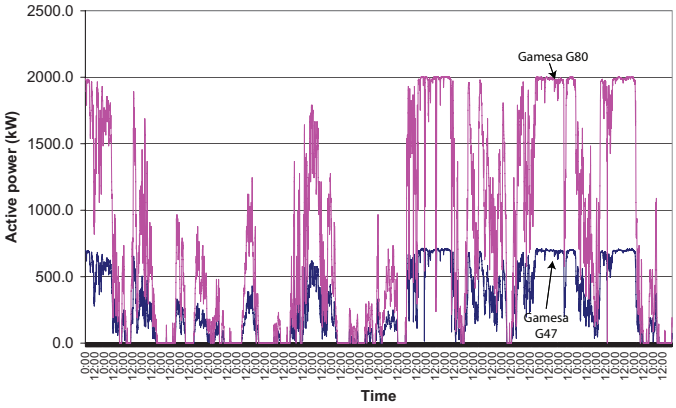

Fig. 5. Generated active power in January

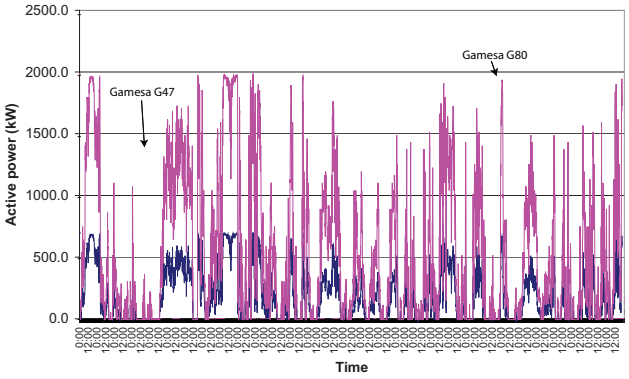

Fig. 6. Generated active power in July

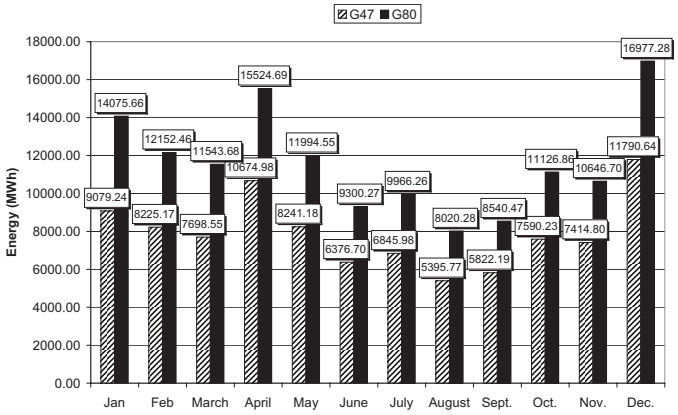

Fig. 7. Generated energy by month

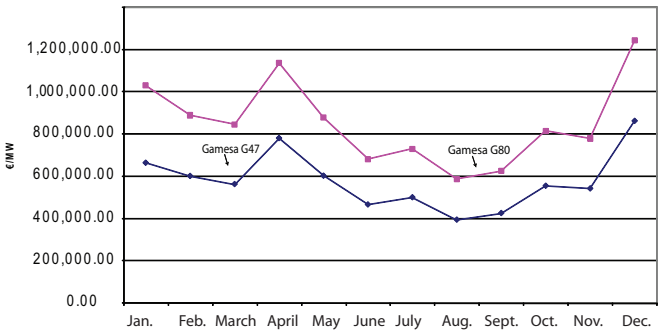

Fig. 8. Benefits by month

7,330 c€/kWh. Consulting some reliable sources (IDAE and AEE) the medium price of the investments has been estimated, first during the year 1998 in an approximate value of 920€/kW installed, secondly for the year 2006 a lightly ascent trend situated this value in 936€/kW installed; it should be noted that both numbers comprise all the necessary requirements to put into operation of a wind farm, included the evacuation electric substructure costs.

Using such data a table summary for the repowering wind farm has been made, from the corresponding cell a global cost for the current installation of 30.360.000€ is derived. To calculate the final cost of the future installation are necessary several previous steps, for instance the residual value of the obsolete wind turbines, the value of the conserved electric substructures and the disbanding expenses of the current wind farm; keeping in mind that the installation is seven years old, the resulting cost is 8.199.794,87€. The wirings also hold an economic value, it is a residual value of 14,42% on the general budget according to the source of the PEE-BCG database of wind farms and projects of wind energy. The dismantling expenses of the wind turbines installed would be the 3,5% of the general budget according to the source of the IDAE. With this amount of items it can be calculated in approximate manner the needed budget to face the new installations, so to setup 50 MW the real cost is 32.912.805,13€.

With the installation final costs, the production accumulated of the current installations and the possible production of the future installations should be considered, thus the annual average production is 95.155,43 MW for the G47 and 139.869,15 MW for the G80 wind turbines. Now it is possible to derive the financial gains of both installations, an annual total of 6.974.892,87€ for the G47 and for the G80 an annual total of 10.252.408,72€ are obtained.

Considering the economic production annual average and depending on the installation final costs, just as has been seen previously, the repayment time of both installations can be achieved. In the case of the G47 wind turbine the repayment time is 4,35 years, whilst in the case of the G80 wind turbine is only 3,21 years as their economic benefits are greater than those of G47, figure 8.

The repowering study is summarized in the Table III.

IV. Conclusions

The number of situable places to install a wind farm in countries like Denmark, Germany and Spain is reduced. The new grid codes [5] are imposing uninterrupted generation throughout power system disturbances, such as the voltage dips [6]. The majory of the wind turbines installed 10 or 8

TABLE III
WIND FARMS ECONOMIC STUDY SUMMARY

Wind Farm Turbines	G47	G80
Setup Year	1998	2006
Service Life (years)	20	20
Unit Power (kW)	660	2000
Number of Units	50	25
Total Power (MW)	33	50
Investment Average Rate (€/kWh)	920	936
Total Cost (€)	30.360.000, 00	46.800.000, 00
Wind Turbine Cost (€)	67, 52%	67, 52%
Dismantling Expenses (€)	3, 50%	-
WT Salvage Value (€)	8.1999.794, 87	-
Conserved Installations Value (€)	14, 42%	14, 42%
Real Cost (€/kWh)	-	32.912.805, 13
Recovery Average Rate (c€/kWh)	7, 33	7, 33
Annual Average Generation (MW)	95.155, 43	139.869, 15
Annual Economic Production (€)	6.974.892, 87	10.252.408, 72
Amortization Time (years)	4, 35	3, 21
Recovery Average Rate to amortize in 4 years (c€/kWh)	7, 98	5, 88

years ago do not accomplished with these grid codes and are placed in an excellent places for the eolic generation.

In this paper, a technical and economic study have been carried out to evaluate the benefits of replacing a wind farm equipped with old-technology wind turbines G47 with the newest G90. The wind turbines technical data have been showed and the main diferences between them has been highlighted.

Finally, an economic evaluation has shown the convenience of repowering in countries like Spain. It shows that repowering has benefits for the sellers countries, they can produce more energy with less cost, and for the buyers countries, they can face the construction of wind farms without a large amount of money or recourses.

ACKNOWLEDGMENT

E. Gómez, M. Cañas and Antonio Pujante acknowledge the support from the "Junta de Comunidades de Castilla-La Mancha" through the grant PCI-05-024.

REFERENCES

[1] N. Peterschmidt, "Wind energy converters in developing countries," in *World Wind Energy Conference*, 2003.

[2] DWIA, "Annual report of the danish industry association," Danish Wind Industry Association, Tech. Rep., 2005.

[3] BWE, "A clean issue-wind energy in Germany," German Wind Industry Association, Tech. Rep., 2006.

[4] W. Klunne, H. J. M. Beurskens, and C. A. Westra, "Wind repowering in the netherlands," in *European Wind Energy Conference and Exhibition*, July 2001.

[5] I. Erlich and U. Bachmann, "Grid code requirements concerning connection and operation of wind turbines in germany," in *IEEE Power Engineering Society General Meeting*, San Francisco, California, June 2005.

[6] M. H. J. Bollen, G. Olguin, and M. Martins, "Voltage dips at the terminals of wind power installations," *Wind Energy*, vol. 8, pp. 307–318, 2005.

Wind Power in Power Markets: Opportunities and Challenges

Nguyen T. H. Anh[1)], Le Anh Tuan[2*)], Ola Carlson[2)]
[1)] Energy Management Faculty, Electric Power University, 235 Hoang Quoc Viet, Hanoi, Vietnam
[2)]Department of Energy and Environment, Chalmers University of Technology, 41296 Gothenburg, Sweden
[*)]Tel: +46-31-772 3832, E-mail: tuan.le@chalmers.se

Abstract — This paper provides a comprehensive review of the opportunities and challenges from trading of wind power in power markets. The opportunities are the low operating costs, government incentive/subsidy program, reduction of market price, reduction of carbon dioxide emission, reduction of network loss, *etc.* The challenges would be technical requirement for power system integration, high investment cost, increased requirement on regulation power due to wind forecast error, more price volatile, more market competition for other generations, *etc.* The opportunities and challenges are discussed from different market players' perspectives. Some suggestions for possible measures to overcome those challenges are presented.

Index Terms — Challenges, opportunities, power market, wind power.

1. INTRODUCTION

In recent years, wind power development in the world has reached a high level in energy industry. At the end of 2006, the wind energy development data from more than 70 countries around the world show that the new installation in this year is 15,197 megawatts (MW), taking the total installed wind energy capacity to 74,223 MW, up from 59,091 MW in 2005 [1]. In terms of economic value, the wind power sector has become firmly as one of the important players in the energy markets (especially in developed countries), with the total value of new generating equipment installed in 2006 reaching US$23 billion [2]. The reasons for this fast development in wind power are due in part to ***e.g.***, i) improved wind power technologies with recent development in wind turbines and converters designs, ii) decreased installed capacity costs, and iii) increased public concern about the climate change problem caused by CO_2 emissions from conventional fossil fuels based generation. It is also important to note that during the last couple of years, the costs of wind turbines have however not gone down due to the lack of production capacity in wind industry. On the other hand, the price of electricity has increased. Therefore, it is possible for the wind power producers to earn more money when the penetration of wind power into the power market grows. This will in turn bring up the development of wind capacity production.

Electricity produced from wind is getting higher and higher in share in total electricity production. However, the amount of wind power participating directly in the liberalized electricity market is still limited. With the liberalization of electricity markets, wind energy producers have the possibility to dispatch their production through electricity pools, rather than having recourse to bilateral contracts. The possibility to trade in the market place would bring more benefit to the wind power producers, which in turn would make wind power more attractive for new investment. However, up to now, the wind generation participates significantly in the electricity markets only in a few countries, e.g., Denmark [3], Spain [4], Alberta in Canada [5], and the New York in USA [6]. In Spain for example, more than 8300 MW of wind energy participated in the market in October 2005 for an installed capacity of about 9300 MW in the Peninsular electric system by that time. In Sweden, the government is financially supporting wind farm projects in the countries. One example is the Lillgrund wind farm. Also the green-certificate program [7] is also making the investment in wind power projects more attractive. The introduction of wind power trading in the market place is just a matter of time.

It has been realized that wind power trading on the one hand has a lot of benefits to the owners of the wind farms as well as to the system as a whole. So, the question is that why wind power has not been largely traded in the electricity market? Participating in an electricity market implies to present bids and to commit the delivery of the agreed amount of energy in a given moment. This has led to several complications in operation of the power market as well as the power delivery system. Wind power trading could, on the one hand, bring about opportunities for the wind investors, to the power system as a whole, and to the environments. It could, on the other hand, make the system more difficult to operate, make the other market players to feel more "economically insecure", and could make the market price more volatile. In this paper, we call these difficulties the challenges which the power sector need to tackle in order to allow for the wind power in the market place which could at the end of the day help to achieve the goal of reducing environmental emission and energy dependence on depletable resources.

There exist opportunities as well as challenges when large-scaled wind power participates in the market place. The central question is that how would we overcome the challenges to allow for maximum levels of wind power traded in the market places. This, at the same time, would mean that the opportunities from wind power can be, to the best extent, utilized. This paper aims at presenting different opportunities and challenges brought about by the possible participation of wind power in the electricity market. The discussions are given from different perspectives, i.e., wind farm owners', network owners', society's perspective.

Figure 1 shows a typical arrangement between the power markets and power system operation. In this figure, wind power is included to show the effects of wind power trading in different components of the overall picture of market and system operation. Once integrated in the markets, one could observe that wind power could have effects on power market itself, on other types of conventional power generations, on the regulation markets, and so on.

The organization of the paper is as follows: The following section will focus on the discussion about the

opportunities. Section 3 will discuss the challenges. Section 4 presents several measures to overcome these challenges. Finally, conclusions are made in Section 5.

2. THE OPPORTUNITIES

2.1. Wind-farm Owners

First, we will study the opportunities from the perspective of wind farm owners. Wind energy is one of the most economical of all renewable energy sources other than hydroelectricity. With wind power plants, they pay operation and maintenance costs, which are less than those of the conventional power plants. The cost of electricity in c/kWh from a wind farm decreases as the annual mean wind speed, turbine size and wind farm size increase. Because wind power is capital intensive, its cost increases significantly as the discount rate (real interest rate) increases. It also increases if a long transmission interconnection to the grid is required. Operation and maintenance costs, comprising land, insurance, regular maintenance, repairs and administration, averaged over the lifetime of a wind farm, may amount to 20–25% of total cost of electricity produced [8]. In the USA in the mid-2000s land-based wind power has an installed capital cost of about US$1000/kW peak [9].

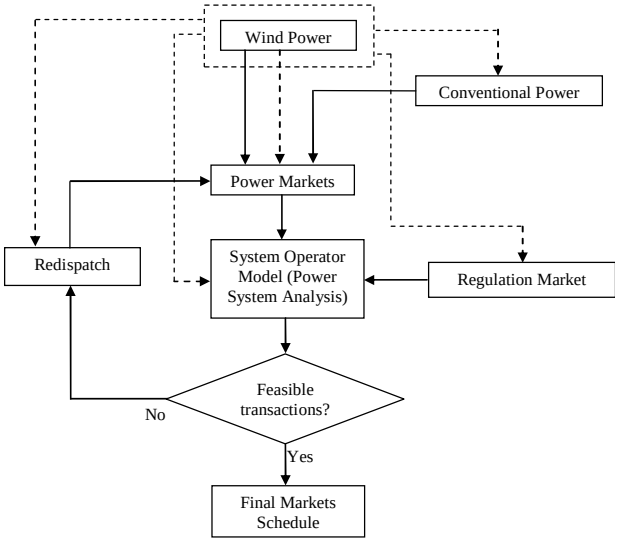

Fig.1: Wind power in power markets

Moreover, they can get more benefits traded energy in the power markets where the market price is settled and paid uniformly to all the selected bidders. The wind power revenues depend on hourly prices for both energy and ancillary services, thus the investors should focus not only on the locations with high wind potentiality but also on the locations with high energy prices [10].

According to [11], feed-in tariff and bonus model can be done for wind power in particular and for renewable power in general. These models consist of paying generators a fixed price or premium for the energy in order to provide a stable long-term price structure and also reduce an important part of the market risks. This can either be done for the electricity (kWh) and wind power together or only a fixed price for wind power. Priority of dispatch is also considered in many electricity markets, especially in Europe. This is clearly established in their national legislation as indicated in the Directive 2001/77/EC [11] (the Directive 2001/77/EC issued by the European Parliament and the Council on the promotion of electricity produced from renewable energy sources in the internal electricity markets). When power system has transmission congestion that may effect both conventional and wind generation, wind (and renewable) generations will receive the priority. In Denmark, the transmission system operator even can restrict the production of conventional power plants in some cases. By that ways, the wind power generation appears to be more attractive in the market place and the wind farm owners could recover their investment faster.

2.2. Other Markets Participants

In general, from the perspective of the power markets, one could say that the sale of generation reflects the marginal production cost. Introducing wind generation would thus generally reduce the market clearing price. A recent study [12] in Nordic power market have shown that the average market price will be reduced with about 5øre/kWh if supply of wind generation is increased to cover 10% of the Nordic power system demand. The electricity users would thus benefit from reduction of the market price.

However, due to the intermittent nature of wind power, the regulation market price may be more volatile or increased. This would probably be an opportunities for those producers who participate in regulation markets.

2.3. Distribution Network Owners

Much of the wind power installation take place as larger wind installation units with a rated power of more than 100 MW and will be connected directly to the 130, 220 or 400 kV grids. However, a substantial amount will be connected into existing local and regional distribution 10-70 kV networks. When the connection point of wind installation is close to the load center, the transmission of power can thus be avoided. This in turn would most likely reduce the transmission losses which would otherwise occur without wind power. Moreover, cost savings can be expected by deferring the needs for transmission and distribution upgrades [13].

2.4. The Environment

From the society's point of view, wind power production would help to reduce total CO_2 emission from conventional fossil-fueled power plants since wind power would replace part of power generation requirement from those conventional plants. According to [14], by the end of 2004, offshore wind power produced more than 2200 GWh in Europe avoiding the equivalent of approximately 1.5 million tones of CO_2 per year to be released into the atmosphere. If we take a rough calculation based on the total world's wind capacity today, the total CO_2 emission avoided in a year could be 88 millions tons of CO_2. Governments are providing policy measures to increase the development of wind power as part of their strategies for the environmental emission reduction goals. As an example, in Sweden, the Act on Electricity Certificate was introduced in 2003 in order to increase the proportion of the electricity produced from renewable energy sources. The producers receive a certificate for each MWh of renewable electricity they produce and they can sell it to get additional revenue [7].

3. THE CHALLENGES

3.1. System Integration and Operation Challenges

We will miss something important if we do not mention about the well-known problems of grid integration of wind power. In general, the main integration issues associated with increasing penetration of wind power include: voltage control at wind power facilities, system stability during fault conditions, need for transmission reinforcements, impacts on operational performance and related market rules. These have been previously studied by many, see for example [15]-[17].

Large-scale integration of wind power into power system operation gives rise to new challenges for the entire system and for transmission system operators in particular. With regard to their system responsibility, the supply of reliable electric power includes the responsibility to maintain a balance between demand and production in the grid. With small wind power penetration levels, wind power can be treated as negative load, e.g., wind power reduces the overall demand, hence the impact on system operation is very small. High wind power penetration levels, however, requires a rethinking of the power system operation methods because wind power cannot be scheduled with the same certainty as conventional power plants. The important wind power fluctuations for the operation of a power system are mainly caused by daily weather patterns, e.g., low pressure zones moving across Europe.

In addition, wind power in large transmission grid may lead to a higher loading of the lines which thus consume more reactive power [11]. The more wind power in-feed, the more reactive power demand in the transmission grid. However at present, wind turbines can not offset the increasing reactive power of the transmission system, especially within transmission system above 110 kV. Moreover, the variable reactive power available in conventional power plants is not designed for the additional reactive power demand of the transmission grid. Thus, some additional elements must be installed into the grid to keep reactive power balance and also power quality and security.

As mentioned above, wind farm generation brings a new challenge for balancing electricity production and consumption, mainly in the grid with high wind penetration. TSOs have to deal with the imperfect generation and consumption forecast. In the case, a system reserve markets has been created as effective solution in order to increase demand side management as well as provide reserve power capacity for maintaining the system balance. The complex of the markets depends on the penetration of wind power, the forecasting techniques and market mechanism, including pricing and penalty mechanism. According to [12], the variations of wind power production will increase the flexibility needed in the system when significant amounts of load are covered by wind power. When studying the incremental effects that varying wind power production imposes on the power system, it is important to study the system as a whole. In Denmark and Finland, the 2000 MW and 4000 MW of wind power would increase the load following requirement by 30-40 MW and 120-160 MW, respectively. The numbers show that the impact on load following reserve requirement (this term is understood as a part of the Fast Contingency Reserve of Nordel) is very small, only around 1.5-4 % of installed wind power capacity. Considering Nordic countries as a whole, the 19,000 MW of wind power would increase the load following requirement by 240-320MW.

Besides, high wind power production far from load centers causes more losses in the transmission grid [11]. The active power losses in the regions with low wind power production are doubled comparing to the regions with high wind power production.

3.2. Market Integration Challenges

A number of studies on market integration of wind power generation have appeared recently. In [18], a strategy for wind producers to present bids under the NETA rules is presented. These rules allow the presentation of bids only a few hours before the operation time, making less necessary the prediction tools. Most of the countries, however, follow different rules. In [19], a study using the rules of the Dutch electricity market is presented. Bids are presented once a day and not updated in subsequent markets. A general study using the Spanish rules under different assumptions, and presenting one bid for each day, with different anticipation times before operation has been done in [20]. They do not use any actual prediction tool, but works with average accuracies. In [21], an analysis of the benefits of the use of short term wind power prediction tool in an electricity market is presented. In the subsequent section, we will present the challenges in more details according to our classification of the problems.

3.2.1. High Investment Costs

The problems which wind-farm owners are facing include high investment cost, imbalance cost trading and technical failures, among other things. At present, the installation cost for both onshore and offshore wind farms are still at high level. For examples, in the UK the costs are about £650/kW (or €900/kW) and £1000/kW (or €1400/kW) for onshore and offshore, respectively [22]. In the EU, based on data from the early 2000s, capital costs were €900–1000/kW and less than 400 € /m^2 of swept area. In Australia, the capital cost of a large installed wind farm in 2005 was about AU$1800/kW (or €1150/kW) and the total levelized cost of electricity at very good to excellent sites was 7.5–8.0 AU$cents/kWh (4.8-5.1 €cents/kWh) [8].

3.2.2. Imbalance Power Cost

The integration of wind power in the power system is quite different from other types of energy sources because their production completely depends on whether, when and how hard the wind blows. In addition, comparing to conventional generators, the production is relatively uncontrollable, variable and especially unpredictable. When wind power producers submit their bids on the power market, if the actual delivered energy differs from the committed, other generators must also change their schedule in order to maintain the balance between generation and load. The cost of this re-scheduling must be paid by those that cause it. Since the power produced by wind power depends largely on wind availability which is difficult to predict, the market value of wind energy is reduced by the cost for regulation [23]. This is one of major the issues which makes wind power trading in the power market difficult.

Any deviations from submitted production plan are penalized, thus wind farm owners must find the ways to

minimize imbalance cost trading, to maximize their benefit also [24]. There are probably two main solutions to this problem. The first solution is to improve the existing forecast techniques for wind power production. This has been dealt with in many studies, see for example, [25] and [26]. The second is to find the proper bidding strategies, in the terms of both how and when submit bids to the market operators.

3.2.3. More Competition for Other Conventional Plants

For conventional power plants, they face the competition from "stronger" competitors, in terms of electricity price and the government's policies as mentioned above. In addition, they must adjust their operating schedule to keep balance between supply and demand in power system at all the time. This could, however, bring the additional revenue for those which participate in regulation markets.

3.2.4. Dealing with Existing Market Rules

Normally, there are three time scales for market scheduling and also for bid submitted in power markets: day- and hour-ahead scheduling; intra-hour balancing and regulation [10]. The scales are important for wind power and intermittent resources in general. Both bidding strategy and forecasting technique of wind generators must be based on these scales to reach the highest revenue. Some bidding strategies are introduced in various power markets from the simplest to the complex strategy.

The simplest way the wind generators can do is to submit no advance schedules to the system operator and only show up in real time (or intra-hour). This strategy is suitable with the wind owners have no effective method to forecast future wind output. By this way, wind owners avoid the penalty caused by forecast errors but the energy price normally is not high as they expect.

Another strategy is to submit bids to the system operator an hour ahead of real time [10]. The wind owners implement this strategy to get more benefit from the payment at higher energy prices than in previous case. The payment in this case may include hour-ahead payments (equal to the wind energy scheduled times hour-ahead price), real time hourly payments (equal to the spot price times the difference between the hour-ahead schedule and the actual wind power distribution), any additional intra-hour charges or payments and regulation charges. In practice, when the wind farm dose not schedule hour-ahead, the price drop can be 31%, this is really signification number. But to deal with forecast errors may lead to the penalty cost, they must develop some forecast methods to eliminate the errors as much as possible. In each period, the wind owner should carefully consider and implement a proper strategy to get high benefit.

However, there has a very efficient strategy for wind owner to get highest revenue in the power market while bidding the most probable value or the expected value of the prediction is not always the best strategy. It is the strategy of wind generating companies and hydro generating companies' cooperation [27]. In the operating practice, they may operate together or separately. If they belong to the same owner, who tries to maximize the joint revenue, they easily come to the combined operation. In this case, the hydro plant would cover the wind power deviations in the joint schedules and bids. Although depending on the penalties for over or under production, the energy prices, etc. it normally shows that the increase of the wind power revenue is bigger than the losses of the hydro power in the total payment. In case they belong to the different owners, who may have different objectives, they will meet some difficulties to operate together. However, the high joint benefits and the active policies of market mechanism will help them operate together easier. This cooperation also helps market operators in energy balance and security issues.

4. MEASURES TO OVERCOME THE CHALLENGES

4.1. Better Wind Power Production Forecast

A number of studies have shown the effects of shorter forecast time would result in better performance of wind generators in the market [19], [20], [28]. Usaola [4] suggested that a wind generator must use a short term wind Power prediction program, if it must participate in the market, presenting bids for the next day in order to minimize the penalty cost due to power imbalance and by that way can maximize its revenue sales. The study also concluded that the most accurate prediction is achieved when bids are updated in intraday markets, using more recent predictions.

4.2. Modify Market Rules for More Wind Power

With the penetration of wind energy, the power markets must adjust their structure because the present power markets are designed for trading conventional generation [29]-[31]. Normally, there are types of market clearing [32]. The first one is uniform market clearing. The second one is pay-as-bid market pricing. In both two market clearing mechanisms, there are two possibilities for integration of wind generators in the competitive electricity market. In option one, they will be allowed to bid into the market and take the market clearing price with some premium. Moreover, they must not be charged the output variability penalty as other dispatchable generators are charged for the same. The risk of getting dispatched in the pay-as bid market is more. Due to government's commitments for green energy this option is not suitable. Moreover, wind generators are not competitive without the government subsidies. Another option, which is more appealing, is that the outputs of wind generators can be taken into the system whenever and wherever, they are available. In this condition the market clearing price (MCP) is to be determined to take care of wind generation output and the variability of wind power as well.

In [33], several changes to the current wholesale electricity market structure have been suggested to encourage the existing and future wind development in Alberta, Canada:

- *Dispatchable Capacity:* Sufficient dispatchable capacity must be available on the system to accommodate large scale integration of wind power, particularly during light load periods when generators may be dispatched off-line, dispatched to minimum MW levels or when the pool price is at zero dollars. Policies or rules may be required to deal with merit order dispatch as a result of wind power ramping that would cause a generator with a long start-up time to be dispatched off.
- *Energy Market Ramp Rate:* Dispatchable generators can provide ramp rate characteristics with their offers and provide certainty of energy market ramp rate capability. The AESO is currently looking at more effective means for generators to provide ramp characteristics in their offers.

- *Biased Operation of Regulating Reserves:* Biased operation of Reserve Regulation (RR) services would reduce the amount of additional reserve regulation. As this would represent a significant change in operation, this matter requires further discussion with industry.
- *New market product, Load or Wind Following:* The studies modeled the behavior of RR, however it is possible that a new product could provide some of the same functionality while not providing all technical aspects of RR such as governor response. Such a new product could create an opportunity for participation by different types of loads or generation technologies.

The electricity market in New York managed by New York Independent System Operator (NYISO) is also expected to modify its rules and structure to allow for about 2800 MW of wind power in the next ten years [6]. Relevant markets are the (i) capacity markets, (ii) day-ahead markets, (iii) real-time or balancing market. No special rules are required for wind power in day-ahead and real-time market.

However, in the capacity market, some modifications to the existing rules are required. Recognizing the apparent mismatch between the time when wind power is most likely available and when electricity is most in demand, three fundamental questions must be asked: (i) should wind resources be allowed to participate in capacity markets where they exist; if so, (ii) how should the capacity be determined, and (iii) what are the obligations of the wind resources? One possible solution to this problem was to allow participation of wind generators in the capacity market but to limit that capacity to the average of that actually measured during selected peak hours. The sale of capacity in New York requires the generator to participate in a day-ahead energy market. This rule seems unduly burdensome to wind resources that, because of the inherent uncertainty of wind forecasts, risk entering into a day-ahead obligation that cannot be satisfied in real-time. The NYISO is exploring the elimination of this requirement for wind generators. Instead, a day-ahead forecast of wind generator output would be used to insure the reliability of the system for the next day, but the wind generator need not take on a day-ahead obligation.

4.3. Modify Market Structure to Accommodate More Wind

Market design can have a strong influence on new, renewable, intermittent production forms like wind power. Holttinen [3] suggested a more flexible market, allowing the bids for wind power to be updated 6–12 hours before, would reduce the regulation costs by 30% and increase the net income by 4% from 20.1 to 20.9 Euro/MWh. An hourly operation, using persistence estimation from 2hours before, would reduce the regulation costs for nearly 70% and increase the net income by 8% to 21.8 Eur/MWh. The study also suggested there is no technical barrier in making the electricity market more flexible that is, shortening the time between the clearing of the market and the delivery. With more flexible mechanisms than what is in use today, *i.e.* 24 hours ahead, there is the possibility to ease the integration of wind power to the system.

A well working after sales market could help both wind power producers and the system operator, in reducing the amount and cost of wind power at the regulating market. However, looking from the power system point of view, only the net imbalance has to be dealt with, so unnecessary trading back and forth for individual producers is not the optimal solution.

4.4. Penalty or Not-Penalty for Wind Generators

The reliable and efficient operation of the power system and the electricity markets depends on the good behavior of generators. Dispatchable generators must follow the dispatch signals of the ISO, self-scheduled generators must notify the ISO of their intended schedule and follow that schedule. Deviations from expected output have a detrimental impact on energy clearing prices. Some markets, such as the NYISO [6], impose penalties on generators who do not follow their schedule within a tolerance. Excessive under-generation is penalized while excessive over-generation is uncompensated. The application of behavioral penalties to generators that have no control of behavior is not productive however. The NYISO has eliminated penalties on classes of generators that have limited control of their output and is currently pursuing the elimination of these penalties on wind generators as well. If we come back to the issues of imbalance cost in the case of Nordic markets, should the imbalance cost due to forecast errors of the wind generators be lift off as well?

While it may be inappropriate to penalize a generator for behavior beyond its control, if that behavior has a quantifiable cost, it is entirely appropriate to assign that cost to the generator. In the case of wind generators there will be a cost associated with the necessary forecasting functions and wind generators will be expected to contribute, at least in part, to this cost. The variability of wind generators may increase the need for regulation and frequency control service.

5. CONCLUSIONS

One may see actual construction of more and more wind farms in the world today, but one may not realize the challenges involved with the integration of wind power generation into the power systems and the electricity markets. The challenges are in the form of technical requirement for integration to power systems to those related to wind power production forecast and the way the electricity market functions today. The degrees of those issues discussed are of course dependent on the penetration level of wind power in the power systems and power markets in different countries. In this paper, we have also reviewed some of the practical solutions for those problems. One obvious observation is that wind power producers could be better off in the market place where they can submit bids in shorter time frame, as suggested by some studies. We could see that it is not infeasible to do so, at least from the technical point of view. This paper is intended to serve as a background for those who would seriously like to do research work in wind power and its integration in the power market. The list of references provided in the paper is, however, in no way complete.

If we can make some forecast, we have seen that wind energy has come a long way in the last ten years, and it will continue to advance over the next ten years. Costs will come down, and turbine technologies will become more capable and more reliable, the markets will be more wind-friendly so that wind power will have a rather "fair" competition to other type of generation technologies.

REFERENCES

[1] Global Wind Energy Council. "Global wind energy markets continue to boom - 2006 another record year", 02/2007.

[2] Global Wind Energy Council. "The Global Wind Energy Report", 2006.

[3] H. Holttinen, "Optimal electricity market for wind power," *Energy Policy*, Vol. 33, No. 16, pp. 2052–2063, Nov. 2004.

[4] J. Usaola, J. Angarita, "Bidding wind energy under uncertainty", International Conference on Clean Electrical Power, 21-23 May 2007 Page(s):754 – 759.

[5] AESO, "Wind Integration Impact Studies, Phase 2, Assessing the impacts of increased wind power on AIES operations and mitigating measures", Revision 2, July 18, 2006.

[6] R. W. de Mello, "Modifying Market Rules to Accommodate High Penetrations of Wind Energy", IEEE Power Systems Conference and Exposition, Oct. 29 2006-Nov. 1 2006, Page(s):223 – 228.

[7] Swedish Energy Agency, "Renewable electricity through electricity certificates", ET2006. Available online at: http://www.energimyndigheten.se/

[8] Mark Disendorf, WWind power in Australia", *International Journal of Environmental Studies*, Vol. 63, No. 6, December 2006, 765–776.

[9] American Wind Energy Association. "The economics of wind energy", 2005.

[10] Eric Hirst, "Interactions of Wind Farm with Bulk-power Operation and Markets". Project for Sustainable FERC Energy Policy, September 2001.

[11] European Transmission Systems Operators, "European Wind Integration Study (EWIS) Towards a Successful Integration of Wind Power into European Electricity Grids", Final-Report *2007-01-15*.

[12] J. O. Tande, "Impact of integrating wind power in the Norwegian power system". SINTEF Energy Research, April 2006.

[13] L. Söder, "The Value of Wind Power", in Wind Power in Power System, Edited by Thomas Eckermann, John Wiley & Sons, 2005.

[14] Danish Energy Authority, "Copenhagen Strategy on Offshore Wind Power Development", European Policy Seminar on Offshore Wind Power, 10/2005.

[15] P.B. Eriksen, T. Ackermann, H. Abildgaard, P. Smith, W. Winter, J.R. García. "System Operation with High Wind Penetration". *IEEE Power and Energy Magazine*, Volume 3, Issue 6, Nov.-Dec. 2005 Page(s): 65 – 74.

[16] J.D. Rose, I. A. Hisken. "Challenges of integrating large amounts of wind Power", 1st Annual IEEE Systems Conference, Hawaii, USA April 9-12, 2007.

[17] H. Bindner, P. Lundsager, "Integration of wind power in the power system", IEEE 2002 28th Annual Conference of the Industrial Electronics Society (IECON 02), Volume 4, 5-8 Nov. 2002, Page(s): 3309 – 3316.

[18] G.N Bathurst, G. Strbac "Trading Wind Generation in Short Term Energy Markets", *IEEE Trans on Power Systems*, Vol. 17, No. 3, 2002.

[19] J. Usaola, et al. "Benefits for wind energy in electricity markets from using short term wind power prediction tools; a simulation study". *Wind Engineering*, Vol. 28, No. 1, 2004.

[20] A. Fabbri, T. Gómez, J. Rivier, V. Méndez "Assessment of the Cost Associated With Wind Generation Prediction Errors in a Liberalized Electricity Market". *IEEE Trans on Power Systems*, Vol. 20, No. 3, 2005.

[21] J. Usaola, J. Angarita "Benefits of short term wind power prediction programs for the integration of wind energy in electricity markets", EWEC 2006. Athens 2006.

[22] G. Strbac, A. Shakoor, M. Black, D. Pudjianto, T. Bopp, "Impacts of Wind Generation on the Operation and Development of the UK Electricity Systems", *Electric Power Systems Research*, Vol. 77 (2007), pp. 1214-1227.

[23] L. H. Nielsen, et al., "Wind power and a liberalised North European electricity exchange," in Proceeding of European Wind Energy Conference (EWEC'99), Nice, France, Mar. 1999, pp. 379–382.

[24] J. Matevosyan, L. Söder, "Minimization of Imbalance Cost Trading Wind Power on the Short-Term Power Market". *IEEE Transactions on Power Systems*, Vol. 21, No. 3, August 2006.

[25] S.M.M. Tafreshi, D. Panahi, "One-hour-ahead Forecasting of Wind Turbine Power Generation Using Artificial Neural Networks", IEWT 2007 (Internationale Energiewirtschaftstagung, an der TU Wien, 14–16 February 2007), available online: http://eeg.tuwien.ac.at/events/iewt/iewt2007/html/poster.html.

[26] A. Fabbri, T. Gómez, J. Rivier, V. Méndez "Assessment of the Cost Associated With Wind Generation Prediction Errors in a Liberalized Electricity Market". *IEEE Trans on Power Systems*, Vol. 20, No. 3, 2005.

[27] J. M. Angarita, J. G. Usaola, "Combining hydro-generation and wind energy-Biddings and operation on electricity spot markets", *Electric Power Systems Research*, Vol. 77 (2007), pp. 393–400.

[28] P. Pinson, C. Chevalier, G. Kariniotakis "Optimizing benefits from wind power participation in electricity markets using advanced tools for wind power forecasting and uncertainty assessment". Proc. of EWEC 2004. London 2004.

[29] J.C. Smith, E.A. DeMeo, B. Parsons, M. Milligan. "Wind Power Impacts on Electric Power System Operating Costs". American Wind Energy Association Global Wind Power Conference March 28-31, 2004, Chicago, Illinois.

[30] H. Holttinen, "The Impact of Large Scale Wind Power Production on the Nordic Electricity System", VTT Publications 554, 2004 (PhD Thesis).

[31] G.N. Bathurst, J. Weatherill, and G. Strbac, "Trading Wind Generation in Short Term Energy Markets". *IEEE Transaction on Power System*, Vol.17, No.3, August 2002.

[32] S. N. Singh, I. Erlich, "Wind Power Trading Options in Competitive Electricity Market", IEEE Power Engineering Society General Meeting, 18-22 June 2006, Page(s):7 pp.

[33] J. Kehler, M. Hu, D. McCrank, "Market Evolution to Accommodate High Wind Power Penetration", 2006 IEEE PES Power Systems Conference and Exposition, Oct. 29 2006-Nov. 1 2006, page(s): 229 – 231.

Design aspects for a fullbridge converter thought for an application in a DC-based wind farm

Lena Max
Chalmers University of Technology, Dept. of Energy and Environment, 412 96 Göteborg, Sweden
tlf. +46 31 7721630, e-mail lena.max@chalmers.se

Abstract — In this paper, design aspects for the fullbridge converter are investigated for the application in a DC-based wind farm. Included in the design is the choice of semiconductor devices and core material of the transformer as well as the chosen switching frequency. The investigated converter is the DC/DC converter for a single wind turbine. It is found that the losses increase with the switching frequency above approximately 1 kHz. Therefore, 1 kHz is chosen as a suitable switching frequency. Using a transformer core made of laminated steel instead of an iron alloy leads to higher losses, especially at lower switching frequencies. Regarding the two IGBT modules, there is no significant difference in the losses. It is also shown that the used analytical method for loss calculations agree well with the losses calculated using results from simulations.

Index Terms — DC wind farm, DC/DC converters, loss calculations.

1. Introduction

The high-power DC/DC converter is a key component for the realization of a DC-based wind farm and will basically have the same function in a DC wind farm as the AC transformer has in the existing AC wind farms of today. An important condition for these DC-based wind farms is that the cost and the losses of the DC/DC converters are not too high. In previous investigations about DC/DC converters in DC-based wind farms, it was found that the fullbridge converter is a suitable choice for this application [2][3]. However, the comparison was based on as identical design conditions as possible for all investigated topologies.

The purpose of this paper is to further investigate the design of the fullbridge DC/DC converter for the application in a DC-based wind farm. The choice of semiconductor components is to be investigated as well as the design of the transformer, including the core material. Also, the switching frequency of the converter is to be investigated. The losses are obtained as an average of the expected operating conditions in a wind farm, and the choice of design is investigated for these operating conditions. Moreover, another goal is to obtain a simplified analytical model for calculating the converter losses.

2. Operating conditions for the converters

For investigating the DC/DC converters for the specific application in a DC-based wind farm, the operating conditions for the converters must be defined. Therefore, a local wind turbine grid with five wind turbines shown in Figure 1 is used to obtain the operating conditions for the converters in the wind turbines [2][3].

Depending on the generator and rectifier in the turbine and also the voltage level for the internal grid, there are three different operating conditions, named positions 1a, 2a and 3a, for the converters in the wind turbines. As seen in the figure, the input voltage to the first DC/DC converter can either be varying with the wind speed between 2 and 5 kV or be constant at 5 kV. This depends on the electrical system in the wind turbine where a diode rectifier gives a varying output voltage while an IGBT rectifier gives a constant output voltage [2][3].

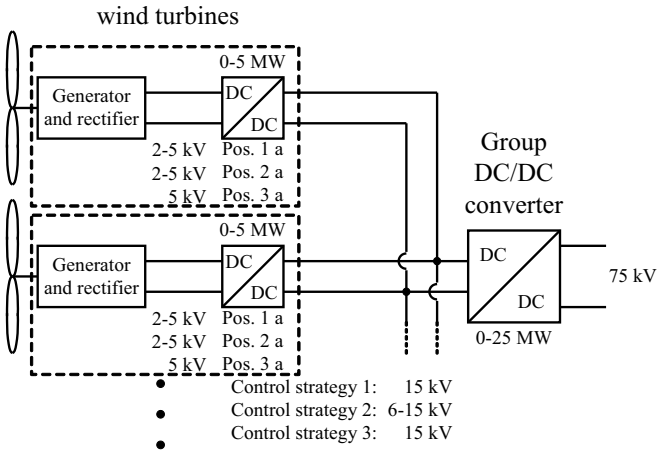

Figure 1. Local wind turbine grid with voltage levels.

The control strategies, that are further explained in [2][3], will in different ways achieve a constant voltage level as output from the group converter. For the first control strategy, the voltage variations are compensated in the wind turbine converter. The second control strategy has basically a fixed voltage ratio for the wind turbine converter and the varying output voltage from the wind turbine converter is compensated for in the group converter. For the third control strategy, the IGBT rectifier gives a constant input voltage to the wind turbine converter and all voltage levels are therefore constant in the local wind turbine grid. Consequently, there are different demands for the converters depending on the control strategy.

3. Control methods for the converters

For the fullbridge converter with a current stiff output, shown in Figure 2 and described in detail in [2], two different control methods are considered, the phase shift control and the duty cycle control.

Using the duty cycle control, the off-state is achieved by turning all switches off and the output current is freewheeling in the output bridge. Consequently, there is no current neither in the transformer nor in the input bridge during the off-state. For this control method, there are no snubber circuits across the transistors in the input bridge and

therefore the turn-off losses can be large, and there can also be oscillations in the input bridge during the off-state.

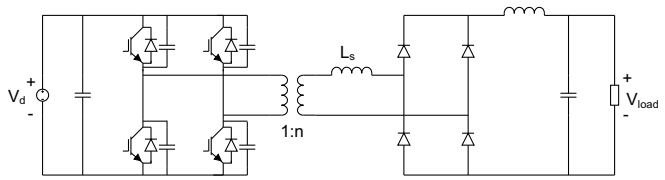

Figure 2. Topology for the fullbridge converter with phase shift control.

The turn-off losses for the transistors can be reduced by connecting snubber capacitors across the transistors and control the converter with phase-shift control as described in [4][5][6]. One transistor and one diode are conducting in the input bridge during the off-state, providing the possibility of soft-switching for the transistors. The switching losses will be reduced but the control of the input bridge will be more complicated. However, as shown in [2], the lagging leg will be hard-switched since the energy stored in the leakage inductance is not enough to achieve soft-switching of the transistors.

4. ANALYTICAL LOSS CALCULATIONS

In previous investigations, the fullbridge converter has been found to be a suitable choice for the wind farm application providing low losses and low contribution to the energy production cost as well as simple design and control [2][3]. These results are based on loss calculations and also an estimation of the contribution to the energy production cost. The losses are calculated using simulated current and voltage waveforms for the converters at each operating point with ideal components. For the predetermined operating conditions, the losses are calculated using known data for the components.

However, these loss calculations are time consuming. First the current and voltage waveforms must be obtained for each wind speed from 4 m/s to 12 m/s. Knowing the operating conditions, the losses can be calculated using known loss data for the components. Since there are three different operating conditions, the number of simulations that needs to be done is increasing. Further, if a number of different switching frequencies should be considered for each converter at each operating point as well as two different control methods for the converters, a large number of simulations are needed.

In order to investigate a large number of operating conditions, analytical loss calculations are preferred since no simulation is needed and all loss calculations for one position can be done with the same calculation file. In this section, the analytical loss calculations will be described and the resulting losses will be compared to the original method for the loss calculations.

4.1. Loss calculations

The analytical loss calculations are based on a simplified model where ideal voltage and current waveforms are assumed in order to achieve the conditions for the semiconductor components and the transformer that are needed for the loss calculations. From the operating conditions, the losses are calculated in the same way as described in [2][3]. In order to simplify the calculations, a number of assumptions are made for the converter. In general, the on-state current is assumed to be constant for all devices due to the current-stiff output. Also, the losses are neglected when calculating the input and output currents.

The input variables needed for the loss calculations are the input voltage V_{in}, the output voltage V_{out}, the input power P_{in}, the transformer ratio n_T and the switching frequency f_s. Also, the data for the transformer design and the number of semiconductor modules must be known.

Knowing the power and the voltage levels, the output current i_{out} is calculated as

$$i_{out} = P_{in} / V_{out}\,, \tag{1}$$

the input current i_{in} is calculated as

$$i_{in} = i_{out} n_T\,, \tag{2}$$

and the duty cycle D is calculated as

$$D = V_{out} / (V_{in} n_T)\,. \tag{3}$$

When calculating the semiconductor switching losses, the voltage $V_{mod,IGBT}$ and current $i_{mod,IGBT}$ for a single IGBT module are used in the calculations. Using the known data for the IGBT module, the energy E_s dissipated during one turn-off is then calculated as

$$E_s = E_{SR} \frac{V_{\mathrm{mod},IGBT}}{V_{ref}} \frac{i_{\mathrm{mod},IGBT}}{i_{ref}}\,, \tag{4}$$

where E_{SR} is the switching energy at voltage V_{ref} and current i_{ref}. The power losses P_{off} resulting from the turn-off losses are calculated as

$$P_{off} = 4 E_s n_s n_p f_s\,, \tag{5}$$

where n_s is the number of IGBT modules connected in series and n_p is the number of IGBT modules connected in parallel in each switch. The diode switching losses are calculated in the same way as shown in [2].

For calculating the conduction losses for the semiconductor components, the currents in one module, $i_{mod,IGBT}$ in the IGBT module and $i_{mod,diode}$ in the diode module are used. The instantaneous power losses for one module, p_{FC} for the output diode, p_{IC} for the IGBT module and p_{ICd} for the IGBT freewheeling diode are then calculated as a function of the currents i_m ($i_{mod,IGBT}$ for the IGBT and $i_{mod,diode}$ for the diode) for one module as

$$p_{FC}(i_m) = V_F i_m = A_F i_m + B_F i^2{}_m + C_F i^3{}_m\,, \tag{6}$$

$$p_{IC}(i_m) = V_{CE} i_m = A_{CE} i_m + B_{CE} i^2{}_m + C_{CE} i^3{}_m \tag{7}$$

and

$$p_{ICd}(i_m) = V_{CE} i_m = A_{CEd} i_m + B_{CEd} i^2{}_m + C_{CEd} i^3{}_m \tag{8}$$

where the values for the constants A_F, B_F, C_F, A_{CE}, B_{CE}, C_{CE}, A_{CEd}, B_{CEd} and C_{CEd} can be obtained from the data sheet for

the diode and the IGBT components.

Regarding the conduction losses, these losses differ depending on the control method used for the converter. For the converter that is controlled by duty cycle control, two diodes are conducting the whole load current during the on-state. At the off-state, the current is freewheeling in the output bridge and the four diodes have half the load current each. The total conduction losses for the output diodes can then be calculated as

$$P_{FC1} = 2Dp_{FC}(i_m)n_{p,o}n_{s,o} + 4(1-D)p_{FC}(i_m/2)n_{p,o}n_{s,o}. \quad (9)$$

Since the IGBT modules are just conducting during the on-state, the total conduction losses P_{IC1} for the IGBT modules are calculated as

$$P_{IC1} = 2Dp_{IC}(i_m)n_{p,in}n_{s,in}. \quad (10)$$

The conduction losses in the freewheeling diodes are assumed to be small.

Using the phase shift control, the transformer carries the total on-state current during the whole duty cycle. This results in that two diodes in the output bridge conduct during the whole duty cycle. The conduction losses P_{FC2} for the diodes in the output bridge are therefore calculated as

$$P_{FC2} = 2p_{FC}(i_m)n_{p,o}n_{s,o}. \quad (11)$$

For the IGBT modules, two IGBT switches are conducting during the on-state while one IGBT switch and one freewheeling diode are conducting during the off-state. Due to this, the losses P_{IC2} in the IGBT modules are

$$P_{IC2} = 2Dp_{IC}(i_m)n_{p,in}n_{s,in} + (1-D)p_{IC}(i_m)n_{p,in}n_{s,in}. \quad (12)$$

Since one of the diodes is conducting at the off-state, the losses in the freewheeling diodes P_{ICd2} can be calculated as

$$P_{ICd2} = (1-D)p_{IC}(i_m)n_{p,in}n_{s,in}. \quad (13)$$

The losses in the transformer consist of both the losses in the windings and the losses in the core material. The losses in the windings differ between the control methods while the core losses are basically the same since the voltage applied at the transformer is the same for both control methods. The losses in the windings are calculated using the resistance in the windings. For the duty cycle control, there is just current in the windings during the on-state and the losses P_{w1} in the windings can therefore be calculated as

$$P_{w1} = D(R_{prim}i_{in}^2 + R_{sec}i_{out}^2), \quad (14)$$

where R_{prim} and R_{sec} are the resistances in the primary and the secondary windings. Using the phase shift control, there is a current in the windings during the on-state as well as the off-state and the losses P_{w2} in the windings can then be calculated as

$$P_{w2} = R_{prim}i_{in}^2 + R_{sec}i_{out}^2. \quad (15)$$

To calculate the core losses, that are similar for both control methods, the peak magnetic field B_{max} in the core is calculated as

$$B_{max} = V_{in}\frac{D}{2f_s}\frac{1}{2N_{prim}A_{core}}, \quad (16)$$

where N_{prim} is the number of primary turns and A_{core} is the area of the core. The core losses are then calculated as

$$P_{core} = K_1 f_s^{K_2} B_{max}^{K_3} V_{core}, \quad (17)$$

using the constants shown in Table 1.

Table 1. Values for the transformer constants.

Core	K_1	K_2	K_3
Steel	298	1.19	1.65
Metglas®	46.7	1.51	1.74

4.2. Comparison of the calculation methods

The resulting losses for the converters are shown in Figure 3 for position 1a, in Figure 4 for position 2a and in Figure 5 for position 3a. Here, the losses are compared between the calculations that use the simulation results and the analytical calculations for both (a) duty cycle control and (b) phase shift control.

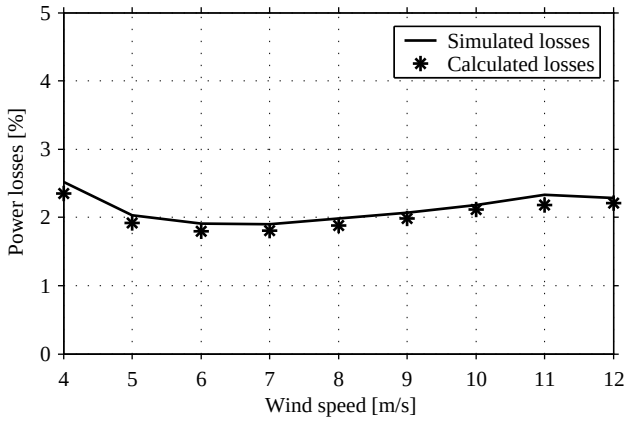

(a) Duty cycle control.

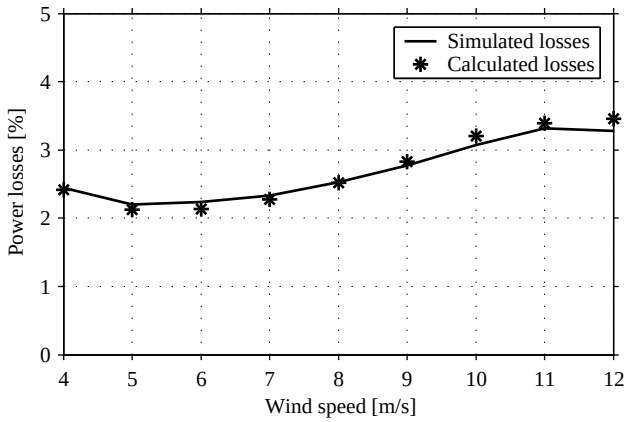

(b) Phase shift control.

Figure 3. Resulting losses from calculations and simulations for position 1a.

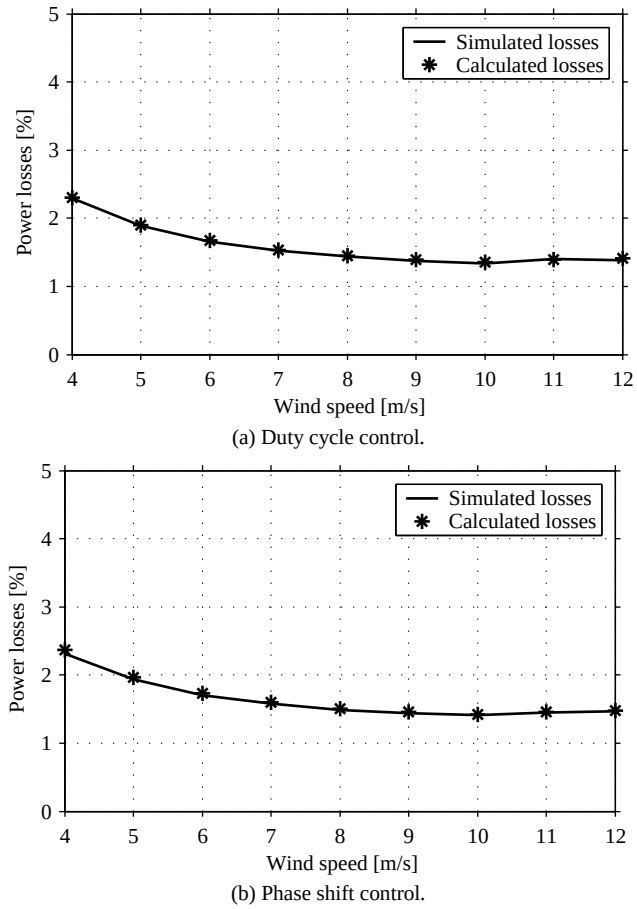

Figure 4. Resulting losses from calculations and simulations for position 2a.

Also, it should be noted that the output power from a wind turbine varies with the wind speed as shown in Figure 6.

From the figures, it can be seen that the results from the analytical calculations agree with the results from the simulations. The only visible deviation is for position 1a for both the duty cycle control and the phase shift control. For this control method, the duty cycle varies for the different operating points and the design of the filter will then affect the ripple in the current and also the resulting turn-off losses and conduction losses. In the analytical calculations, an ideal filter is assumed while there is a ripple in the output current in the simulations. This can cause deviations in the resulting losses as seen in Figure 3. For positions 2a and 3a that have almost full duty cycle for all operating points, the losses agree very well.

Comparing the duty cycle control with the phase shift control, it can be seen that the losses are the same for positions 2a and 3a while the duty cycle control has lower losses at high wind speeds for position 1a. This is due to the low duty cycle at high wind speeds for position 1a. Since the duty cycle control has lower conduction losses at the off state (the load current is freewheeling in the output bridge), the overall losses are clearly lower at a low duty cycle.

5. INVESTIGATION OF THE DESIGN ASPECTS

For investigating different design aspects, the losses are calculated for different switching frequencies and IGBT modules. Further, the choice of core material to the transformer is considered. The losses are presented as average losses for the average value of the wind speed 7.2 m/s, which is considered as a medium wind speed site.

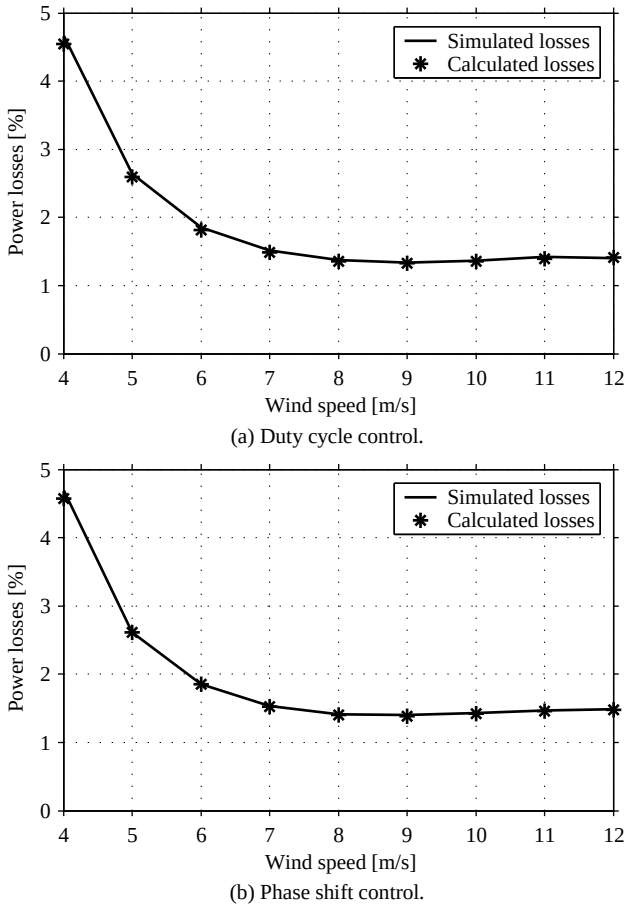

Figure 5. Resulting losses from calculations and simulations for position 3a.

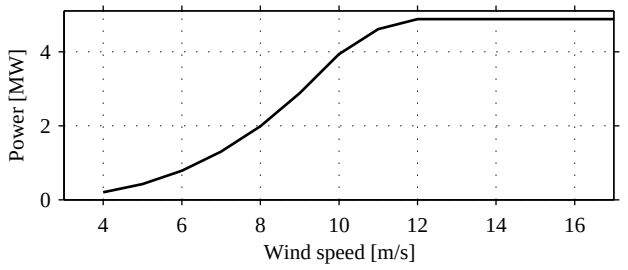

Figure 6. Output power as a function of the wind speed.

5.1. Choice of IGBT modules and switching frequency

For the semiconductor components, the IGBT modules in the input bridge are to be investigated. For the choice of IGBT modules, either the StakPak™ module 5SNR 20H2500, denoted IGBT module 1, with ratings 2500 V and of 2000 A from ABB or the FF200R33KF2C IGBT module, denoted IGBT module 2, rated 3300 V and 200 A from Eupec is to be chosen. Since the current rating of the Eupec module is 200 A, IGBT module 2 is assumed to consist of 10 parallel connected modules giving a current rating of 2000 A. There are some differences between the loss characteristics of these components. IGBT module 1 has lower conduction losses than IGBT module 2, but has on the other hand higher switching losses. A comparison of the two IGBT modules is found in Table 2.

Table 2. Comparison between the IGBT modules.

Value	IGBT module 1	IGBT module 2
$V_{CE,max}$	2.5 kV	3.3 kV
$I_{C,max}$	2 kA	2 kA
E_{on}, 1.25 kV, 2 kA	4.0 J	2.53 J
E_{off}, 1.25 kV, 2 kA	3.6 J	1.77 J
P_c, 2 kA	4.4 kW	8 kW
P_c, 1 kA	1.8 kW	3 kW

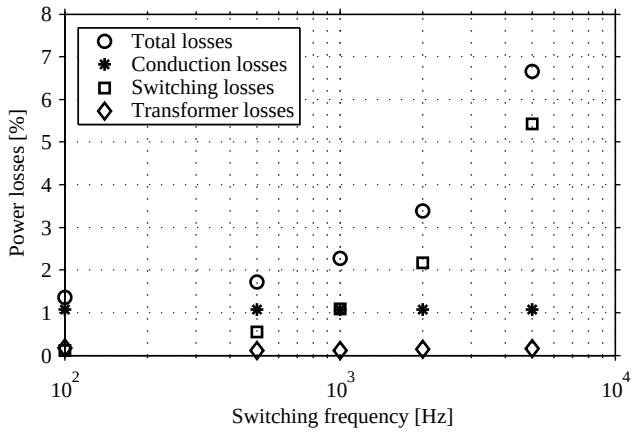

(a) Position 1a.

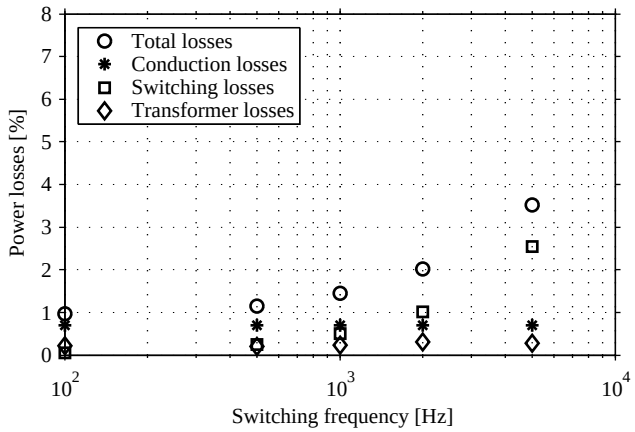

(a) Position 2a.

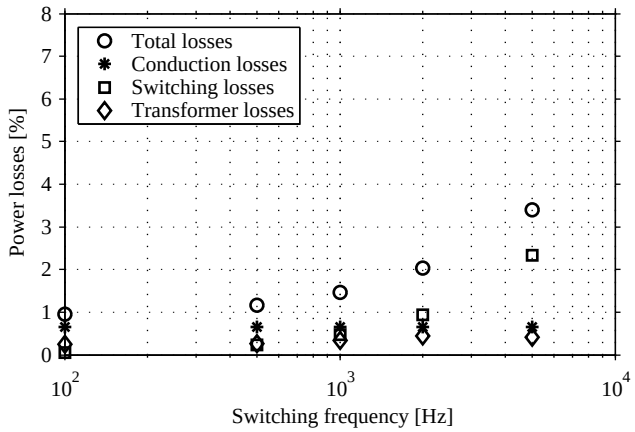

(c) Position 3a.

Figure 7. Loss distribution for IGBT module 1 using duty cycle control at the average wind speed 7.2 m/s.

In the investigations, the losses are calculated using both IGBT modules, and the resulting losses are then compared for the different operating conditions. Also, different switching frequencies are used and the influence on the losses of the semiconductor components is shown.

Knowing that the losses can be accurately calculated using the analytical method, this method is used to obtain the losses as a function of the switching frequency and the choice of IGBT module. The losses are calculated as a function of the switching frequency for both IGBT modules. The average losses at the average wind speed 7.2 m/s are shown in Figure 7 for IGBT module 1 and in Figure 8 for IGBT module 2. A comparison of these modules is made in Figure 9. The core material used for the transformer is a Metglas® POWERLITE® core that is an alloy of steel, boron and silicon.

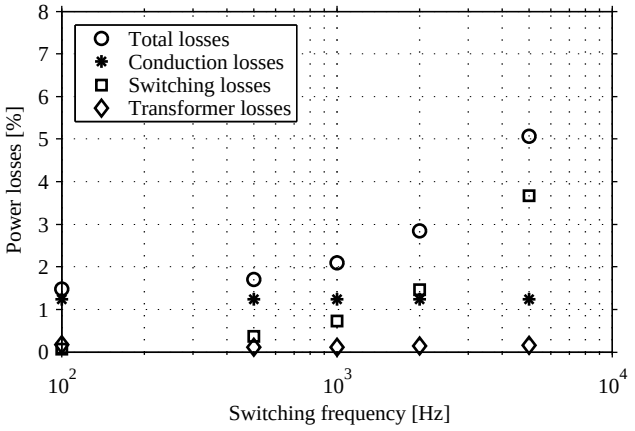

(a) Position 1a.

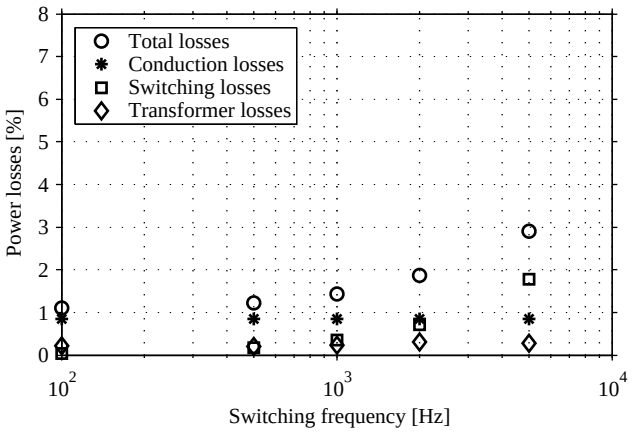

(b) Position 2a.

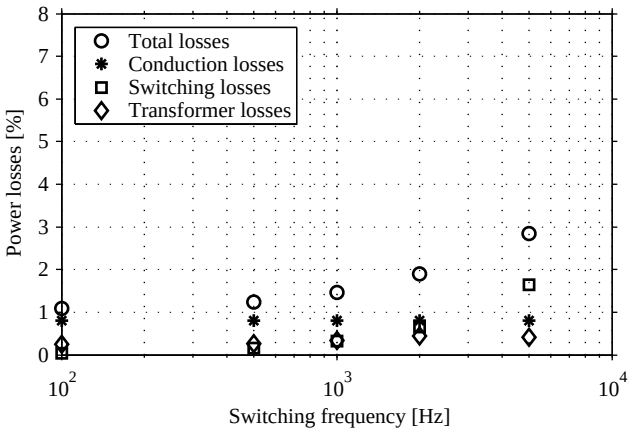

(c) Position 3a.

Figure 8. Loss distribution for IGBT module 2 using duty cycle control at the average wind speed 7.2m/s.

In Figure 7 and Figure 8, it can be seen that the conduction losses are the dominating losses up to a switching frequency of about 1 kHz. At higher switching frequencies, the switching losses increase and become larger than the conduction losses. As a result of this, the total losses are almost constant to about 600 Hz and start to increase significantly above 1 kHz.

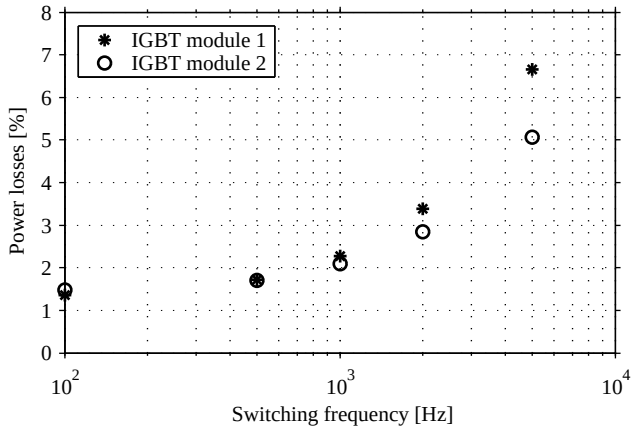

(a) Position 1a.

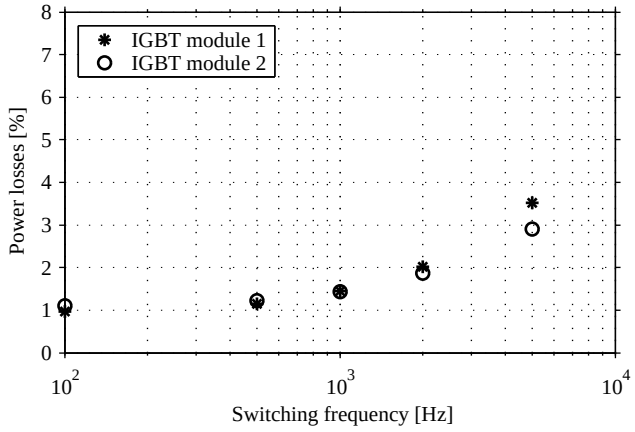

(b) Position 2a.

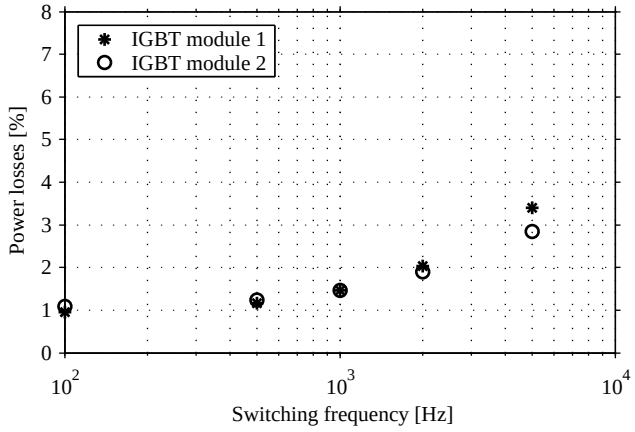

(c) Position 3a.

Figure 9. Loss comparison for the IGBT modules using duty cycle control at the average wind speed 7.2 m/s.

The benefits with a high switching frequency are that the transformer can be made smaller and also the filters can be reduced. However, this should not be made at the expense of drastically increased losses. Considering the resulting losses, a switching frequency of 1 kHz gives a high switching frequency but still acceptable losses. There are also some differences between the different positions in the local wind turbine grid. For position 1a, the losses increase more with increasing switching frequency and the switching frequency that gives the lowest total cost will then be lower for this position than for positions 2a and 3a.

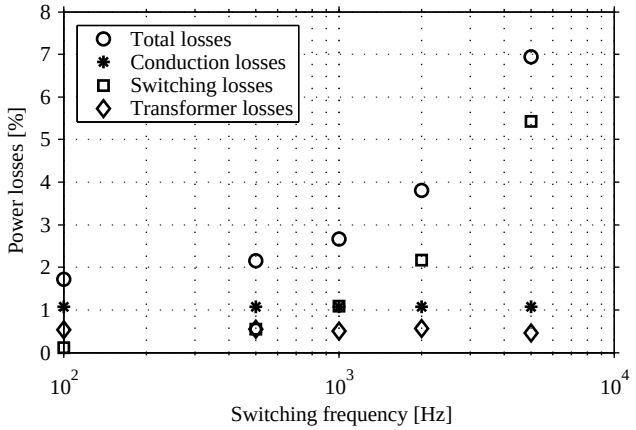

(a) Position 1a.

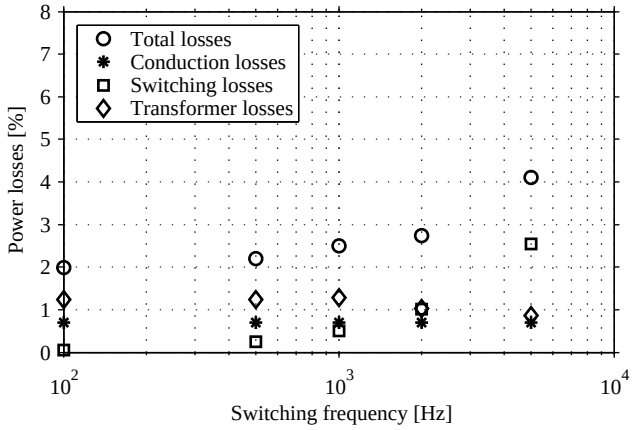

(b) Position 2a.

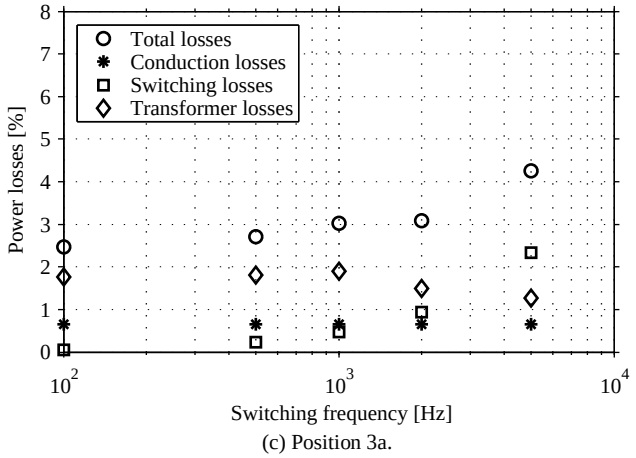

(c) Position 3a.

Figure 10. Loss distribution for IGBT module 1 using duty cycle control at the average wind speed 7.2 m/s using the steel core.

Moreover, Figure 9 shows the losses using the two different IGBT modules. As noted earlier, IGBT module 1 has lower conduction losses and higher switching losses. This results in that IGBT module 1 gives lower losses at low switching frequencies while IGBT module 2 gives lower losses at high switching frequencies. However, at the desired operating frequency 1 kHz, both modules gives similar losses. A suitable switching frequency would be as high

switching frequency as possible without a significant increase in the losses. For position 1a, the losses start to increase significantly above 600 Hz, while positions 2a and 3a have increased losses above 1 kHz.

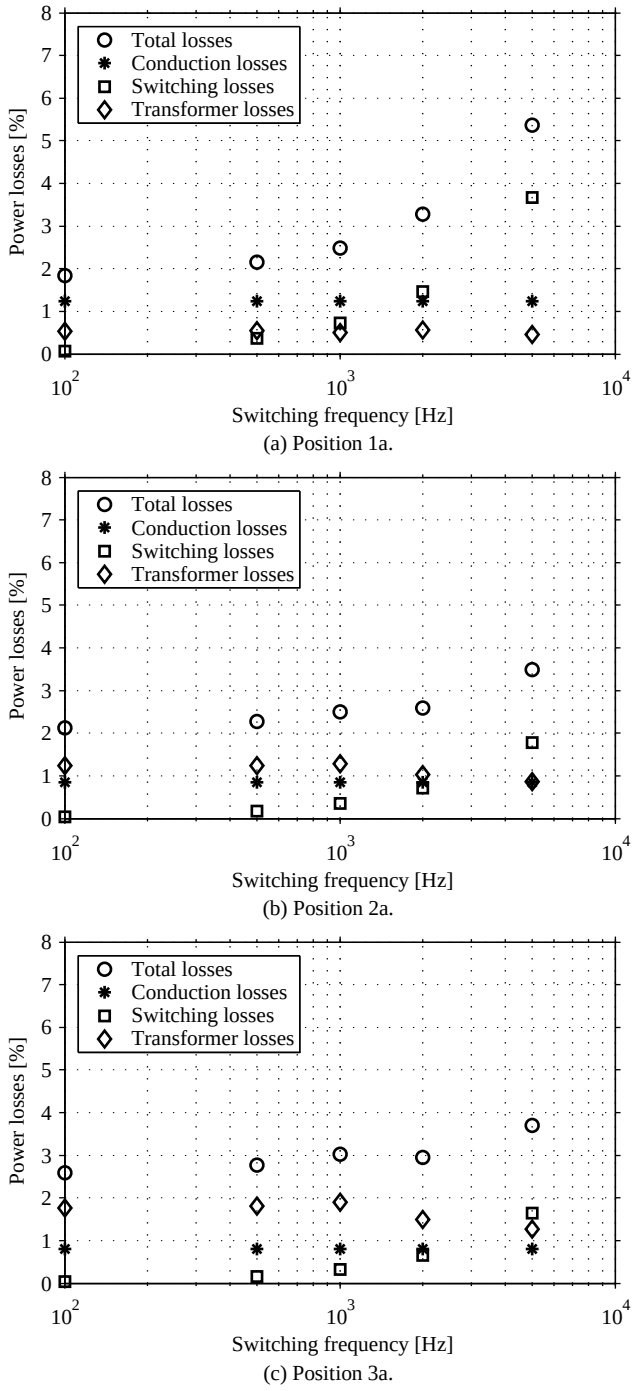

Figure 11. Loss distribution for IGBT module 2 using duty cycle control at the average wind speed 7.2 m/s using the steel core.

5.2. Transformer design

For the transformer, two different core materials are considered. The first material is laminated steel NO12 with a thickness of 0.12 mm, and the second material is the Metglas® POWERLITE® core. The resulting losses will be calculated as in [7] using both core materials. Finally, the effect of a changing switching frequency on the losses of the transformer is investigated.

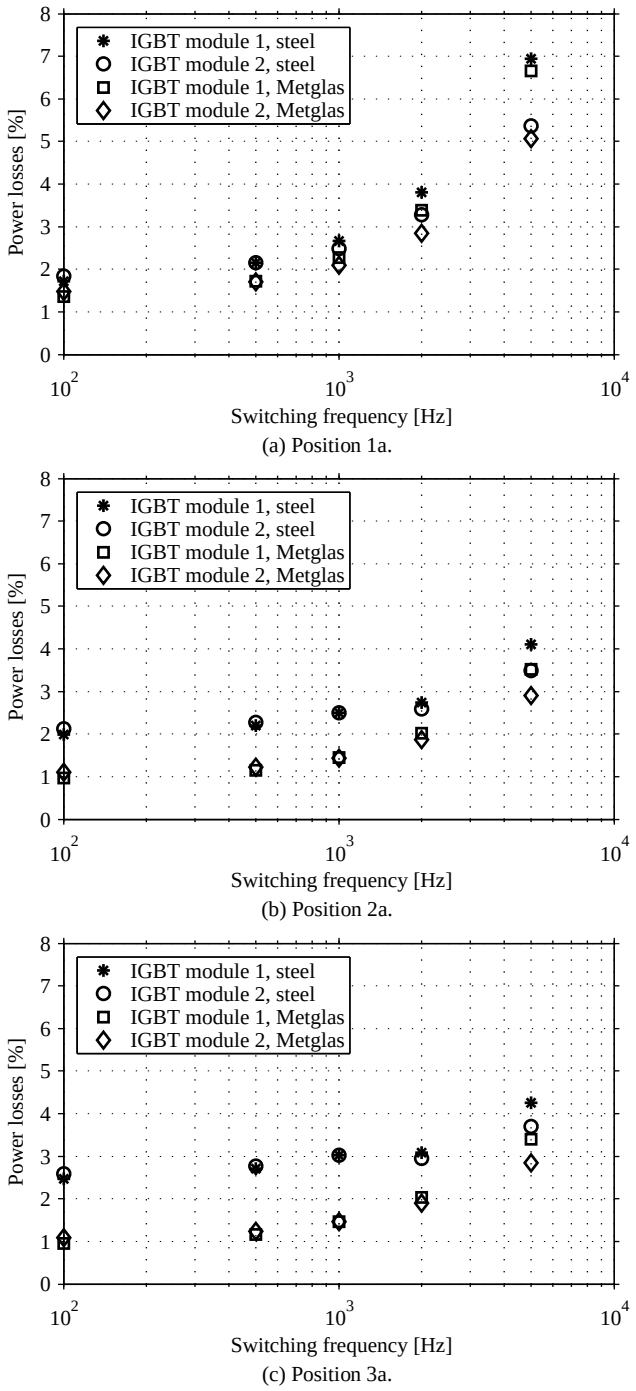

Figure 12. Loss comparison for the IGBT modules using duty cycle control at the average wind speed 7.2 m/s using the steel core compared to the losses using the Metglas® core.

In Figure 7 and Figure 8, the resulting losses are shown for a transformer with a Metglas® POWERLITE® core. Using the steel core for the transformer, the resulting losses are shown in Figure 10 for IGBT module 1 and in Figure 11 for IGBT module 2. Also, a comparison of these modules is made in Figure 12.

For the steel core, the high core losses at low switching frequencies make the total losses for the converter differ from when the Metglas® core is used. For position 1a, the characteristics are similar as for the Metglas® core since the core losses are relatively small as seen in Figure 12 (a). However, for position 2a and especially position 3a, the core

losses increase drastically at low wind speeds and therefore the total losses start to increase at the switching frequency 1.5 kHz for position 2a and at about 2 kHz for position 3a. Consequently, a switching frequency of about 1 kHz will be suitable for the converter using the steel core as well as the converter using the Metglas® core.

In the comparison of the losses between the converter with the steel core and the converter with the Metglas® core in Figure 12, it can be seen that the steel core results in higher losses than the Metglas® core. This increase in losses will also result in an increase in the contribution to the energy production cost from the converter. In Figure 13, the increase in contribution to the energy production cost is shown if the Metglas® core in the transformer is replaced with a steel core. As seen in Figure 12, the steel core gives larger increase in the losses for positions 2a and 3a and consequently these positions also suffer from a large increase in the contribution to the energy production cost when the steel core is used. For positions 2a and 3a, the duty cycle is at maximum at all operating conditions which give high core losses. For position 1a, the duty cycle is lower at high wind speeds and the core losses will therefore also be lower.

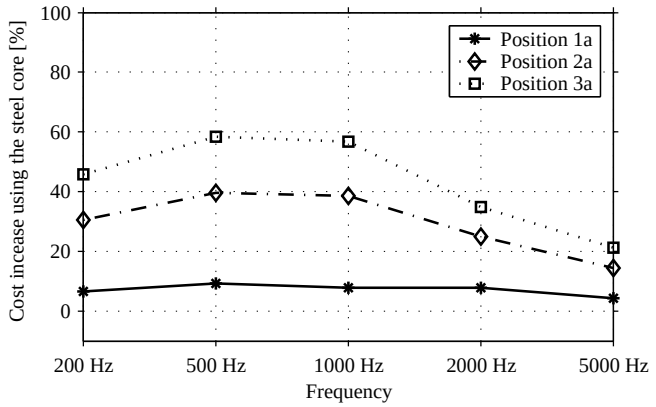

Figure 13. Increase in the contribution to the energy production cost using the steel core.

6. CONCLUSION

In this paper, design factors for the fullbridge converter are studied including choice of IGBT modules, switching frequency and also core material for the transformer. An analytical method is used and is shown to agree well with the loss calculations based on the simulated current and voltage waveforms.

Regarding the choice of IGBT module, there is no major difference in the losses until the switching frequency is well above 1 kHz, and therefore the choice of IGBT module is based on other factors. At higher switching frequencies when the total losses have increased, IGBT module 2 has higher losses due to the high switching losses. The choice of switching frequency depends on the core material used for the transformer. Using the Metglas® core, the transformer losses are relatively small. Due to this, the losses are constant at low frequencies and starts increasing at above 600 Hz for position 1a and above 1 kHz for positions 2a and 3a. For the steel core, the core losses are higher at low switching frequencies, resulting in more similar total losses for different switching frequencies. For position 1a, the losses start to increase at 500 Hz compared to 1.5 kHz for position 2a and 2 kHz for position 3a. The choice of switching frequency will be as high as possible to reduce the size of the transformer and the filters, but with still reasonable losses. Choosing a common switching frequency for all converters, a suitable value can be 1 kHz giving reasonable losses for all converters and also a low weight of the transformer. Regarding the choice of core material, the Metglas® core is a good choice with low losses leading to a low contribution to the energy production cost.

ACKNOWLEDGEMENT

The financial support given by Energimyndigheten (Swedish Energy Agency) is gratefully acknowledged.

REFERENCES

[1] S. Lundberg, "Configuration study of large wind parks", Dep. Power Eng., Chalmers University of Technology, Tech Rep. 474L, 2003.

[2] L. Max, "Energy evaluation for DC/DC converters in DC- based wind farms", Dept. of Energy and Environment, Chalmers University of Technology, Tech. Rep., 2007.

[3] L. Max and S. Lundberg, "System efficiency of a DC/DC converter based wind turbine grid system", in Proc. Nordic Wind Power Conference, NWPC 06, 2006.

[4] R. L. Steigerwald, R. W. De Doncker and H Kheraluwala, "A comparison of high-power DC-DC soft-switched converter topologies", IEEE Trans. Industr Applications, vol. 32, no. 5, pp. 1139-1145, September/October 1996.

[5] A. Bendre, S. Norris, D. Divan, I. Wallace and R. W. Gascoigne, "New high power DC-DC converter with loss limited switching and lossless secondary clamp", IEEE Trans. Power Electronics, vol. 18, no. 4, pp. 1020-1027, July 2003.

[6] R.W. Erickson and D. Maksimović, "Fundamentals of Power Electronics, Second Edition", Massachusetts, USA: Kluwer Academic Publishers, 2002.

[7] M. Sippola and R. E. Sepponen, "Accurate prediction of high-frequency power-transformer losses and temperature rise". IEEE Trans. Power Electronics, vol. 17, no. 5, pp. 835-847, September 2002.

A model for reliability assessment of offshore wind farms

Nicola Barberis Negra[1*)], Ole Holmstrøm[1)], Birgitte Bak-Jensen[2)], Poul Sørensen[3)]
[1)] Dong Energy A/S, Kraftværksvej 53, 7000 Fredericia, Denmark
[*)] Tlf. +45 79 23 32 52, e-mail nibne@dongenergy.dk
[2)] Institute for Energy Technology, Aalborg University, Pontoppidanstræde 101, 9220 Aalborg East, Denmark
[3)] Risø National Laboratory, DTU, 4000 Roskilde, Denmark

Abstract – A model for evaluating the reliability of offshore wind farms is presented in this paper. The need for this representation is justified by the high influence that wind generation has reached nowadays in power system's operation and planning. Several factors, which affect offshore wind generation, are discussed here and implemented into the model. The relevance of each factor is shown by means of the analysis of different cases, which are assessed with a sequential Monte Carlo simulation. Results of the described model can be used to estimate the generation of a wind farm itself or to provide the input for power system reliability assessment.

Index Terms - wind power generation, Monte Carlo methods, reliability modelling

1. INTRODUCTION

With a worldwide increase of installed capacity from 4844 MW in 1995 to 74328 MW at the beginning of 2007 [1,2], wind energy represents the renewable source with the highest growing rate in the last 10 years. Due to this fast development, power system planners and operators have to face new challenges for correctly controlling power systems, to which large wind farms are connected. New elements have to be analysed together with classical ones and well-known methodologies have to be updated and adapted to the new requirements.

Among these elements, the reliability issue plays a relevant role if the overall operation of a power system has to be evaluated. It is necessary to estimate the ability of the system to supply the demand and which are the limitations, to which it is subjected. Moreover, due to variability and randomness of wind generation, alternative solutions and analyses must be considered.

This paper deals with this problematic. In available literature, different models have been discussed for assessing wind generation and its influence on power system reliability. Many aspects have been highlighted, but there is a lack in including all of them into a complete model. Beside this, due to the relatively recent development of offshore wind installations, an upgrade of existing models is needed in order to include some issues that are not relevant onshore, but which affect offshore generation.

According to this, the main scopes of this paper are to describe a suitable method to assess offshore wind reliability and to show which relevant factors affect both modelling and results. These factors are implemented into a complete model and their significance is analysed by considering their influence on reliability results.

2. MODEL DESCRIPTION

When power system reliability is analysed, it is necessary to consider two main issues: the choice of the most suitable technique for the analysis and the choice of the most convenient representation of the system.

Considering available probabilistic techniques for power system reliability assessment, there are two approaches that can be followed, one based on analytical models and one on Monte Carlo simulations. Both methods have advantages and drawbacks and they can be very powerful with proper application [3]. In analytical methods, the system is represented by mathematical models and direct analytical solutions are used to evaluate a-priori reliability indices from the models. Instead, Monte Carlo simulations estimate a-posteriori reliability indices by simulating the actual random behaviour of the system. Both approaches can be based on either chronological (sequential) or non-chronological aspects and the choice of a method depends on the scope of the analysis. As discussed in [4], sequential aspects are more suitable when wind generation is assessed, since the wind varies along hours, days and seasons, and time-related aspects influence the evaluation.

According to [4], a sequential Monte Carlo simulation is used in this paper. Reasons for this choice regard the possibility to have a more flexible analysis and to estimate a broader range of parameters [4]. The main drawback of a Monte Carlo simulation is usually its long computation time: since the studied system is not large, computation time does not represent a problem here.

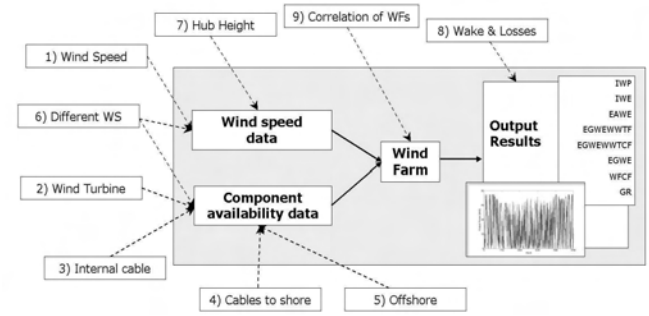

Figure 1. Wind farm reliability model: block diagram and influencing factors.

Regarding modelling issues, it is possible to find many works in available literature on the assessment of wind farm reliability. A generic representation consists usually of four blocks, as it can be observed in Figure 1. The inputs, which are the wind speed data (block a.) and the availability of system components (block b.), are collected by the wind farm model (block c.), where the layout of the wind farm is defined as well as other features of the analysis. Outputs of block c. are the final results (block d.), which can be in form of both hourly power time series and system indices. On the one hand, results as time series are useful because they

preserve the sequential nature of wind generation and they can be utilized as input to other analyses. On the other hand, indices can provide an instantaneous quantification of the yearly generation of the farm; some of the most common ones are listed in the following.

- IWP (Installed Wind Power, [MW]) is the sum of the rated power of all the installed wind turbines.
- IWE (Installed Wind Energy, [GWh]) is the product of the installed wind power and the number of hours in the period under analysis.
- EAWE (Expected Available Wind Energy, [GWh]) is the generated energy without accounting for wind turbine, cable and connector outages.
- EGWEWWTF (Expected Generated Wind Energy With Wind Turbine Failures, [GWh]) is index EAWE including wind turbine failures.
- EGWEWWTCF (Expected Generated Wind Energy With Wind Turbine and Cable Failures, [GWh]) is index EAWE including both wind turbine and cable failures.
- EGWE (Expected Generated Wind Energy, [GWh]) is the sum of the energies that all the available wind turbines can produce in the period under analysis, including wind turbine, cable and connector failures.
- WFCF (Wind Farm Capacity Factor, [-]) is the ratio of EGWE to IWE and it represents the capacity factor of the wind farm.
- GR (Generation Ratio, [-]) is the ratio of the wind power delivered to the Point of Common Coupling (PCC) to the power injection generated by the wind farm

In Figure 1 a set of factors, which influence the generation, is shown as well. These aspects, which are listed in the following, are extracted from available literature [5].

1. Wind speed's randomness and variability
2. Wind turbine technology
3. Power collection grid
4. Grid connection configuration
5. Offshore environment
6. Different wind speeds in the installation site
7. Hub height variations
8. Wake effects and power losses
9. Correlation of output power for different wind farms

As shown in Figure 1, different aspects influence the model in different ways since they are applied to different parts of it. For examples, wind input data in block a. might be affected by the nature of available measurements (aspect 1), which need to be long enough in order to represent properly wind speed conditions at the farm site. In the same way, the height of the measurement's mast can be sensibly different from the hub height (aspect 7): if this issue is not considered, available generation can be underestimated.

Block b. is influenced by several factors, which depends on the used components (aspects 2,3,4), on the layout design (aspects 6,8) and on the environment (aspects 5). For example, the dimension of wind installations becomes an issue in offshore environment. First of all, offshore wind farms have more components, therefore availabilities of internal cables (aspect 3) and connectors to shore (aspect 4), which are not usually considered in onshore assessment, influence the generation (e.g. a failure of a connector to shore may cause the loss of a large portion of the generated power) and the total production might be overestimated if these components are considered as ideal. Secondly, large dimensions imply that wind speed conditions may be different at different wind turbine locations (aspect 6), especially if the machines are far from each other. Usually a single input wind speed is used for all turbines, but this may cause an underestimate of the generation. Large dimensions and high number of components produce also wake effects and power losses (aspect 8), which decrease the total available generation.

If the model is used as input for power system reliability assessment, it must be considered as well that, if there are several wind farms connected, their outputs are somehow correlated (aspect 9).

According to these considerations, the described model is applied to a wind farm and its total generation is assessed in the next sections. Mentioned aspects are included in the model and their different influences on the results are shown.

3. DEFINITION OF THE SIMULATION

In this section the discussed method is applied to a wind farm. The considered layout is based on the Burbo Wind farm, with 25 wind turbines (rated at 3 MW), power collection grid with 22 cables and 3 connectors to shore (Figure 2). Values of components' availability are shown in Table 1; Table 2 defines data for a specific case, as described later in this section. It must be pointed out that these figures are "guesses" of onshore reliability values [9,10]: this is due to the fact that offshore installations are relatively recent and sufficient data have not been collected yet.

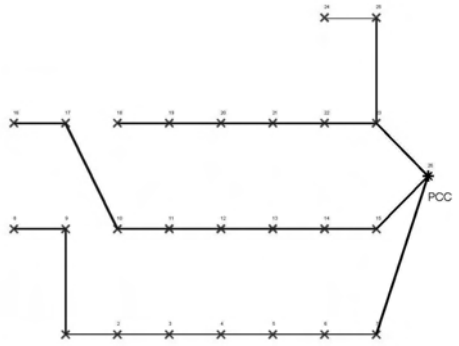

Figure 2. Layout of the wind farm analysed in this paper.

In order to analyse how the discussed factors influence the modelling, different cases have been considered.

- In Case 1), a basic model is studied for the assessment without the inclusion of any of the mentioned aspects. Original wind speed measurements are used as input: these measurements are based on four years of hourly data (2000-2003) recorded at Horns Rev.
- In Case 2), a synthetic wind speed time series generator (aspect 1) simulates the input of block a. The generator is discussed in detail in [6] and wind speed measurements used as input are recorded at Horns Rev during seven years (from May 1999 to May 2006). This case is assumed to be the reference case for the comparisons.
- In Case 3) a monthly variable Mean Time To Repair (MTTR) is added to case 2). This solution is adopted in order to include in the analysis the influence of aspect 5

Table 2. Components' reliability data for basic analyses [9,10].

	Length	Failure rate	MTTR	Availability
Wind turbine	-	1.55 1/y	490 h	92.01 %
Cable	0.7 km	0.015 1/y/km	1440 h	99.83 %
Connector	10 km	0.015 1/y/km	1440 h	99.75 %

Table 2. Components' reliability data for case 6).

	Failure rate	MTTR	Availability
Case 2	1.55 1/y	490 h	92.01 %
Case 6.1	1.10 1/y	490 h	94.19 %
Case 6.2	1.55 1/y	220 h	96.25 %
Case 6.3	1.10 1/y	220 h	97.31 %

(offshore environment) on the MTTR of some components. Considered values of MTTR vary between of 2160 h in winter and 720 h in summer [9,10].

- Case 4) uses an aggregated model, as presented in [7], in order to consider that wind conditions may be different for each wind turbine (aspect 6). The aggregation is applied to both wind turbine power curve and wind speed time series. It is assumed a dimension of the wind farm of 10 km for the definition of the model.
- Case 5) considers that hub and measurement mast heights are different (aspect 7). The following equation is used [8, pp 114-115] to move hourly data between the two heights

$$v_2(h_2) = v_1 \frac{\ln\left(\frac{h_2}{z_0}\right)}{\ln\left(\frac{h_1}{z_0}\right)} \quad (1)$$

where index 1 refers to the measurement height, index 2 to the hub height, v is the wind speed [m/s], h the height (mast height is 62 m, hub height is 100 m) [m] and z_0 is the roughness length [m], which is chosen equal to 0.0001 m [1].

- In Case 6), reliability figures of wind turbines are improved (aspect 3,5) in respect to the reference case, as shown in Table 2. This might be justified [9,10] considering that improvements of components are expected offshore in order to compensate problems caused by the environment.
- In Case 7), an efficiency coefficient equal to 93% is used in order to include wake effects and power losses (aspect 8) into the model [11]. The coefficient is applied to the output power of the wind farm.
- Case 8) uses all considered aspects in order to provide a complete assessment of the wind farm generation.

Aspects 3 and 4 do not require a specific case, since it is sufficient to compare some of the final indices (i.e. EGWA, EGWEWWTF, EGWEWWTCF and EGWE) to observe the influence of cables and connectors' availabilities on the results.

It must be finally noted that aspect 9 is not included in this study. This is due to the fact that its influence becomes relevant when the reliability of a power system with several offshore wind farms is assessed. Since the generation of a single wind farm is analysed here, this aspect cannot be evaluated.

The study of each case is performed with a sequential Monte Carlo simulation considering samples of one year with hourly step. A maximum number of samples equal to 1000 is used as stopping criterion. The choice of not controlling index accuracies to stop the simulation is justified by the intention of having the same large amount of samples for the comparison of results of different cases.

4. Discussion of the results and conclusions

Results of all cases are shown in Table 3, where reliability indices are included as well as the time required for performing each case, the number of samples for which each simulation has been run and the accuracy reached after the indicated number of samples.

Observing the presented results, it is possible to draw the following conclusions.

- The use of a synthetic wind speed generator, which creates a different wind speed time series in each sample, allows to have a more comprehensive power output of the wind farm. This aspect is shown in Figure 3, where probability distribution functions (PDF) of index EGWE in case 1) and 2) are compared. The PDF is smoother in case 2), since the synthetic generator defines different wind speeds for different samples, whereas in case 1) the PDF shows four peaks, since the input wind speed is based on four time series.

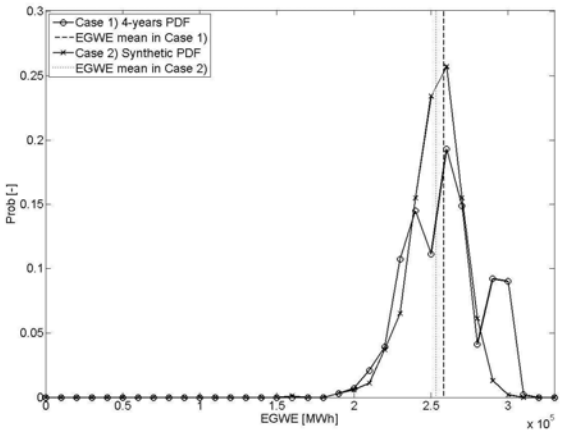

Figure 3. Probability distribution function (PDF) of EGWE in case 1) and case 2).

The use of different wind speed input data explains also the difference in the results of the two cases in Table 3. The average of the four years of data used in case 1) is higher than the total average of the seven years of measurements and therefore higher indices for the generation are expected in case 1)

- Improvements of components' availability produce an increase of wind farm generation (e.g. comparison of cases 6) and 2)). When a monthly-variable MTTR for cables is used instead (case 3), significant variations in the output power cannot be observed. However this depends on the choice of reliability figures: since the average MTTR during the year in case 3) is equal to the constant value of MTTR used in other cases, the

Table 3. Results for the analyzed cases.

	Unit	Case 1	Case 2	Case 3	Case 4.1	Case 5	Case 6.1	Case 6.2	Case 6.3	Case 7	Case 8
IWP	MW	75	75	75	75	75	75	75	75	75	75
IWE	GWh	657.00	657.00	657.00	657.00	657.00	657.00	657.00	657.00	657.00	657.00
EAWE	GWh	285.85	281.17	281.10	300.74	297.50	281.74	281.40	281.39	261.49	296.40
EGWEWWTF	GWh	264.57	259.84	259.92	277.93	275.12	266.29	271.15	271.24	241.65	285.63
EGWEWWTCF	GWh	263.22	258.50	258.70	276.49	273.76	265.10	269.81	269.88	240.40	284.40
EGWE	GWh	258.24	253.28	253.77	270.91	268.81	260.04	265.13	264.76	235.55	278.81
WFCF	-	0.393	0.386	0.386	0.412	0.409	0.396	0.404	0.403	0.359	0.424
GR	-	0.910	0.908	0.910	0.900	0.910	0.929	0.946	0.945	-	-
Time per sample	s	~2540	~3260	~3270	~3220	~3300	~3270	~3270	~3240	-	-
Nr. of samples	-	1000	1000	1000	1000	1000	1000	1000	1000	-	-
Accuracy	%	0.291	0.206	0.210	0.204	0.199	0.206	0.189	0.196	-	-

similarities in the results can be explained.

- If mast height is significantly lower than hub height, equation (1) must be used not to underestimate the total output power, as shown comparing cases 5) and 2). However, if the difference between heights is not too great, this aspect is negligible.
- The inclusion of an aggregated model is useful in order to consider different wind speed conditions for different wind turbines in the park. The effect of this model is to smooth both wind turbine power curves and wind speed time series: this explains why the output energy in case 4) is higher than in the reference case.
- The use of an efficiency coefficient decreases the total output of the wind farm. However, a constant coefficient for all wind speeds only approximates the real behaviour: both power losses and wake effects are dependent on wind speed values. A future improvement of the model may include a more detailed definition of the coefficient as a function of the current wind speed. Furthermore, it is not possible to evaluate index GR in this case: efficiency coefficient includes both electrical losses and wake effects, but GR is influenced by the losses, which are a characteristic of the wind farm grid, but not by the wake effects, which reduce the available wind speed.
- Due to the large number of components in offshore installations, the relevance of the availabilities of cables and connectors can be noted by observing indices EAWE, EGWEWWTF, EGWEWWTCF and EGWE. The inclusion of more types of components that may fail decreases the total generation of the wind farm and this variation of production depends on the used availability figures for the components.

Discussed results show why it is relevant to include the nine factors presented in this paper into the model. Some of them influence the wind data, whereas the others play a role in the definition of components' availabilities and wind farm's layout. In the assessment of the total wind farm generation, the exclusion of any of these factors may cause under- or over- estimate of the output of the wind farm, as shown in Table 3, and this may produce incorrect results.

The outputs of the presented model can be used for assessing the generation of a wind farm itself or as input to reliability models of a power system, to which one or more wind farms are connected. In this second application, it must be kept in mind that some correlation between the outputs of different wind farms must be considered, as discussed in section 3.

ACKNOWLEDGEMENT

This work is part of the project "Offshore wind power – Research related bottlenecks" and was funded by the Danish Research Agency (2104-04-0005), DONG Energy A/S and the Danish Academy of Wind Energy (DAWE).

REFERENCES

[1] Ackermann T (Editor). *Wind Power in Power Systems.* John Wiley & Sons: Chichester, England, 2005.

[2] Wind Power Monthly, *The Windicator*, Vol. 23, No. 1, January 2007, information available at www.windpower-monthly.com/WPM:WINDICATOR:945410.

[3] R. Billinton, R.N. Allan, *Reliability Evaluation of Power Systems,* 2nd ed., Plenum Publishing Corporation, New York, USA, July 1996.

[4] N. Barberis Negra, O. Holmstrøm, B. Bak-Jensen, and P. Sørensen, "Comparison of different techniques for offshore wind farm reliability assessment", Sixth International Workshop on Large-Scale Integration of Wind Power and Transmission Networks for Offshore Wind farms, Delft, The Netherlands, October 2006.

[5] N. Barberis Negra, O. Holmstrøm, B. Bak-Jensen, and P. Sørensen, "Aspects of relevance in offshore wind farm reliability assessment", IEEE Transaction on Power Conversion, Vol. 22, No. 1, March 2007.

[6] N. Barberis Negra, O. Holmstrøm, B. Bak-Jensen, and P. Sørensen, "Model of a synthetic wind speed time series generator", to be published.

[7] H. Holttinne, e P. Norgaard, "A Multi-Machine Power Curve Approach", *Proceedings of Nordic Wind Power Conference 2004*, Chalmers University of Technology, Goteborg, Sweden, March 2004.

[8] R. Gasch and J Twele, "Wind Power Plants – Fundamentals, Design, Construction and Operation", Solarpraxis AG, Germany, 2002.

[9] A. Sannino, H. Breder, and E. K. Nielsen, "Reliability of collection grids for large offshore wind parks", in *Proc. 9th International Conference on Probabilistic Methods Applied to Power Systems*, Stockholm, Sweden, June 11-15, 2006.

[10] Dowec Team, Estimation of turbine reliability figure within the DOWEC project", DOWEC project, Nr 10048, Issue 4, October 2003, Available at www.ecn.nl/en/wind/additional/special-projects/dowec (last visit: Sept. 2007).

[11] J.R. Ubeda and M.A.R. Rodriguez Garcia, "Reliability and production assessment of wind energy production connected to the electric network supply", *IEE Proceeding – Generation, Transmission and Distribution,* Vol. 146, No. 2, March 1999, pp. 169-175.

Adaptive modelling of offshore wind power fluctuations

Pierre Pinson[1,*], Henrik Madsen[1], Poul E. Sørensen[2], Nicolaos A. Cutululis[2]
[1] Technical University of Denmark, Informatics and Mathematical Modelling, Lyngby, Denmark.
[*] tlf. +45 4525 3428, e-mail pp@imm.dtu.dk
[2] Technical University of Denmark, Risø National Laboratory, Wind Energy department, Roskilde, Denmark.

Abstract — Better modelling of power fluctuations at large offshore wind farms may significantly enhance control and management strategies of their power output. The paper introduces a new methodology for modelling and forecasting the short-term (i.e. few minutes ahead) fluctuations of wind generation. This methodology is based on a Markov-switching autoregressive model with time-varying coefficients. An advantage of the method is that one can easily derive full predictive densities along with the usually generated point forecasts. The quality of this methodology is demonstrated from the test case of two large offshore wind farms in Denmark. The exercise consists in 1-step ahead forecasting exercise on time-series of wind generation with a time resolution of 10 minutes. The interest of such modelling approach for better understanding power fluctuations is finally discussed.

Index Terms — forecasting, modelling, offshore, power fluctuations, wind power.

1. Introduction

Future developments of wind power installations are more likely to take place offshore, owing to space availability, less problems with local population acceptance, and more steady winds. This is especially the case for countries that already experience a high wind power penetration onshore, like Germany and Denmark for instance. This latter country hosts the two largest offshore wind farms worldwide: Nysted and Horns Rev, whose nominal capacities are of 165.5 and 160 MW, respectively. Today, each of these wind farms can supply alone 2% of the whole electricity consumption of Denmark [1]. Such large offshore wind farms concentrate a high wind power capacity at a single location. Onshore, the same level of installed capacity is usually spread over an area of significant size, which yields a smoothing of power fluctuations [2]. This smoothing effect is hardly present offshore, and thus the magnitude of power fluctuations may reach very significant levels. Characterizing and modelling the power fluctuations for the specific case of offshore wind farms is a current challenge [3, 4], for better forecasting offshore wind generation, developing control strategies, or alternatively for simulating the combination of wind generation with storage or any form of backup generation. A discussion on these aspects is available in [5].

When inspecting offshore wind power production data averaged at a few-minute rate, one observes variations that are due to slower local atmospheric changes e.g. frontline passages and rain showers [6]. These meteorological phenomena add complexity to the modelling of wind power production, which is already non-linear and bounded owing to the characteristics of the wind-to-power conversion function, the so-called power curve. Such succession of periods with power fluctuations of lower and larger magnitudes calls for the use of regime-switching models. Recently, [7] showed that for the case of the Nysted and Horns Rev wind farms, Markov-switching approaches, i.e. for which the regime sequence is not directly observable but is assumed to be a first-order Markov chain, were more suitable than regime-switching approaches relying on an observable process e.g. using Smooth Transition AutoRegressive (STAR) models. Though, a drawback of the method described in [7] is that model coefficients are not time-varying, while it is known that wind generation is a process with long-term variations due to e.g. changes in the wind farm environment, seasonality or climate change, see e.g. [8]. The main objective of the present paper is to describe a method for adaptive estimation in Markov-switching autoregression that indeed allows for time-varying coefficients. This method utilizes a parameterization inspired by those proposed in [9, 10] and in [11]. Adaptivity in time is achieved with exponential forgetting of past observations. In addition, the formulation of the objective function to be minimized at each time-step includes a regularization term that permits to dampen the variability of the model coefficient estimates. A recursive estimation procedure permits to lower computational costs by updating estimates based on newly available observations only. In parallel, advantage is taken of the possibility to express predictive densities from Markov-switching autoregressive models for associating one-step ahead forecasts with prediction intervals. Predictive densities are given as a mixture of conditional densities in each regime, the quantiles of which can be obtained by numerical integration methods.

The paper is structured as following. A general formulation of the type of models considered, i.e. Markov-switching autoregressions with time-varying coefficients, is introduced in Section 1. The specific model parameterization employed is also described. Then, Section 2 focuses on the adaptive estimation of model coefficients, by first introducing the objective function to be minimized at each time-step, and then deriving an appropriate 3-step recursive estimation procedure. The issue of forecasting is dealt with in Section 4, by describing how one-step ahead point forecasts and quantile forecasts can be obtained, from a formulation of one-step ahead predictive densities. Then, Markov-switching autoregression with time-varying coefficients is applied for modelling power fluctuations at offshore wind farms in Section 5. Data originates from both Nysted and Horns Rev wind farms, and consists in power averages with a 10-minute temporal resolution. The characteristics of the estimated models are discussed. Concluding remarks in Section 6 end the paper.

2. MARKOV-SWITCHING AUTOREGRESSION WITH TIME-VARYING COEFFICIENTS

Let $\{y_t\}$, $t = 1, \ldots, n$, be the time-series of measured power production over a period of n time steps. The power production value at a given time t is defined as the average power over the preceding time interval, i.e. between times $t-1$ and t. For the modelling of offshore wind power fluctuations, the temporal resolution of relevant time-series ranges from 1 to 10 minutes. Hereafter, the notation y_t may be used for denoting either the power production random variable at time t or the measured value.

In parallel, consider $\{z_t\}$ a regime sequence taking a finite number of discrete values, $z_t \in \{1, \ldots, r\}$, $\forall t$. It is assumed that $\{y_t\}$ is an autoregressive process governed by the regime sequence $\{z_t\}$ in the following way

$$y_t = \left(\boldsymbol{\theta}_t^{(z_t)}\right)^\top \mathbf{x}_t + \varepsilon_t^{(z_t)} \tag{1}$$

with

$$\boldsymbol{\theta}_t^{(z)} = [\theta_{t,0}^{(z)} \ \theta_{t,1}^{(z)} \ \ldots \ \theta_{t,p}^{(z)}]^\top \tag{2}$$

$$\mathbf{x}_t = [1 \ y_{t-1} \ y_{t-2} \ \ldots \ y_{t-p}]^\top \tag{3}$$

and where p is the order of the autoregressive process, chosen here to be the same in each regime for simplicity. However, the developed methodology could be extended for having different orders in each regime. The set of parameters for the Markov-switching model introduced above, denoted by $\boldsymbol{\Theta}_t$, is described here. The t-subscript is used for indicating that the autoregressive coefficients are time-dependent, though assumed to be slowly varying. $\{\varepsilon_t^{(z)}\}$ is a white noise process in regime z, i.e. a sequence of independent random variables such that $\mathbb{E}[\varepsilon^{(z)}] = 0$ and $\sigma_t^{(z)} < \infty$. Let us denote by $\eta^{(z)}$ the density function of the innovations in regime z, which we will refer to as a conditional density in the following. For simplicity, it is assumed that innovations in each regime are distributed Gaussian, $\varepsilon_t^{(z)} \sim \mathcal{N}(0, \sigma_t^{(z)})$, $\forall t$, and thus

$$\eta^{(z)}(\varepsilon; \boldsymbol{\Theta}_t) = \frac{1}{\sigma_t^{(z)}\sqrt{2\pi}} \exp\left(-\frac{1}{2}\left(\frac{\varepsilon}{\sigma_t^{(z)}}\right)^2\right) \tag{4}$$

with the t-subscript indicating that standard deviations of conditional densities are allowed to slowly change over time.

In addition, it is assumed that the regime sequence $\{z_t\}$ follows a first order Markov chain on the finite space $\{1, \ldots, r\}$: the regime at time k is determined from the regime at time $k-1$ only, in a probabilistic way

$$p[z_k = j | z_{k-1} = i, z_{k-2}, \ldots, z_0] = p[z_k = j | z_{k-1} = i] \tag{5}$$

All the probabilities governing switches from one regime to the others are gathered in the so-called transition matrix $\mathbf{P}(\boldsymbol{\Theta}_t) = \{p_t^{ij}\}_{i,j=1,\ldots,r}$, for which the element p_t^{ij} represents the probability (given the model coefficients at time t, since transition probabilities are also allowed to slowly change over time) of being in regime j given that the previous regime was i, as formulated in (5). Some constraints need to be imposed on the transition probabilities. Firstly, by definition all the elements on a given row of the transition matrix must sum to 1,

$$\sum_{j=1}^{r} p_t^{ij} = 1 \tag{6}$$

since the r regimes represent all possible states that can be reached at any time. Secondly, all the elements of the matrix are chosen to be positive: $p_t^{ij} \geq 0, \forall i, j, t$, in order to ensure ergodicity, which means that any regime can be reached eventually.

In order for constraint (6) to be met at any time, the transition probabilities are parameterized on a unit sphere, as initially proposed in [9, 10]. Indeed, by having $p_t^{ij} = \left(s_t^{ij}\right)^2$, and for each i, the vector $s_t^{i\cdot} = [s_t^{i1} \ \ldots \ s_t^{ir}]^\top$ describing a location on a r-dimensional sphere, we naturally have

$$\sum_{j=1}^{r} p_t^{ij} = ||s_t^{ij}||_2^2 = 1 \tag{7}$$

For recursive estimation of coefficients in Markov-switching autoregression, [11] argue that a more stable algorithm can be derived by considering the logarithms of the standard deviations of the model innovations, i.e.

$$\tilde{\sigma}_t^{(z)} = \ln\left(\sigma_t^{(z)}\right) \tag{8}$$

In a similar manner, it is also proposed here to consider the logit transform $\tilde{s}_t^{ij}$ of the s_t^{ij} coefficients in order to improve the numerical properties of the information matrix to be used in the recursive estimation scheme,

$$\tilde{s}_t^{ij} = \ln\left(\frac{s_t^{ij}}{1 - s_t^{ij}}\right) \tag{9}$$

Finally, the set of coefficients allowing to fully characterizing the Markov-switching autoregressive model at time t can be summarized as

$$\boldsymbol{\Theta}_t = \left[\boldsymbol{\theta}_t^{(1)\top} \ \ldots \ \boldsymbol{\theta}_t^{(r)\top} \ \tilde{\boldsymbol{\sigma}}_t^\top \ \tilde{\mathbf{s}}^\top\right]^\top \tag{10}$$

where

$$\boldsymbol{\theta}_t^{(j)} = \left[\theta_{t,0}^{(j)} \ \theta_{t,1}^{(j)} \ \ldots \ \theta_{t,p}^{(j)}\right]^\top \tag{11}$$

gives the autoregressive coefficients in regime j and at time t, while

$$\tilde{\boldsymbol{\sigma}}_t = \left[\tilde{\sigma}_t^{(1)} \ \ldots \ \tilde{\sigma}_t^{(r)}\right]^\top \tag{12}$$

corresponds to the natural logarithm of the standard deviations of conditional densities in all regimes at time t, and finally

$$\mathbf{s}_t = \left[\tilde{s}_t^{1\cdot\top} \ \ldots \ \tilde{s}_t^{r\cdot\top}\right]^\top \tag{13}$$

is the vector of logit spherical coefficients summarizing the transition probabilities at that same time.

3. ADAPTIVE ESTIMATION OF THE MODEL COEFFICIENTS

There is a large number of papers in the literature dealing with recursive estimation in hidden Markov models, see e.g. [9, 10, 11]. Most of these estimation methods can be extended

to the case of Markov-switching autoregressions. However, it is often considered that the underlying model is stationary and that recursive estimation is motivated by online applications and reduction of computational costs only. In contrast here, the model coefficients are allowed to be slowly varying owing to the physical characteristics of the wind power generation process. This calls for the introduction of an adaptive estimation method permitting to track such long-term changes in the process characteristics.

Hereafter, it is considered that observations are available up to the current point in time t, and hence that the size of the dataset grows as time increases. The time-dependent objective function to be minimized at each time step is introduced in a first stage, followed by the recursive procedure for updating the set of model coefficients as new observations become available.

3.1. Formulation of the time-dependent objective function

If not seeking for adaptivity of model coefficients, their estimation can be performed (based on a dataset containing observations up to time t) by maximizing the likelihood of the observations given the model. Equivalently, given a chosen model structure, this translates to minimizing the negative log-likelihood of the observations given the set of model coefficients $\boldsymbol{\Theta}$,

$$S_t(\boldsymbol{\Theta}) = -\ln\left(P\left[y_1, y_2, \ldots, y_t \mid \boldsymbol{\Theta}\right]\right) \tag{14}$$

which can be rewritten as

$$S_t(\boldsymbol{\Theta}) = -\sum_{k=1}^{t} \ln\left(u_k(\boldsymbol{\Theta})\right) \tag{15}$$

with

$$u_k(\boldsymbol{\Theta}) = P\left[y_k \mid y_{k-1}, \ldots, y_1; \boldsymbol{\Theta}\right] \tag{16}$$

In contrast, for the case of maximum-likelihood estimation for Markov-switching autoregression with time-varying coefficients, let us introduce the following time-dependent objective function to be minimized at time t

$$S_t(\boldsymbol{\Theta}) = -\frac{1}{n_\lambda}\left(\sum_{k=1}^{t} \lambda^{t-k} \ln\left(u_k(\boldsymbol{\Theta})\right)\right) + \frac{\nu}{2}\boldsymbol{\Theta}\boldsymbol{\Theta}^\top \tag{17}$$

where λ is the forgetting factor, $\lambda \in [0, 1[$, allowing for exponential forgetting of past observations, and where

$$n_\lambda = \frac{1}{1-\lambda} \tag{18}$$

the effective number of observations is used for normalizing the negative log-likelihood part of the objective function. Note that (17) is a regularized version of what would be a usual maximum-likelihood objective function, with ν the regularization parameter. ν controls the balance between likelihood maximization and minimization of the norm of the model estimates. Such type of regularization is commonly known as Tikhonov regularization [12]. It may allow to increase the generalization ability of the model when used for prediction. From a numerical point of view, it will permit to derive acceptable estimates even though the condition number of the information matrix used in the recursive estimation procedure is pretty high. Theoretical and numerical properties of Tikhonov regularization are discussed in [13].

The estimate $\hat{\boldsymbol{\Theta}}_t$ of the model coefficients at time t is finally defined as the set of coefficient values which minimizes (17), i.e.

$$\hat{\boldsymbol{\Theta}}_t = \arg\min_{\boldsymbol{\Theta}} S_t(\boldsymbol{\Theta}) \tag{19}$$

Note that to our knowledge, there is no literature on the properties of model coefficient estimates for Markov-switching autoregressions when the estimation is performed by minimizing (17). We do not aim in the present paper at performing the necessary theoretical developments. A simulation study in [14] shows the nice behaviour of the model estimates.

3.2. Recursive estimation

Imagine being at time t, with the model fully specified by the estimate of model coefficients $\hat{\boldsymbol{\Theta}}_{t-1}$, and a newly available power measure y_t. Our aim in the following is to describe the procedure for updating the model coefficients and thus obtaining $\hat{\boldsymbol{\Theta}}_t$.

Given the definition of the conditional probability u_k in (16), i.e. as the likelihood of the observation y_k given past observations and given the model coefficients (for a chosen model structure), it is straightforward to see that at time t, $u_t(\hat{\boldsymbol{\Theta}}_{t-1})$ can be rewritten as

$$u_t(\hat{\boldsymbol{\Theta}}_{t-1}) = \boldsymbol{\eta}^\top(\boldsymbol{\varepsilon}_t; \hat{\boldsymbol{\Theta}}_{t-1})\mathbf{P}^\top(\hat{\boldsymbol{\Theta}}_{t-1})\boldsymbol{\xi}_{t-1}(\hat{\boldsymbol{\Theta}}_{t-1}) \tag{20}$$

In the above, $\boldsymbol{\varepsilon}_t$ is the vector of residuals in each regime at time t, thus yielding $\boldsymbol{\eta}(\boldsymbol{\varepsilon}_t; \hat{\boldsymbol{\Theta}}_{t-1})$ the related values of conditional density functions (cf. (4)), given the model coefficients at time $t-1$. In addition, $\boldsymbol{\xi}_{t-1}(\hat{\boldsymbol{\Theta}}_{t-1})$ is the vector of probabilities of being in such or such regime at time $t-1$, i.e.

$$\boldsymbol{\xi}_{t-1}(\hat{\boldsymbol{\Theta}}_{t-1}) = \left[\xi_{t-1}^{(1)}(\hat{\boldsymbol{\Theta}}_{t-1}) \;\; \xi_{t-1}^{(2)}(\hat{\boldsymbol{\Theta}}_{t-1}) \;\; \ldots \;\; \xi_{t-1}^{(r)}(\hat{\boldsymbol{\Theta}}_{t-1})\right] \tag{21}$$

given the observations up to that time, and given the most recent estimate of model coefficients, that is, $\hat{\boldsymbol{\Theta}}_{t-1}$

$$\xi_{t-1}^{(j)}(\hat{\boldsymbol{\Theta}}_{t-1}) = p\left[z_{t-1} = j \mid y_{t-1}, y_{t-2}, \ldots, y_1; \hat{\boldsymbol{\Theta}}_{t-1}\right] \tag{22}$$

then making $\mathbf{P}^\top(\hat{\boldsymbol{\Theta}}_{t-1})\boldsymbol{\xi}_{t-1}(\hat{\boldsymbol{\Theta}}_{t-1})$ the forecast issued at time $t-1$ of being in such or such regime at time t.

At this same time t, even if the set of true model coefficients $\boldsymbol{\Theta}_{t-1}$ were known, it would not be possible to readily say what the actual regime is. However, one can use statistical inference for estimating the probability $\xi_t^{(j)}$ of being in regime j at time t. This can indeed be achieved by applying the probabilistic inference filter initially introduced by [15],

$$\boldsymbol{\xi}_t(\hat{\boldsymbol{\Theta}}_{t-1}) = \frac{\boldsymbol{\eta}(\boldsymbol{\varepsilon}_t; \hat{\boldsymbol{\Theta}}_{t-1}) \otimes \mathbf{P}^\top(\hat{\boldsymbol{\Theta}}_{t-1})\boldsymbol{\xi}_{t-1}(\hat{\boldsymbol{\Theta}}_{t-1})}{\boldsymbol{\eta}^\top(\boldsymbol{\varepsilon}_t; \hat{\boldsymbol{\Theta}}_{t-1})\mathbf{P}^\top(\hat{\boldsymbol{\Theta}}_{t-1})\boldsymbol{\xi}_{t-1}(\hat{\boldsymbol{\Theta}}_{t-1})} \tag{23}$$

where $\otimes$ denotes element-by-element multiplication. $\boldsymbol{\xi}_t$ will hence be referred to as the vector of filtered probabilities in the following.

In order to derive the recursive estimation procedure, the method employed is based on using a Newton-Raphson step for obtaining the estimate $\hat{\boldsymbol{\Theta}}_t$ as a function of the previous

estimate $\hat{\boldsymbol{\Theta}}_{t-1}$, see e.g. [16],

$$\hat{\boldsymbol{\Theta}}_t = \hat{\boldsymbol{\Theta}}_{t-1} - \frac{\nabla_{\boldsymbol{\Theta}} S_t(\hat{\boldsymbol{\Theta}}_{t-1})}{\nabla^2_{\boldsymbol{\Theta}} S_t(\hat{\boldsymbol{\Theta}}_{t-1})} \tag{24}$$

After some mathematical developments, which are described in [14], one obtains a 2-step scheme for updating the set of model coefficients at every time step. If denoting by $\mathbf{h}_t$ the information vetor at time t, i.e.

$$\mathbf{h}_t = \nabla_{\boldsymbol{\Theta}} \ln(u_t(\boldsymbol{\Theta}_{t-1})) = \frac{\nabla_{\boldsymbol{\Theta}} u_t(\boldsymbol{\Theta}_{t-1})}{u_t(\boldsymbol{\Theta}_{t-1})} \tag{25}$$

and by $\mathbf{R}_t$ the related inverse covariance matrix, the 2-step updating scheme can be summarized as

$$\mathbf{R}_t = \lambda \mathbf{R}_{t-1} + (1-\lambda)\left(\mathbf{h}_t \mathbf{h}_t^\top + \nu \mathbf{I}\right) \tag{26}$$

$$\hat{\boldsymbol{\Theta}}_t = \pi_s \Big\{ \left(\mathbf{I} + \nu \mathbf{R}_t^{-1}\right)^{-1} \Big[\left(\mathbf{I} + \lambda\nu \mathbf{R}_t^{-1}\right) \hat{\boldsymbol{\Theta}}_{t-1} + (1-\lambda)\mathbf{R}_t^{-1}\mathbf{h}_t \Big] \Big\} \tag{27}$$

where $\mathbf{I}$ is an identity matrix of appropriate dimensions, and π_s a projection operator on the unit spheres defined by the $s^{i\cdot}$ vectors ($i = 1, \ldots, r$). This projection hence concerns transition probabilities only and do not affect autoregressive and standard deviation coefficients. Note that this procedure is applied after having calculated the vector of filtered probabilities $\boldsymbol{\xi}_t$. For that reason, the overall updating procedure is referred to as a 3-step procedure.

One clearly sees in (26)-(27) the effects of regularization. It consists of a constant loading on the diagonal of the inverse covariance matrix, thus permitting to control the condition number of $\mathbf{R}_t$ to be inverted in (27). Then, the second equation for model coefficients includes a dampening of previous estimates before and after updating with new information. Note that when $\nu = 0$ one retrieves a somehow classical updating formula for model coefficients tracked with Recursive Least Squares (RLS) of Recursive Maximum Likelihood (RML) methods. For more details, see e.g. [16].

For initializing the recursive procedure without any information on the process considered, one may use equal probabilities of being in the various states, set the autoregressive coefficients to zero, put a large load on the diagonal elements of the transition matrix, and have sufficiently large standard deviations of conditional densities in each regime so that conditional density values are not too close to zero while having poor knowledge of the process. In parallel, the inverse covariance matrix $\mathbf{R}_0$ can be initialized with a matrix of zeros. Then, for the first few steps of the recursive estimation procedure, only (26) is used for gaining information as long as $\mathbf{R}_t$ is not invertible. After that, (27) can be used for updating model coefficient estimates.

4. Point and density forecasting

Denote by f_t the density function of wind power values at time t. Given the chosen model structure and the set of true model coefficients $\boldsymbol{\Theta}_{t-1}$ estimated at time $t-1$, the one-step ahead predictive density of wind generation $\hat{f}_{t|t-1}$ can easily be expressed as

$$\hat{f}_{t|t-1}(y) = \sum_{j=1}^{r} \hat{\xi}^{(j)}_{t|t-1} \Big[{\boldsymbol{\theta}^{(j)}_{t-1}}^\top \mathbf{x_t} + \eta^{(j)}_{t-1}\left(y - {\boldsymbol{\theta}^{(j)}_{t-1}}^\top \mathbf{x_t}; \boldsymbol{\Theta}_{t-1}\right) \Big] \tag{28}$$

where $\hat{\xi}^{(j)}_{t|t-1}$ is the one-step ahead forecast probability of being in regime j at time t. The vector $\hat{\boldsymbol{\xi}}_{t|t-1}$ containing such forecast for all regimes is given by

$$\hat{\boldsymbol{\xi}}_{t|t-1} = \mathbf{P}^\top(\hat{\boldsymbol{\Theta}}_{t-1})\boldsymbol{\xi}_{t-1}(\boldsymbol{\Theta}_{t-1}) \tag{29}$$

Since the true model coefficients are obviously not available, they are replaced in the above equations by the estimate $\hat{\boldsymbol{\Theta}}_{t-1}$ available at that point in time.

Define $\hat{y}_{t|t-1}$ the one-step ahead point prediction of wind power as the conditional expectation of the random variable y_t, given the information set available at time $t-1$. $\hat{y}_{t|t-1}$ can then be derived from the predictive density definition of (28) as

$$\hat{y}_{t|t-1} = \sum_{j=1}^{r} \hat{\xi}^{(j)}_{t|t-1} {\hat{\boldsymbol{\theta}}^{(j)}_{t-1}}^\top \mathbf{x_t} \tag{30}$$

since the distributions of innovations in each regime are all centred.

In parallel, following the definition of conditional densities in (4), the one-step ahead predictive density $\hat{f}_{t|t-1}$ consists of a mixture of Normal densities. This predictive density can hence be explicitly formulated, and quantile forecasts for given proportions calculated with numerical integration methods. Indeed, if denoting by $\hat{F}_{t|t-1}$ the cumulative distribution function related to the predictive density $\hat{f}_{t|t-1}$, the quantile forecast $\hat{q}^{(\alpha)}_{t|t-1}$ for a given proportion α is

$$\hat{q}^{(\alpha)}_{t|t-1} = {\hat{F}_{t|t-1}}^{-1}(\alpha) \tag{31}$$

The calculation of quantiles for finite mixtures of Normal densities is discussed in [17].

Note that the method proposed here disregards the question of uncertainty in parameter estimation, since it gives the exact formulation of the one-step ahead predictive density $\hat{f}_{t|t-1}$ given the true parameter of the Markov-switching autoregressive model. Accounting for parameter estimation uncertainty for such type of model is a difficult task which, to our knowledge, has not been treated in the relevant literature. The fact that model coefficients are time-varying and the proposed estimation recursive complicates this question even more. However, the use of bootstrap methods may be envisaged, as initially proposed in [18]. And, concerning the recursive estimation issue, one may consider adapting the nonparametric block bootstrap method introduced in [19] to the case of the models considered here.

5. Results

In order to analyze the performance of the proposed Markov-switching autoregressions and related adaptive estimation method for the modelling of offshore wind power fluctuations, they are used on a real-world case study. The exercise

consists in one-step ahead forecasting of time-series of wind power production. Firstly, the data for the offshore wind farm is described. Then, the configuration of the various models and the setup used for estimation purposes are presented. Finally, a collection of results is shown and commented.

5.1. Case studies

The two offshore wind farms are located at Horns Rev and Nysted, off the west coast of Jutland and off the south cost of Zealand in Denmark, respectively. The former has a nominal power of 160 MW, while that of the latter reaches 165.5 MW. The annual energy yield for each of these wind farms is around 600GWh. Today, they represent the two largest offshore wind farms worldwide.

For both wind farms, the original power measurement data consist of one-second measurements for each wind turbine. Focus is given to the total power output at Horns Rev and Nysted. Following [6], it has been chosen to model each wind farm as a single representative wind turbine, the production of which consists of the average of the power generated by all the available wind turbines. These turbines have a nominal capacity P_n of 2000 kW and 2300 kW for Horns Rev and Nysted, respectively. Time series of power production are then normalized by these rated capacities. Hence, power values or error measures are all expressed in percentage of P_n. A sampling procedure has been developed in order to obtain time-series of 10-minute power averages. This sampling rate is selected so that the very fast fluctuations related to the turbulent nature of the wind disappear and reveal slower fluctuations at the minute scale. Because there may be some erroneous or suspicious data in the raw measurements, the sampling procedure has a threshold parameter τ_v, which corresponds to the minimum percentage of data that need to be considered as valid in a given time interval, so that the related power average is considered as valid too. The threshold chosen is $\tau_v = 75\%$. At Horns Rev, the available raw data are from 16$^{\text{th}}$ February 2005 to 25$^{\text{th}}$ January 2006. And, for Nysted, these data have been gathered for the period ranging from 1$^{\text{st}}$ January to 30$^{\text{th}}$ September 2005.

5.2. Model configuration and estimation setup

From the averaged data, it is necessary to define periods that are used for training the statistical models and periods that are used for evaluating what the performance of these models may be in operational conditions. These two types of datasets are referred to as learning and testing sets. We do not want these datasets to have any data considered as not valid. Sufficiently long periods without any invalid data are then identified and permit to define the necessary datasets. For both wind farms, the first 6000 data points are used as a training set, and the remainder for out-of-sample evaluation of the 1-step ahead forecast performance of the Markov-switching autoregressive models. These evaluation sets contain $N_n = 20650$ and $N_h = 21350$ data points for Nysted and Horns Rev, respectively. Over the learning period, a part of the data is used for one-fold cross validation (the last 2000 points) in order to select optimal values of the forgetting factor and regularization parameter. The autoregressive order of the Markov-switching models is arbitrarily set to $p = 3$, and the number of regimes to $r = 3$. For more information on cross validation, we refer to [20]. The error measure that is to be minimized over the cross validation set is the Normalized Root Mean Square Error (NRMSE), since it is aimed at having 1-step ahead forecast that would minimize such criterion over the evaluation set.

For all simulations, the autoregressive coefficients and standard deviations of conditional densities in each regime are initialized as

$$\begin{aligned}
\boldsymbol{\theta}_0^{(1)} &= [0.2\ \ 0\ \ 0\ \ 0]^\top, \quad \sigma_0^{(1)} = 0.15 \\
\boldsymbol{\theta}_0^{(2)} &= [0.5\ \ 0\ \ 0\ \ 0]^\top, \quad \sigma_0^{(2)} = 0.15 \\
\boldsymbol{\theta}_0^{(3)} &= [0.8\ \ 0\ \ 0\ \ 0]^\top, \quad \sigma_0^{(3)} = 0.15
\end{aligned}$$

while the initial matrix of transition probabilities is set to

$$\mathbf{P}_0 = \begin{bmatrix} 0.8 & 0.2 & 0 \\ 0.1 & 0.8 & 0.1 \\ 0 & 0.2 & 0.8 \end{bmatrix}$$

It is considered that the forgetting factor cannot be less than $\lambda = 0.98$, since lower values would correspond to an effective number of observations (cf. (18)) smaller than 50 data points. Such low value of the forgetting factor would then not allow for adaptation with respect to slow variations in the process characteristics, but would serve more for compensating for very bad model specification. No restriction is imposed on the potential range of values for the regularization parameter ν.

5.3. Point forecasting results

The results from the cross-validation procedure, i.e. the values of the forgetting factor λ and regularization parameter ν that minimize the 1-step ahead NRMSE over the validation set, are gathered in Table 1. In both cases, the forgetting factor takes value very close to 1, indicating that changes in process characteristics are indeed slow. The values in the Table correspond to number of effective observations of 500 and 250 for Nysted and Horns Rev, respectively, or seen differently to periods covering the last 3.5 and 1.75 days. Fast and abrupt changes are dealt with thanks to the Markov-switching mechanism. In addition, regularization parameter values are not equal to zero, showing the benefits of the proposal. Note that one could actually increase this value even more if interested in dampening variations in model estimates, though this would affect forecasting performance.

Table 1. Forgetting factor λ and regularization parameter ν obtained from the cross validation procedure for the Nysted and Horns Rev wind farms.

	λ	ν
Nysted	0.998	0.005
Horns Rev	0.996	0.007

For evaluation of out-of-sample forecast accuracy, we follow the approach presented in [21] for the evaluation of short-term wind power forecasts. Focus is given to the use of error measures such as NRMSE and Normalized Mean Absolute Error (NMAE). In addition, forecasts from the proposed Markov-switching autoregressive models are benchmarked against those obtained from persistence. Persistence

is the most simple way of producing a forecast and is based on a random walk model. A 1-step ahead persistence forecast is equal the last power measure. Despite its apparent simplicity, this benchmark method is difficult to beat for short-term look-ahead time such as that considered in the present paper.

The forecast performance assessment over the evaluation set is summarized in Table 2. NMAE and NRMSE criteria have lower values when employing Markov-switching models. This is satisfactory as it was expected that predictions would be hardly better than those from persistence. The reduction in NRMSE and NMAE is higher for the Nysted wind farm than for the Horns Rev wind farm. In addition, the level of error is in general higher for the latter wind farm. This confirms the findings in [7], where it is shown that the level of forecast performance, whatever the chosen approach, is higher at Nysted. The Horns Rev wind farm is located in the North Sea (while Nysted is in the Baltic sea, south of Zealand in Denmark). It may be more exposed to stronger fronts causing fluctuations with larger magnitude, and that are less predictable.

Table 2. One-step ahead forecast performance over the evaluation set for Nysted and Horns Rev. Results are both for persistence and Markov-switching models. Performance is summarized with NMAE and NRMSE criteria, given in percentage of the nominal capacity P_n of the representative single turbine.

	persistence		Markov-switching model	
	NMAE	NRMSE	NMAE	NRMSE
Nysted	2.37	4.11	2.20	3.79
Horns Rev	2.71	5.06	2.70	4.96

An expected interest of the Markov-switching approach is that one can better appraise the characteristics of short-term fluctuations of wind generation offshore by studying the estimated model coefficients, standard deviations of conditional densities, as well as transition probabilities. Autoregressive coefficients may inform on how the persistent nature of power generation may evolve depending on the regime, while standard deviations of conditional densities may tell on the amplitude of wind power fluctuations depending on the regime. Finally, the transition probabilities may tell if such or such regime is more dominant, or if some fast transitions may be expected from certain regimes to the others.

The set of model coefficients at the end of the evaluation set for Nysted can be summarized by the model autoregressive coefficients and related standard deviations of related conditional densities,

$$\boldsymbol{\theta}_{N_n}^{(1)} = [0.0 \;\; 1.361 \;\; -0.351 \;\; -0.019]^\top, \; \sigma_{N_n}^{(1)} = 0.0007$$
$$\boldsymbol{\theta}_{N_n}^{(2)} = [0.013 \;\; 1.508 \;\; -0.778 \;\; 0.244]^\top, \; \sigma_{N_n}^{(2)} = 0.041$$
$$\boldsymbol{\theta}_{N_n}^{(3)} = [-0.001 \;\; 1.435 \;\; -0.491 \;\; 0.056]^\top, \sigma_{N_n}^{(3)} = 0.011$$

while the final matrix of transition probabilities is

$$\mathbf{P}_{N_n} = \begin{bmatrix} 0.888 & 0.036 & 0.076 \\ 0.027 & 0.842 & 0.131 \\ 0.051 & 0.075 & 0.874 \end{bmatrix}$$

In parallel for Horns Rev, the autoregressive coefficients and related standard deviations are

$$\boldsymbol{\theta}_{N_h}^{(1)} = [0.002 \;\; 1.253 \;\; -0.248 \;\; -0.008]^\top, \sigma_{N_h}^{(1)} = 0.023$$
$$\boldsymbol{\theta}_{N_h}^{(2)} = [0.022 \;\; 1.178 \;\; -0.3358 \;\; 0.123]^\top, \sigma_{N_h}^{(2)} = 0.066$$
$$\boldsymbol{\theta}_{N_h}^{(3)} = [0.069 \;\; 0.91 \;\; 0.042 \;\; -0.022]^\top, \sigma_{N_h}^{(3)} = 0.005$$

while the final matrix of transition probabilities is

$$\mathbf{P}_{N_h} = \begin{bmatrix} 0.887 & 0.069 & 0.044 \\ 0.222 & 0.710 & 0.068 \\ 0.173 & 0.138 & 0.689 \end{bmatrix}$$

For both wind farms, the first regime is dominant in the sense that it has the highest probability of keeping on with the same regime when it is reached. However, one could argue that the first regime is more dominant for Horns Rev, as the probabilities of staying in second and third regimes are lower, and as the probabilities of going back to first regime are higher. The dominant regimes have different characteristics for the two wind farms. At Nysted, it is the regime with the lower standard deviation of the conditional density, and thus the regime where fluctuations of smaller magnitude are to be expected. It is not the case at Horns Rev, as the dominant regime is that with the medium value of standard deviations of conditional densities. Such finding confirms the fact that power fluctuations seem to be of larger magnitude at Horns Rev than at Nysted.

Let us study an arbitrarily chosen episode of power generation at the Horns Rev wind farm. For confidentiality reason, the dates defining beginning and end of this period cannot be given. The episode consists of 250 successive time-steps with power measurements and corresponding one-step ahead forecasts as obtained by the fitted Markov-switching autoregressive model. These 250 time steps represent a period of around 42 hours. The time-series of power production over this period is shown in Figure 1, along with corresponding one-step ahead forecasts. In parallel, Figure 2 depicts the evolution of the filtered probabilities, i.e. the probabilities given by the model of being in such or such regime at each time step. Finally, the evolution of the standard deviation of conditional densities in each regime is shown in Figure 3.

First of all, it is important to notice that there is a clear difference between the three regimes in terms of magnitude of potential power fluctuations. There is a ratio 10 between the standard deviations of conditional densities between regime 2 and 3. In addition, these regimes are clearly separated, as there is a smooth evolution of the standard deviation parameters over the episode. If focusing on the power time-series of Figure 1, one observes successive periods with fluctuations of lower and larger magnitude. Then, by comparison with the evolution of filtered probabilities in Figure 2, one sees that periods with highly persistent behaviour of power generation are all associated with very high probability of being in the first regime. This is valid for time steps between 20 and 80 for instance. This also shows that regimes are not bviously related to a certain level of power generation, as it would be the case f using e.g. Self-Exciting Tansition Auto-Regressive (SETAR) or Smooth Transition Auto-Regressive (STAR) models [7]. If looking again at the autogressive coefficients in each regime given above for Horns Rev at the end of the evaluation period, one clearly sees that intercept coefficients are almost zero. While regime 1 appears to be the regime with low mag-

nitude fluctuations, both regime 2 and 3 contribute to periods with larger ones. Studying obtained series of filtered probabilities along with the evolution of some meteorological variables is expected to give useful information for better understanding meteorological phenomena that govern such behaviour. This would then permit to develop prediction methods taking advantage of additional explanatory variables.

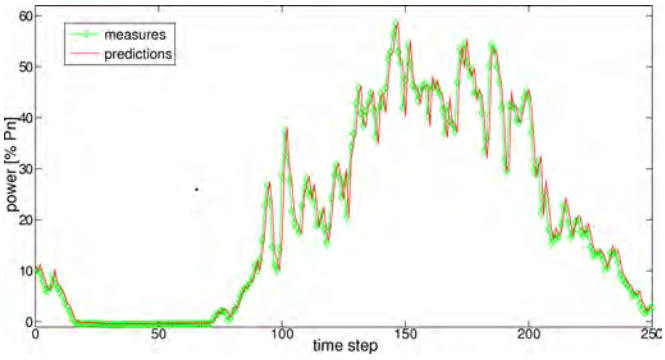

Figure 1. Time-series of normalized power generation at Horns Rev (both measures and one-step ahead predictions) over an arbitrarily chosen episode.

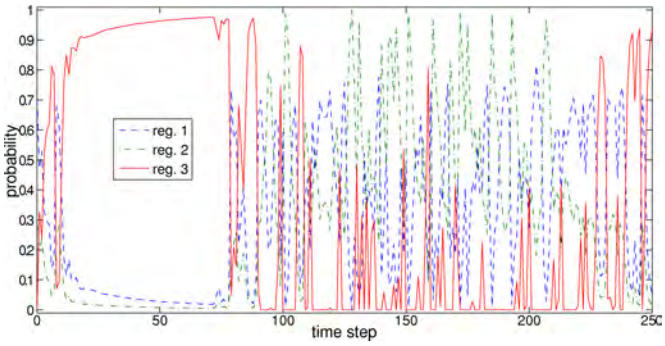

Figure 2. Evolution of filtered probabilities given by the Markov-switching model over the same period.

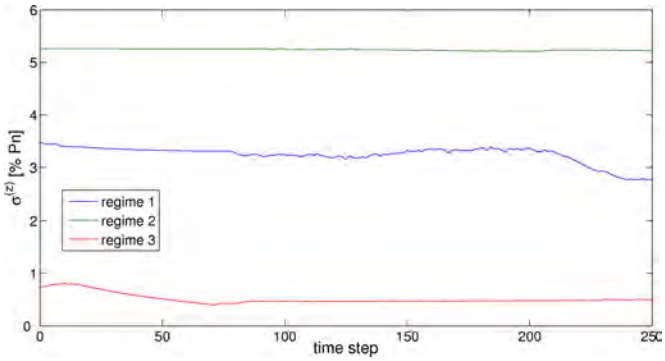

Figure 3. Evolution of the standard deviation of conditional densities in the various regimes for the same episode.

5.4. Interval forecasting results

In a second stage, focus is given to the uncertainty information provided by the Markov-switching autoregressive models. Indeed, even if point predictions in the form of conditional expectations are expected to be relevant for power management purposes, the whole information on fluctuations will actually be given by prediction intervals giving the potential range of power production in the next time-step, with a given probability i.e. their nominal coverage rate. Therefore, the possibility of associating point predictions with central prediction intervals is considered here. Central prediction intervals are intervals that are centred in probability around the median. For instance, a central prediction interval with a nominal coverage rate of 80% has its bounds consisting of the quantile forecasts with nominal proportions 0.1 and 0.9. Therefore, for evaluating the reliability of generated interval forecasts, i.e. their probabilistic correctness, one has to verify the observed proportions of quantiles composing the bounds of intervals. For more information on the evaluation of probabilistic forecasts, and more particularly for the wind power application, we refer to [22, 23].

Table 3. Empirical coverage of the interval forecasts produced from the Markov-switching autoregressive models for Horns Rev and Nysted.

nominal [%]	emp. cov. Horns Rev [%]	emp. cov. Nysted [%]
10	10.09	10.38
20	21.23	19.55
30	31.48	28.69
40	41.67	38.16
50	51.36	48.59
60	61.39	59.18
70	70.45	69.59
80	79.84	79.92
90	89.59	90.92

Prediction intervals are generated over the evaluation set for both Horns Rev and Nysted. The nominal coverage of these intervals range from 10% to 90%, with a 10% increment. This translates to numerically calculating 18 quantiles of the predictive densities obtained from (28). The observed coverage for these various prediction intervals are gathered in Table 3. The agreement between nominal coverage rates and observed one is good, with deviations from perfect reliability overally less than 2%. However as explained above, this valuation has to be carried further by looking at the observed proportions of related quantile forecasts, in order to verify that intervals are indeed properly centred. Such evaluation is performed in Figure 4 by the use of reliability diagrams, which gives the observed proportions of the quantiles against the nominal ones. The closer to the diagonal the better. For both wind farms, the reliability curve lies below the diagonal, indicating that all quantiles are underestimated (in probability). This underestimation is more significant for the central part of predictive densities. Note that for operational applications one would be mainly interested in using prediction intervals with high nominal coverage rates, say larger than 80%, thus corresponding to quantile forecasts that are more reliable in the present evaluation. It seems that the Gaussian assumption for conditional densities allows to have predictive densities (in the form of Normal mixtures) that appropriately capture the shape of the tails of predictive distributions, but not their central parts. Using nonparametric density estimation in each regime may allow to correct for that.

Finally, Figure 5 depicts the same episode with power measures and corresponding one-step ahead point prediction that than shown in Figure 1 for the Horns Rev wind farm, except

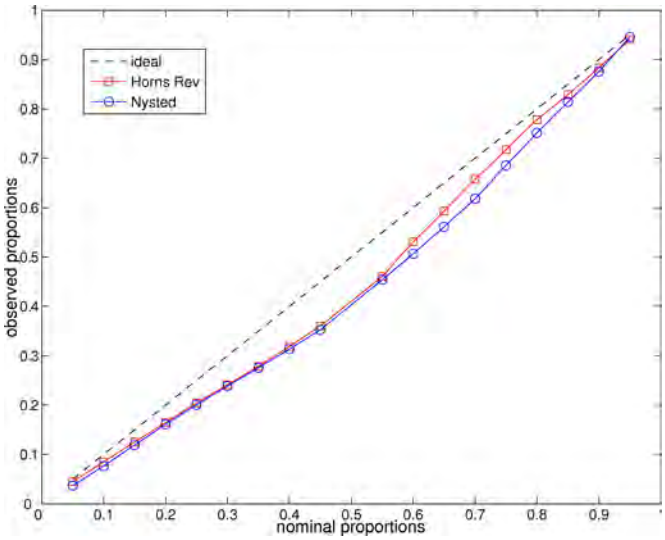

Figure 4. Reliability evaluation of quantile forecasts obtained from the Markov-switching autoregressive models for both Horns Rev and Nysted. Such reliability diagram compare nominal and observed quantile proportions.

that here point predictions are associated with prediction intervals with a nominal coverage rate of 90%. Prediction intervals with such nominal coverage rate are the most relevant for operation applications, and they have been found to be the most reliable in practice. The size of the prediction intervals obviously varies during this 250 time-step period, with their size directly influenced by forecasts of filtered probabilities and standard deviations of conditional densities in each regime (cf. (28)). In addition, prediction intervals are not symmetric, as even if conditional densities are assumed to be Gaussian in each regime, the resulting one-step ahead predictive densities are clearly not. In this episode, prediction intervals are wider during periods with power fluctuations of larger magnitude. Even though point predictions may be less accurate (in a mean square sense) during these periods of larger fluctuations, Markov-switching autoregressive models can provide this valuable information about their potential magnitude.

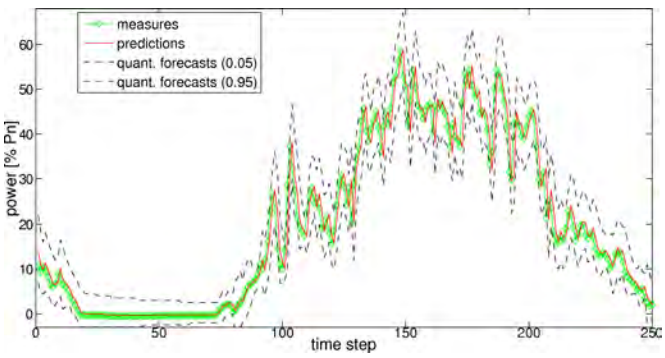

Figure 5. Time-series of normalized power generation at Horns Rev (both measures and one-step ahead predictions) over an arbitrarily chosen episode, accompanied with prediction intervals with a nominal coverage of 90%.

6. Conclusions

Markov-switching autoregressive models are an appealing approach to the modelling of short-term wind power fluctuations at large offshore wind farms. Such models can be used for simulation or forecasting purposes. This class of models has been generalized so that they are allowed to have time-varying coefficients, though slowly varying, in order to follow the long-term variations in the wind generation process characteristics. An appropriate estimation method using recursive maximum likelihood and Tikhonov regularization has been introduced. The proposal for including a regularization term comes from the aim of application to noisy wind power data, for which the use of non-regularized estimation may result in ill-conditioned numerical problems. The convergence and tracking abilities of the method have been shown from simulations. Then, Markov-switching autoregressive models have been employed for characterizing the 10-minute power fluctuations at Horns Rev and Nysted, the two largest offshore wind farms worldwide. The models and related estimation method have been evaluated on a one-step ahead forecasting exercise, with persistence as a benchmark. For both wind farms, the forecast accuracy of the proposed approach is higher than that of persistence, with the additional benefit of informing on the characteristics of such fluctuations. Indeed, it has been possible to identify regimes with different autoregressive behaviours, and more importantly with different variances in conditional densities. This shows the ability of the proposed approach to characterize periods with lower or larger magnitudes of power fluctuations. In the future, the series of state sequences may be compared with the time series of some meteorological variables over the same period, in order to reveal if power fluctuations characteristics can indeed be explained by these meteorological variables.

In addition to generating point predictions of wind generation, it has been shown that the interest of the approach proposed also lied in the possibility of associating prediction intervals or full predictive densities to point predictions. Indeed when focusing on power fluctuations, even if point predictions give useful information, one is mainly interested in the magnitude of potential deviations from these point predictions. It has been shown that for large nominal coverage rates (which are the most appropriate for operational applications) the reliability of prediction intervals was more acceptable than for low nominal coverage rates. It is known that for the wind generation process, noise distributions are not Gaussian, and that the shape of these distributions is influenced by the level of some explanatory variables [24]. Therefore, in order to better shape predictive densities, the Gaussian assumption should be relaxed in the future. Nonparametric density estimation may be achieved with kernel density estimators, as in e.g. [25], though this may introduce some problems in a recursive maximum likelihood estimation framework e.g. multimodality of conditional densities.

One-step ahead predictive densities of power generation have been explicitly formulated. Such densities consist of finite mixtures of conditional densities in each regime. However, it has been explained that the issue of parameter uncertainty was not considered, and that this may also affect the quality of derived conditional densities, especially in an adaptive estimation framework where the quality of parameter estimation may also vary with time. Novel approaches accounting for such parameter uncertainty should hence be proposed. The derivation of analytical formula might be difficult. In contrast,

one may think of employing nonparametric block bootstrap procedures similar to that proposed in [19]. This will be the focus of further research.

ACKNOWLEDGMENTS

The results presented have been generated as a part of the project 'Power Fluctuations in Large Offshore Wind Farms' sponsored by the Danish Public Service Obligation (PSO) fund (PSO 105622 / FU 4104), which is hereby greatly acknowledged. DONG Energy Generation A/S and Vattenfall Danmark A/S are also acknowledged for providing the wind power data for the Nysted and Horns Rev offshore wind farms. Finally, the authors would like to acknowledge Tobias Rydén for fruitful discussions.

References

[1] W. Sweet. Reap the wild wind. IEEE Spectrum, vol. 39, pp. 34-39, 2002.

[2] U. Focken, M. Lange,M. Monnich, H.-P. Waldl, H.-G. Beyer, A. Luig. Short-term prediction of the aggregated power output of wind farms - A statistical analysis of the reduction of the prediction error by spatial smoothing effects. Journal of Wind Engineering and Industrial Aerodynamics, vol. 90, pp. 231-246, 2002.

[3] V. Akhmatov. Influence of wind direction on intense power fluctuations in large offshore windfarms in the North Sea. Wind Engineering, vol. 31, pp. 59-64, 2007.

[4] A.R. Hendersen, C. Morgan, B. Smith B., H.C. Sørensen, R.J. Barthelmie, B. Boesmans. Offshore wind energy in Europe - A review of the state-of-the-art. Wind Energy, vol. 6, pp. 35-52, 2003.

[5] P.E. Sørensen, N.A. Cutululis, A. Vigueras-Rodriguez, L.E. Jensen, J. Hjerrild, M.H. Donovan, H. Madsen. Power fluctuations from large wind farms. IEEE Transactions on Power Systems, vol. 22, pp. 958-965, 2007.

[6] P.E. Sørensen, N.A. Cutululis, A. Vigueras-Rodriguez, H. Madsen, P. Pinson, L.E. Jensen, J. Hjerrild, M.H. Donovan. Modelling of power fluctuations from large offshore wind farms. Wind Energy, to be published, 2007.

[7] P. Pinson, L.E.A. Christensen, H. Madsen, P.E. Sørensen, M.H. Donovan, L.E. Jensen. Regime-switching modelling of the fluctuations of offshore wind generation. Journal of Wind Engineering and Industrial Aerodynamics, submitted for publication, 2006.

[8] G. Giebel, G. Kariniotakis, R. Brownsword. The state of the art in short-term prediction of wind power - A literature overview. Position paper for the ANEMOS project, deliverable report D1.1, available online: http://www.anemos-project.eu, 2003.

[9] I.B. Collings, V. Krishnamurthy, J.B. Moore. On-line identification of hidden Markov models via prediction error techniques. IEEE Transactions on Signal Processing, vol. 42, pp. 3535-3539, 1994.

[10] I.B. Collings, T. Rydén. A new maximum likelihood gradient technique algorithm for on-line hidden Markov model identification. in: Proc. IEEE Int. Conf. Acoust., Speech, Signal Processing, Seattle, 1998.

[11] U. Holst, G. Lindgren, J. Holst, M. Thuvesholmen. Recursive estimation in switching autoregressions with a Markov regime. Journal of Time Series Analysis, vol. 15, pp. 489-506, 1994.

[12] A.N. Tikhonov, V.Y. Arsenin. Solutions of Ill-posed Problems. Wiscon: Washington, DC, 1977.

[13] T.A. Johansen. On Tikhonov regularization, bias and variance in nonlinear system identification. Automatica, vol. 33, pp. 441-446, 1997.

[14] P. Pinson, H. Madsen. Markov-switching autoregression with time-varying coefficients for offshore wind power fluctuations. Technical report, Technical University of Denmark, Informatics and Mathematical Modelling, Denmark, 2007.

[15] J.D. Hamilton. A new approach to the economic analysis of nonstationay time-series and business cycles. Econometrica, vol. 57, pp. 357-384, 1989.

[16] H. Madsen. Time-Series Analysis, Second Edition. Technical University of Denmark: Kgs. Lyngby. ISBN: 87-643-0098-6, 2006.

[17] M. Rahman, R. Rahman, L.R. Pearson. Quantiles for finite mixtures of Normal distributions. International Journal of Mathematical Education in Science and Technology, vol. 37, pp. 352-357, 2006.

[18] B.A. Craig, P.P. Sendi. Estimation of the transition matrix of a discrete-time Markov chain. Health Economics, vol. 11,pp. 33-42, 2002.

[19] V. Corradi, N.R. Swanson. Nonparametric bootstrap procedures for predictive inference based on recursive estimation schemes. International Economic Review, vol. 43, pp. 67-109, 2007.

[20] M. Stone. Cross-validation and assessment of statistical predictions (with discussion). Journal of the Royal Statistical Society B, vol. 36, pp. 111-147, 1974.

[21] H. Madsen, P. Pinson, T.S. Nielsen, H.Aa. Nielsen, G. Kariniotakis. Standardizing the performance evaluation of short-term wind power prediction models. Wind Engineering, vol. 29, pp. 475-489, 2005.

[22] G. Gneiting, F. Balabdaoui, A.E. Raftery. Probabilistic forecasts, calibration and sharpness. Journal of the Royal Statistical Society B, vol. 69, pp. 243-268, 2007.

[23] P. Pinson, H.Aa. Nielsen, J.K. Møller, H. Madsen, G. Kariniotakis. Nonparametric probabilistic forecasts of wind power: required properties and evaluation. Wind Energy, to be published, 2007.

[24] P. Pinson. Estimation of the Uncertainty in Wind Power Forecasting. PhD Thesis, Ecole des Mines de Paris, France, available online: www.pastel.paristech.org, 2006.

[25] C.C.Y. Dorea, L.C. Zhao. Nonparametric density estimation in hidden Markov models. Statistical Inference for Stochastic Processes, vol. 5, pp. 55-64, 2002.

Real-time digital simulation of a VSC-connected offshore wind farm

Patrick P. T. Groenewoud, Delft University of Technology, Netherlands, Patrick.Groenewoud@movares.nl
Ralph L. Hendriks, Delft University of Technology, Netherlands, R.L.Hendriks@tudelft.nl
Bart C. Ummels, Delft University of Technology, Netherlands, B.C.Ummels@tudelft.nl
Wil L. Kling, Delft University of Technology, Netherlands, W.L.Kling@tudelft.nl

Abstract — Multi-terminal high voltage direct-current (MT-HVdc) technology could be an interesting technology for international submarine interconnectors. Synergies may exist between energy trade and the connection of large-scale offshore wind power to onshore grids, since the capacity utilization of the system can be increased.

This paper presents a simplified simulation model of a VSC-connected offshore wind farm for the real-time digital simulator (RTDS). The RTDS works in continuous sustained real-time and is therefore able to perform the simulations fast. The converter bridge is modelled by the assumption of ideal sources. All other components (converter transformer, phase reactors, dc capacitor, etc.) are modelled using their physical representation in standard library blocks. Different operational cases are simulated: normal operation and fault situations in the ac-system.

Index Terms — High Voltage Direct Current, Multi-terminal, Offshore Wind, Real-time Digital Simulator, Voltage-Sourced Converter.

1. Introduction

Offshore wind power has the potential to become an important source of renewable energy in Western Europe. The first projects have been constructed relatively close to shore (<25 km) and have power ratings up to 160 MW. These wind farms are connected to the power system through submarine power cables operated at alternating current (ac). The future holds projects that will be located further away from the shore and have higher power ratings, complicating grid connection. Besides, there is a growing need for electricity trade in Europe, also because of the liberalized electricity market. The combination of these two objectives—grid connection for offshore wind farms and new cross-border interconnection capacity—into a single infrastructure may lead to interesting cost savings. The capacity factor of an offshore wind farm is in the order of 40%; the proposed solution could improve the usage of the electrical infrastructure by facilitating energy transports at times of low wind production.

At transmission distances of about 80 km, the physical limits of ac transmission through submarine cables are reached. Connection through direct-current (dc) technology could overcome these restrictions and seems therefore an interesting technology for the proposed solution. Contrary to most existing HVdc-transmission schemes, the proposed infrastructure is multi-terminal (MT), see figure 1.

Thyristor-based line-commutated converters (LCC) have been used for the conversion between ac and dc for more than 50 years now, for power ratings up to and over 1500 MW. For offshore use this technology has several disadvantages: the converter stations have large space requirements and are therefore difficult to build on offshore platforms, operation is problematic without additional equipment providing a stable ac voltage, and operation at low power produces high valve losses and harmonic currents. DC transmission based on voltage-sourced converters (VSC) with forced commutated switches could overcome these disadvantages. The high switching frequency reduces the ac-side voltage and dc-side current harmonics significantly compared to the LCC, thus requiring less harmonic filters and resulting in a smaller converter footprint. The VSC has inherent black-start capability, enabling energizing of the remote wind farm grid. Besides, the independent control of active and reactive power provides STATCOM-like functionality making it easier to comply with grid connection requirements onshore. Also, more robust operation in MT-configuration is an advantage.

For the study of the behaviour of the MT-VSC transmission system as a part of a power system, various simulation frameworks are available. Delft University of Technology has a real-time digital simulator (RTDS) that enables the simulation of electric networks in real-time. This saves time and allows the user to change system parameters during the simulation. A library with detailed power system-component models is included in the RTDS software. This allows the user to set-up a model that closely resembles the real system. Typical application of the RTDS is the closed-loop verification of control and protection hardware. For real-time operation, the RTDS has a minimum step-size of 50 µs. This step-time limits accurate simulation of circuits switching at frequencies above 1 kHz. To simulate the proposed transmission scheme, reduced VSC models are required.

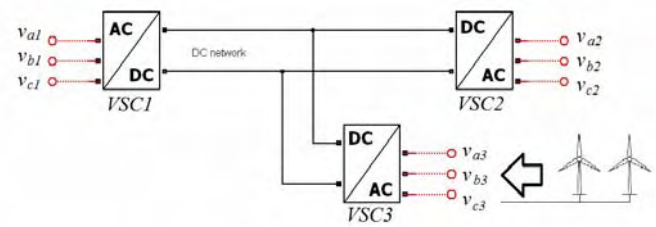

Figure 1 The proposed MT-VSC transmission system, all three converters are rated 300 MW.

The remainder of this paper is organized as follows. In section 2, the operating principles of the VSC are described, after which the control of the VSC is explained in section 3. The RTDS model is discussed in section 4 and in section 5 are different operational cases simulated, regarding the normal operation and fault situations in the ac system.

2. VSC Operating and Modelling Principles

A VSC is a power electronic device that can convert power from the ac to dc side and vice-versa by switching power electronic switches in a controlled manner. The ac side of the

VSC is theoretically able to produce any preferred voltage waveform, only limited by the direct voltage and the switching frequency. For grid purposes, a sinusoidal voltage needs to be produced with the same frequency as the grid's. To produce this waveform, in most cases a pulse-width modulation (PWM) scheme is applied. The VSC is able to exchange active as well as reactive power. To exchange power with the grid, the produced voltage should differ from the ac-grid voltage. "From a system point of view, it acts as a zero-inertia motor or generator that can control active and reactive power almost instantaneously" [1]. In figure 2 a single-phase VSC is shown. The inductance between the grid and the ac side of the VSC is often the leakage inductance of a transformer, or a separately installed converter reactor [2].
For the power electronic switches in VSC transmission systems mainly insulated gate bipolar transistors (IGBT) are applied, and occasionally gate turn-off transistors (GTO) [3]. In case PWM with an infinite switching frequency and ideal switches are assumed, a sinusoidal voltage could be produced by the VSC. Since the minimum step size of the RTDS allows no detailed modelling of the converter bridge, the VSC has been modelled by ideal voltage and current sources. For the ac side, controlled voltage sources are used and a controlled current source has been used for the dc side, whereby the power $P_{ac}=P_{dc}$. See figure 2 for the schematically represented VSC.

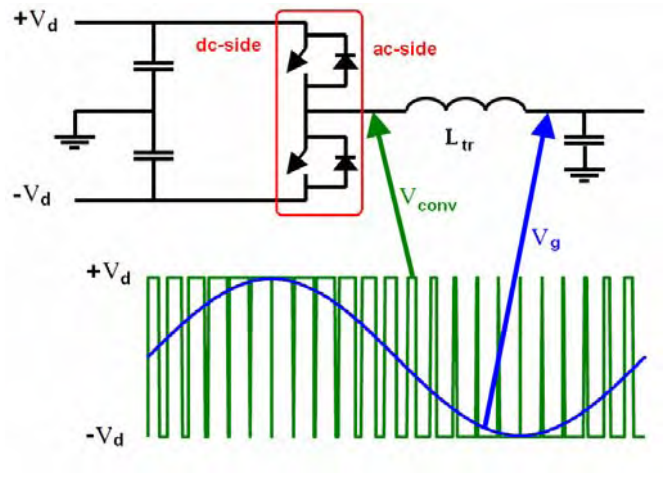

Figure 2 A schematically represented VSC [1].

To exchange power with the ac-grid, the sinusoidal voltage that is produced by the VSC needs to be different from the ac-grid voltage. These well-know formulas describe the power exchange between the VSC and the ac grid

$$P = \frac{V_g V_{conv}}{\omega L_{tr}} \sin\delta \qquad (1)$$

$$Q = \frac{V_g \left(V_g - V_{conv}\cos\delta\right)}{\omega L_{tr}} \qquad (2)$$

in which δ is the angle between V_g and V_{conv}.

3. Control of the VSC

For controlling the VSC, direct control (in which the converter voltage angle δ and amplitude V_{conv} are changed independently) and vector control [5] can be used. Vector control allows developing a controller that is able to control the active power P and the reactive power Q independently. The active and reactive current components are decoupled, which implies consequently no offset in the steady state. (Note: this is not possible with direct control, since a change in the converter voltage angle δ does influence both P and Q, as does a change in V_{conv}; see (1) and (2)). Vector control is therefore used in this work.

With vector control, the *dq*-currents will be tracked to appropriate reference values. For this, the grid-side voltages v_{gd} and v_{gq} are measured and values for converter voltages v_{convd}, and v_{convq} are calculated in such a way that the desired reference values $i_{d,ref}$ and $i_{q,ref}$ are reached. The required converter voltages are then transformed back to the *abc*-reference frame and submitted as an input to the PWM mechanism. An overview of this process is presented in figure 3.

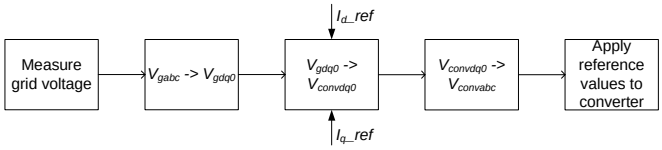

Figure 3 Schematic overview of current control.

The transformation between the *abc*-components and the *dq0*-components is defined by [4]

$$V_{abc} = \boldsymbol{P} V_{dq0}$$

and

$$I_{abc} = \boldsymbol{P} I_{dq0}$$

in which $\boldsymbol{P} = \boldsymbol{AB}$, which is the orthogonal Park transformation

$$\boldsymbol{P} = \sqrt{\frac{2}{3}} \begin{bmatrix} \frac{1}{2}\sqrt{2} & \cos\left(\theta - \frac{2\pi}{3}\right) & -\sin\left(\theta - \frac{2\pi}{3}\right) \\ \frac{1}{2}\sqrt{2} & \cos\left(\theta - \frac{2\pi}{3}\right) & -\sin\left(\theta - \frac{2\pi}{3}\right) \\ \frac{1}{2}\sqrt{2} & \cos\theta & -\sin\theta \end{bmatrix}$$

with $\boldsymbol{P}^{-1} = \boldsymbol{P}^T$.

The angle θ is measured by a phase-locked loop (PLL) system. A d-q-z grid control circuit could be used, which is known to perform robustly: "The d-q-z type of grid control circuit has excellent immunity from either loss of synchronizing voltages or harmonic distortion on the synchronizing voltages" [6].
After the transformation to *dq*-quantities, the voltages v_{convd} and v_{convq} have to be calculated by the current controller. To synthesize the current controller, first the network equations of the ac side will be derived with Kirchhoff's circuit laws, see figure 4.

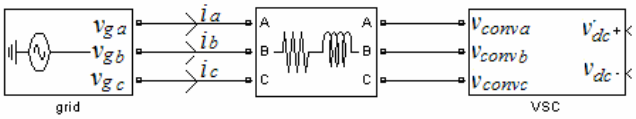

Figure 4 Basic Circuit for the derivation of circuit equations.

Voltages will be in their vector representation

$$\boldsymbol{V} = \begin{bmatrix} v_a \\ v_b \\ v_c \end{bmatrix}, \boldsymbol{V}' = \begin{bmatrix} v_d \\ v_q \\ v_0 \end{bmatrix}, \boldsymbol{V} = \boldsymbol{P}\boldsymbol{V}'$$

The same holds for for **I**.

Applying Kirchhoff's circuit laws and applying the Park-transformation results in

$$\boldsymbol{V_g} = \boldsymbol{RI} + \boldsymbol{L}\frac{d}{dt}(\boldsymbol{I}) + \boldsymbol{V_{conv}}$$

$$\boldsymbol{PV_g}' = \boldsymbol{RPI}' + \boldsymbol{L}\frac{d}{dt}(\boldsymbol{PI}') + \boldsymbol{PV_{conv}}'$$

$$\boldsymbol{V_g}' = \boldsymbol{P^{-1}RPI}' + \boldsymbol{P^{-1}L}\frac{d}{dt}(\boldsymbol{PI}') + \boldsymbol{V_{conv}}'$$

$$\boldsymbol{V_g}' = \boldsymbol{R}'\boldsymbol{I}' + \boldsymbol{P^{-1}L}\frac{d\boldsymbol{P}}{dt}\boldsymbol{I}' + \boldsymbol{P^{-1}LP}\frac{d\boldsymbol{I}'}{dt} + \boldsymbol{V_{conv}}'$$

$$\boldsymbol{V_g}' = \boldsymbol{R}'\boldsymbol{I}' + \boldsymbol{L}'\boldsymbol{P}^{-1}\frac{d\boldsymbol{P}}{dt}\boldsymbol{I}' + \boldsymbol{L}\frac{d\boldsymbol{I}'}{dt} + \boldsymbol{V_{conv}}'$$

$$\begin{bmatrix} v_{gd} \\ v_{gq} \\ v_{g0} \end{bmatrix} = \begin{bmatrix} R & 0 & 0 \\ 0 & R & 0 \\ 0 & 0 & R \end{bmatrix}\begin{bmatrix} i_d \\ i_q \\ i_0 \end{bmatrix} + \begin{bmatrix} 0 & -\omega L & 0 \\ \omega L & 0 & 0 \\ 0 & 0 & 0 \end{bmatrix}\begin{bmatrix} i_d \\ i_q \\ i_0 \end{bmatrix} + \begin{bmatrix} L & 0 & 0 \\ 0 & L & 0 \\ 0 & 0 & L \end{bmatrix}\frac{d}{dt}\begin{bmatrix} i_d \\ i_q \\ i_0 \end{bmatrix} + \begin{bmatrix} v_{convd} \\ v_{convq} \\ v_{conv0} \end{bmatrix}$$

The VSC is connected to the grid through a ΔY-transformer where the converter-sided Y-winding is grounded. The converter star point is not grounded hence no zero-sequence currents can flow in the converter. Because of the delta winding at the grid side of transformer, no zero-sequence currents can flow and will therefore be neglected in the remainder. If i_d and i_q are chosen as state variables, the remaining equations are

$$\frac{di_d}{dt} = \frac{1}{L}v_{gd} - \frac{R}{L}i_d - \omega i_q - \frac{1}{L}v_{convd}$$

$$\frac{di_q}{dt} = \frac{1}{L}v_{gq} - \frac{R}{L}i_q + \omega i_d - \frac{1}{L}v_{convq}$$

In these equations the terms ωi_q and ωi_d cause a cross-coupling between both state variables. For the current controller, these factors will be regarded as external disturbances and fed forward. Two new control inputs can be introduced

$$x_d = v_{gd} - \omega L i_q - v_{convd}$$

$$x_q = v_{gq} + \omega L i_d - v_{convq}$$

From the original expression follows that

$$x_d = (sL + R)\,i_d$$

$$x_q = (sL + R)\,i_q$$

in which s is the Laplace-operator. Now two independent first-order models result that can be controlled by PI-regulators. The current controller is depicted in figure 5.

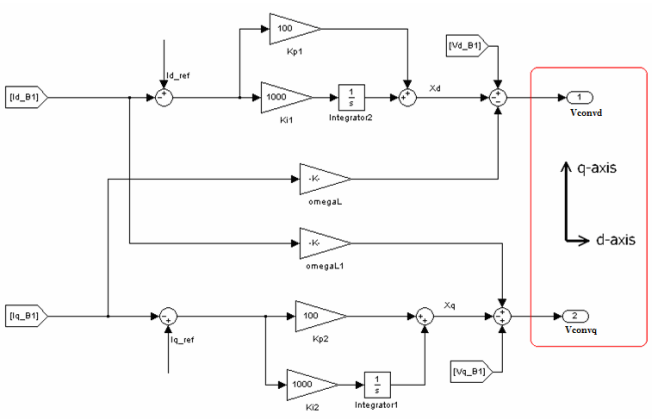

Figure 5 Current controller.

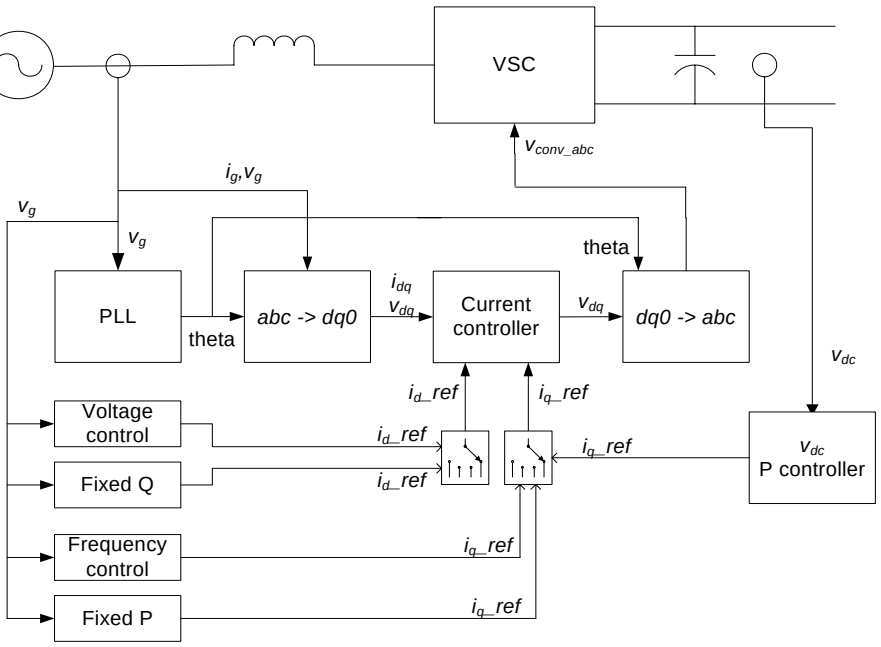

Figure 6 System and controller overview.

Current references $i_{d,ref}$ and $i_{q,ref}$ are obtained from outer controllers. The following control modes can be distinguished (see figure 6):

- Direct-voltage control (i_q);
- fixed amount of active power P (i_q);
- AC-frequency support (i_q);
- fixed amount of reactive power Q (i_d);
- AC-voltage support (i_d).

For reliable operation, at least one of the VSCs in the scheme should control the direct voltage, thus securing power balance in the dc-network. In case only one direct-voltage controlling element is present, direct-voltage control can be implemented as proportional-integral (PI) control. The dc-voltage will then consequently reach the defined reference value after a system disturbance. In case more then one VSC is configured as a direct voltage-controlling element, all direct-voltage controllers need to be implemented as P-control only to prevent unexpected system behaviour. In this work, although only one VSC is configured as a voltage-controlling element, proportional control is applied according

$$i_{q\_ref} = \left(v_{dc\_ref} - v_{dc}\right) k_p$$

In this work VSC1 (as in figure 1) will be in active power-control mode, VSC2 will regulate the direct voltage, and VSC3 is in ac frequency-support mode to ensure that all power produced by the wind farm is injected into the dc system. In case of a fault at the grid side of VSC2, the direct voltage will become incontrollable. VSC2 is not able to exchange sufficient power between the ac and the dc grid. Hence, the direct-voltage will either increase or decrease quickly. The rate of change of the direct voltage depends on the set point of the power controller of VSC1 and the power that is supplied by the wind farm. The direct voltage rises if the set point of the power controller of VSC1 is positive and drops if this set point is negative (in case no power is supplied by the wind farm). Moreover, due to the fast dc-system dynamics, the direct voltage reaches unacceptable values within only a few milliseconds.

To avoid the situation were the direct voltage reaches an unacceptable level, an extra direct voltage controller is added to VSC1, which is only activated when the direct voltage is out of a specified interval. The function of the outer controller shifts from power controller to direct voltage controller if direct voltage is out of this interval. If normal operation is restored and the direct voltage is within the operating boundaries again, VSC1 will change back to power-control mode again. An overview of this process is presented in figure 7.

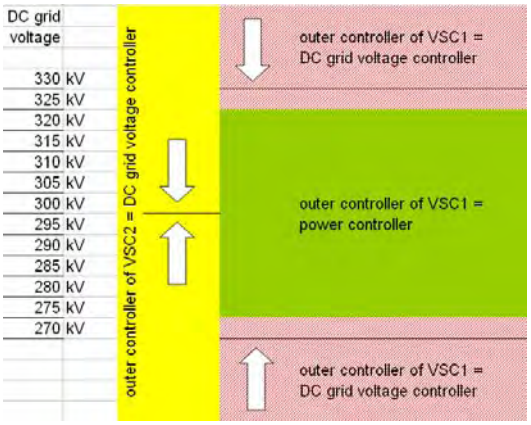

Figure 7 Overview of interaction between outer controllers of VSC1 and VSC2.

4. Model set-up for the RTDS

The transmission system will be implemented for the Real-time Digital Simulator (RTDS) system. The RTDS is a powerful computer that works in continuous, sustained real-time. Hence, simulation of events is just as fast as their occurrence in practice. This saves time, in comparison to other off-line tools, where the simulation of one second would take much more calculation time.

The complete model for the RTDS is shown in figure 8. ACgrid1 is connected via a three-phase circuit breaker and a ΔY-transformer to the ac side of VSC1. The dc side of VSC1 is referred to as "1" in the model section labeled "DCgrid". This also applies for the other VSCs. By changing values for the blocks labeled "RRL" (which are part of a benchmark model for HVdc-transmission systems [7]) the ac grids can represent different short-circuit ratios. The right-hand side of the dc model is used to model energizing of the dc system, as will be explained later. Component values are given in table 1 and are taken from [2].

Table 1 System parameters.

Quantity	Symbol	Value
Rated system power	P_{nom}	300 MW
Rated direct voltage	v_{dc}	300 kV
Rated ac-voltage	v_g	150 kV
Phase reactor inductance	L	35 mH
AC equivalent resistance	R	0 Ω
DC-capacitance	C	40 μF
DC equivalent resistance	R_{dc}	60 kΩ
AC-system rated frequency	f	50 Hz

4.1. Offshore wind farm and collection system

A wind farm consisting of direct drive turbines has been assumed, with a rated power of 300 MW. This wind farm is represented by one VSC. Because of the relatively short simulation time, a constant wind speed has been assumed. The VSC ("direct drive wind farm", figure 8) has been placed in series with two ΔY-transformers. The rated voltage of equivalent wind turbine is 3.5 kV; this voltage is transformed to 20 kV-level in the collection system. From 20 kV, the voltage is transformed to 150 kV.

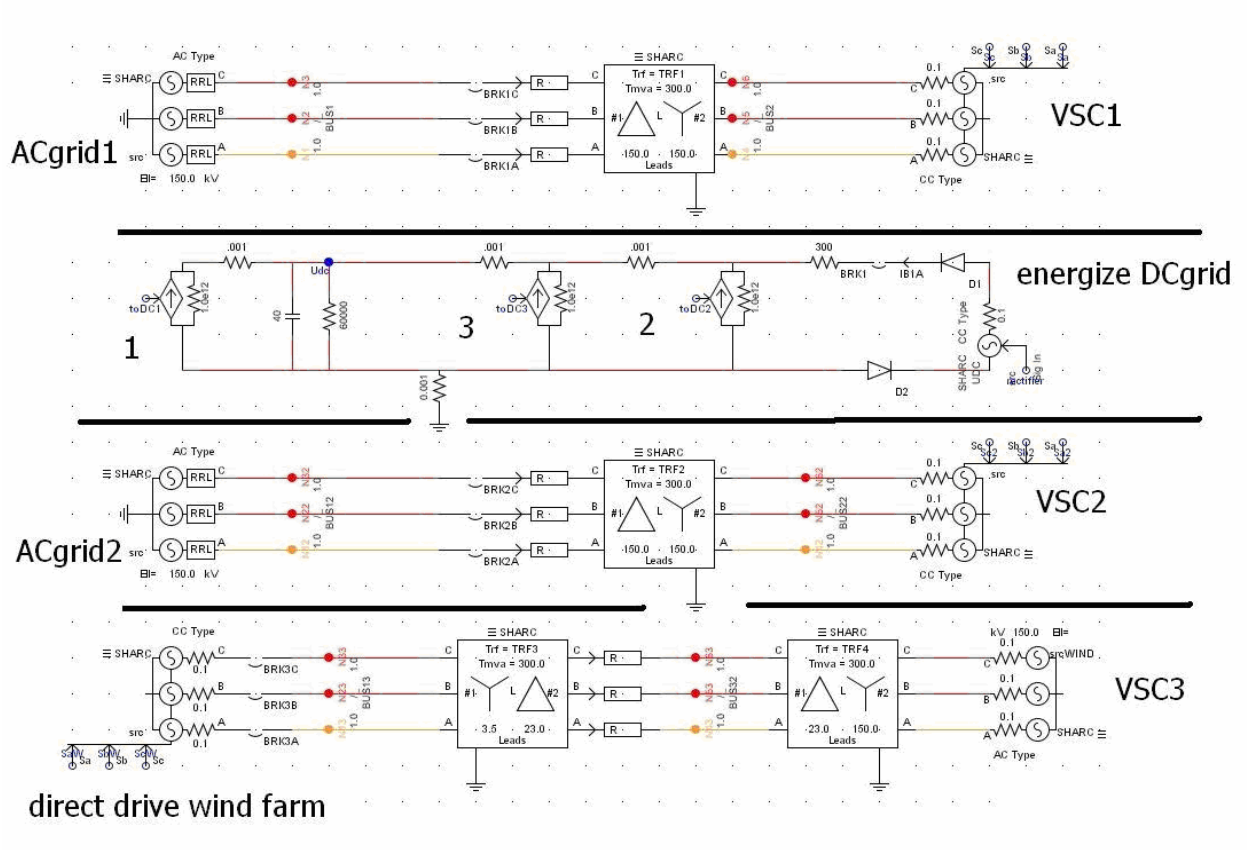

Figure 8 Implementation of the system in the RTDS.

The offshore VSC (VSC3, figure 8) should provide and maintain a stable voltage in the offshore grid. For the generation of the desired system voltage and frequency at the ac-side of the VSC, takes care of the generation of a fixed voltage behind the ΔY (150/23 kV) transformer.

4.2. Energizing of the dc grid and system start-up

The dc system has to be energized before the MT-VSC transmission system can start operation. If the VSC is connected to the ac system without additional measures, high charging currents will flow that could damage the converter. By inserting a current-limiting resistor at system start-up, the converter is protected. When the direct voltage is at its rated value, the resistor is bypassed. The right-hand side of the dc circuit in figure 8 is added to simulate this start-up sequence.

To energize the dc-system the following procedure is followed:

1. Energize the dc grid, close BRK1 (figure 8);
2. Start the PWM of all VSCs and synchronize to the grid voltages;
3. apply a reference for the direct voltage to the direct voltage-controlling VSC;
4. open circuit breaker BRK1 (figure 8); and
5. apply a power reference to the power-controlling VSC.

5. SIMULATION OF SELECTED CASES

In this section different cases will be simulated in order to evaluate the performance of the system. First the power flow during normal operation is evaluated and then different fault situations are considered.

5.1. Power flow during normal operation

During normal operation different power flows in the transmission system can take place. The following power flows are possible:

1. In case the system is only used for energy trade between both interconnected system: from VSC1 to VSC2 or from VSC2 to VSC1;
2. In case wind power is transported to one interconnected system only: from VSC3 to VSC1 or from VSC3 to VSC2;
3. A combination of option of 1 and 2.

As an illustration, a simulation will be performed in which the system is used for energy trade (150 MW from VSC2 to VSC1) and wind power is produced. At a certain moment, the wind power goes up from 100 MW to 200 MW. VSC1 has been equipped with an outer power controller, in order to make sure that 150 MW is drawn by ACgrid1. VSC2 is equipped with a direct-voltage controller as outer controller and will therefore accept the fluctuations in wind power.

Starting value:	After wind gust:
P(VSC1) = −150 MW	P(VSC1) = −150 MW
P(VSC2) = +50 MW	P(VSC2) = −50 MW
P(VSC3) = +100 MW	P(VSC3) = +200 MW

The result of this simulation is presented in figure 9a–b. The system works as expected regarding the power flows.

5.2. Three-phase to ground fault at the grid side of VSC2

In this section, different fault situations will be simulated in order to identify bottlenecks in the system. A three-phase to ground fault will be applied at the grid side of VSC2. As mentioned earlier, VSC2 is unable to control the dc-voltage during the fault and VSC1 should take over this task.

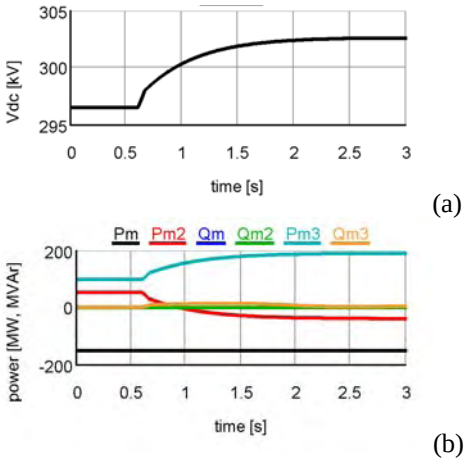

Figure 9 150 MW transported to VSC1, wind power goes up from 100 MW to 200 MW, power fluctuations accepted by VSC2.

Power flow from VSC1 to VSC2

Figure 10a–g shows the system responses to a three-phase to ground fault at the grid side of VSC2, which is cleared after 100 ms. During the fault, the voltage at the grid side of VSC2 is zero (figure 10b). The voltage at the converter side of the transformer however, is not zero (figure 10b). The reason for this is that the current controller of VSC2 still tries to control the current in such a way that the reference value for the direct voltage is reached. This reference value cannot be reached, since ACgrid2 can not deliver power to VSC2. The current through VSC2 remains equal, but the power goes to 0 MW (figure 10e). The current through the valves of VSC2 temporarily reaches a value of 2 kA (figure 10d) at the moment that the fault is applied. It is questionable whether the IGBTs are able to survive this overshoot. A solution would be over dimensioning of the IGBT valves or installation of a larger converter reactor to decrease the rate of rise. The direct voltage increases fast (figure 10f) at the moment that the fault is applied. As can be observed in figure 10f, the outer controller of VSC1 quickly switches from active power-control mode to direct voltage-control mode.

After the fault has been cleared the system remains stable and is able to restore fast (figure 10a–g).

Power flow from VSC2 to VSC1

The same fault as was applied in the previous part will be simulated, but the power is now transported from VSC2 to VSC1. This means that the direct voltage will decrease after the fault has been applied, since VSC2 is the direct voltage-controlling converter. During the fault VSC1 will temporarily take over this function again. The direct voltage reaches a value below 250 kV. However, this is high enough for the system to remain in operation. Other phenomena that occur are similar to what has been explained above and therefore are not included here. The three-phase to ground fault does not result in the shut down of the system. The system remains stable and is able to restore fast.

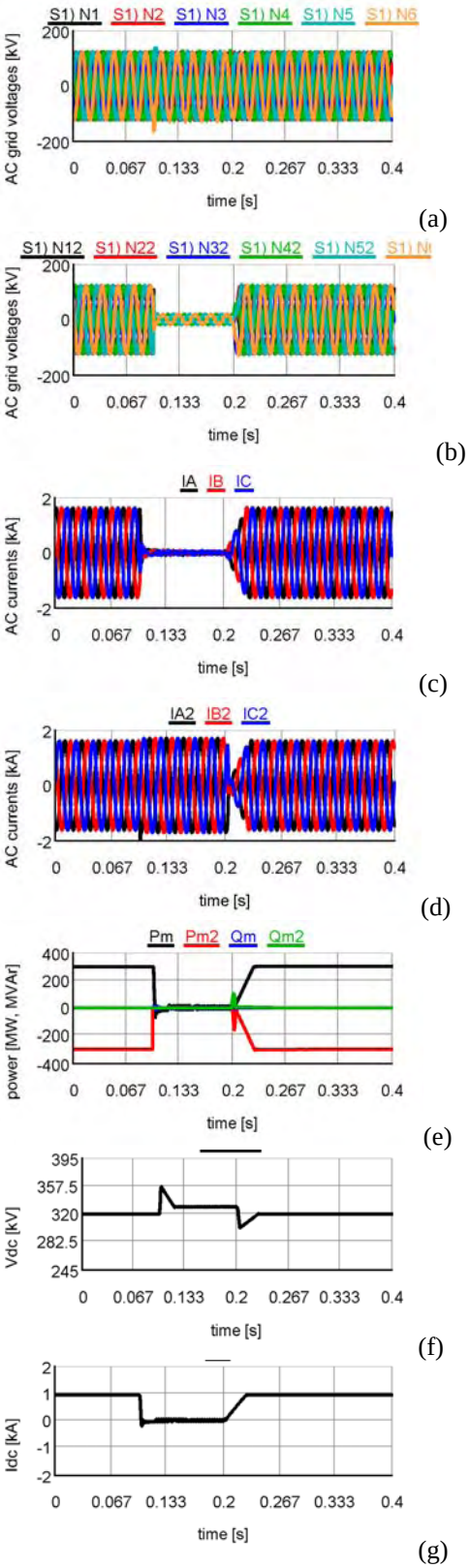

Figure 10 3-phase to ground fault at grid side of VSC2, power flow from VSC1 to VSC2.

6. Conclusion

According to the part of this study concerning steady-state situations, building a MT-VSC transmission system seems to be possible. For multi-terminal purposes, only one VSC can be commanded to control the dc-grid voltage, while the other VSCs are just adding or drawing power to this dc-grid. This interaction between the VSCs can function in a proper way, based on local measurements and without a need for telecommunication.

To control the power flow of each VSC, a current controller (which is able to decouple *P* and *Q*, based on

vector control) with an associated outer controller has been applied to the two VSCs connected to an onshore ac-grid. The VSCs are able to exchange active as well as reactive power with the ac grid and can be used to support the ac grid voltage and frequency.

In order to handle fault situations, the scheme must be expanded in order to protect the VSC and dc-grid from over-voltages and -currents. This is because the defined basic control strategies that are developed in this paper and valid during steady state are not achievable in case a short circuit at the ac-side of the converter occurs, since the converter is simply not able to exchange power with the ac-grid. Thus, in case a short circuit occurs at the ac-side of the VSC controlling the dc-grid voltage, another VSC should control the dc-grid voltage. If this requirement is satisfied, the system is able to restore fast after the ac-short circuit has been cleared.

ACKNOWLEDGEMENT

This research was partly funded under the framework of the Dutch Ministry of Economic Affairs BSIK programme 'Large-scale wind power offshore, towards an innovative and sustainable business', with support from the We@Sea consortium (http://www.we-at-sea.org/).

The research presented in this paper was part of a M.Sc.-project at Delft University of Technology, conducted from December 2006 to August 2007.

REFERENCES

[1] S. Gilje, and L. Carlsson, "Valhall re-development project, power from shore," [Online]. Available: http://library.abb.com/GLOBAL/SCOT/scot221.nsf/VerityDisplay/1BACA5FA5BADC3ECC125718E002F23A8/$File/VALHALL.pdf, p.3 (11-06-2007).

[2] R. L. Hendriks, G. C. Paap, and W. L. Kling, "Control of a multi-terminal VSC transmission scheme for connecting offshore wind farms," *in Proc. 2007 European Wind Energy Conference (EWEC).*

[3] B. R. Anderson, *et al*., "VSC Transmission," CIGRE WG B4.37, Paris, France, 2005, Tech. Rep. 269.

[4] G. C. Paap, "Symmetrical components in the time domain and their application to power network calculations," *IEEE Trans. Power Syst.*, vol. 15, no. 2, pp. 522–528, May 2000.

[5] J. Morren *Grid support by power electronic converters of Distributed Generation units*, 2006, Ph.D. Thesis, Delft University of Technology, Netherlands, 2006.

[6] A. M. Gole, *et al.*, "Validation and analyses of a grid control system using d-q-z transformation for static compensator systems," *Canadian Conference on Electrical and Computer Engineering*, Sept. 17–20, 1989, Montreal, Canada.

[7] M. Szechtman, T. Wess, and C. V. Thio, "First benchmark model for HVDC control studies," *Electra 1991*, vol. 135, pp. 55–73

[8] R. L. Hendriks, G. C. Paap, and W. L. Kling, "Development of a multiterminal VSC Transmission Scheme for Use with Offshore Wind Power," *in Proc 2006 Sixth international workshop on large-scale integration of wind power and transmission networks for offshore wind farms.*

[9] S. Bernet, R. Teichmann, A. Zuckerberger, and P. K. Steimer, "Comparison of high-power IGBTs and hard-driven GTOs for high power inverters," *in Proc. 1999 IEEE Transactions, Industrial Applications*.

[10] L. Tang, and B.-T. Ooi, "Managing zero sequence in voltage source converter," *in Proc. 2002 Conference Record, 37th IAS Annual Meeting, Industry Applications*, vol. 2, pp. 795–802.

[11] S. G. Johansson, G. Asplund, E. Jansson, and R. Rudervall, "Power System Stability Benefits with VSC DC-Transmission System," CIGRE session B4-204, Paris, France, 2004.

Analysis of the experimental spectral coherence in the Nysted Wind Farm

A. Vigueras-Rodríguez[1*)], Poul E. Sørensen[2)], Antonio Viedma[1)], Nicolaos A. Cutululis[2)], M. H. Donovan[3)]
[1)] Universidad Politécnica de Cartagena, 30203 Cartagena (Murcia), Spain
[*)] tlf. +34 968 32 5994, e-mail avigueras.rodriguez@upct.es
[2)] Risø DTU, VEA-118, P.O. Box 49, DK-4000 Roskilde, Denmark
[3)] DONG Energy, Copenhagen, Denmark

Abstract – In this paper, it is analysed the coherence between wind speeds located in a horizontal plane corresponding to hub height of wind turbines in a large wind farm.

The coherence is calculated using real data from Nysted Offshore Wind Farm. Concretely, the wind speed measured in the 72 Wind Turbines and in 2 of the meteorological masts during 9 months. The results are analysed in the characteristic scale of power fluctuations in large offshore wind farms.

This analysis shows the needing of a new spectral coherence model.

Index Terms – wind models, wind coherence, power fluctuation, offshore wind farms

1. INTRODUCTION

Nowadays the concern about the effects of the pollution (like the global warming effect) and the knowledge of the limitations of the fossil resources are creating a strong tendency in Europe towards the use of renewable energy sources. Therefore, there has been a big growth in the Wind Energy development, and it is expected to go on rising. Such growth makes essential to research deeply into this energy technology from the point of view of an important component of the electrical system, instead of considering only the local voltage quality as it was done previously [1].

A major issue in the control and stability of electric power systems is to maintain the balance between generated and consumed power. Because of the fluctuating nature of wind speeds, the increasing use of wind turbines for power generation has risen the interest in the fluctuations of the wind turbines power production, especially when the wind turbines are concentrated geographically in large wind farms. That fluctuation can also be a security issue in the future for systems with weak interconnections like Ireland or the Iberian Peninsula.

As example of the significance of these power fluctuations in Energinet.dk (the Danish Transmission System Operator), according to Akhmatov et al. [2], Energinet.dk has observed that power fluctuations from the 160 MW offshore wind farm Horns Rev in West Denmark introduce several challenges to reliable operation of the power system in West Denmark. And also, that it contributes to deviations from the planned power exchange with the Central European Power System (UCTE). Moreover, it was observed that the time scale of the power fluctuations was from tens of minutes to several hours.

And in those fluctuations the importance of the spatial correlation of the wind speed in that time frame is shown by the fact that the power fluctuations of the 160 MW Wind Farm was significantly greater than the fluctuations in a similar capacity of Wind Turbines (WTs) distributed in smaller onshore Wind Farms. Those conclusions point out that the research of the spatial correlation is a main topic for the power fluctuation analysis.

In this way, models of coherence have been used within the modelling of wind farms regarding power fluctuation. Sørensen et al.[3] developed a wind speed model for a wind farm using a coherence model. In this case, the aim was to simulate the fluctuations in the shorter time scales related with the power quality characteristics.

Later on, an overall model for power fluctuations regarding the "long term" fluctuations described above has been developed [4].

2. COHERENCE MODELS

The spectral coherence between the wind speed in two different points is defined by

$$\gamma(f) = \frac{S_{ab}(f)}{\sqrt{S_{aa}(f)S_{bb}(f)}} \tag{1}$$

where $S_{ab}(f)$ is the crossed power spectral density (CPSD) between the wind speed in points a and b, and $S_{aa}(f)$ and $S_{bb}(f)$ are the power spectral density (PSD) of the wind in each point.

Besides the practical observation of the link between the power fluctuation and the spectral coherence above cited, different theoretical and practical observations have appeared in recent papers [5, 4] confirming that the seeking of power fluctuations models is totally linked with the coherence models in a wind farm frame.

Regarding the current coherence models, most of them are based in modifications to the Davenport model [6]. Davenport's model suggest an exponential behaviour explained by the following expression

$$|\gamma| = e^{-a\frac{d\cdot f}{\bar{V}}} \tag{2}$$

where a, that is usually called decay factor, is a constant.

This model does not explain the inflow angle dependence, and so the usual modifications of this model, based in changing the value of the constant a have the same problem when using them in the scale of a wind farm, where this dependence is essential [7].

Nevertheless, the modifications suggested by Schlez & Infield [8] introduced that dependency expressing a as a function of the inflow angle

$$a = \sqrt{(a_{long}\cdot\cos\alpha)^2 + (a_{lat}\cdot\sin\alpha)^2} \tag{3}$$

being a_{long} and a_{lat} respectively the decay factors for the longitudinal and the lateral situations given by

$$a_{long} = (15 \pm 5)\cdot\frac{\sigma_v}{\bar{V}} \tag{4}$$

$$a_{lat} = (17.5 \pm 5)(m/s)^{-1}\cdot\sigma_v \tag{5}$$

being I_V the turbulent intensity defined by $I_V = \frac{\sigma_v}{\bar{V}}$

However, this empirical model was based on a very limited distance scale and so it does not predict the behaviour in the large wind farms of nowadays [7], so none of the usual models used in Wind Energy suits for studying the Power Fluctuation of Wind Farms. Therefore, in this paper the spectral coherence within a large wind farm is analysed.

3. Experimental procedure of the coherence measuring

The data used in this work is based in the Nysted Wind Farm, which is an offshore Wind Farm compound of 72 Siemens SWT-2.3-82 fixed speed wind turbines, with a global nominal power of 165.6 MW and distances between the wind turbines between 0.48 km and 7.73 km.

The 72 WTs and the 2 Meteorological Masts shown in the figures have been used in this study. In the nacelle of each WT (69 m above ground), it has been measured the wind speed, the active power produced, the yaw angle, the angular velocity and other variables. Furthermore, we have accessed to the wind speed and wind direction data from the meteorological masts at 70 m. above ground.

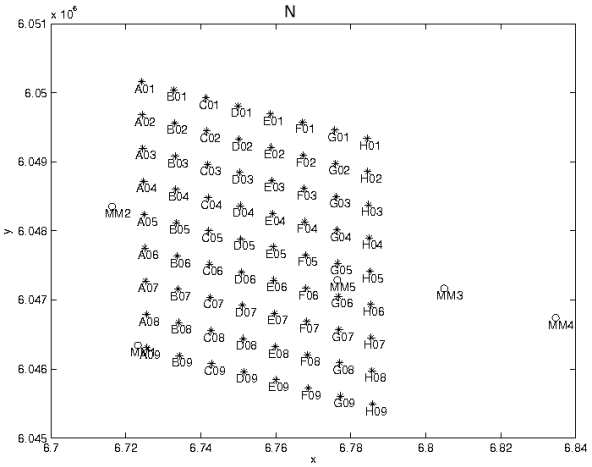

Figure 1. Layout of the Nysted Wind Farm

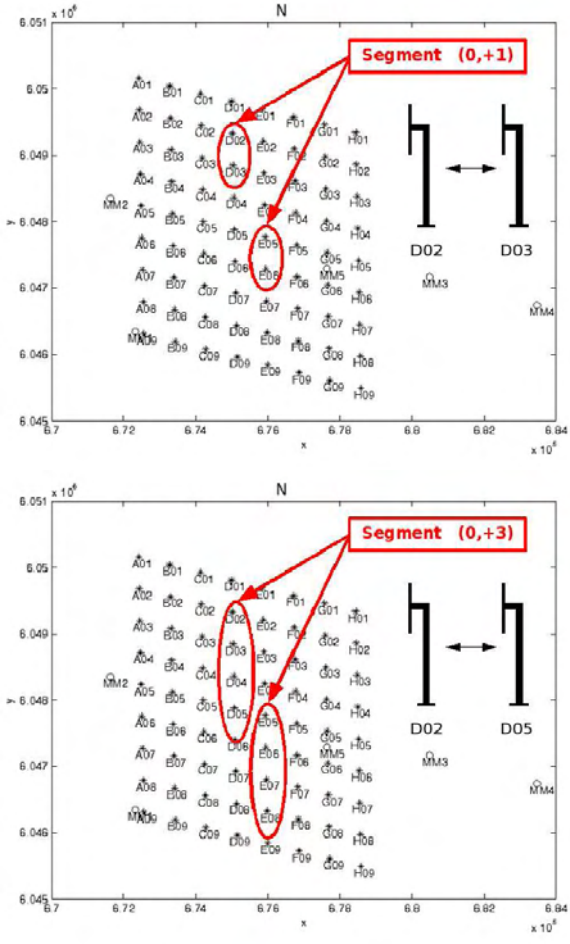

Figure 2. Example of how the segments are assembled.

All of those data have been obtained through a SCADA system used by the wind farm main controller, which logs the data with a 1 Hz sampling frequency.

The data stored that have been used for this work is basically the wind speeds measured by each WT and the velocity and direction of the wind measured in the masts MM2 and MM3 that are shown in the figure 1, corresponding to 9 months in 2005.

All of this data is being processed in 2 hour intervals, so that coherence data is in a suitable time frame for this purpose.

Next, it has been selected only intervals with a 75% of valid data in MM_2 and MM_3. For the single Wind Turbine data a filtering for each Wind Turbine working in a "normal" state has been done by selecting the WTs with at least a 90% of valid data and holes smaller than 3 seconds, so that they can be fulfilled using splines without having any significant influence to the time scale that we are studying.

Then, it has been define similar pairs of WTs with similar distances and angles like A_{01}-A_{02} and C_{03}-C_{04}, calling them geometrical segments.

Following this process, as shown in figure 2, we consider all segments with more than 8 couples, as example some of those segments are shown in the table 1.

Once having selected the intervals, the data in each time interval are processed, averaging the power spectra of each couple of WTs belonging to the same geometrical segment.

For instance, when we consider the segment n compound of m pairs (being $m \geq 8$) of WTs with valid data (a_i, b_i), regarding the convolution property of the Fourier Transform:

$$S_{aa} = \frac{\sum_{i=1}^{m} \mathbf{FFT}(V_{a_i}) \cdot \mathbf{FFT}(V_{a_i})^*}{m} \quad (6)$$

$$S_{bb} = \frac{\sum_{i=1}^{m} \mathbf{FFT}(V_{b_i}) \cdot \mathbf{FFT}(V_{b_i})^*}{m} \quad (7)$$

$$S_{ab} = \frac{\sum_{i=1}^{m} \mathbf{FFT}(V_{a_i}) \cdot \mathbf{FFT}(V_{b_i}^*)}{m} \quad (8)$$

where $S_{aa}(f), S_{bb}(f) \in \mathbb{R}$, as well as $S_{ab}(f) \in \mathbb{C}$. This is done for each segment with enough valid data in each time interval.

Afterwards, the results of each segment data $(S_{aa}(f), S_{bb}(f), S_{ab}(f))$ can be classified depending on the average wind speed $\overline{V}$ and the inflow angle α calculated through the segment angle β and the wind direction ϕ as shown in figure 3.

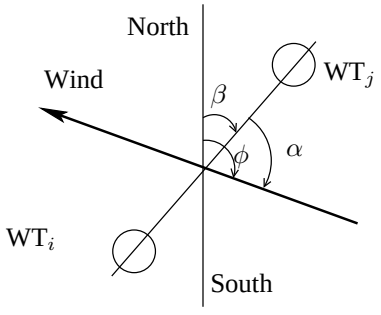

Figure 3. Definition of the inflow (α), segment (β) and wind direction angles (ϕ) used.

Next, the data classified for each segment (n) in the same wind

Δi_{row}	Δi_{column}	d_{xy}(m)	β_{xy}(deg.)	Blocks
0	1	482	-2	64
0	2	964	-2	56
0	3	1445	-2	48
0	4	1927	-2	40
0	5	2409	-2	32
0	6	2890	-2	24
0	7	3372	-2	16
0	8	3854	-2	8
1	0	867	-82	63
1	1	1062	-56	56
1	2	1403	-40	49
1	3	1810	-30	42
1	4	2246	-25	35
1	5	2698	-21	28
1	6	3158	-18	21
1	7	3625	-16	14
⋮	⋮	⋮	⋮	⋮
6	0	5204	-82	18
6	1	5308	-77	16
6	2	5454	-72	14
6	3	5637	-68	12
6	4	5853	-63	10
6	5	6101	-59	8
7	0	6071	-82	9
7	1	6173	-78	8
1	-7	3334	13	14
⋮	⋮	⋮	⋮	⋮
6	-5	5343	71	8
6	-4	5227	76	10
6	-3	5154	82	12
6	-2	5126	87	14
6	-1	5142	-88	16
7	-1	6007	-87	8

Table 1. Example of the 2-point segment characteristics.

speed range (v_m) and inflow angle range (α_k) are used for calculating the coherence $\gamma(n, v_m, \alpha_k, f)$ as follows:

$$\gamma(n, v_m, \alpha_k, f) = \frac{\sum_{i=1}^{N_n} S_{ab}(i, f) \cdot N_i}{\sqrt{\sum_{i=1}^{N_n} S_{aa}(i, f) \cdot N_i \cdot \sum_{i=1}^{N_n} S_{aa}(i, f) \cdot N_i}} \tag{9}$$

where N_i are the number of pairs of WT series of data used previously for calculating the power spectral functions, i.e. the number m in equations 6,7 and 8.

The following 5 inflow angle bins are used $[0, 6, 25, 65, 84, 90]$(deg.), whereas the ranges of wind speed are $2m/s$ intervals from $2m/s$ to $16m/s$.

Finally, using the distance of each segment $d(n)$, we get an experimental $\gamma(d, v_m, \alpha_k, f)$.

In this proceeding the wake has been neglected. That is possible because in most of the pairs consider where both measures are inside of the overall wake, that affects similarly to both series of data and so, it is removed by the definition of the coherence itself (eq. 1). On the other hand, in the cases where the influence of having measures out of the wake and measures in the deep wake could be greater, looking at the expression of power spectral density of the wind inside and out of the wake that is shown in [4], we see that it does not affect to the time scale which we are interested in.

4. RESULTS

As it has been explained previously we have a package of coherence data ($|\gamma(d, v_m, \alpha_k, f)|$ and its argument $\angle\gamma(d, v_m, \alpha_k, f)$), from which in this work we focus in the module part.

Looking into the data, it is found a clear exponential dependence between the coherence and either the frequency f or the dimensionless frequency $\frac{d \cdot f}{V}$, as it is shown in figure 4.

Although looking to the figure 5, where that exponential dependence is represented in 3 different situations, it is also shown that its decay factors are quite different on each situation, and therefore it is not realistic to fit them to a single decay factor.

Then, taking into account the inflow angle, we can focus firstly in the data corresponding to the longitudinal situation ($\alpha_1 \Rightarrow \alpha \in [0,\ 6\,\text{deg}]$) plotted in figure 6, where the decay factor a (see 2) is plotted for different wind speed ranges against the distance. In that figure, it is possible to see that there is not any significant tendency in the variation of that parameter with the distance or the wind speed ($a_{long} \neq f(d, V)$). Therefore, it is possible to assume that a constant value for the longitudinal situation a_{long} (see 4) would be suitable in this distance and time frame. This would agree qualitatively (but not quantitatively) to Schlez & Infield model (Eq. 3).

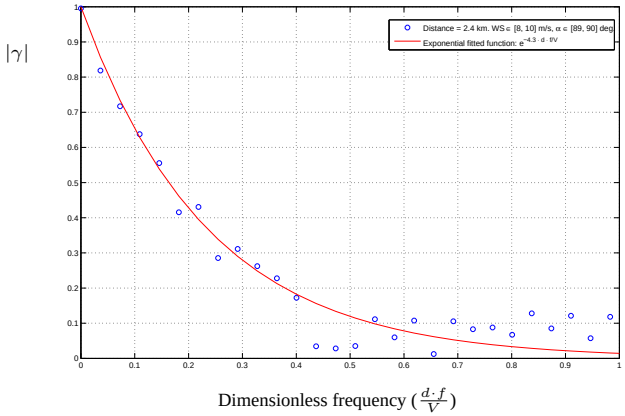

Figure 4. Coherence measured in Nysted Wind Farm in the longitudinal situation and an exponential curve fitted to the data.

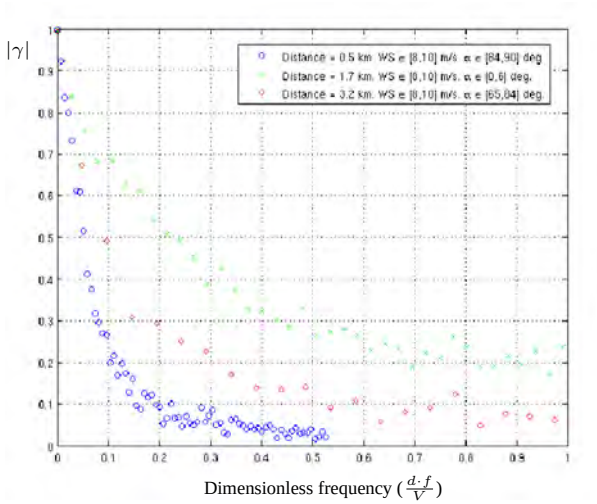

Figure 5. Coherence measured in Nysted Wind Farm in 3 different situations.

However, in the lateral situation ($\alpha_5 \Rightarrow \alpha \in [84,\ 90\,\text{deg}]$), the decay factor parameter depends significantly on the distance and the wind speed ($a_{lat} = f(d, V)$), as it is shown in figure 7 , and this was not predict by the Schlez & Infield model due to the different time

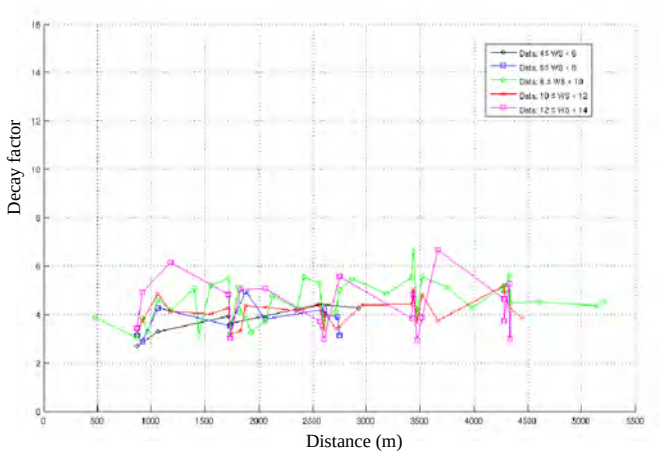

Figure 6. Decay factor of the coherence in the longitudinal situation.

and length scale in the distance between the points (100 m) and in the height above ground (18 m).

Looking into the figure, it is possible to see that a_{lat} gets lower when the distance rises, a_{lat} rises when wind speed gets greater, and those changes of a_{lat} get less significant as the distance gets greater.

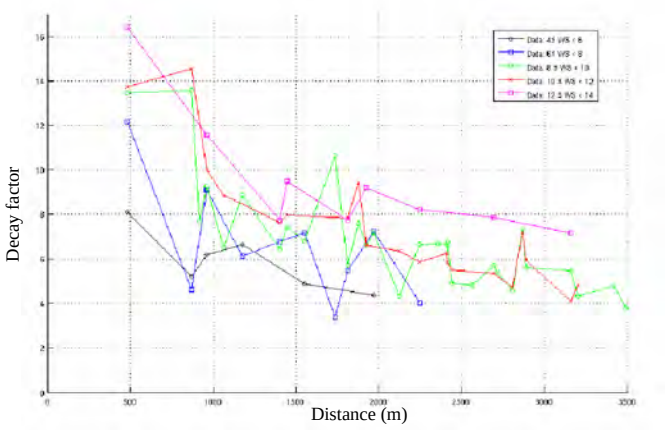

Figure 7. Decay factor of the coherence in the lateral situation.

Looking at the intermediate situations ($\alpha_2, \alpha_3, \alpha_4$), it is possible to see an intermediate behaviour between the longitudinal and the lateral situation, as it was suggested by the Schlez & Infield model.

Therefore, the coherence can be considered explained by eq. 2, where the decay factor is a function $a = a(\alpha, d, V)$ complying the following conditions:

$$\alpha \to 0 \quad \Rightarrow \quad \Delta a(\Delta d, \Delta V) \to 0 \tag{10}$$

$$d \uparrow \quad \Rightarrow \quad a \downarrow \tag{11}$$

$$V \uparrow \quad \Rightarrow \quad a \uparrow \tag{12}$$

$$d \uparrow\uparrow \quad \Rightarrow \quad \Delta a(\Delta d, \Delta V) \downarrow \tag{13}$$

$$\alpha \downarrow \quad \Rightarrow \quad \Delta a(\Delta d, \Delta V) \downarrow \tag{14}$$

5. Conclusion

It has been processed 9 months of real data coming from a Large Offshore Wind Farm, selecting 2 hour intervals. In which the coherence have been calculated. It has been considered all the inflow angle situations and for the whole range of wind speed where the wind farm is often working, and with distances from near 0.5 km to 6 km.

It has been shown that there is a significant dependence between the coherence and the inflow angle, as in the model suggested by Schlez & Infield. However, it was also shown that in the length, height and time scale interesting for studying the power fluctuations of Large Wind Farms, the Schlez & Infield model predicts coherence values that are quite far from the experimental data shown here.

In those experimental data is shown that whereas the longitudinal situation ($\alpha \approx 0$) can be modelled by means of a constant decay factor, there is a strong dependency between the decay factor and the distance and wind speed, being this dependency stronger as the inflow angle gets closer to the lateral situation ($\alpha = \pi/2$).

This analysis has been generalised in a paper submitted to the Journal of Wind Engineering and Industrial Aerodynamics [9].

Acknowledgment

The work presented in this paper has been done in the research project "Power Fluctuations from large offshore wind farms" financed by the Danish Transmission System Operator Energinet.dk as PSO 2004 project number 6506.

A. Vigueras-Rodríguez is supported by the Spanish Ministerio de Educación y Ciencia through the grant program "Becas FPU" and from the national research project "ENE2006-15422-C02-02".

References

[1] P. Sørensen, N. A. Cutululis, T. Lund, A. D. Hansen, T. Sørensen, et al.: Power quality issues on wind power installations in Denmark, in IEEE Power Engineering Society, General Meeting, Tampa, Florida, USA.

[2] V. Akhmatov, J. P. Kjaergaard, H. Abildgaard: Announcement of the large offshore wind farm Horns Rev B and experience from prior projects in Denmark, in European Wind Energy Conference.

[3] P. Sørensen, A. D. Hansen, P. E. C. Rosas: Wind models for simulation of power fluctuations from wind farms, Journal of Wind Engineering and Industrial Aerodynamics vol. 90, 2002, pp. 1381–1402.

[4] P. Sørensen, N. Cutululis, A. Vigueras-Rodríguez, H. Madsen, P. Pinson, et al.: Modelling of power fluctuations from large offshore wind farms, Wind Energy .

[5] T. Nanahara, M. Asari, T. Sato, K. Yamaguchi, M. Shibata, et al.: Smoothing effects of distributed wind turbines. Part 1. Coherence and smoothing effects at a wind farm, Wind Energy vol. 7, 2004, pp. 61–74.

[6] A. G. Davenport: The spectrum of horizontal gustiness near the ground in high winds, Quarterly Journal of Meteorology Society vol. 87, no. 372, 1961, pp. 194–211.

[7] A. Vigueras-Rodríguez, P. Sørensen, A. Viedma: Spectral coherence models for the wind speed in large wind farms, in Proceedings of the 2nd PhD Seminar on Wind Energy in Europe, European Academy of Wind Energy, Roskilde (Denmark).

[8] W. Schlez, D. Infield: Horizontal, two point coherence for separations greater than the measurement height, Boundary-Layer Meteorology vol. 87, 1998, pp. 459–480.

[9] A. Vigueras-Rodríguez, P. Sørensen, A. Viedma, M. H. Donovan: Spectral coherence model for power fluctuations in a wind farm, submitted to Journal of Wind Engineering and Industrial Aerodynamics.

Risø’s research is aimed at solving concrete problems in the society.

Research targets are set through continuous dialogue with business, the political system and researchers.

The effects of our research are sustainable energy supply and new technology for the health sector.